

UC Irvine

UC Irvine Electronic Theses and Dissertations

Title

Synthesis of Epidithiodioxopiperazine Analogues and the Development of a Copper-Catalyzed Stereodivergent 1,3-Dipolar Cycloaddition Reaction

Permalink

<https://escholarship.org/uc/item/52f5b75z>

Author

Walton, Mary Catherine

Publication Date

2015

Peer reviewed|Thesis/dissertation

UNIVERSITY OF CALIFORNIA,
IRVINE

Synthesis of Epidithiodioxopiperazine Analogues and the
Development of a Copper-Catalyzed Stereodivergent 1,3-Dipolar Cycloaddition Reaction

THESIS

submitted in partial satisfaction of the requirements
for the degree of

MASTER OF SCIENCE
in Chemistry

by

Mary Catherine Walton

Thesis Committee:
Professor Larry Overman, Chair
Professor Elizabeth Jarvo
Professor Sergey Pronin

2015

© 2015 Mary C. Walton

Dedication

for my grandfather

Eugene Behun

Table of Contents

	Page
List of Figures	vi
List of Schemes	vii
List of Tables	viii
List of Equations	x
Acknowledgments	xi
Abstract of the Thesis	xii
Chapter 1: Synthesis and Biological Testing of Novel Epidithiodioxopiperazine Derivatives	1
1.1 Introduction	1
1.1.1 ETP Natural Products' Mechanisms of Toxicity	1
1.1.2 Anticancer Activity of ETP Natural Products	4
1.2 Synthesis and Biological Testing of Novel ETP Analogues	5
1.2.1 Overview of the Synthetic Route	6
1.2.2 SAR Trends	7
1.2.3 Substrate Synthesis	11
1.2.4 Determination of ETP Anticancer Activity	14
1.3 Conclusion	15
1.4 Appendix A: Experimental Procedures	16
1.4.1 Materials and Methods	16
1.4.2 Synthesis of Imines	17
1.4.3 Synthesis of Pyrrolidines	18
1.4.4 Synthesis of Dioxopiperazines	21

1.4.5 Synthesis of Epidithiodioxopiperazines	24
1.5 Appendix B: NMR Spectral Data	28
1.6 References and Notes	51
Chapter 2: Studies Toward the Development of a Diastereo- and Enantioselective Catalytic 1,3-Dipolar Cycloaddition for the Synthesis of Pyrrolidine Derivatives	56
2.1 Relative and Absolute Configuration are Important Factors in the Potency of Epidithiodioxopiperazine Analogues	56
2.2. Chiral Lewis Acids in 1,3-DCs of Azomethine Ylides	58
2.2.1 Ag(I)-Catalyzed 1,3-DC Reactions	62
2.2.2 Cu(I)-Catalyzed 1,3-DC Reactions	65
2.3 Investigation of Ligand Types	66
2.3.1 Phosphoramidite Ligands	68
2.3.2 Phosphine Ligands	72
2.3.3 Phosphite Ligands	77
2.4 Conclusion	81
2.5 Appendix A: Experimental Procedures	82
2.5.1 Materials and Methods	82
2.5.2 Synthesis of Imine 2.5	83
2.5.3 Ag(I)-Catalyzed 1,3-DC Reactions	84
2.5.4 Cu(I)-Catalyzed 1,3-DC Reactions	86
2.5.5 Ligand Synthesis	88
2.6 Appendix B: NMR Spectral Data	92
2.7 Appendix C: Enantioselective HPLC Chromatograms	109
2.8 References and Notes	126

Chapter 3: Catalytic Diastereoselective Synthesis of Pyrrolidine Derivatives by 1,3-Dipolar Cycloaddition with Methacrylonitrile	134
3.1 Introduction	134
3.1.1 Switching 1,3-DC Diastereoselectivity by Changing the Metal Salt	135
3.1.2 Catalyst-Controlled Diastereoselectivity	136
3.1.3 Ligand-Directed Diastereodivergence	137
3.2 Optimization of Reaction Conditions	139
3.3 Investigation of Imine Reactivity	145
3.4 Transition State Calculations	148
3.5 Utilization of Different Dipolarophiles	151
3.6 Conclusion	154
3.7 Appendix A: Experimental Procedures	155
3.7.1 Materials and Methods	155
3.7.2 Synthesis of Imines	156
3.7.3 Cu(I)-Catalyzed 1,3-DC Reaction Using Various Imine Substrates	161
3.7.4 Cu(I)-Catalyzed 1,3-DC Reaction Using Various Dipolarophiles	174
3.7.5 Verification of Cu(I)/PCy ₃ Catalyst	180
3.8 Appendix B: NMR Spectral Data	182
3.9 Appendix C: Representative GC-FID Chromatograms	277
3.10 Appendix D: Representative Analytical ¹ H NMR Spectral Data	288
3.11 References and Notes	291

List of Figures

	Page
Figure 1.1. Generic Structure of ETP Alkaloids and Three Well Studied ETP Natural Products	2
Figure 1.2. Mechanisms of ETP Toxicity	3
Figure 1.3. Influence of C7 Substitution on Anticancer Activity	8
Figure 1.4. Effects of Aromatic Substitution Patterns on ETP Anticancer Activity	9
Figure 1.5. Anticancer Activity of ETP Derivatives with Different Polysulfide Bridge Lengths	9
Figure 1.6. Effect of C3 Substitution on ETP Analogue Anticancer Activity	10
Figure 1.7. Alkyl Group Substitutions at the N2 Position	10
Figure 1.8. IC ₅₀ Values of ETP Analogues 1.40 , 1.41 , 1.42 , and 1.17	15
Figure 2.1. IC ₅₀ Values for Four ETP Diastereomers against Two Cancer Cell Lines	57
Figure 2.2. IC ₅₀ Values of Enantiopure (+)- and (-)- 2.1 Against Two Cancer Cell Lines	57
Figure 2.3. 1,3-DC between a “W-Shaped” Azomethine Ylide and an Electron-Deficient Olefin	58
Figure 2.4. Zhang’s Ag(I)/xylyl-FAP-Catalyzed Synthesis of Enantioenriched Pyrrolidines	59
Figure 2.5. Jørgensen’s Zn(II)/ <i>t</i> -Bu-BOX Catalyst System	61
Figure 3.1. Transition State Energies Calculated for a Cu(I)-Phosphite-Ylide Complex	149
Figure 3.2. Calculated Endo Transition State with Phosphite Ligand	149
Figure 3.3. Transition State Energies Calculated for a Cu(I)-PCy ₃ -Ylide Complex	150
Figure 3.4. Transition State Energies Calculated for a Cu(I)-DavePhos-Ylide Complex	151

List of Schemes

	Page
Scheme 1.1. Retrosynthetic Analysis for Novel ETP Analogues	6
Scheme 1.2. Five-Step Sequence to Access Highly Substituted ETP Analogues	7
Scheme 1.3. Synthesis of ETPs 1.40 and 1.41	11
Scheme 1.4. Unsuccessful Strategies to Access Pyrrolidine 1.43	12
Scheme 1.5. Synthesis of Oxime 1.46	13
Scheme 1.6. Attempts to Access Pyrrolidine 1.43 by Dehydration of Oxime 1.46	13
Scheme 1.7. Completion of ETP 1.42	14
Scheme 2.1. Key Reaction to Develop a Highly Selective Synthesis of ETP (+)- 2.1	62
Scheme 3.1. Martín's Stereodifferentiation of Fulleropyrrolidines	137
Scheme 3.2. Carretero's <i>P,P'</i> -Biaryl Ligand-Induced Diastereoselectivity Changes	139

List of Tables

	Page
Table 2.1. Condition Screening for Ag(I)-Catalyzed 1,3-DC using Methacrylonitrile	63
Table 2.2. Competition Experiments to Test Nitrile–Ag(I) Compatibility	64
Table 2.3. Investigation of Solvent to Selectively Access Pyrrolidine 2.6	66
Table 2.4. <i>P,S-</i> , <i>P,N-</i> , HASPO, NHC, and Pyridine-Based Ligands	67
Table 2.5. Chiral Phosphoric Acid Ligands	68
Table 2.6. Phosphoramidite Ligands Used with PhMe as the Reaction Solvent	69
Table 2.7. Phosphoramidite Ligands Used with THF as the Reaction Solvent	71
Table 2.8. Achiral Monodentate Phosphines	73
Table 2.9. Achiral Bidentate Phosphine Ligands	74
Table 2.10. Achiral Polydentate Phosphine Ligands in THF	75
Table 2.11. Chiral Diphosphine Ligands Tested in the Cu(I)-Catalyzed 1,3-DC	76
Table 2.12. Achiral Phosphite Ligands Used in the Cu(I)-Catalyzed 1,3-DC	78
Table 2.13. Achiral Monodentate Phosphite Ligands Run in THF	79
Table 2.14. Chiral and Racemic Phosphite Ligands	80
Table 2.15. Ligand-Controlled Diastereodivergence	81
Table 3.1. Ligand-Controlled Diastereodivergence	134
Table 3.2. Töke’s Metal-Induced Diastereoselectivity Changes	136
Table 3.3. Hou’s <i>P,N</i> -Ferrocenyl Ligand-Induced Diastereoselectivity Changes	138
Table 3.4. Solvent Screen	140
Table 3.5. Negative Controls	140
Table 3.6. Equivalents of Dipolarophile	141

Table 3.7. Base Optimization	142
Table 3.8. Temperature Effects on Yield and Diastereoselectivity	143
Table 3.9. Catalyst Loading and Reaction Concentration	144
Table 3.10. Optimization of Reaction Time	145
Table 3.11. Diastereodivergence using Different Imines	147
Table 3.12. Increased Catalyst Loading to Access Pyrrolidines 3.17 and 3.18	148
Table 3.13. Pyridine Poisons Cu(I) Catalysts	148
Table 3.14. Nitrile-Containing Dipolarophiles	152
Table 3.15. Acrylate Dipolarophiles	154
Table 3.16. ^{31}P NMR Shifts of PCy ₃ Derivatives	181
Table 3.17. Testing PCy ₃ Ligands	181
Table 3.18. GC-FID Response Factors for Starting Materials	277

List of Equations

	Page
Equation 2.1	58
Equation 2.2	59
Equation 2.3	65
Equation 2.4	65
Equation 2.5	66
Equation 3.1	150
Equation 3.2	153

Acknowledgments

While the yearlong sunshine and lack of snow attracted me to pursue my graduate studies at UC Irvine, the opportunity to work with Professor Larry Overman proved to be the most alluring. It was an enormous honor to work in Larry's group. I thank Larry for his mentorship and support, but most importantly, for believing in me.

Additionally, I would like to thank my committee members, Professors Liz Jarvo and Sergey Pronin. Liz, your course was one of my favorites at UC Irvine. Sergey, I have had a great time getting to know you and was happy to be involved in the transition as you set up your new lab. I learned a lot from both of you and am honored to have you on my thesis committee.

I also wish to thank Professors Chris Vanderwal and Scott Rychnovsky for their guidance and mentorship during my second year report and oral examination. I have enjoyed the experience of recently integrating with the Vanderwal and Rychnovsky labs on the fourth floor.

It has been a privilege to be a member of the Overman group. My coworkers are very driven and have inspired me to become a better chemist. A special thanks is extended to Carol Schwarz. Carol's support for the Overman group was unique and will be dearly missed.

I have met many interesting people over the past three years and I thank them for their support and their friendship: Kyle, for being there every step of the way, from the very beginning; Michael, for his friendship and mentorship; Jess, a diamond in the rough; Greg and Allen for their help and advice during my search for a career; Jacob, for always helping me to see the bright side of any situation; Brian, for always listening; Alyssa and Nancy, my ice cream gang; and friends in the Vanderwal lab for helpful (but more often entertaining) conversations.

The collaborative and open environment at UC Irvine provided the opportunity for me to share ideas with chemists from other research groups and form many friendships in the process. I wish to thank the Rychnovsky, Jarvo, Shea, and Dong labs for helping provide chiral ligands and instrumental support for the work described herein.

I am grateful for the GAANN and NSF GRFP fellowships that generously supported me during my graduate studies. Thank you to our collaborators Dr. David Horne and Dr. Sangkil Nam at City of Hope for performing cytotoxicity studies and Professor Kendall Houk, Dr. Xin Hong, and Dr. Yunfeng Yang at UCLA for their computational support. Thank you to the excellent facilities at UC Irvine: Dr. John Greaves, Dr. Beniam Berhane, Shirin Sorooshian, Dr. Philip Dennison, and Jorg Meyer. Your work is highly valued and greatly appreciated.

Endless thanks to my loving family for their unconditional support.

Finally, I extend a special thanks to Kyle, Michael, and Brian for proofreading this thesis. Your input greatly improved its content.

Abstract of the Thesis

Synthesis of Epidithiodioxopiperazine Analogues and the
Development of a Copper-Catalyzed Stereodivergent 1,3-Dipolar Cycloaddition Reaction

By

Mary C. Walton

Master of Science in Chemistry

University of California, Irvine, 2015

Professor Larry E. Overman, Chair

In Chapter 1, epipolythiodioxopiperazine (ETP) natural products and a short synthesis of novel ETP analogues are introduced. Analogue synthesis and structure-activity relationship studies of their anticancer activity are described.

In Chapter 2, studies toward the development of a catalytic, diastereoselective, and enantioselective 1,3-dipolar cycloaddition (1,3-DC) reaction to improve upon the synthesis of ETP analogues are described. Over 75 different ligands were tested for their effectiveness in accomplishing this goal. A trend between catalyst electronic structure and the reaction diastereoselectivity was discovered where the use of an electron-deficient phosphite ligand resulted in a highly endo adduct-selective reaction. Alternatively, when a bulky electron-rich phosphine was used, the diastereoselectivity reversed to favor the exo cycloadduct.

In Chapter 3, the generality of the diastereodivergent 1,3-DC reactions are explored by investigating aryl imine starting materials with different electronic properties as well as different dipolarophiles. Computational studies performed by our collaborators at UCLA are also described. It was shown that methacrylonitrile is the ideal dipolarophile to exhibit the dramatic changes in diastereoselectivity depending on the ligand used in the catalytic 1,3-DC reaction.

Chapter 1: Synthesis and Biological Testing of Novel Epidithiodioxopiperazine Derivatives

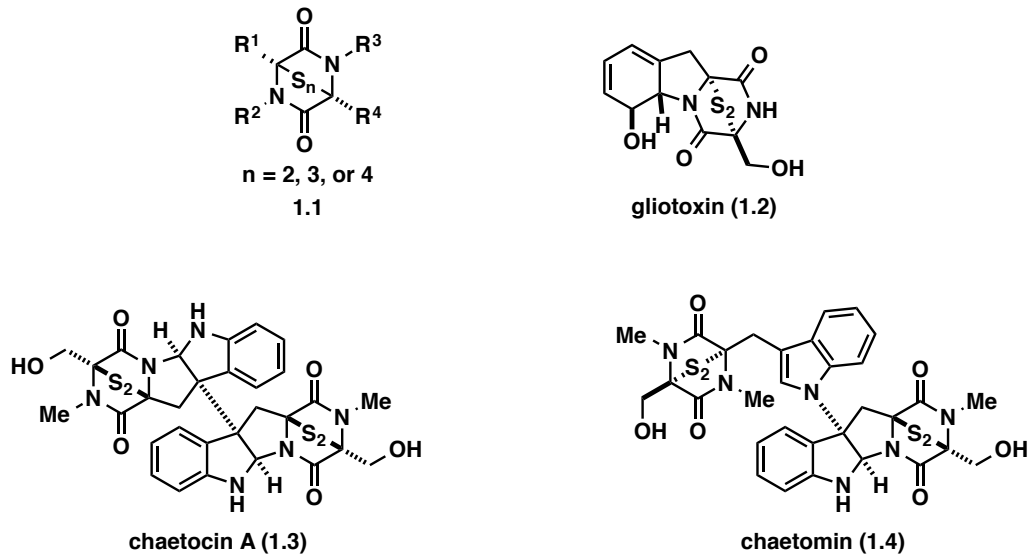
1.1 Introduction

Epipolythiodioxopiperazine (ETP) natural products are a class of alkaloids with intriguing structural features and diverse biological activities.¹ Their general structure is described by a 2,5-dioxopiperazine core² with a bridging polysulfide unit, where in natural sources, the number of sulfur atoms can range between two and four (**1.1**, Figure 1.1). ETPs are amino acid-derived³ secondary metabolites that are isolated from filamentous fungi.⁴ While the role of ETP secondary metabolites is presently not well understood, the variety of ETP bioactivities as well as their isolation from a phylogenetically diverse range of fungi⁵ suggests their importance in the defense and survival of the organisms that produce them. Recent studies have described a broad range of bioactivities attributed to ETPs, and their potent anticancer activity is of particular interest.¹ The complex and diverse array of structural features of ETPs, as well as the underexplored reports of structure-activity relationship studies,⁶ have intrigued organic chemists to direct synthetic efforts toward this unique class of alkaloids.

1.1.1 ETP Natural Products' Mechanisms of Toxicity

Weindling reported the first isolated ETP natural product, gliotoxin (**1.2**, Figure 1.1), in 1932.⁷ Since its discovery, gliotoxin has remained one of the most studied ETP alkaloids in terms of its structure,⁸ synthesis,^{9,10} and biological activity.¹¹ Similarly, ETPs chaetocin A¹² (**1.3**) and chaetomin¹³ (**1.4**) have been used to elucidate the mechanisms of ETP toxicity, which have been attributed to the labile bridging disulfide moiety of these natural products.^{14,15} Three common mechanisms of toxicity have been described: (1) Generation of reactive oxygen species

via redox cycling,¹⁶ (2) formation of mixed thiol species by thiol-disulfide exchange with essential thiol groups on proteins,¹⁷ and (3) chelation and extrusion of metal cofactors from proteins (Figure 1.2).¹⁸



**Figure 1.1. Generic Structure of ETP Alkaloids and
Three Well Studied ETP Natural Products**

The internal disulfide bridge of an ETP can be reduced *in vivo* to the corresponding dithiol species. This reduction is thought to occur by glutathione,¹⁹ a ubiquitous intracellular tripeptide that has antioxidant properties because of its ability to undergo redox cycling between a reduced form (GSH) and a dimeric oxidized form (GSSG) (Figure 1.2A).²⁰ The resulting reduced ETP is aerobically unstable and undergoes facile single-electron oxidation by molecular oxygen.²¹ This process results in reformation of the parent ETP disulfide bridge, but also generates superoxide anion radicals. Further processing of superoxide anion radicals results in the formation of highly reactive hydrogen peroxide or hydroxyl radicals, which cause oxidative cellular damage.²² Studies have shown that rapid oxidative cell death occurs in cells treated with ETP and a large excess of GSSG, which is thought to promote formation of reduced ETP,

thereby supporting this proposed mechanism of ETP toxicity.²³ The redox properties of ETP analogues therefore suggest a possible mechanism of cellular damage and death.

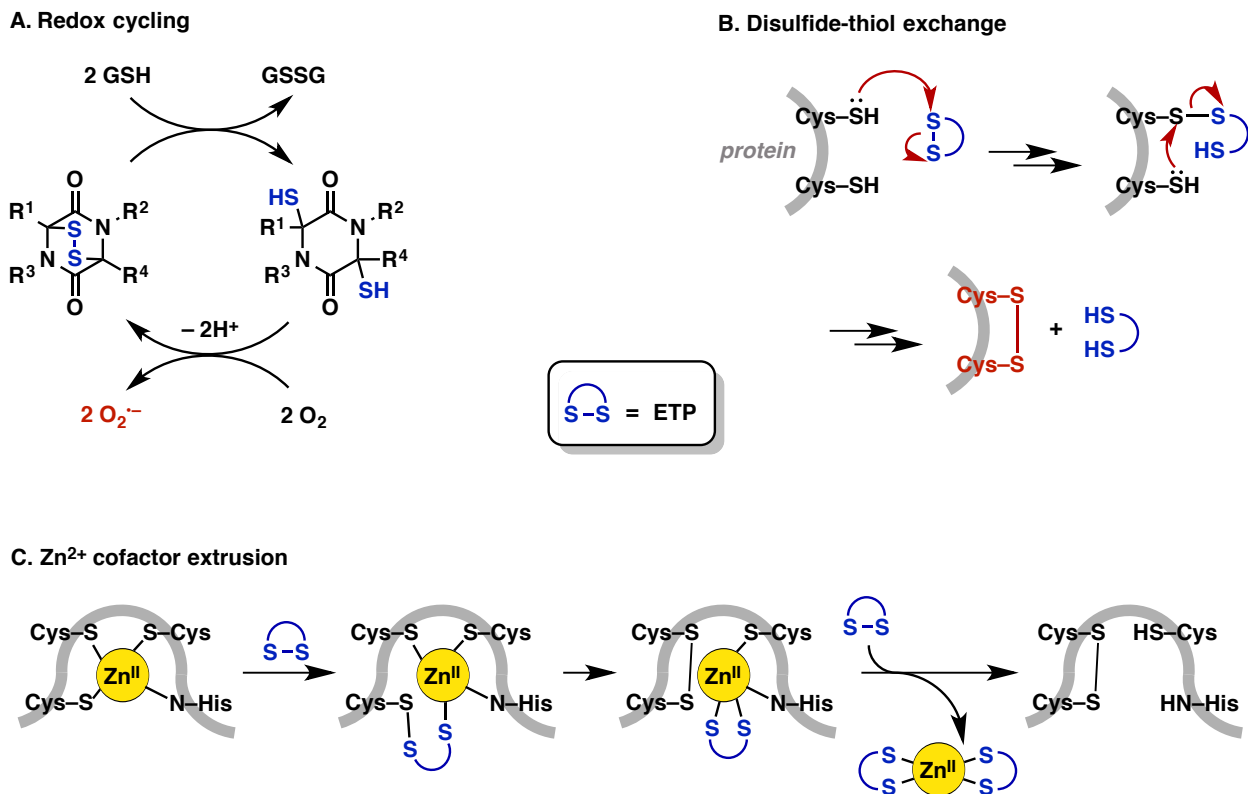


Figure 1.2. Mechanisms of ETP Toxicity

Additionally, the episulfide moiety of ETP analogues is subject to nucleophilic attack by thiol groups on proteins (Figure 1.2B). Such attack results in the formation of mixed polysulfide species, which may be directly toxic, or, in the presence of a second nearby thiol residue, can result in extrusion of reduced ETP while forming an internal polysulfide bridge within the protein. Both of these mechanisms result in detrimental changes to the protein's tertiary structure, which may result in loss of activity. Radiolabeling studies have demonstrated that gliotoxin forms protein adducts with bovine serum albumin,^{14c} creatine kinase,²⁴ viral RNA polymerase 3D^{pol},²⁵ alcohol dehydrogenase,^{11a} farnesyl transferase,²⁶ and transcription factor

NF- κ B.²⁷ Together with loss of function data, these studies demonstrate that gliotoxin inactivates certain proteins by the formation of mixed thiol adducts.

The sulfur atoms of ETP natural products have also been shown to chelate Zn²⁺ ions in the CH1 domain of p300 protein (Figure 1.2C).^{28,29} Schofield and coworkers studied this interaction specifically by treating CH1 with increasing equivalents of gliotoxin.²⁹ It was observed that the Zn²⁺ cofactor was completely extruded from the protein when treated with a large excess of gliotoxin (20 equiv). Partial zinc ejection was observed by treating CH1 with structurally simplified synthetic ETPs, demonstrating that the observed effect is attributed to the simple ETP disulfide core **1.1**. Toxic effects of ETPs were relieved when zinc supplementation was enforced.²⁹ This observation is consistent with reports of reversing toxic effects in grazing animals affected by sporidesmin³⁰ poisoning.³¹ While this third potential mechanism of ETP toxicity is comparatively less explored, the interaction of sulfur with metal cofactors may help explain the selective toxicity profiles of ETPs.

1.1.2 Anticancer Activity of ETP Natural Products

While the toxicity of natural ETPs gliotoxin, chaetomin, and chaetocin A is broad, recent studies have elucidated specific anticancer activity of ETP alkaloids. ETPs have been shown to be important inhibitors of two distinct pathways: Hypoxic cell signaling and epigenetic modifications dictated by histone methylation. In hypoxic cellular microenvironments, such as those in solid tumors, levels of the protein hypoxia-inducible factor 1- α (HIF-1 α) accumulate. HIF-1 α is translocated into the nucleus and binds to hypoxia response elements, along with proteins ARNT, CREB, p300, and cJUN. This assembly enables the transcription of genes that lead to the production of proteins that are essential for cell survival in a hypoxic environment.³² As mentioned in the previous section, gliotoxin has been shown to extrude Zn²⁺ ions from the

CH1 domain of protein p300, resulting in HIF-1 α /p300 binding inhibition.²⁹ Disruption of HIF-1 α /p300 binding exhibited by ETPs has demonstrated antiproliferative effects in vivo studies.^{6a,33} Therefore, the development of HIF inhibitors is an attractive target for anticancer therapy.³⁴

Chaetocin A has been the subject of many studies as a result of its documented inhibition of the SUV39 family of histone methyl transferases.^{35,36} Histone methyl transferases are important enzymes involved in epigenetic regulation of chromatin organization and gene expression, making them attractive targets for anticancer therapy.³⁷ For example, G9a,³⁸ a histone lysine methyl transferase (HKMT), has been shown to be inhibited by a variety of natural and synthetic ETPs in vitro.^{6c,39} Additionally, chaetocin A has been demonstrated to form covalent adducts with HKMT G9a in vitro.⁴⁰ A hypothesis for the selective HKMT inhibition of ETPs is proposed to be due to their ability to coordinate to Zn²⁺ ions; Zn²⁺ ions have been reported to be present in HKMTs SU(VAR)3–9 and G9a, but not SET7/9, thus positively correlating with the ETP HKMT toxicity profile.^{1b} Studies directly linking ETP anti-HKMT activity to anticancer activity are, however, yet to be disclosed.

1.2 Synthesis and Biological Testing of Novel ETP Analogues

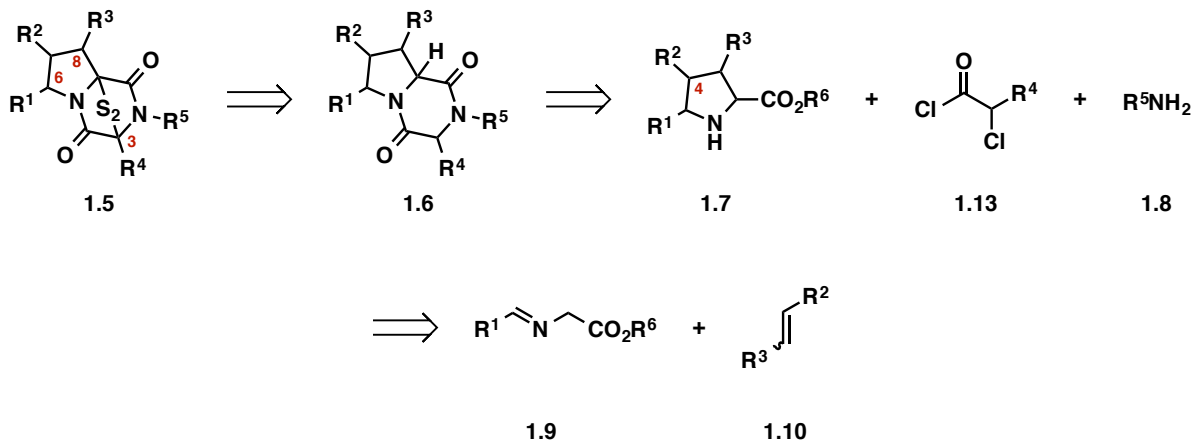
The Overman group became interested in the synthesis of ETP natural products to not only address the challenges associated with their structural complexity⁴¹ but also because of their promising anticancer activity.^{6e,42} As described previously, natural ETP alkaloids exhibit potent anticancer activity, but their therapeutic applications are limited as a result of their broader toxicity.^{34b} We hypothesized that more selective anticancer activity could be accomplished by truncating the ETP scaffold to focus on the activity-bearing polysulfide bridge. Consequently,

a short and modular synthesis of unnatural ETP analogues was developed, and collaboration was established with the City of Hope National Medical Center in order to explore SAR trends.

1.2.1 Overview of the Synthetic Route

Because of the conservation of a fused pyrrolidine-dioxopiperazine core in ETP natural products with potent anticancer activity (Figure 1.1), our goal was to develop structurally simplified synthetic ETP analogues that contain this motif (**1.5**, Scheme 1.1). Retrosynthetic analysis of this structure led us to investigate late-stage installation of the labile polysulfide bridge. The dioxopiperazine core **1.6** was proposed to be easily accessed by acylation of a C2-ester-substituted pyrrolidine **1.7**, with ring closure being accomplished through reaction with a primary amine **1.8**. Substituted pyrrolidines are routinely synthesized by 1,3-dipolar cycloaddition reactions between imines **1.9** and electron-deficient olefins **1.10**.

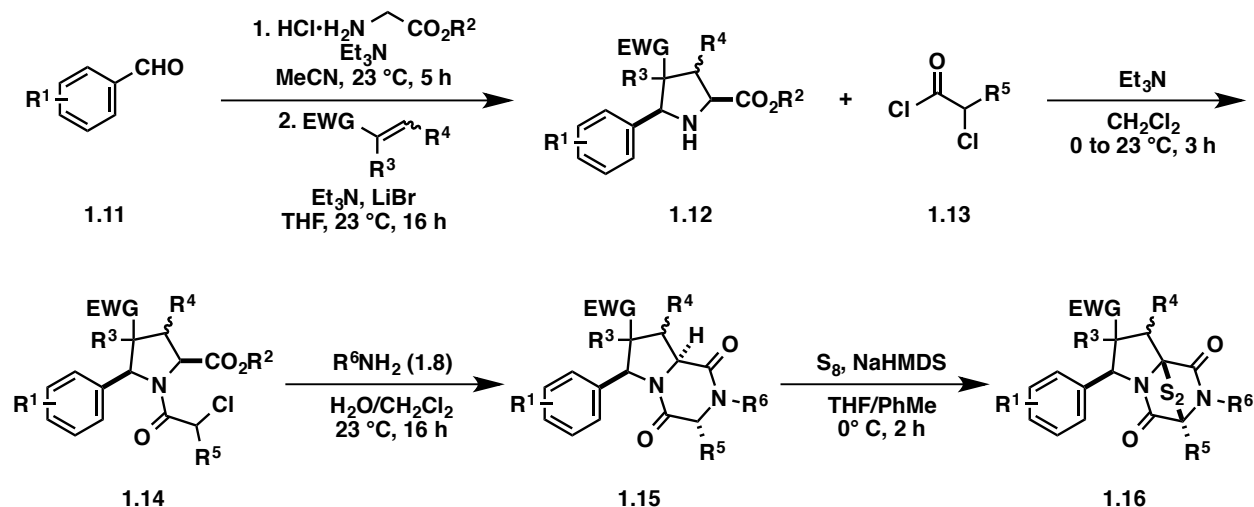
Scheme 1.1. Retrosynthetic Analysis for Novel ETP Analogues



A two-step process to access substituted pyrrolidines was developed by first preparing imines from condensation between aromatic aldehydes **1.11** and glycine ester salts in acetonitrile (Scheme 1.2). Subsequent 1,3-dipolar cycloaddition with electron-deficient olefins was promoted by the addition of superstoichiometric LiBr and Et₃N in THF,⁴³ affording pyrrolidine products **1.12** harboring C4 substitution. The dioxopiperazine core was synthesized by acylation of the

secondary amine with 2-chloroacetyl chlorides **1.13** to generate reactive α -chloroamides **1.14**, which underwent facile cyclization with primary amines **1.8** to afford dioxopiperazines **1.15**. Successful installation of the sulfide bridge to access epidithiodioxopiperazines **1.16** was accomplished utilizing conditions described by Nicolaou and coworkers.⁴⁴ Using this route, over 70 unique ETP derivatives have been synthesized and their anticancer activity has been tested.

Scheme 1.2. Five-Step Sequence to Access Highly Substituted ETP Analogues



1.2.2 SAR Trends

The development of a short and modular synthesis of novel ETP analogues led to us to quickly prepare a number of diverse products that were subsequently screened for anticancer activity against two common cancer cell lines, PC3 human prostate DU145 and human melanoma A2058.⁴² Early in our SAR studies, we identified ETP **1.17** as a particularly potent analogue against the tested cancer cell lines (Figure 1.3). The importance of nitrile substitution at the C7 position was illustrated by comparing the biological data of ETP analogues **1.17** and **1.18**, where methyl ester-substituted congener **1.18** exhibited no observable cell growth inhibition at the tested concentrations. Additional acrylate-derived ETPs **1.19** and **1.20** were inactive against DU145 and A2058 cancer cell lines. Synthetic efforts were then directed toward accessing

C7-nitrile-substituted ETPs derived from the pyrrolidine products of a 1,3-dipolar cycloaddition between imines **1.9** and methacrylonitrile.

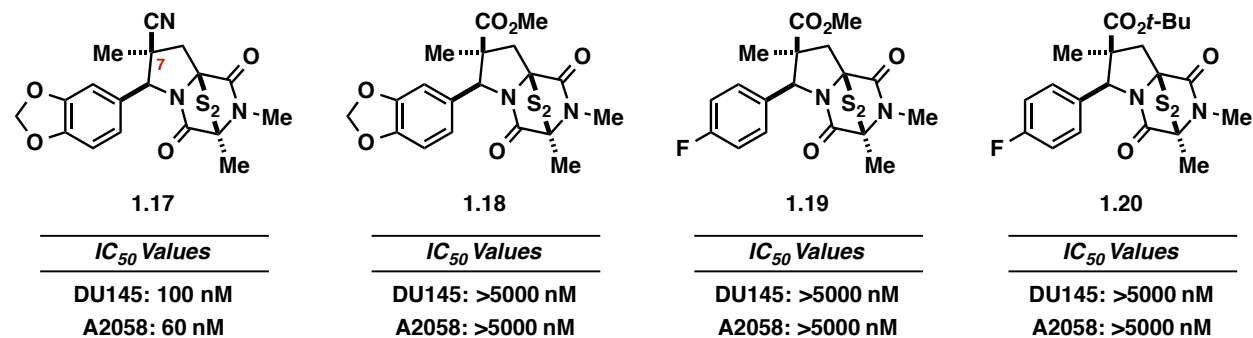


Figure 1.3. Influence of C7 Substitution on Anticancer Activity

After demonstrating the importance of the C7 nitrile functionality for the biological activity of ETP analogues, a number of such derivatives were synthesized. The effect of aromatic substitution on ETP anticancer activity was explored by using various aromatic aldehydes **1.11** (Scheme 1.2). 5-Bromo-2-methoxyphenyl ETP **1.21** exhibited IC₅₀ values of 3700 nM and 2000 nM against DU145 and A2058 cell lines, respectively (Figure 1.4). 3,4-Dichlorophenyl ETP **1.22** displayed 5- and 15-fold decreases in potency against DU145 and A2058 cell lines compared to **1.17**, respectively, suggesting that oxygen substitution is important to the observed potency of analogue **1.17**. 2,3-Methylenedioxyphenyl ETP **1.23** is not as potent as 3,4-methylenedioxyphenyl analogue **1.17**, indicating that oxygen functionality at positions C3 and C4 on the aromatic ring are necessary to access ETPs of high potency. The importance of the methylene bridge of **1.17** was demonstrated by synthesizing derivative **1.24**, which possesses an ethylene bridge; **1.17** was twice as potent as **1.24** against both of the tested cell lines. As a result, future ETP analogue syntheses focused on the use of piperonal as the parent aldehyde (Scheme 1.2).

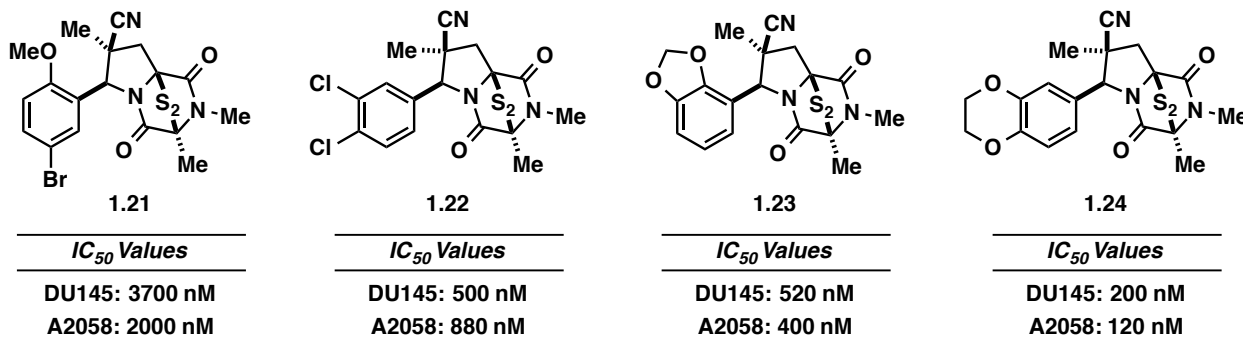


Figure 1.4. Effects of Aromatic Substitution Patterns on ETP Anticancer Activity

The effect of the number of sulfur atoms in the polysulfide bridge on ETP cytotoxicity was investigated (Figure 1.5). The anticancer activity of dioxopiperazine **1.25** and monosulfide **1.26** were tested against the prostate cancer and melanoma cell lines and it was observed that both compounds lacked activity. Trisulfide **1.27**, which was isolated as a byproduct in the sulfenylation reaction to access disulfide **1.17**,^{45,46} exhibited IC₅₀ values of 460 nM and 240 nM against DU145 and A2058 cell lines, respectively. As a result, future synthetic efforts were focused on accessing the more potent ETP disulfide products.

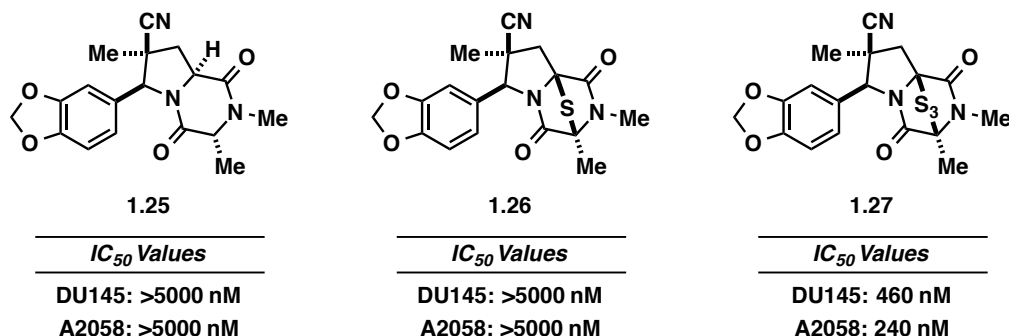


Figure 1.5. Anticancer Activity of ETP Derivatives with Different Polysulfide Bridge Lengths

Utilizing different 2-chloroacetyl chlorides **1.13**, ETPs **1.28** and **1.29** were synthesized with ethyl and benzyl substitution at position C3, respectively (Scheme 1.2). Comparing the IC₅₀ values of analogues **1.28** and **1.29** to those of lead compound **1.17**, it was determined that

incorporation of larger alkyl groups at position C3 resulted in decreased potency against both of the tested cell lines (Figure 1.6). Additionally, various primary amines **1.8** were employed to synthesize ETPs **1.30–1.33** (Scheme 1.2). Products derived from ethylamine (**1.30**) and cyclopropylamine (**1.31**) exhibited slightly higher IC₅₀ values than derivative **1.17**. *N*-Allyl and *N*-butyl ETPs **1.32** and **1.33** were even less potent than analogue **1.17** (Figure 1.7). The corresponding anticancer activities of these analogues demonstrate that smaller alkyl groups are tolerated at the N2 position, but substitution with larger allyl and *n*-butyl groups results in significantly increased IC₅₀ values. While ETP **1.17** remains the most potent analogue tested to date, new analogues are still being synthesized in order to discover new ETP derivatives with potent anticancer activity.

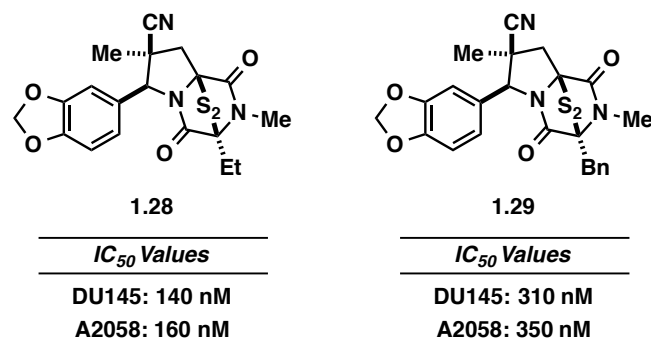


Figure 1.6. Effect of C3 Substitution on ETP Analogue Anticancer Activity

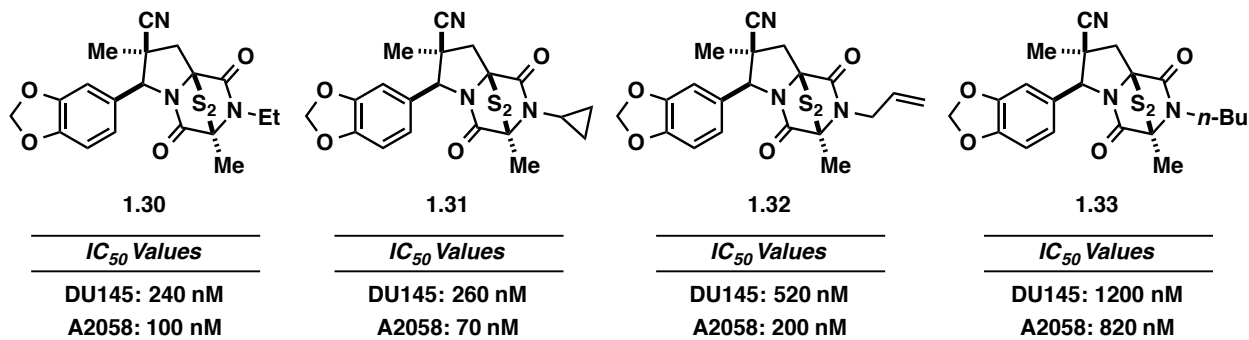
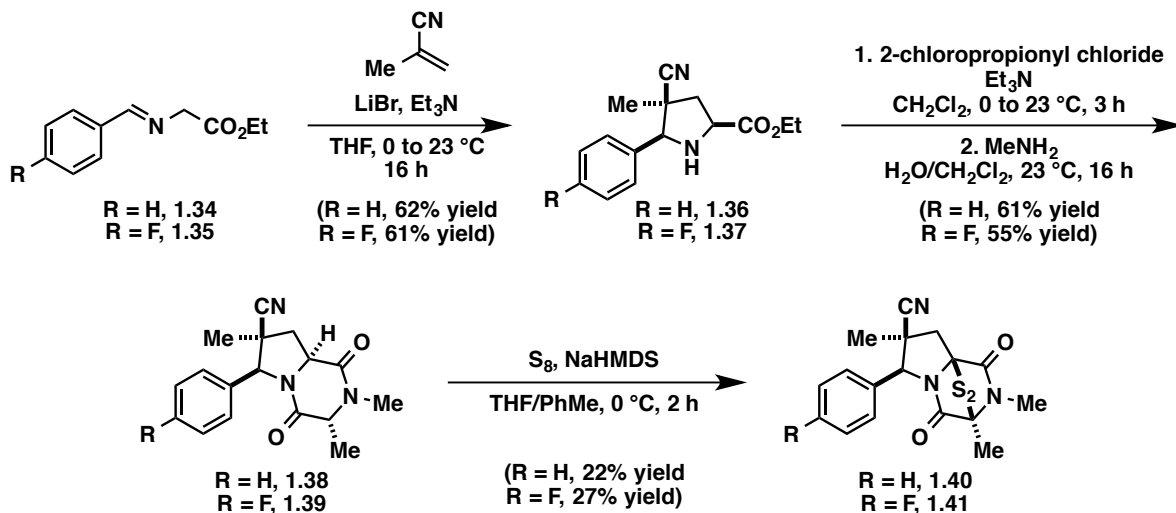


Figure 1.7. Alkyl Group Substitutions at the N2 Position

1.2.3 Substrate Synthesis

Using the route outlined in Scheme 1.2, three new nitrile-containing ETP analogues were synthesized for subsequent evaluation at City of Hope. The 1,3-dipolar cycloaddition between benzaldehyde-derived imine **1.34** and methacrylonitrile afforded pyrrolidine product **1.36** in 62% yield and a 3.3:1 endo:exo adduct ratio (Scheme 1.3). Endo pyrrolidine adduct **1.36** was carried forward in the synthesis:⁴⁷ Acylation with 2-chloropropionyl chloride and cyclization using aqueous methylamine afforded dioxopiperazine **1.38** in 61% yield over two steps, after trituration from MeOH. Disulfenylation of **1.38** with S₈ and NaHMDS afforded ETP **1.40** in 22% yield after tedious purification.⁴⁸ Similarly, ETP **1.41** was prepared in 9% overall yield from 4-fluorobenzaldehyde.

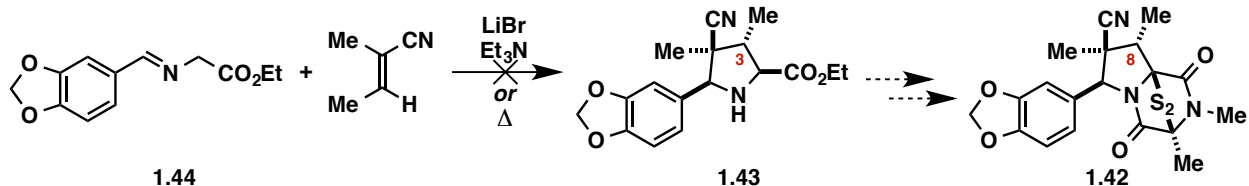
Scheme 1.3. Synthesis of ETPs 1.40 and 1.41



To broaden our SAR studies, the synthesis of C8-methyl-substituted ETP analogue **1.42** was pursued (Scheme 1.4). Previous experiments were attempted to directly access C3-methyl pyrrolidine **1.43** by 1,3-dipolar cycloaddition between imine **1.44** and 2-methyl-2-butenenitrile using the LiBr and Et₃N (Scheme 1.2); however, this resulted in recovery of starting material.⁴⁹

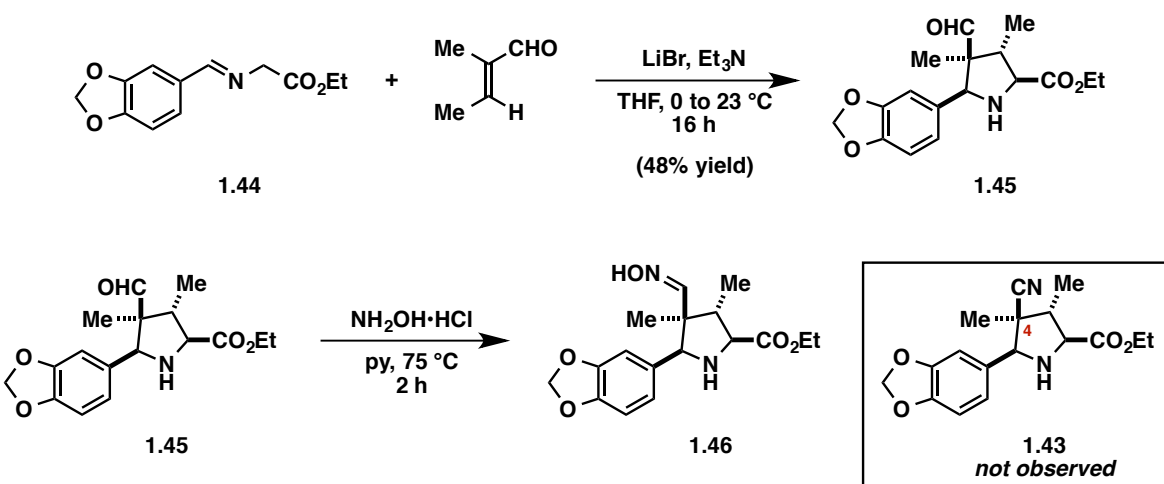
A thermal 1,3-dipolar cycloaddition was then pursued, but was met without success.⁵⁰ This required a revision to the original synthetic plan in order to access desired ETP **1.42**.

Scheme 1.4. Unsuccessful Strategies to Access Pyrrolidine **1.43**

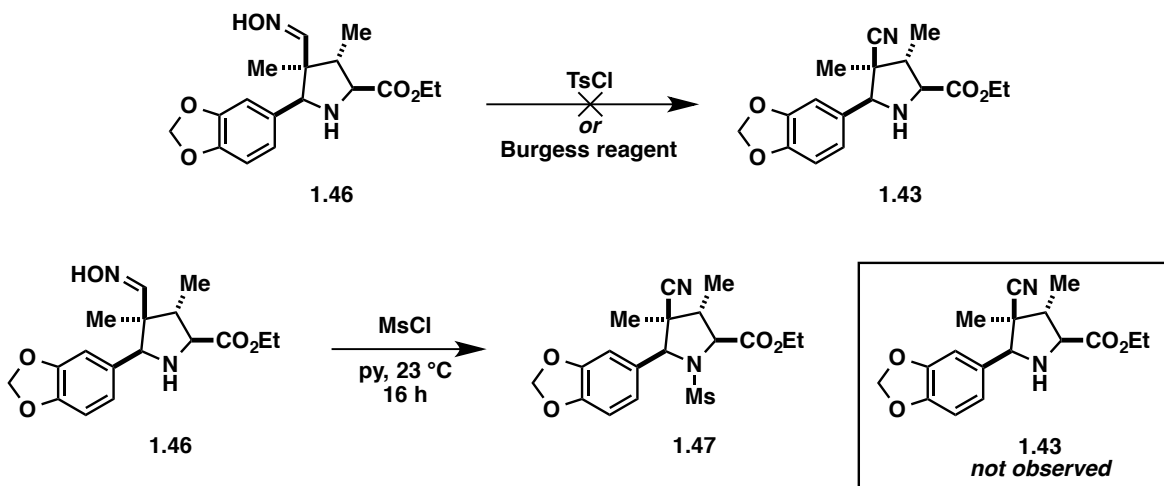


A 1,3-dipolar cycloaddition was successfully achieved between imine **1.44** and *trans*-2-methyl-2-butenal, affording endo cycloadduct **1.45** in 48% yield and a 4:1 dr. While treatment of pyrrolidine **1.45** with hydroxylamine hydrochloride in DMSO did not directly access desired product **1.43**,⁵¹ oxime **1.46** was synthesized by this method (Scheme 1.5). Next, dehydration conditions were investigated in order to access the desired nitrile functionality at the C4 position of the pyrrolidine ring. Dehydration was initially attempted using tosyl chloride (TsCl);⁵² however, these conditions resulted in a complex mixture of unidentifiable products (Scheme 1.6). Similarly unproductive dehydration attempts were made using the Burgess reagent.⁵³ The use of mesyl chloride (MsCl) as a dehydrating agent promoted the desired transformation of the oxime to nitrile functionality,⁵⁴ but resulted in undesired mesylation of the secondary amine, affording *N*-Ms pyrrolidine **1.47**. Dehydration was ultimately accomplished by treating oxime **1.46** with an excess of 2-chloropropionyl chloride to afford α -chloroamide **1.48** with the desired nitrile functionality at C4 (Scheme 1.7). With the desired C4-methyl-substituted pyrrolidine core in hand, unpurified α -chloroamide **1.48** was treated with aqueous methylamine to afford dioxopiperazine **1.49** as a 2:1 mixture of epimers at C3. This mixture was carried forward in the disulfenylation reaction, affording ETP **1.42** in 3% yield over four steps.

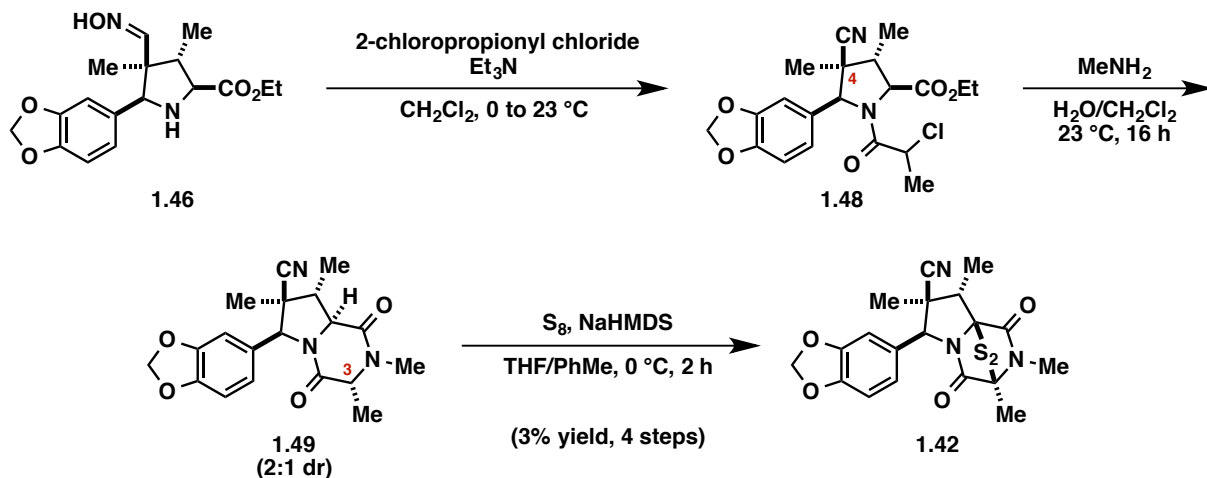
Scheme 1.5. Synthesis of Oxime 1.46



Scheme 1.6. Attempts to Access Pyrrolidine 1.43 by Dehydration of Oxime 1.46



Scheme 1.7. Completion of ETP 1.42



1.2.4 Determination of ETP Anticancer Activity

Growth inhibition assays were performed at the City of Hope National Medical Center by our collaborators Dr. Sangkil Nam and Dr. David Horne. Thus, the anticancer activities of over 70 ETP analogues **1.5** against PC3 human prostate DU145 and human melanoma A2058 cancer cell lines have been determined. The IC₅₀ values of novel analogues **1.40**, **1.41**, and **1.42** were compared to those of lead compound **1.17** (Figure 1.8). Analogues **1.40** and **1.41** exhibited lower potency than ETP **1.17**, which supports our previous observations that 3,4-dioxy substitution on the aromatic ring is important in accessing high potency anticancer agents.⁴² Finally, the installation of a methyl group at the C8 position resulted in dramatic increases in IC₅₀ values for ETP **1.42** against the two cell lines. While analogues **1.40**, **1.41**, and **1.42** supplied us with important SAR data, ETP **1.17** still harnesses the most potent anticancer activity observed to date.

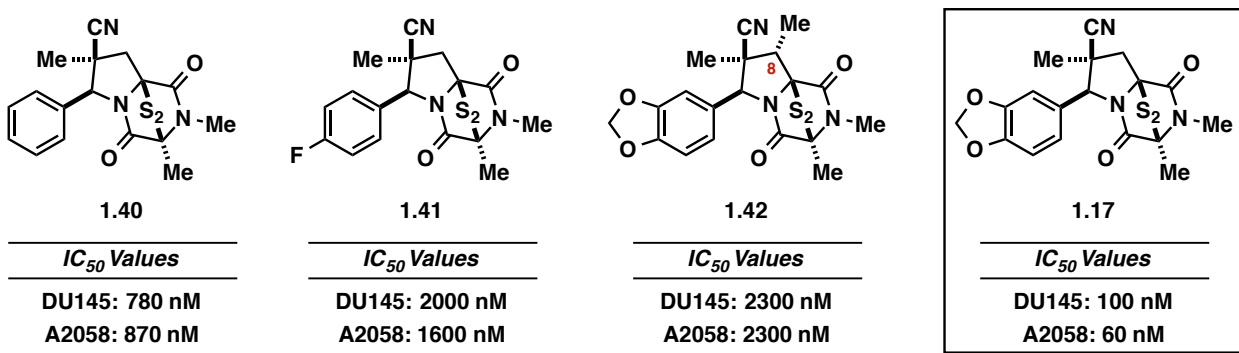


Figure 1.8. IC₅₀ Values of ETP Analogues 1.40, 1.41, 1.42, and 1.17

1.3 Conclusion

Synthetic endeavors toward ETP natural products have been revived in recent years as a result of more detailed studies of their potent anticancer activity being described.¹ As the cytotoxic activity of ETPs has been elucidated to arise from the labile polysulfide bridge,^{14,15} the Overman group pursued a study on accessing unnatural ETP analogues with increased potency with regard to anticancer activity while reducing broad toxicity.⁴²

Using the short and robust ETP analogue synthesis developed by our group, three new ETP products were accessed. Congeners **1.40** and **1.41** were synthesized without incident, while C8-methyl ETP **1.42** demanded the use of an aldehyde in the 1,3-dipolar cycloaddition step. Consequently, the development of appropriate dehydration conditions was required to access the desired nitrile functionality at the C4 position of the resulting pyrrolidine core. The IC₅₀ values of ETPs **1.40**, **1.41**, and **1.42** were determined at City of Hope to establish SAR trends in efforts to develop ETP analogues with potent anticancer activity.

1.4 Appendix A: Experimental Procedures

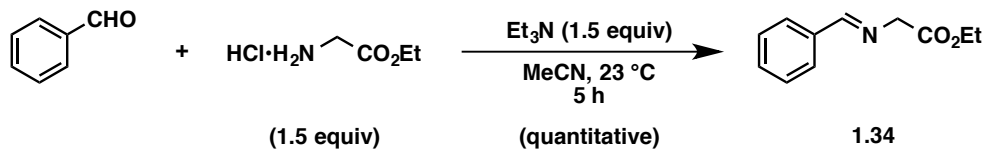
1.4.1 Materials and Methods

Unless stated otherwise, reactions were conducted in flame- or oven-dried glassware under a positive pressure of nitrogen (N_2) or argon (Ar) using anhydrous solvents (dried by passing through activated alumina columns under a positive pressure of Ar). All commercially obtained reagents were used as received. Reaction temperatures were controlled using an IKAmag temperature modulator, and unless stated otherwise, reactions were performed at room temperature (approximately 23 °C). Analytical thin-layer chromatography (TLC) and preparative thin-layer chromatography (PTLC) were conducted on EMD silica gel 60 F₂₅₄ glass-backed plates (250 μm and 500 μm, respectively) and visualized by exposure to UV light (254 nm), or by Dragendorff–Munier or potassium permanganate staining. Flash chromatography was performed using forced flow of the indicated solvent system on EMD Geduran® silica gel 60 (particle size 0.040–0.063 mm). NMR spectra were recorded at 298 K on Bruker FT-NMR spectrometers at the indicated frequencies. Chemical shifts (δ) are reported in parts per million (ppm) relative to residual deuterated solvent signals ($CDCl_3$). Data for 1H NMR spectra are reported as follows: chemical shift (δ ppm), multiplicity, coupling constant [J , reported in Hertz (Hz)], and integration. Splitting patterns are abbreviated as follows: singlet (s), doublet (d), triplet (t), quartet (q), multiplet (m), apparent (app), and broad (br). Carbon multiplicity was determined by a combination of DEPTQ and HMQC experiments. Chemical shifts (δ) for ^{19}F NMR spectra are reported in parts per million (ppm) and referenced to the corresponding calibrated 1H NMR spectrum. Infrared (IR) spectra were recorded on a Varian 640-IR spectrometer as thin films in CH_2Cl_2 on KBr plates and are reported in terms of frequency of absorption (cm^{-1}). High-resolution mass spectra (HRMS) were obtained from the

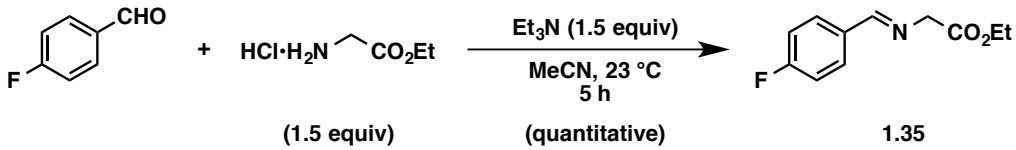
UC Irvine Mass Spectrometry Facility with a Micromass LCT spectrometer. Melting points (mp) were determined on a melting point apparatus (Thomas Hoover, Uni-Melt) and are uncorrected. Abbreviations used can be found on the Internet at:

http://pubs.acs.org/paragonplus/submission/joceah/joceah_abbreviations.pdf.

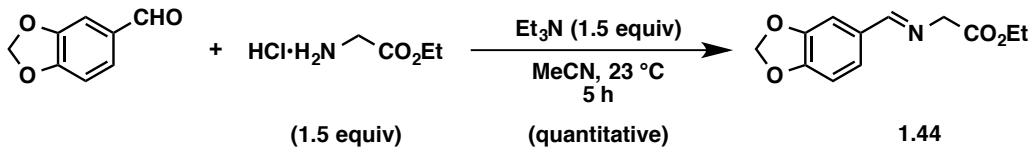
1.4.2 Synthesis of Imines



Ethyl (E)-2-(benzylideneamino)acetate (1.34). A 50 mL round-bottom flask was charged with a magnetic stir bar and glycine ethyl ester hydrochloride (525 mg, 3.75 mmol, 1.50 equiv). MeCN (4.2 mL, 0.6 M) and benzaldehyde (250 μL , 2.5 mmol, 1.0 equiv) were then added, followed by Et_3N (520 μL , 3.75 mmol, 1.50 equiv). The resulting heterogeneous mixture was vigorously stirred at 23°C for 5 h. Concentration of the reaction mixture under reduced pressure afforded an amorphous colorless solid, which was transferred to a separatory funnel using CH_2Cl_2 (15 mL) and H_2O (30 mL). The layers of the resulting biphasic mixture were partitioned and the organic layer was extracted with H_2O (30 mL) and brine (30 mL). The organic layer was dried over Na_2SO_4 , filtered, and concentrated to afford imine **1.34** (480 mg, quantitative yield) as a clear oil. Imine **1.34** was carried further in subsequent reactions without further purification.⁵⁵ ^1H NMR (500 MHz, CDCl_3): δ 8.30 (s, 1H), 7.79–7.77 (m, 2H), 7.47–7.40 (m, 3H), 4.40 (s, 2H), 4.24 (q, $J = 7.2$, 2H), 1.31 (t, $J = 7.2$, 3H).

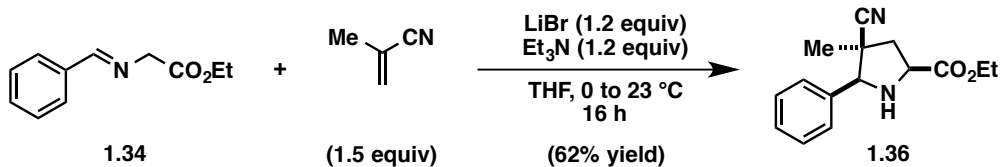


Ethyl (E)-2-((4-fluorobenzylidene)amino)acetate (1.35). According to the procedure described for the synthesis of imine **1.34**, imine **1.35** was prepared from 4-fluorobenzaldehyde (270 μL , 2.5 mmol, 1.0 equiv) and received as a light yellow oil (520 mg, quantitative yield). Imine **1.35** was carried further in subsequent reactions without further purification. ^1H NMR (500 MHz, CDCl_3): δ 8.26 (s, 1H), 7.78 (app dd, $J = 8.6, 5.9$, 2H), 7.11 (app t, $J = 8.6$, 2H), 4.39 (s, 2H), 4.24 (q, $J = 7.2$, 2H), 1.31 (t, $J = 7.2$, 3H).



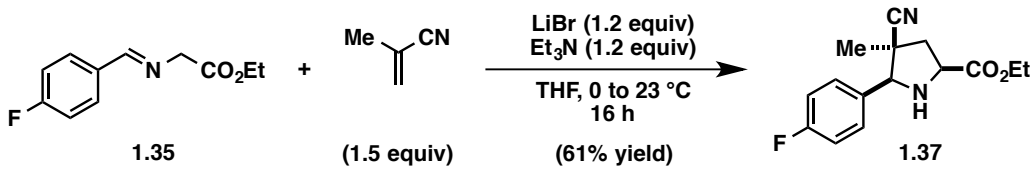
Ethyl (E)-2-((benzo[d][1,3]dioxol-5-ylmethylene)amino)acetate (1.44). According to the procedure described for the synthesis of imine **1.34**, imine **1.44** was prepared from piperonal (375 mg, 2.50 mmol, 1.00 equiv) and obtained as a light yellow oil⁵⁶ (588 mg, quantitative yield). Imine **1.44** was carried further in subsequent reactions without further purification. ^1H NMR (600 MHz, CDCl_3): δ 8.16 (s, 1H), 7.41 (s, 1H), 7.15 (d, $J = 7.9$, 1H), 6.83 (d, $J = 7.9$, 1H), 6.01 (s, 2H), 4.35 (s, 2H), 4.23 (q, $J = 6.8$, 2H), 1.30 (t, $J = 6.8$, 3H).

1.4.3 Synthesis of Pyrrolidines



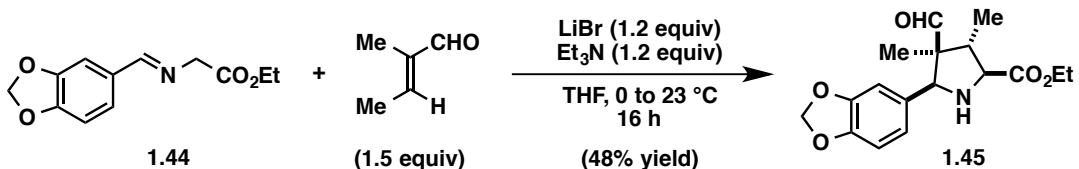
Ethyl *rac*-(2*S*,4*S*,5*S*)-4-cyano-4-methyl-5-phenylpyrrolidine-2-carboxylate (1.36). A 100 mL round-bottom flask was charged with a magnetic stir bar, imine **1.34** (2.9 g, 15 mmol,

1.0 equiv), LiBr (1.6 g, 18 mmol, 1.2 equiv), THF (25 mL, 0.6 M), and Et₃N (2.5 mL, 18 mmol, 1.2 equiv). The mixture was cooled to 0 °C in an ice-water bath. After 5 min, methacrylonitrile (1.90 mL, 22.5 mmol, 1.50 equiv) was added dropwise. The resulting heterogeneous yellow mixture slowly warmed to 23 °C and was maintained at this temperature for 16 h. The volatile components were removed under reduced pressure and the resulting oil was transferred to a separatory funnel with CH₂Cl₂ (25 mL) and H₂O (40 mL). The layers of the resulting biphasic mixture were partitioned and the aqueous layer was extracted with CH₂Cl₂ (2 × 15 mL). The combined organic layers were washed with brine (40 mL), dried over Na₂SO₄, filtered, and concentrated under reduced pressure. ¹H NMR analysis of the resulting residue indicated a 3.3:1 mixture of endo:exo cycloadducts. The residue was purified by flash chromatography (1:1 hexanes:EtOAc) to yield pyrrolidine endo adduct **1.36** (2.4 g, 62% yield) as a clear oil. R_f 0.32 (1:1 hexanes:EtOAc); ¹H NMR (500 MHz, CDCl₃): δ 7.52 (app d, J = 7.1, 2H), 7.41–7.34 (m, 3H), 4.34–4.24 (m, 2H), 3.98 (dd, J = 9.6, 4.2, 1H), 3.93 (s, 1H), 2.90 (br s, 1H), 2.82 (dd, J = 13.6, 4.2, 1H), 2.29 (dd, J = 13.6, 9.6, 1H), 1.42 (s, 3H), 1.34 (t, J = 7.1, 3H); ¹³C NMR (125 MHz, CDCl₃): δ 173.0 (C), 136.5 (C), 128.9 (CH), 128.6 (2CH), 127.6 (2CH), 121.9 (C), 72.4 (CH), 61.7 (CH₂), 57.3 (CH), 44.1 (C), 42.4 (CH₂), 22.0 (CH₃), 14.2 (CH₃); IR (thin film): 3348, 2980, 2234, 1734, 1454 cm⁻¹; HRMS-ESI (*m/z*) [M + Na]⁺ calculated for C₁₅H₁₈N₂O₂Na, 281.1266; found, 281.1263. Characterization data are consistent with those previously reported.⁴²



Ethyl *rac*-(2*S*,4*S*,5*S*)-4-cyano-5-(4-fluorophenyl)-4-methylpyrrolidine-2-carboxylate (1.37).

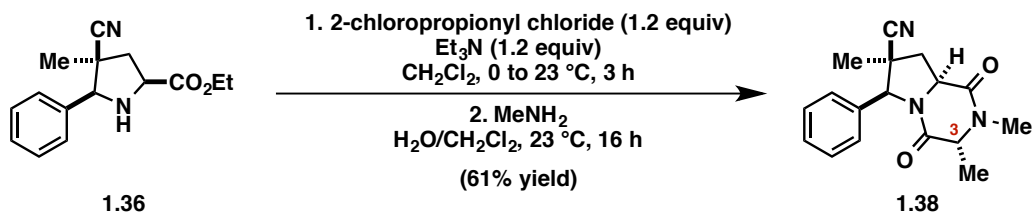
According to the procedure described for the synthesis of pyrrolidine **1.36**, endo cycloadduct **1.37** was prepared from imine **1.35** (3.1 g, 15 mmol, 1.0 equiv) and methacrylonitrile (1.90 mL, 22.5 mmol, 1.50 equiv) and isolated as a clear oil (2.5 g, 61% yield). R_f 0.29 (1:1 hexanes:EtOAc); ^1H NMR (500 MHz, CDCl_3): δ 7.52 (app dd, $J = 8.7, 5.4$, 2H), 7.09 (app t, $J = 8.7$, 2H), 4.34–4.24 (m, 2H), 3.99 (dd, $J = 9.6, 4.2$, 1H), 3.95 (s, 1H), 2.83 (dd, $J = 13.7, 4.2$, 1H), 2.82 (br s, 1H), 2.29 (dd, $J = 13.7, 9.6$, 1H), 1.41 (s, 3H), 1.34 (t, $J = 7.1$, 3H); ^{13}C NMR (125 MHz, CDCl_3): δ 172.9 (C), 163.2 (d, $J_{\text{C}-\text{F}} = 245.8$, C), 132.4 (C), 129.4 (d, $J_{\text{C}-\text{F}} = 8.3$, 2CH), 121.8 (C), 115.7 (d, $J_{\text{C}-\text{F}} = 21.5$, 2CH), 71.7 (CH), 61.9 (CH_2), 57.3 (CH), 44.0 (C), 42.2 (CH_2), 22.0 (CH_3), 14.3 (CH_3); ^{19}F NMR (376.5 MHz, CDCl_3): δ –112.7; IR (thin film): 3348, 2982, 2235, 1736, 1605, 1510 cm^{-1} ; HRMS-ESI (m/z) [M + Na] $^+$ calculated for $\text{C}_{15}\text{H}_{17}\text{FN}_2\text{O}_2\text{Na}$, 299.1172; found, 299.1177. Characterization data are consistent with those previously reported.⁴²



Ethyl *rac*-(2*S*,3*S*,4*S*,5*S*)-5-(benzo[d][1,3]dioxol-5-yl)-4-formyl-3,4-dimethylpyrrolidine-2-carboxylate (1.45). According to the procedure described for the synthesis of pyrrolidine **1.36**, endo cycloadduct **1.45** was prepared from imine **1.44** (3.5 g, 15 mmol, 1.0 equiv) and *trans*-2-methyl-2-butenal (2.20 mL, 22.5 mmol, 1.50 equiv) and isolated as an orange oil (2.3 g, 48% yield). R_f 0.16 (30% EtOAc/hexanes); ^1H NMR (600 MHz, CDCl_3): δ 9.06 (s, 1H), 6.91 (s, 1H), 6.83 (d, $J = 7.9$, 1H), 6.75 (d, $J = 7.9$, 1H), 5.94 (s, 2H), 4.34–4.24 (m, 2H), 4.09

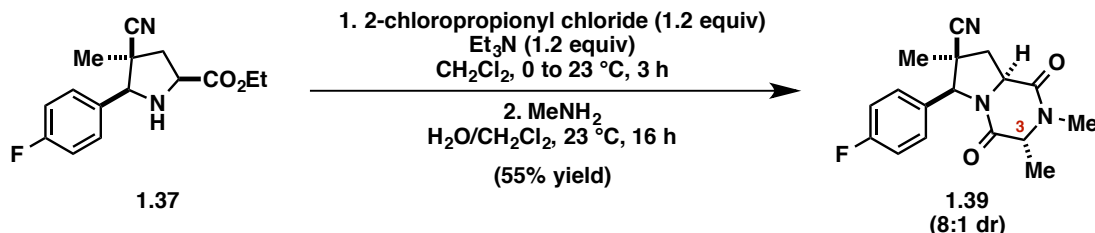
(s, 1H), 3.57 (d, J = 8.8, 1H), 2.73 (dq, J = 8.8, 7.1, 1H), 2.59 (br s, 1H), 1.35 (t, J = 7.1, 3H), 1.16 (s, 3H), 1.06 (d, J = 7.1, 3H); ^{13}C NMR (125 MHz, CDCl_3): δ 204.0, 173.5, 148.2, 147.5, 132.4, 120.5, 108.4, 107.7, 101.3, 71.9, 66.3, 61.4, 58.8, 40.8, 15.6, 14.4, 13.5; IR (thin film): 3344, 2976, 2902, 2726, 1721, 1504, 1488 cm^{-1} ; HRMS-ESI (m/z) [M + Na] $^+$ calculated for $\text{C}_{17}\text{H}_{21}\text{NO}_5\text{Na}$, 342.1317; found, 342.1306.

1.4.4 Synthesis of Dioxopiperazines



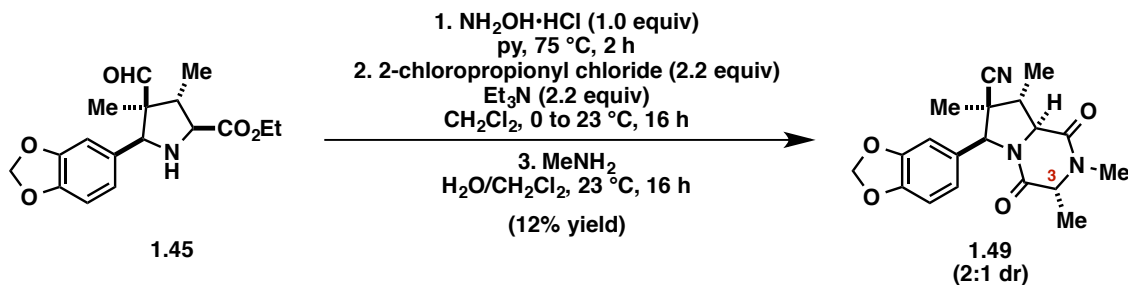
Rac-(3*R*,6*S*,7*S*,8*aS*)-2,3,7-trimethyl-1,4-dioxo-6-phenyloctahydropyrrolo[1,2-*a*]pyrazine-7-carbonitrile (1.38). A 100 mL round-bottom flask was charged with pyrrolidine **1.36** (2.4 g, 9.3 mmol, 1.0 equiv), a magnetic stir bar, and CH_2Cl_2 (20 mL, 0.5 M). The solution was cooled to 0 °C in an ice-water bath. Et_3N was added (1.60 mL, 11.2 mmol, 1.20 equiv), followed by dropwise addition of 2-chloropropionyl chloride (1.10 mL, 11.2 mmol, 1.20 equiv). The reaction was maintained at 0 °C for 5 min, then at 23 °C for 3 h. The reaction was quenched with H_2O (25 mL). The resulting phases were partitioned in a separatory funnel and the aqueous layer was extracted with CH_2Cl_2 (2 × 25 mL). Combined extracts were dried over Na_2SO_4 , filtered, and concentrated under reduced pressure. The resulting yellow foam was dissolved in CH_2Cl_2 (20 mL) and a solution of MeNH_2 (20 mL, 40% in H_2O) was added. The biphasic mixture was vigorously stirred at 23 °C for 16 h. The phases were partitioned in a separatory funnel and the aqueous layer was extracted with CH_2Cl_2 (2 × 25 mL). Combined extracts were washed with brine (25 mL), dried over Na_2SO_4 , filtered, and concentrated under reduced pressure. ^1H NMR analysis of the unpurified material indicated a 10:1 mixture of C3-methyl epimers. The pale

yellow foam was dissolved in CH₂Cl₂ (10 mL) and MeOH (10 mL) was added. The solution was stirred under a stream of air until it became a thick slurry (ca. 3 mL solvent remaining). Subsequent filtration afforded dioxopiperazine **1.38** as a colorless powder (1.7 g, 61% yield, single diastereomer, mp = 258–262 °C). R_f 0.58 (4:1 EtOAc:MeOH); ¹H NMR (600 MHz, CDCl₃): δ 7.39–7.33 (m, 3H), 7.12 (app d, J = 7.2, 2H), 4.91 (s, 1H), 4.40 (dd, J = 11.2, 6.6, 1H), 3.91 (q, J = 7.2, 1H), 3.05 (s, 3H), 2.79 (dd, J = 13.0, 11.2, 1H), 2.46 (dd, J = 13.0, 6.6, 1H), 1.69 (s, 3H), 1.48 (d, J = 7.2, 3H); ¹³C NMR (125 MHz, CDCl₃): δ 166.7 (C), 166.2 (C), 136.9 (C), 129.2 (2CH), 129.1 (2CH), 126.1 (CH), 119.9 (C), 69.8 (CH), 60.9 (CH), 56.3 (CH), 42.6 (C), 36.7 (CH₂), 32.2 (CH₃), 25.3 (CH₃), 15.4 (CH₃); IR (thin film): 2981, 2937, 2244, 1673 cm⁻¹; HRMS-ESI (m/z) [M + Na]⁺ calculated for C₁₇H₁₉N₃O₂Na, 320.1375; found, 320.1380. Characterization data are consistent with those previously reported.⁴²



Rac-(3*R*,6*S*,7*S*,8*aS*)-6-(4-fluorophenyl)-2,3,7-trimethyl-1,4-dioxo-octahydropyrrolo-[1,2*a*]pyrazine-7-carbonitrile (1.39**).** According to the procedure described for the synthesis of dioxopiperazine **1.38**, dioxopiperazine **1.39** was prepared from pyrrolidine **1.37** (2.5 g, 9.2 mmol, 1.0 equiv), 2-chloropropionyl chloride (1.1 mL, 11 mmol, 1.2 equiv), and MeNH₂ (18 mL, 40% in H₂O) and isolated as a colorless powder (1.6 g, 55% yield, ca. 8:1 mixture of C3-methyl epimers). The 8:1 epimeric mixture was carried forward in the next step without further purification. R_f 0.58 (4:1 EtOAc:MeOH); ¹H NMR (ca. 8:1 mixture of diastereomers, 500 MHz, CDCl₃): δ 7.13–7.05 (m, 4H), 4.90 (s, 1H), 4.39 (dd, J = 11.4, 6.6, 1H), 3.91 (q, J = 7.2, 1H), 3.06 (s, 3H), 2.76 (dd, J = 13.4, 11.4, 1H), 2.47 (dd, J = 13.4, 6.6, 1H), 1.69 (s, 3H), 1.49

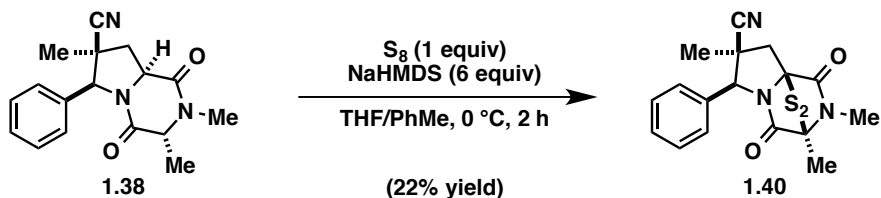
(d, $J = 7.2$, 3H); ^{13}C NMR (ca. 8:1 mixture of diastereomers, 125 MHz, CDCl_3): δ 166.8 (C), 166.1 (C), 163.0 (d, $J_{\text{C-F}} = 245.5$, C), 132.8 (d, $J_{\text{C-F}} = 3.1$, C), 127.9 (d, $J_{\text{C-F}} = 8.4$, 2CH), 119.8 (C), 116.2 (d, $J_{\text{C-F}} = 21.8$, 2CH), 69.2 (CH), 60.9 (CH), 56.3 (CH), 42.6 (C), 36.8 (CH_2), 32.2 (CH_3), 25.3 (CH_3), 15.4 (CH_3); ^{19}F NMR (376.5 MHz, CDCl_3): δ -112.4; IR (thin film): 2989, 2940, 2241, 1681 cm^{-1} ; HRMS-ESI (m/z) [M + Na] $^+$ calculated for $\text{C}_{17}\text{H}_{18}\text{FN}_3\text{O}_2\text{Na}$, 338.1281; found, 338.1283. Characterization data are consistent with those previously reported.⁴²



Rac-(3*R*,6*S*,7*S*,8*S*,8a*S*)-6-(benzo[*d*][1,3]dioxol-5-yl)-2,3,7,8-tetramethyl-1,4-dioxooctahydropyrrolo[1,2-*a*]pyrazine-7-carbonitrile (1.49). A 25 mL round-bottom flask was charged with a magnetic stir bar, pyrrolidine **1.45** (320 mg, 1.0 mmol, 1.0 equiv), and hydroxylamine hydrochloride (69 mg, 1.0 mmol, 1.0 equiv). Pyridine (10 mL, 0.1 M) was added and the resulting solution was maintained at 75 °C for 2 h. After cooling to 23 °C, the solution was transferred to a separatory funnel with Et₂O (80 mL) and H₂O (15 mL). The layers of the resulting biphasic mixture were partitioned and the organic phase was extracted with sat. aq. NH₄Cl (15 mL) and sat. aq. NaHCO₃ (15 mL). The organic layer was dried over MgSO₄, filtered, and concentrated under reduced pressure. Azeotropic removal of pyridine with PhMe afforded an oil that was transferred to a 50 mL round-bottom flask. The oil was dissolved in CH₂Cl₂ (2 mL) and the resulting solution was cooled to 0 °C in an ice-water bath. Et₃N (310 µL, 2.2 mmol, 2.2 equiv) was added in one portion, followed by the dropwise addition of 2-chloropropionyl chloride (210 µL, 2.2 mmol, 2.2 equiv). After 5 min, the reaction vessel was

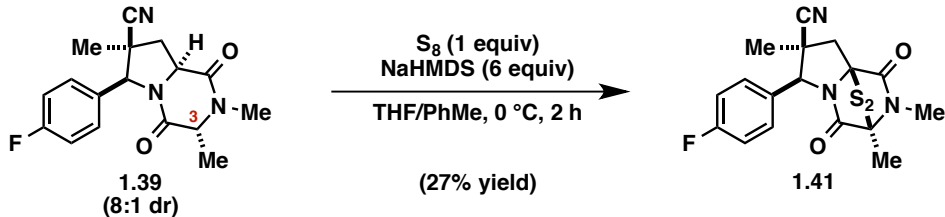
removed from the ice-water bath and the solution was maintained at 23 °C for 16 h. The reaction was quenched with H₂O (20 mL). The resulting phases were partitioned in a separatory funnel and the aqueous layer was extracted with CH₂Cl₂ (2 × 20 mL). The combined extracts were dried over Na₂SO₄, filtered, and concentrated under reduced pressure. The resulting brown foam was dissolved in CH₂Cl₂ (2 mL) and a solution of MeNH₂ (2 mL, 40% in H₂O) was added. The biphasic mixture was vigorously stirred at 23 °C for 16 h. The biphasic mixture was transferred to a separatory funnel with CH₂Cl₂ (20 mL) and H₂O (20 mL) and the phases were partitioned. The aqueous layer was extracted with CH₂Cl₂ (2 × 20 mL). Combined extracts were washed with brine (25 mL), dried over Na₂SO₄, filtered, and concentrated under reduced pressure. The resulting oil was dissolved in CH₂Cl₂ (10 mL) and MeOH (5 mL) was added. The solution was stirred under a stream of air until a precipitate formed. Filtration afforded impure dioxopiperazine **1.49** (43 mg, 12% yield, ca. 2:1 mixture of C3-methyl epimers) as a colorless powder which was carried forward without further purification. ¹H NMR (ca. 2:1 mixture of diastereomers, 600 MHz, CDCl₃): δ 6.78 (d, *J* = 8.0, 1H), 6.59 (dd, *J* = 8.0, 1.1, 1H), 6.54 (d, *J* = 1.1, 1H), 5.963 (s, 1H), 5.960 (s, 1H), 4.90 (s, 1H), 4.11 (q, *J* = 6.5, 1H), 3.84 (d, *J* = 10.3, 1H), 3.07 (s, 3H), 3.04–3.01 (m, 1H), 1.54 (d, *J* = 6.5, 3H), 1.52 (s, 3H), 1.41 (d, *J* = 6.5, 3H).

1.4.5 Synthesis of Epidithiodioxopiperazines

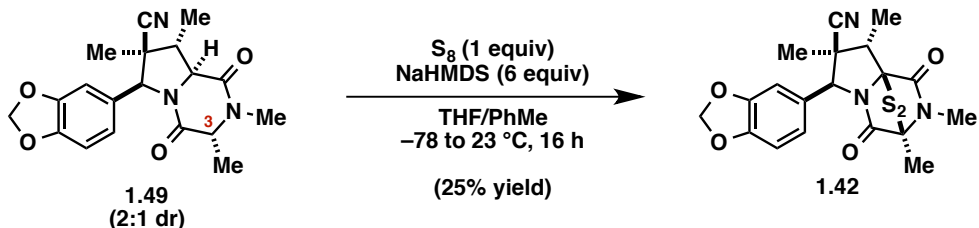


*Rac-(3S,6S,7S,8aS)-2,3,7-trimethyl-1,4-dioxo-6-phenylhexahydro-6*H*-3,8a-epidithiopyrrolo-[1,2-*a*]pyrazine-7-carbonitrile (**1.40**).* Dioxopiperazine **1.38** (100 mg, 0.34 mmol, 1.0 equiv) and S₈ (90 mg, 0.34 mmol, 1.0 equiv) were added to a 25 mL round-bottom flask and

azeotropically dried with PhMe (3 × 3 mL). The solids were suspended in THF (3.4 mL, 0.10 M) and the heterogeneous mixture was sparged with Ar for 10 min. The suspension was cooled to 0 °C for 5 min, then NaHMDS (0.60 M in PhMe, 3.4 mL, 2.0 mmol, 6.0 equiv) was added dropwise over 2 min with vigorous stirring. The reaction was maintained at 0 °C for 2 h, then quenched at 23 °C with sat. aq. NH₄Cl (10 mL) and extracted with EtOAc (3 × 10 mL). Combined extracts were dried over Na₂SO₄, filtered, and concentrated under reduced pressure. The resulting residue was dissolved in MeCN (15 mL) and washed with hexanes (3 × 10 mL) in a separatory funnel to remove HMDS-related byproducts. The MeCN layer was dried over Na₂SO₄, then concentrated in vacuo. Flash chromatography (2% EtOAc/CH₂Cl₂) afforded ETP **1.40** as a colorless powder (27 mg, 22% yield, mp = 243–246 °C). R_f 0.30 (3% EtOAc/CH₂Cl₂); ¹H NMR (500 MHz, CDCl₃): δ 7.46–7.38 (m, 5H), 4.91 (s, 1H), 3.32 (d, *J* = 14.7, 1H), 3.09 (s, 3H), 3.00 (d, *J* = 14.7, 1H), 1.94 (s, 3H), 1.69 (s, 3H); ¹³C NMR (125 MHz, CDCl₃): δ 165.7 (C), 162.2 (C), 133.8 (C), 129.6 (CH), 129.1 (2CH), 126.9 (2CH), 120.2 (C), 73.4 (C), 72.5 (CH), 44.5 (C), 43.0 (CH₂), 29.8 (C), 27.9 (CH₃), 24.9 (CH₃), 18.2 (CH₃); IR (thin film): 2917, 2849, 2240, 1705, 1680 cm⁻¹; HRMS-ESI (*m/z*) [M + Na]⁺ calculated for C₁₇H₁₇N₃O₂S₂Na, 382.0660; found, 382.0671. Characterization data are consistent with those previously reported.⁴²



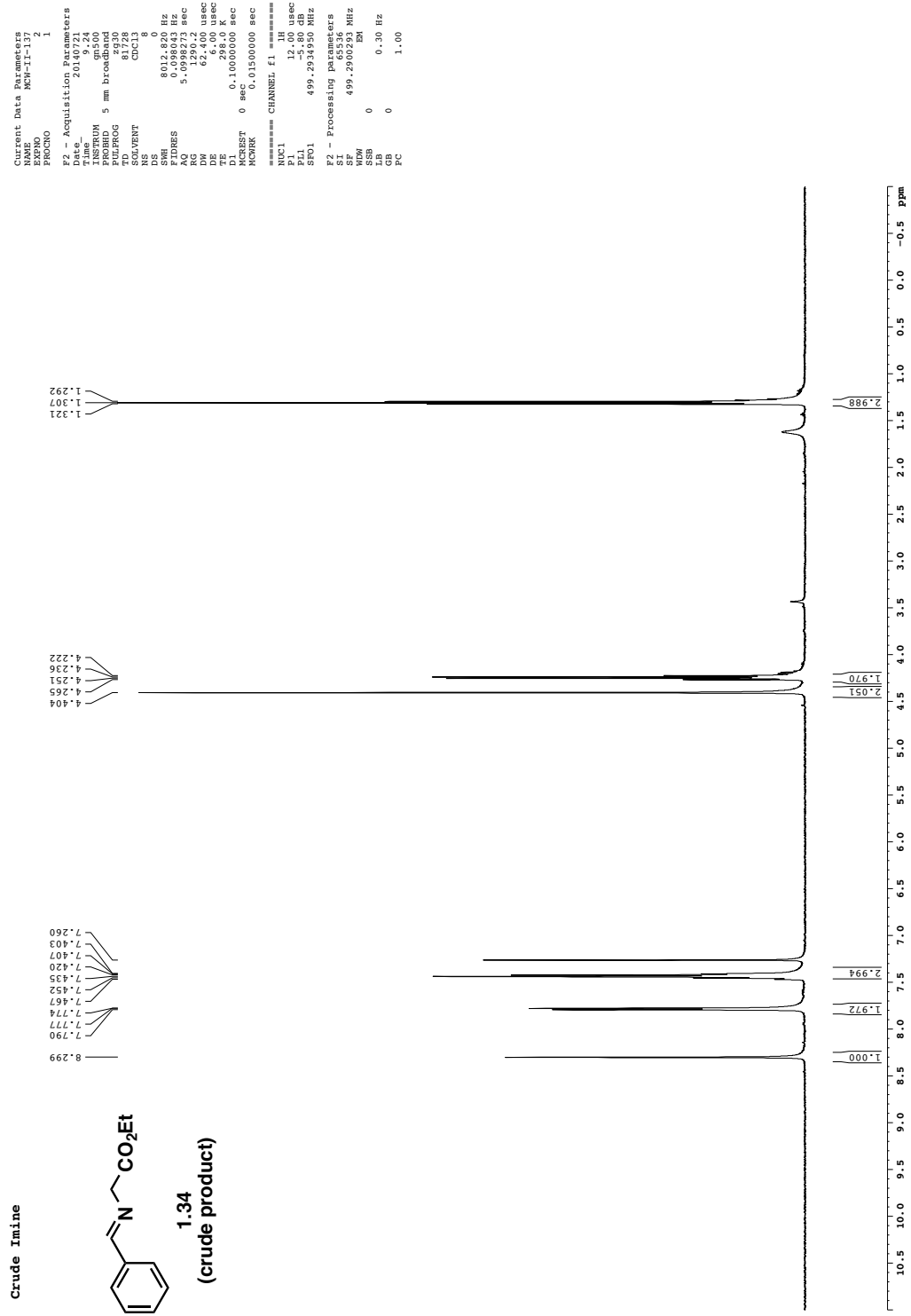
Rac-(3*S*,6*S*,7*S*,8*aS*)-6-(4-fluorophenyl)-2,3,7-trimethyl-1,4-dioxohexahydro-6*H*-3,8*a*-epithiopyrrolo[1,2-*a*]pyrazine-7-carbonitrile (1.41). According to the procedure described for the synthesis of ETP **1.40**, ETP **1.41** was prepared from dioxopiperazine **1.39** (110 mg, 0.34 mmol, 1.0 equiv) and accessed as a colorless powder (35 mg, 27% yield, mp = 221–223 °C). R_f 0.18 (3% EtOAc/CH₂Cl₂); ¹H NMR (500 MHz, CDCl₃): δ 7.37 (app dd, *J* = 8.6, 5.2, 2H), 7.13 (app t, *J* = 8.6, 2H), 4.89 (s, 1H), 3.31 (d, *J* = 15.0, 1H), 3.08 (s, 3H), 2.99 (d, *J* = 15.0, 1H), 1.94 (s, 3H), 1.68 (s, 3H); ¹³C NMR (125 MHz, CDCl₃): δ 165.6 (C), 163.4 (d, *J*_{C-F} = 248.2, C), 162.2 (C), 129.6 (d, *J*_{C-F} = 3.1, C), 128.8 (d, *J*_{C-F} = 8.5, 2CH), 120.2 (C), 116.2 (d, *J*_{C-F} = 22.1, 2CH), 73.52 (C), 73.46 (C), 71.9 (CH), 44.5 (C), 42.9 (CH₂), 27.9 (CH₃), 24.7 (CH₃), 18.2 (CH₃); ¹⁹F NMR (376.5 MHz, CDCl₃): δ -112.0; IR (thin film): 2988, 2926, 2239, 1703, 1687, 1511 cm⁻¹; HRMS-ESI (*m/z*) [M + Na]⁺ calculated for C₁₇H₁₆FN₃O₂S₂Na, 400.0566; found, 400.0559. Characterization data are consistent with those previously reported.⁴²



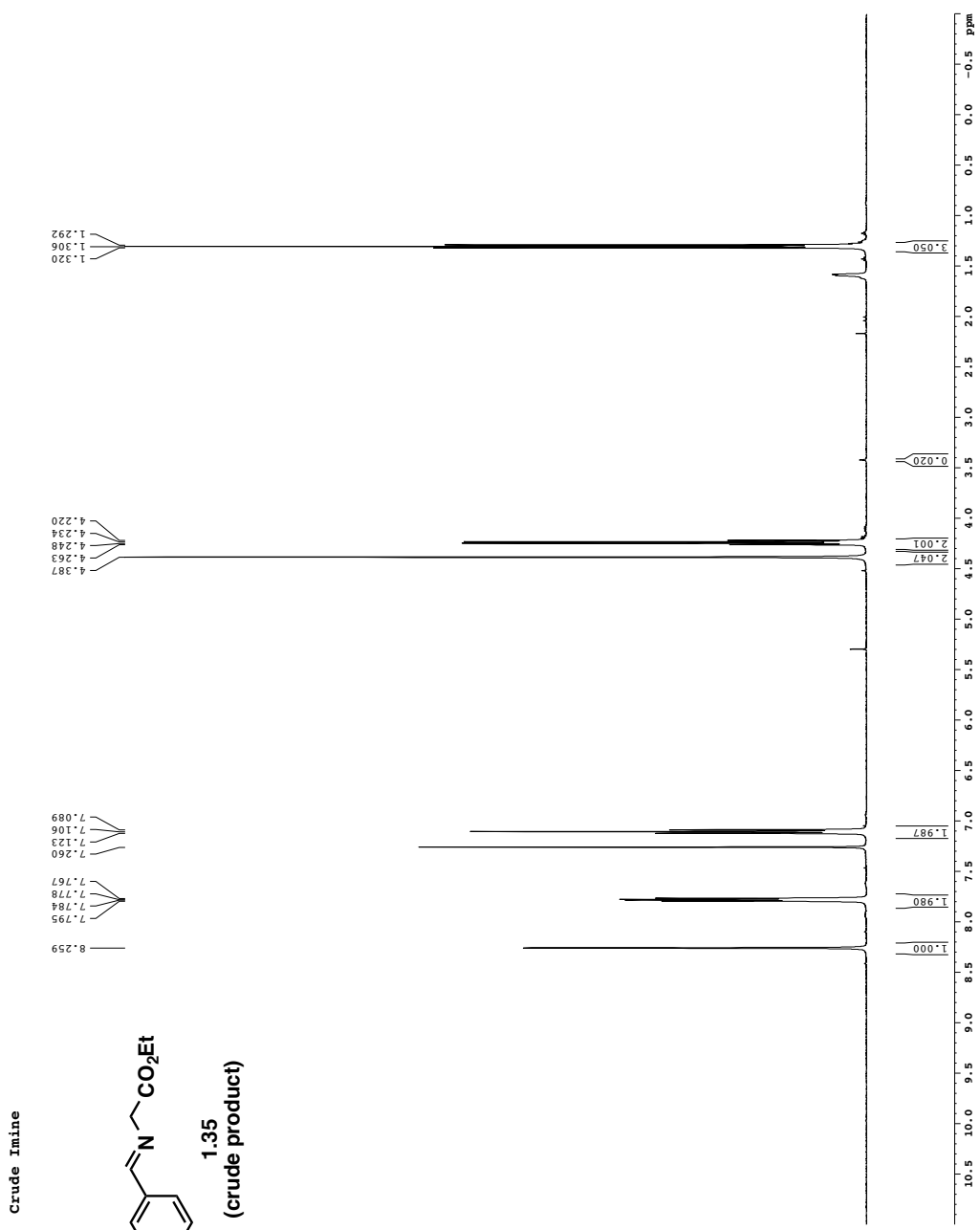
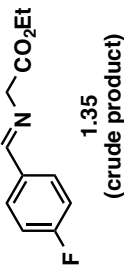
Rac-(3*S*,6*S*,7*S*,8*S*,8*aS*)-6-(benzo[d][1,3]dioxol-5-yl)-2,3,7,8-tetramethyl-1,4-dioxohexahydro-6*H*-3,8*a*-epithiopyrrolo[1,2-*a*]pyrazine-7-carbonitrile 9-sulfide (1.42). A 15 mL round-bottom flask was charged with a magnetic stir bar, impure dioxopiperazine **1.49** (43 mg, 0.12 mmol, 1.0 equiv), S₈ (37 mg, 0.15 mmol, 1.2 equiv), and THF (1.2 mL, 0.10 M). The resulting

suspension was cooled to $-78\text{ }^{\circ}\text{C}$ for 5 min, then NaHMDS (0.60 M in PhMe, 1.2 mL, 0.73 mmol, 6.0 equiv) was added dropwise over 3 min with vigorous stirring. The resulting yellow-orange heterogeneous solution was slowly warmed to $23\text{ }^{\circ}\text{C}$ and stirred for 16 h. The reaction was quenched by the addition of sat. aq. NH₄Cl (5 mL). The resulting biphasic solution was transferred to a separatory funnel with CH₂Cl₂ (10 mL) and H₂O (20 mL) and the layers were separated. The aqueous layer was extracted with CH₂Cl₂ (2 \times 10 mL), then the organic layers were combined, dried over Na₂SO₄, and concentrated under reduced pressure to yield an amorphous brown residue. This residue was dissolved in MeCN (10 mL) and washed with hexanes (3 \times 20 mL) in a separatory funnel. The MeCN layer was dried over Na₂SO₄, then concentrated in vacuo. The residue was purified by PTLC (1% EtOAc/CH₂Cl₂). The desired ETP **1.42** was isolated as a colorless solid (12 mg, 25% yield, mp = 212–214 °C) after concentration in vacuo. R_f 0.47 (3% EtOAc/CH₂Cl₂); ¹H NMR (600 MHz, CDCl₃): δ 6.80 (d, *J* = 8.1, 1H), 6.58 (d, *J* = 8.1, 1H), 6.52 (s, 1H), 5.98 (s, 1H), 5.97 (s, 1H), 5.03 (s, 1H), 3.83 (q, *J* = 7.0, 1H), 3.10 (s, 3H), 1.96 (s, 3H), 1.90 (s, 3H), 1.50 (d, *J* = 7.0, 3H); ¹³C NMR (125 MHz, CDCl₃): δ 165.3 (C), 162.5 (C), 148.62 (C), 148.58 (C), 129.9 (C), 119.7 (CH), 119.6 (C), 109.1 (CH), 106.2 (CH), 101.7 (C), 77.3 (C), 72.8 (C), 70.5 (CH), 47.8 (CH₂), 44.3 (CH), 27.8 (CH₃), 21.9 (CH₃), 18.3 (CH₃), 10.1 (CH₃); IR (thin film): 2984, 2917, 2849, 2244, 1695, 1505, 1491 cm⁻¹; HRMS-ESI (*m/z*) [M + Na]⁺ calculated for C₁₉H₁₉N₃O₄S₂Na, 440.0715; found, 440.0719.

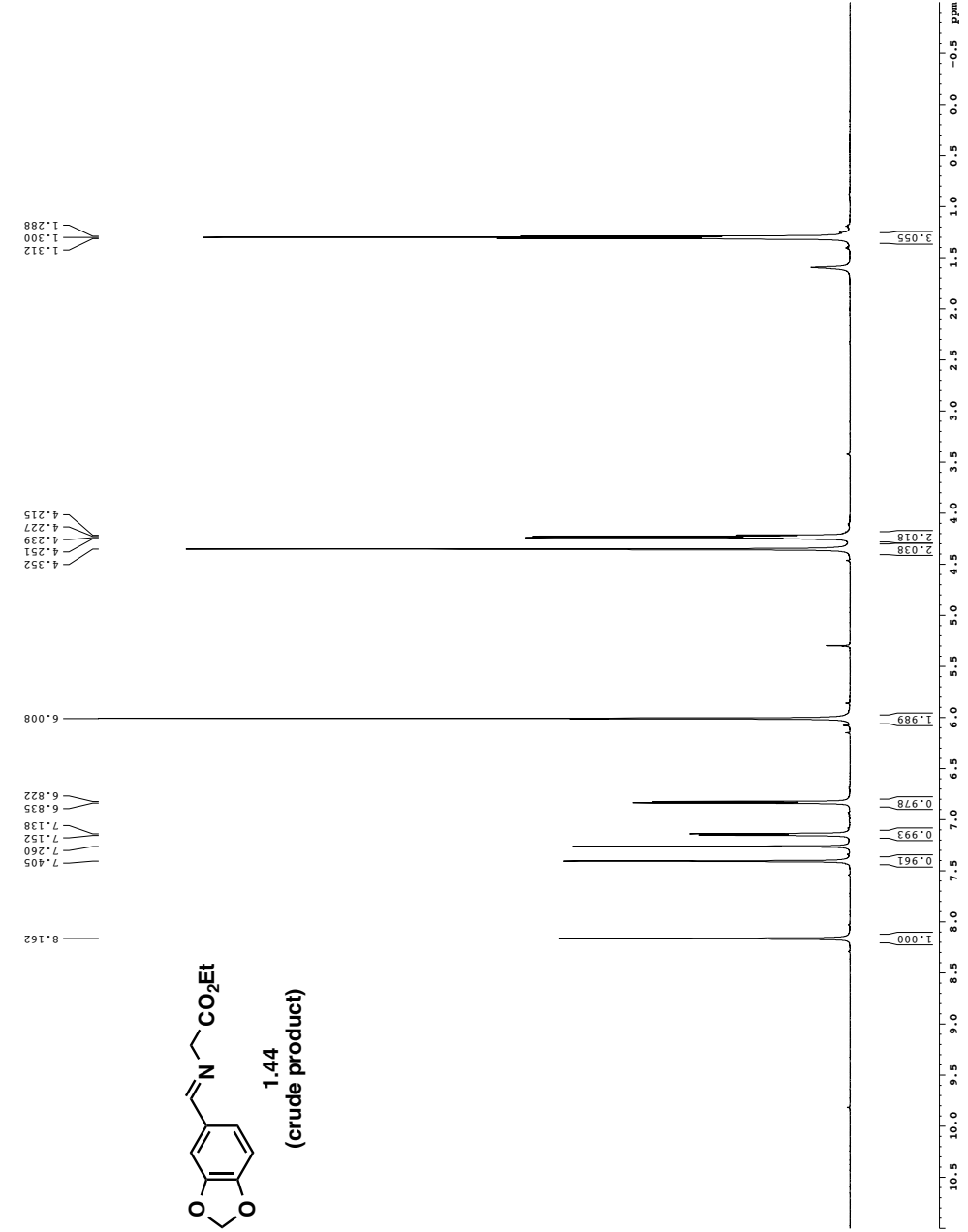
1.5 Appendix B: NMR Spectral Data



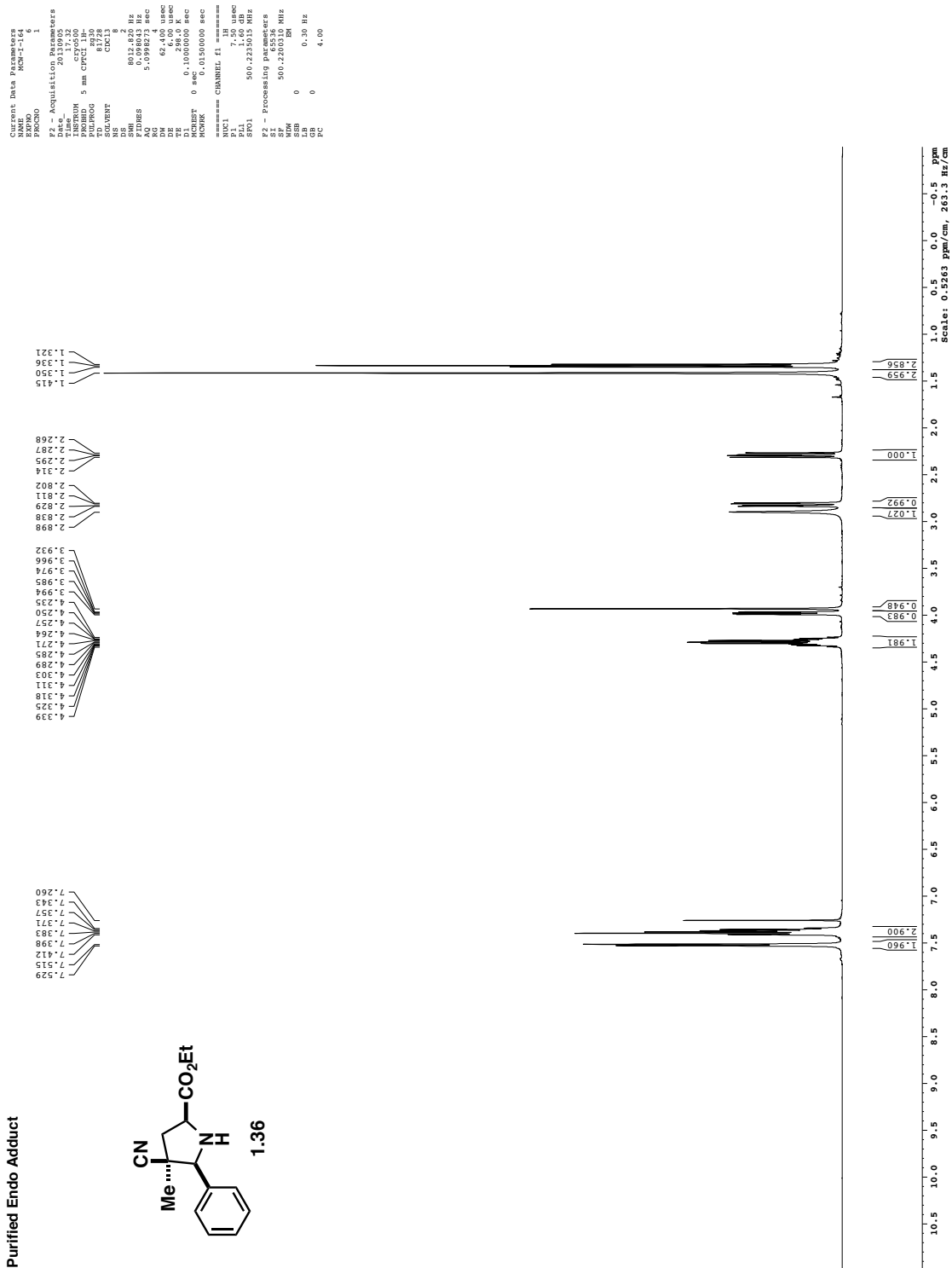
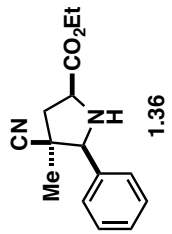
Crude Imine



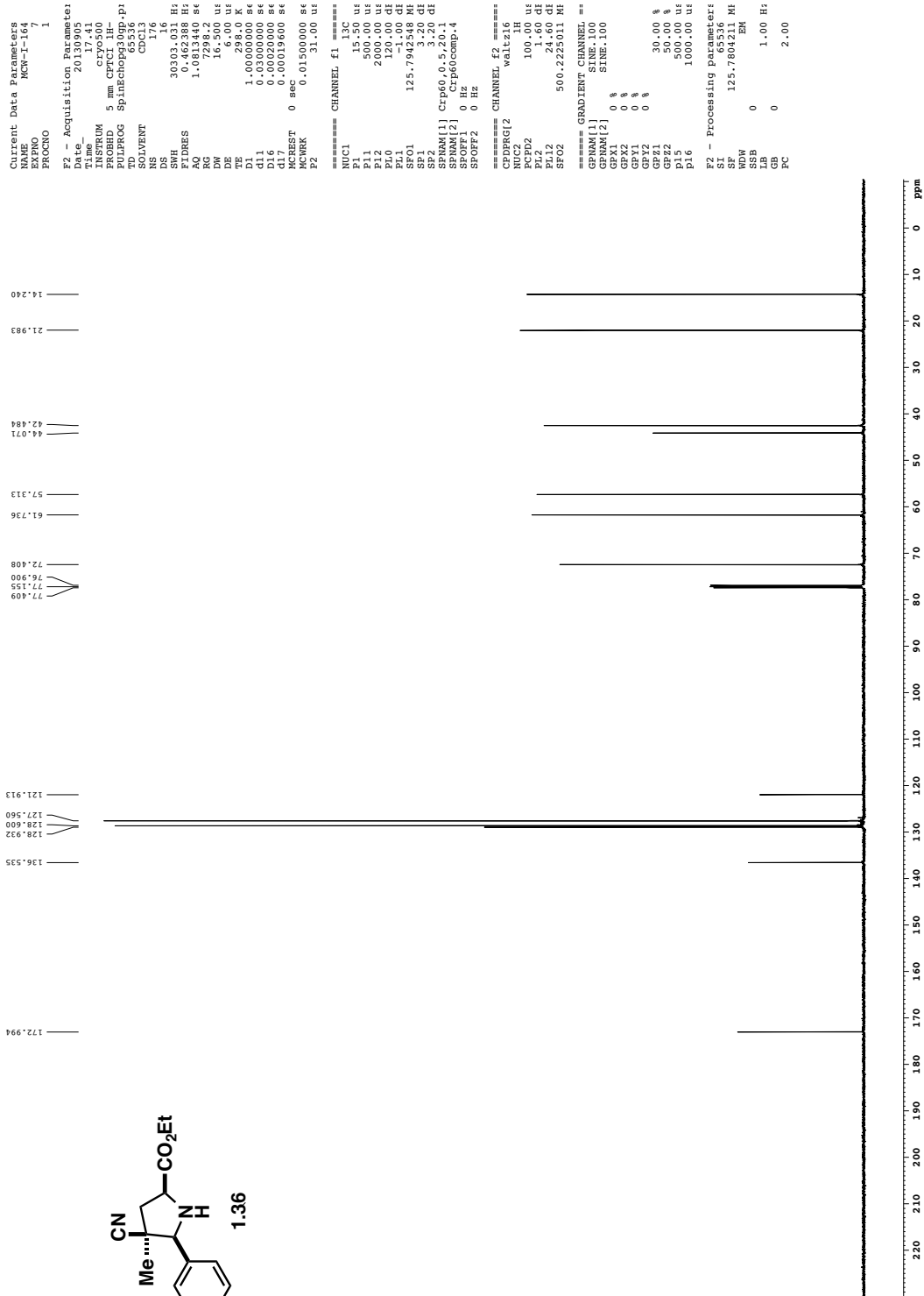
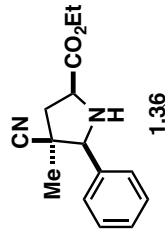
Crude Imine



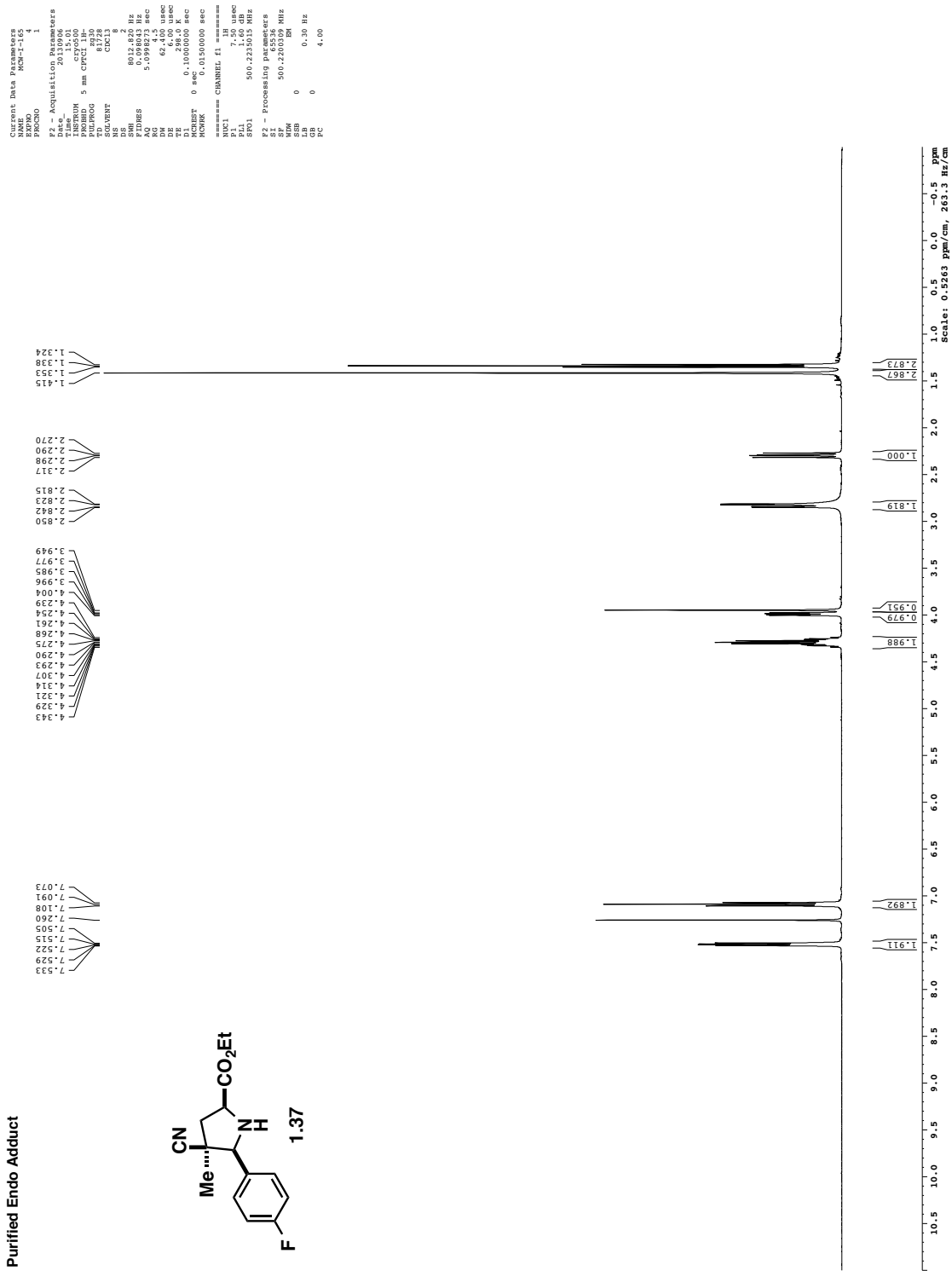
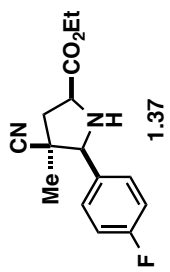
Purified Endo Adduct



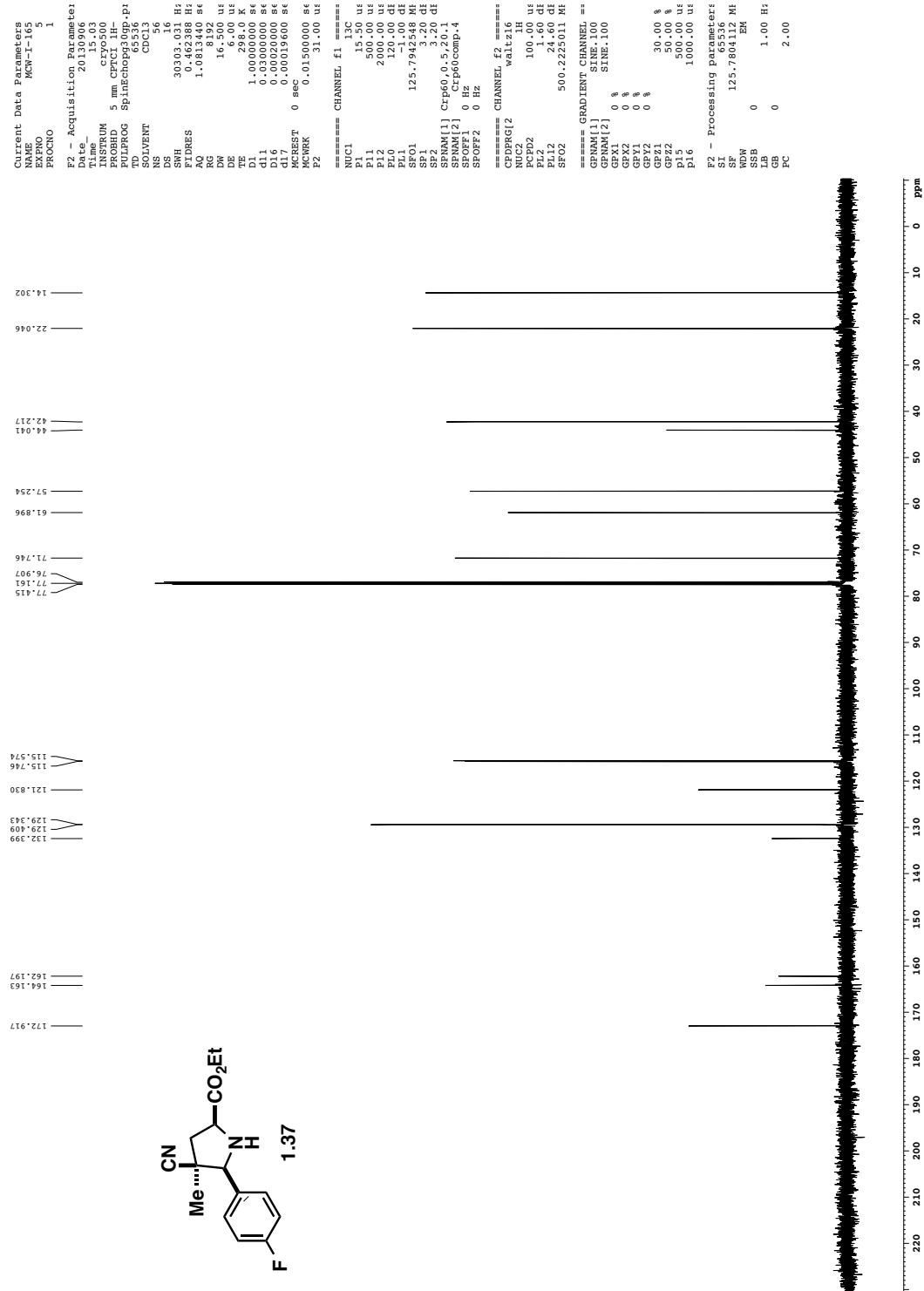
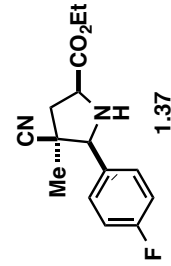
Purified Endo Adduct



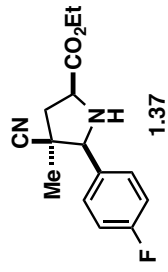
Purified Endo Adduct



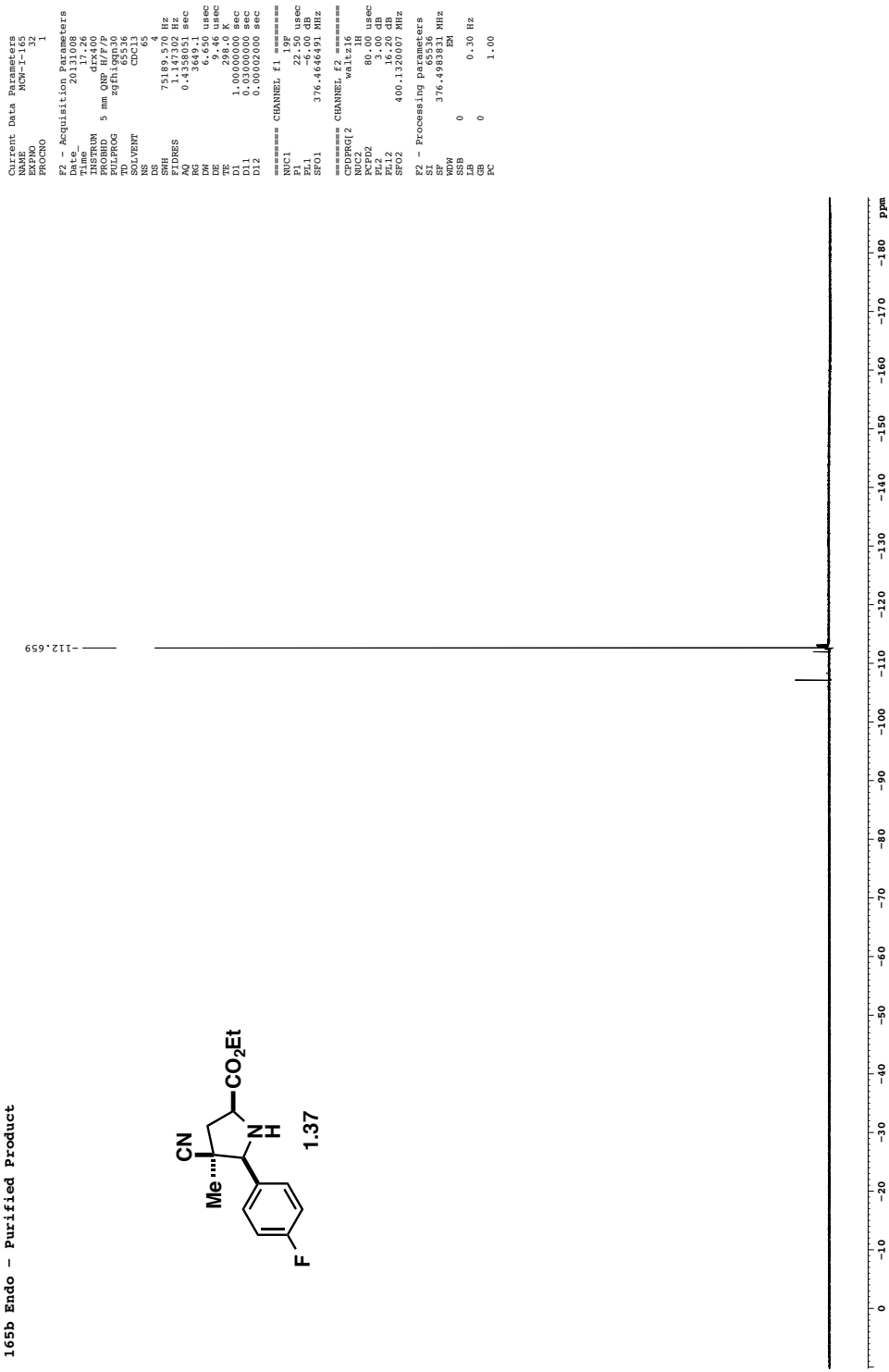
Purified Endo Adduct



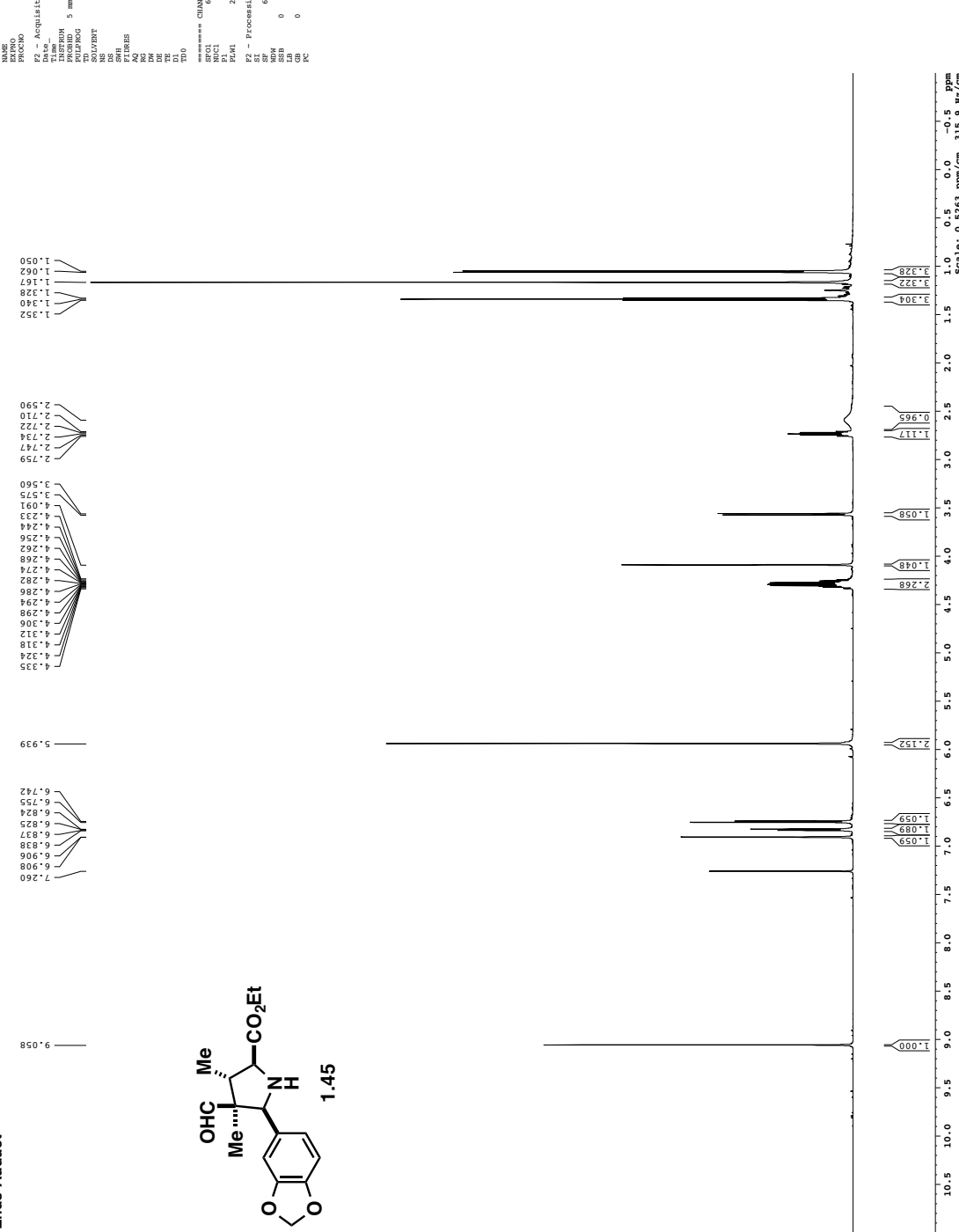
165b Endo - Purified Product



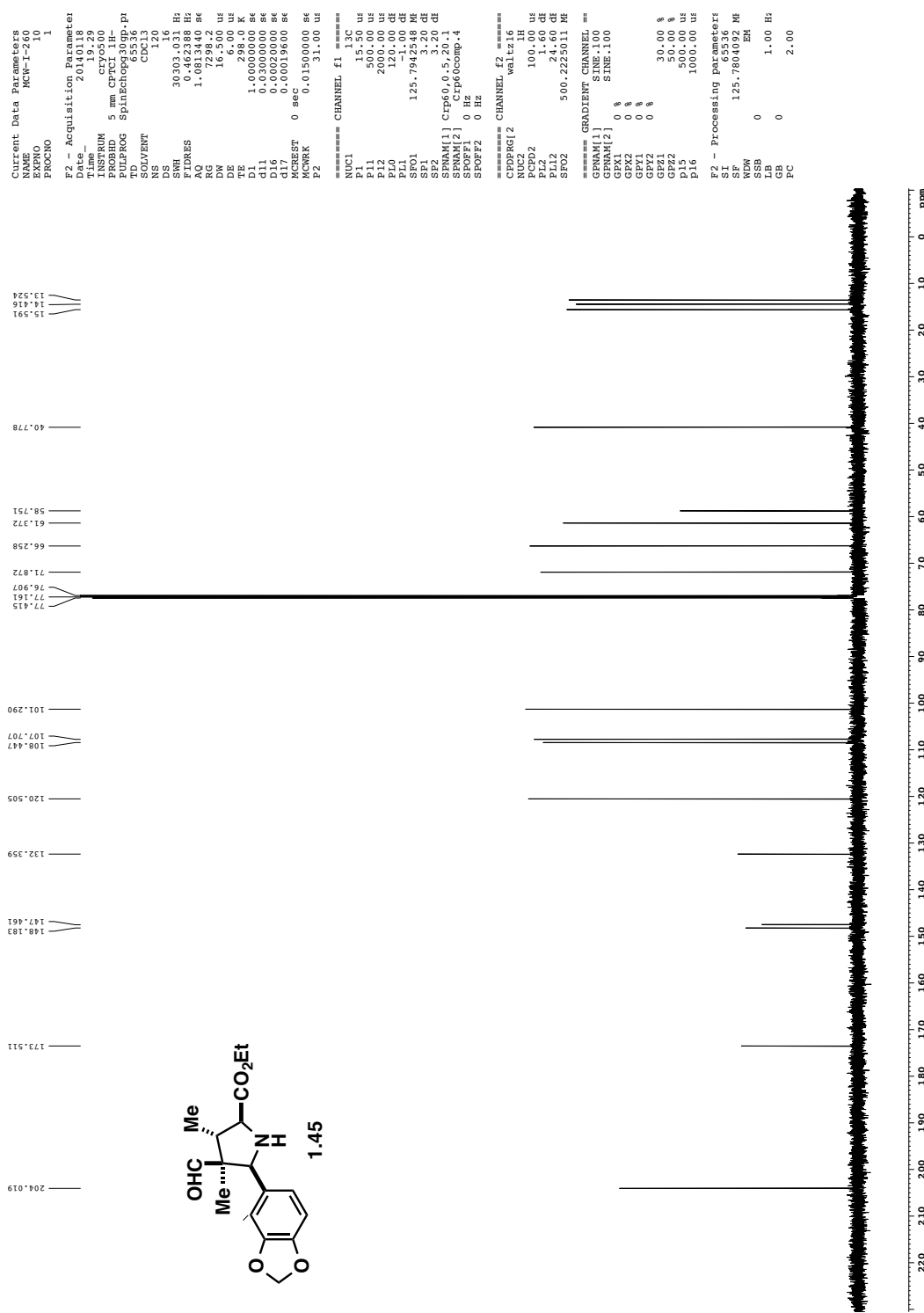
-112.659



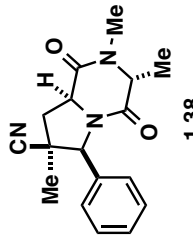
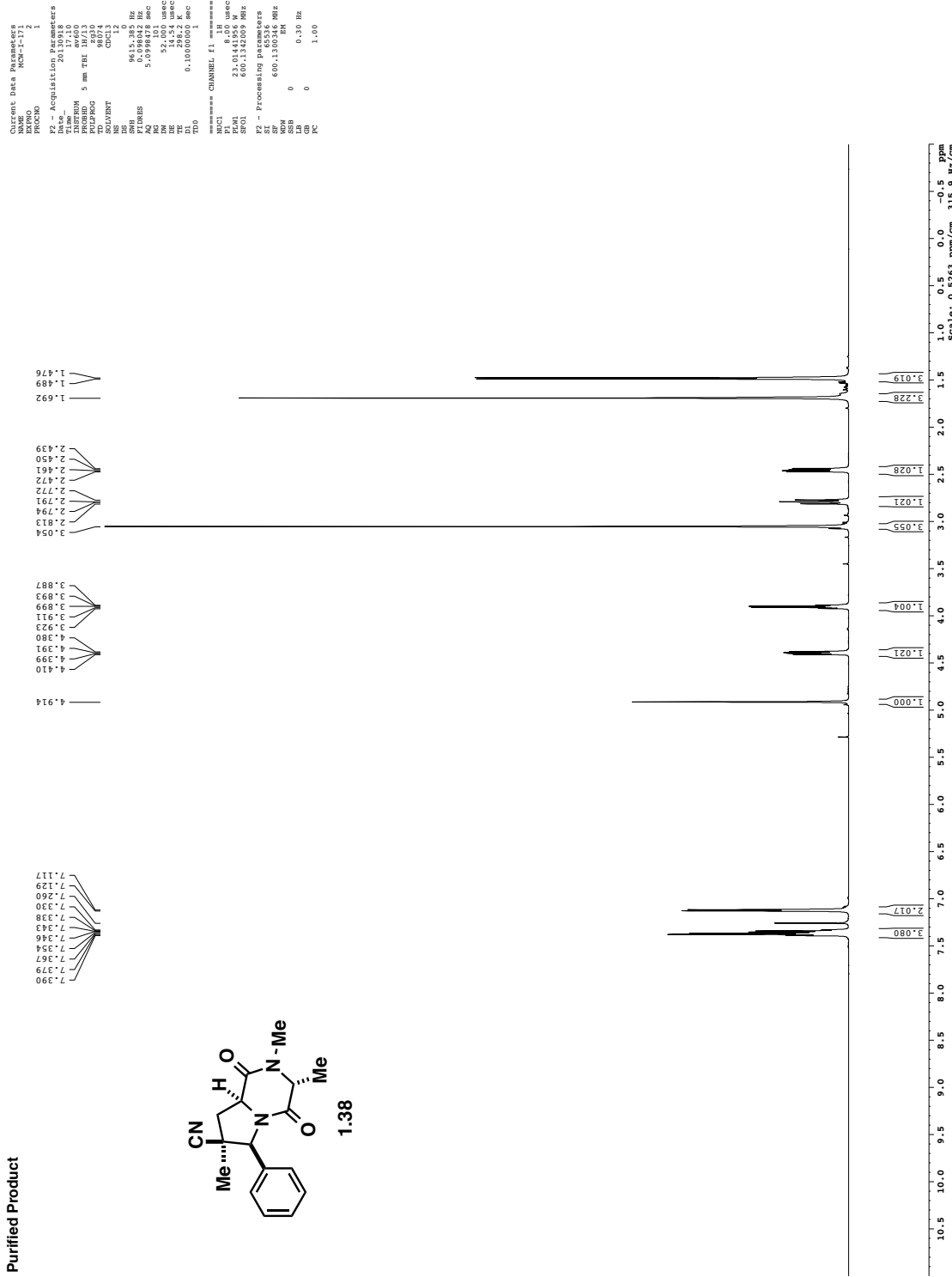
Endo Adduct



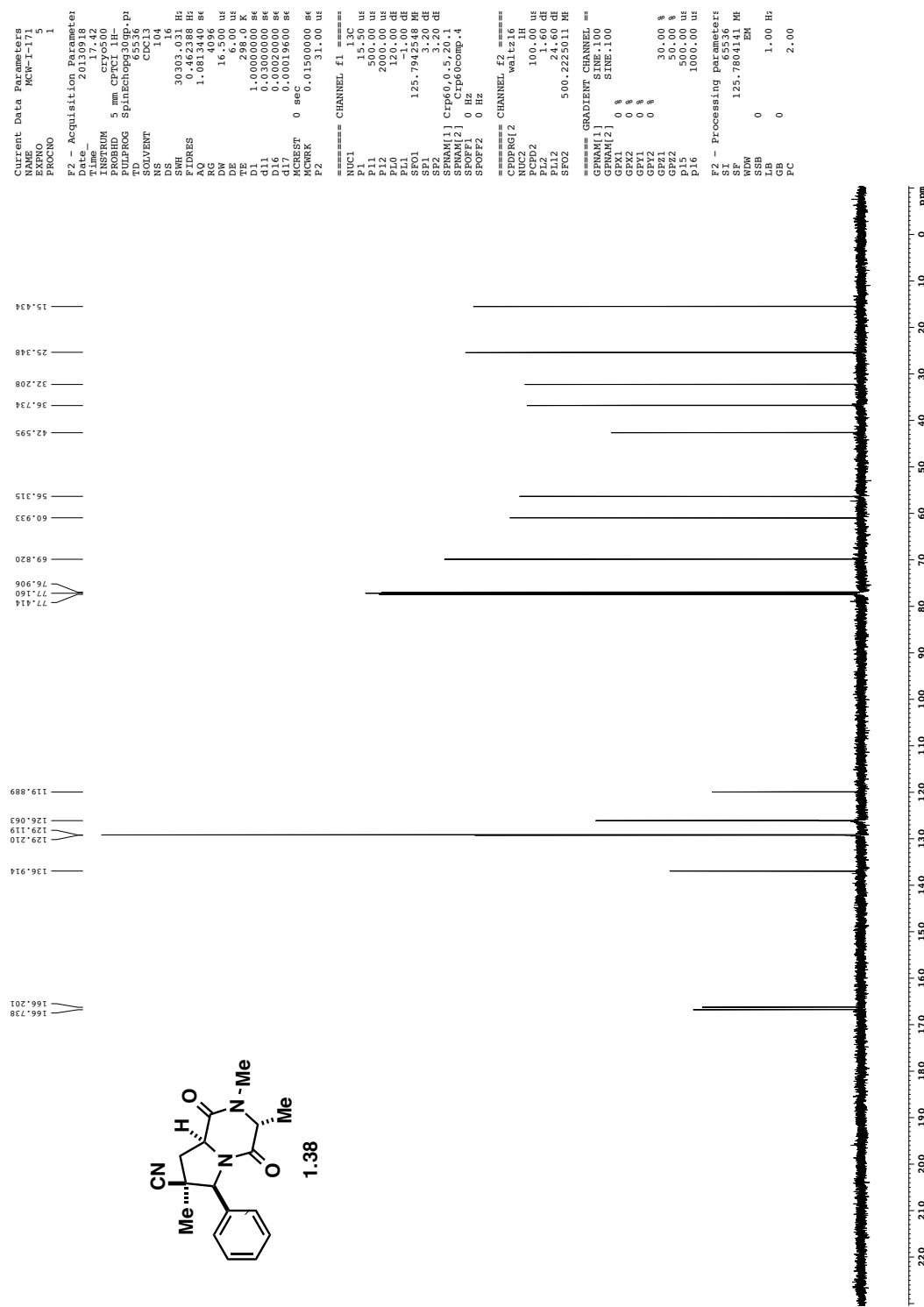
Purified Endo Adduct



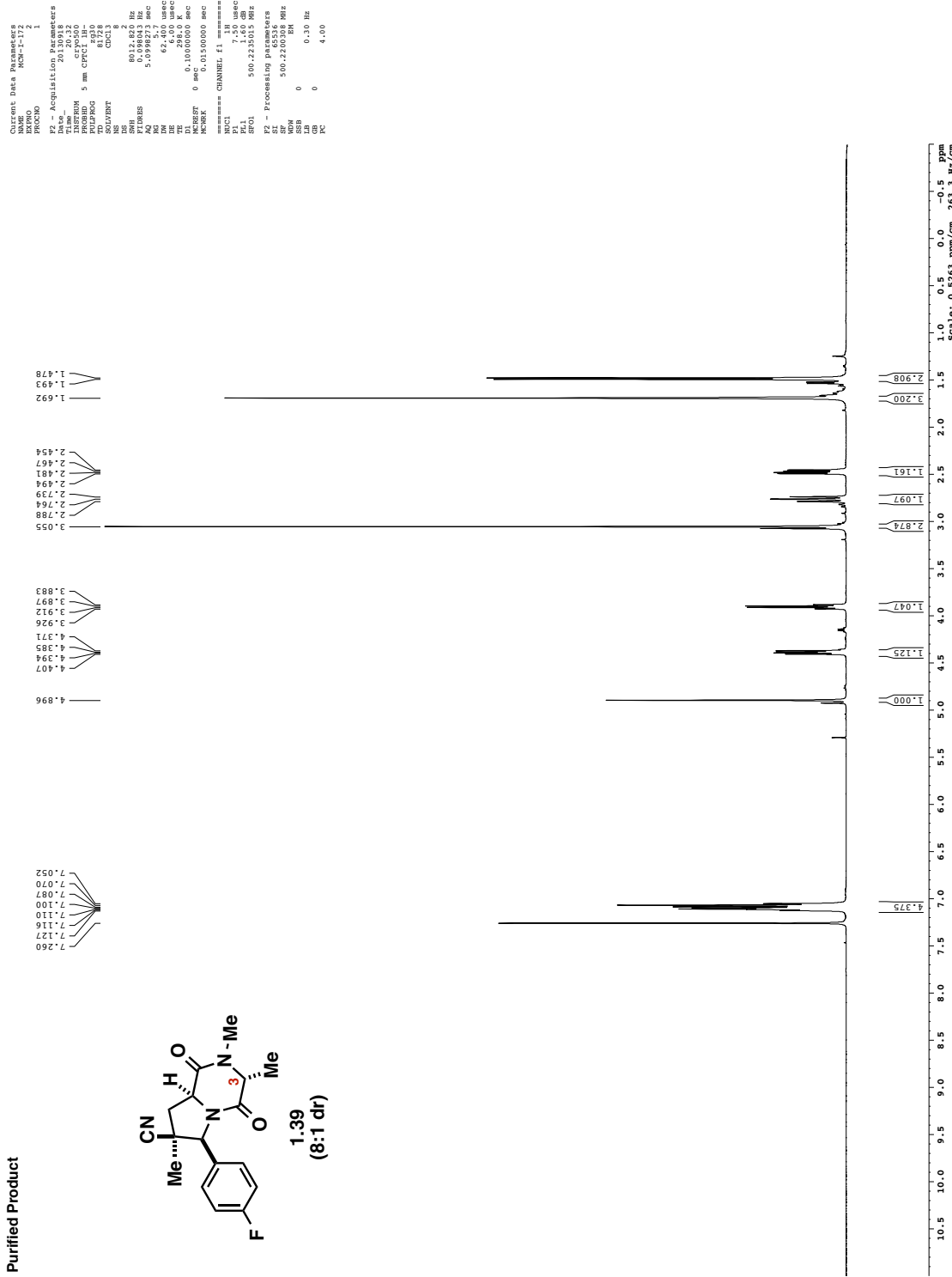
Purified Product



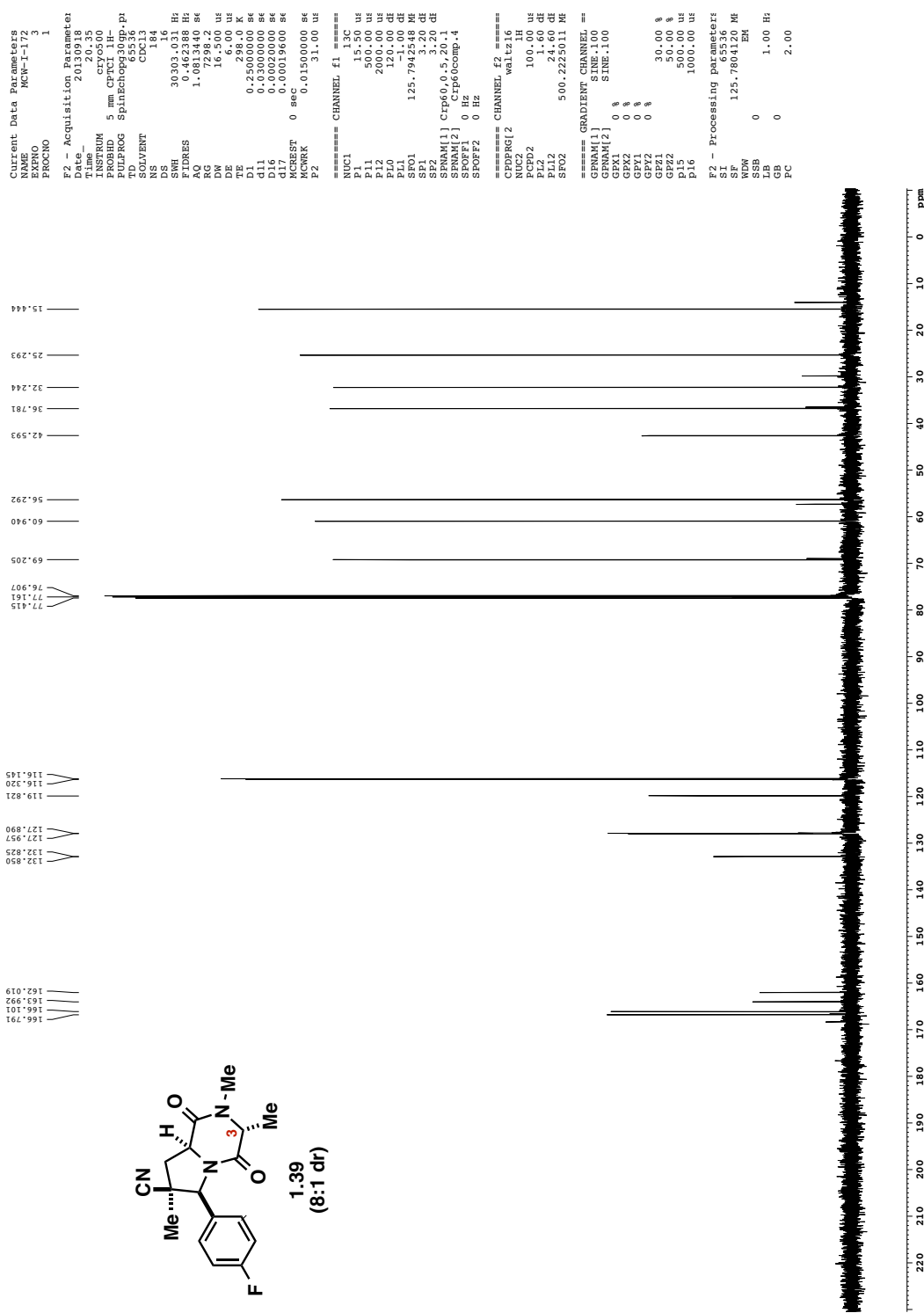
Purified Product



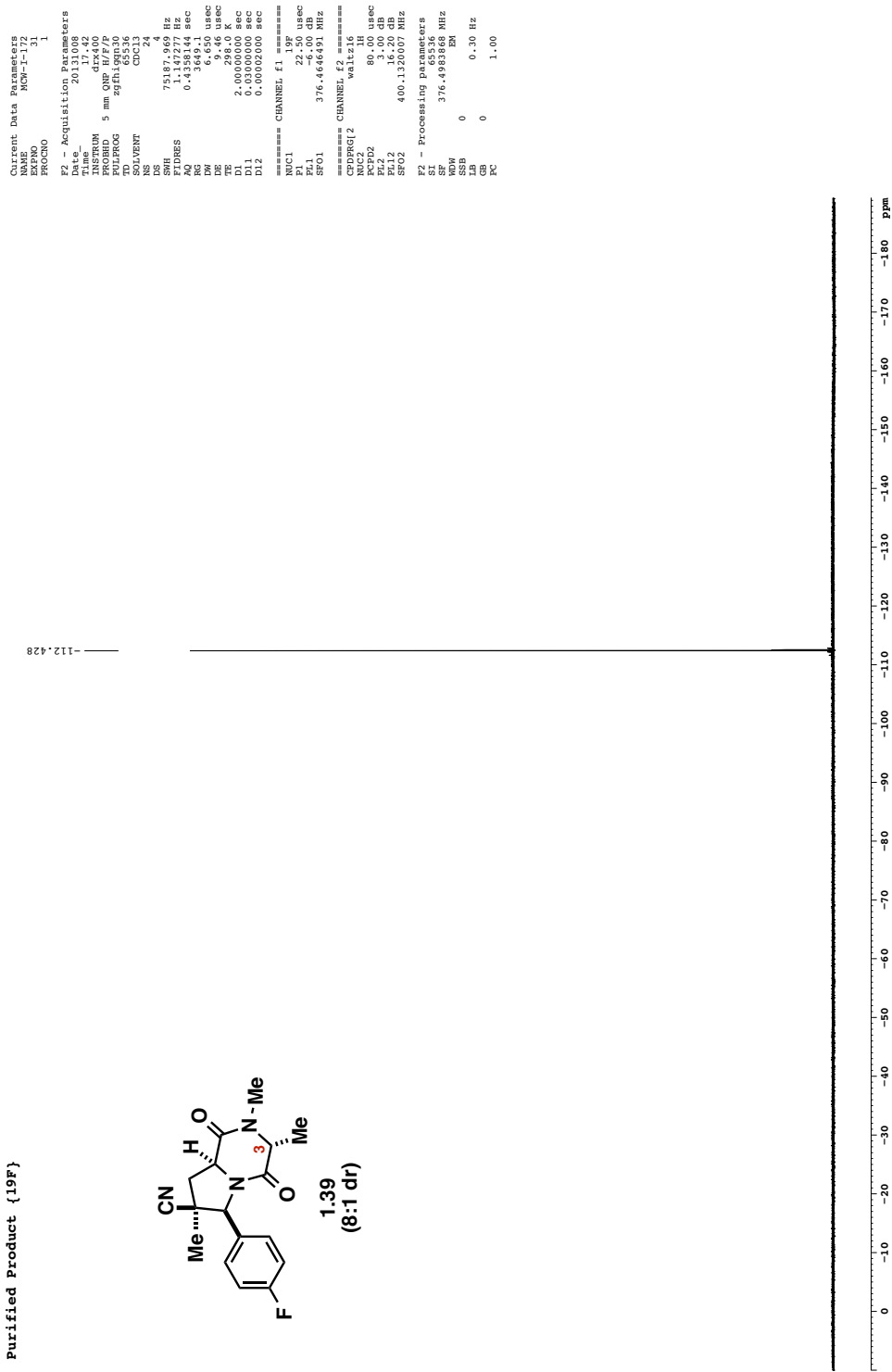
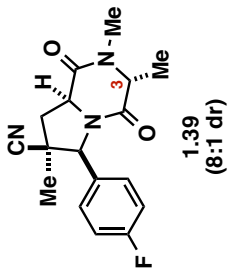
Purified Product



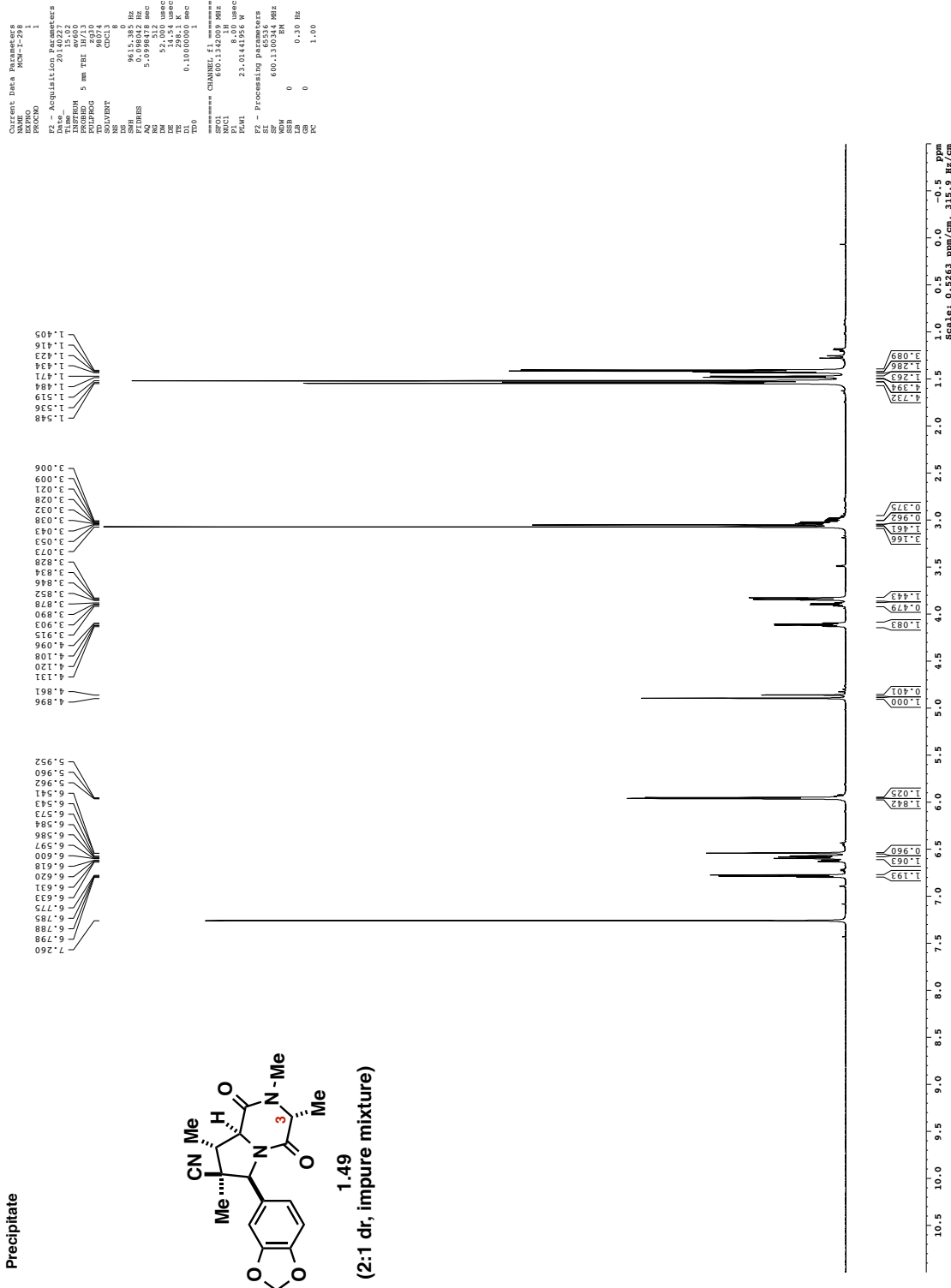
Purified Product



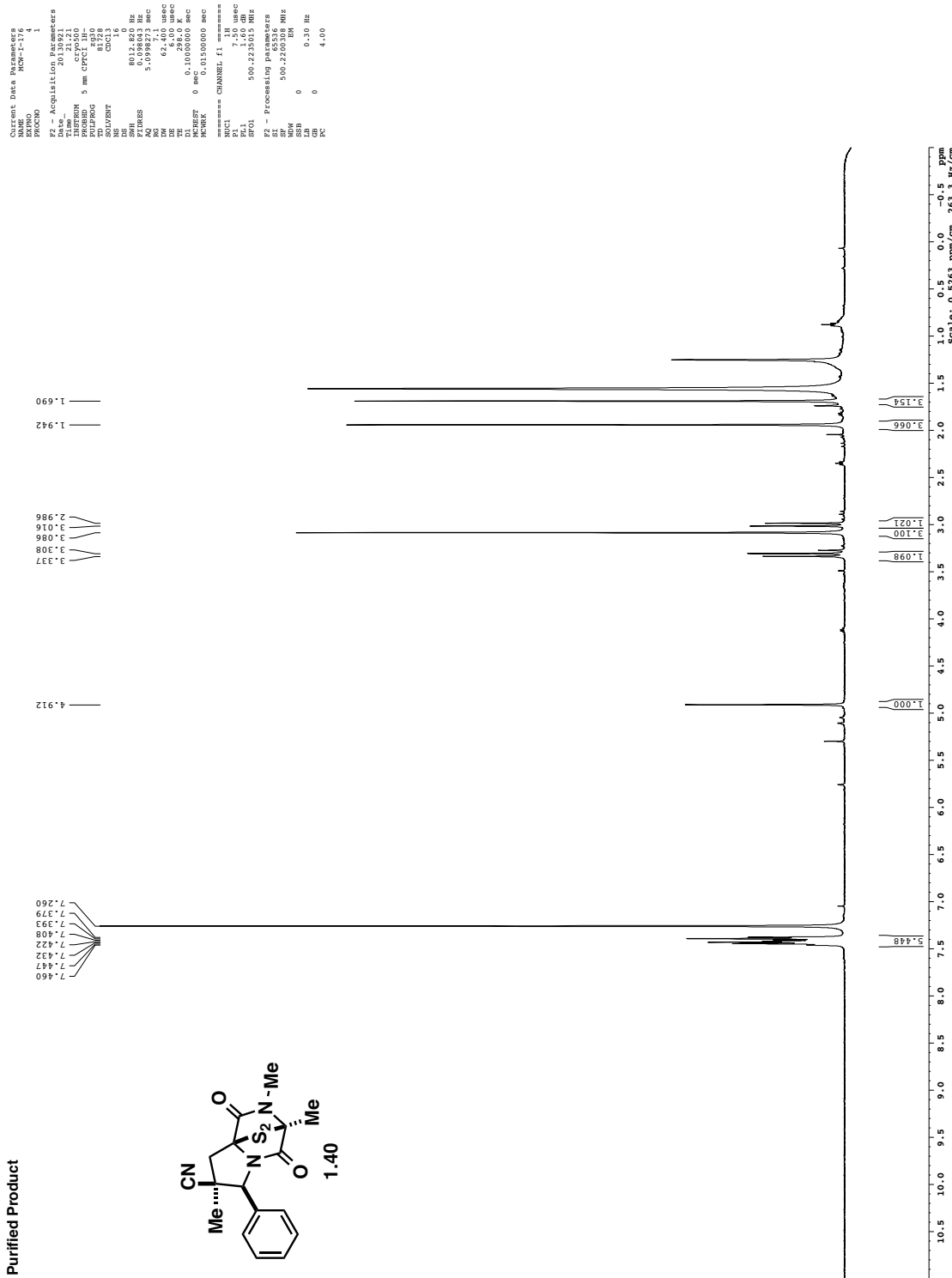
Purified Product {¹⁹F}



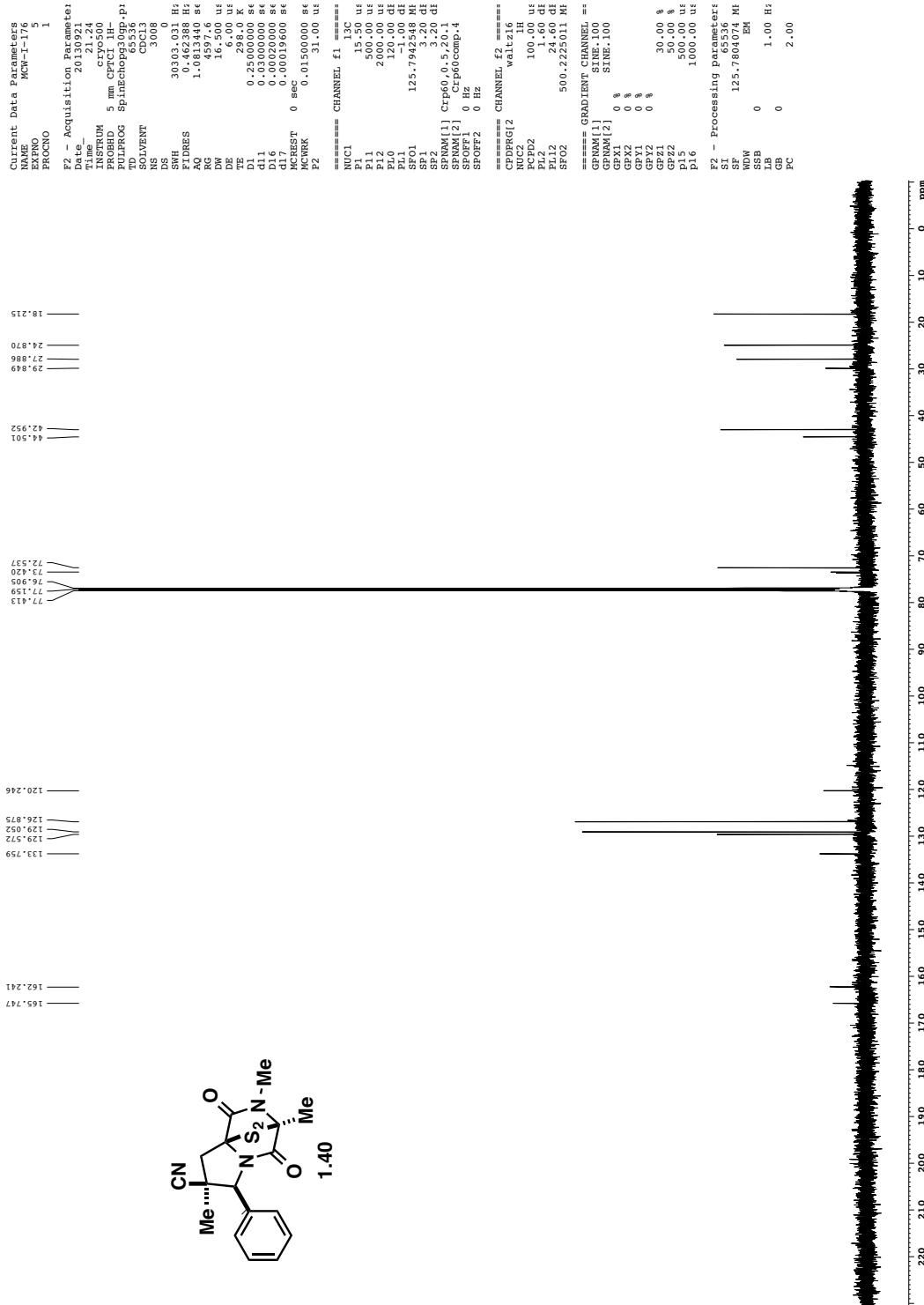
Precipitate



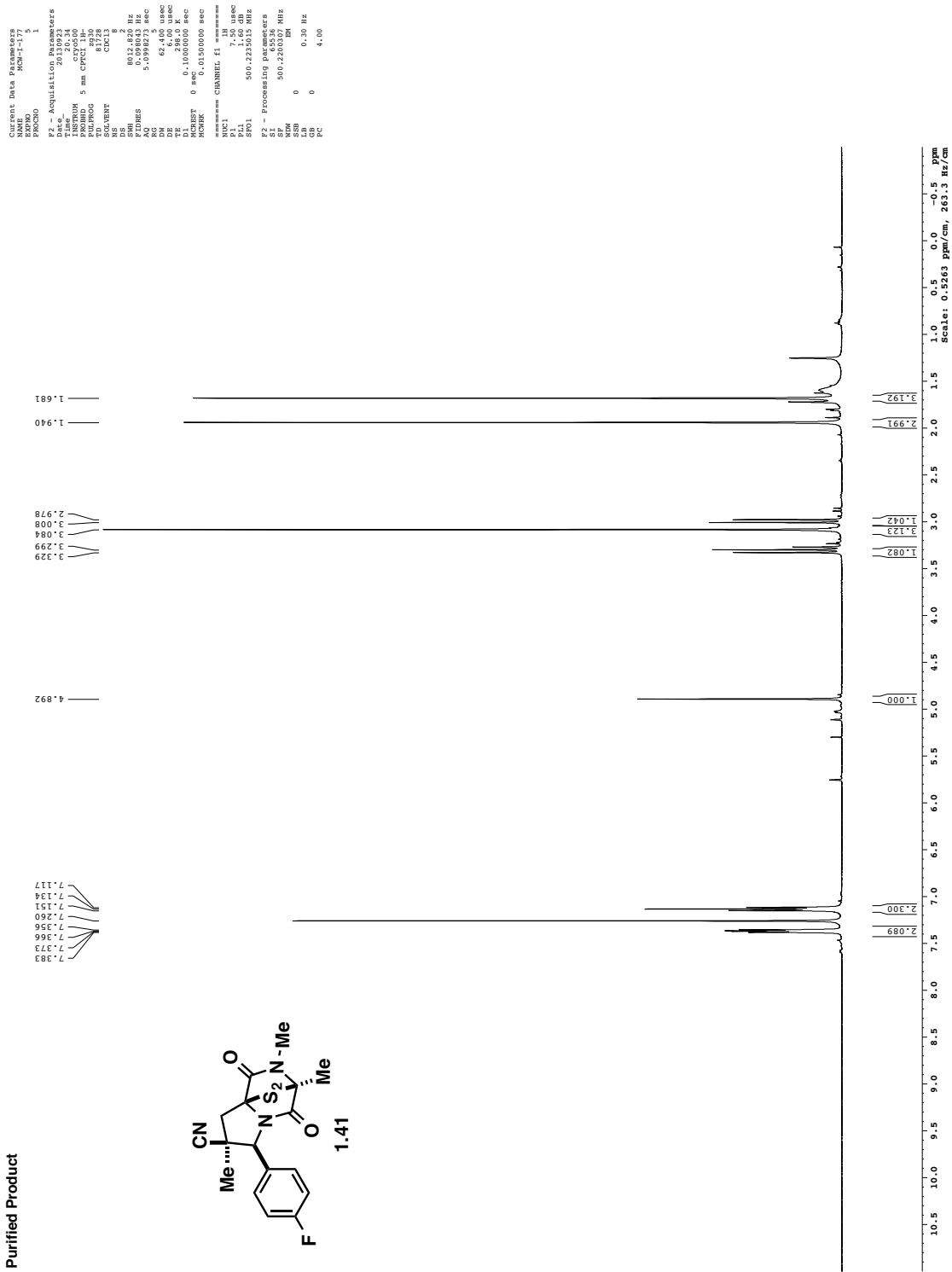
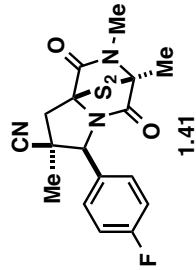
Purified Product



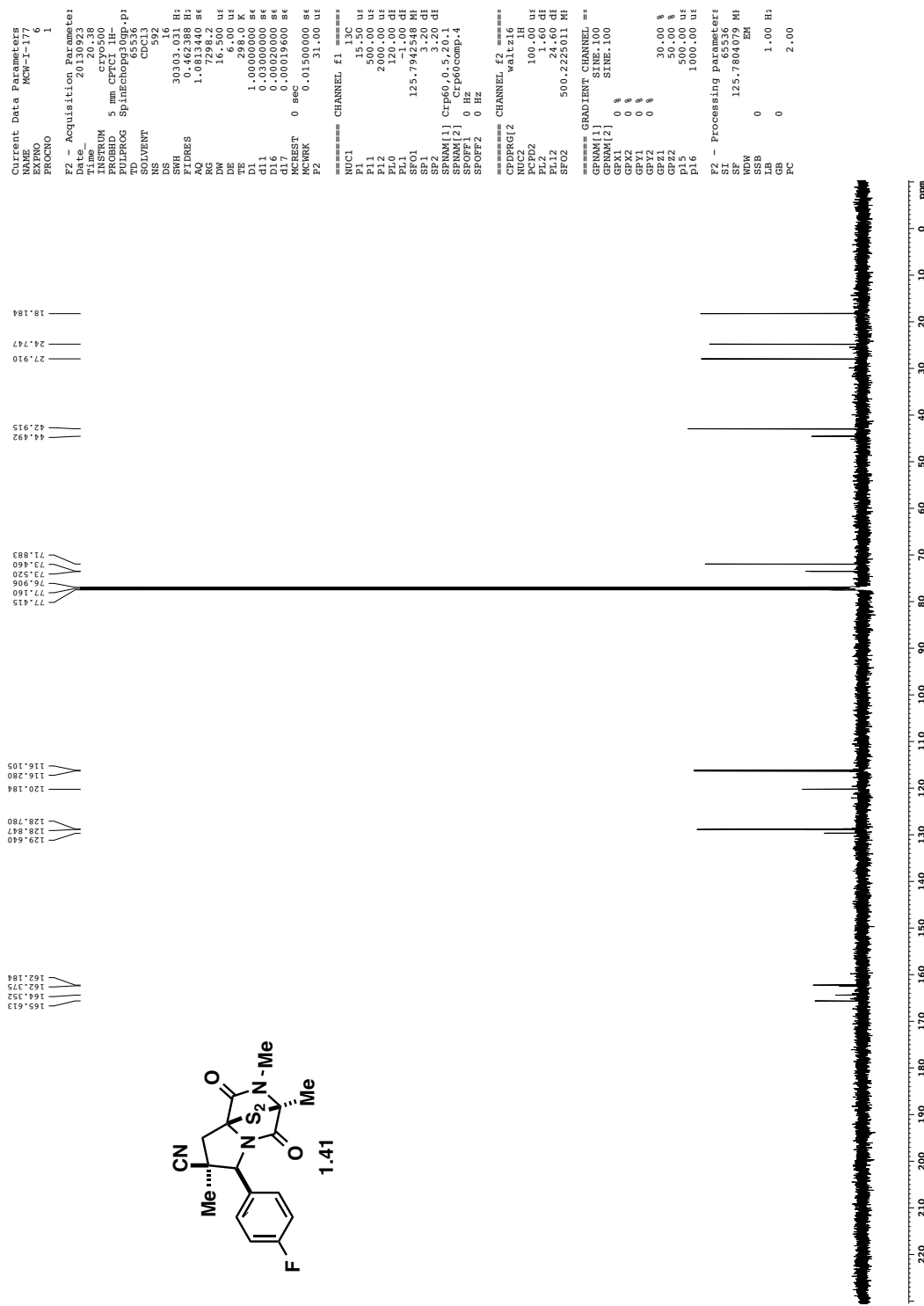
Purified Product



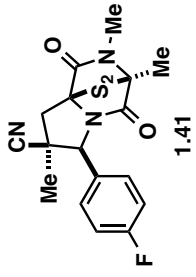
Purified Product



Purified Product



Purified Product {¹⁹F}



— 111.983 —

```

Current Data Parameters
NAME      MCW-T-177
PROCNO    31
1

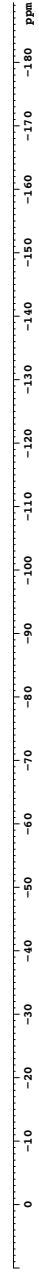
E2 = Acquisition Parameters
Date_     2013.068
Time_     17:38
INSTRUM  5 mm QNP400
RFIDR    251.0630
TD       6536
SOLVENT   CDCl3
NS        32
SWH      75187.969 Hz
FIDRES   1.14277 Hz
AQ       0.435144 sec
RG       186.2
DE       6.50 usec
TE       298.0 K
TSP      2.000000 sec
D1L      0.000000 sec
D1ZD    0.0000200 sec

CHANNEL F1 = 1H
NUC1    1H
P1      22.30 usec
PL1    -4.00 dB
SFO1    376.464491 MHz

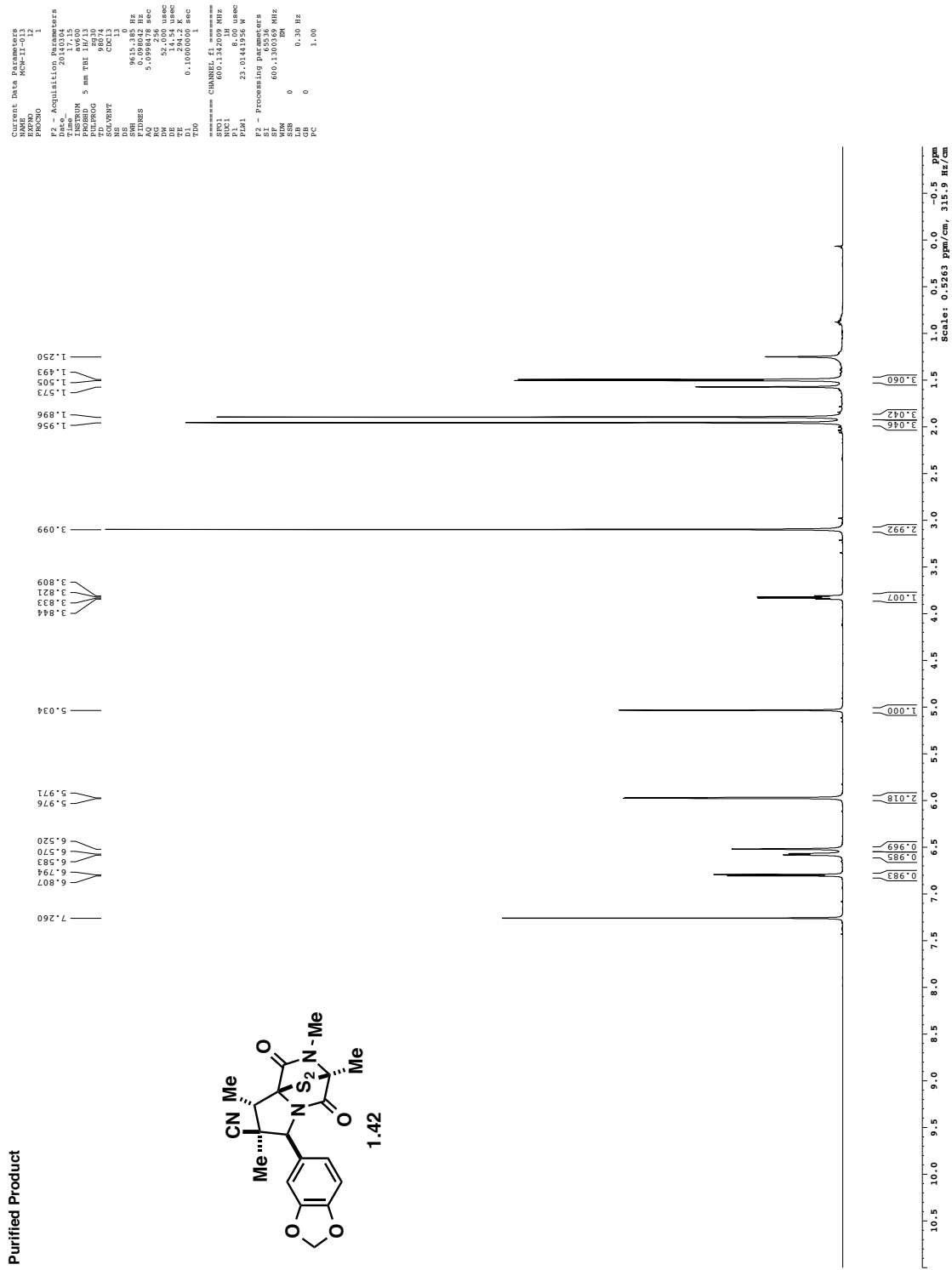
CHANNEL F2 = 1H
NUC2    1H
PCPD2  80.00 usec
P2      3.00 dB
RF2    4006.1426007 MHz

E2 = Processing parameters
IS      376.464491 MHz
SF      376.464491 MHz
WDW    EN
SSB      0
LB      0.30 Hz
PE      0
AC      1.00

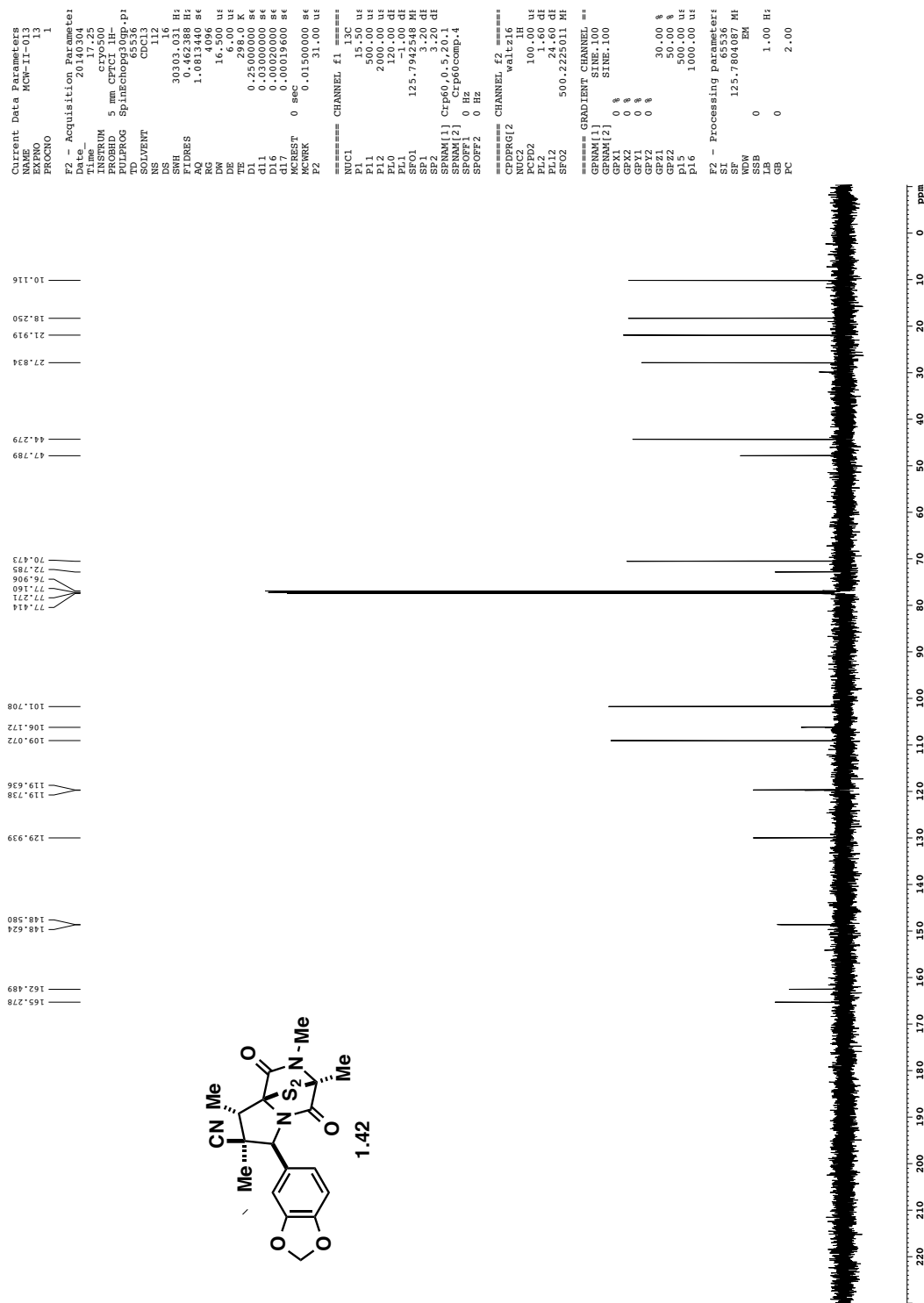
```



Purified Product



Purified Product



1.6 References and Notes

¹ For recent reviews on ETP total syntheses and biological activity studies, see: (a) Gardiner, D. M.; Waring, P.; Howlett, B. J. *Microbiology* **2005**, *151*, 1021. (b) Iwasa, E.; Hamashima, Y.; Sodeoka, M. *Isr. J. Chem.* **2011**, *51*, 420. (c) Jiang, C.-S.; Müller, W. E. G.; Schröder, H. C.; Guo, Y.-W. *Chem. Rev.* **2012**, *112*, 2179. (d) Welch, T. R.; Williams, R. M. *Nat. Prod. Rep.* **2014**, *31*, 1376.

² (a) Shimazaki, N.; Shima, I.; Hemmi, K.; Tsurumi, Y.; Hashimoto, M. *Chem. Pharm. Bull.* **1987**, *35*, 3527. (b) Martins, M. B.; Carvalho, I. *Tetrahedron* **2007**, *63*, 9923. (c) Huang, R.; Zhou, X.; Xu, T.; Yang, X.; Liu, Y. *Chem. Biodiversity* **2010**, *7*, 2809. (d) Borthwick, A. D. *Chem. Rev.* **2012**, *112*, 3641.

³ (a) Kirby, G. W.; Patrick, G. L.; Robins, D. J. *J. Chem. Soc., Perkin Trans. I* **1978**, 1336. (b) Balibar, C. J.; Walsh, C. T. *Biochemistry* **2006**, *45*, 15029.

⁴ Jordan, T. W.; Cordiner, S. J. *Trends Pharmacol. Sci.* **1987**, *8*, 144.

⁵ Patron, N. J.; Waller, R. F.; Cozijnsen, A. J.; Straney, D. C.; Gardiner, D. M.; Nierman, W. C.; Howlett, B. J. *BMC Evol. Bio.* **2007**, *7*, 174.

⁶ (a) Block, K. M.; Wang, H.; Szabó, L. Z.; Polaske, N. W.; Henchey, L. K.; Dubey, R.; Kushal, S.; László, C. F.; Makhoul, J.; Song, Z.; Meuillet, E. J.; Olenyuk, B. Z. *J. Am. Chem. Soc.* **2009**, *131*, 18078. (b) Sodeoka, M.; Dodo, K.; Teng, Y.; Iuchi, K.; Hamashima, Y.; Iwasa, E.; Fujishiro, S. *Pure Appl. Chem.* **2012**, *84*, 1369. (c) Fujishiro, S.; Dodo, K.; Iwasa, E.; Teng, Y.; Sohtome, Y.; Hamashima, Y.; Ito, A.; Yoshida, M.; Sodeoka, M. *Bioorg. Med. Chem. Lett.* **2013**, *23*, 733. (d) Boyer, N.; Morrison, K. C.; Kim, J.; Hergenrother, P. J.; Movassaghi, M. *Chem. Sci.* **2013**, *4*, 1646. (e) DeLorbe, J. E.; Horne, D.; Jove, R.; Mennen, S. M.; Nam, S.; Zhang, F.-L.; Overman, L. E. *J. Am. Chem. Soc.* **2013**, *135*, 4117. (f) Dubey, R.; Levin, M. D.; Szabo, L. Z.; Kushal, S.; Singh, J. B.; Oh, P.; Schnitzer, J. E.; Olenyuk, B. Z. *J. Am. Chem. Soc.* **2013**, *135*, 4537.

⁷ (a) Weindling, R. *Phytopathology* **1932**, *22*, 837. (b) Weindling, R.; Emerson, O. H. *Phytopathology* **1936**, *26*, 1068. (c) Johnson, J. R.; Bruce, W. F.; Dutcher, J. D. *J. Am. Chem. Soc.* **1943**, *65*, 2005.

⁸ (a) Johnson, J. R.; Buchanan, J. B. *J. Am. Chem. Soc.* **1953**, *75*, 2103. (b) Bell, M. R.; Johnson, J. R.; Wildi, B. S.; Woodward, R. B. *J. Am. Chem. Soc.* **1958**, *80*, 1001. (c) Beecham, A. F.; Fridrichsons, J.; Mathieson, A. McL. *Tetrahedron Lett.* **1966**, 3131.

⁹ For total syntheses, see: (a) Fukuyama, T.; Kishi, Y. *J. Am. Chem. Soc.* **1976**, *98*, 6723. (b) Fukuyama, T.; Nakatsuka, S.-I.; Kishi, Y. *Tetrahedron* **1981**, *37*, 2045. (c) Nicolaou, K. C.; Lu, M.; Totokotsopoulos, S.; Heretsch, P.; Giguère, D.; Sun, Y.-P.; Sarlah, D.; Nguyen, T. H.; Wolf, I. C.; Smee, D. F.; Day, C. W.; Bopp, S.; Winzeler, E. A. *J. Am. Chem. Soc.* **2012**, *134*, 17320.

¹⁰ For biosynthesis studies, see: (a) Schrettl, M.; Carberry, S.; Kavanagh, K.; Haas, H.; Jones, G. W.; O'Brien, J.; Nolan, A.; Stephens, J.; Fenelon, O.; Doyle, S. *PLoS Pathog.* **2010**, *6*, e1000952. (b) Scharf, D. H.; Remme, N.; Heinekamp, T.; Hortschansky, P.; Brakhage, A. A.; Hertweck, C. *J. Am. Chem. Soc.* **2010**, *132*, 10136. (c) Scharf, D. H.; Remme, N.; Habel, A.; Chankhamjon, P.; Scherlach, K.; Heinekamp, T.; Hortschansky, P.; Brakhage, A. A.; Hertweck, C. *J. Am. Chem. Soc.* **2011**, *133*, 12322. (d) Davis, C.; Carberry, S.; Schrettl, M.; Singh, I.; Stephens, J. C.; Barry, S. M.; Kavanagh, K.; Challis, G. L.; Brougham, D.; Doyle, S. *Chem. Biol.* **2011**, *18*, 542. (e) Forseth, R. R.; Fox, E. M.; Chung, D.; Howlett, B. J.; Keller, N. P.; Schroeder, F. C. *J. Am. Chem. Soc.* **2011**, *133*, 9678. (f) Scharf, D. H.; Chankhamjon, P.; Scherlach, K.; Heinekamp, T.; Roth, M.; Brakhage, A. A.; Hertweck, C. *Angew. Chem. Int. Ed.* **2012**, *51*, 10064. (g) Scharf, D. H.; Chankhamjon, P.; Scherlach, K.; Heinekamp, T.; Willing, K.; Brakhage, A. A.; Hertweck, C. *Angew. Chem. Int. Ed.* **2013**, *52*, 11092. (h) Scharf, D. H.; Habel, A.; Heinekamp, T.; Brakhage, A. A.; Hertweck, C. *J. Am. Chem. Soc.* **2014**, *136*, 11674. (i) Scharf, D. H.; Groll, M.; Habel, A.; Heinekamp, T.; Hertweck, C.; Brakhage, A. A.; Huber, E. M. *Angew. Chem. Int. Ed.* **2014**, *53*, 2221. (j) Amatov, T.; Jahn, U. *Angew. Chem. Int. Ed.* **2014**, *53*, 3312. (k) Dolan, S. K.; O'Keefe, G.; Jones, G. W.; Doyle, S. *Trends Microbiol.* **2015**, *23*, 419.

¹¹ (a) Waring, P.; Sjaarda, A.; Lin, Q. H. *Biochem. Pharmacol.* **1995**, *49*, 1195. (b) Waring, P.; Beaver, J. *Gen. Pharmacol.* **1996**, *27*, 1311. (c) Vigushin, D. M.; Mirsaidi, N.; Brooke, G.; Sun, C.; Pace, P.; Inman, L.; Moody, C. J.; Coombes, R. C. *Med. Oncol.* **2004**, *21*, 21. (d) Kupfahl, C.; Michalka, A.; Lass-Flörl, C.; Fischer, G.; Haase, G.; Ruppert, T.; Geginat, G.; Hof, H. *Int. J. Med. Microbiol.* **2008**, *298*, 319. (e) Takahashi, M.; Takemoto, Y.; Shimazu, T.; Kawasaki, H.; Tachibana, M.; Shinkai, Y.; Takagi, M.; Shin-ya, K.; Igarashi, Y.; Ito, A.; Yoshida, M. *J. Antibiot.* **2012**, *65*, 263. (f) Vargas, W. A.; Mukherjee, P. K.; Laughlin, D.; Wiest, A.; Moran-Diez, M. E.; Kenerley, C. M. *Microbiology* **2014**, *160*, 2319. (g) Sakamoto, H.; Egashira, S.; Saito, N.; Kirisako, T.; Miller, S.; Sasaki, Y.; Matsumoto, T.; Shimonishi, M.; Komatsu, T.; Terai, T.; Ueno, T.; Hanaoka, K.; Kojima, H.; Okabe, T.; Wakatsuki, S.; Iwai, K.; Nagano, T. *ACS Chem. Biol.* **2015**, *10*, 675.

¹² von Hauser, D.; Weber, H. P.; Sigg, H. P. *Helv. Chim. Acta* **1970**, *53*, 1061.

¹³ (a) Waksman, S. A.; Bugie, E. *J. Bacteriol.* **1944**, *48*, 527. (b) McInnes, A. G.; Taylor, A.; Walter, J. A. *J. Am. Chem. Soc.* **1976**, *98*, 6741.

¹⁴ For selected early studies showing that removal of the episulfide functionality results in loss of observed biological activity, see: (a) Trown, P. W.; Bilello, J. A. *Antimicrob. Agents Chemother.* **1972**, *2*, 261. (b) Middleton, M. C. *Biochem. Pharmacol.* **1974**, *23*, 811. (c) Waring, P.; Eichner, R. D.; Müllbacher, A. *Med. Res. Rev.* **1988**, *8*, 499.

¹⁵ For an early study demonstrating that simple ETP analogues exhibit biological activity, see: Müllbacher, A.; Waring, P.; Tiwari-Palni, U.; Eichner, R. D. *Mol. Immunol.* **1986**, *23*, 231.

¹⁶ Chai, C. L. L.; Waring, P. *Redox. Rep.* **2000**, *5*, 257.

¹⁷ For studies on thiol-disulfide exchange equilibria, see: (a) Whitesides, G. M.; Houk, J.; Patterson, M. A. K. *J. Org. Chem.* **1983**, *48*, 112. (b) Gilbert, H. F. *Methods Enzymol.* **1995**, *251*, 8.

¹⁸ For early studies of ETP metal complexes, see: (a) Woodcock, J. C.; Henderson, W.; Miles, C. O.; Nicholson, B. K. *J. Inorg. Biochem.* **2001**, *84*, 225. (b) Woodcock, J. C.; Henderson, W.; Miles, C. O. *J. Inorg. Biochem.* **2001**, *85*, 187.

¹⁹ (a) Bernardo, P. H.; Chai, C. L. L.; Deeble, G. J.; Liu, X.-M.; Waring, P. *Bioorg. Med. Chem. Lett.* **2001**, *11*, 483. (b) Bernardo, P. H.; Brasch, N.; Chai, C. L. L.; Waring, P. *J. Biol. Chem.* **2003**, *278*, 46549.

²⁰ Szajewski, R. P.; Whitesides, G. M. *J. Am. Chem. Soc.* **1980**, *102*, 2011.

²¹ Chai, C. L. L.; Heath, G. A.; Huleatt, P. B.; O'Shea, G. A. *J. Chem. Soc., Perkin Trans. 2* **1999**, 389.

²² (a) Ames, B. N. *Science* **1983**, *221*, 1256. (b) Eichner, R. D.; Waring, P.; Geue, A. M.; Braithwaite, A. W.; Müllbacher, A. *J. Biol. Chem.* **1988**, *263*, 3772.

²³ Munday, R. *J. Appl. Toxicol.* **1984**, *4*, 182.

²⁴ Hurne, A. M.; Chai, C. L. L.; Waring, P. *J. Biol. Chem.* **2000**, *275*, 25202.

²⁵ Rodriguez, P. L.; Carrasco, L. *J. Virol.* **1992**, *66*, 1971.

²⁶ Van der Pyl, D.; Inokoshi, J.; Shiomi, K.; Yang, H.; Takeshima, H.; Omura, S. *J. Antibiotic.* **1992**, *11*, 1802.

²⁷ Pahl, H. L.; Krauss, B.; Schulze-Osthoff, K.; Decker, T.; Traenckner, E. B.-M.; Vogt, M.; Myers, C.; Parks, T.; Warring, P.; Müllbacher, A.; Czernilofsky, A.-P.; Baeuerle, P. A. *J. Exp. Med.* **1996**, *183*, 1829.

²⁸ Kung, A. L.; Zabludoff, S. D.; France, D. S.; Freedman, S. J.; Tanner, E. A.; Vieira, A.; Cornell-Kennon, S.; Lee, J.; Wang, B.; Wang, J.; Memmert, K.; Naegeli, H.-U.; Petersen, F.; Eck, M. J.; Bair, K. W.; Wood, A. W.; Livingston, D. M. *Cancer Cell* **2004**, *6*, 33.

²⁹ Cook, K. M.; Hilton, S. T.; Mecinovic, J.; Motherwell, W. B.; Figg, W. D.; Schofield, C. J. *J. Biol. Chem.* **2009**, *284*, 26831.

³⁰ Synge, R. L. M.; White, E. P. *Chem. and Ind.* **1959**, *1546*.

³¹ (a) Towers, N. R.; Smith, B. L. *N. Z. Vet. J.* **1978**, *26*, 199. (b) Munday, R.; Manns, E.; Mortimer, P. H. *Proc. New Zeal. Soc. An.* **1983**, *43*, 209. (c) Waring, P.; Egan, M.; Braithwaite, A.; Mullbacher, A.; Sjaarda, A. *Int. J. Immunopharmac.* **1990**, *12*, 445.

³² (a) Suzuki, H.; Tomida, A.; Tsuruo, T. *Oncogene* **2001**, *20*, 5779. (b) Semenza, G. L. *Nat. Rev. Cancer* **2003**, *3*, 721. (c) Thirlwell, C.; Schulz, L. K. E.; Beck, S. *Clin. Epigenetics* **2011**, *3*, 9.

³³ Reece, K. M.; Richardson, E. D.; Cook, K. M.; Campbell, T. J.; Pisle, S. T.; Holly, A. J.; Venzon, D. J.; Liewehr, D. J.; Chau, C. H.; Price, D. K.; Figg, W. D. *Mol. Cancer* **2014**, *13*, 91.

³⁴ (a) Kung, A. L.; Wang, S.; Klco, J. M.; Kaelin, W. G., Jr.; Livingston, D. M. *Nat. Med.* **2000**, *6*, 1335. (b) Onnis, B.; Rapisarda, A.; Melillo, G. *J. Cell. Mol. Med.* **2009**, *13*, 2780. (c) Lin, S.-C.; Liao, W.-L.; Lee, J.-C.; Tsai, S.-J. *Exp. Biol. Med.* **2014**, *239*, 779.

³⁵ Greiner, D.; Bonaldi, T.; Eskeland, R.; Roemer, E.; Imhof, A. *Nat. Chem. Biol.* **2005**, *1*, 143.

³⁶ Cherblanc, F. L.; Chapman, K. L.; Brown, R.; Fuchter, M. J. *Nat. Chem. Biol.* **2013**, *9*, 136.

³⁷ (a) Rea, S.; Eisenhaber, F.; O'Carroll, D.; Strahl, B. D.; Sun, Z.-W.; Schmid, M.; Opravil, S.; Mechtedler, K.; Ponting, C. P.; Allis, C. D.; Jenuwein, T. *Nature* **2000**, *406*, 593. (b) Zhang, Y.; Reinberg, D. *Genes Dev.* **2001**, *15*, 2343. (c) Hake, S. B.; Xiao, A.; Allis, C. D. *Br. J. Cancer* **2004**, *90*, 761. (d) Martin, C.; Zhang, Y. *Mol. Cell Biol.* **2005**, *6*, 838. (d) Copeland, R. A.; Solomon, M. E.; Richon, V. M. *Nat. Rev. Drug Discov.* **2009**, *8*, 724. (e) Copeland, R. A. *Drug Discovery Today: Ther. Strategies* **2012**, *9*, 83.

³⁸ (a) Kondo, Y.; Shen, L.; Ahmed, S.; Boumber, Y.; Sekido, Y.; Haddad, B. R.; Issa, J. P. *PLoS ONE* **2008**, *3*, e2037. (b) Watanabe, H.; Soejima, K.; Yasuda, H.; Kawada, I.; Nakachi, I.; Yoda, S.; Naoki, K.; Ishizaka, A. *Cancer Cell Int.* **2008**, *8*, 15.

³⁹ Iwasa, E.; Hamashima, Y.; Fujishiro, S.; Higuchi, E.; Ito, A.; Yoshida, M.; Sodeoka, M. *J. Am. Chem. Soc.* **2010**, *132*, 4078.

⁴⁰ Cherblanc, F. L.; Chapman, K. L.; Reid, J.; Borg, A. J.; Sundriyal, S.; Alcazar-Fuoli, L.; Bignell, E.; Demetriades, M.; Schofield, C. J.; DiMaggio, P. A., Jr.; Brown, R.; Fuchter, M. J. *J. Med. Chem.* **2013**, *56*, 8616.

⁴¹ (a) Overman, L. E.; Sato, T. *Org. Lett.* **2007**, *9*, 5267. (b) DeLorbe, J. E.; Jabri, S. Y.; Mennen, S. M.; Overman, L. E.; Zhang, F.-L. *J. Am. Chem. Soc.* **2011**, *133*, 6549. (c) Jabri, S. Y.; Overman, L. E. *J. Am. Chem. Soc.* **2013**, *135*, 4231. (d) Jabri, S. Y.; Overman, L. E. *J. Org. Chem.* **2013**, *78*, 8766.

⁴² (a) Overman, L. E.; Baumann, M.; Nam, S.; Horne, D.; Jove, R.; Xie, J.; Kowolik, C. ETP Derivatives. PCT Int. Appl. WO 2014066435 A1, 22 October 2012. (b) Baumann, M.; Dieskau, A. P.; Loertscher, B. M.; Walton, M. C.; Nam, S.; Xie, J.; Horne, D.; Overman, L. E. *Chem. Sci.* **2015**, *6*, 4451.

⁴³ Tsuge, O.; Kanemasa, S.; Yoshioka, M. *J. Org. Chem.* **1988**, *53*, 1384.

⁴⁴ Nicolaou, K. C.; Giguère, D.; Totokotsopoulos, S.; Sun, Y.-P. *Angew. Chem. Int. Ed.* **2012**, *51*, 728.

⁴⁵ In contrast to the synthesis of tetrasulfide products accomplished by the Nicolaou and Reisman groups, we observed the disulfide derivative as the major sulfenylation product in our studies. We attribute this to the nonplanar topology of our ETP derivatives, which may not allow for the incorporation of a large tetrasulfide bridge. Alternatively, planar ETP products are common synthetic targets in the Nicolaou and Reisman groups, which may explain their observance of tetrasulfides as the major sulfenylation products (see references 44 and 46).

⁴⁶ Codelli, J. A.; Puchlopek, A. L. A.; Reisman, S. E. *J. Am. Chem. Soc.* **2012**, *134*, 1930.

⁴⁷ See Chapter 2 for studies relating the importance of relative and absolute stereochemistry to the potency of our novel ETP analogues.

⁴⁸ The sulfenylation procedure used resulted in the formation of many sulfenylated products. The desired epidithiodioxopiperazines were difficult to purely separate from the corresponding epitrithiodioxopiperazine products, resulting in low isolated yields of the target compounds.

⁴⁹ Baumann attempted twice to accomplish the desired 1,3-dipolar cycloaddition but in each case an overnight reaction resulted in 90% recovery of imine starting material **1.44** (unpublished studies, UC Irvine, MB2-141).

⁵⁰ As described previously by Baumann (unpublished studies, UC Irvine, MB2-148), treatment of imine **1.44** with 2-methyl-2-butenenitrile in MeCN at 85 °C for 6 h resulted in ca. 90% recovery of unreacted starting material.

⁵¹ Augustine, J. K.; Bombrun, A.; Atta, R. N. *Synlett* **2011**, *15*, 2223.

⁵² Adapted from the procedure described by Quasdorf (unpublished studies, UC Irvine, KQ2-187).

⁵³ Tse, B. 4-Cyano-4-Deformylsodaricin Derivatives. PCT Int. Appl. WO 1999009975 A1, March 4, 1999.

⁵⁴ Kubota, Y.; Ishizaki, N.; Haraguchi, K.; Hamasaki, T.; Baba, M.; Tanaka, H. *Bioorg. Med. Chem.* **2010**, *18*, 7186.

⁵⁵ Attempts to purify crude imine products to remove residual unreacted aldehyde (filtration through SiO₂, alumina, Celite, or Florisil, and bulb-to-bulb distillation) resulted in hydrolysis or dimerization of the desired material. If left concentrated for more than a few hours, slow decomposition of the imine was observed.

⁵⁶ Solidifies at –20 °C.

Chapter 2: Studies Toward the Development of a Diastereo- and Enantioselective Catalytic 1,3-Dipolar Cycloaddition for the Synthesis of Pyrrolidine Derivatives

2.1. Relative and Absolute Configuration are Important Factors in the Potency of Epidithiodioxopiperazine Analogues

As described in the previous chapter, the Overman group has developed a short synthetic sequence to access epipolythiodioxopiperazine (ETP) analogues that exhibit promising anticancer activity.¹ SAR studies identified ETP analogue **2.1** as the most potent analogue tested to date. Three additional diastereomers—**2.2**, **2.3**, and **2.4**—were synthesized and their anticancer activity was determined in order to investigate the effect of the relative configuration of the pyrrolidine ring substituents and the disulfide bridge on the corresponding IC₅₀ value (Figure 2.1). Isomer **2.2**, where the disulfide bridge is trans to both the 3,4-methylenedioxyphenyl and nitrile groups, and congener **2.3**, which possesses a trans relationship between the nitrile group to both the disulfide bridge and the aryl group, both exhibited decreased potency against DU145 prostate cancer and A2058 melanoma cell lines compared to ETP **2.1**. Derivative **2.4**, a product retaining the cis relationship between the nitrile group and disulfide bridge but both of which are trans to the aryl group, exhibited the lowest potency of this series, with IC₅₀ values of 2200 nM and 3750 nM against DU145 and A2058 cell lines, respectively. These data illustrated the importance of the relative configuration of the disulfide bridge, the 3,4-methylenedioxyphenyl group, and the nitrile substituent on the ETP skeleton.

(±)-2.1	(±)-2.2	(±)-2.3	(±)-2.4
<i>IC₅₀</i> Values	<i>IC₅₀</i> Values	<i>IC₅₀</i> Values	<i>IC₅₀</i> Values
DU145: 100 nM A2058: 60 nM	DU145: 750 nM A2058: 220 nM	DU145: 870 nM A2058: 510 nM	DU145: 2200 nM A2058: 3750 nM

Figure 2.1. IC₅₀ Values for Four ETP Diastereomers against Two Cancer Cell Lines

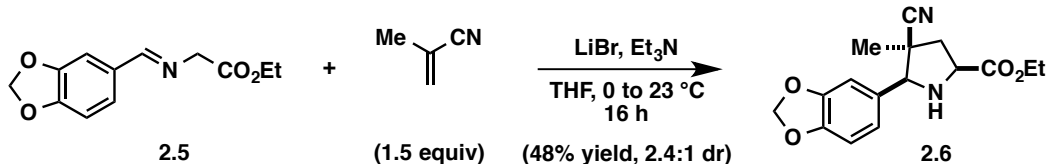
Racemic **2.1** was separated into its corresponding enantiomers using enantioselective HPLC.^{1a} Growth inhibition assays were run using the resulting enantiopure ETPs, which demonstrated that enantiomer **(+)-2.1** is six times more potent at inhibiting DU145 prostate cancer cells than **(-)-2.1** and 13 times more potent against A2058 cells (Figure 2.2). Collectively, these experiments demonstrate, in addition to relative stereochemistry, that absolute stereochemistry is important in the anticancer activity in this series of ETP analogues.

The synthetic route was reevaluated in order to more efficiently access ETP analogues in a diastereo- and enantioselective manner. As the 1,3-dipolar cycloaddition (1,3-DC) between imine **2.5** and methacrylonitrile is the first step in the sequence to **2.1** that introduces chiral centers (eq 2.1),² optimization of this step to synthesize endo pyrrolidine adduct **2.6** in a diastereo- and enantioselective fashion was initiated.

(+)-2.1	(-)-2.1
<i>IC₅₀</i> Values	<i>IC₅₀</i> Values
DU145: 130 nM A2058: 60 nM	DU145: 810 nM A2058: 750 nM

Figure 2.2. IC₅₀ Values of Enantiopure (+)- and (-)-2.1 Against Two Cancer Cell Lines

Equation 2.1



2.2. Chiral Lewis Acids in 1,3-DCs of Azomethine Ylides

Grigg and coworkers pioneered the early development of metallo-azomethine ylides for regio- and stereoselective 1,3-DC reactions.^{3,4} Ester-derived metallo-azomethine ylides adopt a “W-shaped” conformation when coordinated to a Lewis acid (LA, Figure 2.3).⁵ Consequently, pyrrolidines formed via the endo transition state contain an all-*cis* relationship between substituents at C2, C4, and C5. In 1991, Grigg and Allway published the first report using a chiral Lewis acid to synthesize enantioenriched pyrrolidines from aryl aldehyde-derived imines.⁶ The authors found that CoCl₂ and (1*R*,2*S*)-1-phenyl-2-(1-pyrrolidinyl)-1-propanol formed a suitable chiral catalyst that was used to synthesize pyrrolidine **2.7** in 83% yield and 96% ee (eq 2.2). Two major drawbacks exist in this method: The cobalt complex was used in stoichiometric amounts and, in order to prevent decomposition of the starting material, the dipolarophile methyl acrylate was used as the solvent. Nonetheless, this report inspired further investigations into the development of catalytic asymmetric 1,3-DC reactions.

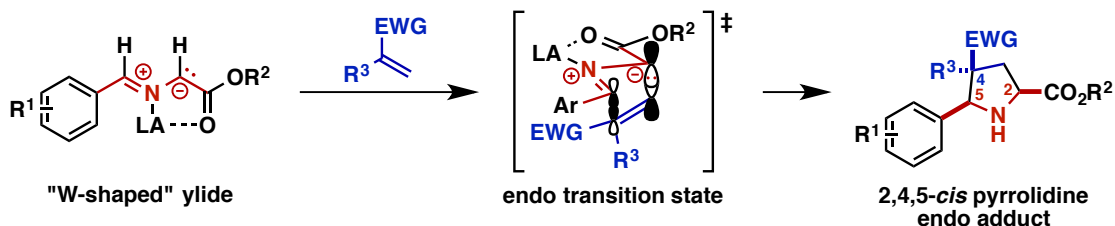
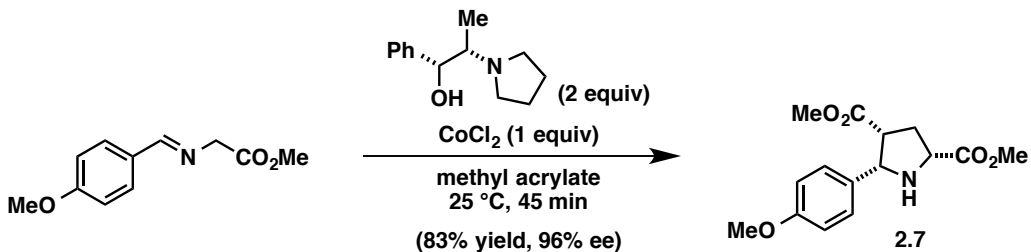


Figure 2.3. 1,3-DC between a “W-Shaped” Azomethine Ylide and an Electron-Deficient Olefin

Equation 2.2



Eleven years after Grigg's development of an asymmetric synthesis of pyrrolidines by 1,3-DC,⁶ the first reports of asymmetric 1,3-DC reactions using substoichiometric amounts of catalyst were independently described by the Zhang⁷ and Jørgensen⁸ groups. The Zhang group described endo adduct-selective syntheses of chiral pyrrolidines using the Ag(I)/xylyl-bis-ferrocenyl amide phosphine (FAP)⁹ catalyst **2.8** (Figure 2.4). The authors noted increased enantioenrichment of pyrrolidine **2.9** when using bulky xylyl-FAP ligand **2.8** over FAP (**2.10**) as well as when more sterically demanding dipolarophiles like *tert*-butyl acrylate were employed (compare **2.11** to **2.12**). Using this method, Zhang and coworkers synthesized endo pyrrolidine adducts from 13 different imine substrates and six dipolarophiles with up to 97% ee.⁷

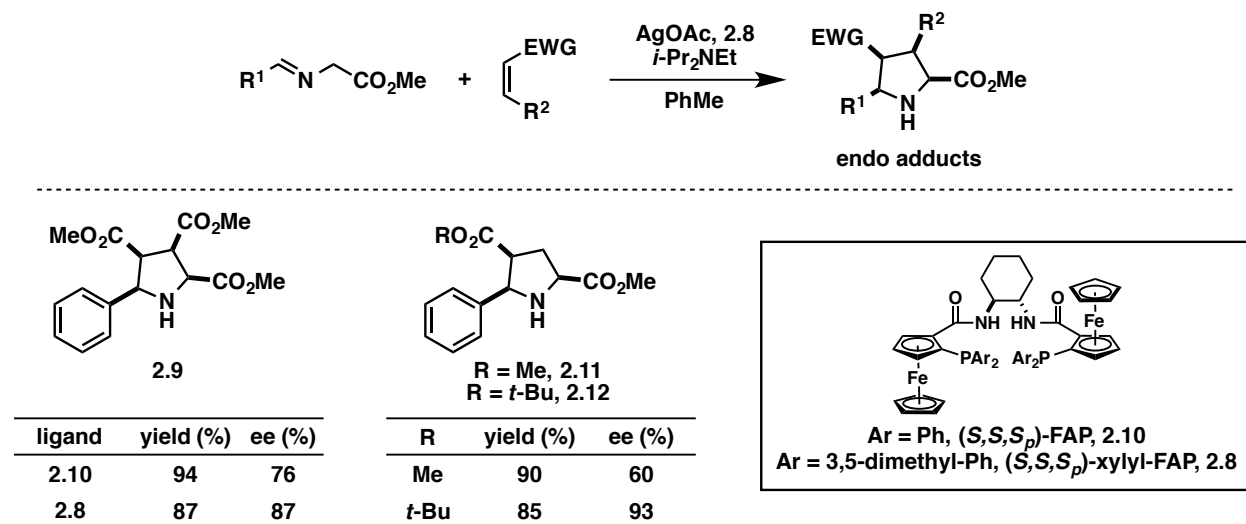


Figure 2.4. Zhang's Ag(I)/xylyl-FAP-Catalyzed Synthesis of Enantioenriched Pyrrolidines

Alternatively, the Jørgensen group reported decreased optical purity of pyrrolidines accessed from acrylates by increasing steric bulk.⁸ Using a Zn(II)/*t*-Bu-bisoxazoline (*t*-Bu-BOX) catalyst, endo pyrrolidine adducts were diastereoselectively synthesized from *N*-arylglycines and acrylates or dimethyl fumarate (Figure 2.5A). The authors proposed a transition state model to explain both the diastereoselectivity and enantioselectivity trends observed in their experiments (Figure 2.5B). This model conforms to the hypothesis where the carbonyl group of the α,β -unsaturated dipolarophile occupies a coordination site on the metal, thereby activating the dipolarophile for the subsequent cycloaddition step. This model also rationalizes the effect of the acrylate bulkiness on yield and enantioenrichment of the corresponding pyrrolidine product (Figure 2.5C). Pyrrolidine **2.13** was synthesized from methyl acrylate in 93% yield with 78% ee. Using ethyl acrylate to access product **2.14**, however, resulted in a lower yield of 76% and a 10% drop in ee. Finally, cycloadduct **2.15** was formed in only 12% yield with enantioenrichment of <5%. The authors rationalize the proposed stabilized endo transition state by observing that *sp*² hybridization of the dipolarophile vinyl carbon is important in achieving high endo selectivity.¹⁰ Although not supported by X-ray crystal structure analysis or theoretical calculations, the hypothesized endo transition state depicted in Jørgesen's report inspired the development of more selective 1,3-DCs using α,β -unsaturated carbonyl compounds as dipolarophiles.

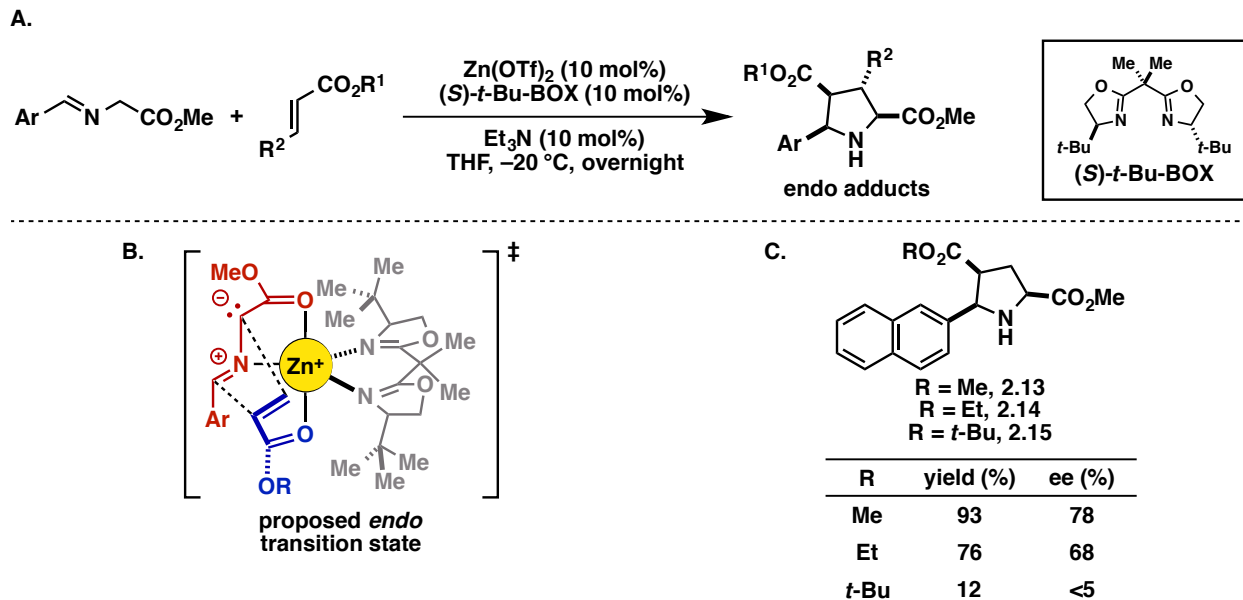


Figure 2.5. Jørgensen's Zn(II)/*t*-Bu-BOX Catalyst System

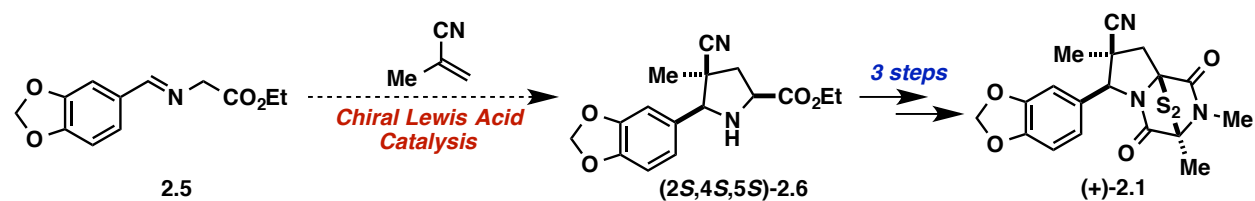
With an aim to develop a more available catalyst system for the asymmetric synthesis of pyrrolidine derivatives,¹¹ Schreiber and coworkers published a report in 2003 describing a Ag(I)/QUINAP¹² catalyst system.¹³ This new catalyst proved to be highly reactive, as pyrrolidine products were synthesized from aryl imines and *tert*-butyl acrylate using only 3 mol % catalyst at -45°C . Yields were typically high (89–95%) and up to 96% ee was reported. Notably, Schreiber's catalytic system allowed for the first synthesis of enantioenriched pyrrolidine products bearing a quaternary center at the C2 position, although higher reaction temperature and catalyst loading were required for this to be accomplished.

Currently, the catalytic asymmetric 1,3-DC literature utilizing azomethine ylides is dominated by the use of α,β -unsaturated carbonyl compounds as dipolarophiles and the pyrrolidine products formed are derived from the endo transition state in the majority of cases. A variety of different chiral Lewis acid complexes have been described to access optically active pyrrolidine products using salts of Ag(I),¹⁴ Cu(I),¹⁵ Cu(II),¹⁶ Au(I),^{17,18} Zn(II),^{8,19} Ni(II),²⁰ or Ca(II).²¹ Asymmetric organocatalytic methods have also been reported.^{3c,22} Many reports access

exo pyrrolidine adducts from α,β -unsaturated carbonyl dipolarophiles using Cu(I)^{15a,c,d,g,i,j,l,n,p,u} and Cu(II)^{16a,d–f,j,k} salts while others have found success using bulky ligands on Ag(I) such as TF-BIPHAMPPhos,^{14v} DTBM-SEGPHOS,^{14w,x,ai;15y,16e} and atropisomeric amides.^{14ak} However, far fewer examples exist of 1,3-DC reactions between azomethine ylides and α,β -unsaturated nitrile dipolarophiles.

The Overman lab aspires to selectively synthesize ETP (+)-**2.1** in large quantities in order to pursue more detailed biological studies. This goal can be quickly accomplished though elaboration of enantiopure pyrrolidine (2*S*,4*S*,5*S*)-**2.6** (Scheme 2.1). We wish to develop a diastereo- and enantioselective 1,3-DC between imine **2.5** and methacrylonitrile using chiral Lewis acid catalysis. The deficiency of reports describing the use and behavior of α,β -unsaturated nitrile dipolarophiles in catalytic asymmetric 1,3-DC reactions presents us with the opportunity to explore and better understand the reactivity of this underrepresented class of dipolarophile in catalytic asymmetric 1,3-DC reactions.

Scheme 2.1. Key Reaction to Develop a Highly Selective Synthesis of ETP (+)-2.1



2.2.1 Ag(I)-Catalyzed 1,3-DC Reactions

Because Ag(I) salts are commonly used in catalytic asymmetric 1,3-DC reactions, initial efforts were focused on utilizing the conditions developed by Schreiber.¹³ Thus, using 3 mol % Ag(I)/(*R*)-QUINAP catalyst, 1,3-DC between imine **2.5** and methacrylonitrile was attempted; however, no reaction proceeded under the precedented conditions (Table 2.1, entry 1). Reaction temperature (entry 2), catalyst loading (entries 3–9), superstoichiometric Lewis acid

(entries 10–14), solvent (entries 3–6), and organic base (entries 7, 10–14) were varied in order to accomplish the desired transformation. However, all attempts were met without success; unreacted starting material remained after each Ag(I)-catalyzed reaction tested. This indicated that the nitrile functionality of the dipolarophile might be poisoning the Ag(I) catalyst.

Table 2.1. Condition Screening for Ag(I)-Catalyzed 1,3-DC using Methacrylonitrile

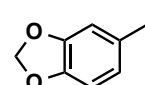
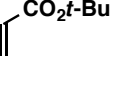
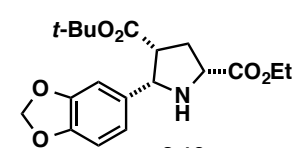
entry	catalyst (mol %)	base (mol %)	solvent	temp (°C)	time (h)	conversion (%) ^a	dr (endo:exo)
1	AgOAc/(R)-QUINAP (3)	<i>i</i> -Pr ₂ NEt (10)	THF	-45	20	0	-
2	AgOAc/(R)-QUINAP (3)	<i>i</i> -Pr ₂ NEt (10)	THF	0 to 23	16	0	-
3	AgOAc/(R)-QUINAP (5)	<i>i</i> -Pr ₂ NEt (17)	THF	-45	20	0	-
4	AgOAc/(R)-QUINAP (5)	<i>i</i> -Pr ₂ NEt (17)	PhMe	-45	20	0	-
5	AgOAc/(R)-QUINAP (5)	<i>i</i> -Pr ₂ NEt (17)	CH ₂ Cl ₂	-45	20	0	-
6	AgOAc/(R)-QUINAP (5)	<i>i</i> -Pr ₂ NEt (17)	Et ₂ O	-45	20	0	-
7	AgOAc/(S)-QUINAP (5)	Et ₃ N (17)	THF	-45	20	0	-
8	AgOAc/(S)-QUINAP (5)	-	THF	-45	20	0	-
9	AgOAc/(R)-QUINAP (20)	<i>i</i> -Pr ₂ NEt (50)	THF	-45	20	0	-
10	LiBr (120)	Et ₃ N (120)	THF	-45	20	33	71:29
11	LiBr (120)	Et ₃ N (120)	THF	0 to 23	16	80	80:20
12	LiBr (120)	<i>i</i> -Pr ₂ NEt (120)	THF	0 to 23	16	25	75:25
13	AgOAc (120)	<i>i</i> -Pr ₂ NEt (120)	THF	0 to 23	16	0	-
14	AgOAc (120)	Et ₃ N (120)	THF	0 to 23	16	0	-

^aConversion of starting material to product determined by relative integration in ¹H NMR spectrum of the crude reaction mixture.

A set of competition experiments was designed in order to test whether the nitrile functionality of the dipolarophile was inhibiting the reactivity of the Ag(I)/QUINAP catalyst (Table 2.2). As the reaction between imine **2.5** and *tert*-butyl acrylate succeeded in 32% yield with exclusive formation of endo pyrrolidine adduct **2.16** (90% ee, entry 1),²³ this cycloaddition reaction was run with the inclusion of a nitrile-containing additive. Methacrylonitrile,

acetonitrile, and isobutyronitrile were chosen as the three additives, allowing the effect of both the nitrile functionality and steric hindrance on catalyst activity to be determined. No desired reactivity was observed with the inclusion of methacrylonitrile (entry 2). The addition of acetonitrile allowed for 5% pyrrolidine **2.16** to be formed, as determined by ¹H NMR (entry 3). Finally, the use of isobutyronitrile resulted in a 19% ¹H NMR yield of desired product **2.16** (entry 4).

Table 2.2. Competition Experiments to Test Nitrile–Ag(I) Compatibility

2.5	 + 	additive (1.5 equiv) AgOAc/(R)-QUINAP (3 mol %) <i>i</i> -Pr ₂ NEt (10 mol %) THF, -45 °C, 20 h		
		(1.5 equiv)		
1	none		32	90
2	methacrylonitrile		0	—
3	acetonitrile		5	nd
4	isobutyronitrile ^c		19	nd

^aYield determined by ¹H NMR using DMF as an external standard. ^bDetermined by enantioselective HPLC.

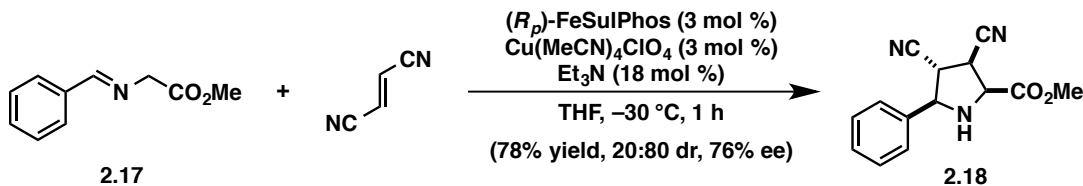
^cReaction run using (S)-QUINAP. nd = not determined.

Collectively, the results of the competition experiments indicate that the nitrile functionality is interfering with the desired 1,3-DC reactivity and that dipolarophile sterics as well as conjugation are important factors in poisoning the silver catalyst. These results are consistent with a study by the Kühn group, who tested the effect of metal–nitrile bond strengths on the activity of a cyclopropanation catalyst with MeCN ligands.²⁴ Kühn’s results indicated that the strong MeCN–Ag bond²⁵ inhibited reactivity while the weaker MeCN–Cu bond allowed Cu(I) complexes to be catalytically active. Thus, the focus of the reaction development was shifted to investigate the effectiveness of Cu(I) catalysts in the desired transformation.

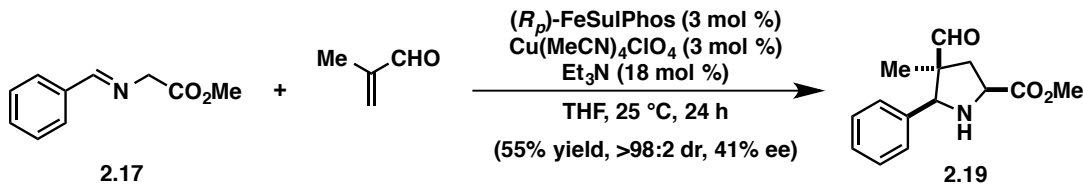
2.2.2 Cu(I)-Catalyzed 1,3-DC Reactions

Carretero and coworkers accomplished asymmetric 1,3-DCs with fumaronitrile to form nitrile-containing pyrrolidines using $\text{Cu}(\text{MeCN})_4\text{ClO}_4$ and enantiopure FeSulPhos ligands.^{15b,e;26} Although the reaction of imine **2.17** with fumaronitrile preferentially formed exo pyrrolidine adduct **2.18** in 78% yield, 20:80 dr (endo:exo), and 76% ee (eq 2.3), Carretero showed that reaction of imine **2.17** with methacrolein selectively afforded endo adduct **2.19** in 55% yield and >98:2 dr (eq 2.4). Encouraged by Carretero's results using a nitrile-containing dipolarophile and separately an α -substituted dipolarophile, the Cu(I)/(*R*_p)-FeSulPhos-catalyzed²⁷ 1,3-DC between imine **2.5** and methacrylonitrile was studied.

Equation 2.3



Equation 2.4



The Cu(I)/(*R*_p)-FeSulPhos-catalyzed 1,3-DC between imine **2.5** and methacrylonitrile resulted in the formation of the minor endo cycloadduct **2.6** in a 18:82 dr and 50% ee (eq 2.5). Based on conversion and diastereoselectivity of the 1,3-DC using 10 mol % Cu(I)/(*R*_p)-FeSulPhos catalyst, toluene (PhMe) was chosen as the solvent to be used in subsequent reactions (Table 2.3).

Equation 2.5

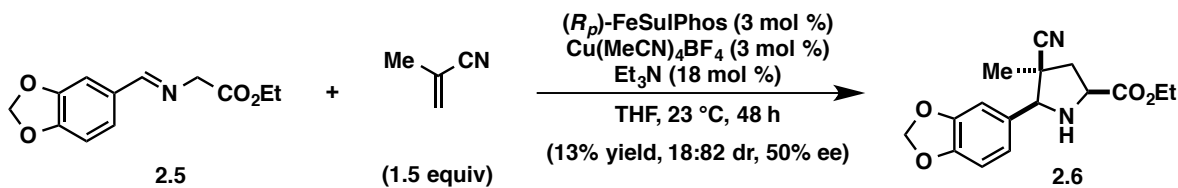


Table 2.3. Investigation of Solvent to Selectively Access Pyrrolidine 2.6

entry	solvent	conversion (%) ^a	dr (endo:exo)
1	THF	>95	17:83
2	DME	>95	17:83
3	Et ₂ O	95	21:79
4	CH ₂ Cl ₂	94	14:86
5	PhMe	>95	29:71
6	PhH	89	33:67
7	MeOH	>95	28:72
8	MeCN	0	—
9	DMF	0	—

^aConversion of starting material to product determined by relative integration in ¹H NMR spectrum of the crude reaction mixture.

2.3 Investigation of Ligand Types

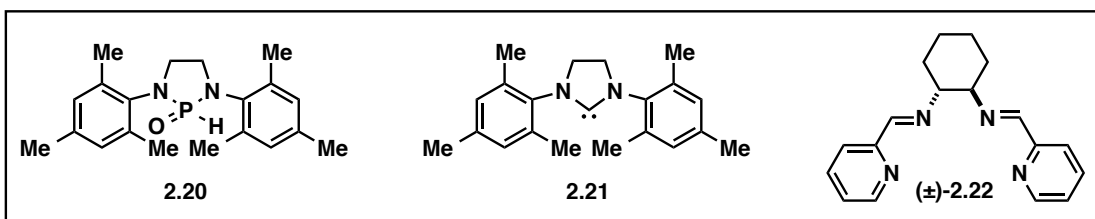
A variety of different ligand types was investigated in order to identify a catalyst that exhibits the desired endo adduct selectivity in the 1,3-DC between imine **2.5** and methacrylonitrile (Table 2.4). Using a catalyst loading of 10 mol % and PhMe as the solvent, the 1,3-DC catalyzed by Cu(I)/(*R*_p)-FeSulPhos resulted in a 29:71 dr and a 38% ee of the endo pyrrolidine adduct **2.6** (entry 1). *P,N*-ligands (*S*)-QUINAP and 2-dicyclohexylphosphino-2'-(*N,N*-dimethylamino)biphenyl (DavePhos) were also tested. These reactions offered low-to-no conversion to product and no diastereoselectivity (entries 2 and 3). Heteroatom-substituted

phosphine oxide (HASPO) ligand **2.20** and *N*-heterocyclic carbene (NHC) **2.21** were also examined in the 1,3-DC, both of which resulted in low conversion (entries 4 and 5).

Table 2.4. *P,S-*, *P,N-*, HASPO, NHC, and Pyridine-Based Ligands

entry	ligand (mol %)	conversion (%) ^a	dr (endo:exo)	ee _{endo} (%) ^b
1	(<i>R_p</i>)-FeSulPhos (10)	>95	29:71	38
2	(<i>S</i>)-QUINAP (10)	0	—	nd
3	DavePhos (10)	57	50:50	—
4	HASPO 2.20 (20)	33	70:30	—
5	NHC 2.21 (20) ^c	31	60:40	—
6	bpy (10)	0	—	—
7	1,10-phenanthroline (10)	5	nd	—
8	(+)-PyBOX (10)	<5	nd	nd
9	(±)-2.22 (10)	22	74:26	—

^aConversion of starting material to product determined by relative integration in ¹H NMR spectrum of the crude reaction mixture. ^bDetermined by enantioselective HPLC. ^cTHF was used as the reaction solvent. nd = not determined.



N,N'-Bidentate ligands are common in copper catalysis;²⁸ thus, the efficacy of select bipyridyl, bisoxazoline (BOX),²⁹ and diimine ligands were explored (Table 2.4). 2,2'-Bipyridyl (bpy), 1,10-phenanthroline, and (+)-PyBOX were ineffective ligands for the Cu(I)-catalyzed 1,3-DC, resulting in <5% conversion to desired product **2.6** (entries 6–8). The reaction run using racemic diimine ligand **2.22**³⁰ resulted in preferential formation of the endo cycloadduct (74:26 dr), but proceeded with a low 22% conversion (entry 9). As a result of the low reactivity

of pyridine-type ligands in the target reaction, the implementation of phosphorus-based ligands was studied next.

The effectiveness of chiral phosphoric acids as ligands was also explored (Table 2.5).³¹

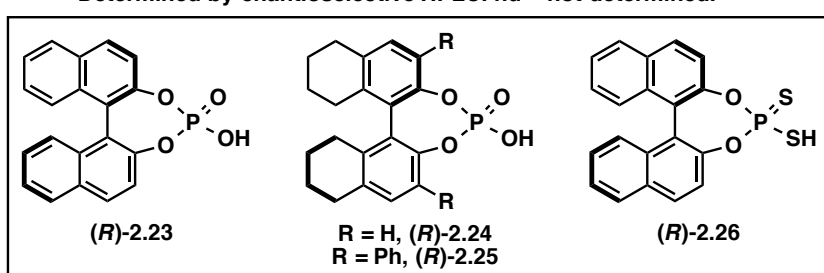
While reactions employing ligands *(R)*-**2.23**–*(R)*-**2.25** were selective for the endo adduct (ca. 85:15 dr), overall reactivity and resulting ee of product **2.6** were low (entries 1–3). Using dithiophosphoric acid ligand *(R)*-**2.26** resulted in no desired reactivity (entry 4). Thus, the reactivity of ligand classes other than chiral phosphoric acids was further explored.

Table 2.5. Chiral Phosphoric Acid Ligands

entry	ligand	conversion (%) ^a	dr (endo:exo)	ee _{endo} (%) ^b
1	<i>(R)</i> - 2.23	33	86:14	0
2	<i>(R)</i> - 2.24	49	84:16	2
3	<i>(R)</i> - 2.25	51	87:13	0
4	<i>(R)</i> - 2.26	<5	nd	nd

^aConversion of starting material to product determined by relative integration in ¹H NMR spectrum of the crude reaction mixture.

^bDetermined by enantioselective HPLC. nd = not determined.



2.3.1 Phosphoramidite Ligands

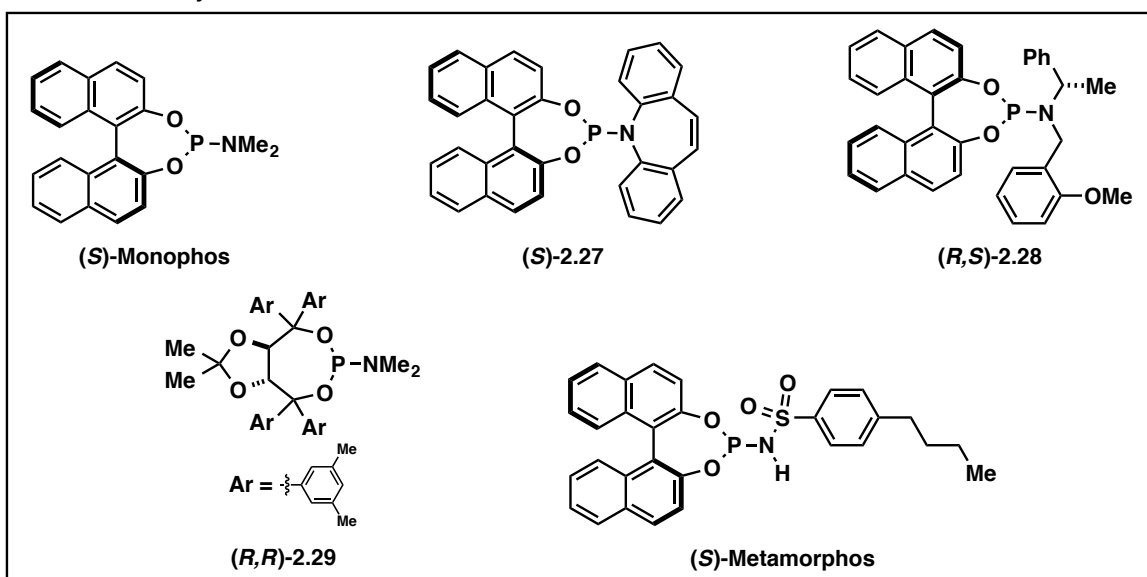
Phosphoramidites are privileged ligands in asymmetric catalysis.³² Their synthesis is robust and many research groups have accessed large libraries of chiral non-racemic phosphoramidite ligands.³³ Five phosphoramidite ligands were initially used in the Cu(I)-

catalyzed 1,3-DC reaction between imine **2.5** and methacrylonitrile (Table 2.6). Reactions run using BINOL-derived ligands (*S*)-Monophos,³⁴ (*S*)-**2.27**, and (*R,S*)-**2.28**³⁵ resulted in a non-selective mixture of endo and exo cycloadducts (ca. 62:38 dr) with 37–90% conversion and 22–43% ee of desired endo adduct **2.6** (entries 1–3). Using TADDOL-derived ligand^{36,37} (*R,R*)-**2.29** resulted in no desired product (entry 4) and (*S*)-Metamorphos³⁵ proved to be an equally ineffective ligand (entry 5). In order to increase catalyst solubility and generalize the further use of phosphoramidite ligands, the reaction solvent was changed to THF.

Table 2.6. Phosphoramidite Ligands Used with PhMe as the Reaction Solvent

entry	ligand (mol %)	conversion (%) ^a	dr (endo:exo)	ee _{endo} (%) ^b
1	(<i>S</i>)-Monophos	90	64:36	36
2	(<i>S</i>)- 2.27	37	62:38	22
3	(<i>R,S</i>)- 2.28	72	62:38	43
4	(<i>R,R</i>)- 2.29	0	—	—
5	(<i>S</i>)-Metamorphos	<5%	nd	nd

^aConversion of starting material to product determined by relative integration in ¹H NMR spectrum of the crude reaction mixture. ^bDetermined by enantioselective HPLC. nd = not determined.

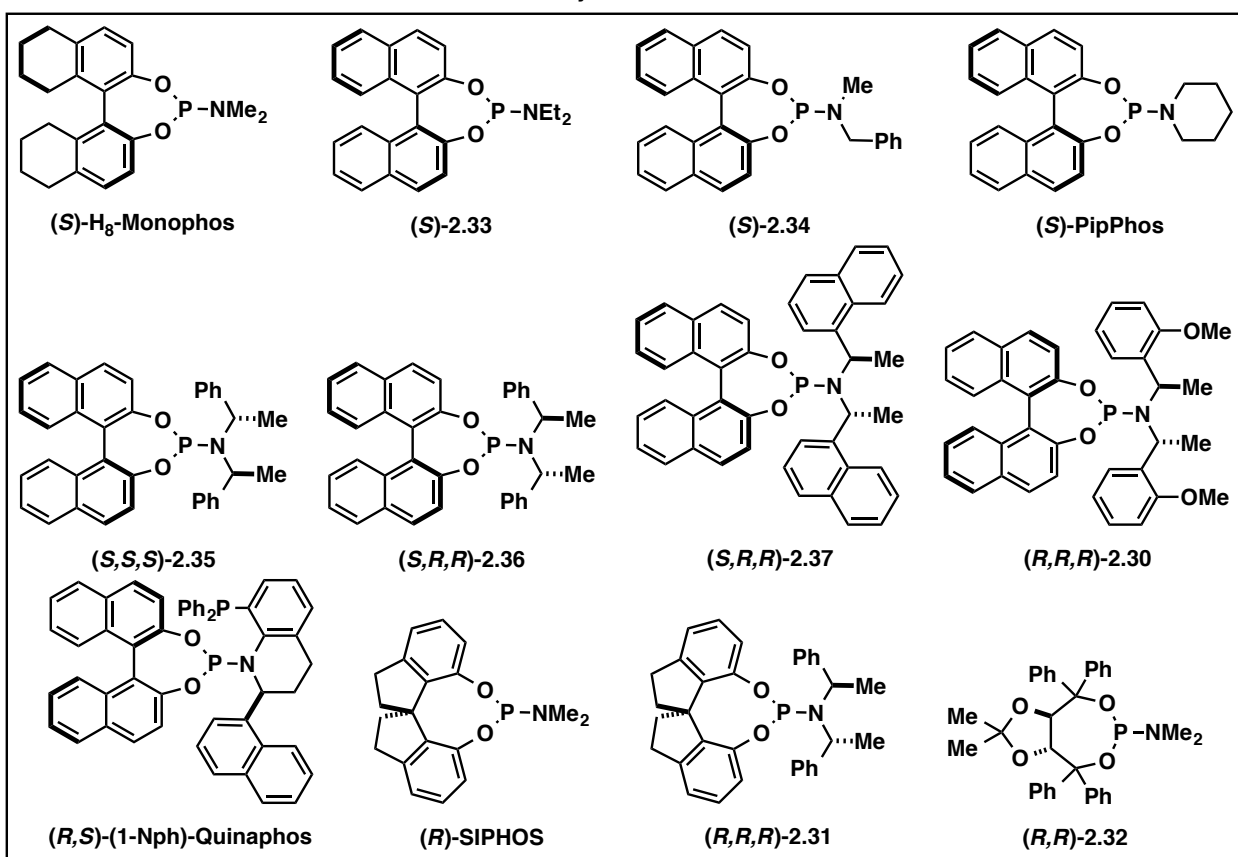


After modifying the reaction between imine **2.5** and methacrylonitrile to run for 6 h in THF, a library of phosphoramidite ligands was tested (Table 2.7). Reactions performed using BINOL-achiral amine ligands resulted in poor diastereo- and enantioselectivity for endo adduct **2.6** (entries 1–4). The implementation of BINOL-chiral amine ligands resulted in reactions that were overall more selective for the exo cycloadduct (entries 5–8), yet pyrrolidine **2.6** was accessed with 58% ee when ligand (*R,R,R*)-**2.30** was used (entry 8). The highest ee was achieved when (*R,S*)-(1-Nph)-Quinaphos was used as the ligand (72% ee); however, this reaction was highly selective for the undesired exo cycloadduct (10:90 dr, entry 9). When the (*R*)-SIPHOS³⁸ ligand was used, product **2.6** was accessed with 26% ee but the reaction was not selective (49:51 dr, entry 10). The use of ligand (*R,R,R*)-**2.31** eroded the ee to 0% and the reaction favored the formation of the exo cycloadduct (29:71 dr, entry 11). Finally, when TADDOL-dimethylamine phosphoramidite (*R,R*)-**2.32** was used as the ligand, the reaction was not diastereoselective (45:55 dr), but endo adduct **2.6** was synthesized with 38% ee (entry 12). Although the reaction run using the Cu(I)/(*R,S*)-(1-Nph)-Quinaphos catalyst afforded desired product **2.6** in the highest ee, the diastereoselectivity was undesired. As a result, other ligand types were investigated using the new reaction conditions in THF.

Table 2.7. Phosphoramidite Ligands Used with THF as the Reaction Solvent

 2.5	 (1.5 equiv)	ligand (10 or 20 mol %) $\text{Cu}(\text{MeCN})_4\text{BF}_4$ (10 mol %) Et ₃ N (60 mol %) THF, 23 °C, 6 h	 2.6
entry	ligand (mol %)	conversion (%) ^a	dr (endo:exo)
1	(S)-H ₈ -Monophos (20)	74	35:65
2	(S)-2.33 (20)	28	45:55
3	(S)-2.34 (20)	36	50:50
4	(S)-PipPhos (20)	11	50:50
5	(S,S,S)-2.35 (20)	95	22:78
6	(S,R,R)-2.36 (20)	57	49:51
7	(S,R,R)-2.37 (20)	98	27:73
8	(R,R,R)-2.30 (20)	95	26:74
9	(R,S)-(1-Nph)-Quinaphos (10)	96	10:90
10	(R)-SIPHOS (20)	97	49:51
11	(R,R,R)-2.31 (20)	98	29:71
12	(R,R)-2.32 (20)	70	45:55
			<i>ee</i> _{endo} (%) ^b
			8
			nd
			29
			nd
			8
			4
			2
			58
			72
			26
			0
			38

^aConversion of starting material to product determined by relative integration in ¹H NMR spectrum of the crude reaction mixture. ^bDetermined by enantioselective HPLC. nd = not determined.



2.3.2 Phosphine Ligands

Monodentate phosphines were next explored as ligands in the desired 1,3-DC reaction (Table 2.8). The use of triphenylphosphine as the ligand resulted in a low conversion to pyrrolidine products and a nonselective 58:42 dr (entry 1). A trend was observed when using fluorine-substituted ligands tris(*p*-fluorophenyl)phosphine and tris(pentafluorophenyl)phosphine. Conversions increased to over 90% and the diastereoselectivity of the reaction favored endo adduct **2.6** with increasing fluorine substitution on the ligand (entries 2 and 3). Three phosphines with substitution at the *ortho* position were also examined (entries 10–12). Ligands tri(*o*-tolyl)phosphine (entry 4) and tri(2-furyl)phosphine (entry 5) resulted in a 1,3-DC that proceeded in 52% and 68% conversion to product and 75:25 and 50:50 dr, respectively. The reaction run using (2-cyanophenyl)diphenylphosphine as the ligand proceeded with a low 29% conversion yet favored endo adduct **2.6** in a 79:21 dr (entry 6). Interestingly, the use of electron-rich tricyclohexylphosphine as the ligand favored the exo pyrrolidine adduct in an 18:82 dr with a 98% conversion to product (entry 7). Finally, the reaction catalyzed by a Cu(I)/tris(hydroxymethyl)phosphine resulted in no desired reactivity (entry 8). This set of experiments revealed an interesting trend between ligand electronic effects and the diastereoselectivity of the 1,3-DC reaction. In order to further investigate this breakthrough observation, achiral and chiral polydentate phosphines were tested.

Table 2.8. Achiral Monodentate Phosphines

entry	ligand	conversion (%) ^a	dr (endo:exo)
1	triphenylphosphine	12	58:42
2	tris(<i>p</i> -fluorophenyl)phosphine	97	63:37
3	tris(pentafluorophenyl)phosphine	94	80:20
4	tri(<i>o</i> -tolyl)phosphine	52	75:25
5	tri(2-furyl)phosphine	68	50:50
6	(2-cyanophenyl)diphenylphosphine	29	79:21
7	tricyclohexylphosphine	98	18:82
8	tris(hydroxymethyl)phosphine	0	—

^aConversion of starting material to product determined by relative integration in ¹H NMR spectrum of the crude reaction mixture.

The selectivity trends of achiral polydentate phosphines in the targeted 1,3-DC were next explored (Table 2.9). The Cu(I)/1,2-bis(diphenylphosphino)ethane (dppe) complex catalyzed an endo adduct-selective 1,3-DC (entry 1). The use of the more electron-deficient variant 1,2-bis[bis(pentafluorophenyl)phosphino]ethane (dfppe) as the ligand resulted in a slower reaction and offered no improved endo selectivity (entry 2), unlike the trend observed with achiral monodentate phosphines. 1,3-Bis(diphenylphosphino)propane (dppp), whose extra methylene unit increased the bite angle to 91° (dppe = 85°), resulted in an erosion of endo selectivity (compare entries 1 and 3). Further increasing the bite angle of the ligand to 97° resulted in a dramatic loss of catalytic activity, as the reaction using a Cu(I)/1,4-bis(diphenylphosphino)butane (dppb) catalyst resulted in almost complete recovery of starting material (entry 4). The use of either 1,2-bis(diphenylphosphino)benzene (dppbz) or 1,1'-bis(diphenylphosphino)ferrocene (dppf) as the ligand resulted in low reactivity and endo selectivities near 70:30 dr (entries 5 and 6). As the bite angles of dppbz and dppf are 83° and 96°,

respectively, these studies do not indicate a trend relating diphosphine bite angle and reaction selectivity (entries 1–6).³⁹ DPEPhos and NIXANTPHOS were ineffective ligands to catalyze the reaction (entry 7 and 8), and XANTPHOS⁴⁰ and *t*-Bu-XANTPHOS promoted the desired transformation to only 26% and 48% conversion, respectively, after 24 h (entries 9 and 10).

Table 2.9. Achiral Bidentate Phosphine Ligands

2.e	(1.5 equiv)	ligand (10 mol %) $\text{Cu}(\text{MeCN})_4\text{BF}_4$ (10 mol %) Et ₃ N (60 mol %) PhMe, 23 °C, 24 h	2.f
entry	ligand	conversion (%) ^a	dr (endo:exo)
1	dppe	92	81:19
2	dpppe	40	79:21
3	dppp	94	68:32
4	dppb	<5	nd
5	dppbz	40	66:34
6	dppf	8	71:29
7	DPEPhos	0	—
8	NIXANTPHOS	0	—
9	XANTPHOS	26	69:31
10	<i>t</i> -Bu-XANTPHOS	48	48:52

^aConversion of starting material to product determined by relative integration in ¹H NMR spectrum of the crude reaction mixture. nd = not determined.

Bis(diphenylphosphine) ligands of various chain lengths and two tridentate phosphines were tested in THF (Table 2.10). Reactions that used dppe, dppp, and dppb as ligands resulted in high conversion to product and high endo selectivity (ca. 95% conversion and 85:15 dr, entries 1–3). Reactivity and endo selectivity were increased in the cases of dppp and dppb compared to the same reaction run in PhMe for 24 h (see Table 2.9, entries 3 and 4). Endo selectivity was lower for reactions using either 1,5-bis(diphenyl-phosphino)pentane (dpppe) or 1,6-bis(diphenylphosphino)hexane as the ligand (67:33 dr, entries 4 and 5). The diastereoselectivity was reversed when using either bis(2-diphenylphosphinoethyl)phenylphosphine (90:10 dr,

entry 6) or 1,1,1-tris(diphenylphosphinomethyl)ethane (8:92 dr, entry 7), although the nature of this switch is not well understood at this time. This set of experiments demonstrates the effectiveness of select achiral polydentate phosphine ligands to diastereoselectively access endo pyrrolidine adduct **2.6** in high conversion, although no clear trend relating structure and selectivity could be established.

Table 2.10. Achiral Polydentate Phosphine Ligands in THF

entry	ligand (mol %)	conversion (%) ^a	dr (endo:exo)
1	dppe	93	84:16
2	dppp	96	87:13
3	dppb	95	82:18
4	dpppe	96	67:33
5	1,6-bis(diphenylphosphino)hexane	94	67:33
6	bis(2-diphenylphosphinoethyl)phenylphosphine	97	90:10
7	1,1,1-tris(diphenylphosphinomethyl)ethane	95	8:92

^aConversion of starting material to product determined by relative integration in ¹H NMR spectrum of the crude reaction mixture.

The ability of chiral bisphosphine ligands to induce enantioselection in the Cu(I)-catalyzed 1,3-DC reaction was investigated next (Table 2.11). The reaction utilizing chiral ferrocenyldiphosphine Josiphos ligand⁴¹ SL-J002-2 resulted in a 61% conversion to product, poor diastereoselectivity (42:58 dr), and a low 7% enantioenrichment of the desired endo adduct **2.6** (entry 1). While the use of ligand (*S,S*)-DIOP^{42,43} in the reaction allowed for high conversion to the desired pyrrolidine products, the endo adduct diastereo- and enantioselectivities were low (entry 2). The use of (*R,R*)-Me-DUPHOS⁴⁴ resulted in lower reactivity and no diastereoselectivity; however the ee of the endo pyrrolidine adduct was increased to 44% (entry 3). The 1,3-DC reaction using (*S,S*)-DACH-phenyl Trost ligand⁴⁵ resulted in a 69:31 dr

and 50% ee of endo cycloadduct **2.6**. Cu(I)/(*S*)-BINAP^{46,47} or Cu(I)/(*S*)-TolBINAP⁴⁸ complexes possessed high reactivity but favored the exo pyrrolidine cycloadduct in 26:74 or 30:70 dr, respectively (entries 5 and 6).

Table 2.11. Chiral Diphosphine Ligands Tested in the Cu(I)-Catalyzed 1,3-DC

entry	ligand	conversion (%) ^a	dr (endo:exo)	ee _{endo} (%) ^b
1	SL-J002-2	61	42:58	7
2	(<i>S,S</i>)-DIOP	92	40:60	25
3	(<i>R,R</i>)-Me-DUPHOS	37	60:40	44
4	(<i>S,S</i>)-DACH-phenyl	39	69:31	50
5	(<i>S</i>)-BINAP	93	26:74	42
6	(<i>R</i>)-TolBINAP	95	30:70	32
7	BIPHEP	96	34:66	–
8	(<i>R</i>)-MeOBIPHEP	94	27:73	6
9	(<i>R</i>)-3,5- <i>i</i> -Pr-MeOBIPHEP	83	11:89	36
10	(<i>R</i>)-3,5-xyl-MeOBIPHEP	22	73:27	2
11	(<i>R</i>)-SEGPHOS	9	32:68	nd
12	(<i>R</i>)-DIFLUOROPHOS	91	40:60	14

^aConversion of starting material to product determined by relative integration in ¹H NMR spectrum of the crude reaction mixture. ^bDetermined by enantioselective HPLC. nd = not determined.

Substitution effects were examined using achiral BIPHEP⁴⁹ and three chiral MeOBIPHEP ligands⁵⁰ (Table 2.11, entries 7–10). Initially, it seemed that exo adduct selectivity improved with increasing bulkiness of the MeOBIPHEP ligand; however, the reaction catalyzed by the Cu(I)/(*R*)-3,5-xyl-MeOBIPHEP complex favored the endo adduct in a 73:27 dr, but with little enantioinduction (2% ee, entry 10). Finally, the effects of SEGPHOS⁵¹ and DPEPhos⁵² ligands were tested. While the introduction of difluoromethylene groups in (*R*)-DIFLUOROPHOS⁵³ increased the reactivity compared to using (*R*)-SEGPHOS, the

diastereoselectivity of the two reactions were similar, despite the difference in their electronic properties (entries 11 and 12). Of the polydentate phosphine ligands used, bis(2-diphenylphosphinoethyl)phenylphosphine resulted in the highest endo adduct selectivity (90:10 dr, Table 2.10, entry 6). The highest ee of endo adduct **2.6**, 44%, was achieved using (*R,R*)-Me-DUPHOS as the ligand on Cu(I), yet the overall reaction lacked diastereoselectivity (Table 2.11, entry 3).

In summary, an interesting trend was discovered when achiral phosphine ligands were tested in the Cu(I)-catalyzed 1,3-DC reaction. Endo adduct selectivity increased with increased fluorine substitution on the triphenylphosphine backbone. It was also shown that electron-rich, bulky ligands like tricyclohexylphosphine were highly selective for the exo cycloadduct. Because no additional trends were recognized with the other phosphine ligands tested, phosphite ligands were chosen as the next ligand class to investigate.

2.3.3 Phosphite Ligands

Phosphite ligands are good π -acceptor ligands, which gives them a unique electron-withdrawing property that is not shared with phosphines.⁵⁴ High endo adduct selectivity was discovered while testing achiral monodentate phosphite ligands in the desired Cu(I)-catalyzed 1,3-DC reaction (Table 2.12). Using triphenyl phosphite as the ligand, pyrrolidine **2.6** was synthesized in 91% conversion with a 94:6 dr (entry 1). The use of either tris(2,4-di-*tert*-butylphenyl) phosphite or trimethyl phosphite resulted in slight erosion of endo selectivity to approximately 75:25 dr (entries 2 and 3). Dimethyl phosphite, a ligand which contains a P=O and P–H bond, did not allow for the desired transformation to occur (entry 4). Interestingly, the diastereoselectivity of the reaction was reversed to a 26:74 dr when the triisopropyl phosphite ligand was employed (entry 5). The highest endo adduct selectivity was achieved by using

tris(2,2,2-trifluoroethyl) phosphite as a monodentate ligand, where cycloadduct **2.6** was selectively synthesized in a >94:6 dr and 94% conversion (entry 6).

Table 2.12. Achiral Phosphite Ligands Used in the Cu(I)-Catalyzed 1,3-DC

entry	ligand (mol %)	conversion (%) ^a	dr (endo:exo)
1	triphenyl phosphite	91	94:6
2	tris(2,4-di- <i>tert</i> -butylphenyl) phosphite	94	75:25
3	trimethyl phosphite	83	76:24
4	dimethyl phosphite	0	—
5	triisopropyl phosphite	36	26:74
6	tris(2,2,2-trifluoroethyl) phosphite	94	>94:6

^aConversion of starting material to product determined by relative integration in ¹H NMR spectrum of the crude reaction mixture.

Achiral monodentate phosphite ligands were reexamined in the 1,3-DC between imine **2.5** and methacrylonitrile using THF instead of PhMe as the solvent and a reaction time of 6 h (Table 2.13). The endo adduct selectivities of reactions run using triphenyl phosphite, trimethyl phosphite, and tris(2,2,2-trifluoroethyl) phosphite were lower than those reactions run using the previous reaction conditions (compare Table 2.13, entries 1–3 to Table 2.12, entries 1, 3, and 6). Interestingly, the reaction run using triethyl phosphite as the ligand proceeded much more slowly and with a reversal of diastereoselectivity when compared to the same reaction run using electron-deficient tris(2,2,2-trifluoroethyl) phosphite (Table 2.13, compare entries 3 and 4). These experiments also indicate an important correlation between the electronic properties of the ligand and the resulting 1,3-DC reaction diastereoselectivity (see Table 2.8, entries 1–3). As a result of the observed drop in endo adduct selectivity for reactions run in THF, further studies were made with phosphite ligands using PhMe as the solvent.

Table 2.13. Achiral Monodentate Phosphite Ligands Run in THF

entry	ligand (mol %)	conversion (%) ^a	dr (endo:exo)
1	triphenyl phosphite	93	71:29
2	trimethyl phosphite	74	48:52
3	tris(2,2,2-trifluoroethyl) phosphite	96	93:7
4	triethyl phosphite	34	35:65
5	tributyl phosphite	87	68:32

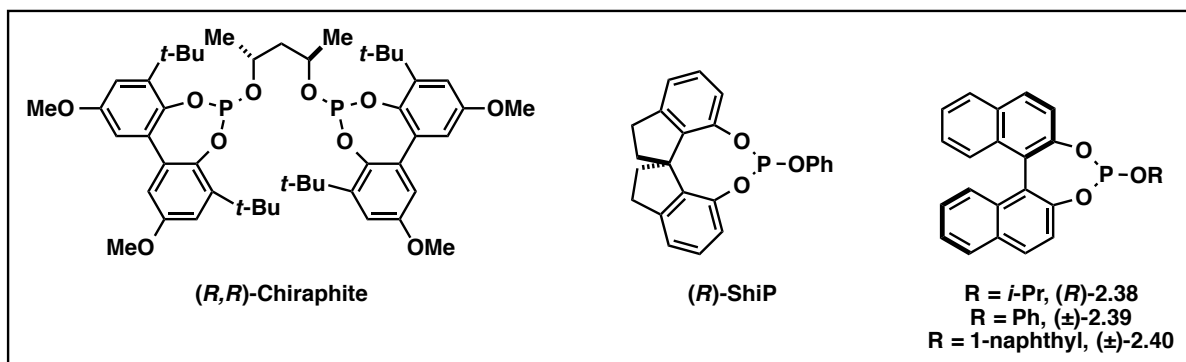
^aConversion of starting material to product determined by relative integration in ¹H NMR spectrum of the crude reaction mixture.

After demonstrating that phosphite ligands complexed with Cu(I) can be highly selective for the endo cycloadduct, three commercially available chiral phosphite ligands were chosen in order to investigate ee of pyrrolidine product **2.6** (Table 2.14). When using bulky bidentate (*R,R*)-Chiraphite, the reaction proceeded to only 50% conversion. Endo adduct **2.6** was formed selectively in a 78:22 dr, but without enantioenrichment (entry 1). SPINOL-derived^{55,56} ligand (*R*)-ShiP allowed for 21% ee to be accomplished (entry 2), but using BINOL-derived⁵⁷ (*R*)-**2.38** resulted in only 8% ee of endo adduct **2.6** (entry 3).

Table 2.14. Chiral and Racemic Phosphite Ligands

entry	ligand (mol %)	conversion (%) ^a	dr (endo:exo)	ee _{endo} (%) ^b
1	(R,R)-Chiraphite (10)	50	78:22	0
2	(R)-ShiP (20)	61	73:27	21
3	(R)-2.38 (20)	90	93:7	8
4	(±)-2.39 (20)	97	85:15	—
5	(±)-2.40 (20)	92	83:17	—

^aConversion of starting material to product determined by relative integration in ¹H NMR spectrum of the crude reaction mixture. ^bDetermined by enantioselective HPLC. nd = not determined.



Because of the low selection and high price of commercial chiral phosphite ligands, the synthesis of a library of ligands was attempted by following the procedure described by Laschat and coworkers.^{58,59} Purification of the desired phosphite ligands resulted in significant hydrolysis and only low yields of pure product were obtained, thus racemic BINOL was used in these early studies. Ligands **(±)-2.39** and **(±)-2.40** were successfully synthesized and used in the Cu(I)-catalyzed 1,3-DC reaction (Table 2.14, entries 4 and 5). While both reactions proceeded with >90% conversion and ca. 84:16 dr, attempts to prepare chiral phosphite ligands were suspended as a result of the difficulty of their synthesis and purification.

2.4 Conclusion

SAR studies have indicated the importance in accessing potent ETP analogue (+)-**2.1** in both a diastereo- and enantioselective manner. Over 75 ligands across a variety of ligand families were tested in our efforts to optimize the 1,3-DC step of the short ETP analogue synthesis. A positive correlation between the electron deficiency of the ligand and the 1,3-DC reaction endo adduct selectivity was observed. Achiral monodentate phosphite ligands have been identified as being able to accomplish the desired transformation with high endo adduct selectivity (>94:6 dr). This high selectivity may be attributed the π -accepting nature of this ligand class. Once chiral phosphite ligands are more readily accessible, an investigation of substitution pattern effects of chiral phosphite ligands on 1,3-DC reaction diastereo- and enantioselectivity will be initiated.

An interesting diastereodivergent trend was observed while investigating various ligand classes. We identified three ligands, each from a different class, which result in a different diastereomeric mixture of pyrrolidine products under otherwise identical reaction conditions (Table 2.15). This phenomenon is explained in further detail in Chapter 3.

Table 2.15. Ligand-Controlled Diastereodivergence

entry	ligand (mol %)	conversion (%) ^a	dr (endo:exo)
1	tris(2,2,2-trifluoroethyl) phosphite (20)	94	>94:6
2	tricyclohexylphosphine (20)	98	18:82
3	DavePhos (10)	57	50:50

^aConversion of starting material to product determined by relative integration in ¹H NMR spectrum of the crude reaction mixture.

2.5 Appendix A: Experimental Procedures

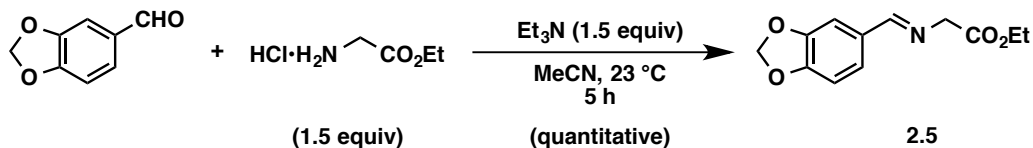
2.5.1 Materials and Methods

Unless stated otherwise, reactions were conducted in flame- or oven-dried glassware under a positive pressure of nitrogen (N₂) or argon (Ar) using anhydrous solvents (dried by passing through activated alumina columns under a positive pressure of Ar). Oxygen-sensitive reactions were carried out in solvents that were degassed by three freeze-pump-thaw cycles. Catalyst components and imine starting materials for the asymmetric 1,3-dipolar cycloaddition ligand screening reactions were weighed out in a MBraun Unilab 2000 glove box with a N₂ atmosphere. *tert*-Butyl acrylate and methacrylonitrile were distilled directly prior to use. All other commercially obtained reagents were used as received. Reaction temperatures were controlled using an IKAmag temperature modulator or Neslab Cryobath CB-80, and unless stated otherwise, reactions were performed at room temperature (approximately 23 °C). Analytical thin-layer chromatography (TLC) was conducted on EMD silica gel 60 F₂₅₄ glass-backed plates (250 μm) and visualized by exposure to UV light (254 nm), or by potassium permanganate or ceric ammonium molybdate staining. Flash chromatography was performed using forced flow of the indicated solvent system on EMD Geduran® silica gel 60 (particle size 0.040–0.063 mm). Analytical enantioselective HPLC was performed on an Agilent 1100 Series HPLC utilizing Chiralcel columns (0.46 cm φ × 25 cm) obtained from Daicel Chemical Industries, Ltd. with visualization at 254 nm. NMR spectra were recorded at 298 K on Bruker FT-NMR spectrometers at the indicated frequencies. Chemical shifts (δ) are reported in parts per million (ppm) relative to residual deuterated solvent signals (CDCl₃). Data for ¹H NMR spectra are reported as follows: chemical shift (δ ppm), multiplicity, coupling constant [J , reported in Hertz (Hz)], and integration. Splitting patterns are abbreviated as follows: singlet (s), doublet (d),

triplet (t), quartet (q), multiplet (m), apparent (app), and broad (br). Carbon multiplicity was determined by a combination of DEPTQ and HMQC experiments. Chemical shifts (δ) for ^{31}P NMR spectra are reported in parts per million (ppm) and referenced to the corresponding calibrated ^1H NMR spectrum. Infrared (IR) spectra were recorded on a Varian 640-IR spectrometer as thin films in CH_2Cl_2 on KBr plates and are reported in terms of frequency of absorption (cm^{-1}). High-resolution mass spectra (HRMS) were obtained from the UC Irvine Mass Spectrometry Facility with a Micromass LCT spectrometer. Melting points (mp) were determined on a melting point apparatus (Thomas Hoover, Uni-Melt) and are uncorrected. Abbreviations used can be found on the Internet at:

http://pubs.acs.org/paragonplus/submission/joceah/joceah_abbreviations.pdf.

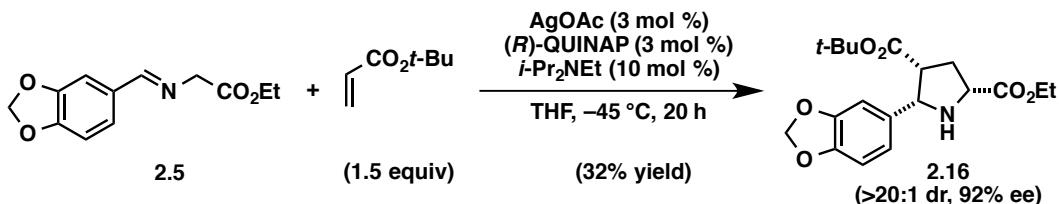
2.5.2 Synthesis of Imine 2.5



Ethyl (E)-2-((benzo[d][1,3]dioxol-5-ylmethylene)amino)acetate (2.5). A 50 mL round-bottom flask was charged with a magnetic stir bar, glycine ethyl ester hydrochloride (525 mg, 3.75 mmol, 1.50 equiv), and piperonal (375 mg, 2.50 mmol, 1.00 equiv). MeCN (4.2 mL, 0.6 M) and Et_3N (520 μL , 3.75 mmol, 1.50 equiv) were sequentially added and the resulting heterogeneous mixture was vigorously stirred at 23 $^\circ\text{C}$ for 5 h. Concentration of the reaction mixture under reduced pressure afforded an amorphous colorless solid, which was transferred to a separatory funnel using CH_2Cl_2 (15 mL) and H_2O (30 mL). The layers of the resulting biphasic mixture were partitioned and the organic layer was extracted with H_2O (30 mL) and brine (30 mL). The organic layer was dried over Na_2SO_4 , filtered, and concentrated to afford imine 2.5 (590 mg, quantitative yield) as a light yellow oil.⁶⁰ Imine 2.5 was carried further in subsequent

reactions without further purification. ^1H NMR (600 MHz, CDCl_3): δ 8.16 (s, 1H), 7.41 (s, 1H), 7.15 (d, J = 7.9, 1H), 6.83 (d, J = 7.9, 1H), 6.01 (s, 2H), 4.35 (s, 2H), 4.23 (q, J = 6.8, 2H), 1.30 (t, J = 6.8, 3H).

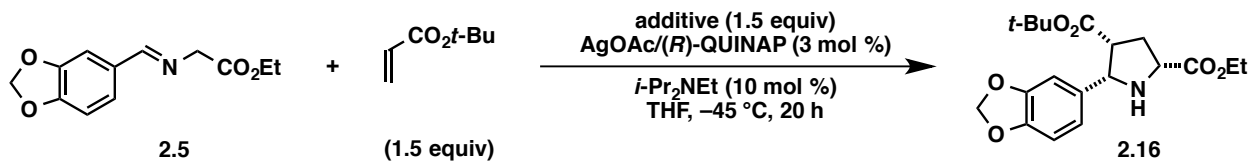
2.5.3 Ag(I)-Catalyzed 1,3-DC Reactions



4-(*tert*-Butyl) 2-ethyl (*2R,4R,5S*)-5-(benzo[*d*][1,3]dioxol-5-yl)pyrrolidine-2,4-dicarboxylate (2.16).

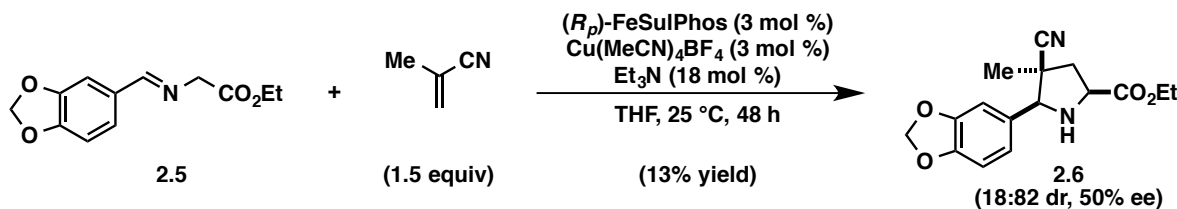
The enantioselective synthesis of pyrrolidine **2.16** was performed using the procedure reported by Schreiber and coworkers.¹³ In the glove box, a foil-wrapped 1-dram vial was charged with a magnetic stir bar, AgOAc (1 mg, 0.005 mmol, 0.03 equiv), and (*R*)-QUINAP (2 mg, 0.005 mmol, 0.03 equiv). The vial was sealed with a Teflon-lined cap, removed from the glove box, and placed under an atmosphere of Ar. THF (0.52 mL) was added to the vial and the resulting catalyst solution was stirred at 23 °C for 5 h. The catalyst solution was then added to a vial containing a solution of imine **2.5** [41 mg, 0.17 mmol, 1.0 equiv; azeotropically dried with PhMe (3 × 0.5 mL)] in THF (1.2 mL) at -45 °C. *tert*-Butyl acrylate (38 μL, 0.26 mmol, 1.5 equiv) and *i*-Pr₂NEt (3 μL, 0.02 mmol, 0.1 equiv) were sequentially added and the reaction mixture was stirred at -45 °C for 20 h. The reaction mixture was quenched at 23 °C with 0.1 mL of a 10:1 v/v THF:glacial acetic acid solution, then concentrated under reduced pressure. The resulting residue was dissolved in CH₂Cl₂ (10 mL) and transferred to a separatory funnel with H₂O (10 mL). The layers of the resulting biphasic mixture were separated and the aqueous layer was extracted with CH₂Cl₂ (2 × 10 mL). The combined extracts were dried over Na₂SO₄ and concentrated under reduced pressure. The resulting residue was purified by flash

chromatography (1:1 hexanes:EtOAc) to yield pyrrolidine **2.16** (20 mg, 32% yield) as a clear oil in >20:1 dr and 92% ee. Enantiomeric excess was determined by HPLC: Daicel Chiralpak AS, *i*-PrOH/*n*-hexane 60:40, flow rate 1.0 mL/min, $\lambda = 254$ nm, $t_R = 9.2$ min (major isomer), 12.5 min (minor isomer).⁶¹ R_f 0.60 (1:1 hexanes:EtOAc); ¹H NMR (600 MHz, CDCl₃): δ 6.87 (s, 1H), 6.83 (d, $J = 7.9$, 1H), 6.74 (d, $J = 7.9$, 1H), 5.91 (s, 2H), 4.42 (d, $J = 7.9$, 1H), 4.26 (q, $J = 7.0$, 2H), 3.91 (t, $J = 8.5$, 1H), 3.21 (q, $J = 7.6$, 1H), 2.97 (br s, 1H), 2.42–2.37 (m, 1H), 2.31–2.27 (m, 1H), 1.31 (t, $J = 7.0$, 3H), 1.12 (s, 9H); ¹³C NMR (125 MHz, CDCl₃): δ 173.3, 171.7, 147.6, 146.9, 133.6, 120.6, 108.3, 108.0, 101.1, 80.8, 65.3, 61.4, 60.0, 50.4, 33.9, 27.8, 14.4; IR (thin film): 2978, 2932, 2904, 1730, 1489 cm^{−1}; HRMS-ESI (*m/z*) [M + Na]⁺ calculated for C₁₉H₂₅NO₆Na, 386.1580; found, 386.1570.



4-(*tert*-Butyl) 2-ethyl (2*R*,4*R*,5*S*)-5-(benzo[*d*][1,3]dioxol-5-yl)pyrrolidine-2,4-dicarboxylate (2.16**).** The competition experiments described in Table 2.2 were conducted following the procedure for the enantioselective synthesis of **2.16**. The additive [either methacrylonitrile (22 μ L, 0.26 mmol, 1.5 equiv), acetonitrile (14 μ L, 0.26 mmol, 1.5 equiv), or isobutyronitrile (23 μ L, 0.26 mmol, 1.5 equiv)] was introduced to the reaction vial simultaneously with *tert*-butyl acrylate. ¹H NMR yields were determined in CDCl₃ from the unpurified reaction residue using 3 μ L DMF as the external standard.

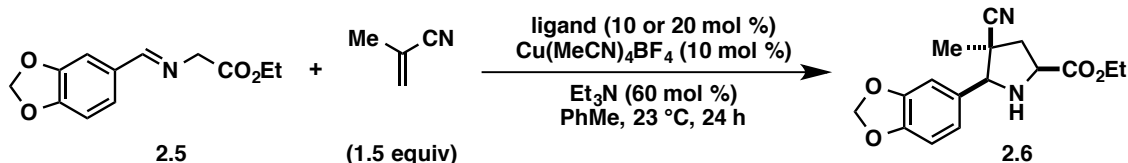
2.5.4 Cu(I)-Catalyzed 1,3-DC Reactions



Ethyl (2*S*,4*S*,5*S*)-5-(benzo[*d*][1,3]dioxol-5-yl)-4-cyano-4-methylpyrrolidine-2-carboxylate (2.6).

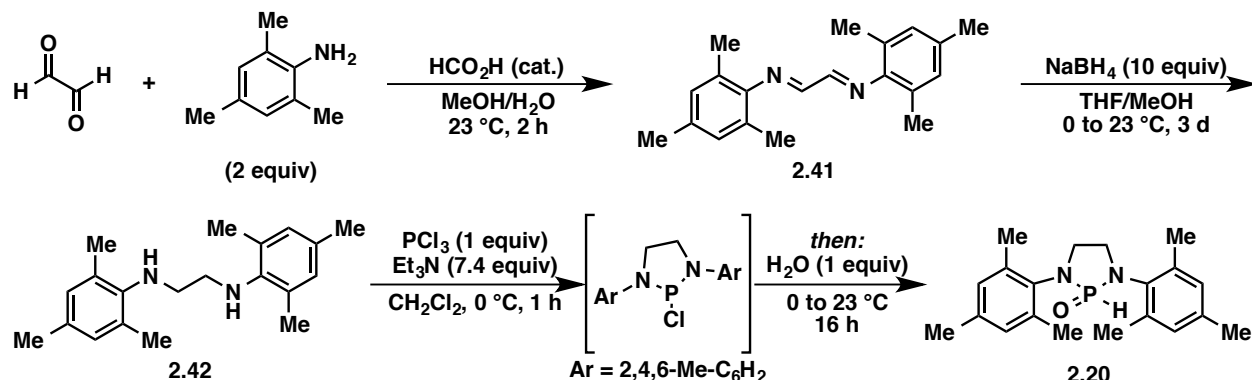
The enantioselective synthesis of pyrrolidine **2.6** was performed using the procedure reported by Carretero and coworkers.^{15e} In the glove box, a 1-dram vial was charged with (R_p) -FeSulPhos (3 mg, 0.006 mmol, 0.03 equiv), $\text{Cu}(\text{MeCN})_4\text{BF}_4$ (2 mg, 0.006 mmol, 0.03 equiv), and a magnetic stir bar. Also in the glove box, a second 1-dram vial was charged with imine **2.5** (47 mg, 0.20 mmol, 1.0 equiv). The vials were each sealed with a Teflon-lined cap, removed from the glove box, and placed under an atmosphere of Ar. THF (0.5 mL) was added to each vial. The vial containing the catalyst solution was cooled to –30 °C before the sequential addition of the imine solution, Et_3N (5.0 μL , 0.035 mmol, 0.18 equiv), and methacrylonitrile (25 μL , 0.30 mmol, 1.5 equiv). The reaction mixture stirred at –30 °C for 1 h, after which time TLC indicated no formation of product. The reaction mixture was then allowed to warm to 23 °C and product was detected by TLC after 1 h. The reaction mixture continued stirring at 23 °C for 48 h, after which time it was transferred to a separatory funnel with CH_2Cl_2 (10 mL) and H_2O (10 mL). The layers of the resulting biphasic mixture were separated and the aqueous layer was extracted with CH_2Cl_2 (2 \times 10 mL). The combined extracts were dried over Na_2SO_4 and concentrated under reduced pressure. The resulting residue was purified by flash chromatography (1:1 hexanes:EtOAc) to afford pyrrolidine **2.6** (8 mg, 13% yield) as a yellow oil in 50% ee. Enantiomeric excess was determined by HPLC: Daicel Chiralpak OD-H III,

i-PrOH/*n*-hexane 20:80, flow rate 1.0 mL/min, $\lambda = 254$ nm, $t_R = 17.2$ min (*2S,4S,5S*)-isomer, 19.8 min (*2S,4R,5S*)-isomer.



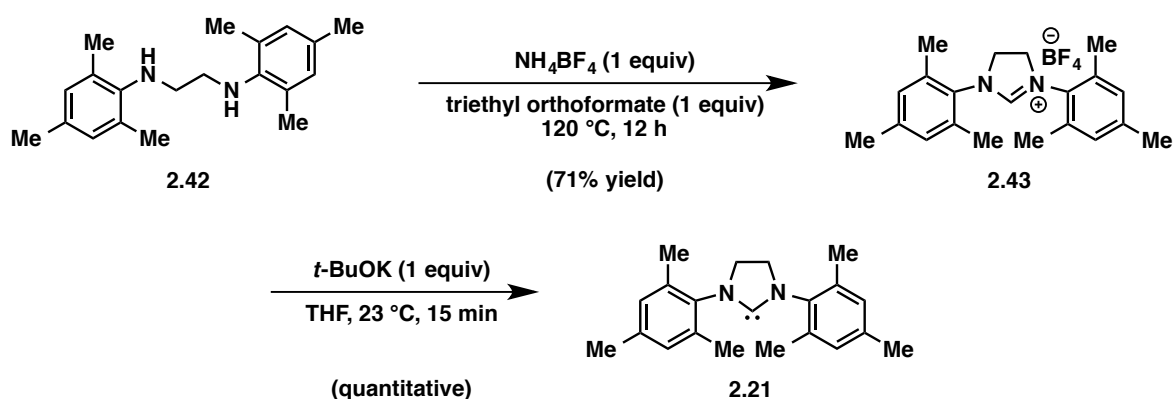
General Procedure for Investigating Cu(I) Catalysts. In the glove box, a 1-dram vial was charged with $\text{Cu}(\text{MeCN})_4\text{BF}_4$ (3 mg, 0.01 mmol, 0.1 equiv), ligand (bi- or tridentate, 0.01 mmol, 0.1 equiv; monodentate, 0.02 mmol, 0.2 equiv), a magnetic stir bar, and PhMe (0.25 mL). Also in the glove box, a second 1-dram vial was charged with imine **2.5** (24 mg, 0.10 mmol, 1.0 equiv) and PhMe (0.25 mL). The vials were each sealed with a Teflon-lined cap, removed from the glove box, and placed under an atmosphere of Ar. To the vial containing catalyst solution was sequentially added the solution of imine **2.5**, Et_3N (8 μL , 0.06 mmol, 0.6 equiv), and methacrylonitrile (13 μL , 0.15 mmol, 1.5 equiv). After stirring for 24 h at 23 °C, the solution was filtered through 310 mg of SiO_2 with EtOAc (10 mL). After removal of the volatile components in vacuo, the resulting residues were analyzed by ^1H NMR to determine the starting material-to-product conversion and the endo:exo cycloadduct ratio via signal integration of the diagnostic pyrrolidine methylene group signals [endo adduct **2.6**: δ 2.81 (dd, J = 13.6, 4.3, 1H), δ 2.27 (dd, J = 13.6, 9.6, 1H); exo adduct: δ 2.72 (dd, J = 13.3, 9.9, 1H), δ 2.21 (dd, J = 13.5, 6.2, 1H)] against the imidoyl imine **2.5** signal [δ 8.16 (s, 1H)] and piperonal aldehydic signal [δ 9.81 (s, 1H); from hydrolysis of unreacted imine **2.5** starting material]. Reactions represented in Tables 2.7, 2.10, and 2.13 were run in a similar manner to those described in this procedure, with modifications of the solvent (THF) and the reaction time (6 h). Enantiomeric excess was determined by HPLC: Daicel Chiraldak OD-H III, *i*-PrOH/*n*-hexane 10:90, flow rate 1.0 mL/min, λ = 254 nm, t_R = 32.9 min (*2S,4S,5S*)-isomer, 40.1 min (*2S,4R,5S*)-isomer.

2.5.5 Ligand Synthesis

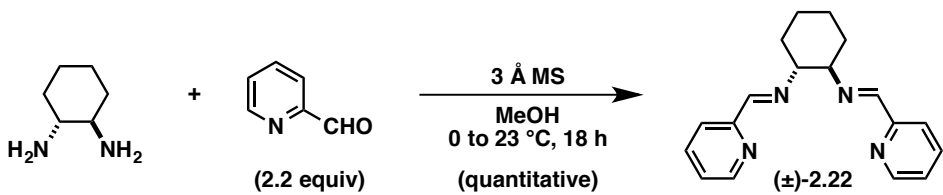


1,3-Dimesityl-1,3,2-diazaphospholidine 2-oxide (2.20). HASPO ligand **2.20** was prepared as described by Dieskau.⁶² Glyoxal (2.3 mL, 20 mmol, 1.0 equiv, 40 wt % in H₂O) and 2,4,6-trimethylaniline (5.6 mL, 40 mmol, 2.0 equiv) were dissolved in a minimal amount of MeOH (0.4 mL) in a 250 mL round-bottom flask charged with a magnetic stir bar. Three drops of formic acid were added to initiate the formation of a dark brown precipitate. After stirring for 2 h, the brown precipitate was filtered through a Büchner funnel to afford diimine intermediate **2.41** as a bright yellow-orange solid, which was used immediately in the following transformation. A 250 mL three-neck flask was charged with diimine **2.41** (5.8 g, 20 mmol, 1.0 equiv) and a magnetic stir bar, followed by the addition of MeOH (40 mL) and THF (80 mL). The solution was cooled to 0 °C and NaBH₄ (7.60 g, 200 mmol, 10.0 equiv) was added portion-wise. The heterogeneous mixture was allowed to warm to 23 °C. After 3 days, the resulting clear solution was quenched with sat. aq. NH₄Cl (10 mL). The resulting biphasic mixture was extracted with EtOAc (3 × 50 mL) and the organic layers were combined, washed with brine (100 mL), and dried over Na₂SO₄. The volatile components were removed under reduced pressure to afford diamine **2.42** (4.3 g, 73% yield over 2 steps) as a dark orange oil, which was used directly in the following transformation. A 25 mL round-bottom flask was charged with diamine **2.42** (1.5 g, 5.0 mmol, 1.0 equiv), a magnetic stir bar, and Et₃N (5.2 mL,

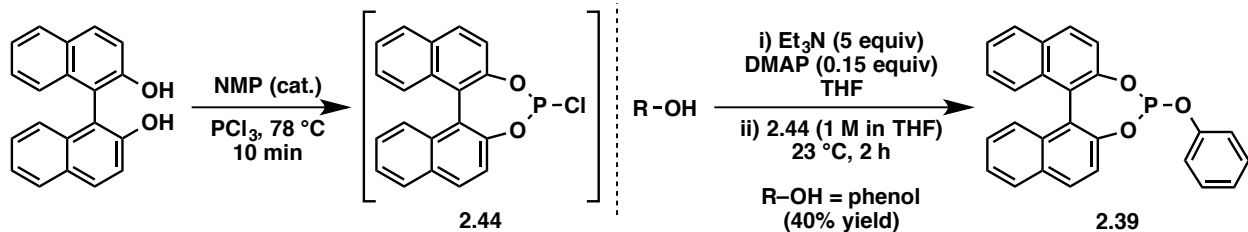
37 mmol, 7.4 equiv). The resulting mixture was dissolved in CH₂Cl₂ (8.3 mL) and cooled to 0 °C. PCl₃ (0.44 mL, 5.0 mmol, 1.0 equiv) was added dropwise over 20 min. The reaction temperature was maintained at 0 °C for 1 h before the dropwise addition of H₂O (90 µL, 5.0 mmol, 1.0 equiv). The resulting heterogeneous solution was allowed to warm to 23 °C and maintained at that temperature for 16 h. After filtration through Celite and concentration under reduced pressure, the residue was purified by flash chromatography (3:1 hexanes:EtOAc) to yield HASPO ligand **2.20** (1.6 g, 94%) as a colorless solid (mp = 160–162 °C). Spectral data match those previously reported.⁶³



1,3-Dimesityl-4,5-dihydro-1*H*-imidazol-3-ium-2-ide (2.21). NHC ligand **2.21** was prepared following the procedure published by Kingsbury and Hoveyda.⁶⁴ A 10 mL round-bottom flask was charged with diamine **2.42** (1.8 g, 6.0 mmol, 1.0 equiv), ammonium tetrafluoroborate (0.60 g, 6.0 mmol, 1.0 equiv), and a magnetic stir bar. Triethyl orthoformate (1.0 mL, 6.0 mmol, 1.0 equiv) was then added and the resulting homogenous mixture was maintained at 120 °C for 12 h. Upon cooling to 23 °C, a purple solid formed, which was then suspended in EtOH (4 mL) and filtered with pentane, affording tetrafluoroborate salt **2.43** as a light purple solid (1.7 g, 71% yield). NHC ligand **2.21** was generated *in situ* immediately before use by stirring tetrafluoroborate salt **2.43** (8 mg, 0.02 mmol, 0.2 equiv) with *t*-BuOK (2 mg, 0.02 mmol, 0.2 equiv) in THF (0.25 mL, 0.40 M) for 15 min.

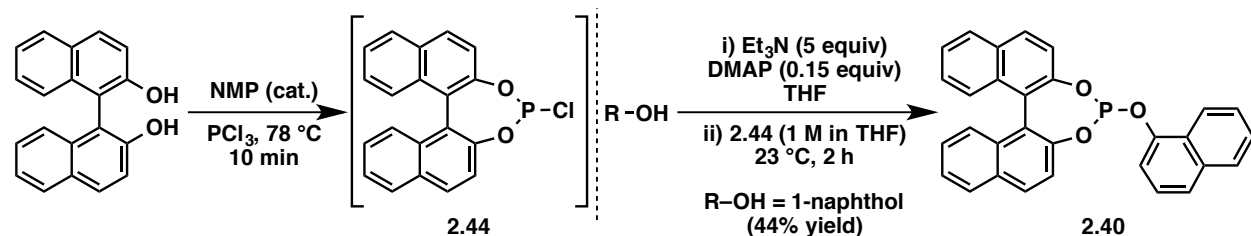


Rac-*N,N'*-cyclohexane-1,2-diyl bis(1-(pyridin-2-yl)methanimine) [(\pm)-2.22]. Diimine ligand (\pm)-2.22 was prepared as described by Thomas and coworkers.³⁰ A 25 mL round-bottom flask was charged with a magnetic stir bar, 3 Å MS, (\pm)-*trans*-diaminocyclohexane (120 μ L, 1.0 mmol, 1.0 equiv), and MeOH (2.5 mL, 0.4 M). The resulting heterogeneous mixture was cooled to 0 °C in an ice-water bath, then a methanolic solution of 2-pyridinecarboxaldehyde (210 μ L, 2.2 mmol, 2.2 equiv in 2.5 mL MeOH) was added dropwise. The mixture was warmed to 23 °C and maintained at this temperature for 18 h. The reaction mixture was filtered through Celite with MeOH. Concentration of the filtrate afforded diimine ligand (\pm)-2.22 (290 mg, quantitative yield) as an amorphous yellow solid, which was used without further purification.



Rac-4-phenoxydinaphtho[2,1-d:1',2'-f][1,3,2]dioxaphosphepine (2.39). Phosphites 2.39 and 2.40 were prepared according to the procedure described by Laschat and coworkers.⁵⁸ A 10 mL round-bottom flask was charged with (\pm)-BINOL [570 mg, 2.0 mmol, 1.0 equiv; azeotropically dried with PhMe (3 x 2 mL)], a magnetic stir bar, PCl_3 (2 mL), and NMP (1 drop). The homogenous reaction mixture was heated at reflux for 10 min. The reaction mixture was cooled to 23 °C and excess PCl_3 was azeotropically removed under reduced pressure and inert atmosphere to yield 2.44 as an orange oil, which was then dissolved in THF (2 mL). A 15 mL round-bottom flask was charged with phenol (190 mg, 2.0 mmol, 1.0 equiv), DMAP

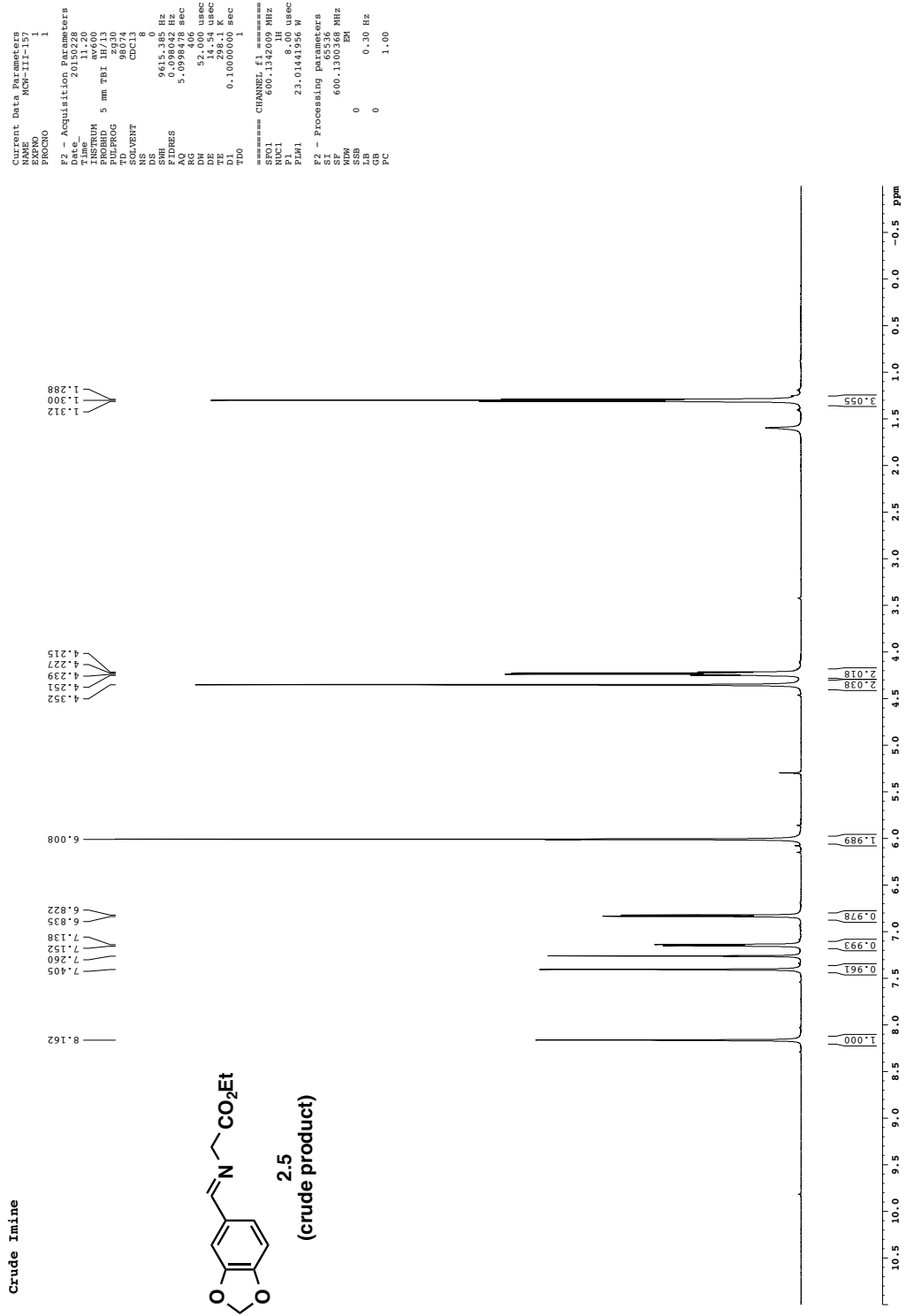
(37 mg, 0.30 mmol, 0.15 equiv), a magnetic stir bar, and Et₃N (1.4 mL, 10 mmol, 5.0 equiv). The solution of **2.44** was then added dropwise to the homogenous reaction mixture at 23 °C. The resulting homogenous reaction mixture stirred at ambient temperature for 2 h. The reaction mixture was concentrated under reduced pressure and purified by flash chromatography (10:1 hexanes:EtOAc) to yield phosphite ligand **2.39** (165 mg, 40% yield) as an amorphous colorless solid. ¹H, ¹³C, and ³¹P NMR spectra of the product are consistent with those previously reported.⁶⁵



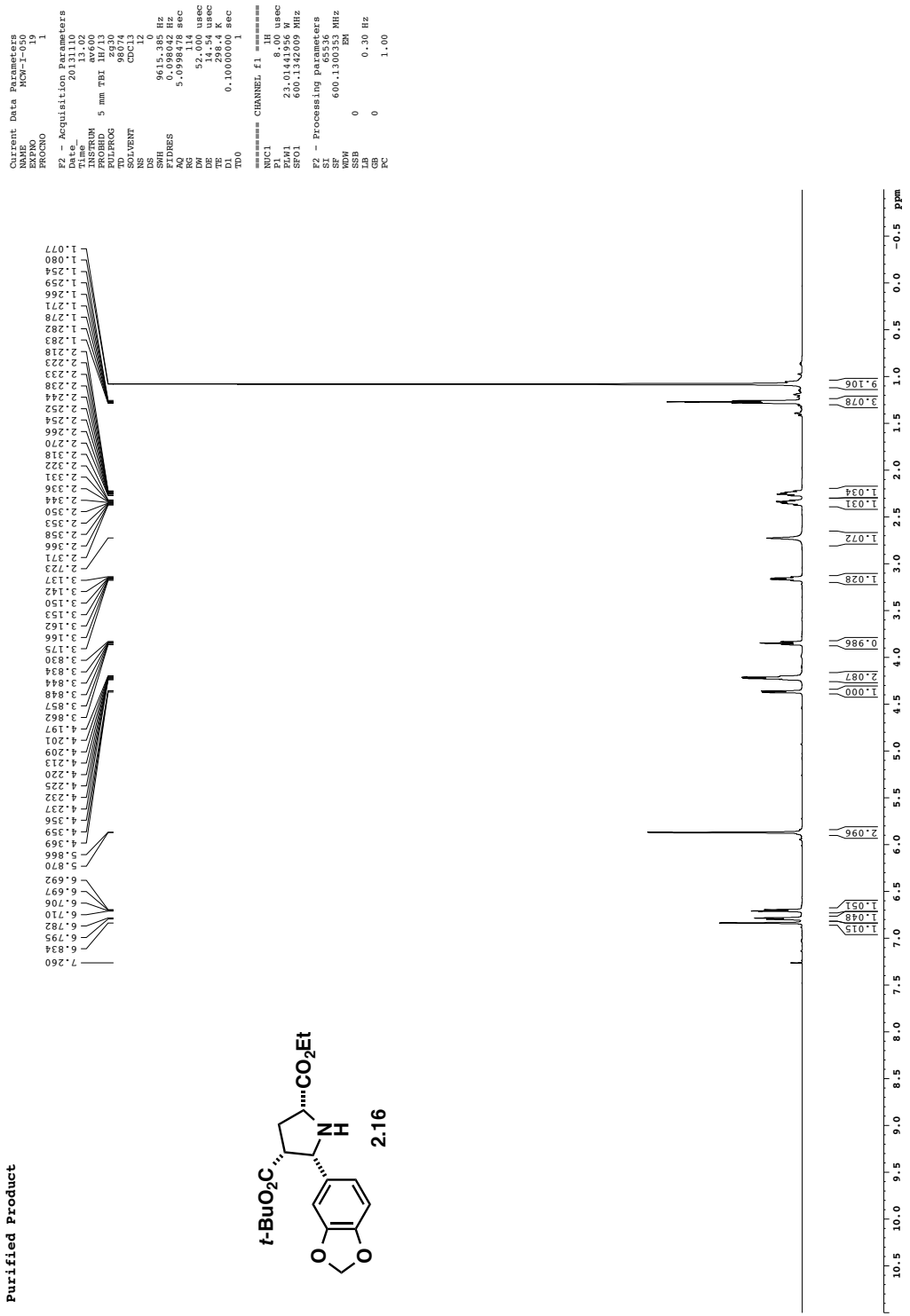
Rac-4-(naphthalen-1-yloxy)dinaphtho[2,1-d:1',2'-f][1,3,2]dioxaphosphepine (2.40).

Phosphite ligand **2.40** was prepared following the procedure described for ligand **2.39** using 1-naphthol (290 mg, 2.0 mmol, 1.0 equiv) and accessed as an amorphous colorless solid (400 mg, 44% yield). ¹H, ¹³C, and ³¹P NMR spectra of the product are consistent with those previously reported.^{59f}

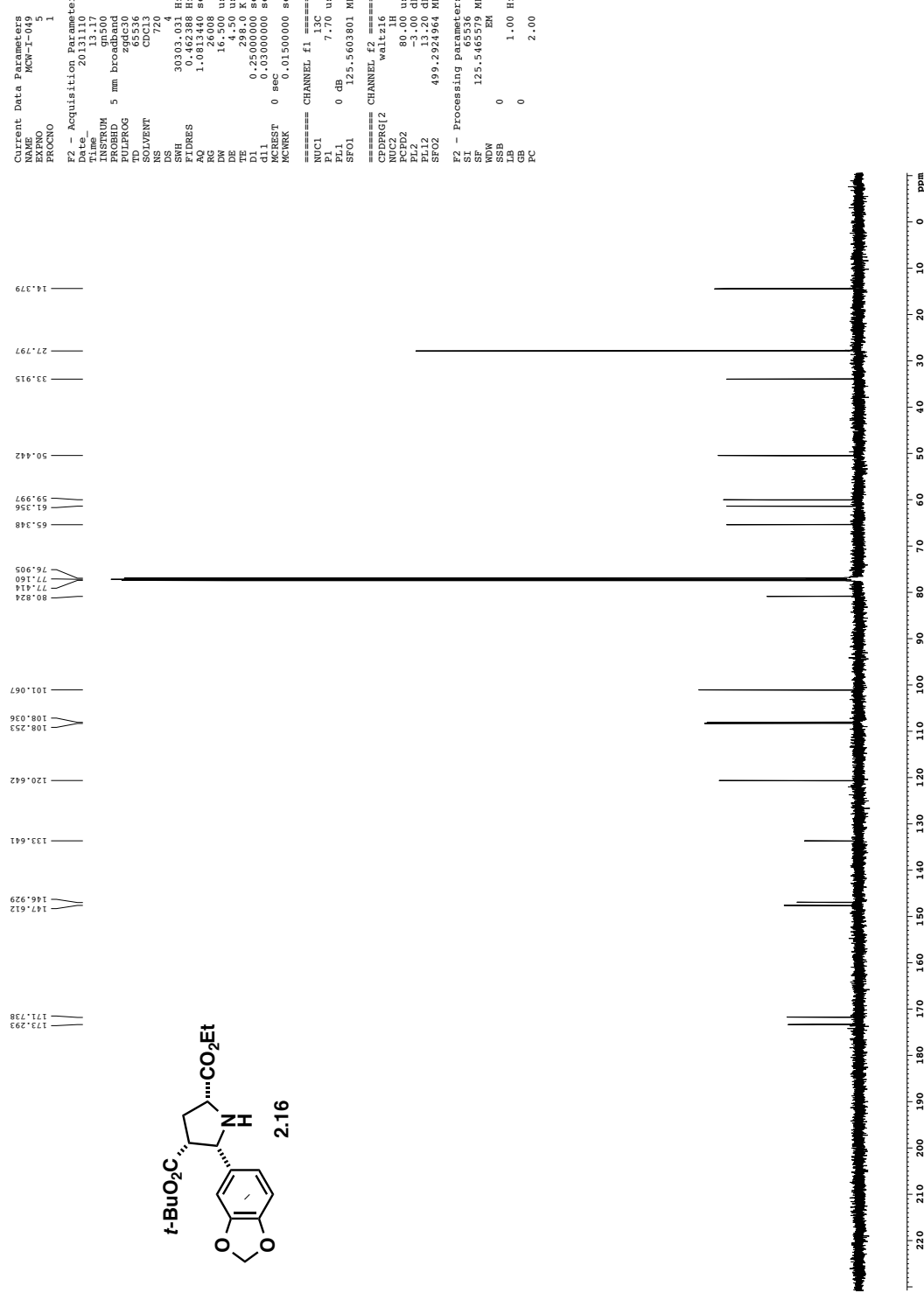
2.6 Appendix B: NMR Spectral Data



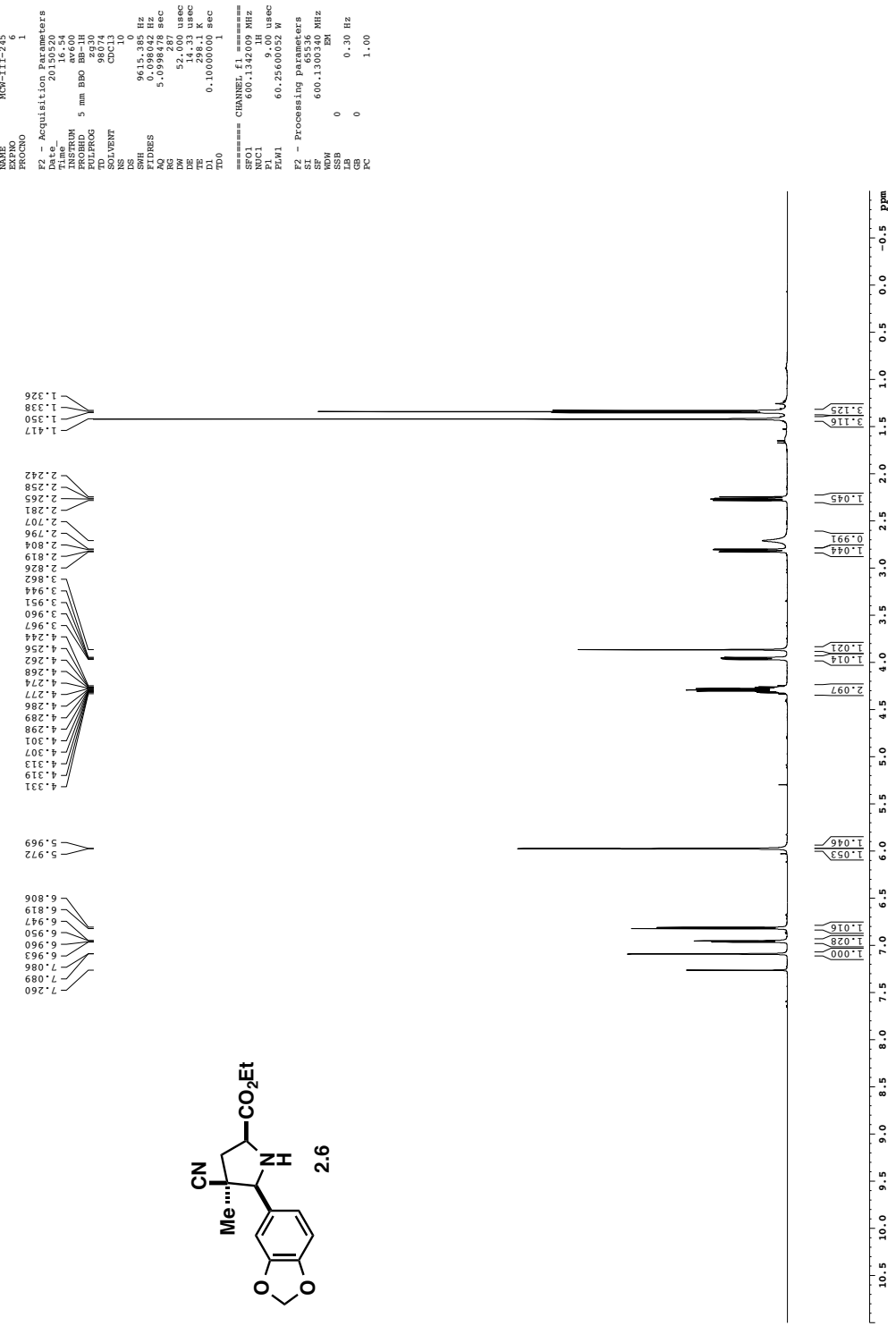
Purified Product



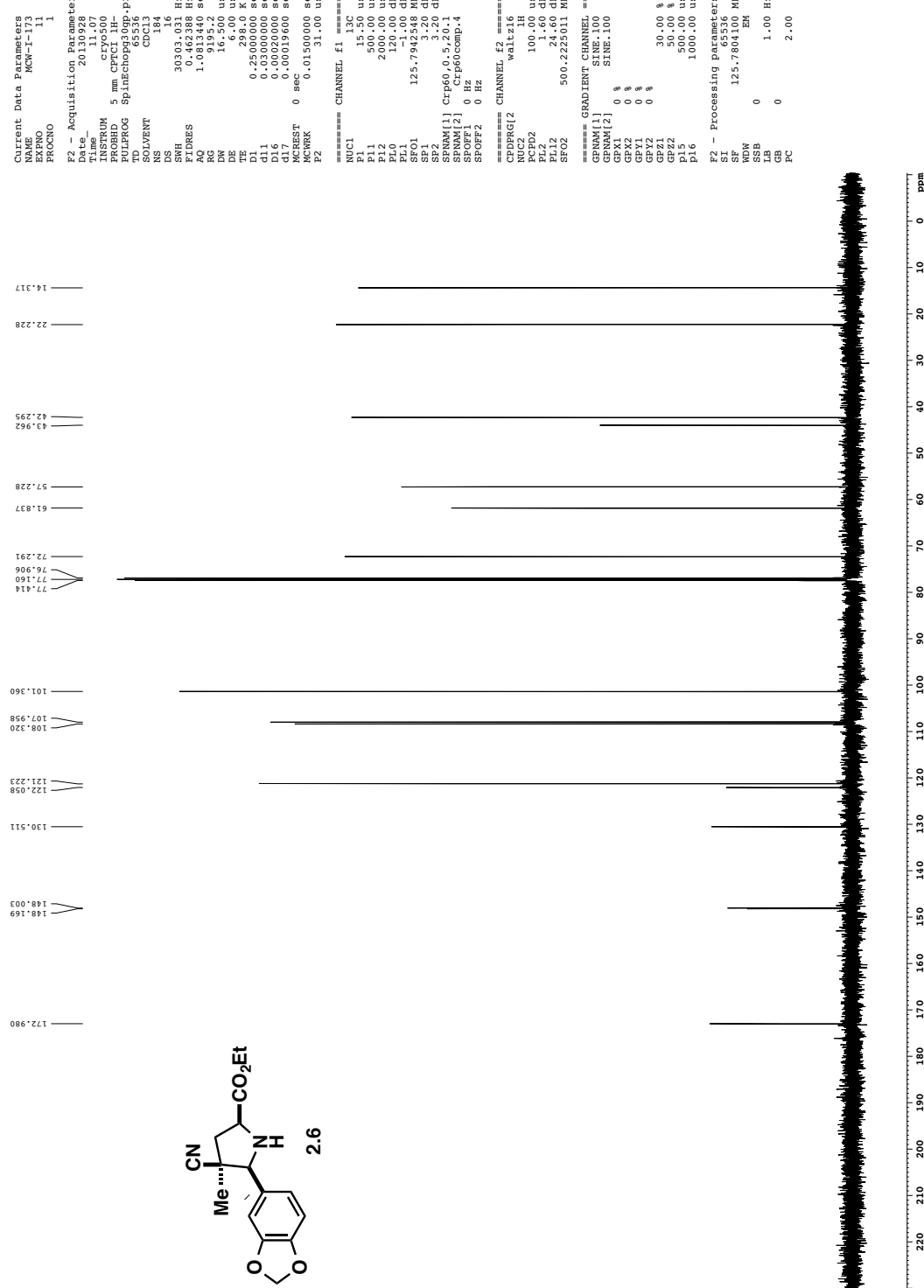
Purified Product



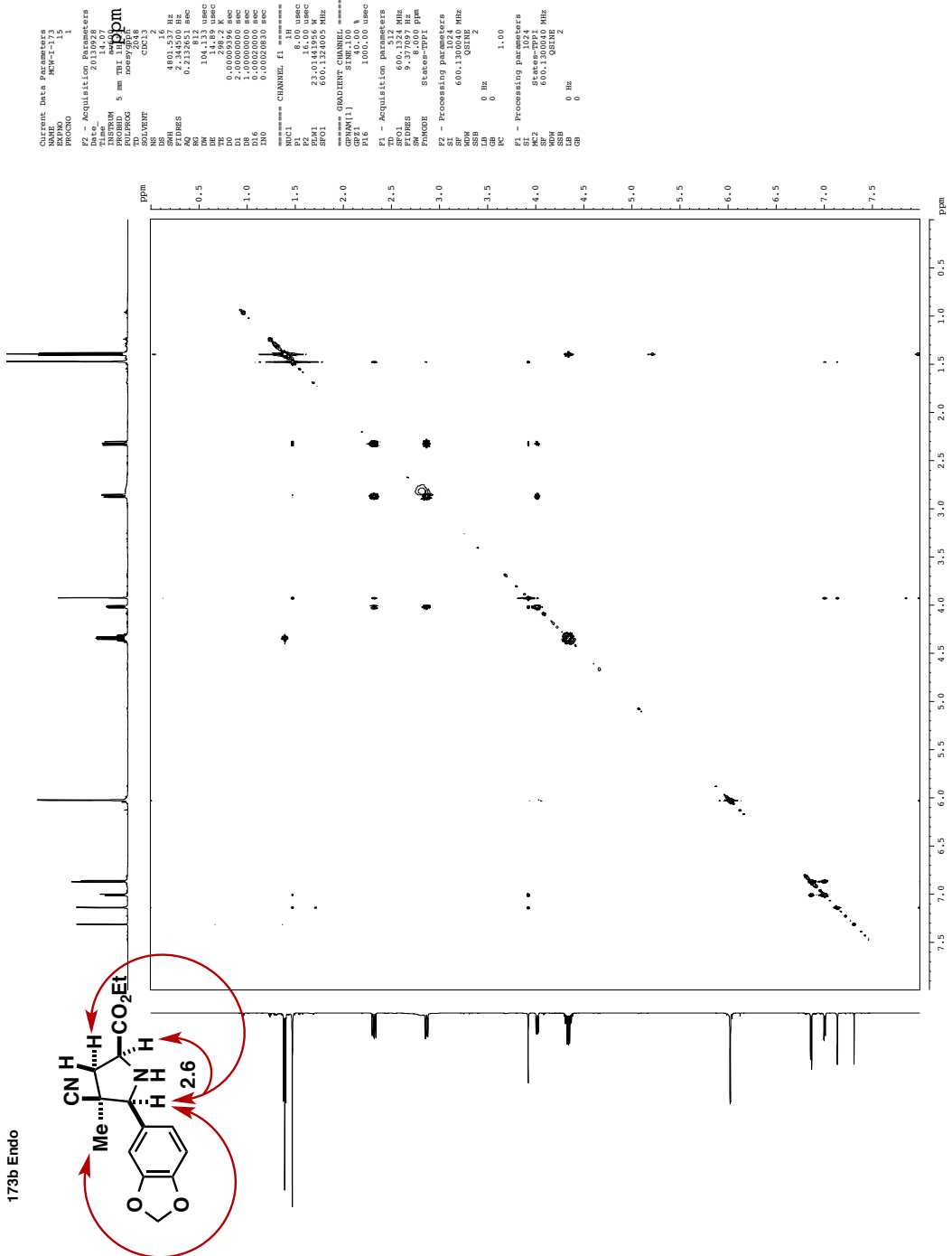
Endo Adduct



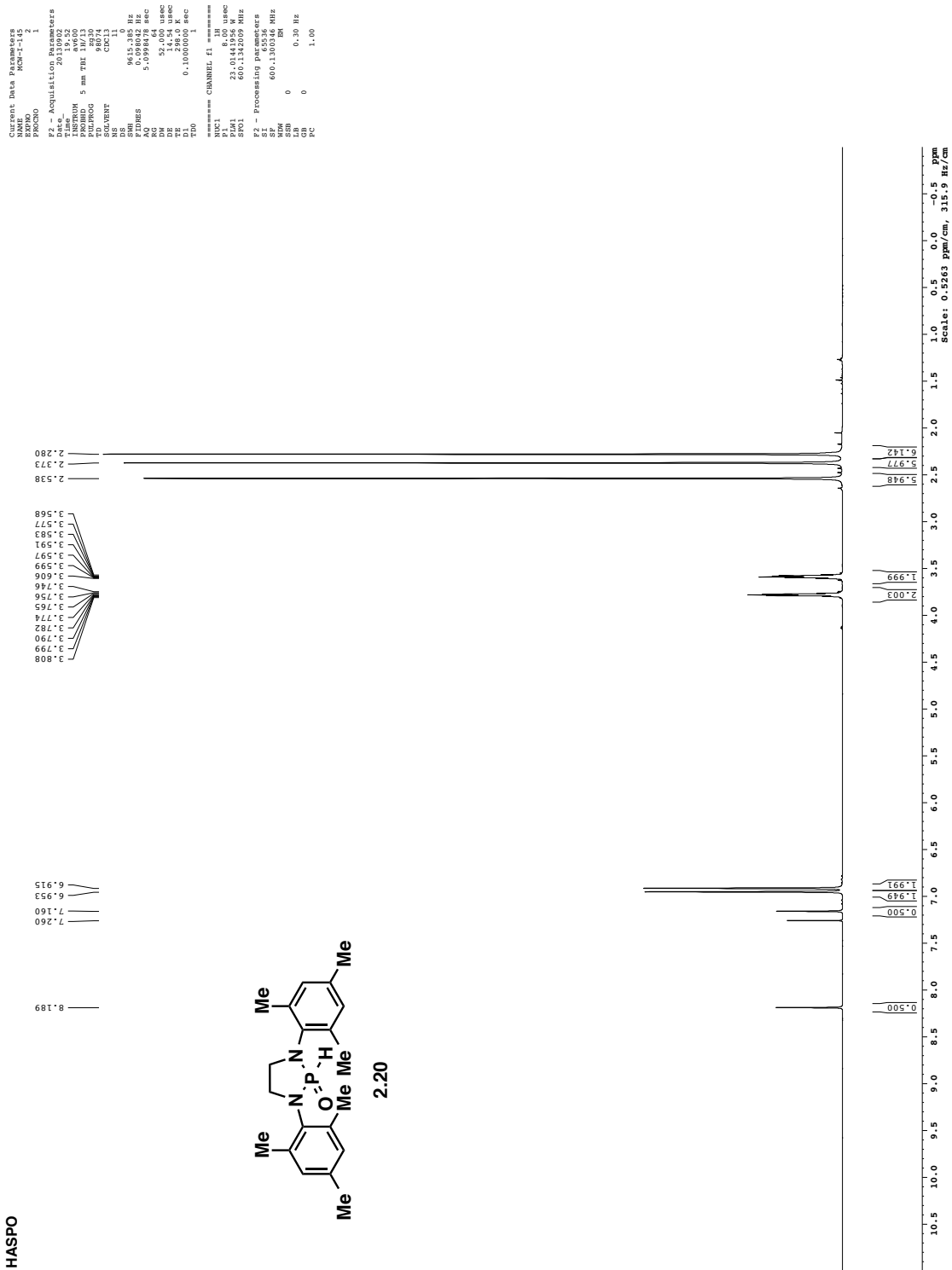
Purified Endo Product

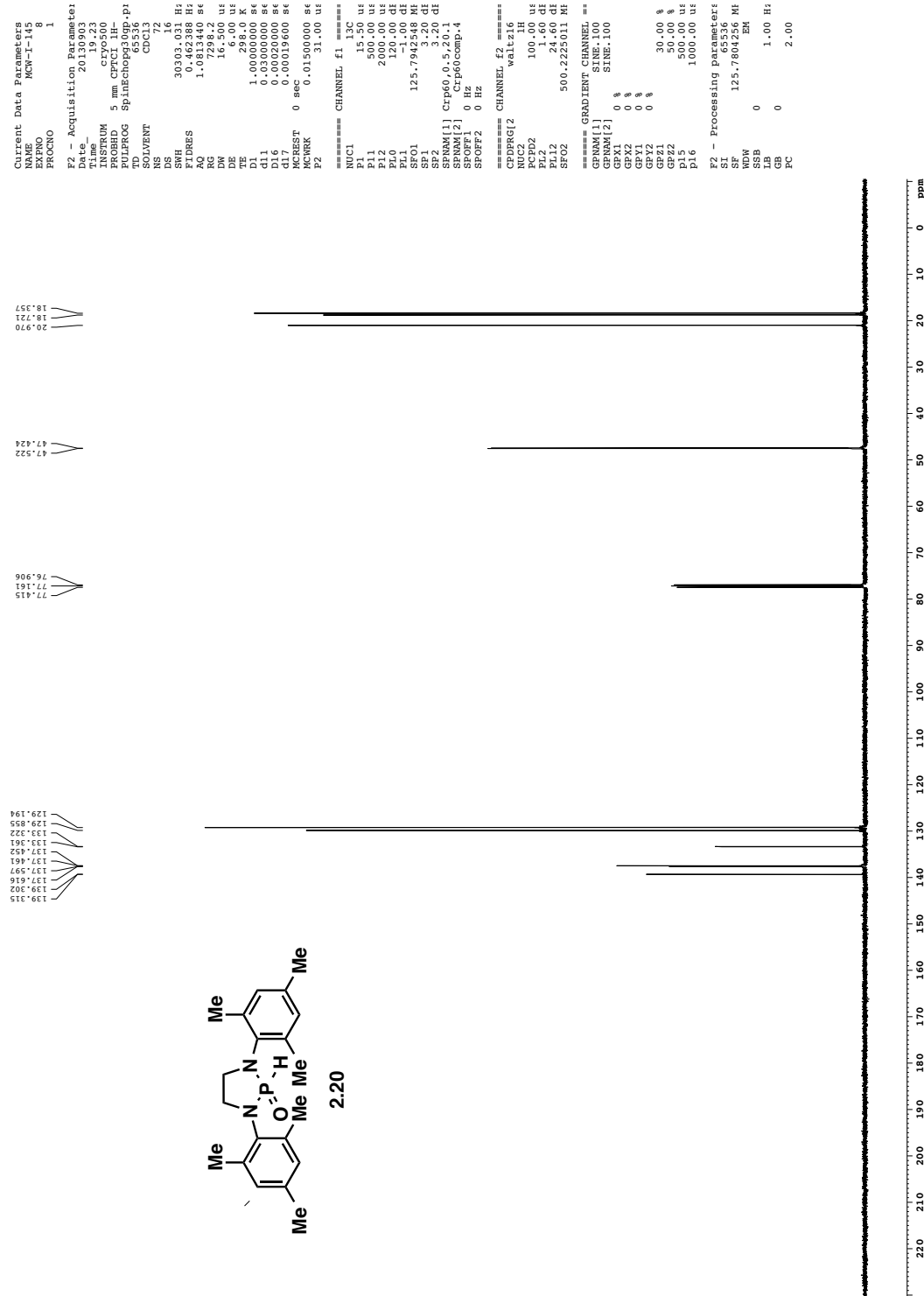


173b Endo

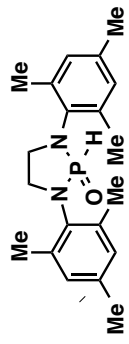


HASPO

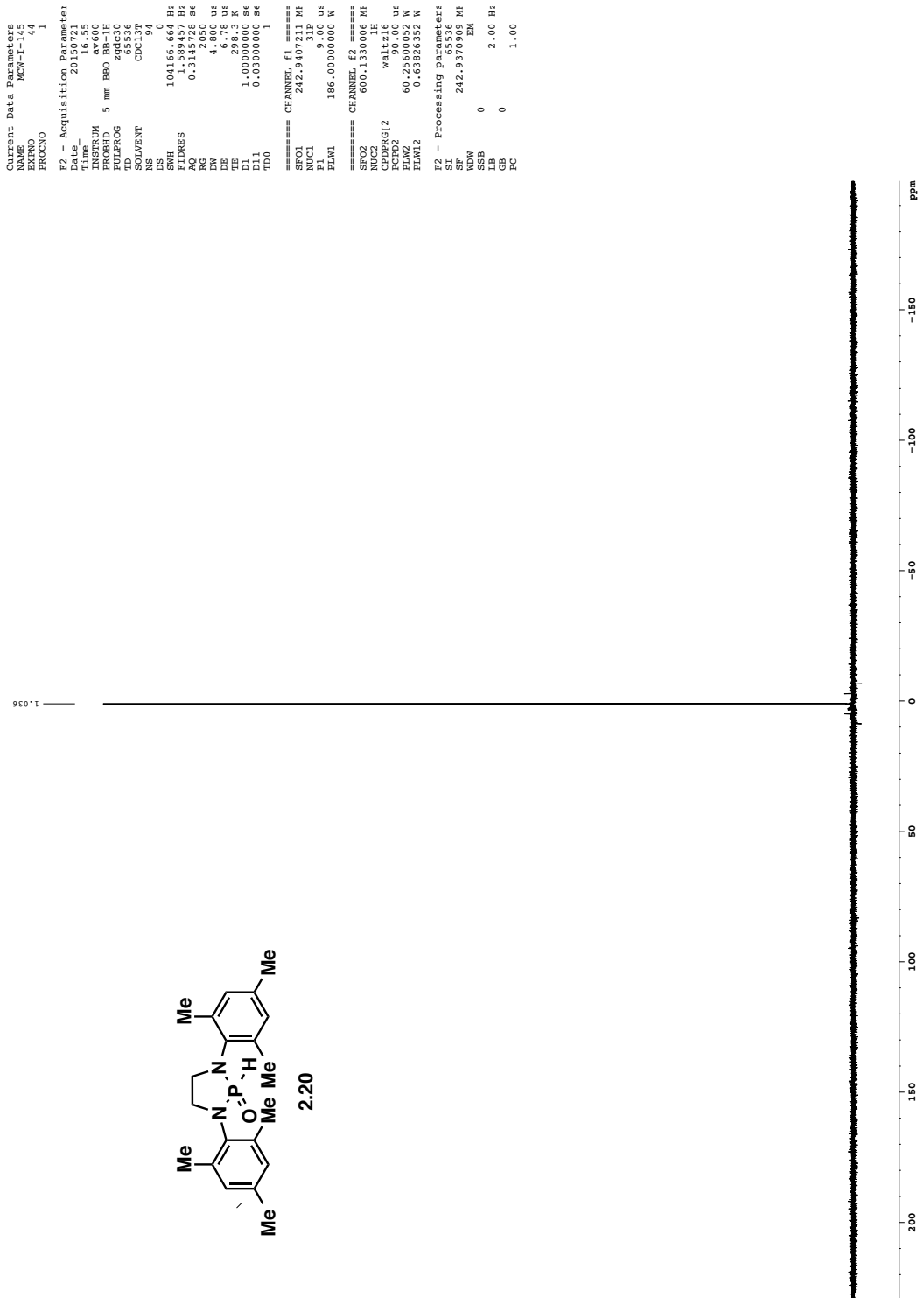




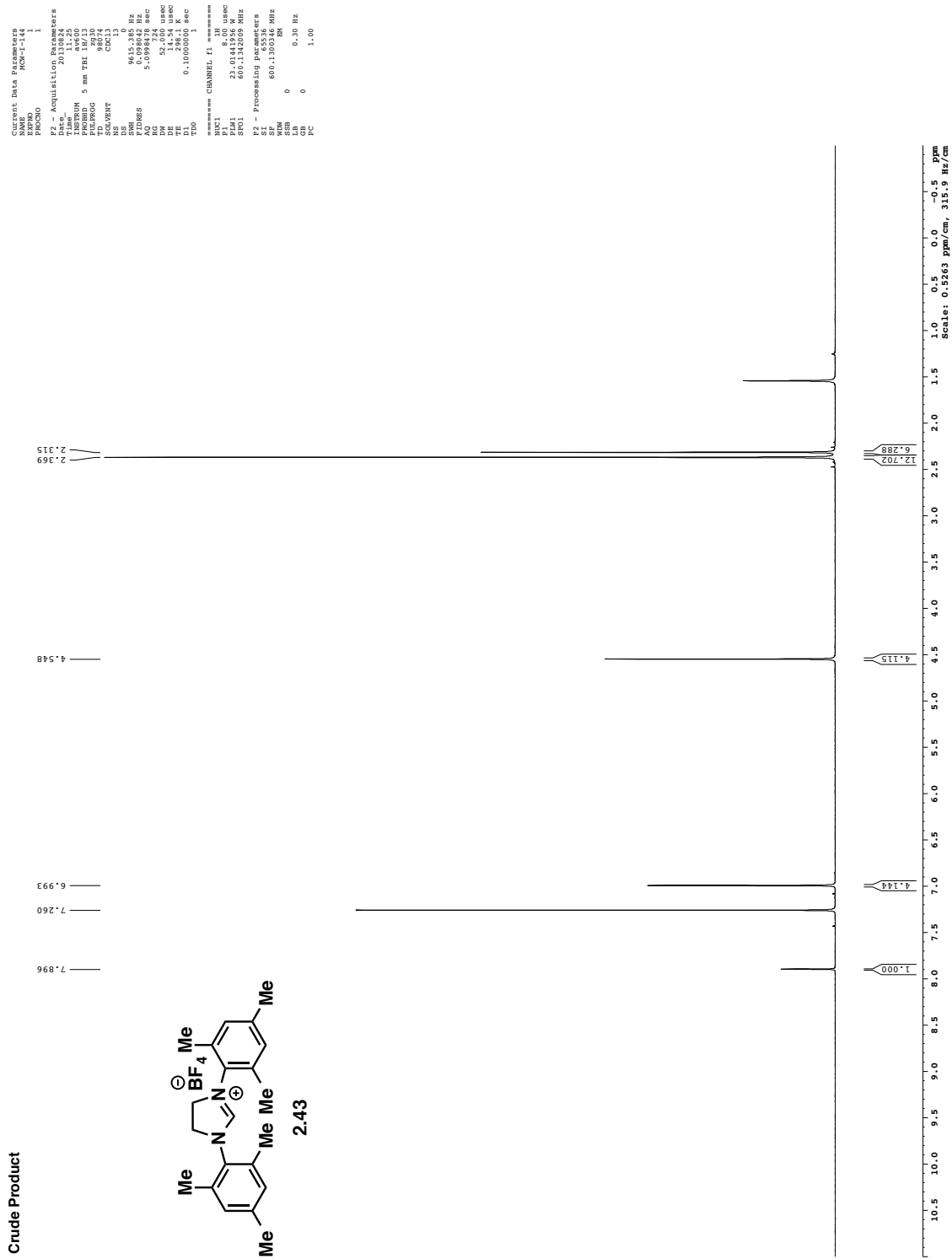
HASPO



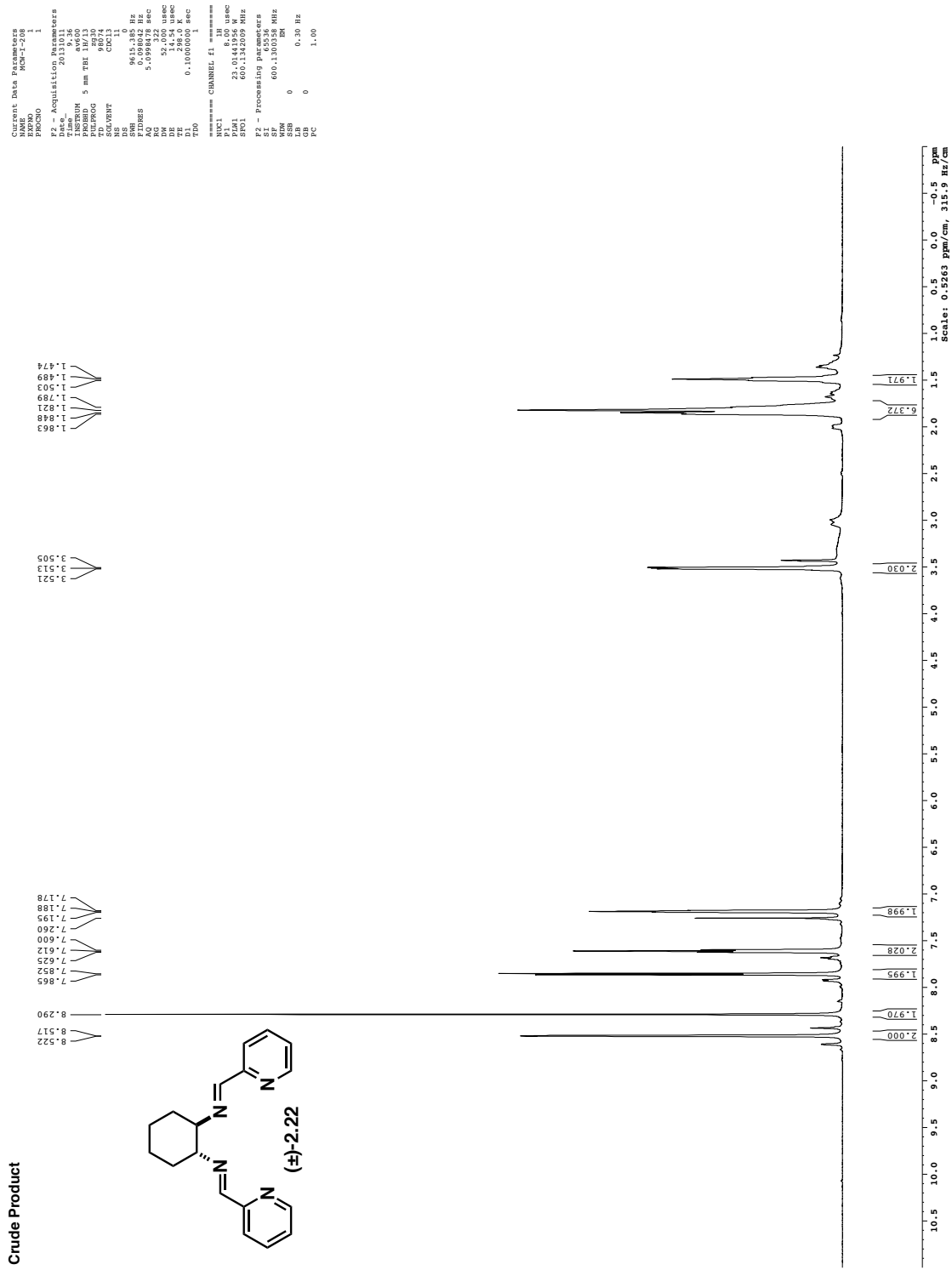
2.20



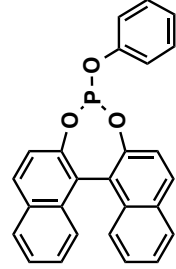
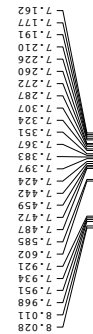
Crude Product



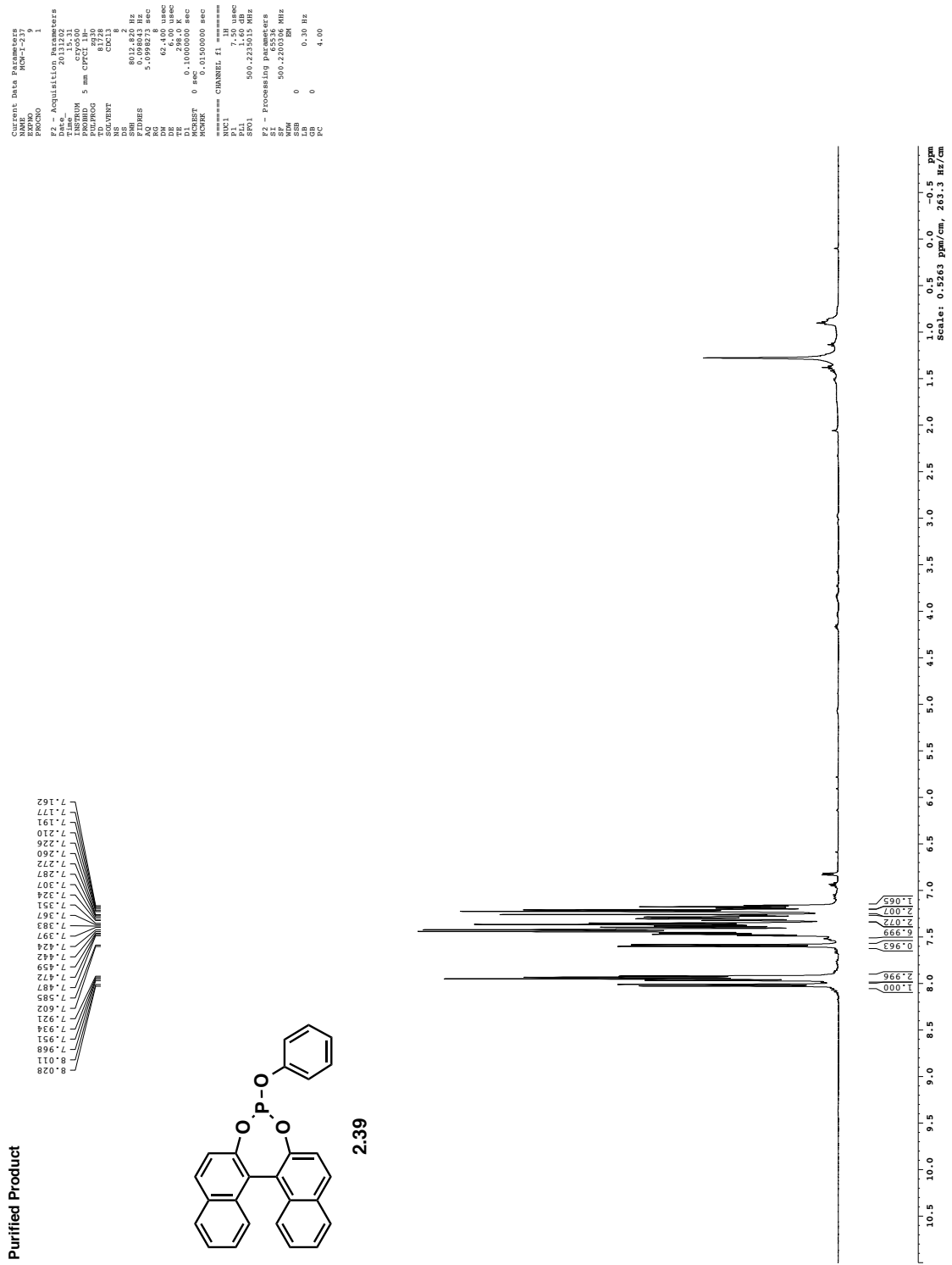
Crude Product



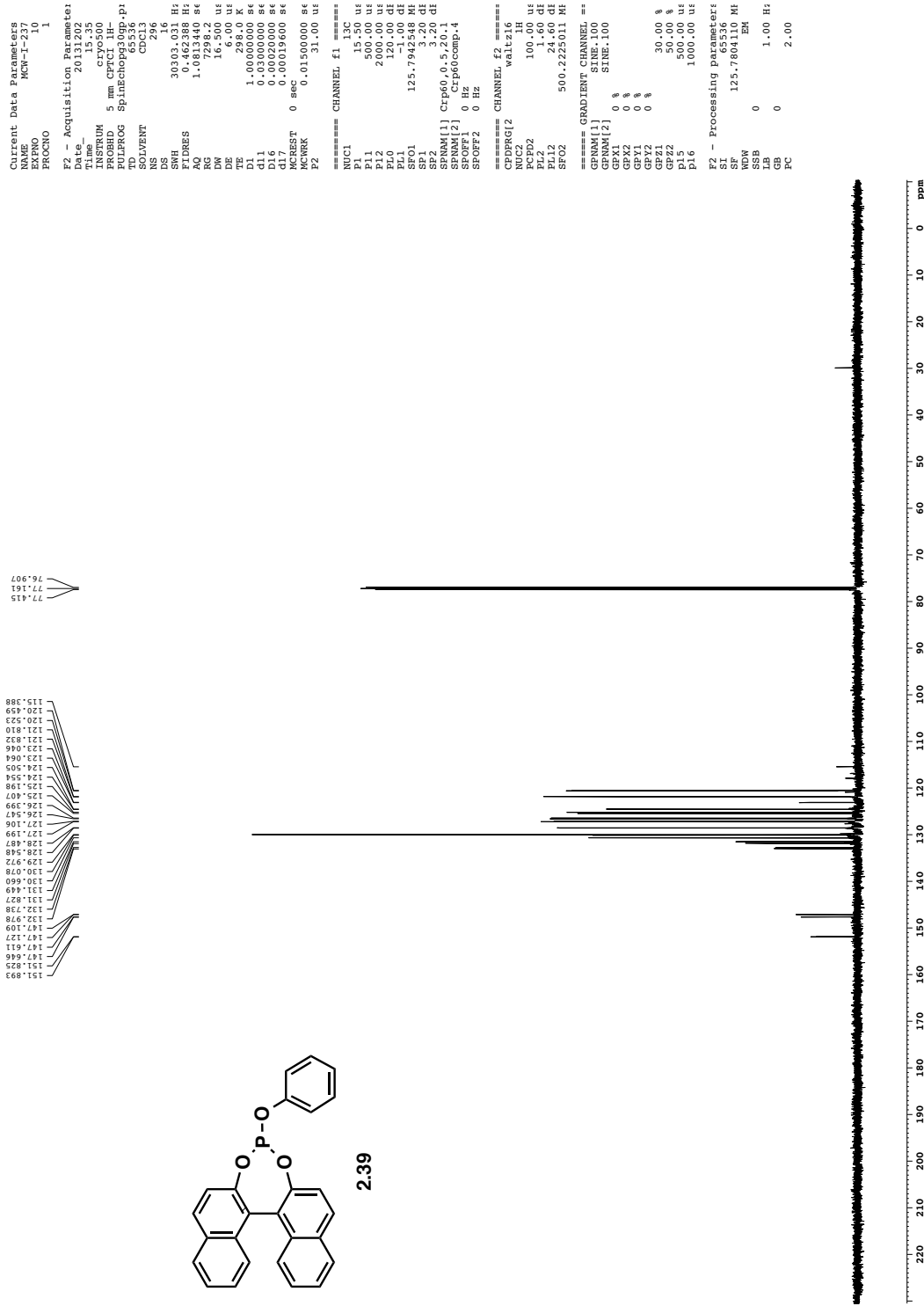
Purified Product



2.39

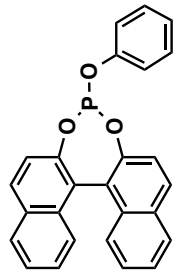


Purified Product



Purified Product

98.85%

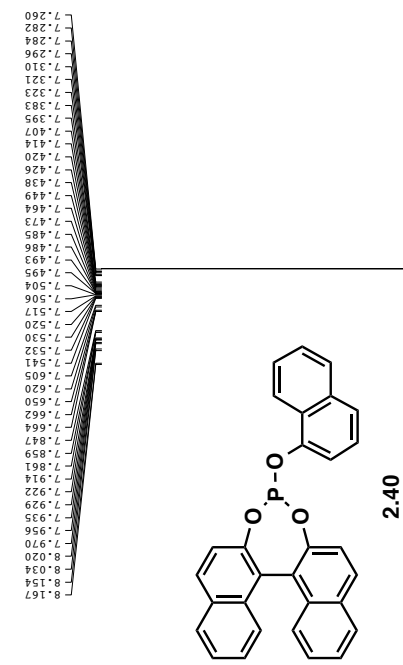


2.39

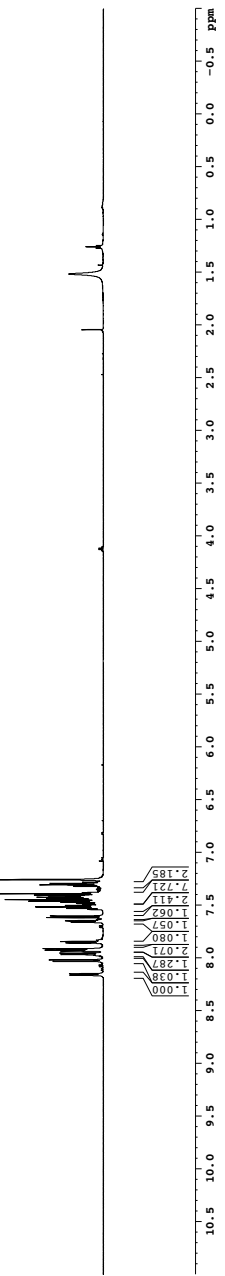
Current Data Parameters
NMR-T 277
EXPNO 8
PROCNO 1
F2 - Acquisition Parameters
Date 20131202
Time 11:35
INSTRUM TBI
PROBHD 5 mm TBI AW110
BPPROG 65930
TD 65536
SOLVENT CDCl3
NS 35
DS 4
SWH 101166.64 Hz
ETRATES 0.13944 Hz
AQ 0.34728 sec
RG 2050
DW 4.800 us
DE 6.69 us
TE 294.5 K
D1 1.0000000 sec
TD0 ===== CHANNEL f1 =====
NUC1 P1 31P
PLM1 173.41079712 W
SFO1 242.9407210 MHz
F2 - Processing Parameters
SI 65536
SP 242.9370912 MHz
WDW 0
SSB 0
LB 2.00 Hz
GB 0
PC 1.00



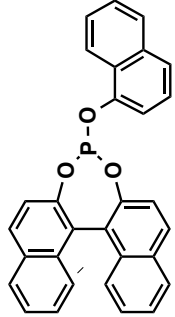
Purified Product



Current Data Parameters
NAME: MCM-T-236
PROCNO: 1
Date: 2013.12.01
Time: 9:34
INSTRUM: 5 mm TBI
PROBOD: 1H
PULPROG: TD
SOLVENT: CDCl₃
NS: 15
SWH: 961.35 Hz
FIDRES: 0.098042 Hz
AQ: 5.0998478 sec
RG: 35
DE: 52.00 usec
TE: 14.54 usec
D1: 298.1 K
TD0: 0.1000000 sec
==== CHANNEL F1 ======
NUC1: 1H
P1: 2.3.01449.00 usec
SP01: 600.1342099 MHz
==== Processing Parameters ====
PS: 600.1300322 MHz
SF: 600.1300322 MHz
NDW: 0
SSB: 0
LB: 0.30 Hz
GB: 0
PC: 1.00

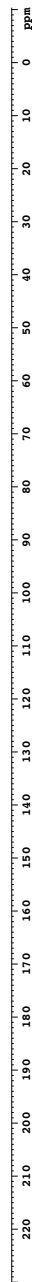


Purified Product



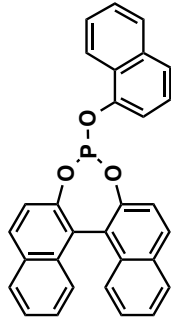
240

77.413	77.159	76.905
17.954	17.787	17.620
17.787	17.620	17.453
17.620	17.453	17.286
17.453	17.286	17.119
17.286	17.119	16.952
17.119	16.952	16.785
16.952	16.785	16.618
16.785	16.618	16.451
16.618	16.451	16.294
16.451	16.294	16.127
16.294	16.127	15.950
16.127	15.950	15.783
15.950	15.783	15.616
15.783	15.616	15.449
15.616	15.449	15.282
15.449	15.282	15.115
15.282	15.115	14.948
15.115	14.948	14.781
14.948	14.781	14.614
14.781	14.614	14.447
14.614	14.447	14.280
14.447	14.280	14.113
14.280	14.113	13.946
14.113	13.946	13.779
13.946	13.779	13.612
13.779	13.612	13.445
13.612	13.445	13.278
13.445	13.278	13.111
13.278	13.111	12.944
13.111	12.944	12.777
12.944	12.777	12.610
12.777	12.610	12.443
12.610	12.443	12.246
12.443	12.246	12.079
12.246	12.079	11.912
12.079	11.912	11.745
11.912	11.745	11.578
11.745	11.578	11.411
11.578	11.411	11.244
11.411	11.244	11.077
11.244	11.077	10.910
11.077	10.910	10.753
10.910	10.753	10.586
10.753	10.586	10.419
10.586	10.419	10.252
10.419	10.252	10.095
10.252	10.095	9.928
10.095	9.928	9.761
9.928	9.761	9.594
9.761	9.594	9.427
9.594	9.427	9.260
9.427	9.260	9.093
9.260	9.093	8.926
9.093	8.926	8.759
8.926	8.759	8.592
8.759	8.592	8.425
8.592	8.425	8.258
8.425	8.258	8.091
8.258	8.091	7.924
8.091	7.924	7.757
7.924	7.757	7.590
7.757	7.590	7.423
7.590	7.423	7.256
7.423	7.256	7.099
7.256	7.099	6.932
7.099	6.932	6.765
6.932	6.765	6.598
6.765	6.598	6.431
6.598	6.431	6.264
6.765	6.598	6.197
6.431	6.264	6.129
6.598	6.431	6.062
6.264	6.129	5.995
6.431	6.264	5.928
6.129	6.062	5.861
6.264	6.129	5.794
6.062	5.995	5.727
6.129	6.062	5.660
6.264	6.129	5.593
6.129	6.062	5.526
6.062	5.995	5.459
6.129	6.062	5.392
6.264	6.129	5.325
6.129	6.062	5.258
6.062	5.995	5.191
6.129	6.062	5.124
6.264	6.129	5.057
6.129	6.062	4.990
6.062	5.995	4.923
6.129	6.062	4.856
6.264	6.129	4.789
6.129	6.062	4.722
6.062	5.995	4.655
6.129	6.062	4.588
6.264	6.129	4.521
6.129	6.062	4.454
6.062	5.995	4.387
6.129	6.062	4.320
6.264	6.129	4.253
6.129	6.062	4.186
6.062	5.995	4.119
6.129	6.062	4.052
6.264	6.129	3.985
6.129	6.062	3.918
6.062	5.995	3.851
6.129	6.062	3.784
6.264	6.129	3.717
6.129	6.062	3.650
6.062	5.995	3.583
6.129	6.062	3.516
6.264	6.129	3.449
6.129	6.062	3.382
6.062	5.995	3.315
6.129	6.062	3.248
6.264	6.129	3.181
6.129	6.062	3.114
6.062	5.995	3.047
6.129	6.062	2.980
6.264	6.129	2.913
6.129	6.062	2.846
6.062	5.995	2.779
6.129	6.062	2.712
6.264	6.129	2.645
6.129	6.062	2.578
6.062	5.995	2.511
6.129	6.062	2.444
6.264	6.129	2.377
6.129	6.062	2.310
6.062	5.995	2.243
6.129	6.062	2.173
6.264	6.129	2.106
6.129	6.062	2.039
6.062	5.995	1.972
6.129	6.062	1.905
6.264	6.129	1.838
6.129	6.062	1.771
6.062	5.995	1.704
6.129	6.062	1.637
6.264	6.129	1.570
6.129	6.062	1.503
6.062	5.995	1.436
6.129	6.062	1.369
6.264	6.129	1.302
6.129	6.062	1.235
6.062	5.995	1.168
6.129	6.062	1.101
6.264	6.129	1.034
6.129	6.062	0.967
6.062	5.995	0.900
6.129	6.062	0.833
6.264	6.129	0.766
6.129	6.062	0.700
6.062	5.995	0.633
6.129	6.062	0.566
6.264	6.129	0.500
6.129	6.062	0.433
6.062	5.995	0.366
6.129	6.062	0.300
6.264	6.129	0.233
6.129	6.062	0.166
6.062	5.995	0.100
6.129	6.062	0.033
6.264	6.129	-0.133
6.129	6.062	-0.200
6.062	5.995	-0.267
6.129	6.062	-0.333
6.264	6.129	-0.400
6.129	6.062	-0.467
6.062	5.995	-0.533
6.129	6.062	-0.600
6.264	6.129	-0.667
6.129	6.062	-0.733
6.062	5.995	-0.800
6.129	6.062	-0.867
6.264	6.129	-0.933
6.129	6.062	-1.000
6.062	5.995	-1.067
6.129	6.062	-1.133
6.264	6.129	-1.200
6.129	6.062	-1.267
6.062	5.995	-1.333
6.129	6.062	-1.400
6.264	6.129	-1.467
6.129	6.062	-1.533
6.062	5.995	-1.600
6.129	6.062	-1.667
6.264	6.129	-1.733
6.129	6.062	-1.800
6.062	5.995	-1.867
6.129	6.062	-1.933
6.264	6.129	-2.000
6.129	6.062	-2.067
6.062	5.995	-2.133
6.129	6.062	-2.200
6.264	6.129	-2.267
6.129	6.062	-2.333
6.062	5.995	-2.400
6.129	6.062	-2.467
6.264	6.129	-2.533
6.129	6.062	-2.600
6.062	5.995	-2.667
6.129	6.062	-2.733
6.264	6.129	-2.800
6.129	6.062	-2.867
6.062	5.995	-2.933
6.129	6.062	-3.000
6.264	6.129	-3.067
6.129	6.062	-3.133
6.062	5.995	-3.200
6.129	6.062	-3.267
6.264	6.129	-3.333
6.129	6.062	-3.400
6.062	5.995	-3.467
6.129	6.062	-3.533
6.264	6.129	-3.600
6.129	6.062	-3.667
6.062	5.995	-3.733
6.129	6.062	-3.800
6.264	6.129	-3.867
6.129	6.062	-3.933
6.062	5.995	-4.000
6.129	6.062	-4.067
6.264	6.129	-4.133
6.129	6.062	-4.200
6.062	5.995	-4.267
6.129	6.062	-4.333
6.264	6.129	-4.400
6.129	6.062	-4.467
6.062	5.995	-4.533
6.129	6.062	-4.600
6.264	6.129	-4.667
6.129	6.062	-4.733
6.062	5.995	-4.800
6.129	6.062	-4.867
6.264	6.129	-4.933
6.129	6.062	-5.000
6.062	5.995	-5.067
6.129	6.062	-5.133
6.264	6.129	-5.200
6.129	6.062	-5.267
6.062	5.995	-5.333
6.129	6.062	-5.400
6.264	6.129	-5.467
6.129	6.062	-5.533
6.062	5.995	-5.600
6.129	6.062	-5.667
6.264	6.129	-5.733
6.129	6.062	-5.800
6.062	5.995	-5.867
6.129	6.062	-5.933
6.264	6.129	-6.000
6.129	6.062	-6.067
6.062	5.995	-6.133
6.129	6.062	-6.200
6.264	6.129	-6.267
6.129	6.062	-6.333
6.062	5.995	-6.400
6.129	6.062	-6.467
6.264	6.129	-6.533
6.129	6.062	-6.600
6.062	5.995	-6.667
6.129	6.062	-6.733
6.264	6.129	-6.800
6.129	6.062	-6.867
6.062	5.995	-6.933
6.129	6.062	-7.000
6.264	6.129	-7.067
6.129	6.062	-7.133
6.062	5.995	-7.200
6.129	6.062	-7.267
6.264	6.129	-7.333
6.129	6.062	-7.400
6.062	5.995	-7.467
6.129	6.062	-7.533
6.264	6.129	-7.600
6.129	6.062	-7.667
6.062	5.995	-7.733
6.129	6.062	-7.800
6.264	6.129	-7.867
6.129	6.062	-7.933
6.062	5.995	-8.000
6.129	6.062	-8.067
6.264	6.129	-8.133
6.129	6.062	-8.200
6.062	5.995	-8.267
6.129	6.062	-8.333
6.264	6.129	-8.400
6.129	6.062	-8.467
6.062	5.995	-8.533
6.129	6.062	-8.600
6.264	6.129	-8.667
6.129	6.062	-8.733
6.062	5.995	-8.800
6.129	6.062	-8.867
6.264	6.129	-8.933
6.129	6.062	-9.000
6.062	5.995	-9.067
6.129	6.062	-9.133
6.264	6.129	-9.200
6.129	6.062	-9.267
6.062	5.995	-9.333
6.129	6.062	-9.400
6.264	6.129	-9.467
6.129	6.062	-9.533
6.062	5.995	-9.600
6.129	6.062	-9.667
6.264	6.129	-9.733
6.129	6.062	-9.800
6.062	5.995	-9.867
6.129	6.062	-9.933
6.264	6.129	-10.000
6.129	6.062	-10.067
6.062	5.995	-10.133
6.129	6.062	-10.200
6.264	6.129	-10.267
6.129	6.062	-10.333
6.062	5.995	-10.400
6.129	6.062	-10.467
6.264	6.129	-10.533
6.129	6.062	-10.600
6.062	5.995	-10.667
6.129	6.062	-10.733
6.264	6.129	-10.800
6.129	6.062	-10.867
6.062	5.995	-10.933
6.129	6.062	-11.000
6.264	6.129	-11.067
6.129	6.062	-11.133
6.062	5.995	-11.200
6.129	6.062	-11.267
6.264	6.129	-11.333
6.129	6.062	-11.400
6.062	5.995	-11.467
6.129	6.062	-11.533
6.264	6.129	-11.600
6.129	6.062	-11.667
6.062	5.995	-11.733
6.129	6.062	-11.800
6.264	6.129	-11.867
6.129	6.062	-11.933
6.062	5.995	-12.000
6.129	6.062	-12.067
6.264	6.129	-12.133
6.129	6.062	-12.200
6.062	5.995	-12.267
6.129	6.062	-12.333
6.264	6.129	-12.400
6.129	6.062	-12.467
6.062	5.995	-12.533
6.129	6.062	-12.600
6.264	6	



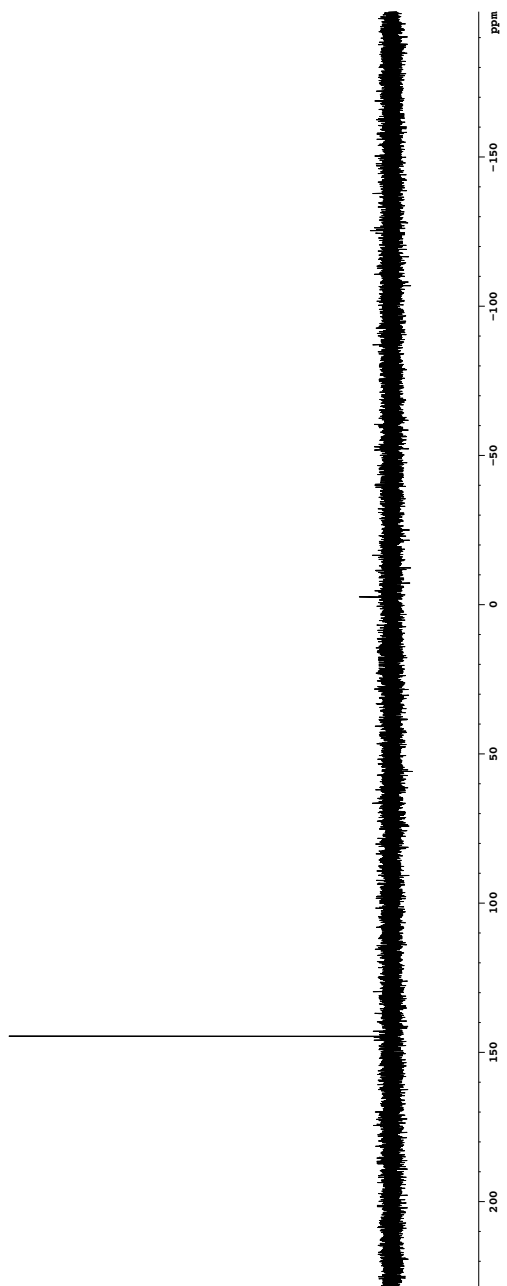
Purified Product

144.571



2.40

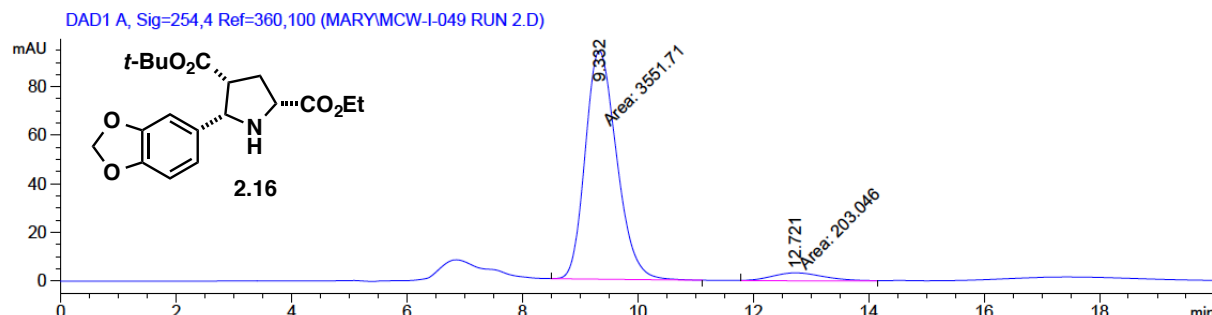
Current Data Parameters
NMR-T-216
EXPNO 1
PROCNO 1
F2 - Acquisition Parameters
Date 20131201
Time 9:37
INSTRUM TBI
PROBHD 5 mm TBI AW13
BPPRGR 65930
TD 65536
DS 54
NS 104166
SWH 6.64 Hz
ETDRES 0.13944 s
AQ 2050
RG 4,800 us
DE 6.69 us
TE 298.0 K
D1 1.0000000 se
TD0 1
===== CHANNEL f1 =====
NUC1 P1 31P
PLM1 173.41079712 W
SFO1 242.9407210 MHz
F2 - Processing Parameters
SI 65536
SP 242.9469071 MHz
WDW 0
SSB 0
LB 2.00 Hz
GB 0
PC 1.00



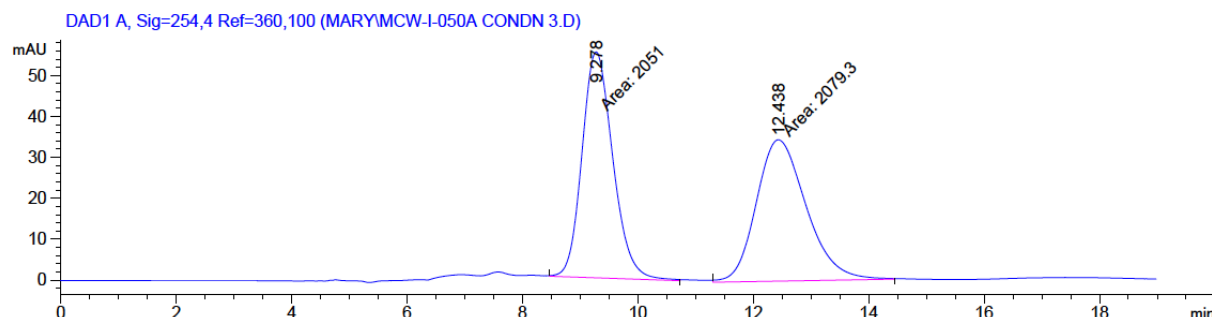
2.7 Appendix C: Enantioselective HPLC Chromatograms

2.16, Table 2.2, entry 1 [(*R*)-QUINAP], 90% ee:

Daicel Chiralpak AS, *i*-PrOH/*n*-hexane 60:40, flow rate 1.0 mL/min, $\lambda = 254$ nm.

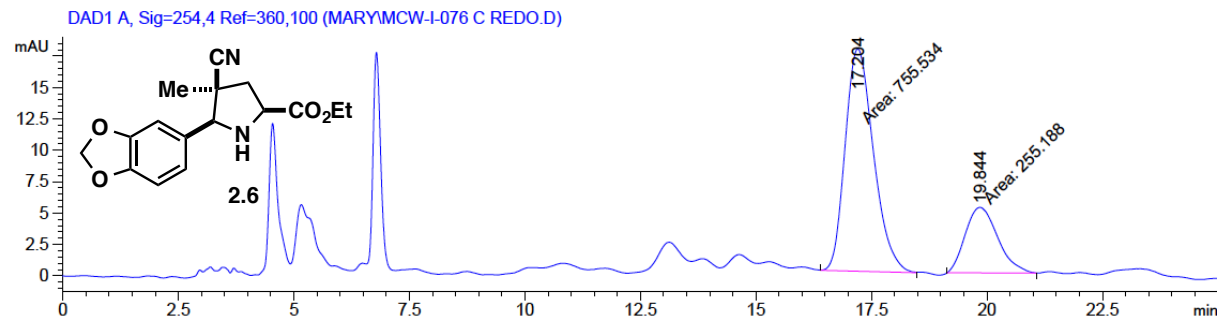


2.16, racemic standard:



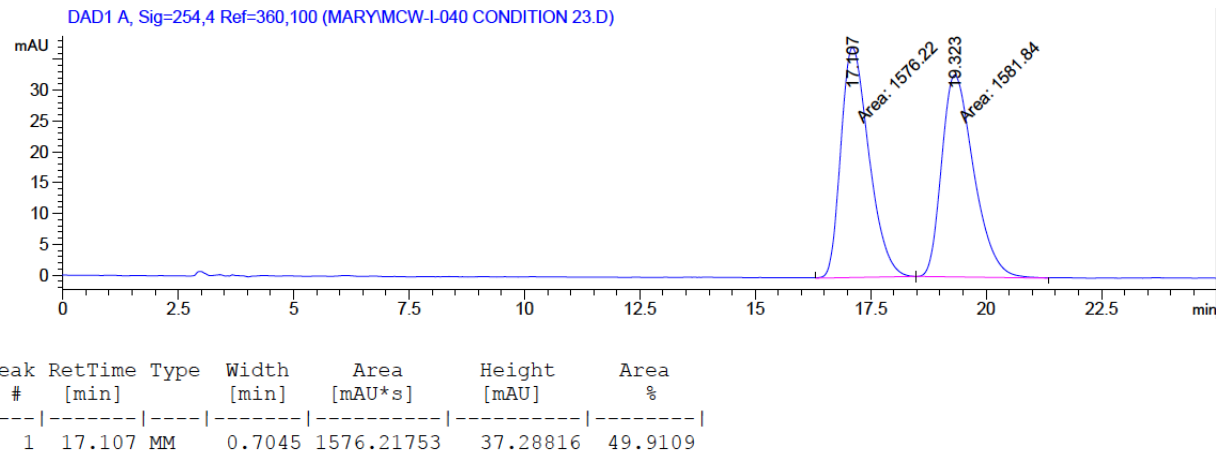
2.6, eq 2.5 [(R_p) -FeSulPhos], 50% ee:

Daicel Chiralpak OD-H III column; flow: 1.0 mL/min; 20:80 *i*-PrOH:*n*-hexane; $\lambda = 254$ nm.



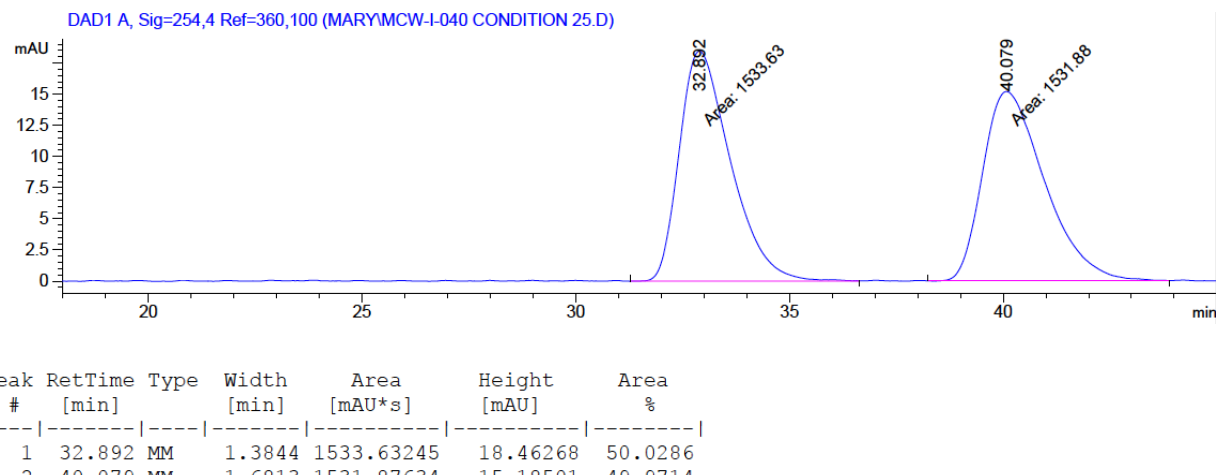
Peak	RetTime	Type	Width	Area	Height	Area %
#	[min]		[min]	[mAU*s]	[mAU]	%
1	17.204	MM	0.7111	755.53387	17.70918	74.7519
2	19.844	MM	0.8149	255.18791	5.21936	25.2481

2.6, racemic standard:

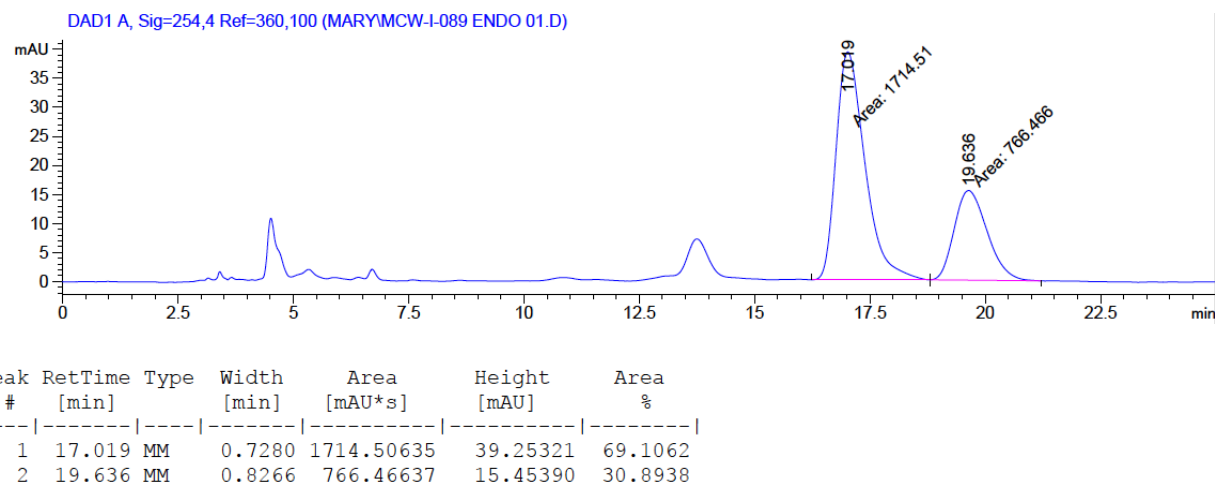


2.6, racemic standard:

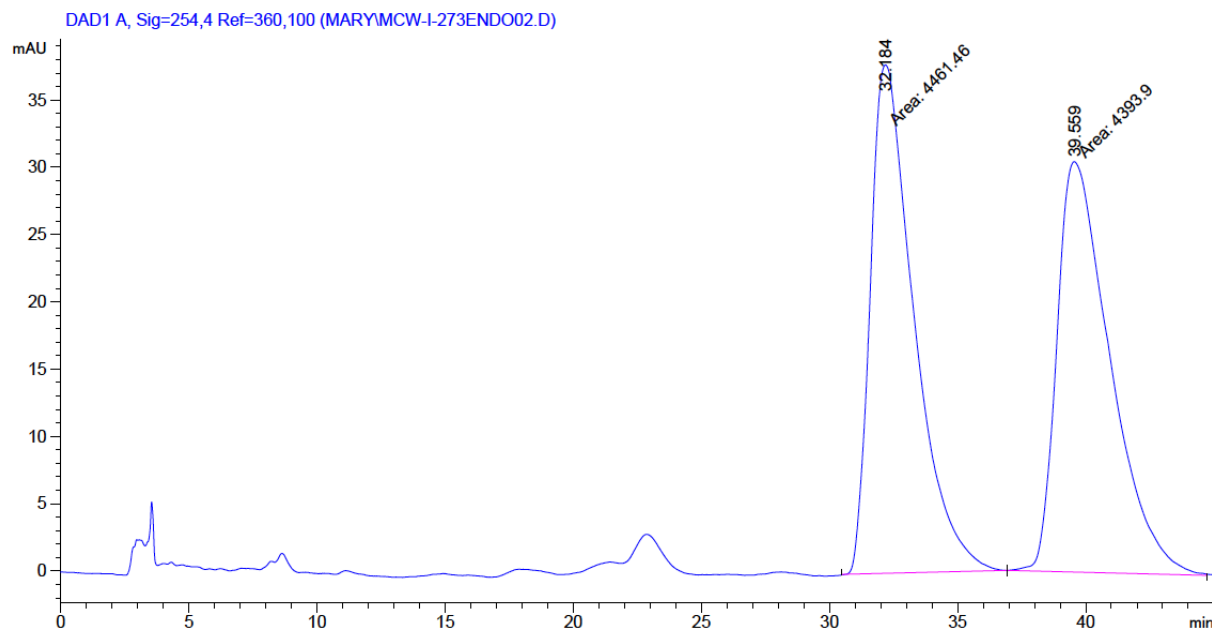
Daicel Chiralpak OD-H III column; flow: 1.0 mL/min; 10:90 *i*-PrOH:*n*-hexane; $\lambda = 254$ nm.



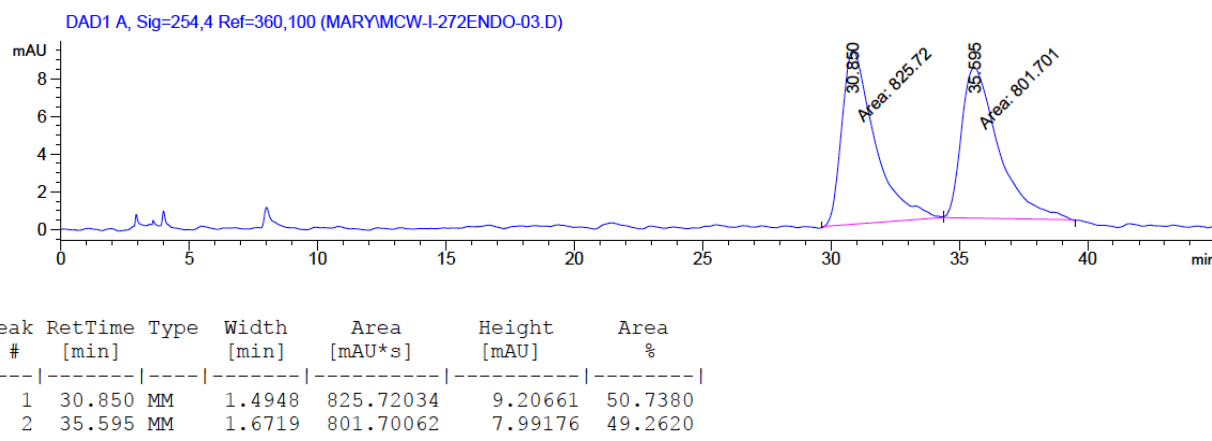
2.6, Table 2.4, entry 1 [(R_p) -FeSulPhos], 38% ee:



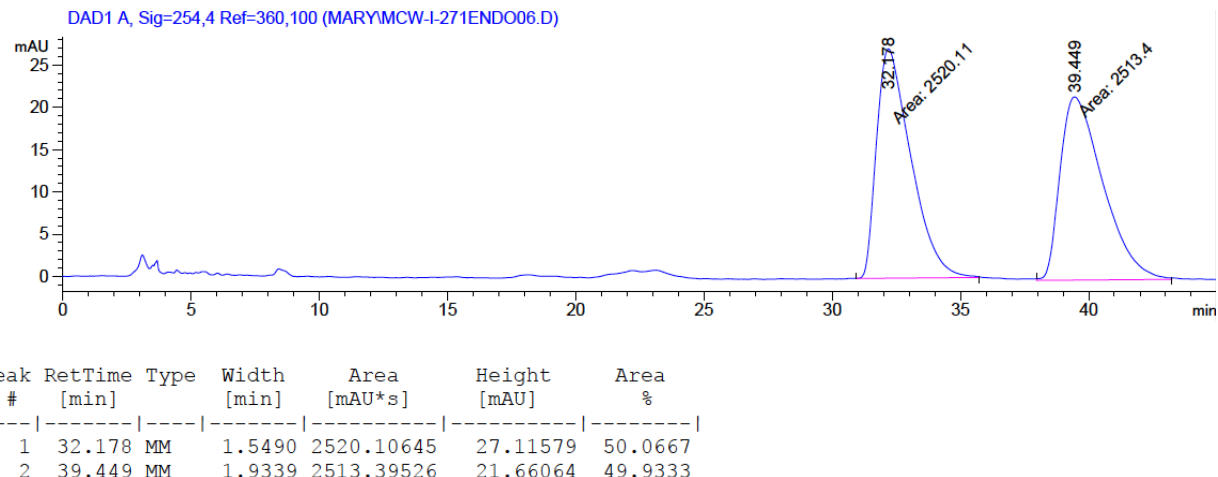
2.6, Table 2.5, entry 1 [(R)-2.23], 0% ee:



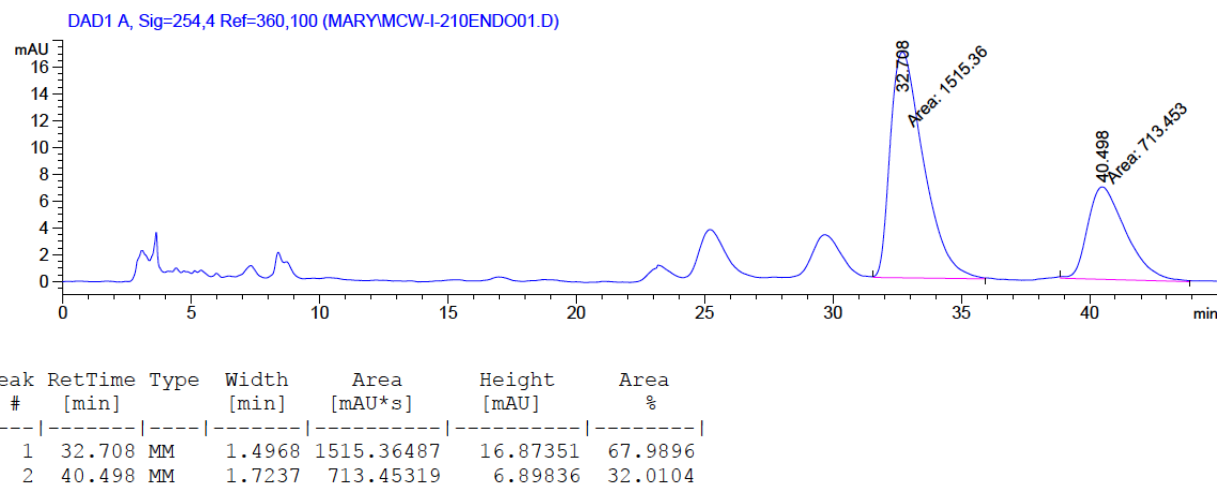
2.6, Table 2.5, entry 2 [(R)-2.24], 2% ee:



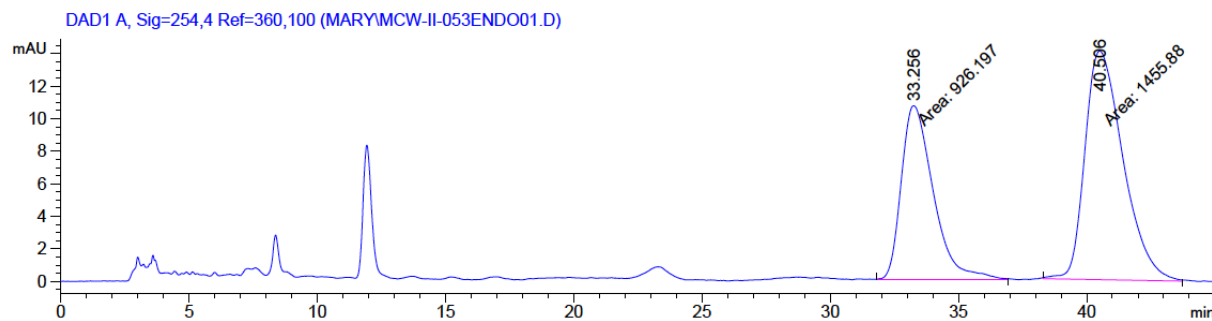
2.6, Table 2.5, entry 3 [(R)-2.25**], 0% ee:**



2.6, Table 2.6, entry 1 [(S)-Monophos], 36% ee:

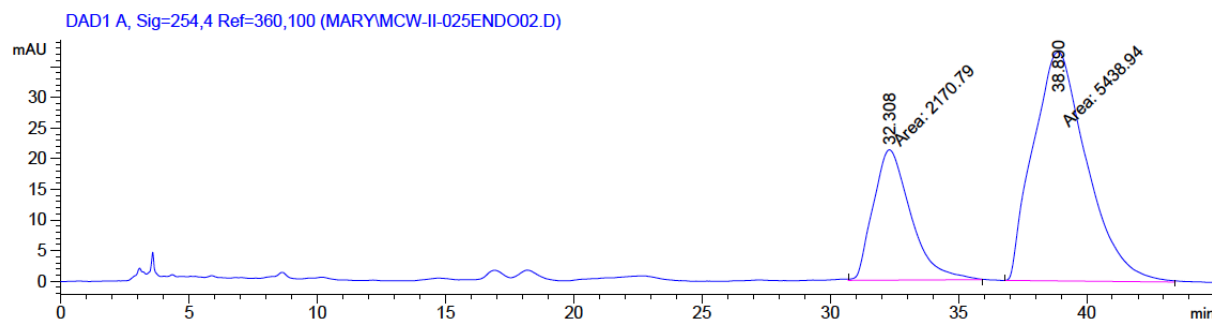


2.6, Table 2.6, entry 2 [(S)-2.27], 22% ee:



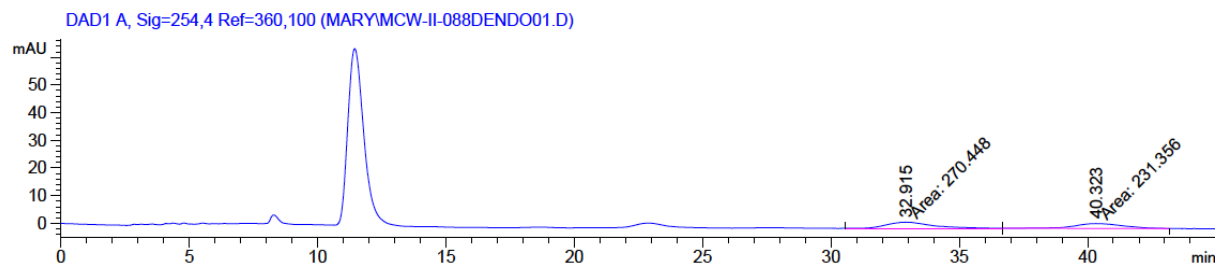
Peak #	RetTime [min]	Type	Width [min]	Area [mAU*s]	Height [mAU]	Area %
1	33.256	MM	1.4456	926.19733	10.67804	38.8819
2	40.506	MM	1.7254	1455.88086	14.06330	61.1181

2.6, Table 2.6, entry 3 [(R,S)-2.28], 43% ee:



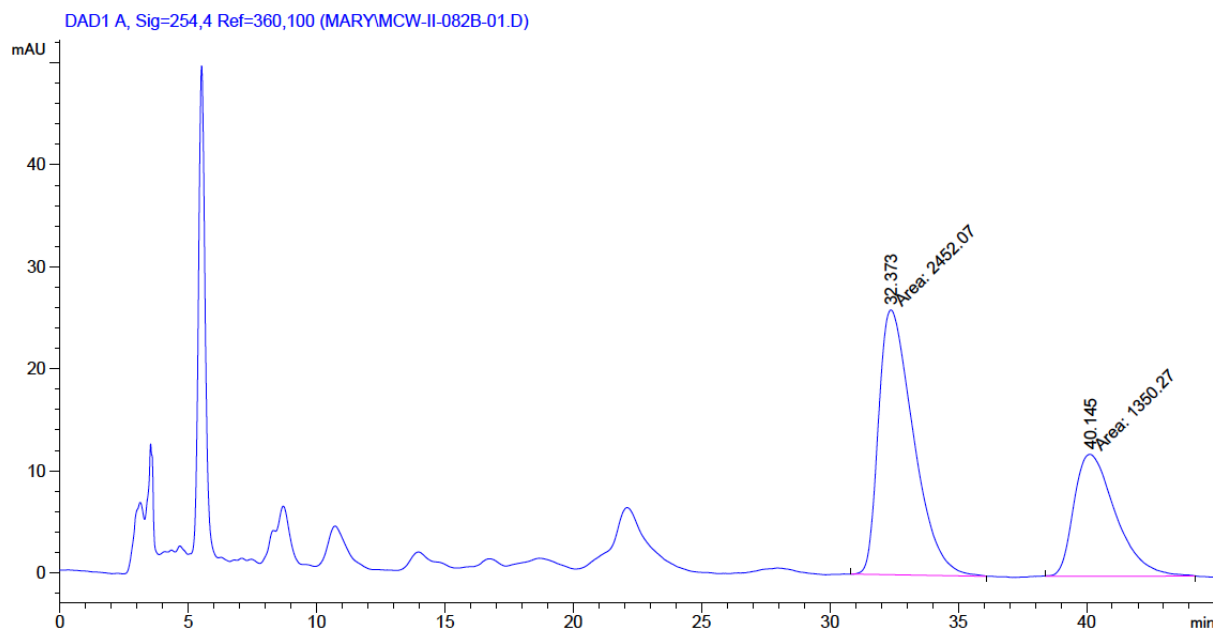
Peak #	RetTime [min]	Type	Width [min]	Area [mAU*s]	Height [mAU]	Area %
1	32.308	MM	1.7009	2170.79370	21.27077	28.5265
2	38.890	MM	2.4261	5438.94141	37.36426	71.4735

2.6, Table 2.7, entry 1 [(S)-H₈-Monophos], 8% ee:



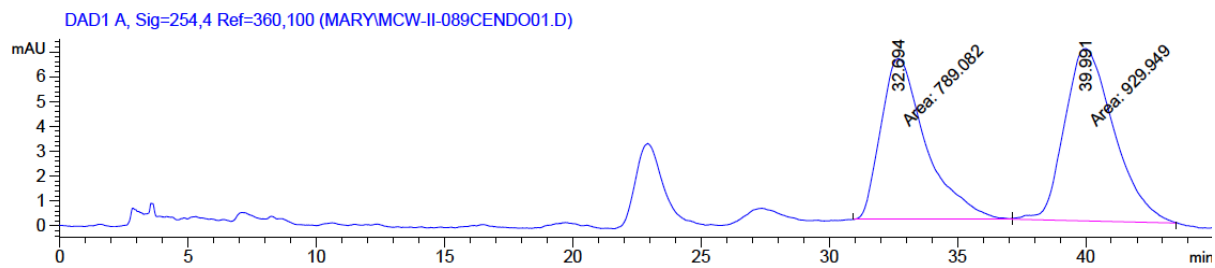
Peak #	RetTime [min]	Type	Width [min]	Area [mAU*s]	Height [mAU]	Area %
1	32.915	MM	2.0348	270.44794	2.21514	53.8951
2	40.323	MM	2.2183	231.35614	1.73826	46.1049

2.6, Table 2.7, entry 3 [(S)-2.34], 29% ee:

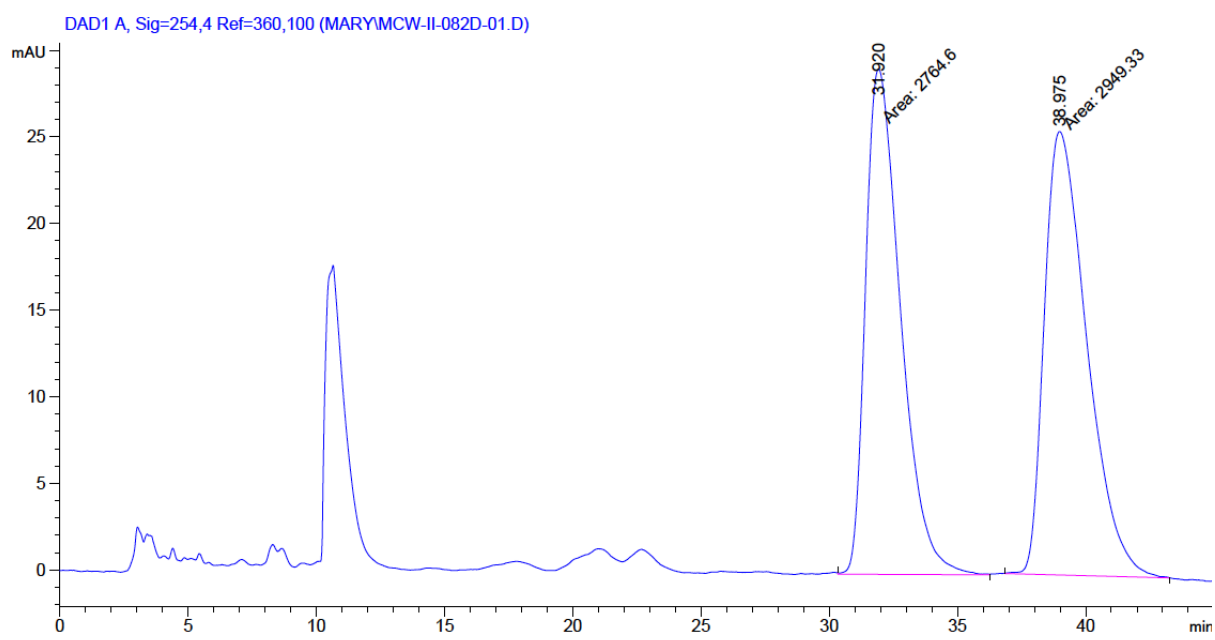


Peak #	RetTime [min]	Type	Width [min]	Area [mAU*s]	Height [mAU]	Area %
1	32.373	MM	1.5741	2452.07227	25.96318	64.4884
2	40.145	MM	1.8827	1350.27161	11.95354	35.5116

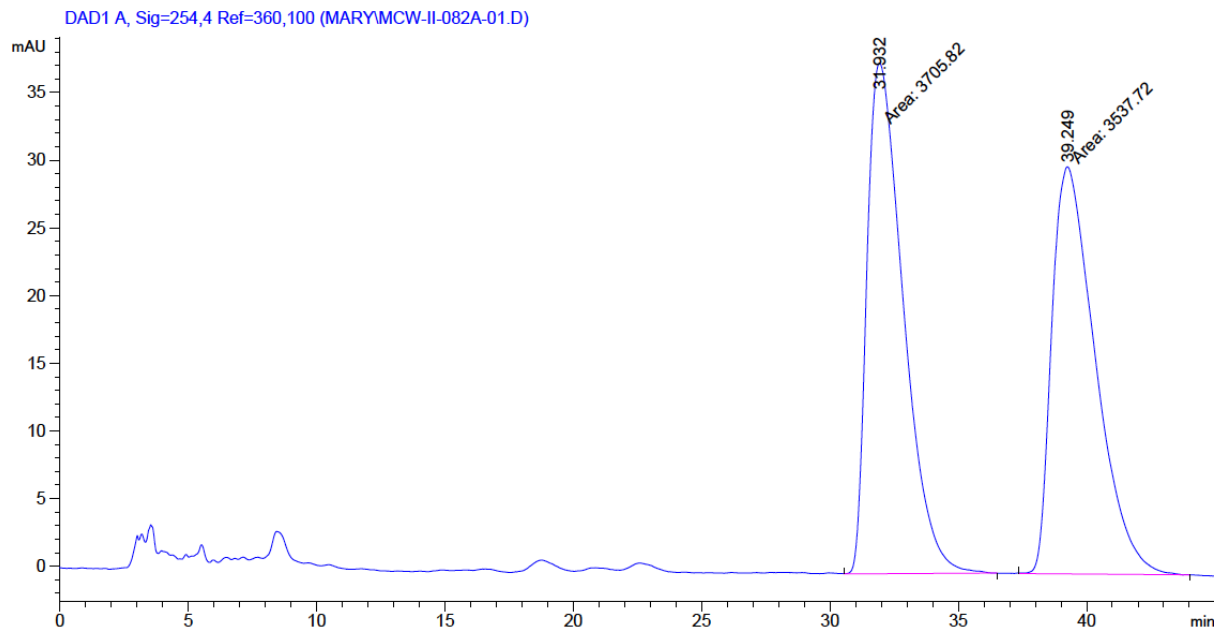
2.6, Table 2.7, entry 5 [(S,S,S)-2.35], 8% ee:



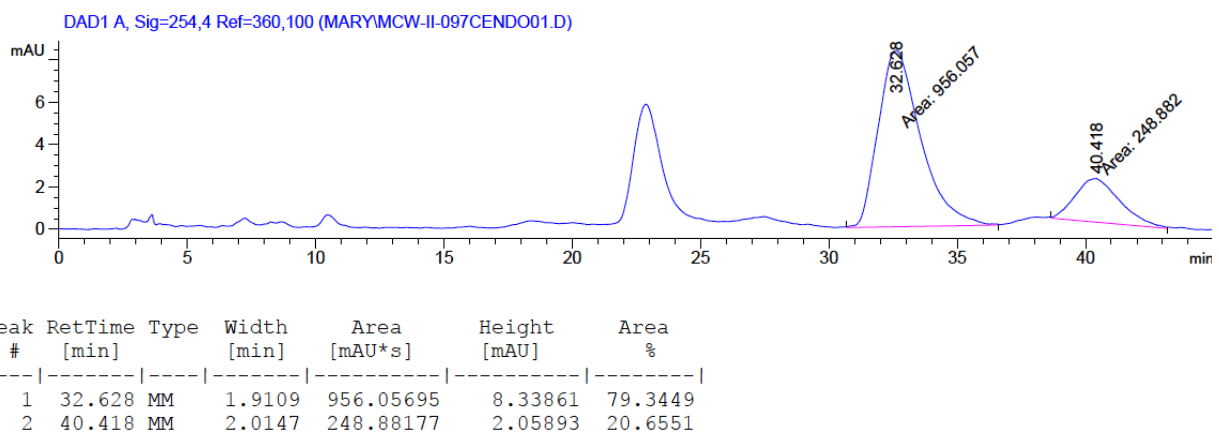
2.6, Table 2.7, entry 6 [(S,R,R)-2.36], 4% ee:



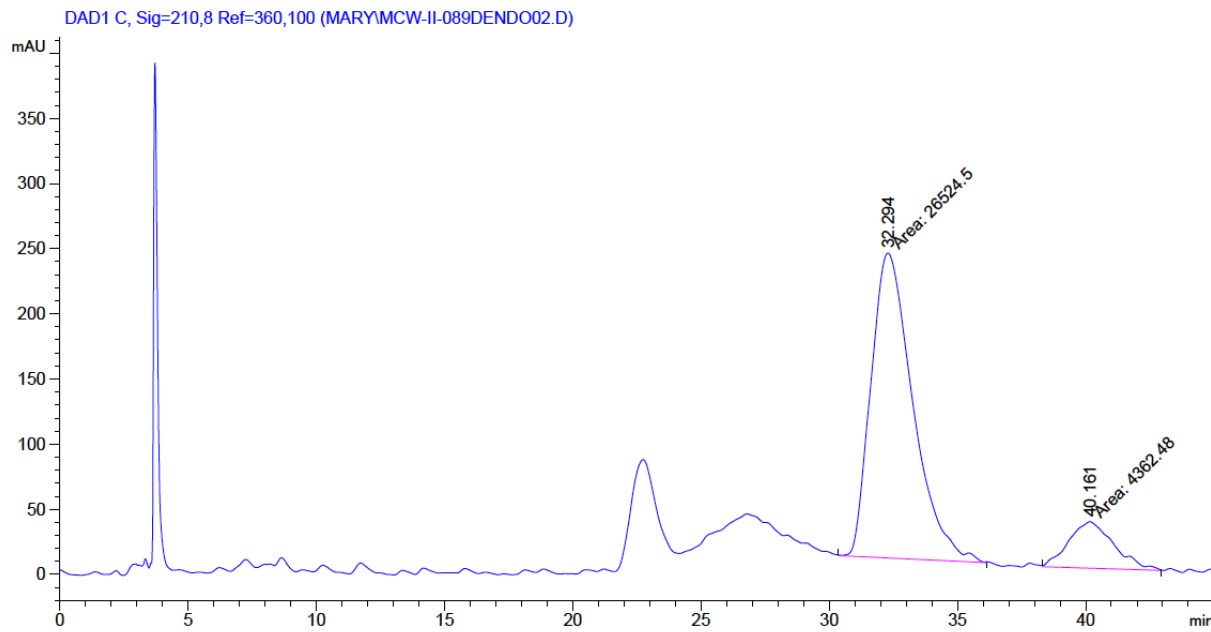
2.6, Table 2.7, entry 7 [(S,R,R)-2.37], 2% ee:



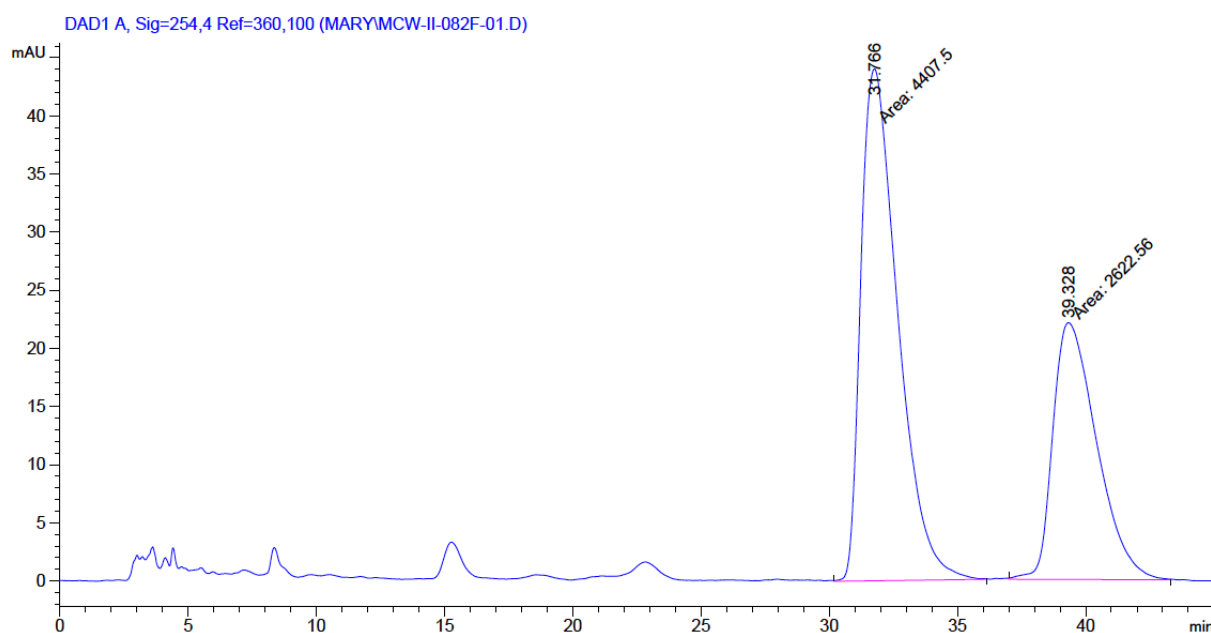
2.6, Table 2.7, entry 8 [(R,R,R)-2.30], 58% ee:



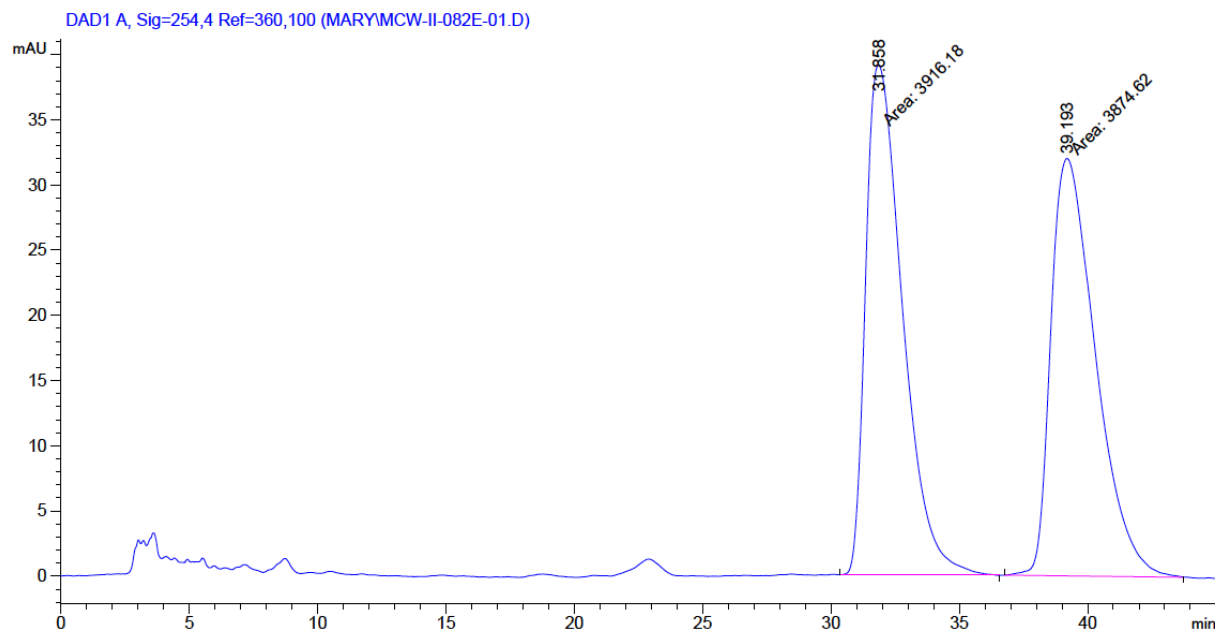
2.6, Table 2.7, entry 9 [(R,S)-(1-Nph)-Quinaphos], 72% ee:



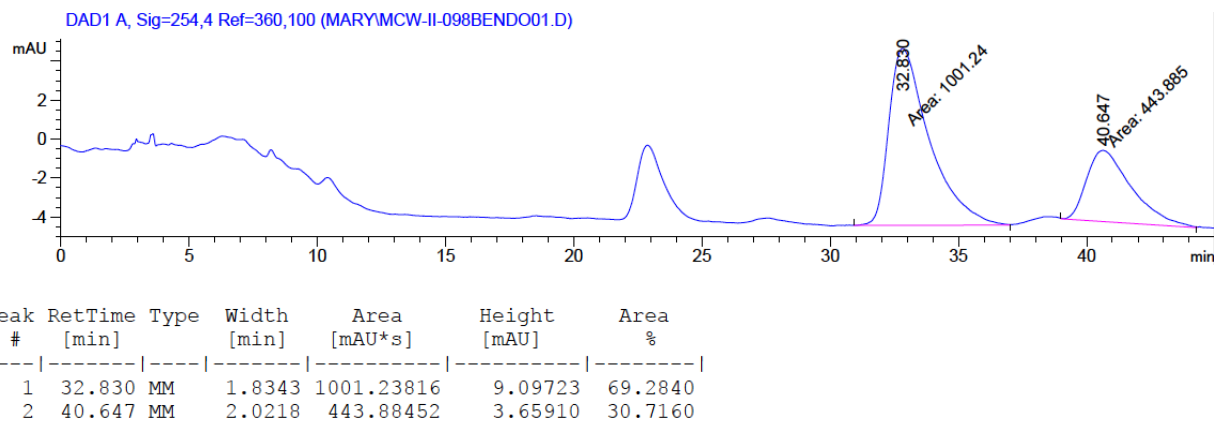
2.6, Table 2.7, entry 10 [(R)-SIPHOS], 26% ee:



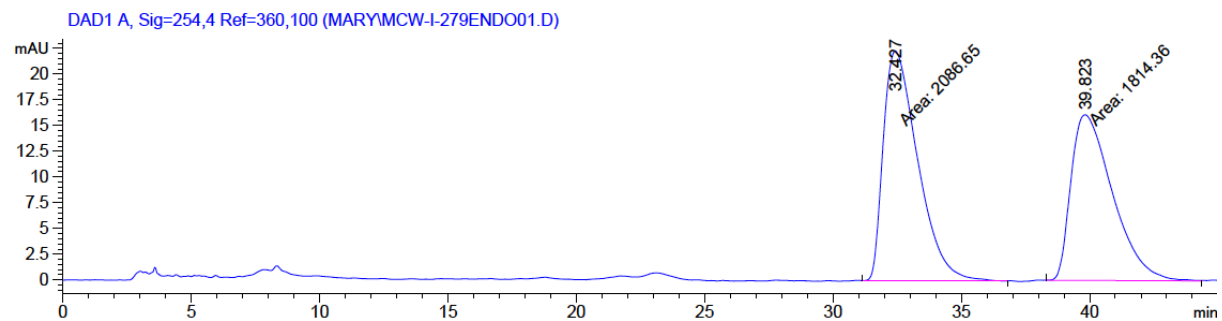
2.6, Table 2.7, entry 11 [(R,R,R)-2.31], 0% ee:



2.6, Table 2.7, entry 12 [(R,R)-2.32], 38% ee:

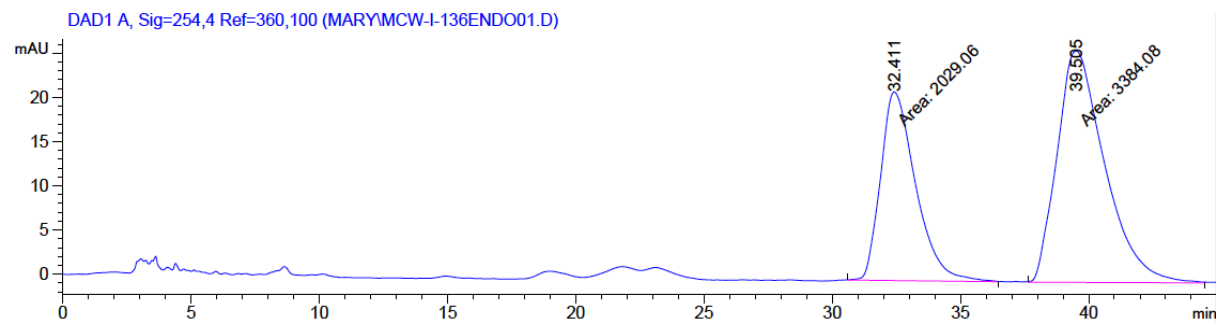


2.6, Table 2.11, entry 1 (SL-J002-2), 7% ee:



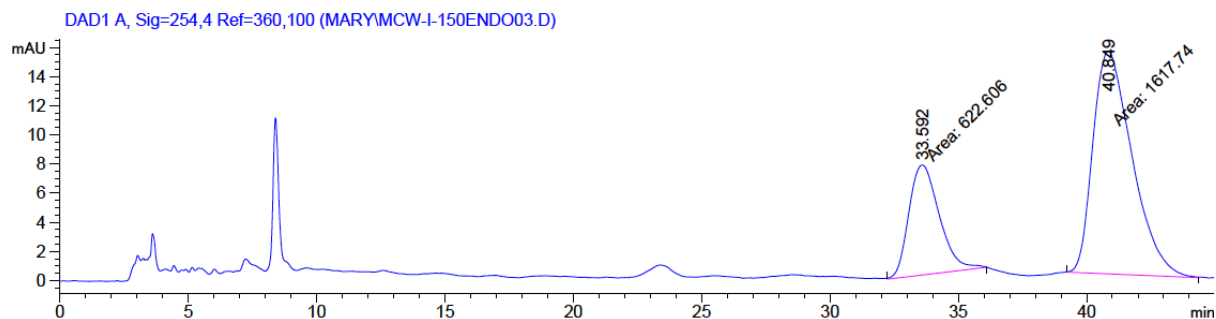
Peak #	RetTime [min]	Type	Width [min]	Area [mAU*s]	Height [mAU]	Area %
1	32.427	MM	1.5561	2086.65234	22.34980	53.4900
2	39.823	MM	1.8785	1814.36462	16.09728	46.5100

2.6, Table 2.11, entry 2 [(S,S)-DIOP], 25% ee:



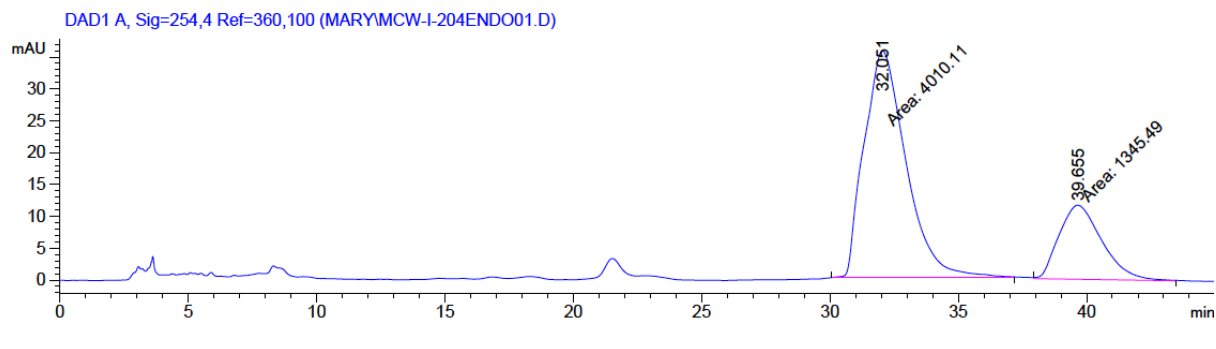
Peak #	RetTime [min]	Type	Width [min]	Area [mAU*s]	Height [mAU]	Area %
1	32.411	MM	1.5839	2029.05505	21.35107	37.4839
2	39.505	MM	2.1531	3384.07886	26.19565	62.5161

2.6, Table 2.11, entry 3 [(R,R)-Me-DUPHOS], 44% ee:



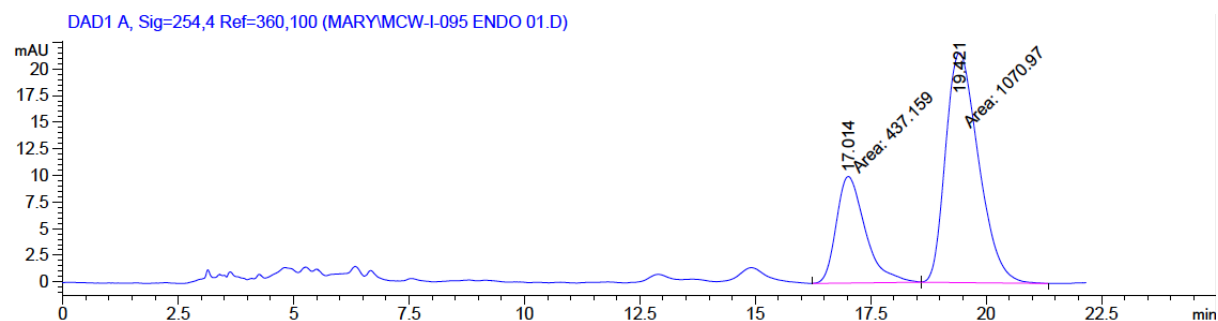
Peak #	RetTime [min]	Type	Width [min]	Area [mAU*s]	Height [mAU]	Area %
1	33.592	MM	1.3743	622.60614	7.55071	27.7906
2	40.849	MM	1.7623	1617.73853	15.29978	72.2094

2.6, Table 2.11, entry 4 [(S,S)-DACH-phenyl], 50% ee:



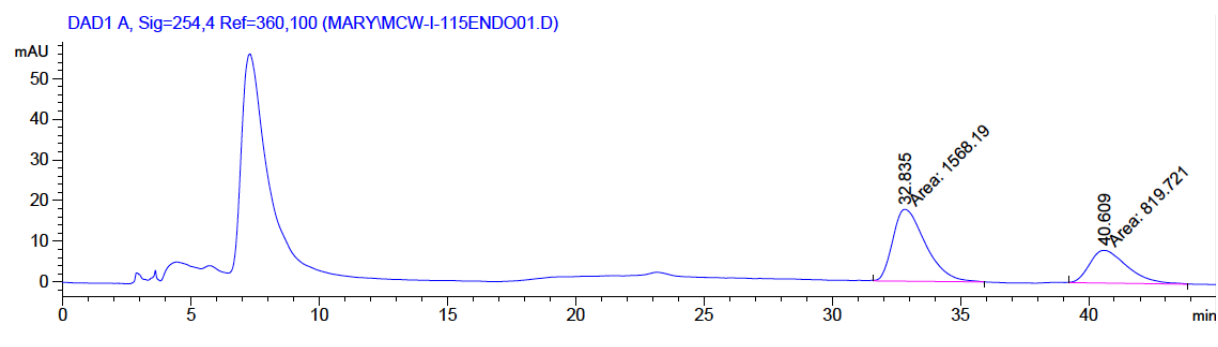
Peak #	RetTime [min]	Type	Width [min]	Area [mAU*s]	Height [mAU]	Area %
1	32.051	MM	1.8828	4010.11475	35.49694	74.8770
2	39.655	MM	1.9291	1345.48645	11.62436	25.1230

2.6, Table 2.11, entry 5 [(S)-BINAP], 42% ee:



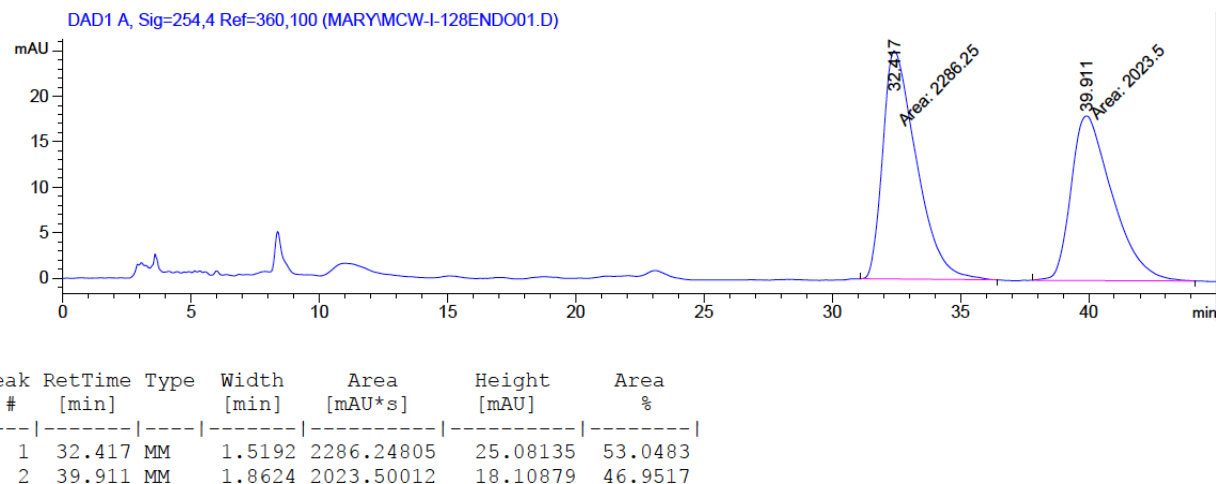
Peak #	RetTime [min]	Type	Width [min]	Area [mAU*s]	Height [mAU]	Area %
1	17.014	MM	0.7279	437.15881	10.00983	28.9868
2	19.421	MM	0.8269	1070.97400	21.58552	71.0132

2.6, Table 2.11, entry 6 [(R)-TolBINAP], 32% ee:

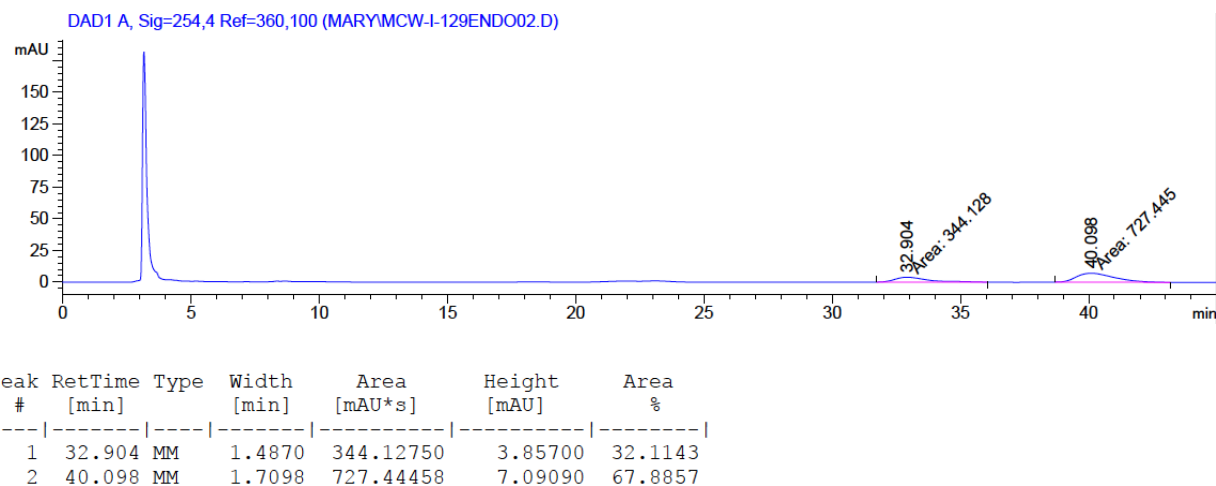


Peak #	RetTime [min]	Type	Width [min]	Area [mAU*s]	Height [mAU]	Area %
1	32.835	MM	1.4781	1568.19141	17.68276	65.6721
2	40.609	MM	1.6980	819.72076	8.04581	34.3279

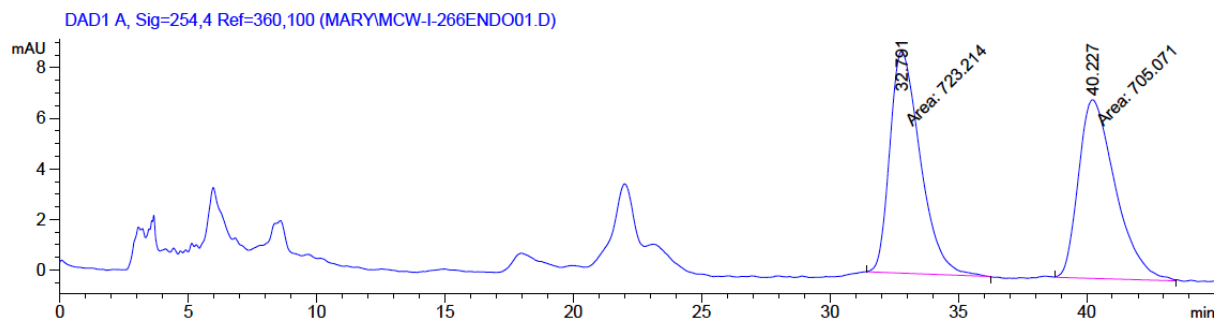
2.6, Table 2.11, entry 8 [(*R*)-MeOBIPHEP], 6% ee:



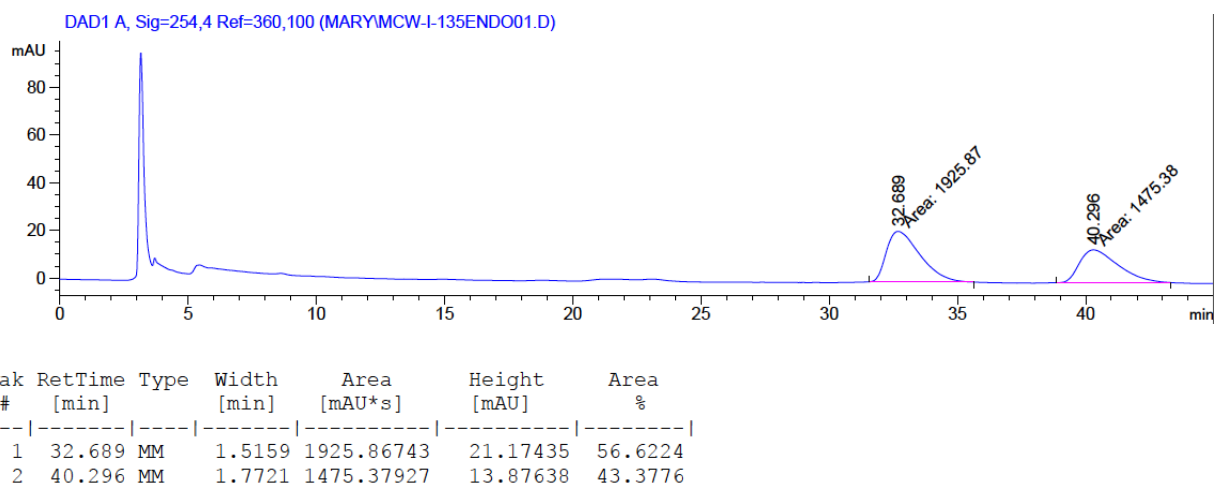
2.6, Table 2.11, entry 9 [(*R*)-3,5-*i*-Pr-MeOBIPHEP], 36% ee:



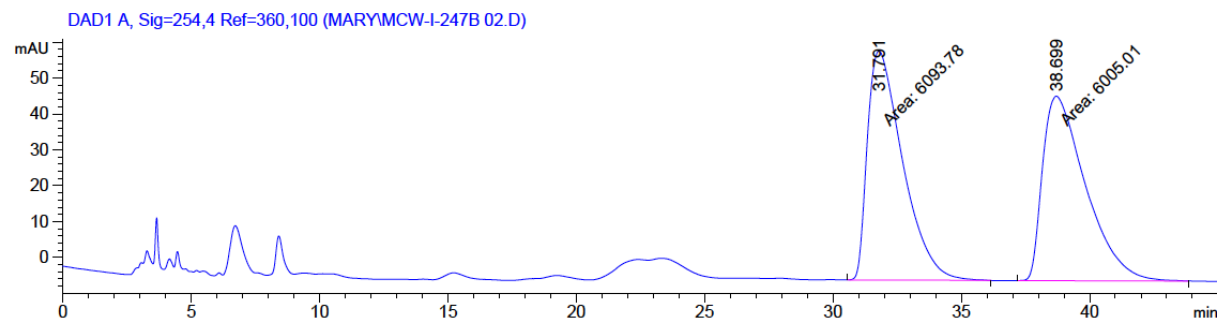
2.6, Table 2.11, entry 10 [(R)-3,5-xyl-MeOBIPHEP], 2% ee:



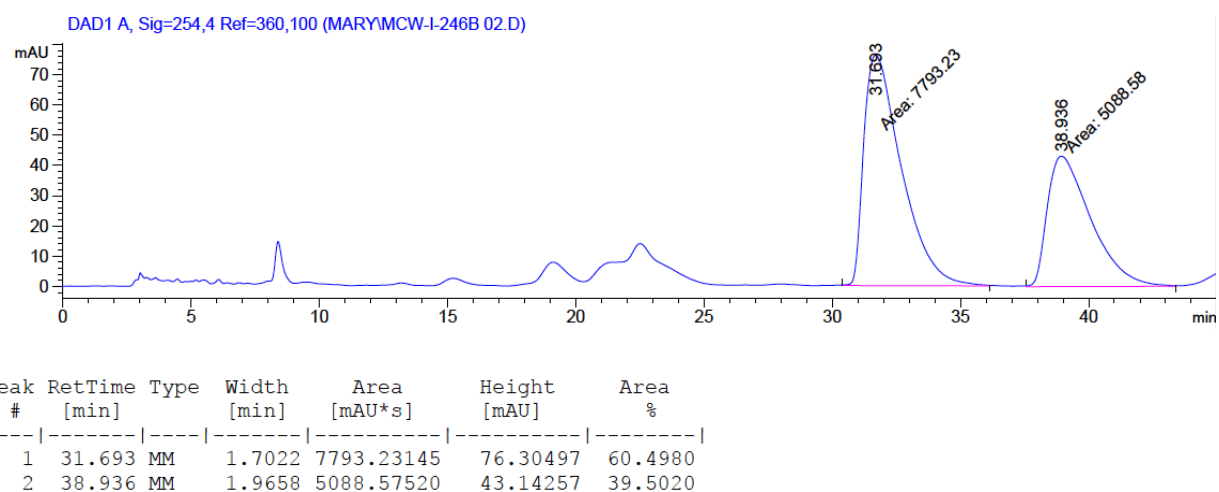
2.6, Table 2.11, entry 12 [(R)-DUFLUOROPHOS], 14% ee:



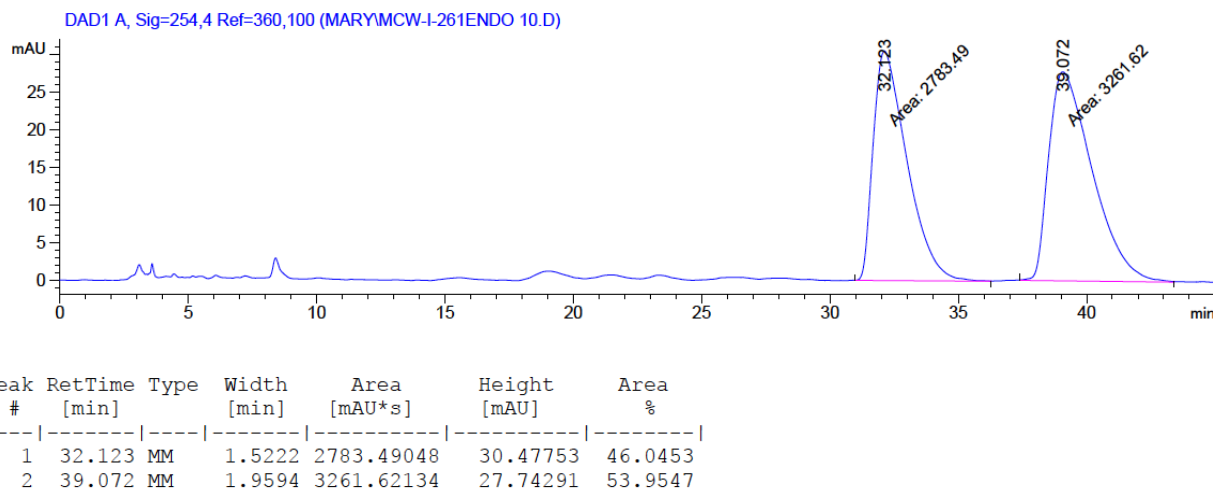
2.6, Table 2.14, entry 1 [(R,R)-Chiraphite], 0% ee:



2.6, Table 2.14, entry 2 [(R)-ShiP], 21% ee:



2.6, Table 2.14, entry 3 [(R)-2.38], 8% ee:



2.8 References and Notes

¹ (a) Overman, L. E.; Baumann, M.; Nam, S.; Horne, D.; Jove, R.; Xie, J.; Kowolik, C. ETP Derivatives. PCT Int. Appl. WO 2014066435 A1, October 22, 2012. (b) Baumann, M.; Dieskau, A. P.; Loertscher, B. M.; Walton, M. C.; Nam, S.; Xie, J.; Horne, D.; Overman, L. E. *Chem. Sci.* **2015**, *6*, 4451.

² See Chapter 1 for a thorough description of our route to access novel ETP analogues.

³ (a) Grigg, R.; Sridharan, V.; Thianpatanagul, S. *J. Chem. Soc., Perkin Trans. I* **1986**, 1669. (b) Grigg, R.; Delvin, J. *J. Chem. Soc. Chem. Commun.* **1986**, 631. (c) Grigg, R.; Gunaratne, H. Q. N.; Sridharan, V. *Tetrahedron* **1987**, *43*, 5887. (d) Barr, D. A.; Grigg, R.; Gunaratne, H. Q. N.; Kemp, J.; McMeekin, P.; Sridharan, V. *Tetrahedron* **1988**, *44*, 557. (e) Barr, D. A.; Donegan, G.; Grigg, R. *J. Chem. Soc., Perkin Trans. I* **1989**, 1550. (f) Barr, D. A.; Grigg, R.; Sridharan, V. *Tetrahedron Lett.* **1989**, *30*, 4727. (g) Amornraksa, K.; Barr, D.; Donegan, G.; Grigg, R.; Ratananukul, P.; Sridharan, V. *Tetrahedron* **1989**, *45*, 4649. (h) Barr, D. A.; Dorrity, M. J.; Grigg, R.; Malone, J. F.; Montgomery, J.; Rajviroongit, S.; Stevenson, P. *Tetrahedron Lett.* **1990**, *31*, 6569. (i) Grigg, R.; Montgomery, J.; Somasunderam, A. *Tetrahedron* **1992**, *48*, 10431. (j) Grigg, R. *Tetrahedron: Asymmetry* **1995**, *6*, 2475.

⁴ Tsuge, Kanemasa, and coworkers also contributed to early studies of metallo-azomethine ylides: (a) Tsuge, O.; Kanemasa, S.; Yoshioka, M. *J. Org. Chem.* **1988**, *53*, 1384. (b) Kanemasa, S.; Yoshioka, M.; Tsuge, O. *Bull. Chem. Soc. Jpn.* **1989**, *62*, 869. (c) Kanemasa, S.; Yamamoto, H. *Tetrahedron Lett.* **1990**, *31*, 3633.

⁵ For reviews on 1,3-DC reactions, see: (a) Kanemasa, S. *Synlett* **2002**, 1371. (b) Coldham, I.; Hufton, R. *Chem. Rev.* **2005**, *105*, 2765. (c) Nájera, C.; Sansano, J. *Angew. Chem. Int. Ed.* **2005**, *44*, 6272. (d) Husinec, S.; Savic, V. *Tetrahedron: Asymmetry* **2005**, *16*, 2047. (e) Pandey, G.; Banerjee, P.; Gadre, S. R. *Chem. Rev.* **2006**, *106*, 4484. (f) Adrio, J.; Carretero, J. C. *Chem.*

Commun. **2011**, *47*, 6784. (g) Nájera, C.; Sansano, J. M. *Monatsh. Chem.* **2011**, *142*, 659. (h) Nájera, C.; Sansano, J. M. *J. Organomet. Chem.* **2014**, *771*, 78. (i) Narayan, R.; Potowski, M.; Jia, Z.-J.; Antonchick, A. P.; Waldmann, H. *Acc. Chem. Res.* **2014**, *47*, 1296. (j) Adrio, J.; Carretero, J. C. *Chem. Commun.* **2014**, *50*, 12434. (k) Hashimoto, T.; Maruoka, K. *Chem. Rev.* **2015**, *115*, 5366.

⁶ Allway, P.; Grigg, R. *Tetrahedron Lett.* **1991**, *32*, 5817.

⁷ Longmire, J. M.; Wang, B.; Zhang, X. *J. Am. Chem. Soc.* **2002**, *124*, 13400.

⁸ Gothelf, A. S.; Gothelf, K. V.; Hazell, R. G.; Jørgensen, K. A. *Angew. Chem. Int. Ed.* **2002**, *41*, 4236.

⁹ (a) Longmire, J. M.; Wang, B.; Zhang, X. *Tetrahedron Lett.* **2000**, *41*, 5435. (b) You, S.-L.; Hou, X.-L.; Dai, L.-X.; Gao, B.-X.; Sun, J. *Chem. Commun.* **2000**, 1933.

¹⁰ For examples where the dipolarophile carbonyl group is proposed to coordinate to the catalyst metal center, thereby lowering the energy of the endo transition state, see references 3j; 4a ,b; 8; 14h, n, x; 15c, v, x; 16i; and 19b.

¹¹ At the time of Schreiber's publication, only (*S,S*)-*t*-Bu-BOX was commercially available, and the shortest synthesis of xylyl-FAP consisted of eight steps (see references 7 and 9).

¹² Alcock, N. W.; Brown, J. M.; Hulmes, D. L. *Tetrahedron: Asymmetry* **1993**, *4*, 743.

¹³ Chen, C.; Li, X.; Schreiber, S. L. *J. Am. Chem. Soc.* **2003**, *125*, 10174.

¹⁴ (a) Knöpfel, T. F.; Aschwanden, P.; Ichikawa, T.; Watanabe, T.; Carreira, E. M. *Angew. Chem. Int. Ed.* **2004**, *43*, 5971. (b) Stohlner, R.; Wahl, F.; Pfaltz, A. *Synthesis* **2005**, 1431. (c) Zeng, W.; Zhou, Y.-G. *Org. Lett.* **2005**, *7*, 5055. (d) Alemparte, C.; Blay, G.; Jørgensen, K. A. *Org. Lett.* **2005**, *7*, 4569. (e) Bonini, B. F.; Boschi, F.; Franchini, M. C.; Fochi, M.; Fini, F.; Mazzanti, A.; Ricci, A. *Synlett* **2006**, 543. (f) Nájera, C.; de Gracia Retamosa, M.; Sansano, J. M. *Org. Lett.* **2007**, *9*, 4025. (g) Zeng, W.; Zhou, Y.-G. *Tetrahedron Lett.* **2007**, *48*, 4619. (h) Zeng, W.; Chen, G.-Y.; Zhou, Y.-G.; Li, Y.-X. *J. Am. Chem. Soc.* **2007**, *129*, 750. (i) Nájera, C.; de Gracia Retamosa, M.; Sansano, J. M.; de Cázar, A.; Cossío, F. P. *Tetrahedron: Asymmetry* **2008**, *19*, 2913. (j) Nájera, C.; de Gracia Retamosa, M.; Sansano, J. M. *Angew. Chem. Int. Ed.* **2008**, *47*, 6055. (k) Agbodjan, A. A.; Cooley, B. E.; Copley, R. C. B.; Corfield, J. A.; Flanagan, R. C.; Glover, B. N.; Guidetti, R.; Haigh, D.; Howes, P. D.; Jackson, M. M.; Matsuoka, R. T.; Medhurst, K. J.; Millar, A.; Sharp, M. J.; Slater, M. J.; Toczko, J. F.; Xie, S. *J. Org. Chem.* **2008**, *73*, 3094. (l) Hernández-Toribio, J.; Arrayás, R. G.; Martín-Matute, B.; Carretero, J. C. *Org. Lett.* **2009**, *11*, 393. (m) Yu, S.-B.; Hu, X.-P.; Deng, J.; Wang, D.-Y.; Duan, Z.-C.; Zheng, Z. *Tetrahedron: Asymmetry* **2009**, *20*, 621. (n) Nájera, C.; de Gracia Retamosa, M.; Martín-Rodríguez, M.; Sansano, J. M.; de Cázar, A.; Cossío, F. P. *Eur. J. Org. Chem.* **2009**, 5622. (o) Wang, C.-J.; Xue, Z.-Y.; Liang, G.; Lu, Z. *Chem. Commun.* **2009**, 2905. (p) Liang, G.; Tong, M.-C.; Wang, C.-J. *Adv. Synth. Catal.* **2009**, *351*, 3101. (q) Robles-Machín, R.; Alonso, I.; Adrio, J.; Carretero, J. C. *Chem. Eur. J.* **2010**, *16*, 5286. (r) Oura, I.; Shimizu, K.; Ogata, K.;

Fukuzawa, S. *Org. Lett.* **2010**, *12*, 1752. (s) Martín-Rodríguez, M.; Nájera, C.; Sansano, J. M.; Costa, P. R. R.; de Lima, E. C.; Dias, A. G. *Synlett* **2010**, 962. (t) Shimizu, K.; Ogata, K.; Fukuzawa, S. *Tetrahedron Lett.* **2010**, *51*, 5068. (u) Eröksüz, S.; Dogan, Ö.; Garner, P. P. *Tetrahedron: Asymmetry* **2010**, *21*, 2535. (v) Xue, Z.-Y.; Liu, T.-L.; Lu, Z.; Huang, H.; Tao, H.-Y.; Wang, C.-J. *Chem. Commun.* **2010**, *46*, 1727. (w) Yamashita, Y.; Imaizumi, T.; Kobayashi, S. *Angew. Chem. Int. Ed.* **2011**, *50*, 4893. (x) Yamashita, Y.; Imaizumi, T.; Guo, X.-X.; Kobayashi, S. *Chem. Asian J.* **2011**, *6*, 2550. (y) Liu, T.-L.; Xue, Z.-Y.; Tao, H.-Y.; Wang, C.-J. *Org. Biomol. Chem.* **2011**, *9*, 1980. (z) Tong, M.-C.; Li, J.; Tao, H.-Y.; Li, Y.-X.; Wang, C.-J. *Chem. Eur. J.* **2011**, *17*, 12922. (aa) Liu, T.-L.; He, Z.-L.; Li, Q.-H.; Tao, H.-Y.; Wang, C.-J. *Adv. Synth. Catal.* **2011**, *353*, 1713. (ab) Xue, Z.-Y.; Fang, X.; Wang, C.-J. *Org. Biomol. Chem.* **2011**, *9*, 3622. (ac) Imae, K.; Konno, T.; Ogata, K.; Fukuzawa, S. *Org. Lett.* **2012**, *14*, 4410. (ad) Han, M.-L.; Wang, D.-Y.; Zeng, P.-W.; Zheng, Z.; Hu, X.-P. *Tetrahedron: Asymmetry* **2012**, *23*, 306. (ae) González-Esguevillas, M.; Adiro, J.; Carretero, J. C. *Chem. Commun.* **2013**, *49*, 4649. (af) Lim, A. D.; Codelli, J. A.; Reisman, S. E. *Chem. Sci.* **2013**, *4*, 650. (ag) Liu, K.; Teng, H.-L.; Yao, L.; Tao, H.-Y.; Wang, C.-J. *Org. Lett.* **2013**, *15*, 2250. (ah) Wang, Z.; Luo, S.; Zhang, S.; Yang, W.-L.; Liu, Y.-Z.; Li, H.; Luo, X.; Deng, W.-P. *Chem. Eur. J.* **2013**, *19*, 6739. (ai) Yamashita, Y.; Kobayashi, S. *Chem. Eur. J.* **2013**, *19*, 9420. (aj) Mancebo-Aracil, J.; Nájera, C.; Sansano, J. M. *Tetrahedron: Asymmetry* **2015**, *26*, 674. (ak) Bai, X.-F.; Song, T.; Xu, Z.; Xia, C.-G.; Huang, W.-S.; Xu, L.-W. *Angew. Chem. Int. Ed.* **2015**, *54*, 5255.

¹⁵ (a) Gao, W.; Zhang, X.; Raghunath, M. *Org. Lett.* **2005**, *7*, 4241. (b) Cabrera, S.; Arrayás, R. G.; Carretero, J. C. *J. Am. Chem. Soc.* **2005**, *127*, 16394. (c) Yan, X.-X.; Peng, Q.; Zhang, Y.; Zhang, K.; Hong, W.; Hou, X.-L.; Wu, Y.-D. *Angew. Chem. Int. Ed.* **2006**, *45*, 1979. (d) Llamas, T.; Arrayás, R. G.; Carretero, J. C. *Org. Lett.* **2006**, *8*, 1795. (e) Cabrera, S.; Arrayás, R. G.; Martín-Matute, B.; Cossío, F. P.; Carretero, J. C. *Tetrahedron* **2007**, *63*, 6587. (f) Martín-Matute, B.; Pereira, S. I.; Peña-Cabrera, E.; Adiro, J.; Silva, A. M. S.; Carretero, J. C. *Adv. Synth. Catal.* **2007**, *349*, 1714. (g) Llamas, T.; Arrayás, R. G.; Carretero, J. C. *Synthesis* **2007**, 950. (h) Shi, M.; Shi, J.-W. *Tetrahedron: Asymmetry* **2007**, *18*, 645. (i) Fukizawa, S.; Oki, H. *Org. Lett.* **2008**, *10*, 1747. (j) López-Pérez, A.; Adiro, J.; Carretero, J. C. *J. Am. Chem. Soc.* **2008**, *130*, 10084. (k) Wang, C.-J.; Liang, G.; Xue, Z.-Y.; Gao, F. *J. Am. Chem. Soc.* **2008**, *130*, 17250. (l) Hernández-Toribio, J.; Arrayás, R. G.; Martín-Matute, B.; Carretero, J. C. *Org. Lett.* **2009**, *11*, 393. (m) Kim, H. Y.; Shih, H.-J.; Knabe, W. E.; Oh, K. *Angew. Chem. Int. Ed.* **2009**, *48*, 7420. (n) López-Pérez, A.; Adrio, J.; Carretero, J. C. *Angew. Chem. Int. Ed.* **2009**, *48*, 340. (o) Zhang, C.; Yu, S.-B.; Hu, X.-P.; Wang, D.-Y.; Zheng, Z. *Org. Lett.* **2010**, *12*, 5542. (p) Padilla, S.; Tejero, R.; Adrio, J.; Carretero, J. C. *Org. Lett.* **2010**, *12*, 5608. (q) Liu, T.-L.; He, Z.-L.; Tao, H.-Y.; Cai, Y.-P.; Wang, C.-J. *Chem. Commun.* **2011**, *47*, 2616. (r) Teng, H.-L.; Huang, H.; Tao, H.-Y.; Wang, C.-J. *Chem. Commun.* **2011**, *47*, 5494. (s) Liu, T.-L.; He, Z.-L.; Wang, C.-J. *Chem. Commun.* **2011**, *47*, 9600. (t) Li, Q.-H.; Tong, M.-C.; Li, J.; Tao, H.-Y.; Wang, C.-J. *Chem. Commun.* **2011**, *47*, 11110. (u) Wang, M.; Wang, C.-J.; Lin, Z. *Organometallics* **2012**, *31*, 7870. (v) Yan, D.; Li, Q.; Wang, C. *Chin. J. Chem.* **2012**, *30*, 2714. (w) He, Z.; Liu, T.; Tao, H.; Wang, C.-J. *Org. Lett.* **2012**, *14*, 6230. (x) Tao, H.-Y.; He, Z.-L.; Yang, Y.; Wang, C.-J. *RSC Adv.* **2014**, *4*, 16899. (y) González-Esguevillas, M.; Pascual-Escudero, A.; Adrio, J.; Carretero, J. C. *Chem. Eur. J.* **2015**, *21*, 4561. (z) Li, J.-Y.; Kim, H. Y.; Oh, K. *Org. Lett.* **2015**, *17*, 1288.

¹⁶ (a) Oderaotoshi, Y.; Cheng, W.; Fujitomi, S.; Kasano, Y.; Minakata, S.; Komatsu, M. *Org. Lett.* **2003**, *5*, 5043. (b) Filippone, S.; Maroto, E. E.; Martín-Domenech, A.; Suarez, M.; Martín,

N. *Nat. Chem.* **2009**, *1*, 578. (c) Arai, T.; Mishiro, A.; Yokoyama, N.; Suzuki, K.; Sato, H. *J. Am. Chem. Soc.* **2010**, *132*, 5338. (d) Wang, M.; Wang, Z.; Shi, Y.-H.; Shi, X.-X.; Fossey, J. S.; Deng, W.-P. *Angew. Chem. Int. Ed.* **2011**, *50*, 4897. (e) Maroto, E. E.; Filippone, S.; Martín-Domenech, A.; Suárez, M.; Martín, N. *J. Am. Chem. Soc.* **2012**, *134*, 12936. (f) Castelló, L. M.; Nájera, C.; Sansano, J. M.; Larrañaga, O.; de Cózar, A.; Cossío, F. P. *Org. Lett.* **2013**, *15*, 2902. (g) Chaulagain, M. R.; Felten, A. E.; Gilbert, K.; Aron, Z. D. *J. Org. Chem.* **2013**, *78*, 9471. (h) Maroto, E. E.; Filippone, S.; Suárez, M.; Martínez-Álvarez, R.; de Cózar, A.; Cossío, F. P.; Martín, N. *J. Am. Chem. Soc.* **2014**, *136*, 705. (i) Wang, Z.; Yu, X.; Tian, B.-X.; Payne, D. T.; Yang, W.-L.; Liu, Y.-Z.; Fossey, J. S.; Deng, W.-P. *Chem. Eur. J.* **2015**, *21*, 10457. (j) Castelló, L. M.; Nájera, C.; Sansano, J. M.; Larrañaga, O.; de Cózar, A.; Cossío, F. P. *Synthesis* **2015**, *47*, 934. (k) Dai, L.; Xu, D.; Tang, L.-W.; Zhou, Z.-M. *ChemCatChem* **2015**, *7*, 1078.

¹⁷ (a) Martín-Rodríguez, M.; Nájera, C.; Sansano, J. M.; Wu, F.-L. *Tetrahedron: Asymmetry* **2010**, *21*, 1184 and corrigendum: *Tetrahedron: Asymmetry* **2010**, *21*, 2559. (b) Martín-Rodríguez, M.; Nájera, C.; Sansano, J. M.; de Cózar, A.; Cossío, F. P. *Chem. Eur. J.* **2011**, *17*, 14224. (c) Martín-Rodríguez, M.; Nájera, C.; Sansano, J. M.; de Cózar, A.; Cossío, F. P. *Beilstein J. Org. Chem.* **2011**, *7*, 988.

¹⁸ For a procedure describing the synthesis of Au(I)/diphosphine complexes, see: Wheaton, C. A.; Jennings, M. C.; Puddephatt, R. J. *Z. Naturforsch.* **2009**, *64b*, 1469.

¹⁹ (a) Dogan, Ö.; Koyuncu, H.; Garner, P.; Bulut, A.; Youngs, W. J.; Panzer, M. *Org. Lett.* **2006**, *8*, 4687. (b) Dogan, Ö.; Koyuncu, H.; Kaniskan, Ü. *Turkish J. Chem.* **2001**, *25*, 365. (c) Ayan, S.; Dogan, Ö.; Ivantcova, P. M.; Datsuk, N. G.; Shulga, D. A.; Chupakhin, V. I.; Zabolotnev, D. V.; Kudryavtsev, K. V. *Tetrahedron: Asymmetry* **2013**, *24*, 838.

²⁰ (a) Shi, J.-W.; Zhao, M.-X.; Lei, Z.-Y.; Shi, M. *J. Org. Chem.* **2008**, *73*, 305. (b) Arai, T.; Yokoyama, N.; Mishiro, A.; Sato, H. *Angew. Chem. Int. Ed.* **2010**, *49*, 7895. (c) Awata, A.; Arai, T. *Chem. Eur. J.* **2012**, *18*, 8278.

²¹ (a) Saito, S.; Tsubogo, T.; Kobayashi, S. *J. Am. Chem. Soc.* **2007**, *129*, 5364. (b) Tsubogo, T.; Saito, S.; Seki, K.; Yamashita, Y.; Kobayashi, S. *J. Am. Chem. Soc.* **2008**, *130*, 13321. (c) Chaulagain, M. R.; Aron, Z. D. *J. Org. Chem.* **2010**, *75*, 8271. (d) Hut'ka, M.; Tsubogo, T.; Kobayashi, S. *Adv. Synth. Catal.* **2013**, *355*, 1561.

²² For examples using proline derivatives, see: (a) *Angew. Chem. Int. Ed.* **2007**, *46*, 5168. (b) Ibrahim, I.; Rios, R.; Vesely, J.; Córdova, A. *Tetrahedron Lett.* **2007**, *48*, 6252. (c) Lin, S.; Deiana, L.; Zhao, G.-L.; Sun, J.; Córdona, A. *Angew. Chem. Int. Ed.* **2011**, *50*, 7624. (d) Reboredo, S.; Vicario, J. L.; Badía, D.; Carrillo, L.; Reyes, E. *Adv. Synth. Catal.* **2011**, *353*, 3307. (e) Reboredo, S.; Reyes, E.; Vicario, J. L.; Badía, D.; Carrillo, L.; De Cozar, A.; Cossío, F. P. *Chem. Eur. J.* **2012**, *18*, 7179. (f) Reboredo, S.; Vicario, J. L.; Carrillo, L.; Reyes, E.; Uria, U. *Synthesis* **2013**, 2669. (g) Xiao, J.-A.; Liu, Q.; Ren, J.-W.; Liu, J.; Carter, R. G.; Chen, X.-Q.; Yang, H. *Eur. J. Org. Chem.* **2014**, 5700. For an example using imidazolidinones, see: (h) Fernandez, N.; Carrillo, L.; Vicario, J. L.; Badía, D.; Reyes, E. *Chem. Commun.* **2011**, *47*, 12313. For examples using Brønsted acids, see: (i) Grigg, R.; Gunaratne, H. Q. N. *J. Chem. Soc. Chem. Commun.* **1982**, 384. (j) Chen, X.-H.; Zhang, W.-Q.; Gong, L.-Z. *J. Am. Chem. Soc.* **2008**,

130, 5652. (k) Chen, X.-H.; Wei, Q.; Luo, S.-W.; Xiao, H.; Gong, L.-Z. *J. Am. Chem. Soc.* **2009**, 131, 13819. (l) Yu, J.; He, L.; Chen, X.-H.; Song, J.; Chen, W.-J.; Gong, L.-Z. *Org. Lett.* **2009**, 11, 4946. (m) Yu, J.; Chen, W.-J.; Gong, L.-Z. *Org. Lett.* **2010**, 12, 4050. (n) Wang, C.; Chen, X.-H.; Zhou, S.-M.; Gong, L.-Z. *Chem. Commun.* **2010**, 46, 1275. (o) Cheng, M.-N.; Wang, H.; Gong, L.-Z. *Org. Lett.* **2011**, 13, 2418. (p) He, L.; Chen, X.-H.; Wang, D.-N.; Luo, S.-W.; Zhang, W.-Q.; Yu, J.; Ren, L.; Gong, L.-Z. *J. Am. Chem. Soc.* **2011**, 133, 13504. (q) Cheng, Y.; Liu, Y.-N.; Ye, J.; He, L.; Kang, T.-R.; Liu, Q.-Z. *Tetrahedron Lett.* **2012**, 53, 6775. (r) Shi, F.; Tao, Z.-L.; Luo, S.-W.; Tu, S.-J.; Gong, L.-Z. *Chem. Eur. J.* **2012**, 18, 6885. (s) Guo, C.; Song, J.; Gong, L.-Z. *Org. Lett.* **2013**, 15, 2676. (t) Luo, W.; Lin, Y.; Yang, D.; He, L. *Tetrahedron: Asymmetry* **2014**, 25, 787. For examples using thioureas, see: (u) Xue, M.-X.; Zhang, X.-M.; Gong, L.-Z. *Synlett* **2008**, 691. (v) Xie, J.; Yoshida, K.; Takasu, K.; Takemoto, Y. *Tetrahedron Lett.* **2008**, 49, 6910. (x) Liu, Y.-K.; Liu, H.; Du, W.; Yue, L.; Chen, Y.-C. *Chem. Eur. J.* **2008**, 14, 9873. (y) Bai, J. F.; Wang, L. L.; Peng, L.; Guo, Y. L.; Ming, J. N.; Wang, F. Y.; Xu, X. Y.; Wang, L. X. *Eur. J. Org. Chem.* **2011**, 4472. For an example using guanidines, see: (z) Nakano, M.; Terada, M. *Synlett* **2009**, 1670. For example using an NHC, see: (aa) Yang, Y.-J.; Zhang, H.-R.; Zhu, S.-Y.; Zhu, P.; Hui, X.-P. *Org. Lett.* **2014**, 16, 5048.

²³ Absolute configuration was assigned by analogy to products reported in the literature (see reference 13).

²⁴ Zhang, Y.; Sun, W.; Freund, C.; Santos, A. M.; Herdtweck, E.; Mink, J.; Kühn, F. E. *Inorg. Chim. Acta* **2006**, 359, 4723.

²⁵ Calculations performed by the Cossío group also indicate strong coordination between Ag(I) ions and nitrile groups: Ayerbe, M.; Arrieta, A.; Cossío, F. P. *J. Org. Chem.* **1998**, 63, 1795.

²⁶ Priego, J.; Mancheño, O. G.; Cabrera, S.; Arrayás, R. G.; Llamas, T.; Carretero, J. C. *Chem. Commun.* **2002**, 2512.

²⁷ As a safer alternative, commercially available Cu(MeCN)₄BF₄ was substituted for Cu(MeCN)₄ClO₄.

²⁸ For reviews, see: (a) Johnson, J. S.; Evans, D. A. *Acc. Chem. Res.* **2000**, 33, 325. (b) Stanley, L. M.; Sibi, M. P. *Chem. Rev.* **2008**, 108, 2887. (c) Rasappan, R.; Laventine, D.; Reiser, O. *Coord. Chem. Rev.* **2008**, 252, 702. (d) Surry, D. S.; Buchwald, S. L. *Chem. Sci.* **2010**, 1, 13.

²⁹ Nishiyama, H.; Sakaguchi, H.; Nakamura, T.; Horihata, M.; Kondo, M.; Itoh, K. *Organometallics* **1989**, 8, 846.

³⁰ Le Bailly, B. A. F.; Greenhalgh, M. D.; Thomas, S. P. *Chem. Commun.* **2012**, 48, 1580.

³¹ Ligand (*R*)-**2.23** was prepared by Plaza according to the following procedure: Shen, K.; Liu, X.; Lin, L.; Feng, X. *Chem. Eur. J.* **2009**, 15, 6008. Ligands (*R*)-**2.24**–(*R*)-**2.26** were prepared by May.

³² Gual, A.; Godard, C.; de la Fuente, V.; Castillón, S.; Lefront, L.; de Vries, J. G. Phosphorus(III) Ligands in Homogenous Catalysis: Design and Synthesis. Kamer, P. C. J., van Leeuwen, P. W. N. M., Eds.; Wiley: West Sussex, 2012; pp 133–157.

³³ For an example of library synthesis, see: Jagt, R. B. C.; Toullec, P. Y.; Schudde, E. P.; de Vries, J. G.; Feringa, B. L.; Minnaard, A. J. *J. Comb. Chem.* **2007**, *9*, 407. For an excellent review on the synthesis and applications of phosphoramidite ligands, see: Teichert, J. F.; Feringa, B. L. *Angew. Chem. Int. Ed.* **2010**, *49*, 2486.

³⁴ Hulst, R.; de Vries, N. K.; Feringa, B. L. *Tetrahedron: Asymmetry* **1994**, *5*, 699.

³⁵ Ligands (*R,S*)-**2.28** and (*S*)-Metamorphos were generously provided to us from the group of Professor John Wolfe at the University of Michigan.

³⁶ TADDOL = 2,2-dimethyl- $\alpha,\alpha,\alpha',\alpha'$ -tetraphenyldioxolane-4,5-dimethanol.

³⁷ For a review on TADDOL ligands, see: Seebach, D.; Beck, A. K.; Heckel, A. *Angew. Chem. Int. Ed.* **2001**, *40*, 92. For a general method to access TADDOL-derived phosphorus(III) ligands, see: Mewald, M.; Weickgenannt, A.; Frölich, R.; Oestreich, M. *Tetrahedron: Asymmetry* **2010**, *21*, 1232.

³⁸ Fu, Y.; Xie, J.-H.; Hu, A.-G.; Zhou, H.; Wang, L.-X.; Zhou, Q.-L. *Chem. Commun.* **2002**, 480.

³⁹ Dierkes, P.; van Leeuwen, P. W. N. M. *J. Chem. Soc., Dalton Trans.* **1999**, 1519.

⁴⁰ XANTPHOS = 4,5-bis(diphenylphosphino)-9,9-dimethylxanthene.

⁴¹ Togni, A.; Breutel, C.; Schnyder, A.; Spindler, F.; Landert, H.; Tijani, A. *J. Am. Chem. Soc.* **1994**, *116*, 4062.

⁴² DIOP = 2,3-*O*-isopropylidene-2,3-dihydroxy-1,4-bis(diphenylphosphino)butane.

⁴³ (a) Dang, T. P.; Kagan, H. B. *Chem. Commun.* **1971**, 481. (b) Kagan, H. B.; Dang, T.-P. *J. Am. Chem. Soc.* **1972**, *94*, 6429.

⁴⁴ Burk, M. *J. Am. Chem. Soc.* **1991**, *113*, 8518.

⁴⁵ DACH = 1,2-diaminocyclohexane.

⁴⁶ BINAP = 2,2'-bis(diphenylphosphino)-1,1'-binaphthyl.

⁴⁷ (a) Miyashita, A.; Yasuda, A.; Takaya, H.; Toriumi, K.; Ito, T.; Souchi, T.; Noyori, R. *J. Am. Chem. Soc.* **1980**, *102*, 7932. (b) Miyashita, A.; Takaya, H.; Souchi, T.; Noyori, R. *Tetrahedron* **1984**, *40*, 1245. (c) Takaya, H.; Mashima, K.; Koyano, K.; Yagi, M.; Kumobayashi, H.; Taketomi, T.; Akutagawa, S.; Noyori, R. *J. Org. Chem.* **1986**, *51*, 629.

⁴⁸ Mashima, K.; Kusano, K.; Sato, N.; Matsumura, Y.; Nozaki, K.; Kumobayashi, H.; Sayo, N.; Hori, Y.; Ishizaki, T.; Akutagawa, S.; Takaya, H. *J. Org. Chem.* **1994**, *59*, 3064.

⁴⁹ BIPHEP = 2,2'-bis(diphenylphosphino)-1,1'-biphenyl.

⁵⁰ Schmid, R.; Foricher, J.; Cereghetti, M.; Schönholzer, P. *Helv. Chim. Acta* **1991**, *74*, 370.

⁵¹ (a) Saito, T.; Yokozawa, T.; Zhang, X.; Sayo, N. Chiral diphosphine compound intermediate for preparing the same transition metal complex having the same diphosphine compound as ligand and asymmetric hydrogenation catalyst. U.S. Patent 5,872,273, February 16, 1999. (b) Saito, T.; Yokozawa, T.; Ishizaki, T.; Moroi, T.; Sayo, N.; Miura, T.; Kumobayashi, H. *Adv. Synth. Catal.* **2001**, *343*, 264.

⁵² DPEPhos = bis-[2-(diphenylphosphino)phenyl]ether.

⁵³ (a) Jeulin, S.; de Paule, S. D.; Ratovelomanana-Vidal, V.; Genêt, J.-P.; Campion, N.; Dellis, P. *Angew. Chem. Int. Ed.* **2004**, *43*, 320. (b) Genet, J.-P.; Ayad, T.; Ratovelomanana-Vidal, V. *Chem. Rev.* **2014**, *114*, 2824.

⁵⁴ Gual, A.; Godard, C.; de la Fuente, V.; Castillón, S.; Lefront, L.; de Vries, J. G. Phosphorus(III) Ligands in Homogenous Catalysis: Design and Synthesis. Kamer, P. C. J., van Leeuwen, P. W. N. M., Eds.; Wiley: West Sussex, 2012; pp 81–131.

⁵⁵ SPINOL = 1,1'-spirobiindane-7,7'-diol.

⁵⁶ (a) Birman, V. B.; Rheingold, A. L.; Lam, K.-C. *Tetrahedron: Asymmetry* **1999**, *10*, 125. (b) Zhang, J.-H.; Liao, J.; Cui, X.; Yu, K.-B.; Zhu, J.; Deng, J.-G.; Zhu, S.-F.; Wang, L.-X.; Zhou, Q.-L.; Chung, L. W.; Ye, T. *Tetrahedron: Asymmetry* **2002**, *13*, 1363.

⁵⁷ BINOL = 1,1'-bi-2-naphthol.

⁵⁸ Cramer, N.; Laschat, S.; Baro, A. *Organometallics* **2006**, *25*, 2284.

⁵⁹ Other procedures, and variations thereof, used to access phosphite derivatives were tried but met with decomposition of phosphite products upon purification included: (a) Brunel, J. M.; Buono, G. *J. Org. Chem.* **1993**, *58*, 7313. (b) de Vries, A. H. M.; Meetsma, A.; Feringa, B. L. *Angew. Chem. Int. Ed.* **1996**, *20*, 2374. (c) Alexakis, A.; Burton, J.; Vastra, J.; Benhaim, C.; Fournoux, X.; van den Heuvel, A.; Levêque, J.-M.; Mazé, F.; Rosset, S. *Eur. J. Org. Chem.* **2000**, *24*, 4011. (d) Blume, F.; Zemolka, S.; Fey, T.; Kranich, R.; Schmalz, H.-G. *Adv. Synth. Catal.* **2002**, *344*, 868. (e) Hu, Y.; Liang, X.; Wang, J.; Zheng, Z.; Hu, X. *J. Org. Chem.* **2003**, *68*, 4542. (f) Kawasaki, M.; Li, P.; Yamamoto, H. *Angew. Chem. Int. Ed.* **2008**, *47*, 3795. (g) Wassenaar, J.; de Bruin, B.; Reek, J. N. H. *Organometallics* **2010**, *29*, 2767.

⁶⁰ Solidifies at –20 °C.

⁶¹ To determine enantioselective HPLC conditions required for the separation of pyrrolidine **2.16** enantiomers, racemic **2.16** was prepared following a procedure described by Overman (see reference 1). Imine **2.5** (700 mg, 3 mmol, 1 equiv) and *tert*-butyl acrylate (0.66 mL, 4.5 mmol, 1.5 equiv) were converted to racemic pyrrolidine **2.16** (480 mg, 44%) as a clear oil in a 2:1 endo:exo cycloadduct ratio.

⁶² Dieskau, A. P. Nachhaltige Metallkatalyse mit niedervalenten Eisen-Komplexen: Von Allylischen Substitutionen zu selektiven C–C-Bindungsaktivierungen. Ph.D. Thesis, Universität Stuttgart, July 2012.

⁶³ Ackermann, L.; Born, R. *Angew. Chem. Int. Ed.* **2005**, *44*, 2444.

⁶⁴ Kingsbury, J. S.; Hoveyda, A. H. *J. Am. Chem. Soc.* **2005**, *127*, 4510.

⁶⁵ Morin, M. S. T.; Arndtsen, B. A. *Org. Lett.* **2014**, *16*, 1056.

Chapter 3: Catalytic Diastereoselective Synthesis of Pyrrolidine Derivatives by 1,3-Dipolar Cycloaddition with Methacrylonitrile

3.1 Introduction

As described in Chapter 2, conditions for a Cu(I)-catalyzed 1,3-dipolar cycloaddition (1,3-DC) reaction between imine **3.1** and methacrylonitrile have been developed where the diastereoselectivity can be reversed by changing the ligand (Table 3.1). It was shown that when the electron-deficient π -accepting ligand tris(2,2,2-trifluoroethyl) phosphite [$P(OCH_2CF_3)_3$] was used, the reaction was selective for endo pyrrolidine product **3.2** (entry 1). Alternatively, utilization of the electron-rich σ -donating phosphine ligand tricyclohexylphosphine (PCy_3) yielded exo adduct **3.3** with high diastereoselectivity (entry 2). When P,N -ligand 2-dicyclohexylphosphino-2'-(*N,N*-dimethylamino)biphenyl (DavePhos) was the ligand employed, the 1,3-DC reaction afforded both diastereomers as a non-selective mixture (entry 3). The results of the studies described in Chapter 2 were of particular interest because such dramatic ligand effects on reaction diastereoselectivity have rarely been reported.^{1,2,3}

Table 3.1. Ligand-Controlled Diastereodivergence

The reaction scheme shows the 1,3-dipolar cycloaddition of imine **3.1** (2-((E)-2-(ethoxycarbonyl)vinyl)benzaldehyde) and methacrylonitrile (1.5 equiv) in the presence of a ligand/Cu(I) catalyst (10 mol %) and Et₃N (60 mol %) in PhMe at 23 °C for 24 h. The products are endo-3.2 and exo-3.3, which are diastereomeric pyrrolidines. Endo-3.2 has the methyl group (Me) and cyano group (CN) in axial positions, while exo-3.3 has them in equatorial positions.

entry ^a	ligand	conversion (%) ^{d,e}	dr (endo:exo) ^e
1	tris(2,2,2-trifluoroethyl) phosphite ^b	94	>94:6
2	tricyclohexylphosphine ^b	98	18:82
3	DavePhos ^c	57	50:50

^aReactions were performed using imine **3.1** (0.10 mmol), methacrylonitrile (0.15 mmol), $Cu(MeCN)_4BF_4$ (10 mol %), and Et_3N (0.12 mmol) at a concentration of 0.2 M in PhMe. ^bReactions were performed using 20 mol % ligand.

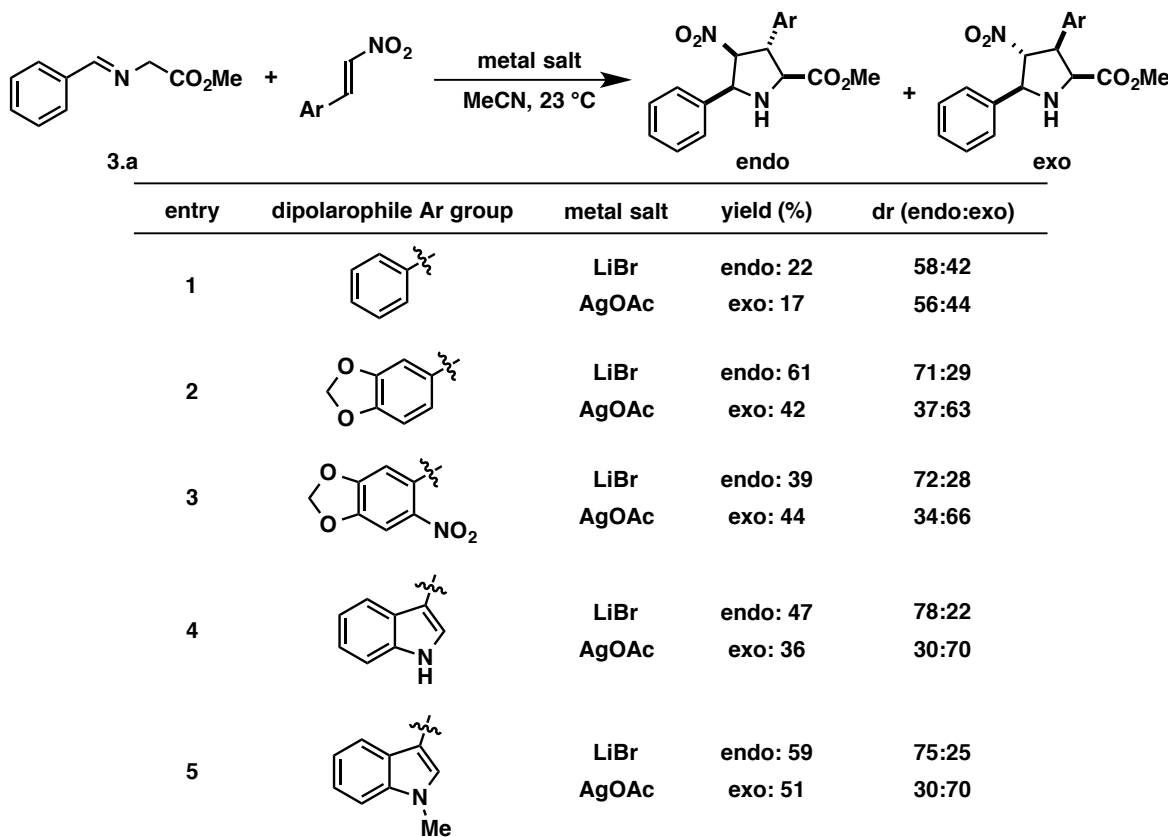
^cReactions were performed using 10 mol % ligand. ^dConversion is defined by comparing the relative amount of product to unreacted starting material. ^eDetermined by relative integration in the ¹H NMR spectrum of the crude reaction mixture.

3.1.1 Switching 1,3-DC Diastereoselectivity by Changing the Metal Salt

Early studies of metal-promoted 1,3-DC reactions reported success using Li(I)⁴ or Ag(I) salts^{5,6} in the formation of *N*-metalated azomethine ylide precursors. While these reports describe the selective synthesis of endo pyrrolidine cycloadducts using α,β -unsaturated carbonyl dipolarophiles, a report by Töke and coworkers described a difference in diastereoselectivity when either Li(I) or Ag(I) salts were used in 1,3-DC reactions between metallo-azomethine ylides and aryl nitroolefins.⁷ Among the five examples listed, the greatest diastereoselectivity change was a 78:22 dr (endo:exo) when LiBr was used to promote the cycloaddition; instead, AgOAc induced a 30:70 dr, favoring the exo adduct (Table 3.2, entry 4). The authors propose that secondary orbital interactions of the dipolarophile aryl group with Ag(I) and dipolarophile coordination to Li(I)^{4e} may result in the observed switch in diastereoselectivity.

Intrigued by the Töke report,⁷ the Cossío group further investigated the effect of the metal on the diastereochemical outcome of 1,3-DC reactions involving nitroalkenes.⁸ Through a combination of experimental and computational results, it was determined that the observed endo adduct selectivity of the reactions performed using LiClO₄ as the Lewis acid was indeed due to a lower energy endo transition state from coordination of the nitro group of the dipolarophile to the metal center. Competitive coordination for the metal binding sites was observed when the reactions were performed using AgOAc in acetonitrile; the nitrile groups of the solvent coordinated to Ag(I) more strongly than the nitro group of the dipolarophile. The corresponding lack of nitro group coordination resulted in a higher energy endo transition state when using Ag(I) compared to Li(I), explaining the exo adduct selectivity observed when utilizing AgOAc.

Table 3.2. Töke's Metal-Induced Diastereoselectivity Changes

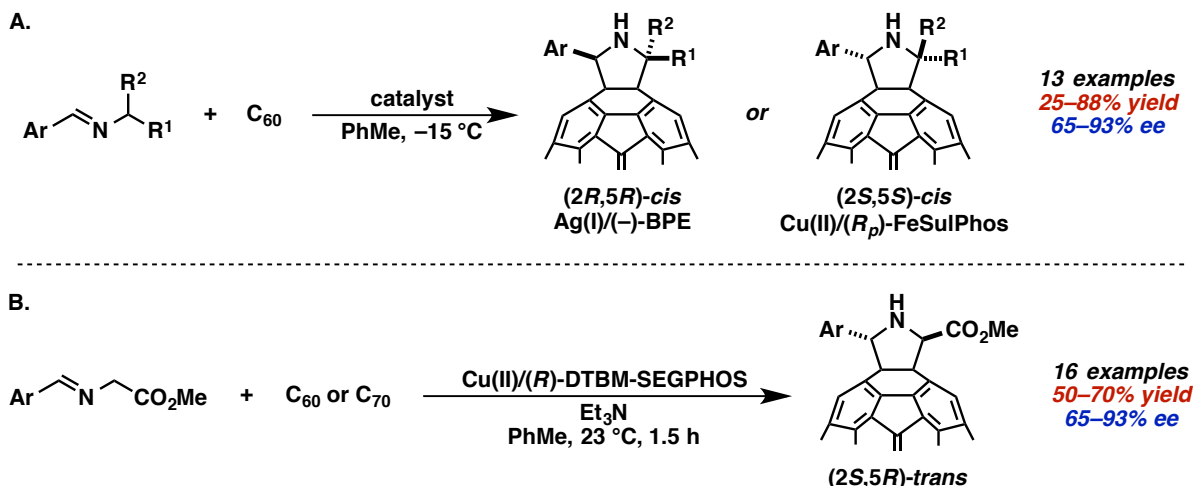


3.1.2 Catalyst-Controlled Diastereoselectivity

$\text{Ag(I)}^{3a,9}$ and $\text{Cu(II)}^{1,2c,10}$ salts are common Lewis acids used in catalytic asymmetric 1,3-DC reactions. Martín and coworkers have studied the effects of switching the enantioselectivity of 1,3-DC reactions between azomethine ylides and fullerenes by using either a Ag(I) ($-$)-BPE or a Cu(II) $/(R_p)$ -FeSulPhos catalyst,^{10a} resulting in the formation of ($2R,5R$)-*cis* or ($2S,5S$)-*cis* fulleropyrrolidines, respectively (Scheme 3.1A). Fullerenes are unique dipolarophiles as the π -system is noncoordinating and curved and the 1,3-DC endo/exo nomenclature does not apply to these systems. Therefore, the breakthrough discovery of a Cu(II) $/(±)$ -BINAP¹¹ system¹ that synthesized 2,5-*trans* pyrrolidine fullerenes indicated a step-wise 1,3-DC reaction mechanism for this particular system. The Martín group further

elaborated this methodology using a Cu(II)/(*R*)-DTBM-SEGPHOS catalyst to synthesize enantioenriched 2,5-*trans* fulleropyrrolidines (Scheme 3.1B).^{10d}

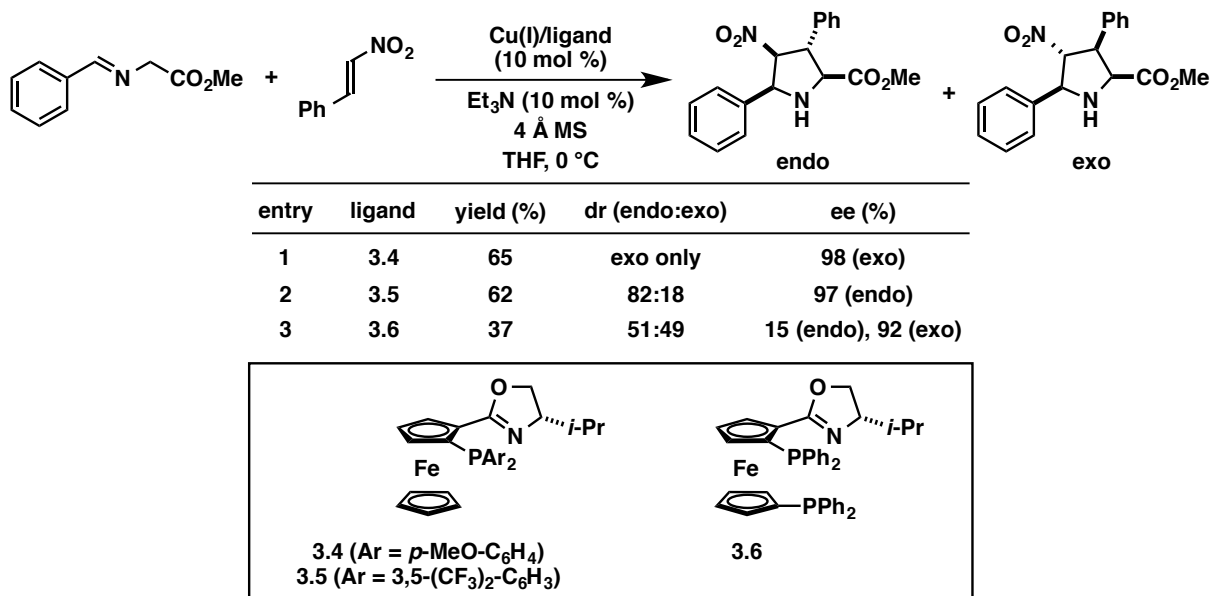
Scheme 3.1. Martín's Stereodifferentiation of Fulleropyrrolidines



3.1.3 Ligand-Directed Diastereodivergence

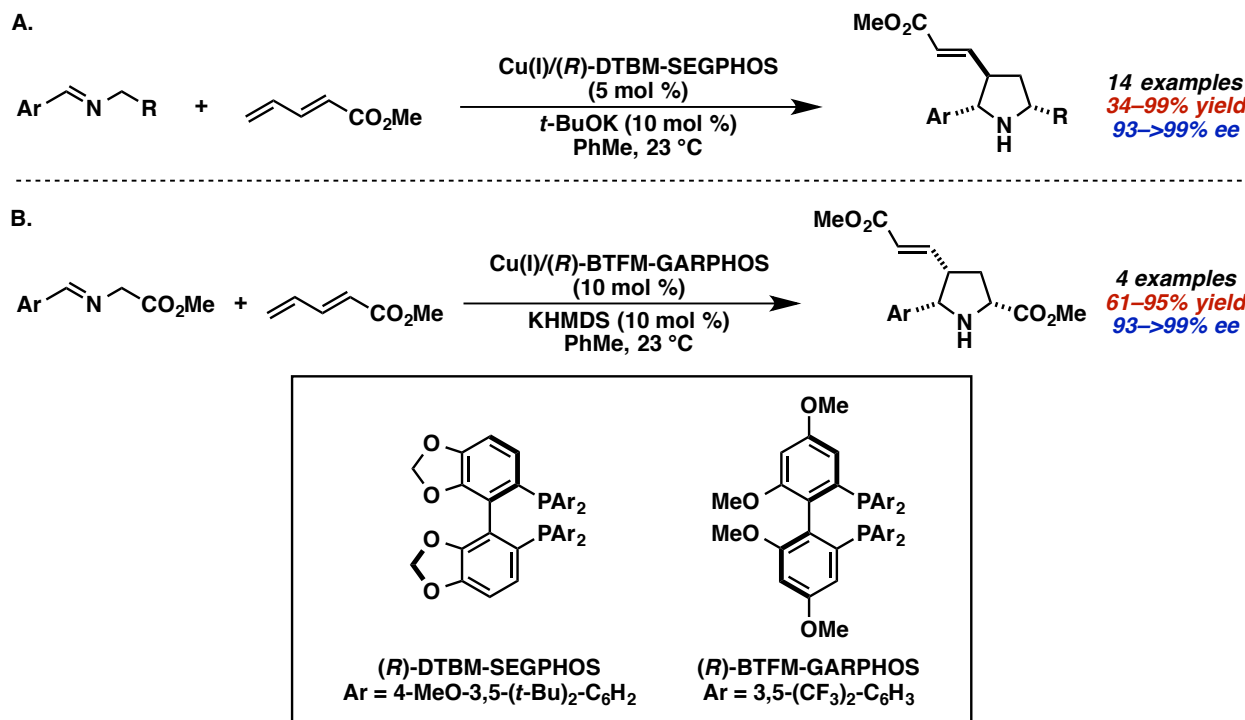
In 2006, Hou and coworkers published a report where the endo/exo diastereoselectivity of a Cu(I)-catalyzed 1,3-DC between azomethine ylides and nitroalkenes could be switched by tuning electronics on the *P,N*-ferrocenyl ligand (Table 3.3).¹² When the aromatic group on the ligand phosphine moiety was electron-rich (**3.4**), the pyrrolidine exo adduct was selectively synthesized. Alternatively, the endo pyrrolidine adduct could be accessed by utilizing electron-deficient phosphine groups on the ligand (**3.5**). A non-selective mixture of both endo and exo pyrrolidine cycloadducts was formed when diphosphine ligand **3.6** was used. Yields were moderate (ca. 60%) due to competitive formation of the Michael addition product. While such electronic trends were observed in our diastereoselective 1,3-DC reaction, the reaction system developed by our group varies from that of the Hou group because we identified ligands from different ligand classes that accomplish the observed switches in endo/exo selectivity.

Table 3.3. Hou's *P,N*-Ferrocenyl Ligand-Induced Diastereoselectivity Changes



One final example is a recent report from the Carretero group where the diastereoselectivity of a Cu(I)-catalyzed 1,3-DC between azomethine ylides and acyclic 1,3-dienes was achieved using two different *P,P'*-biaryl phosphine ligands (Scheme 3.2).¹³ Strong bases were required in order to accomplish selective reactivity at the terminal double bond of the diene. When Cs₂CO₃ was tested as the base, the 1,6-addition product was formed instead of the expected cycloadduct. This result suggested that this reaction proceeds step-wise. While no detailed discussion on the nature of diastereodivergence was provided in this report, it is possible that the diastereodetermining step is the Mannich-type cyclization, where the Cu(I) ligand can dictate the resulting C4 stereochemistry.

Scheme 3.2. Carretero's *P,P'*-Biaryl Ligand-Induced Diastereoselectivity Changes



3.2 Optimization of Reaction Conditions

After discovering the unique diastereoselectivity effects of different ligand types in the Cu(I)-catalyzed 1,3-DC (Table 3.1), reaction optimization was initiated. Higher yields and diastereoselectivity for reactions using $\text{P}(\text{OCH}_2\text{CF}_3)_3$ and PCy_3 were observed in THF than in PhMe or MeCN. (Table 3.4, entries 1–9). The reaction profiles using THF and CH_2Cl_2 were very similar (compare entries 1–3 and 10–12), but THF was chosen as the preferred solvent. With the exception of entry 6,^{14,15} no reaction proceeds in the absence of Cu(I) salt, ligand, or base (Table 3.5). It was also demonstrated that the amount of the dipolarophile could be reduced to 1.1 equiv without compromising yield or altering the diastereoselectivity (Table 3.6).

Table 3.4. Solvent Screen

The reaction scheme shows the addition of methacrylonitrile (1.5 equiv) to imine 3.1 in the presence of ligand/Cu(I) (10 mol %) and Et₃N (60 mol %) in THF at 23 °C for 3 h. The products are diastereomeric cyclopropanes 3.2 and 3.3.

entry ^a	ligand	solvent	unreacted 3.1 (%) ^d	yield (%) ^d	dr (endo:exo) ^e
1	P(OCH ₂ CF ₃) ₃ ^b		7	74	98:2
2	PCy ₃ ^b	THF	4	89	10:90
3	DavePhos ^c		4	85	41:59
4	P(OCH ₂ CF ₃) ₃ ^b		99	0	—
5	PCy ₃ ^b	PhMe	7	89	16:84
6	DavePhos ^c		87	12	50:50
7	P(OCH ₂ CF ₃) ₃ ^b		65	5	78:22
8	PCy ₃ ^b	MeCN	93	5	20:80
9	DavePhos ^c		83	7	62:38
10	P(OCH ₂ CF ₃) ₃ ^b		20	77	96:4
11	PCy ₃ ^b	CH ₂ Cl ₂	4	97	11:89
12	DavePhos ^c		21	74	40:60

^aReactions were performed using imine 3.1 (0.2 mmol), methacrylonitrile (0.3 mmol), Cu(MeCN)₄BF₄ (10 mol %), and Et₃N (0.12 mmol) at a concentration of 0.2 M in the indicated solvent. ^bReactions were performed using 22 mol % ligand. ^cReactions were performed using 11 mol % ligand. ^dGC yields using 1,3,5-trimethoxybenzene as external standard (\pm 5% error). ^eRatios determined by GC-FID analysis.

Table 3.5. Negative Controls

The reaction scheme shows the addition of methacrylonitrile (1.5 equiv) to imine 3.1 in the presence of ligand/Cu(I) (10 mol %) and Et₃N (60 mol %) in THF at 23 °C for 3 h. The products are diastereomeric cyclopropanes 3.2 and 3.3.

entry ^a	ligand	mol % Cu(I)	mol % Et ₃ N	unreacted 3.1 (%) ^d	yield (%) ^d	dr (endo:exo) ^e
1	none	0	60	98	0	—
2	P(OCH ₂ CF ₃) ₃ ^b	0	60	93	0	—
3	PCy ₃ ^b	0	60	94	0	—
4	DavePhos ^c	0	60	93	0	—
5	P(OCH ₂ CF ₃) ₃ ^b	10	0	89	0	—
6	PCy ₃ ^b	10	0	38	60	10:90
7	DavePhos ^c	10	0	88	0	—

^aReactions were performed using imine 3.1 (0.2 mmol) and methacrylonitrile (0.3 mmol) at a concentration of 0.2 M in THF. ^bReactions were performed using 22 mol % ligand. ^cReactions were performed using 11 mol % ligand. ^dGC yields using 1,3,5-trimethoxybenzene as external standard (\pm 5% error). ^eRatios determined by GC-FID analysis.

Table 3.6. Equivalents of Dipolarophile

The reaction scheme shows the Diels-Alder reaction between imine 3.1 (1,3,5-trimethoxybenzene derivative with an N-(2-ethoxycarbonyl)ethyl imine group) and methacrylonitrile. The reaction conditions are ligand/Cu(I) (10 mol %), Et₃N (60 mol %), THF, 23 °C, 3 h. The products are two diastereomeric cycloadducts, 3.2 and 3.3, which differ in the stereochemistry at the new carbon atom.

entry ^a	ligand	equiv methacrylonitrile	unreacted 3.1 (%) ^d	yield (%) ^d	dr (endo:exo) ^e
1	P(OCH ₂ CF ₃) ₃ ^b		6	84	98:2
2	PCy ₃ ^b	1.1	4	93	10:90
3	DavePhos ^c		3	93	40:60
4	P(OCH ₂ CF ₃) ₃ ^b		5	83	98:2
5	PCy ₃ ^b	1.5	4	90	10:90
6	DavePhos ^c		4	85	41:59
7	P(OCH ₂ CF ₃) ₃ ^b		4	85	97:3
8	PCy ₃ ^b	2.0	3	97	10:90
9	DavePhos ^c		3	93	42:58

^aReactions were performed using imine 3.1 (0.2 mmol), Cu(MeCN)₄BF₄ (10 mol %), and Et₃N (0.12 mmol) at a concentration of 0.2 M in THF. ^bReactions were performed using 22 mol % ligand. ^cReactions were performed using 11 mol % ligand. ^dGC yields using 1,3,5-trimethoxybenzene as external standard (\pm 5% error). ^eRatios determined by GC-FID analysis.

The effects of the nature of the base were next investigated (Table 3.7). When the strong organic base 1,8-diazabicyclo[5.4.0]undec-7-ene (DBU) was used instead of Et₃N, yields of cycloadducts and diastereoselectivity eroded (entries 1–6). The efficacy of Cs₂CO₃ and KHMDS were also explored. Cs₂CO₃ proved to promote the 1,3-DC reaction well when ligands P(OCH₂CF₃)₃ and DavePhos were used (entries 7 and 9); however, the reaction run using PCy₃ as the ligand proceeded in a lower yield with a loss of diastereoselectivity compared to the same reaction using Et₃N (compare entries 2 and 8). Finally, the use of KHMDS resulted in very low yields of the desired products (entries 10–12). Using a catalytic amount of Et₃N maintained high conversion and desired diastereoselectivities (compare entries 1–3 to 13–15).

Table 3.7. Base Optimization

entry ^a	ligand	base (equiv)	unreacted 3.1 (%) ^d	yield (%) ^d	dr (endo:exo) ^e
1	P(OCH ₂ CF ₃) ₃ ^b		6	84	98:2
2	PCy ₃ ^b	Et ₃ N (0.60)	4	93	10:90
3	DavePhos ^c		3	93	40:60
4	P(OCH ₂ CF ₃) ₃ ^b		73	12	65:35
5	PCy ₃ ^b	DBU (0.60)	47	40	62:38
6	DavePhos ^c		13	67	45:55
7	P(OCH ₂ CF ₃) ₃ ^b		6	82	97:3
8	PCy ₃ ^b	Cs ₂ CO ₃ (0.60)	5	78	49:51
9	DavePhos ^c		2	86	47:53
10	P(OCH ₂ CF ₃) ₃ ^b		1	20	94:6
11	PCy ₃ ^b	KHMDS (0.60)	13	6	nd
12	DavePhos ^c		1	2	nd
13 ^f	P(OCH ₂ CF ₃) ₃ ^b		5	81	98:2
14 ^f	PCy ₃ ^b	Et ₃ N (1.1)	4	93	10:90
15 ^f	DavePhos ^c		3	91	42:58

^aReactions were performed using imine 3.1 (0.20 mmol), methacrylonitrile (0.22 mmol), and Cu(MeCN)₄BF₄ (10 mol %) at a concentration of 0.2 M in THF. ^bReactions were performed using 22 mol % ligand. ^cReactions were performed using 11 mol % ligand. ^dGC yields using 1,3,5-trimethoxybenzene as external standard (\pm 5% error). ^eRatios determined by GC-FID analysis. ^fReactions run using 1.5 equiv methacrylonitrile. nd = not determined.

The 1,3-DC reaction was run at lower temperatures to determine whether an improvement of diastereoselectivity could be achieved (Table 3.8). Surprisingly, lower temperatures had no effect on the diastereoselectivity for any of the three reactions tested. Yields of the cycloadducts were lower as the reaction temperature was decreased (entries 1–6). Conveniently, ambient temperature proved to be the most effective temperature to carry out the desired transformation (entries 7–9).

Table 3.8. Temperature Effects on Yield and Diastereoselectivity

entry ^a	ligand	temp (°C)	unreacted 3.1 (%) ^d	yield (%) ^d	dr (endo:exo) ^e
1	P(OCH ₂ CF ₃) ₃ ^b		38	33	94:6
2	PCy ₃ ^b	-20	44	56	9:91
3	DavePhos ^c		14	79	48:52
4	P(OCH ₂ CF ₃) ₃ ^b		21	54	96:4
5	PCy ₃ ^b	0	15	81	10:90
6	DavePhos ^c		3	88	44:56
7	P(OCH ₂ CF ₃) ₃ ^b		6	84	98:2
8	PCy ₃ ^b	23	4	93	10:90
9	DavePhos ^c		3	93	40:60

^aReactions were performed using imine 3.1 (0.20 mmol), methacrylonitrile (0.22 mmol), Cu(MeCN)₄BF₄ (10 mol %), and Et₃N (0.12 mmol) at a concentration of 0.2 M in THF. ^bReactions were performed using 22 mol % ligand.

^cReactions were performed using 11 mol % ligand. ^dGC yields using 1,3,5-trimethoxybenzene as external standard (\pm 5% error). ^eRatios determined by GC-FID analysis.

The optimal catalyst loading, reaction time, and reaction concentration were next determined (Table 3.9). Running the reaction at a concentration of 0.2 M and using a 10 mol % catalyst loading for 1 h proved insufficient (entries 1–3), as did a 1 mol % catalyst loading for a reaction time of 12 h (entries 4–6). A catalyst loading of 5 mol % was adapted and the effect of concentration was explored over a 2 h reaction time (entries 7–24). Not surprisingly, yields increased as the reaction concentration was increased from 0.1 M to 1 M. Using P(OCH₂CF₃)₃ as the ligand, endo adduct selectivity slowly degraded as the reaction concentration was increased above 0.4 M (compare entry 13 to entries 16, 19, and 22). A concentration of 0.6 M was chosen for reactions run using the phosphite ligand as the results showed a reasonable compromise between yield and endo adduct selectivity. The reactions run using PCy₃ as the ligand showed good reactivity and exo adduct selectivity at a concentration of 1 M (entry 23), and a

concentration of 0.4 M was chosen to further study 1,3-DC reactions using DavePhos as the ligand (entry 15).

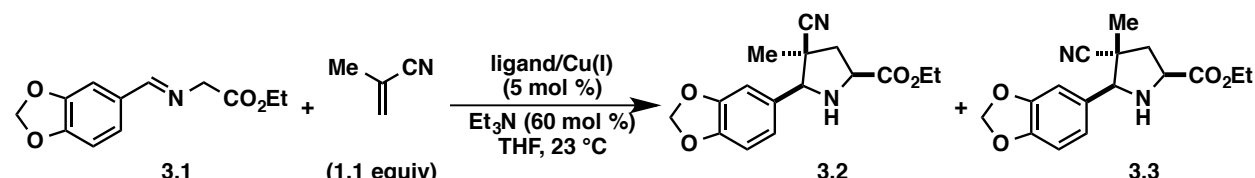
Table 3.9. Catalyst Loading and Reaction Concentration

entry ^a	ligand	catalyst loading	concentration	time	unreacted 3.1 (%) ^d	yield (%) ^d	dr (endo:exo) ^e
1	P(OCH ₂ CF ₃) ₃ ^b				50	25	96:4
2	PCy ₃ ^b	10 mol %	0.2 M	1 h	27	66	11:89
3	DavePhos ^c				4	86	40:60
4	P(OCH ₂ CF ₃) ₃ ^b				65	7	97:3
5	PCy ₃ ^b	1 mol %	0.2 M	12 h	52	36	13:87
6	DavePhos ^c				80	1	nd
7	P(OCH ₂ CF ₃) ₃ ^b				68	9	97:3
8	PCy ₃ ^b	5 mol %	0.1 M	2 h	27	62	12:88
9	DavePhos ^c				51	30	46:54
10	P(OCH ₂ CF ₃) ₃ ^b				59	16	97:3
11	PCy ₃ ^b	5 mol %	0.2 M	2 h	13	76	11:89
12	DavePhos ^c				19	63	43:57
13	P(OCH ₂ CF ₃) ₃ ^b				49	35	98:2
14	PCy ₃ ^b	5 mol %	0.4 M	2 h	7	88	10:90
15	DavePhos ^c				5	94	39:61
16	P(OCH ₂ CF ₃) ₃ ^b				20	72	96:4
17	PCy ₃ ^b	5 mol %	0.6 M	2 h	6	98	10:90
18	DavePhos ^c				2	98	39:61
19	P(OCH ₂ CF ₃) ₃ ^b				17	71	94:6
20	PCy ₃ ^b	5 mol %	0.8 M	2 h	3	97	10:90
21	DavePhos ^c				3	96	38:62
22	P(OCH ₂ CF ₃) ₃ ^b				8	84	93:7
23	PCy ₃ ^b	5 mol %	1.0 M	2 h	3	99	9:91
24	DavePhos ^c				2	95	39:61

^aReactions were performed using imine 3.1 (0.20 mmol), methacrylonitrile (0.22 mmol), and Et₃N (0.12 mmol) with the indicated catalyst loading and at the indicated concentration in THF. ^bReactions were performed using a 2.2:1 ligand-to-Cu(I) ratio. ^cReactions were performed using a 1.1:1 ligand-to-Cu(I) ratio. ^dGC yields using 1,3,5-trimethoxybenzene as external standard (\pm 5% error). ^eRatios determined by GC-FID analysis. nd = not determined.

Next, the reaction time was optimized using each of the three ligands based on the optimal concentration (Table 3.10). Focusing on four different time points, a reaction time of 5 h was chosen for reactions using the phosphite ligand as the highest conversion was achieved (entries 1–4). The high reactivity of the Cu(I)/*PCy*₃ catalyst was demonstrated by running the 1,3-DC for 0.5–2 h (entries 5–8) and a 1 h reaction time was chosen for this catalyst system. Finally, after probing the reactivity of the Cu(I)/DavePhos catalyst from 2–5 h at a concentration of 0.4 M, a 3 h reaction time was shown to accomplish desirable reactivity (entries 9–12).

Table 3.10. Optimization of Reaction Time



entry ^a	ligand	concentration	time	unreacted 3.1 (%) ^d	yield (%) ^d	dr (endo:exo) ^e
1	<i>P</i> (OCH ₂ CF ₃) ₃ ^b	0.6 M	2 h	23	64	97:3
2			3 h	14	73	97:3
3			4 h	6	84	96:4
4			5 h	8	86	96:4
5	<i>PCy</i> ₃ ^b	1.0 M	30 min	14	86	9:91
6			60 min	5	95	9:91
7			90 min	4	>99	9:91
8			120 min	3	99	9:91
9	DavePhos ^c	0.4 M	2 h	7	91	38:62
10			3 h	3	95	38:62
11			4 h	3	96	37:63
12			5 h	2	96	38:62

^aReactions were performed using imine 3.1 (0.20 mmol), methacrylonitrile (0.22 mmol), Et₃N (0.12 mmol), and Cu(MeCN)₄BF₄ (5 mol %) for the indicated time and at the indicated concentration in THF. ^bReactions were performed using 11 mol % ligand. ^cReactions were performed using 5.5 mol % ligand. ^dGC yields using 1,3,5-trimethoxybenzene as external standard (\pm 5% error). ^eRatios determined by GC-FID analysis.

3.3 Investigation of Imine Reactivity

After optimizing the 1,3-DC reaction for each catalyst system at a 5 mol % catalyst loading, three different methods were developed: Method A, where P(OCH₂CF₃)₃ was used as the ligand (11 mol %) and the reaction was run at a concentration of 0.6 M for 5 h; method B,

where PCy₃ was used as the ligand (11 mol %) at a 1.0 M concentration for a 1 h reaction time; and method C, where ligand DavePhos (5.5 mol %), a 3 h reaction time, and a 0.4 M concentration were used. Relative configuration of the cycloadducts was assigned by 2D ¹H NMR experiments (see Appendix B for details).

The results of cycloadditions of nine imine substrates with methacrylonitrile under these reaction conditions are summarized in Table 3.11. Electron-rich (**3.1**, **3.7**, **3.10**; entries 1–9), electron-neutral (**3.13**, entries 10–12), and electron-deficient (**3.16**, **3.19**, **3.22**, **3.25**, **3.28**; entries 13–27) aryl imines were used as substrates. Methods A and B preferentially provided the endo and exo cycloadducts, respectively. These results demonstrated that the diastereoselectivity trends are controlled by the catalyst.

As pyridyl groups are common ligands for copper,¹⁶ it was not surprising that 3-pyridyl imine **3.16** was a poor substrate for this reaction (Table 3.11, entries 13–15). To test the hypothesis that the pyridyl group coordinates to the Cu(I) catalyst, the catalyst loading was increased from 5 mol % to 10 mol %, which resulted in increased yields of desired pyrrolidine products **3.17** or **3.18** (Table 3.12). Additionally, the three 1,3-DC reactions between phenyl imine **3.13** and methacrylonitrile were conducted in the presence of 1 equiv pyridine (Table 3.13). Compared to the results of these reactions run in the absence of pyridine, yields of pyrrolidine products **3.14** and **3.15** were significantly decreased. Collectively, these two sets of experiments indicate that pyridyl-derived imine substrates are not suitable for the Cu(I)-catalyzed 1,3-DC reaction, as they can reduce the activity of the catalyst.

Table 3.11. Diastereodivergence using Different Imines

The reaction scheme illustrates the Diels-Alder reaction between a substituted imine (R-phenyl-C(=N)CH₂CO₂E_t) and methacrylonitrile (Me-CH=CH-CN). The reaction conditions are ligand/Cu(I) (5 mol %), Et₃N (60 mol %), THF, 23 °C, 1.1 equiv of imine. The products are the endo adduct (with Me and CN on the same side) and the exo adduct (with Me and CN on opposite sides).

entry ^a	aryl group	method	GC yield (%) ^e	cycloadducts	dr (endo:exo) ^f	isolated yield (dr, endo:exo) ^g
1		A ^b	88		96:4	79% (94:6)
2	3.1	B ^c	97	endo = 3.2 exo = 3.3	9:91	82% (11:89)
3	3.1	C ^d	95		39:61	
4		A ^b	58		94:6	
5	3.7	B ^c	>99	endo = 3.8 exo = 3.9	12:88	
6	3.7	C ^d	96		35:65	
7	3.10	A ^b	91		94:6	
8	3.10	B ^c	93	endo = 3.11 exo = 3.12	9:91	
9	3.10	C ^d	93		40:60	
10	3.13	A ^b	76		98:2	76% (96:4)
11	3.13	B ^c	97	endo = 3.14 exo = 3.15	11:89	83% (12:88)
12	3.13	C ^d	94		38:62	
13	3.16	A ^b	14		86:14	
14	3.16	B ^c	52	endo = 3.17 exo = 3.18	12:88	
15	3.16	C ^d	46		49:51	
16	3.19	A ^b	84		96:4	
17	3.19	B ^c	>99	endo = 3.20 exo = 3.21	12:88	
18	3.19	C ^d	>99		41:59	
19	3.22	A ^b	88		96:4	74% (96:4)
20	3.22	B ^c	92	endo = 3.23 exo = 3.24	14:86	78% (15:85)
21	3.22	C ^d	98		47:53	
22	3.25	A ^b	78		96:4	
23	3.25	B ^c	95	endo = 3.26 exo = 3.27	12:88	
24	3.25	C ^d	98		56:44	
25	3.28	A ^b	91		98:2	76% (98:2)
26	3.28	B ^c	>99	endo = 3.29 exo = 3.30	14:86	73% (15:85)
27	3.28	C ^d	>99		61:39	

^aReactions were performed using imine (0.20 mmol), methacrylonitrile (0.22 mmol), Et₃N (0.12 mmol), and Cu(MeCN)₄BF₄ (5 mol %), at the indicated concentration in THF. ^bReactions run at 0.6 M for 5 h using P(OCH₂CF₃)₃ as the ligand (11 mol %). ^cReactions run at 1.0 M for 1 h using PCy₃ as the ligand (11 mol %). ^dReactions run at 0.4 M for 3 h using DavePhos as the ligand (5.5 mol %). ^eGC yields determined using 1,3,5-trimethoxybenzene as external standard (average of two experiments, ± 5% error). ^fRatios determined by GC-FID analysis (average of two experiments). ^gRatios determined by ¹H NMR analysis of the crude reaction mixture.

Table 3.12. Increased Catalyst Loading to Access Pyrrolidines 3.17 and 3.18

entry ^a	method	unreacted 3.16 (%) ^e	yield (%) ^e	dr (endo:exo) ^f
1	A ^b	52	39	76:24
2	B ^c	35	73	9:91
3	C ^d	33	67	44:56

^aReactions were performed using imine 3.16 (0.20 mmol), methacrylonitrile (0.22 mmol), Et₃N (0.12 mmol), and Cu(MeCN)₄BF₄ (10 mol %) at the indicated concentration in THF. ^bReactions run at 0.6 M for 5 h using P(OCH₂CF₃)₃ as the ligand (22 mol %). ^cReactions run at 1.0 M for 1 h using PCy₃ as the ligand (22 mol %). ^dReactions run at 0.4 M for 3 h using DavePhos as the ligand (11 mol %). ^eGC yields determined using 1,3,5-trimethoxybenzene as external standard (\pm 5% error). ^fRatios determined by GC-FID analysis.

Table 3.13. Pyridine Poisons Cu(I) Catalysts

entry ^a	method	unreacted 3.13 (%) ^e	yield (%) ^e	dr (endo:exo) ^f
1	A ^b	79	<5	nd
2	B ^c	45	49	10:90
3	C ^d	57	31	40:60

^aReactions were performed using imine 3.13 (0.20 mmol), methacrylonitrile (0.22 mmol), pyridine (0.20 mmol), Et₃N (0.12 mmol), and Cu(MeCN)₄BF₄ (5 mol %) at the indicated concentration in THF. ^bReactions run at 0.6 M for 5 h using P(OCH₂CF₃)₃ as the ligand (11 mol %). ^cReactions run at 1.0 M for 1 h using PCy₃ as the ligand (11 mol %). ^dReactions run at 0.4 M for 3 h using DavePhos as the ligand (5.5 mol %). ^eGC yields determined using 1,3,5-trimethoxybenzene as external standard (\pm 5% error). ^fRatios determined by GC-FID analysis. nd = not determined.

3.4 Transition State Calculations

A collaboration with the Houk group at UCLA was established in order to gain a better understanding of the catalyst control of the diastereoselectivity of the Cu(I)-catalyzed 1,3-DC reaction. Using the B3LYP-D3/6-311+G(d,p)/SDD,CPCM//B3LYP/6-31G*/LANL2DZ computational method, endo and exo adduct transition states were calculated for each Cu(I)-ligand-ylide complex.¹⁷ The endo transition state was calculated to be 0.9 kcal/mol lower in energy than the corresponding exo transition state with the P(OCH₂CF₃)₃ ligand (Figure 3.1).

In the endo transitions state, a favorable electrostatic interaction between the ESP-negative nitrogen atom in methacrylonitrile and the ESP-positive methylene protons on the phosphite ligand was observed (Figure 3.2). This stabilizing interaction is absent in the exo transition state and therefore may account for the lower energy calculated for the endo transition state using $\text{P}(\text{OCH}_2\text{CF}_3)_3$ as the ligand.

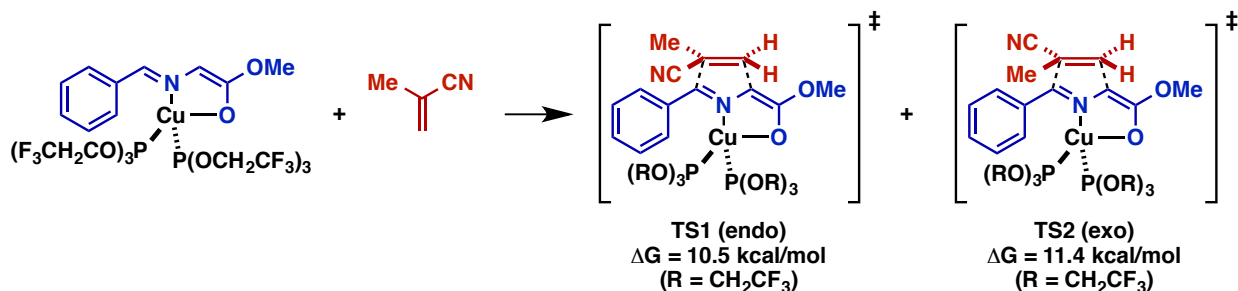


Figure 3.1. Transition State Energies Calculated for a Cu(I)-Phosphite-Ylide Complex

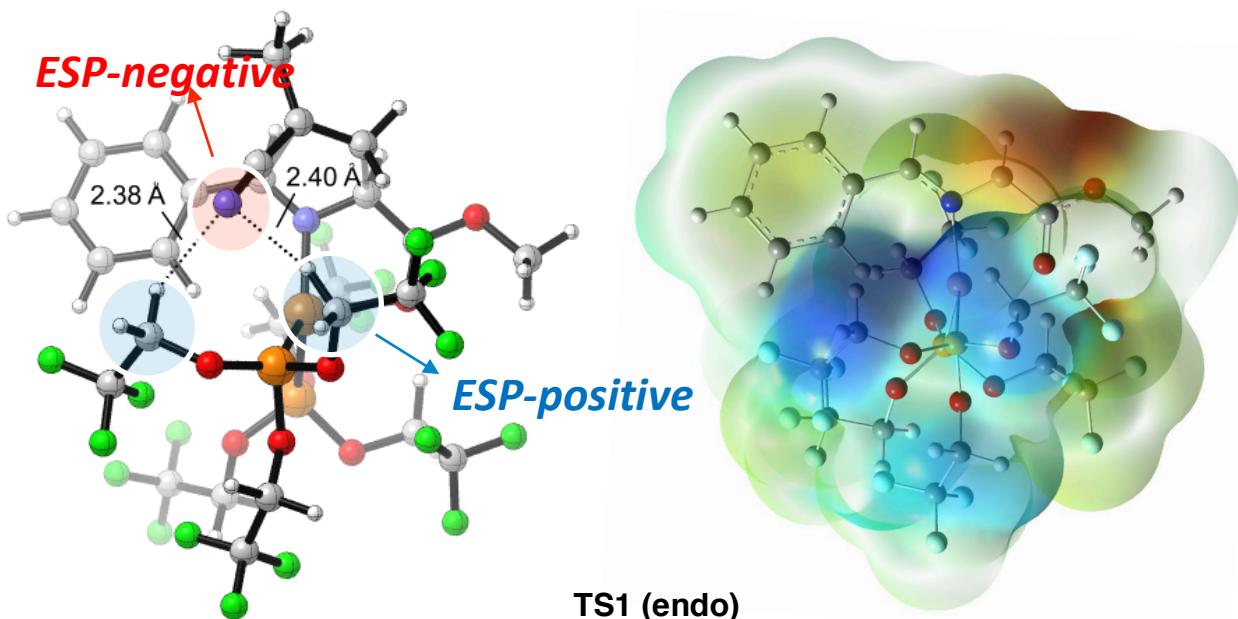
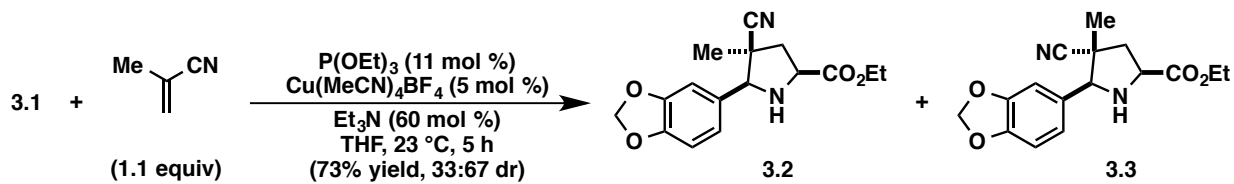


Figure 3.2. Calculated Endo Transition State with Phosphite Ligand

The endo transition state-stabilizing electrostatic interaction hypothesis was tested by running a similar calculation using triethyl phosphite $[\text{P}(\text{OEt})_3]$ as the ligand. The resulting endo and exo transition states were calculated to differ by only 0.5 kcal/mol and indicated a more

stable exo transition state; this difference is thought to be the result of the ESP-neutral character of the P(OEt)₃ methylene protons. This hypothesis was also tested experimentally (eq 3.1). The 1,3-DC reaction using P(OEt)₃ as the ligand accessed products **3.2** and **3.3** in a 73% yield and 33:67 dr (endo:exo). The disrupted endo adduct selectivity of this reaction supports the electrostatic interaction hypothesis.

Equation 3.1



The exo transition state was calculated to be 1.1 kcal/mol lower in energy than the endo transition state when PCy₃ was used as the ligand (Figure 3.3). This energy difference is proposed to be the result of steric interactions between the bulky cyclohexyl groups on the phosphine ligand and the nitrile group of the dipolarophile. These theoretical results are in corroboration with the experimental results using PCy₃ as the ligand.

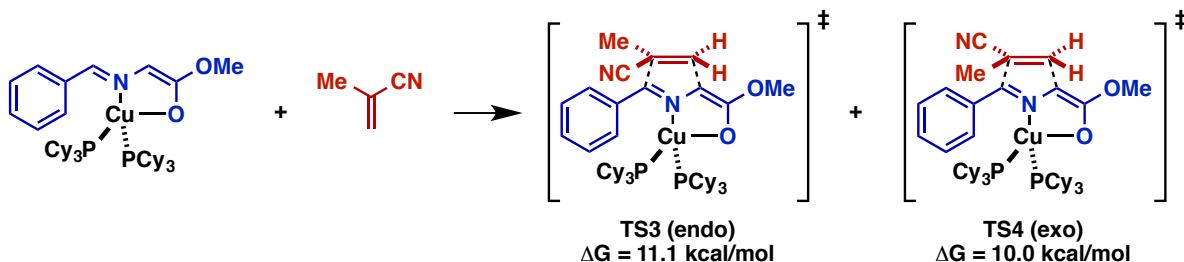


Figure 3.3. Transition State Energies Calculated for a Cu(I)-PCy₃-Ylide Complex

Eight transition states for the Cu(I)-DavePhos complex were found as a result of two diastereomeric Cu(I)/DavePhos complexes, **3.31** and **3.32**, and four possible approaches of the dipolarophile for each catalyst configuration (bottom or top approach and exo or endo coordination; Figure 3.4). The lowest energy endo and exo transition states, TS5 and TS6,

respectively, differed by only 0.5 kcal/mol. No significant stabilizing electrostatic or destabilizing steric interactions were detected. Collectively, the calculations performed on the Cu(I)-DavePhos-ylide complex offer an explanation for the poor diastereoselectivity that is observed experimentally.

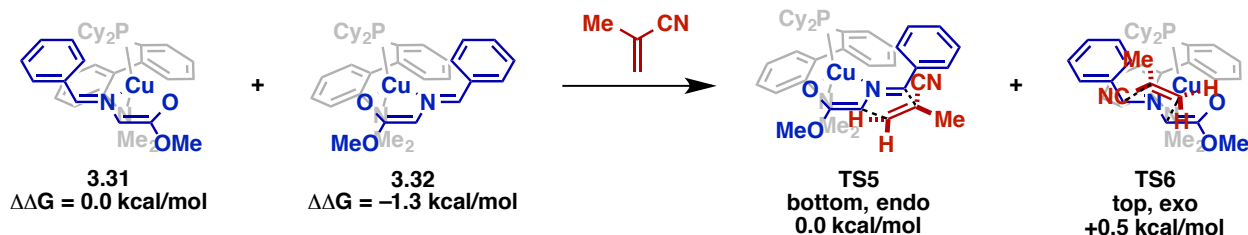


Figure 3.4. Transition State Energies Calculated for a Cu(I)-DavePhos-Ylide Complex

In summary, the theoretical calculations performed by the Houk group clearly demonstrate that the nitrile functionality of the dipolarophile is a key factor in differentiating the endo and exo transition states for the endo adduct-selective ligand $P(OCH_2CF_3)_3$ and the exo adduct-selective ligand PCy_3 .

3.5 Utilization of Different Dipolarophiles

Nitrile-containing dipolarophiles are underrepresented in the catalytic 1,3-DC literature compared to α,β -unsaturated carbonyl compounds,¹⁸ and the majority of such reports involve the use of either acrylonitrile^{4e;9h,t,v,w,ah;10d,f;19} or highly electron-deficient fumaronitrile.^{1,2a,6b,20,21} While the original goal to developing a highly diastereoselective 1,3-DC with methacrylonitrile was for the epidithiodioxopiperazine research program,²² we embraced the opportunity to address the deficit of nitrile-containing dipolarophiles used in catalytic 1,3-DC reactions. The reaction between imine **3.13** and acrylonitrile was performed using the optimized conditions (Table 3.14). Endo adduct selectivity was not as pronounced as when methacrylonitrile was used (69:31 dr, entry 1).²³ As predicted by transition state calculations using methacrylonitrile, steric interactions with the α -methyl group increase the exo transition state energy when $P(OCH_2CF_3)_3$

is used as the ligand. The lack of substitution at the α -position on acrylonitrile may result in a relatively lower energy exo transition state, resulting in a less endo adduct-selective reaction using method A. However, using method B, exo pyrrolidine adduct **3.34** was selectively synthesized (8:92 dr, entry 2). This result was expected when considering the analogous lack of a stabilizing electrostatic interaction in the calculated endo transition state. Finally, in the reaction using DavePhos as the ligand, exo cycloadduct **3.34** was preferentially accessed in a 19:81 ratio (entry 3). This result also suggests the importance of α -substitution on the dipolarophile in the corresponding transition state energies.

Table 3.14. Nitrile-Containing Dipolarophiles

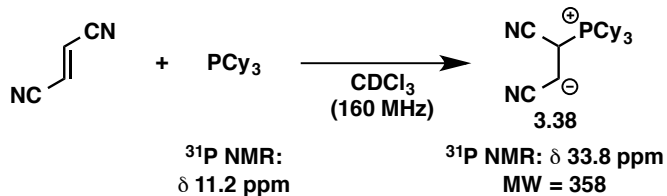
entry ^a	dipolarophile	method	yield (%) ^e	cycloadducts	dr (endo:exo) ^f
1	acrylonitrile (R = H)	A ^b	93 ^g		69:31 ^g
2		B ^c	85 ^g	endo = 3.33, exo = 3.34	8:92 ^g
3		C ^d	>99 ^g		19:81 ^g
4	fumaronitrile (R = CN)	A ^b	61 (3.35, exo)	3.36	
5		B ^c	65 (3.35, exo)	3.37	
6		C ^d	76 (3.35, exo)		

^aReactions were performed using imine **3.13** (0.20 mmol), dipolarophile (0.22 mmol), Et₃N (0.12 mmol), and Cu(MeCN)₄BF₄ (5 mol %), at the indicated concentration in THF. ^bReactions run at 0.6 M for 5 h using P(OCH₂CF₃)₃ as the ligand (11 mol %). ^cReactions run at 1.0 M for 1 h using PCy₃ as the ligand (11 mol %). ^dReactions run at 0.4 M for 3 h using DavePhos as the ligand (5.5 mol %). ^eGC yields determined using 1,3,5-trimethoxybenzene as external standard (\pm 5% error). ^fRatios determined by GC-FID analysis. ^gAverage of two experiments.

Fumaronitrile was used as a dipolarophile in the optimized 1,3-DC reactions (Table 3.14). Despite the method used, exo cycloadduct **3.35** was accessed as the major product. The endo cycloadduct was not observed and additional diastereomers **3.36** and **3.37** were detected in small amounts (<10%),²⁴ indicating isomerization of the dipolarophile component.²⁵ Treatment of fumaronitrile with 1 equiv PCy₃ resulted in one signal observed by ³¹P NMR and ESI-MS

indicated the formation of zwitterionic species **3.38** (eq 3.2). These results indicate that either a stepwise Michael addition-intramolecular Mannich-type reaction pathway occurs when using fumaronitrile, or that the dipolarophile isomerizes prior to cycloaddition due to reaction with other reaction components. Thus, the use of fumaronitrile in this reaction was no longer pursued.

Equation 3.2



The reactivity of α,β -unsaturated carbonyl dipolarophiles methyl acrylate and methyl methacrylate were also examined in the Cu(I)-catalyzed reaction (Table 3.15). Reactions run using methyl acrylate resulted in preferential formation of endo pyrrolidine adduct **3.39** regardless of the method used (entries 1–3). While the reaction run using PCy_3 did not afford significant amounts of exo cycloadduct **3.40** (entry 2), pyrrolidine **3.40** was accessed non-selectively when method C was used (entry 3). Similar results were obtained using methyl methacrylate as the dipolarophile, but with lower overall yields (entries 4–6). While the Cu(I)-catalyzed 1,3-DC reaction with novel catalyst-controlled diastereoselectivity works well with acrylonitrile and methacrylonitrile dipolarophiles, reactions performed using acrylates with or without α -substitution were selective for the endo cycloadduct.

Table 3.15. Acrylate Dipolarophiles

The reaction scheme shows the cycloaddition of imine 3.13 (a benzylidene imine derivative) with a general acrylate dipolarophile (R-C(=O)CH₂CO₂Me). The reaction conditions are ligand/Cu(I) (5 mol %), Et₃N (60 mol %), THF, 23 °C. The products are the endo and exo adducts, which are bicyclic structures where the imine nitrogen is bonded to the aromatic ring and the acrylate carbon, with the methyl ester group and R group in specific stereochemical positions.

entry ^a	dipolarophile	method	yield (%) ^e	cycloadducts	dr (endo:exo) ^f
1	methyl acrylate (R = H)	A ^b	87		97:3
2		B ^c	85	endo = 3.39, exo = 3.40	94:6
3		C ^d	93		69:31
4	methyl methacrylate (R = Me)	A ^b	61		99:1
5		B ^c	75	endo = 3.41, exo = 3.42	97:3
6		C ^d	87		78:22

^aReactions were performed using imine 3.13 (0.20 mmol), dipolarophile (0.22 mmol), Et₃N (0.12 mmol), and Cu(MeCN)₄BF₄ (5 mol %), at the indicated concentration in THF. ^bReactions run at 0.6 M for 5 h using P(OCH₂CF₃)₃ as the ligand (11 mol %). ^cReactions run at 1.0 M for 1 h using PCy₃ as the ligand (11 mol %).

^dReactions run at 0.4 M for 3 h using DavePhos as the ligand (5.5 mol %). ^e¹H NMR yields determined using 5,6-dibromo-1,3-benzodioxole as external standard (average of two experiments). ^fRatios determined by ¹H NMR analysis of the crude reaction mixture (average of two experiments).

3.6 Conclusion

In conclusion, we have developed a catalytic 1,3-DC reaction to access nitrile-containing pyrrolidine products in high diastereoselectivity by changing only the ligand. Theoretical transition state energy calculations suggest a stabilizing electrostatic interaction in the endo transition state using P(OCH₂CF₃)₃ as the ligand and destabilizing steric interactions in the endo transition state when PCy₃ is used. The calculations explain the experimental selectivity trends using methacrylonitrile as the dipolarophile. The observed trends for acrylonitrile and methacrylonitrile dipolarophiles, however, did not apply to reactions using fumaronitrile or acrylates. Further development of this reaction to incorporate chiral ligands to achieve asymmetric induction is currently the future focus of this project.

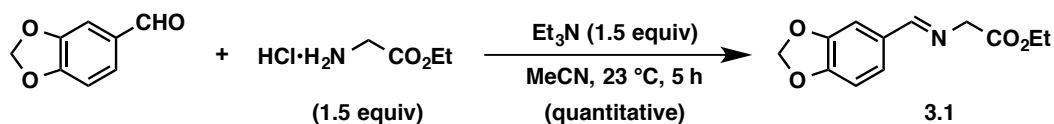
3.7 Appendix A: Experimental Procedures

3.7.1 Materials and Methods

Unless stated otherwise, reactions were conducted in flame- or oven-dried glassware under a positive pressure of nitrogen (N_2) or argon (Ar) using anhydrous solvents (dried by passing through activated alumina columns under a positive pressure of Ar). Oxygen-sensitive reactions were carried out in solvents that were degassed by three freeze-pump-thaw cycles. Catalyst components and imine starting materials for the 1,3-dipolar cycloaddition reactions were weighed out in an MBraun Unilab 2000 glove box with a N_2 atmosphere. Aldehydes were distilled neat prior to use. Methacrylonitrile, acrylonitrile, methyl acrylate, methyl methacrylate, and tris(2,2,2-trifluoroethyl) phosphite [$P(OCH_2CF_3)_3$] were sparged with Ar for 5 min before distilling neat prior to use. All other commercially obtained reagents were used as received. Reaction temperatures were controlled using an IKAmag temperature modulator, and unless stated otherwise, reactions were performed at room temperature (approximately 23 °C). Analytical thin-layer chromatography (TLC) was conducted on EMD silica gel 60 F₂₅₄ glass-backed plates (250 µm) and visualized by exposure to UV light (254 nm), or by Dragendorff–Munier and potassium permanganate staining. Flash chromatography was performed using forced flow of the indicated solvent system on EMD Geduran® silica gel 60 (particle size 0.040–0.063 mm). NMR spectra were recorded at 298 K on Bruker FT-NMR spectrometers at the indicated frequencies. Chemical shifts (δ) are reported in parts per million (ppm) relative to residual deuterated solvent signals ($CDCl_3$ or acetone-d₆). Data for ¹H NMR spectra are reported as follows: chemical shift (δ ppm), multiplicity, coupling constant [J , reported in Hertz (Hz)], and integration. Splitting patterns are abbreviated as follows: singlet (s), doublet (d), triplet (t), quartet (q), multiplet (m), apparent (app), and broad (br). Carbon multiplicity was determined by

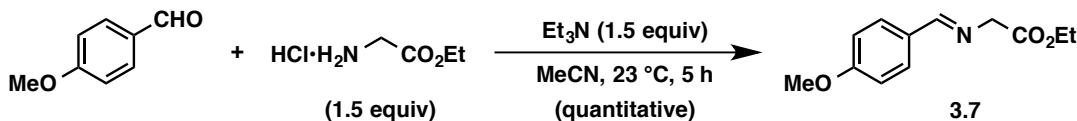
a combination of DEPTQ and HMQC experiments. Chemical shifts (δ) for ^{19}F and ^{31}P NMR spectra are reported in parts per million (ppm) and referenced to the corresponding calibrated ^1H NMR spectrum. GC-FID analysis was performed on an Agilent 7890A GC System equipped with a Flame Ionization Detector (FID) and Cyclodex-B capillary column (30 m length, 0.25 mm ID, 0.25 μm film). Infrared (IR) spectra were recorded on a Varian 640-IR spectrometer as thin films in CH_2Cl_2 on KBr plates and are reported in terms of frequency of absorption (cm^{-1}). High-resolution mass spectra (HRMS) were obtained from the UC Irvine Mass Spectrometry Facility with a Micromass LCT spectrometer. Melting points (mp) were determined on a melting point apparatus (Thomas Hoover, Uni-Melt) and are uncorrected. Abbreviations used can be found on the Internet at: http://pubs.acs.org/paragonplus/submission/joceah/joceah_abbreviations.pdf.

3.7.2 Synthesis of Imines

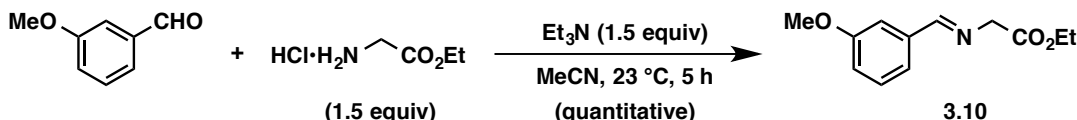


Ethyl (E)-2-((benzo[*d*][1,3]dioxol-5-ylmethylene)amino)acetate (3.1). A 50 mL round-bottom flask was charged with a magnetic stir bar and glycine ethyl ester hydrochloride (525 mg, 3.75 mmol, 1.50 equiv) and piperonal (375 mg, 2.50 mmol, 1.00 equiv). MeCN (4.2 mL, 0.6 M) and Et_3N (520 μL , 3.75 mmol, 1.50 equiv) were sequentially added and the resulting heterogeneous mixture was vigorously stirred at 23 °C for 5 h. Concentration of the reaction mixture under reduced pressure afforded an amorphous colorless solid, which was transferred to a separatory funnel using CH_2Cl_2 (15 mL) and H_2O (30 mL). The layers of the resulting biphasic mixture were partitioned and the organic layer was extracted with H_2O (30 mL) and brine (30 mL). The organic layer was dried over Na_2SO_4 , filtered, and concentrated to afford imine **3.1** (588 mg, quantitative yield) as a light yellow oil.²⁶ Imine **3.1** was carried

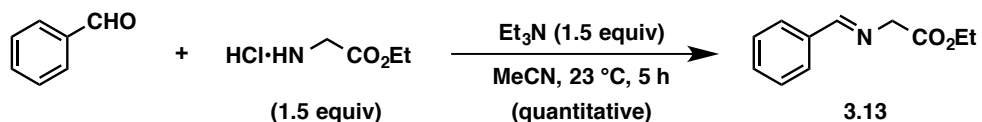
further in subsequent reactions without further purification. ^1H NMR (600 MHz, CDCl_3): δ 8.16 (s, 1H), 7.41 (s, 1H), 7.15 (d, $J = 7.9$, 1H), 6.83 (d, $J = 7.9$, 1H), 6.01 (s, 2H), 4.35 (s, 2H), 4.23 (q, $J = 6.8$, 2H), 1.30 (t, $J = 6.8$, 3H).



Ethyl (E)-2-((4-methoxybenzylidene)amino)acetate (3.7). According to the procedure described for the synthesis of imine **3.1**, imine **3.7** was prepared from 4-methoxybenzaldehyde (300 μL , 2.5 mmol, 1.0 equiv) as a yellow oil (550 mg, quantitative yield). Imine **3.7** was carried further in subsequent reactions without further purification. ^1H NMR (600 MHz, CDCl_3): δ 8.21 (s, 1H), 7.73 (app d, $J = 8.6$, 2H), 6.93 (app d, $J = 8.6$, 2H), 4.36 (s, 2H), 4.23 (q, $J = 7.1$, 2H), 3.85 (s, 3H), 1.30 (t, $J = 7.1$, 3H).

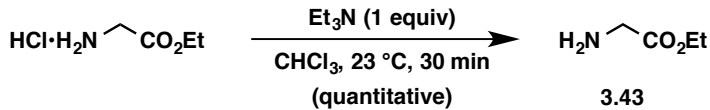


Ethyl (E)-2-((3-methoxybenzylidene)amino)acetate (3.10). According to the procedure described for the synthesis of imine **3.1**, imine **3.10** was prepared from 3-methoxybenzaldehyde (300 μL , 2.5 mmol, 1.0 equiv) as a light yellow oil (550 mg, quantitative yield). Imine **3.10** was carried further in subsequent reactions without further purification. ^1H NMR (600 MHz, CDCl_3): δ 8.27 (s, 1H), 7.39 (br s, 1 H), 7.33 (t, $J = 7.7$, 1H), 7.29 (br d, $J = 7.7$, 1H), 7.01 (dd, $J = 7.7$, 1.8, 1H), 4.40 (s, 2H), 4.24 (q, $J = 7.2$, 2H), 3.85 (s, 3H), 1.31 (t, $J = 7.2$, 3H).

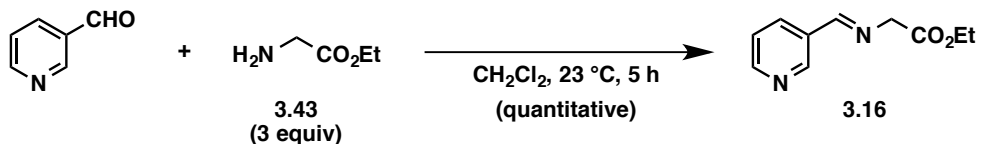


Ethyl (E)-2-(benzylideneamino)acetate (3.13). According to the procedure described for the synthesis of imine **3.1**, imine **3.13** was prepared from benzaldehyde (250 μL , 2.5 mmol,

1.0 equiv) as a clear oil (480 mg, quantitative yield). Imine **3.13** was carried further in subsequent reactions without further purification. ^1H NMR (500 MHz, CDCl_3): δ 8.30 (s, 1H), 7.79–7.77 (m, 2H), 7.47–7.40 (m, 3H), 4.40 (s, 2H), 4.24 ($q, J = 7.2$, 2H), 1.31 ($t, J = 7.2$, 3H).

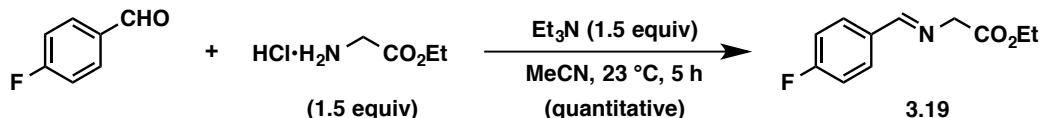


Glycine ethyl ester (3.43). Amine base **3.43** was prepared using modifications to the procedure of Al-Rawi and coworkers.²⁷ A 50 mL round-bottom flask was charged with a magnetic stir bar, glycine ethyl ester hydrochloride (1.7 g, 12 mmol, 1.0 equiv), and CHCl_3 (15 mL, 0.70 M). Et_3N (1.7 mL, 12 mmol, 1.0 equiv) was added in one portion and the resulting heterogeneous mixture stirred vigorously open to air at 23 °C for 30 min. The mixture was concentrated under reduced pressure and the resulting colorless solid was filtered through Celite using Et_2O (50 mL). Concentration of the filtrate afforded **3.43** as a light yellow oil which was carried forward without purification. ^1H NMR (600 MHz, CDCl_3): δ 4.19 ($q, J = 7.1$, 2H), 3.42 (s, 2H), 1.48 (br s, 2H), 1.28 ($t, J = 7.1$, 3H).

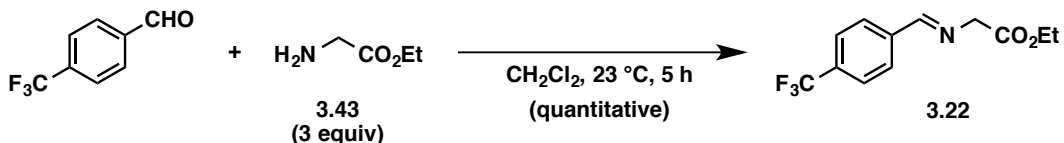


Ethyl (E)-2-((pyridin-3-ylmethylene)amino)acetate (3.16). A 50 mL round-bottom flask was charged with a magnetic stir bar, **3.43** (770 mg, 7.5 mmol, 3.0 equiv), and CH_2Cl_2 (4.2 mL, 0.6 M). 3-Pyridinecarboxaldehyde (230 μL , 2.5 mmol, 1.0 equiv) was then added in one portion. The resulting homogeneous mixture was maintained at 23 °C for 5 h. The reaction mixture was transferred to a separatory funnel using CH_2Cl_2 (10 mL) and H_2O (30 mL). The layers of the resulting biphasic mixture were partitioned and the organic layer was extracted with H_2O (30 mL) and brine (30 mL). The organic layer was dried over Na_2SO_4 , filtered, and

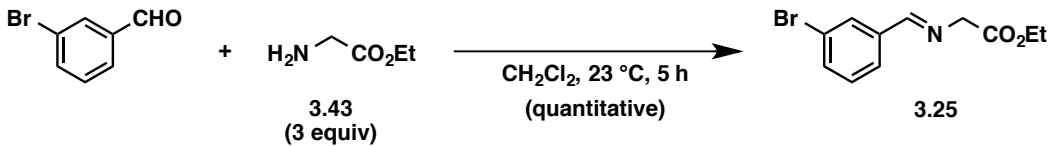
concentrated to afford imine **3.16** (480 mg, quantitative yield) as a light yellow oil. Imine **3.16** was carried further in subsequent reactions without further purification.²⁸ ¹H NMR (600 MHz, CDCl₃): δ 8.89 (app d, *J* = 1.5, 1H), 8.68 (app dd, *J* = 4.8, 1.5, 1H), 8.35 (s, 1H), 8.19 (app dt, *J* = 7.9, 1.5, 1H), 7.37 (dd, *J* = 7.9, 4.8, 1H), 4.43 (s, 2H), 4.25 (q, *J* = 7.1, 2H), 1.31 (t, *J* = 7.1, 3H).



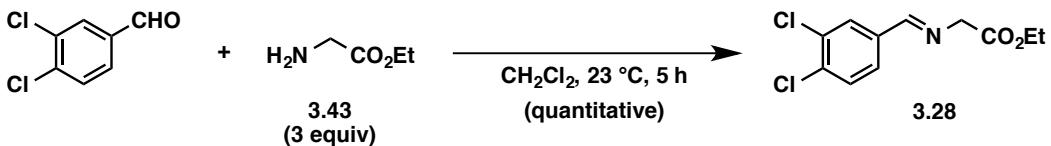
Ethyl (E)-2-((4-fluorobenzylidene)amino)acetate (3.19). According to the procedure described for the synthesis of imine **3.1**, imine **3.19** was prepared from 4-fluorobenzaldehyde (270 μL, 2.5 mmol, 1.0 equiv) as a light yellow oil (520 mg, quantitative yield). Imine **3.19** was carried further in subsequent reactions without further purification. ¹H NMR (500 MHz, CDCl₃): δ 8.26 (s, 1H), 7.78 (app dd, *J* = 8.6, 5.9, 2H), 7.11 (app t, *J* = 8.6, 2H), 4.39 (s, 2H), 4.24 (q, *J* = 7.2, 2H), 1.31 (t, *J* = 7.2, 3H).



Ethyl (E)-2-((4-(trifluoromethyl)benzylidene)amino)acetate (3.22). According to the procedure described for the synthesis of imine **3.16**, imine **3.22** was prepared from 4-(trifluoromethyl)benzaldehyde (340 μL, 2.5 mmol, 1.0 equiv) as a colorless semi-solid (650 mg, quantitative yield). Imine **3.22** was carried further in subsequent reactions without further purification. ¹H NMR (600 MHz, CDCl₃): δ 8.35 (s, 1H), 7.90 (d, *J* = 8.1, 2H), 7.68 (d, *J* = 8.1, 2H), 4.44 (s, 2H), 4.25 (q, *J* = 7.1, 2H), 1.31 (t, *J* = 7.1, 3H).

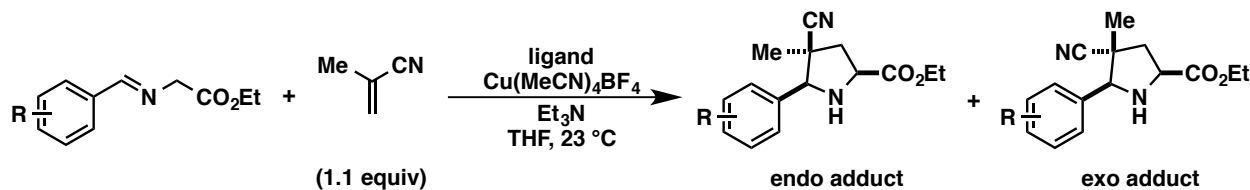


Ethyl (E)-2-((3-bromobenzylidene)amino)acetate (3.25). According to the procedure described for the synthesis of imine **3.16**, imine **3.25** was prepared from 3-bromobenzaldehyde (290 μ L, 2.5 mmol, 1.0 equiv) as a yellow oil (670 mg, quantitative yield). Imine **3.25** was carried further in subsequent reactions without further purification. ^1H NMR (500 MHz, CDCl_3): δ 8.23 (s, 1H), 7.98 (br s, 1H), 7.67 (app d, $J = 7.9$, 1H), 7.57 (app d, $J = 7.9$, 1H), 7.30 (app t, $J = 7.9$, 1H), 4.40 (s, 2H), 4.25 (q, $J = 7.1$, 2H), 1.31 (t, $J = 7.1$, 3H).



Ethyl (E)-2-((3,4-dichlorobenzylidene)amino)acetate (3.28). According to the procedure described for the synthesis of imine **3.16**, imine **3.28** was prepared from 3,4-dichlorobenzaldehyde (440 mg, 2.5 mmol, 1.0 equiv) as a yellow oil (650 mg, quantitative yield). Imine **3.28** was carried further in subsequent reactions without further purification. ^1H NMR (600 MHz, CDCl_3): δ 8.22 (s, 1H), 7.91 (d, $J = 1.5$, 1H), 7.59 (dd, $J = 8.3, 1.5$, 1H), 7.50 (d, $J = 8.3$, 1H), 4.40 (s, 2H), 4.25 (q, $J = 7.1$, 2H), 1.31 (t, $J = 7.1$, 3H).

3.7.3 Cu(I)-Catalyzed 1,3-DC Reaction Using Various Imine Substrates



General Procedure 1. The catalyst and imine components of these reactions were partially prepared in separate 1-dram screw-top vials inside a glove box with a N₂ atmosphere. The reaction vial was charged with a magnetic stir bar and neat imine (0.20 mmol, 1.0 equiv). The catalyst and reaction vials were each sealed with a Teflon-lined cap, then brought outside the glove box where the Teflon-lined caps were each covered with an inverted 14/20 joint rubber septum under a balloon of Ar. **Method A:** In the glove box, the catalyst vial was charged with tetrakis(acetonitrile)copper(I) tetrafluoroborate (12.6 mg, 0.0400 mmol). Outside of the glove box, the catalyst vial was charged with THF (1.33 mL, freeze-pump-thawed) and tris(2,2,2-trifluoroethyl) phosphite (19.4 μ L, 0.0880 mmol). An aliquot of the catalyst solution (0.33 mL, 0.60 M; 0.010 mmol, 0.050 equiv Cu(I) and 0.022 mmol, 0.11 equiv ligand), Et₃N (16.7 μ L, 0.120 mmol, 0.600 equiv), and methacrylonitrile (18.4 μ L, 0.220 mmol, 1.10 equiv) were added to the reaction vial via syringe. The resulting homogenous mixture was maintained at 23 °C for 5 h. The reaction was quenched by opening the vial to air and filtering the reaction mixture through a plug of SiO₂ (200 mg) using EtOAc (8.7 mL, HPLC grade). For yield and diastereomeric ratio analysis using GC-FID instrumentation, 1 mL of a GC standard solution [0.1 M solution of 1,3,5-trimethoxybenzene in EtOAc (HPLC grade)] was added to the filtrate. For analysis by ¹H NMR, ca. 28 mg 5,6-dibromo-1,3-benzodioxole was added to the filtrate as an external standard and the concentrated residue was analyzed in CDCl₃, acetone-d₆, C₆D₆, or CD₃OD. **Method B:** In the glove box, the catalyst vial was charged with

tetrakis(acetonitrile)copper(I) tetrafluoroborate (12.6 mg, 0.0400 mmol) and tricyclohexylphosphine (24.6 mg, 0.0880 mmol). Outside of the glove box, the catalyst vial was charged with THF (0.80 mL, freeze-pump-thawed). An aliquot of the catalyst solution (0.20 mL, 1.0 M; 0.010 mmol, 0.050 equiv Cu(I) and 0.022 mmol, 0.11 equiv ligand), Et₃N (16.7 μL, 0.120 mmol, 0.600 equiv), and methacrylonitrile (18.4 μL, 0.220 mmol, 1.10 equiv) were added to the reaction vial via syringe. The resulting homogenous mixture was maintained at 23 °C for 1 h. The reaction was quenched by opening the vial to air and filtering the reaction mixture through a plug of SiO₂ (200 mg) using EtOAc (8.2 mL, HPLC grade). For yield and diastereomeric ratio analysis using GC-FID instrumentation, 1 mL of a GC standard solution [0.1 M solution of 1,3,5-trimethoxybenzene in EtOAc (HPLC grade)] was added to the filtrate. For analysis by ¹H NMR, ca. 28 mg 5,6-dibromo-1,3-benzodioxole was added to the filtrate as an external standard and the concentrated residue was analyzed in CDCl₃, acetone-d₆, C₆D₆, or CD₃OD. **Method C:** In the glove box, the catalyst vial was charged with tetrakis(acetonitrile)-copper(I) tetrafluoroborate (12.6 mg, 0.0400 mmol) and DavePhos (17.3 mg, 0.0440 mmol). Outside of the glove box, the catalyst vial was charged with THF (2.0 mL, freeze-pump-thawed). An aliquot of the catalyst solution (0.50 mL, 0.4 M; 0.010 mmol, 0.050 equiv Cu(I) and 0.011 mmol, 0.055 equiv ligand), Et₃N (16.7 μL, 0.120 mmol, 0.600 equiv), and methacrylonitrile (18.4 μL, 0.220 mmol, 1.10 equiv) were added to the reaction vial via syringe. The resulting homogenous mixture was maintained at 23 °C for 3 h. The reaction was quenched by opening the vial to air and filtering the reaction mixture through a plug of SiO₂ (200 mg) using EtOAc (8.5 mL, HPLC grade). For yield and diastereomeric ratio analysis using GC-FID instrumentation, 1 mL of a GC standard solution [0.1 M solution of 1,3,5-trimethoxybenzene in EtOAc (HPLC grade)] was added to the filtrate. For analysis by ¹H NMR, ca. 28 mg

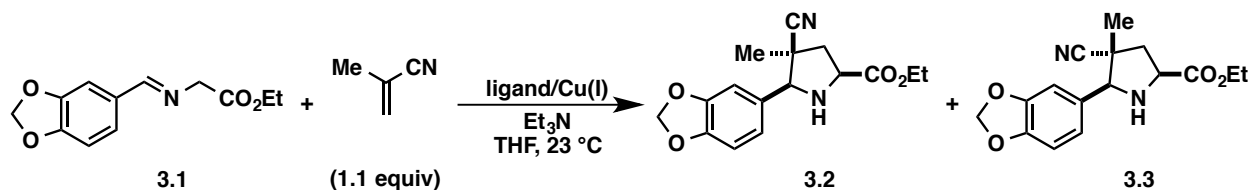
5,6-dibromo-1,3-benzodioxole was added to the filtrate as an external standard and the concentrated residue was analyzed in CDCl₃, acetone-d₆, C₆D₆, or CD₃OD.

Preparative Scale Experiments (General Procedure 2). The imine and catalyst components of these reactions were partially prepared in separate 1-dram screw-top vials inside a glove box with a N₂ atmosphere. The reaction vial was charged with a magnetic stir bar and neat imine (0.50 mmol, 1.0 equiv). The catalyst and reaction vials were each sealed with a Teflon-lined cap, then brought outside the glove box where the Teflon-lined caps were each covered with an inverted 14/20 joint rubber septum under a balloon of Ar.

Method A: In the glove box, the catalyst vial was charged with tetrakis(acetonitrile)copper(I) tetrafluoroborate (15.8 mg, 0.0500 mmol). Outside of the glove box, the catalyst vial was charged with THF (1.7 mL, freeze-pump-thawed) and tris(2,2,2-trifluoroethyl) phosphite (24 μL, 0.11 mmol). An aliquot of the catalyst solution (0.83 mL, 0.60 M; 0.025 mmol, 0.050 equiv Cu(I) and 0.055 mmol, 0.11 equiv ligand), Et₃N (42 μL, 0.30 mmol, 0.60 equiv), and methacrylonitrile (46 μL, 0.55 mmol, 1.1 equiv) were added to the reaction vial via syringe. The resulting homogenous mixture was maintained at 23 °C for 5 h. The reaction was quenched by opening the vial to air and filtering the reaction mixture through a plug of SiO₂ (400 mg) using EtOAc (15 mL). Concentration of the filtrate under reduced pressure afforded a residue that was purified by flash chromatography (2:1 hexanes:EtOAc).

Method B: In the glove box, the catalyst vial was charged with tetrakis(acetonitrile)copper(I) tetrafluoroborate (15.8 mg, 0.0500 mmol) and tricyclohexylphosphine (30.8 mg, 0.110 mmol). Outside of the glove box, the catalyst vial was charged with THF (1.0 mL, freeze-pump-thawed). An aliquot of the catalyst solution (0.50 mL, 1.0 M; 0.025 mmol, 0.050 equiv Cu(I) and 0.055 mmol, 0.11 equiv ligand), Et₃N (42 μL, 0.30 mmol, 0.60 equiv), and methacrylonitrile (46 μL, 0.55 mmol, 1.1 equiv) were added to the

reaction vial via syringe. The resulting homogenous mixture was maintained at 23 °C for 1 h. The reaction was quenched by opening the vial to air and filtering the reaction mixture through a plug of SiO₂ (400 mg) using EtOAc (15 mL). Concentration of the filtrate under reduced pressure afforded a residue that was purified by flash chromatography (4:1 hexanes:EtOAc).

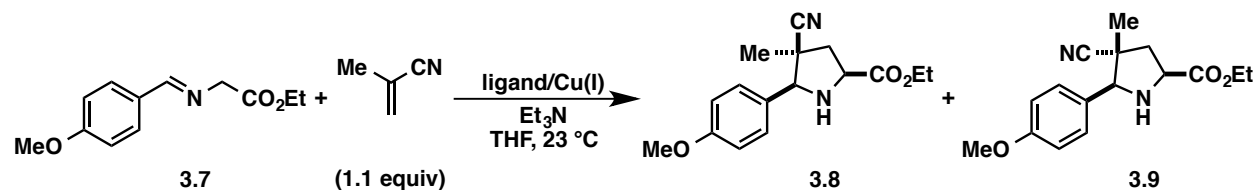


Ethyl *rac*-(2*S*,4*S*,5*S*)-5-(benzo[*d*][1,3]dioxol-5-yl)-4-cyano-4-methylpyrrolidine-2-carboxylate (3.2) and **ethyl *rac*-(2*S*,4*R*,5*S*)-5-(benzo[*d*][1,3]dioxol-5-yl)-4-cyano-4-methylpyrrolidine-2-carboxylate (3.3)**.

Using **General Procedure 1**, pyrrolidines **3.2** and **3.3** were accessed via various methods from imine **3.1** (47.0 mg, 0.200 mmol, 1.00 equiv) and methacrylonitrile (18.4 μL, 0.220 mmol, 1.10 equiv) in the following yields and diastereomeric ratios (endo:exo). **Method A:** 88% yield, 96:4 dr; **Method B:** 97% yield, 9:91 dr; **Method C:** 95% yield, 39:61 dr. Using **General Procedure 2**, **Method A**, pyrrolidine **3.2** was isolated as a yellow oil (120 mg, 79% yield) from a crude reaction mixture with a 94:6 dr. Using **General Procedure 2**, **Method B**, pyrrolidine **3.3** was isolated as a yellow oil (123 mg, 82% yield) from a crude reaction mixture with a 11:89 dr.

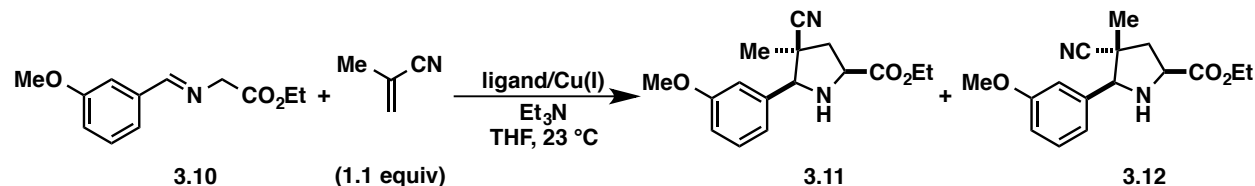
3.2 (endo adduct): R_f 0.12 (2:1 hexanes:EtOAc); ¹H NMR (600 MHz, CDCl₃): δ 7.09 (d, J = 1.6, 1H), 6.96 (dd, J = 8.0, 1.6, 1H), 6.81 (d, J = 8.0, 1H), 5.97 (d, J = 1.9, 2H), 4.33–4.25 (m, 2H), 3.96 (dd, J = 9.6, 4.3, 1H), 3.87 (s, 1H), 2.81 (dd, J = 13.6, 4.3, 1H), 2.71 (br s, 1H), 2.27 (dd, J = 13.6, 9.6, 1H), 1.42 (s, 3H), 1.34 (t, J = 7.2, 3H); ¹³C NMR (125 MHz, CDCl₃): δ 173.0 (C), 148.2 (C), 148.0 (C), 130.5 (C), 122.1 (C), 121.2 (CH), 108.3 (CH), 108.0 (CH), 101.4 (CH₂), 72.3 (CH), 61.8 (CH₂), 57.2 (CH), 44.0 (C), 42.3 (CH₂), 22.2 (CH₃), 14.3 (CH₃); IR (thin film): 3351, 2980, 2901, 2234, 1734, 1490, 1445 cm⁻¹;

HRMS-ESI (*m/z*) [M + Na]⁺ calculated for C₁₆H₁₈N₂O₄Na, 325.1164; found, 325.1157. Spectral data match those previously reported.²² **3.3 (exo adduct):** R_f 0.29 (2:1 hexanes:EtOAc); ¹H NMR (600 MHz, CDCl₃): δ 6.98 (d, *J* = 1.6, 1H), 6.93 (dd, *J* = 8.1, 1.4, 1H), 6.80 (d, *J* = 8.0, 1H), 5.96 (s, 2H), 4.50 (s, 1H), 4.24 (q, *J* = 7.1, 2H), 4.05–4.02 (m, 1H), 2.72 (dd, *J* = 13.3, 9.9, 1H), 2.63 (br s, 1H), 2.21 (dd, *J* = 13.5, 6.2, 1H), 1.31 (t, *J* = 7.3, 3H), 1.00 (s, 3H); ¹³C NMR (125 MHz, CDCl₃): δ 173.1 (C), 147.9 (C), 147.7 (C), 130.5 (C), 124.1 (C), 120.7 (CH), 108.4 (CH), 107.7 (CH), 101.3 (CH₂), 69.3 (CH), 61.7 (CH₂), 57.2 (CH), 41.5 (CH₂), 40.2 (C), 20.6 (CH₃), 14.3 (CH₃); IR (thin film): 3348, 2982, 2901, 2234, 1735, 1490, 1445 cm⁻¹; HRMS-ESI (*m/z*) [M + Na]⁺ calculated for C₁₆H₁₈N₂O₄Na, 325.1164; found, 325.1156. Spectral data match those previously reported.²²



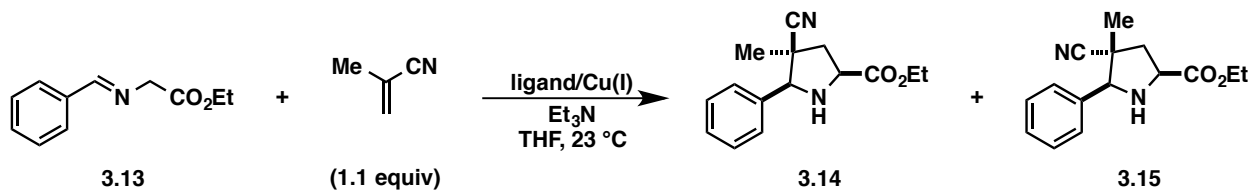
Ethyl *rac*-(2*S*,4*S*,5*S*)-4-cyano-5-(4-methoxyphenyl)-4-methylpyrrolidine-2-carboxylate (3.8) and **ethyl *rac*-(2*S*,4*R*,5*S*)-4-cyano-5-(4-methoxyphenyl)-4-methylpyrrolidine-2-carboxylate (3.9).** Using **General Procedure 1**, pyrrolidines **3.8** and **3.9** were accessed via various methods from imine **3.7** (44.2 mg, 0.200 mmol, 1.00 equiv) and methacrylonitrile (18.4 μL, 0.220 mmol, 1.10 equiv) in the following yields and diastereomeric ratios (endo:exo). **Method A:** 58% yield, 94:6 dr; **Method B:** >99% yield, 12:88 dr; **Method C:** 96% yield, 35:65 dr. **3.8 (endo adduct):** R_f 0.30 (1:1 hexanes:EtOAc); ¹H NMR (500 MHz, CDCl₃): δ 7.45 (d, *J* = 8.8, 2H), 6.93 (d, *J* = 8.8, 2H), 4.35–4.24 (m, 2H), 3.97 (dd, *J* = 9.8, 1H), 3.89 (s, 1H), 3.81 (s, 3H), 2.82 (dd, *J* = 13.4, 4.1, 1H), 2.46 (br s, 1H), 2.28 (dd, *J* = 13.4, 9.8, 1H), 1.40 (s, 3H), 1.34 (t, *J* = 7.2, 3H); ¹³C NMR (125 MHz, CDCl₃): δ 173.2 (C), 160.1 (C), 128.8 (2CH₂), 128.5 (C), 122.2 (C),

144.1 (2CH₂), 72.2 (CH), 61.8 (CH₂), 57.4 (CH), 55.4 (CH₃), 44.1 (C), 42.5 (CH₂), 22.0 (CH₃), 14.3 (CH₃); IR (thin film): 3350, 2979, 2838, 2234, 1735, 1514, 1249 cm⁻¹; HRMS-ESI (*m/z*) [M + Na]⁺ calculated for C₁₆H₂₀N₂O₃Na, 311.1372; found, 311.1362. Spectral data match those previously reported.²² **3.9 (exo adduct):** R_f 0.50 (1:1 hexanes:EtOAc); ¹H NMR (600 MHz, CDCl₃): δ 7.38 (d, *J* = 8.6, 2H), 6.90 (d, *J* = 8.6, 2H), 4.53 (s, 1H), 4.25 (q, *J* = 7.1, 2H), 4.04 (dd, *J* = 9.7, 6.2, 1H), 3.81 (s, 3H), 2.74 (dd, *J* = 13.5, 9.7, 1H), 2.53 (br s, 1H), 2.21 (dd, *J* = 13.5, 6.2, 1H), 1.31 (t, *J* = 7.1, 3H), 0.97 (s, 3H); ¹³C NMR (125 MHz, CDCl₃): δ 173.3 (C), 159.7 (C), 128.6 (C), 128.4 (2CH), 124.2 (C), 114.0 (2CH), 69.2 (CH), 61.6 (CH₂), 57.3 (CH), 55.4 (CH₃), 41.8 (CH₂), 40.2 (C), 20.5 (CH₃), 14.3 (CH₃); IR (thin film): 3346, 2982, 2838, 2234, 1613, 1736, 1514, 1458, 1249 cm⁻¹; HRMS-ESI (*m/z*) [M + Na]⁺ calculated for C₁₆H₂₀N₂O₃Na, 311.1372; found, 311.1371. Spectral data match those previously reported.²²



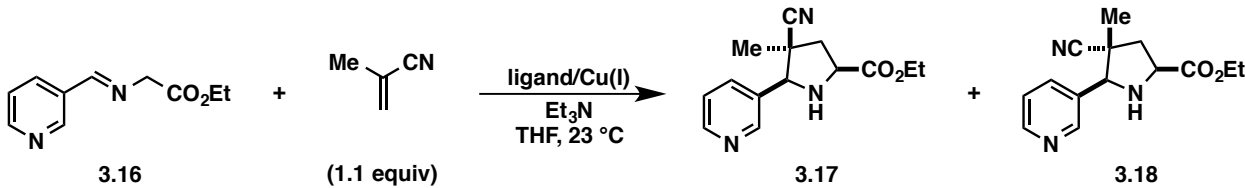
Ethyl *rac*-(2*S*,4*S*,5*S*)-4-cyano-5-(3-methoxyphenyl)-4-methylpyrrolidine-2-carboxylate (3.11) and ethyl *rac*-(2*S*,4*R*,5*S*)-4-cyano-5-(3-methoxyphenyl)-4-methylpyrrolidine-2-carboxylate (3.12). Using **General Procedure 1**, pyrrolidines **3.11** and **3.12** were accessed via various methods from imine **3.10** (44.2 mg, 0.200 mmol, 1.00 equiv) and methacrylonitrile (18.4 μL, 0.220 mmol, 1.10 equiv) in the following yields and diastereomeric ratios (endo:exo). **Method A:** 91% yield, 94:6 dr; **Method B:** 93% yield, 9:91 dr; **Method C:** 93% yield, 40:60 dr. **3.11 (endo adduct):** R_f 0.27 (1:1 hexanes:EtOAc); ¹H NMR (500 MHz, CDCl₃): δ 7.31 (t, *J* = 7.8, 1H), 7.13–7.12 (m, 1H), 7.09 (br d, *J* = 7.8, 1H), 6.91 (dd, *J* = 8.2, 2.2, 1H), 4.35–4.25 (m, 2H), 3.99 (dd, *J* = 9.6, 4.2, 1H), 3.91 (s, 1H), 3.84 (s, 3H), 2.83 (dd, *J* = 13.5, 4.2, 1H), 2.82

(br s, 1H), 2.29 (dd, J = 13.5, 9.6, 1H), 1.44 (s, 3H), 1.34 (t, J = 7.0, 3H); ^{13}C NMR (125 MHz, CDCl_3): δ 173.1 (C), 159.8 (C), 138.3 (C), 129.7 (CH), 122.0 (C), 119.9 (CH), 114.6 (CH), 113.2 (CH), 72.5 (CH), 61.8 (CH₂), 57.5 (CH), 55.4 (CH₃), 44.1 (C), 42.6 (CH₂), 22.2 (CH₃), 14.3 (CH₃); IR (thin film): 3348, 2979, 2939, 2837, 2234, 1734, 1602, 1586, 1490, 1455 cm^{-1} ; HRMS-CI (m/z) [M + H]⁺ calculated for $\text{C}_{16}\text{H}_{21}\text{N}_2\text{O}_3$, 289.1552; found, 289.1551. Spectral data match those previously reported.²² **3.12 (exo adduct):** R_f 0.54 (1:1 hexanes:EtOAc); ^1H NMR (600 MHz, CDCl_3): δ 7.28 (t, J = 8.0, 1H), 7.043 (d, J = 8.0, 1H), 7.036 (s, 1H), 6.87–6.86 (m, 1H), 4.55 (s, 1H), 4.25 (q, J = 7.0, 2H), 4.06 (dd, J = 9.6, 6.3, 1H), 3.82 (s, 3H), 2.74 (dd, J = 13.5, 9.6, 1H), 2.67 (br s, 1H), 2.22 (dd, J = 13.5, 6.3, 1H), 1.32 (t, J = 7.0, 3H), 0.99 (s, 3H); ^{13}C NMR (125 MHz, CDCl_3): δ 173.2 (C), 159.9 (C), 138.5 (C), 129.7 (CH), 124.2 (C), 119.5 (CH), 113.9 (CH), 112.8 (CH), 69.4 (CH), 61.6 (CH₂), 57.4 (CH), 55.4 (CH₃), 41.8 (CH₂), 40.2 (C), 20.6 (CH₃), 14.3 (CH₃); IR (thin film): 3345, 2981, 2939, 2837, 2234, 1736, 1602, 1586, 1489, 1456 cm^{-1} ; HRMS-ESI (m/z) [M + Na]⁺ calculated for $\text{C}_{16}\text{H}_{20}\text{N}_2\text{O}_3\text{Na}$, 311.1372; found, 311.1368. Spectral data match those previously reported.²²



Ethyl *rac*-(2*S*,4*S*,5*S*)-4-cyano-4-methyl-5-phenylpyrrolidine-2-carboxylate (3.14) and ethyl *rac*-(2*S*,4*R*,5*S*)-4-cyano-4-methyl-5-phenylpyrrolidine-2-carboxylate (3.15). Using **General Procedure 1**, pyrrolidines **3.14** and **3.15** were accessed via various methods from imine **3.13** (38.2 mg, 0.200 mmol, 1.00 equiv) and methacrylonitrile (18.4 μL , 0.220 mmol, 1.10 equiv) in the following yields and diastereomeric ratios (endo:exo). **Method A:** 76% yield, 98:2 dr; **Method B:** 97% yield, 11:89 dr; **Method C:** 94% yield, 38:62 dr. Using **General Procedure 2**,

Method A, pyrrolidine **3.14** was isolated as a clear oil (98 mg, 76% yield) from a crude reaction mixture with a 96:4 dr. Using **General Procedure 2, Method B**, pyrrolidine **3.15** was isolated as a colorless solid (107 mg, 83% yield; mp = 74–76 °C) from a crude reaction mixture with a 12:88 dr. **3.14 (endo adduct)**: R_f 0.32 (1:1 hexanes:EtOAc); ¹H NMR (500 MHz, CDCl₃): δ 7.52 (app d, J = 7.1, 2H), 7.41–7.34 (m, 3H), 4.34–4.24 (m, 2H), 3.98 (dd, J = 9.6, 4.2, 1H), 3.93 (s, 1H), 2.90 (br s, 1H), 2.82 (dd, J = 13.6, 4.2, 1H), 2.29 (dd, J = 13.6, 9.6, 1H), 1.42 (s, 3H), 1.34 (t, J = 7.1, 3H); ¹³C NMR (125 MHz, CDCl₃): δ 173.0 (C), 136.5 (C), 128.9 (CH), 128.6 (2CH), 127.6 (2CH), 121.9 (C), 72.4 (CH), 61.7 (CH₂), 57.3 (CH), 44.1 (C), 42.4 (CH₂), 22.0 (CH₃), 14.2 (CH₃); IR (thin film): 3348, 2980, 2234, 1734, 1454 cm⁻¹; HRMS-ESI (*m/z*) [M + Na]⁺ calculated for C₁₅H₁₈N₂O₂Na, 281.1266; found, 281.1263. Spectral data match those previously reported.²² **3.15 (exo adduct)**: R_f 0.25 (3:1 hexanes:EtOAc); ¹H NMR (500 MHz, CDCl₃): δ 7.45 (d, J = 7.3, 2H), 7.37–7.29 (m, 3H), 4.55 (s, 1H), 4.23 (q, J = 6.9, 2H), 4.04 (dd, J = 9.7, 6.2, 1H), 2.73 (dd, J = 13.4, 9.8, 1H), 2.67 (br s, 1H), 2.21 (dd, J = 13.5, 6.1, 1H), 1.30 (t, J = 7.1, 3H), 0.95 (s, 3H); ¹³C NMR (125 MHz, CDCl₃): δ 173.1 (C), 136.6 (C), 128.5 (CH), 128.3 (2CH), 127.1 (2CH), 124.0 (C), 69.4 (CH), 61.5 (CH₂), 57.2 (CH), 41.7 (C), 40.0 (CH₂), 20.4 (CH₃), 14.2 (CH₃); IR (thin film): 3346, 2982, 2235, 1736, 1455 cm⁻¹; HRMS-ESI (*m/z*) [M + Na]⁺ calculated for C₁₅H₁₈N₂O₂Na, 281.1266; found, 281.1275. Spectral data match those previously reported.²²

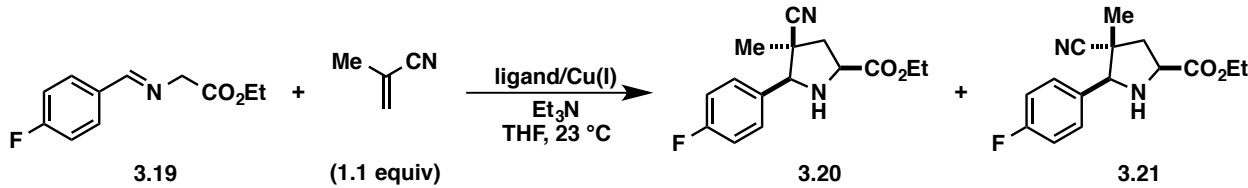


Ethyl *rac*-(2*S*,4*S*,5*S*)-4-cyano-4-methyl-5-(pyridin-3-yl)pyrrolidine-2-carboxylate (3.17) and **ethyl *rac*-(2*S*,4*R*,5*S*)-4-cyano-4-methyl-5-(pyridin-3-yl)pyrrolidine-2-carboxylate (3.18)**.

Using **General Procedure 1**, pyrrolidines **3.17** and **3.18** were accessed via various methods from imine **3.16** (38.4 mg, 0.200 mmol, 1.00 equiv) and methacrylonitrile (18.4 µL, 0.220 mmol, 1.10 equiv) in the following yields and diastereomeric ratios (endo:exo). **Method A:** 14% yield, 86:14 dr; **Method B:** 52% yield, 12:88 dr; **Method C:** 46% yield, 49:51 dr.

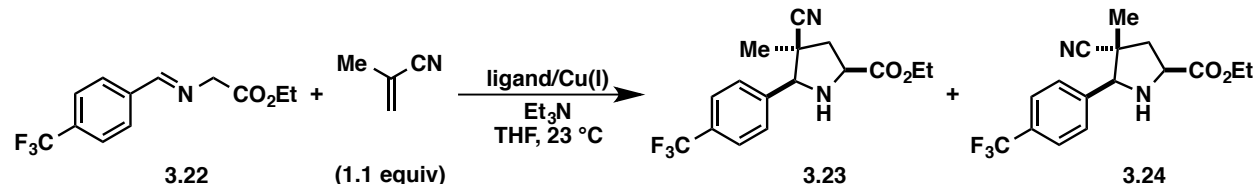
3.17 (endo adduct): R_f 0.24 (1:1 hexanes:acetone); ¹H NMR (600 MHz, CDCl₃): δ 8.60 (s, 1H), 8.57 (s, 1H), 8.08 (d, J = 7.7, 1H), 7.38–7.36 (m, 2H), 4.32–4.23 (m, 2H), 3.97 (dd, J = 9.3, 3.3, 1H), 3.95 (s, 1H), 2.85 (dd, J = 13.8, 3.3, 2H), 2.72 (br s, 1H), 2.31 (dd, J = 13.8, 9.3, 1H), 1.43 (s, 3H), 1.32 (t, J = 6.8, 3H); ¹³C NMR (125 MHz, CDCl₃): δ 172.7 (C), 150.4 (CH), 149.3 (CH), 135.0 (CH), 132.6 (C), 123.7 (CH), 121.5 (C), 69.7 (CH), 61.7 (CH₂), 57.1 (CH), 43.9 (C), 41.9 (CH₂), 21.8 (CH₃), 14.2 (CH₃); IR (thin film): 3345, 2982, 2235, 1735, 1450, 1206 cm⁻¹; HRMS-ESI (*m/z*) [M + Na]⁺ calculated for C₁₄H₁₇N₃O₂Na, 282.1219; found, 282.1216.

3.18 (exo adduct): R_f 0.41 (1:1 hexanes:acetone); ¹H NMR (600 MHz, CDCl₃): δ 8.72 (s, 1H), 8.59 (d, J = 4.1, 1H), 7.83 (d, J = 8.1, 1H), 7.31 (dd, J = 4.1, 1H), 4.61 (s, 1H), 4.25 (q, J = 7.1, 2H), 4.09 (dd, J = 9.5, 6.1, 1H), 2.76 (dd, J = 13.5, 9.5, 1H), 2.54 (br s, 1H), 2.26 (dd, J = 13.5, 6.1, 1H), 1.31 (t, J = 7.1, 3H), 1.01 (s, 3H); ¹³C NMR (125 MHz, CDCl₃): δ 172.8 (C), 150.0 (CH), 148.9 (CH), 135.1 (CH), 132.6 (C), 123.54 (C), 123.52 (CH), 67.4 (CH), 61.7 (CH₂), 57.3 (CH), 41.4 (CH₂), 40.1 (C), 20.6 (CH₃), 14.3 (CH₃); IR (thin film): 3340, 2982, 2235, 1736, 1451, 1201 cm⁻¹; HRMS-ESI (*m/z*) [M + Na]⁺ calculated for C₁₄H₁₇N₃O₂Na, 282.1219; found, 282.1223.



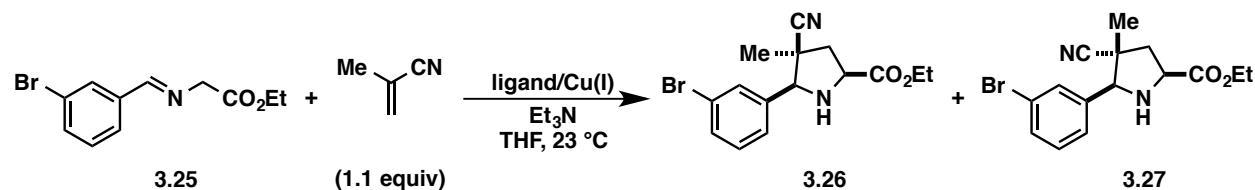
Ethyl *rac*-(2*S*,4*S*,5*S*)-4-cyano-5-(4-fluorophenyl)-4-methylpyrrolidine-2-carboxylate (3.20) and **ethyl *rac*-(2*S*,4*R*,5*S*)-4-cyano-5-(4-fluorophenyl)-4-methylpyrrolidine-2-carboxylate (3.21)**. Using **General Procedure 1**, pyrrolidines **3.20** and **3.21** were accessed via various methods from imine **3.19** (41.8 mg, 0.200 mmol, 1.00 equiv) and methacrylonitrile (18.4 µL, 0.220 mmol, 1.10 equiv) in the following yields and diastereomeric ratios (endo:exo). **Method A:** 84% yield, 96:4 dr; **Method B:** >99% yield, 12:88 dr; **Method C:** >99% yield, 41:59 dr. **3.20 (endo adduct):** R_f 0.29 (1:1 hexanes:EtOAc); ¹H NMR (500 MHz, CDCl₃): δ 7.52 (dd, J = 8.7, 5.4, 2H), 7.09 (t, J = 8.7, 2H), 4.34–4.24 (m, 2H), 4.00 (dd, J = 9.6, 4.2, 1H), 3.95 (s, 1H), 2.83 (dd, J = 13.7, 4.2, 1H), 2.82 (br s, 1H), 2.30 (dd, J = 13.7, 9.6, 1H), 1.41 (s, 3H), 1.34 (t, J = 7.1, 3H); ¹³C NMR (125 MHz, CDCl₃): δ 172.9 (C), 163.2 (d, J_{C-F} = 245.8, C), 132.4 (C), 129.4 (d, J_{C-F} = 8.3, CH), 121.8 (C), 115.7 (d, J_{C-F} = 21.5, CH), 71.7 (CH), 61.9 (CH₂), 57.3 (CH), 44.0 (C), 42.2 (CH₂), 22.0 (CH₃), 14.3 (CH₃); ¹⁹F NMR (376.5 MHz, CDCl₃): δ –112.7; IR (thin film): 3348, 2982, 2235, 1736, 1605, 1510 cm^{–1}; HRMS-ESI (*m/z*) [M + Na]⁺ calculated for C₁₅H₁₇FN₂O₂Na, 299.1172; found, 299.1177. Spectral data match those previously reported.²² **3.21 (exo adduct):** R_f 0.28 (3:1 hexanes:EtOAc); ¹H NMR (600 MHz, CDCl₃): δ 7.45 (dd, J = 7.2, 4.5, 2H), 7.06 (t, J = 7.2, 2H), 4.56 (s, 1H), 4.24 (q, J = 6.0, 2H), 4.05 (dd, J = 8.1, 5.1, 1H), 2.74 (dd, J = 11.3, 8.1, 1H), 2.57 (br s, 1H), 2.23 (dd, J = 11.3, 5.1, 1H), 1.31 (t, J = 6.0, 3H), 0.96 (s, 3H); ¹³C NMR (125 MHz, CDCl₃): δ 173.1 (C), 162.8 (d, J_{C-F} = 245.5, C), 132.5 (d, J_{C-F} = 3.1, C), 128.9 (d, J_{C-F} = 8.1, 2CH), 124.0 (C), 115.5 (d, J_{C-F} = 21.3, 2CH), 68.8 (CH), 61.6 (CH₂), 57.2 (CH), 41.5 (CH₂), 40.0 (C), 20.5 (CH₃), 14.3 (CH₃); ¹⁹F NMR

(376.5 MHz, CDCl₃): δ -113.7; IR (thin film): 3347, 2983, 2938, 2235, 1737, 1605, 1510 cm⁻¹; HRMS-Cl (*m/z*) [M + H]⁺ calculated for C₁₅H₁₈FO₂N₂, 277.1352; found, 277.1361. Spectral data match those previously reported.²²



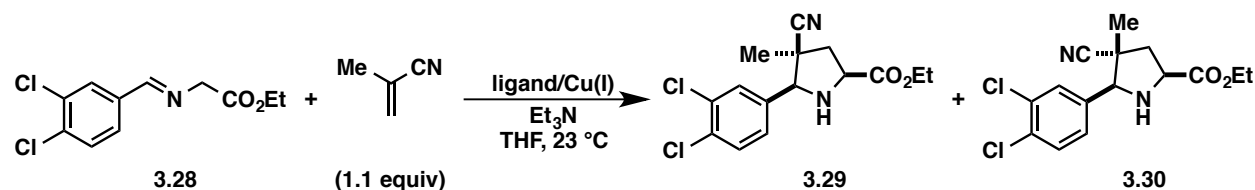
Ethyl *rac*-(2*S,4S,5S*)-4-cyano-4-methyl-5-(4-(trifluoromethyl)phenyl)pyrrolidine-2-carboxylate (3.23) and ethyl *rac*-(2*S,4R,5S*)-4-cyano-4-methyl-5-(4-(trifluoromethyl)phenyl)pyrrolidine-2-carboxylate (3.24). Using **General Procedure 1**, pyrrolidines **3.23** and **3.24** were accessed via various methods from imine **3.22** (51.8 mg, 0.200 mmol, 1.00 equiv) and methacrylonitrile (18.4 μL, 0.220 mmol, 1.10 equiv) in the following yields and diastereomeric ratios (endo:exo). **Method A:** 88% yield, 96:4 dr; **Method B:** 92% yield, 14:86 dr; **Method C:** 98% yield, 47:53 dr. Using **General Procedure 2**, **Method A**, pyrrolidine **3.23** was isolated as a colorless solid (120 mg, 74% yield; mp = 98–100 °C) from a crude reaction mixture with a 96:4 dr. Using **General Procedure 2**, **Method B**, pyrrolidine **3.24** was isolated as a yellow solid (127 mg, 78% yield; mp = 69–71 °C) from a crude reaction mixture with a 15:85 dr. **3.23 (endo adduct):** R_f 0.31 (1:1 hexanes:EtOAc); ¹H NMR (500 MHz, CDCl₃): δ 7.67 (app s, 4H), 4.35–4.25 (m, 2H), 4.03 (s, 1H), 4.02 (dd, *J* = 9.6, 3.8, 1H), 2.86 (dd, *J* = 13.5, 3.8, 1H), 2.79 (br s, 1H), 2.32 (dd, *J* = 13.5, 9.6, 1H), 1.45 (s, 3H), 1.35 (t, *J* = 7.3, 3H); ¹³C NMR (125 MHz, CDCl₃): δ 172.8 (C), 141.0 (C), 131.2 (q, *J*_{C-F} = 32.4, C), 128.1 (2CH), 125.7 (q, *J*_{C-F} = 3.7, 2CH), 124.1 (q, *J*_{C-F} = 273.1, C), 121.6 (C), 71.9 (CH), 61.9 (CH₂), 57.3 (CH), 44.1 (C), 42.2 (CH₂), 22.1 (CH₃), 14.3 (CH₃); ¹⁹F NMR (376.5 MHz, CDCl₃): δ -62.7; IR (thin film): 3351, 2983, 2907, 2878, 2236, 1738, 1620, 1326 cm⁻¹; HRMS-Cl (*m/z*) [M + H]⁺

calculated for $C_{16}H_{18}F_3N_2O_2$, 327.1320; found, 327.1310. **3.24 (exo adduct):** R_f 0.58 (1:1 hexanes:EtOAc); 1H NMR (600 MHz, $CDCl_3$): δ 7.64–7.61 (m, 4H), 4.64 (s, 1H), 4.25 (q, $J = 7.2$, 2H), 4.08 (dd, $J = 9.5$, 6.5, 1H), 2.77 (dd, $J = 13.3$, 9.5, 1H), 2.66 (br s, 1H), 2.26 (dd, $J = 13.3$, 6.5, 1H), 1.31 (t, $J = 7.2$, 3H), 0.97 (s, 3H); ^{13}C NMR (125 MHz, $CDCl_3$): 173.0 (C), 141.1 (C), 130.8 (q, $J_{C-F} = 32.2$, C), 127.8 (CH), 125.7 (q, $J_{C-F} = 3.7$, C), 124.2 (q, $J_{C-F} = 272.2$, C), 123.8 (CH), 69.0 (CH), 61.8 (CH₂), 57.3 (CH), 41.6 (CH₂), 40.1 (C), 20.7 (CH₃), 14.4 (CH₃); ^{19}F NMR (376.5 MHz, $CDCl_3$): δ –62.6; IR (thin film): 3344, 2985, 2905, 2880, 2237, 1738, 1620, 1326 cm⁻¹; HRMS-ESI (m/z) [M + Na]⁺ calculated for $C_{16}H_{17}F_3N_2O_2Na$, 327.1320; found, 327.1314.



Ethyl *rac*-(2*S*,4*S*,5*S*)-5-(3-bromophenyl)-4-cyano-4-methylpyrrolidine-2-carboxylate (3.26) and **ethyl *rac*-(2*S*,4*R*,5*S*)-5-(3-bromophenyl)-4-cyano-4-methylpyrrolidine-2-carboxylate (3.27).** Using **General Procedure 1**, pyrrolidines **3.26** and **3.27** were accessed via various methods from imine **3.25** (53.8 mg, 0.200 mmol, 1.00 equiv) and methacrylonitrile (18.4 μL, 0.220 mmol, 1.10 equiv) in the following yields and diastereomeric ratios (endo:exo). **Method A:** 78% yield, 96:4 dr; **Method B:** 95% yield, 12:88 dr; **Method C:** 98% yield, 56:44 dr. **3.26 (endo adduct):** R_f 0.32 (1:1 hexanes:EtOAc); 1H NMR (600 MHz, $CDCl_3$): δ 7.64 (br s, 1H), 7.52–7.49 (m, 2H), 7.28 (t, $J = 8.0$, 1H), 4.33–4.25 (m, 2H), 3.99 (dd, $J = 9.7$, 4.4, 1H), 3.92 (s, 1H), 2.83 (dd, $J = 13.3$, 4.4, 1H), 2.65 (br s, 1H), 2.29 (dd, $J = 13.3$, 9.7, 1H), 1.44 (s, 3H), 1.34 (t, $J = 7.3$, 3H); ^{13}C NMR (125 MHz, $CDCl_3$): δ 172.8 (C), 139.3 (C), 132.1 (CH), 130.9 (CH), 130.3 (CH), 126.2 (CH), 122.7 (C), 121.6 (C), 71.7 (CH), 61.9 (CH₂), 57.3 (CH), 44.0 (C),

42.2 (CH₂), 22.2 (CH₃), 14.3 (CH₃); IR (thin film): 3345, 2980, 2938, 2877, 2235, 1736, 1568, 1449, 1204 cm⁻¹; HRMS-Cl (*m/z*) [M + H]⁺ calculated for C₁₅H₁₈BrN₂O₂, 337.0552; found, 337.0555. **3.27 (exo adduct):** R_f 0.62 (1:1 hexanes:EtOAc); ¹H NMR (600 MHz, CDCl₃): δ 7.65 (br s, 1H), 7.47 (br d, *J* = 7.9, 1H), 7.41 (br d, *J* = 7.9, 1H), 7.25 (t, *J* = 7.9, 1H), 4.56 (s, 1H), 4.26 (q, *J* = 7.0, 2H), 4.07 (dd, *J* = 9.7, 6.3, 1H), 2.75 (dd, *J* = 13.4, 9.7, 1H), 2.68 (br s, 1H), 2.25 (dd, *J* = 13.4, 6.3, 1H), 1.33 (t, *J* = 7.0, 3H), 1.00 (s, 3H); ¹³C NMR (125 MHz, CDCl₃): δ 172.9 (C), 139.3 (C), 131.7 (CH), 130.2 (2CH), 126.1 (CH), 123.8 (C), 122.9 (C), 68.8 (CH₂), 61.7 (CH), 57.2 (CH₂), 41.4 (CH), 40.0 (C), 20.7 (CH₃), 14.3 (CH₃); IR (thin film): 3345, 2982, 2937, 2874, 2235, 1736, 1568, 1378 cm⁻¹; HRMS-Cl (*m/z*) [M + H]⁺ calculated for C₁₅H₁₈BrN₂O₂, 337.0552; found, 337.0546.

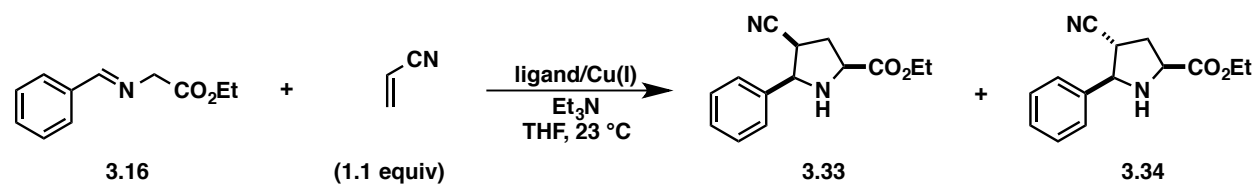


Ethyl *rac*-(2*S*,4*S*,5*S*)-4-cyano-5-(3,4-dichlorophenyl)-4-methylpyrrolidine-2-carboxylate (3.29) and **ethyl *rac*-(2*S*,4*R*,5*S*)-4-cyano-5-(3,4-dichlorophenyl)-4-methylpyrrolidine-2-carboxylate (3.30)**. Using **General Procedure 1**, pyrrolidines **3.29** and **3.30** were accessed via various methods from imine **3.28** (51.8 mg, 0.200 mmol, 1.00 equiv) and methacrylonitrile (18.4 μL, 0.220 mmol, 1.10 equiv) in the following yields and diastereomeric ratios (endo:exo). **Method A:** 91% yield, 98:2 dr; **Method B:** >99% yield, 14:86 dr; **Method C:** >99% yield, 61:39 dr. Using **General Procedure 2**, **Method A**, pyrrolidine **3.29** was isolated as a colorless solid (124 mg, 76% yield; mp = 71–72 °C) from a crude reaction mixture with a 98:2 dr. Using **General Procedure 2**, **Method B**, pyrrolidine **3.30** was isolated as a clear oil (118 mg, 73% yield) from a crude reaction mixture with a 15:85 dr. **3.29 (endo adduct):** R_f 0.38

(1:1 hexanes:EtOAc); ^1H NMR (500 MHz, CDCl_3): δ 7.61 (s, 1H), 7.47 (d, $J = 8.5$, 1H), 7.42 (d, $J = 8.5$, 1H), 4.31–4.24 (m, 2H), 3.98 (dd, $J = 9.5, 4.5$, 1H), 3.92 (s, 1H), 2.83 (dd, $J = 13.5$, 4.5, 1H), 2.69 (br s, 1H), 2.28 (dd, $J = 13.5, 9.5$, 1H), 1.43 (s, 3H), 1.33 (t, $J = 7.5$, 3H); ^{13}C NMR (125 MHz, CDCl_3): δ 172.7 (C), 137.4 (C), 133.0 (C), 132.7 (C), 130.7 (CH), 129.7 (CH), 126.9 (CH), 121.5 (C), 71.0 (CH), 61.8 (CH₂), 57.1 (CH), 43.9 (C), 41.8 (CH₂), 22.2 (CH₃), 14.3 (CH₃); IR (thin film): 3350, 2981, 2938, 2236, 1737, 1469, 1205 cm^{-1} ; HRMS-ESI (m/z) [M + Na]⁺ calculated for $\text{C}_{15}\text{H}_{16}\text{Cl}_2\text{N}_2\text{O}_2\text{Na}$, 349.0486; found, 349.0490.

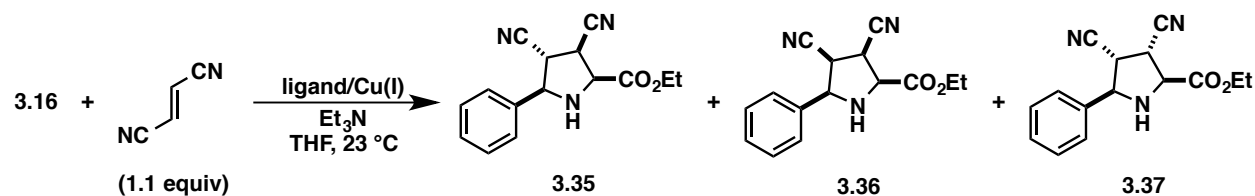
3.30 (exo adduct): R_f 0.59 (1:1 hexanes:EtOAc); ^1H NMR (600 MHz, CDCl_3): δ 7.62 (s, 1H), 7.45 (d, $J = 8.2$, 1H), 7.33 (d, $J = 8.2$, 1H), 4.55 (s, 1H), 4.25 (q, $J = 7.1$, 2H), 4.09–4.06 (m, 1H), 2.75 (dd, $J = 13.2, 9.5$, 1H), 2.58 (br s, 1H), 2.25 (dd, $J = 13.2, 6.1$, 1H), 1.32 (t, $J = 7.1$, 3H), 1.01 (s, 3H); ^{13}C NMR (125 MHz, CDCl_3): δ 172.8 (C), 137.4 (C), 133.0 (C), 132.6 (C), 130.6 (CH), 129.2 (CH), 126.7 (CH), 123.7 (C), 68.3 (CH), 61.7 (CH₂), 57.1 (CH), 41.3 (CH₂), 40.0 (C), 20.7 (CH₃), 14.3 (CH₃); IR (thin film): 3348, 2982, 2938, 2235, 1736, 1469, 1201 cm^{-1} ; HRMS-Cl (m/z) [M + H]⁺ calculated for $\text{C}_{15}\text{H}_{17}\text{Cl}_2\text{N}_2\text{O}_2$, 327.0667; found, 327.0670.

3.7.4 Cu(I)-Catalyzed 1,3-DC Reaction Using Various Dipolarophiles



Ethyl *rac*-(2*S,4S,5R*)-4-cyano-5-phenylpyrrolidine-2-carboxylate (3.33) and ethyl *rac*-(2*S,4R,5R*)-4-cyano-5-phenylpyrrolidine-2-carboxylate (3.34). Using General Procedure 1, pyrrolidines **3.33** and **3.34** were accessed via various methods from imine **3.16** (38.2 mg, 0.200 mmol, 1.00 equiv) and acrylonitrile (14.5 μL , 0.220 mmol, 1.10 equiv) in the following yields and diastereomeric ratios (endo:exo). **Method A:** 93% yield, 69:31 dr; **Method B:**

85% yield, 8:92 dr; **Method C**: >99% yield, 19:81 dr. **3.33 (endo adduct)**: R_f 0.29 (1:1 hexanes:EtOAc); ^1H NMR (600 MHz, CDCl_3): δ 7.48 (app d, $J = 7.6$, 2H), 7.40 (app t, $J = 7.6$, 2H), 7.39 (app t, $J = 7.6$, 1H), 4.41 (d, $J = 6.4$, 1H), 4.33–4.23 (m, 2H), 3.96 (dd, $J = 8.8$, 6.4, 1H), 3.29–3.26 (m, 1H), 2.66 (br s, 1H), 2.63–2.56 (m, 1H), 2.51–2.47 (m, 1H), 1.33 (t, $J = 7.0$, 3H); ^{13}C NMR (125 MHz, CDCl_3): δ 172.6 (C), 137.8 (C), 128.7 (2CH), 128.6 (CH), 127.1 (2CH), 119.3 (C), 64.8 (CH), 61.7 (CH_2), 58.8 (CH), 36.0 (CH), 34.4 (CH_2), 14.2 (CH_3); IR (thin film): 3339, 2980, 2846, 2241, 1740, 1454, 1204 cm^{-1} ; HRMS-ESI (m/z) [M + Na] $^+$ calculated for $\text{C}_{14}\text{H}_{16}\text{N}_2\text{O}_2\text{Na}$, 267.1110; found, 267.1114. **3.34 (exo adduct)**: R_f 0.49 (1:1 hexanes:EtOAc); ^1H NMR (600 MHz, CDCl_3): δ 7.50 (app d, $J = 7.5$, 2H), 7.39 (app t, $J = 7.5$, 2H), 7.34 (app t, $J = 7.5$, 1H), 4.38 (d, $J = 9.0$, 1H), 4.25 (q, $J = 7.3$, 2H), 4.07 (dd, $J = 9.0$, 4.8, 1H), 2.83 (q, $J = 9.0$, 1H), 2.59–2.50 (m, 2H), 2.39 (br s, 1H), 1.32 (t, $J = 7.3$, 3H); ^{13}C NMR (125 MHz, CDCl_3): δ 173.4 (C), 138.8 (C), 129.1 (2CH), 128.8 (CH), 126.8 (2CH), 119.8 (C), 67.5 (CH), 61.8 (CH_2), 58.8 (CH), 36.5 (CH), 34.6 (CH_2), 14.3 (CH_3); IR (thin film): 3350, 3062, 3031, 2983, 2917, 2849, 2243, 1734, 1455, 1378, 1273, 1206 cm^{-1} ; HRMS-ESI (m/z) [M + Na] $^+$ calculated for $\text{C}_{14}\text{H}_{16}\text{N}_2\text{O}_2\text{Na}$, 267.1110; found, 267.1110.

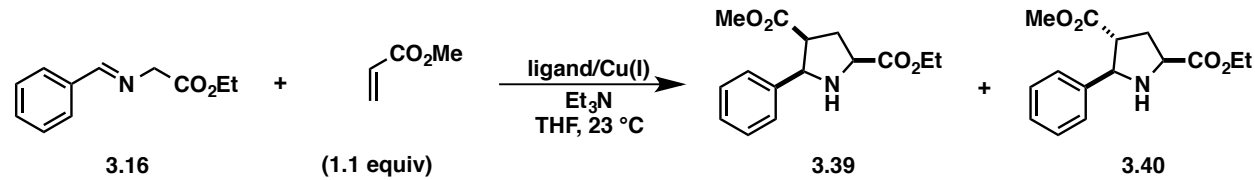


Ethyl *rac*-(2*S*,3*R*,4*R*,5*R*)-3,4-dicyano-5-phenylpyrrolidine-2-carboxylate (3.35). Exo pyrrolidine adduct **3.35** was synthesized using the following adaptations to **General Procedure 1**. The catalyst and imine components of these reactions were partially prepared in separate 1-dram screw-top vials inside a glove box with a N_2 atmosphere. The reagent vial was charged with neat imine **3.16** (38.2 mg, 0.200 mmol, 1.00 equiv). The catalyst and reagent vials were

each sealed with a Teflon-lined cap, then brought outside the glove box where the Teflon-lined caps were each covered with an inverted 14/20 joint rubber septum under a balloon of Ar. Outside of the glove box, a 1-dram vial was charged with fumaronitrile [17.2 mg, 0.220 mmol, 1.10 equiv; azeotropically dried with PhMe (3 x 2 mL)] and a magnetic stir bar, which was then sealed with a Teflon-lined cap and covered with an inverted 14/20 joint rubber septum under an atmosphere of Ar. **Method A:** In the glove box, the catalyst vial was charged with tetrakis(acetonitrile)copper(I) tetrafluoroborate (12.6 mg, 0.0400 mmol). Outside of the glove box, the catalyst vial was charged with THF (1.33 mL, freeze-pump-thawed) and tris(2,2,2-trifluoroethyl) phosphite (19.4 μ L, 0.0880 mmol). An aliquot of the catalyst solution (0.33 mL, 0.60 M; 0.010 mmol, 0.050 equiv Cu(I) and 0.022 mmol, 0.11 equiv ligand) and Et₃N (16.7 μ L, 0.120 mmol, 0.600 equiv) were added to the vial containing imine **3.16** via syringe. The homogenous mixture was transferred via syringe to the vial containing fumaronitrile. The resulting heterogeneous mixture was stirred at 23 °C for 5 h. The reaction was quenched by opening the vial to air and filtering the reaction mixture through a plug of SiO₂ (200 mg) using EtOAc (8.7 mL, HPLC grade). Exo adduct **3.35** was accessed in 61% yield as determined by GC-FID analysis by adding 1 mL of a GC standard solution [0.1 M solution of 1,3,5-trimethoxybenzene in EtOAc (HPLC grade)] to the filtrate. **Method B:** In the glove box, the catalyst vial was charged with tetrakis(acetonitrile)copper(I) tetrafluoroborate (12.6 mg, 0.0400 mmol) and tricyclohexylphosphine (24.6 mg, 0.0880 mmol). Outside of the glove box, the catalyst vial was charged with THF (0.80 mL, freeze-pump-thawed). An aliquot of the catalyst solution (0.20 mL, 1.0 M; 0.010 mmol, 0.050 equiv Cu(I) and 0.022 mmol, 0.11 equiv ligand) and Et₃N (16.7 μ L, 0.120 mmol, 0.600 equiv) were added to the vial containing imine **3.16** via syringe. The homogenous mixture was transferred via syringe to the vial containing

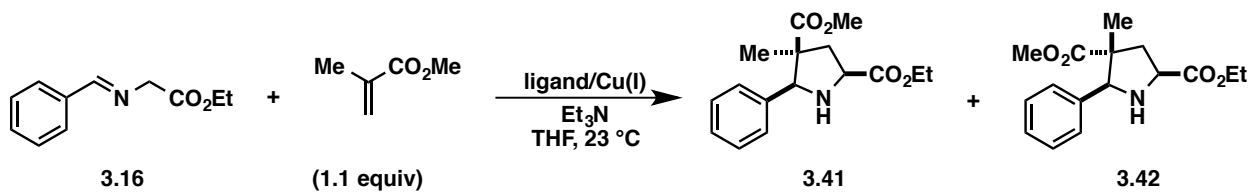
fumaronitrile. The resulting heterogeneous mixture was stirred at 23 °C for 1 h. The reaction was quenched by opening the vial to air and filtering the reaction mixture through a plug of SiO₂ (200 mg) using EtOAc (8.2 mL, HPLC grade). Exo adduct **3.35** was accessed in 65% yield as determined by GC-FID analysis by adding 1 mL of a GC standard solution [0.1 M solution of 1,3,5-trimethoxybenzene in EtOAc (HPLC grade)] to the filtrate. **Method C:** In the glove box, the catalyst vial was charged with tetrakis(acetonitrile)copper(I) tetrafluoroborate (12.6 mg, 0.0400 mmol) and DavePhos (17.3 mg, 0.0440 mmol). Outside of the glove box, the catalyst vial was charged with THF (2.0 mL, freeze-pump-thawed). An aliquot of the catalyst solution (0.50 mL, 0.4 M; 0.010 mmol, 0.050 equiv Cu(I) and 0.011 mmol, 0.055 equiv ligand) and Et₃N (16.7 µL, 0.120 mmol, 0.600 equiv) were added to the vial containing imine **3.16** via syringe. The homogenous mixture was transferred via syringe to the vial containing fumaronitrile. The resulting heterogeneous mixture was stirred at 23 °C for 3 h. The reaction was quenched by opening the vial to air and filtering the reaction mixture through a plug of SiO₂ (200 mg) using EtOAc (8.5 mL, HPLC grade). Exo adduct **3.35** was accessed in 76% yield as determined by GC-FID analysis by adding 1 mL of a GC standard solution [0.1 M solution of 1,3,5-trimethoxybenzene in EtOAc (HPLC grade)] to the filtrate. In addition to exo adduct **3.35**, cycloadducts **3.36** and **3.37** were isolated by flash chromatography (4:1 hexanes:EtOAc to 100% EtOAc, gradient elution) but insufficient quantities of these two cycloadducts could be isolated for adequate characterization.²⁴ The endo cycloadduct was not detected. **3.35 (exo adduct):** Colorless solid (mp = 81–83 °C); R_f 0.54 (1:1 hexanes:EtOAc); ¹H NMR (500 MHz, CDCl₃): δ 7.51 (app dd, J = 8.2, 1.2, 2H), 7.45–7.39 (m, 3H), 4.44–4.31 (m, 3H), 4.27 (app t, J = 7.4, 1H), 3.69 (app t, J = 8.6, 1H), 3.22 (app t, J = 8.6, 1H), 2.78 (app t, J = 7.8, 1H), 1.38 (t, J = 7.4, 3H); ¹³C NMR (125 MHz, CDCl₃): δ 169.3 (C), 136.5 (C), 129.6 (CH), 129.5 (2CH), 126.8

(2CH), 116.9 (C), 116.2 (C), 67.1 (CH), 63.0 (CH₂), 61.8 (CH), 41.6 (CH), 37.5 (CH), 14.2 (CH₃); IR (thin film): 3351, 3064, 3032, 2983, 2940, 2873, 2248, 1738, 1457, 1378, 1211 cm⁻¹; HRMS-ESI (*m/z*) [M + Na]⁺ calculated for C₁₅H₁₅N₃O₂Na, 292.1062; found, 292.1068. **3.36 (with minor impurities):** ¹H NMR (600 MHz, CDCl₃): δ 7.47–7.46 (m, 2H), 7.42–7.36 (m, 3H), 4.64 (dd, *J* = 9.1, 6.7, 1H), 4.33–4.29 (m, 2H), 3.74 (dd, *J* = 8.5, 5.1, 1H), 3.16 (app t, *J* = 9.1, 1H), 2.76 (app t, *J* = 6.4, 1H), 1.35 (t, *J* = 7.3, 3H); ¹³C NMR (125 MHz, CDCl₃): δ 169.9 (C), 136.9 (C), 129.5 (CH), 129.3 (2CH), 126.7 (2CH), 116.6 (C), 115.9 (C), 66.1 (CH), 62.9 (CH₂), 62.8 (CH), 40.7 (CH), 35.9 (CH), 14.3 (CH₃); **3.37 (with minor impurities):** ¹H NMR (600 MHz, CDCl₃): δ 7.46–7.38 (m, 5H), 4.66 (app t, *J* = 6.1, 1H), 4.36 (q, *J* = 7.1, 2H), 4.18 (app t, *J* = 6.1, 1H), 3.72 (dd, *J* = 6.1, 4.4, 1H), 3.58 (dd, *J* = 6.1, 4.4, 1H), 2.82 (br s, 1H), 1.38 (t, *J* = 7.1, 3H); ¹³C NMR (125 MHz, CDCl₃): δ 169.0 (C), 135.4 (C), 129.5 (CH), 129.1 (2CH), 127.1 (2CH), 117.7 (C), 116.4 (C), 64.3 (CH), 63.2 (CH), 63.0 (CH₂), 41.0 (CH), 36.5 (CH), 14.3 (CH₃).



2-Ethyl 4-methyl *rac*-(2*S*,4*S*,5*R*)-5-phenylpyrrolidine-2,4-dicarboxylate (3.39) and 2-ethyl 4-methyl *rac*-(2*S*,4*R*,5*R*)-5-phenylpyrrolidine-2,4-dicarboxylate (3.40). Using General Procedure 1, pyrrolidines **3.39** and **3.40** were accessed via various methods from imine **3.16** (38.2 mg, 0.200 mmol, 1.00 equiv) and methyl acrylate (19.8 μL, 0.220 mmol, 1.10 equiv) in the following yields and diastereomeric ratios (endo:exo). **Method A:** 87% yield, 97:3 dr; **Method B:** 85% yield, 94:6 dr; **Method C:** 93% yield, 69:31 dr. **3.39 (endo adduct):** R_f 0.27 (1:1 hexanes:EtOAc); ¹H NMR (600 MHz, CDCl₃): δ 7.33–7.29 (m, 4H), 7.26–7.23 (m, 1H), 4.54 (d, *J* = 7.8, 1H), 4.29 (q, *J* = 7.1, 2H), 3.96 (app t, *J* = 8.3, 1H), 3.32 (q, *J* = 7.8, 1H), 3.22

(s, 3H), 2.89 (br s, 1H), 2.45–2.37 (m, 2H), 1.34 (t, J = 7.1, 3H); ^{13}C NMR (125 MHz, CDCl_3): δ 173.4 (C), 173.0 (C), 139.2 (C), 128.2 (2CH), 127.6 (CH), 126.8 (2CH), 65.9 (CH), 61.2 (CH₂), 60.1 (CH), 51.3 (CH₃), 49.8 (CH), 33.4 (CH₂), 14.3 (CH₃); IR (thin film): 3346, 3062, 3028, 2983, 2950, 2906, 1735, 1454, 1437, 1203, 1168 cm^{-1} ; HRMS-ESI (m/z) [M + Na]⁺ calculated for $\text{C}_{15}\text{H}_{19}\text{NO}_4\text{Na}$, 300.1212; found, 300.1209. ^1H NMR spectral data are consistent with those previously reported.^{19l} **3.40 (exo adduct):** R_f 0.40 (1:1 hexanes:EtOAc); ^1H NMR (500 MHz, CDCl_3): δ 7.44 (app d, J = 7.6, 2H), 7.33 (app t, J = 7.6, 2H), 7.27 (app t, J = 7.6, 1H), 4.40 (d, J = 8.7, 1H), 4.23 (q, J = 7.1, 2H), 4.02 (dd, J = 8.9, 5.4, 1H), 3.63 (s, 3H), 2.91 (q, J = 8.9, 1H), 2.54–2.48 (m, 1H), 2.43 (br s, 1H), 2.40–2.35 (m, 1H), 1.30 (t, J = 7.1, 3H); ^{13}C NMR (125 MHz, CDCl_3): δ 174.3 (C), 173.9 (C), 141.2 (C), 128.7 (2CH), 127.9 (CH), 127.0 (2CH), 66.9 (CH), 61.4 (CH₂), 59.5 (CH), 52.0 (CH₃), 51.4 (CH), 34.9 (CH₂), 14.3 (CH₃); IR (thin film): 3345, 3028, 2982, 2953, 2904, 1732, 1437, 1196, 1168 cm^{-1} ; HRMS-ESI (m/z) [M + H]⁺ calculated for $\text{C}_{15}\text{H}_{20}\text{NO}_4$, 278.1392; found, 278.1384.



2-Ethyl 4-methyl *rac*-(2*S*,4*S*,5*S*)-4-methyl-5-phenylpyrrolidine-2,4-dicarboxylate (3.41) and 2-ethyl 4-methyl *rac*-(2*S*,4*R*,5*S*)-4-methyl-5-phenylpyrrolidine-2,4-dicarboxylate (3.42). Using **General Procedure 1**, pyrrolidines **3.41** and **3.42** were accessed via various methods from imine **3.16** (38.2 mg, 0.200 mmol, 1.00 equiv) and methyl methacrylate (23.5 μL , 0.220 mmol, 1.10 equiv) in the following yields and diastereomeric ratios (endo:exo). **Method A:** 61% yield, 99:1 dr; **Method B:** 75% yield, 97:3 dr; **Method C:** 87% yield, 78:22 dr. **3.41 (endo adduct):** R_f 0.35 (1:1 hexanes:EtOAc); ^1H NMR (500 MHz, CDCl_3): δ 7.32–7.24 (m, 5H), 4.29

(q, $J = 7.1$, 2H), 4.06 (s, 1H), 4.02 (dd, $J = 8.7$, 7.2, 1H), 3.21 (s, 3H), 3.00 (br s, 1H), 2.72 (dd, $J = 13.2$, 7.2, 1H), 2.12 (dd, $J = 13.2$, 8.7, 1H), 1.41 (s, 3H), 1.33 (t, $J = 7.1$, 3H); ^{13}C NMR (125 MHz, CDCl_3): δ 174.9 (C), 174.0 (C), 138.9 (C), 128.3 (2CH), 128.0 (CH), 126.8 (2CH), 74.2 (CH), 61.3 (CH₂), 59.3 (CH), 54.9 (C), 51.5 (CH₃), 41.7 (CH₂), 22.8 (CH₃), 14.4 (CH₃); IR (thin film): 3348, 3028, 2981, 2878, 1734, 1455, 1240, 1217 cm^{-1} ; HRMS-ESI (m/z) [M + Na]⁺ calculated for $\text{C}_{16}\text{H}_{21}\text{NO}_4\text{Na}$, 314.1368; found, 314.1363. **3.42 (exo adduct):** R_f 0.61 (1:1 hexanes:EtOAc); ^1H NMR (500 MHz, CDCl_3): δ 7.34–7.30 (m, 4H), 7.27–7.24 (m, 1H), 4.70 (s, 1H), 4.25 (dq, $J = 7.2$, 1.1, 2H), 4.02 (dd, $J = 9.1$, 7.3, 1H), 3.74 (s, 3H), 2.76 (dd, $J = 13.0$, 9.1, 1H), 2.65 (br s, 1H), 1.97 (dd, $J = 13.0$, 7.3, 1H), 1.31 (t, $J = 7.2$, 3H), 0.85 (s, 3H); ^{13}C NMR (125 MHz, CDCl_3): δ 176.9 (C), 174.2 (C), 139.3 (C), 128.2 (2CH), 127.6 (CH), 127.4 (2CH), 68.9 (CH), 61.3 (CH₂), 58.1 (CH), 52.7 (C), 52.4 (CH₃), 42.0 (CH₂), 19.7 (CH₃), 14.4 (CH₃); IR (thin film): 3344, 3029, 2981, 2935, 1730, 1455, 1273, 1197 cm^{-1} ; HRMS-Cl (m/z) [M + H]⁺ calculated for $\text{C}_{16}\text{H}_{22}\text{NO}_4$, 292.1549; found, 292.1553.

3.7.5 Verification of Cu(I)/PCy₃ Catalyst

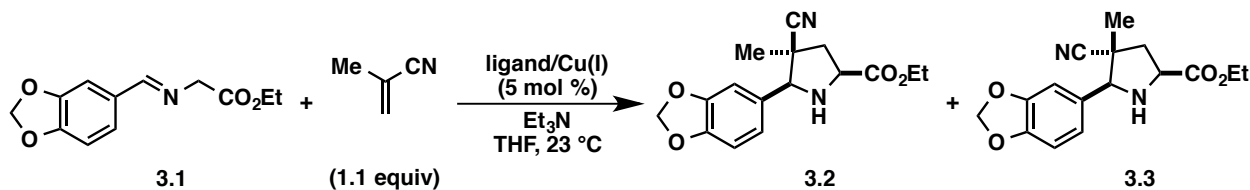
PCy₃ is a sensitive ligand because it readily oxidizes. A series of experiments was performed in order to verify that Cu(I)/PCy₃ was the active catalyst in the 1,3-DC reactions run using PCy₃ as the ligand. Tricyclohexylphosphonium tetrafluoroborate (PCy₃•HBF₄) is an air-stable salt from which PCy₃ is easily liberated by the addition of Et₃N (Table 3.16, entry 3). The 1,3-DC reaction was run using PCy₃•HBF₄ (Table 3.17, entry 2). The reaction proceeded more sluggishly but the dr was consistent with the reaction run using PCy₃. Increasing the reaction time to 19 h resulted in a higher yield (entry 3), but the yield did not compare to that using PCy₃ (entry 1). Pretreating the Cu(I)/PCy₃•HBF₄ catalyst solution with Et₃N (22 mol %) did not affect reactivity (entry 4). These results suggested that the Et₃N•HBF₄ byproduct may inhibit desired

reactivity. This hypothesis was supported by running the Cu(I)/ PCy_3 -catalyzed reaction with $\text{Et}_3\text{N}\bullet\text{HBF}_4$ ²⁹ as an additive. Yields were lower when increased amounts of $\text{Et}_3\text{N}\bullet\text{HBF}_4$ were added to the reaction but the dr was consistent at 10:90 (entries 5 and 6). Finally, it was shown that the reaction run using tricyclohexylphosphine oxide ($\text{O}=\text{PCy}_3$) was slower and less diastereoselective than running the same reaction with PCy_3 as the ligand (entry 7). Collectively, these results support that the reactions run in this report are indeed catalyzed by a Cu(I)/ PCy_3 complex where the ligand has not been oxidized.

Table 3.16. ^{31}P NMR Shifts of PCy_3 Derivatives

entry	compound	^{31}P NMR (δ ppm in CDCl_3)
1	PCy_3	11.2
2	$\text{PCy}_3\bullet\text{HBF}_4$	27.8
3	$\text{PCy}_3\bullet\text{HBF}_4 + \text{Et}_3\text{N}$ (1:1)	11.2
4	$\text{O}=\text{PCy}_3$	50.3

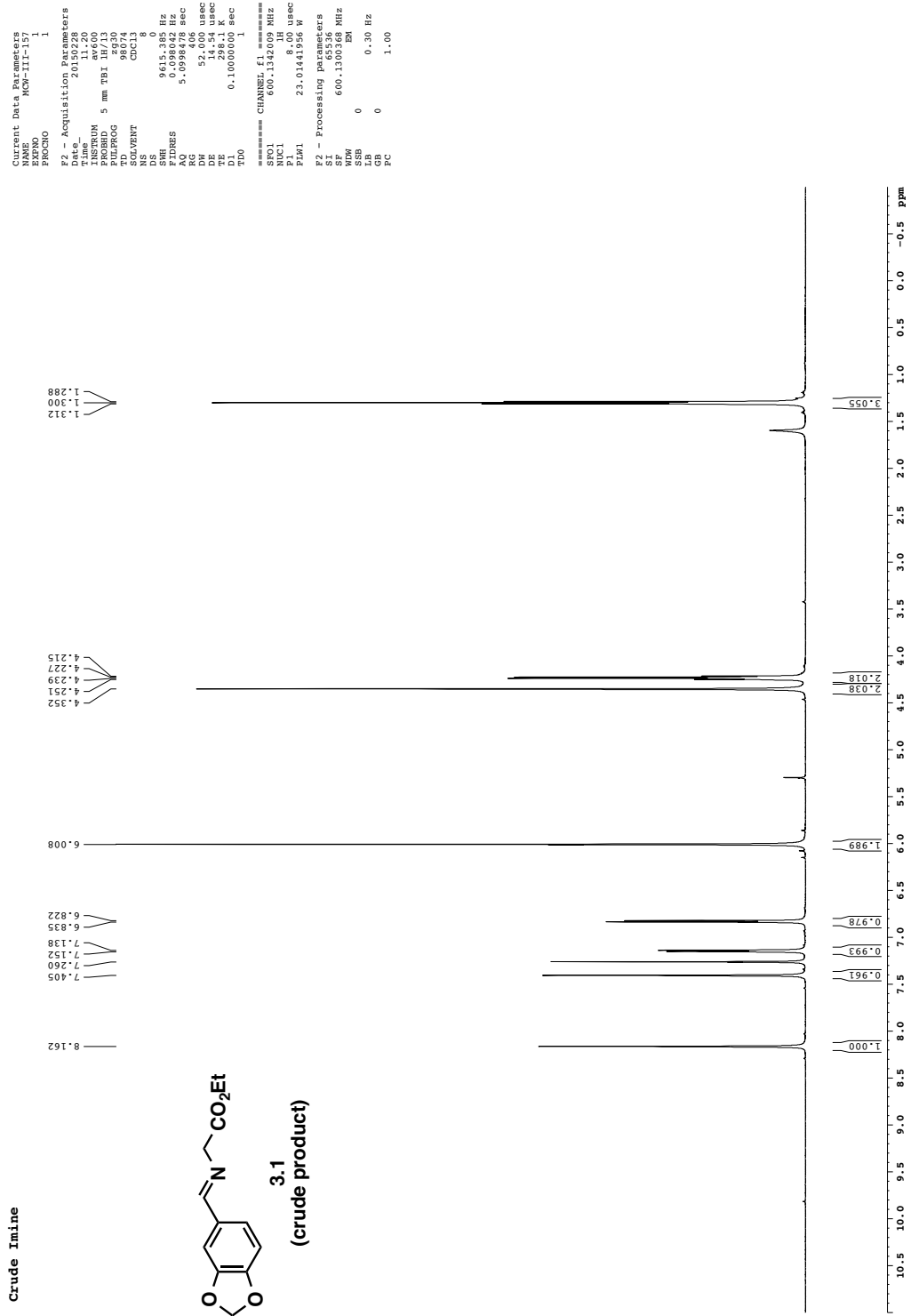
Table 3.17. Testing PCy_3 Ligands



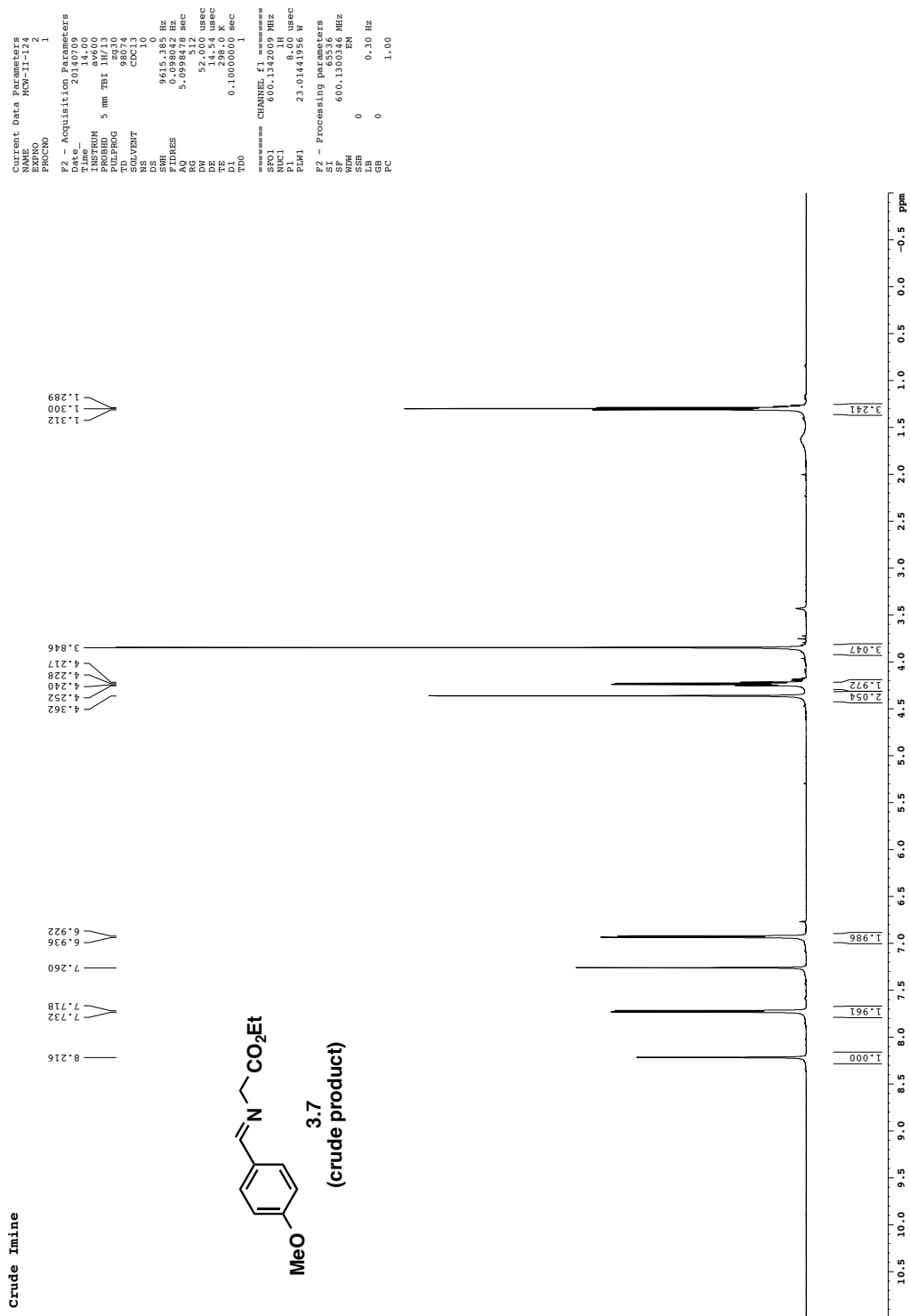
entry ^a	ligand (11 mol %)	additive	reaction time (h)	unreacted 3.1 (%) ^b	yield (%) ^b	dr (endo:exo) ^c
1	PCy_3	–	1	3	95	9:91
2	$\text{PCy}_3\bullet\text{HBF}_4$	–	1	69	25	9:91
3	$\text{PCy}_3\bullet\text{HBF}_4$	–	19	13	64	11:89
4	$\text{PCy}_3\bullet\text{HBF}_4^d$	–	1	66	29	9:91
5	PCy_3	$\text{Et}_3\text{N}\bullet\text{HBF}_4$ (11 mol %)	1	38	57	10:90
6	PCy_3	$\text{Et}_3\text{N}\bullet\text{HBF}_4$ (22 mol %)	1	50	40	10:90
7	$\text{O}=\text{PCy}_3$	–	1	29	49	21:79

^aReactions were performed using imine 3.1 (0.20 mmol) and methacrylonitrile (0.22 mmol) at a concentration of 0.2 M in THF. ^bGC yields using 1,3,5-trimethoxybenzene as external standard ($\pm 5\%$ error). ^cRatios determined by GC-FID analysis. ^dPretreated catalyst solution with Et_3N (22 mol %).

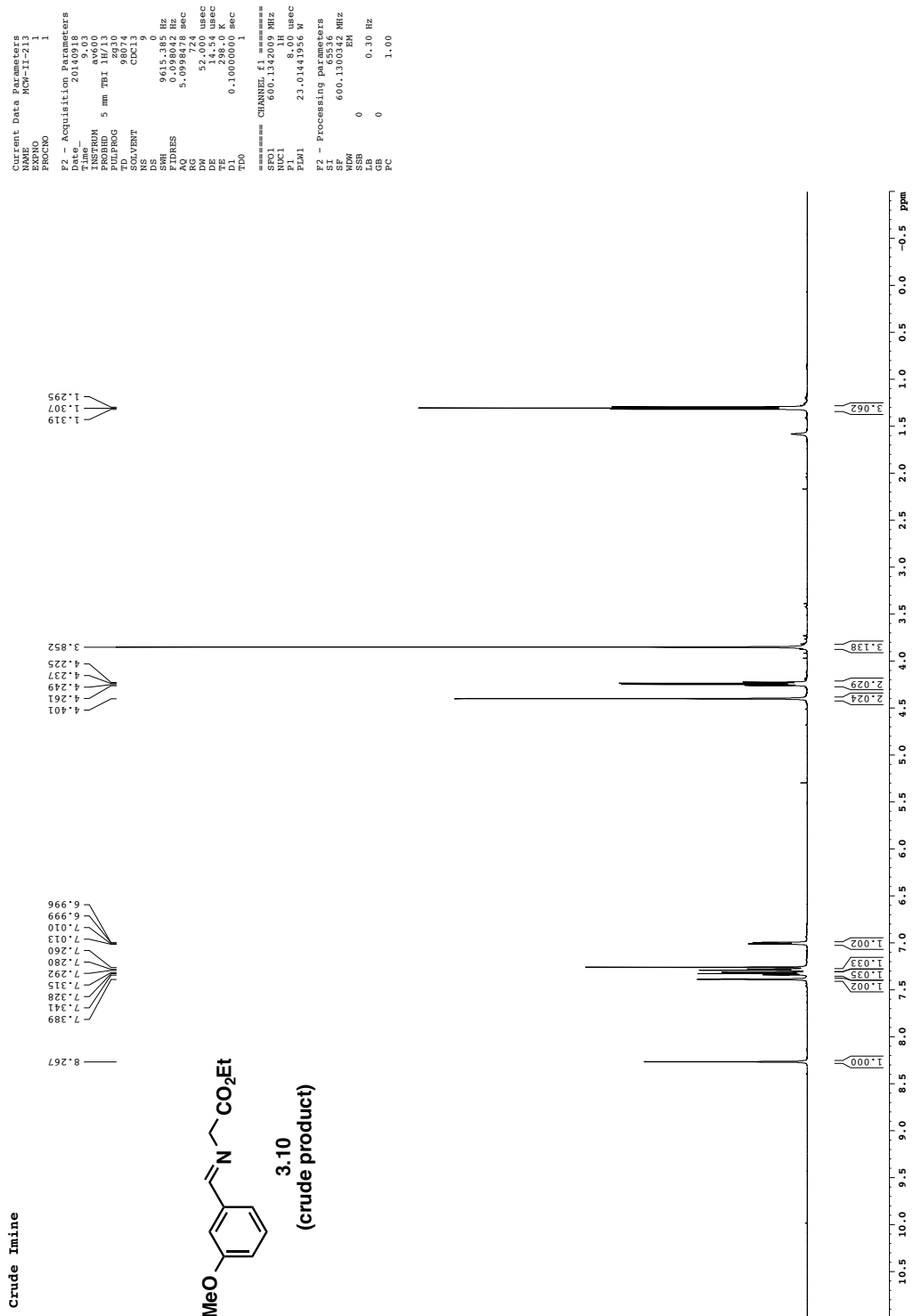
3.8 Appendix B: NMR Spectral Data



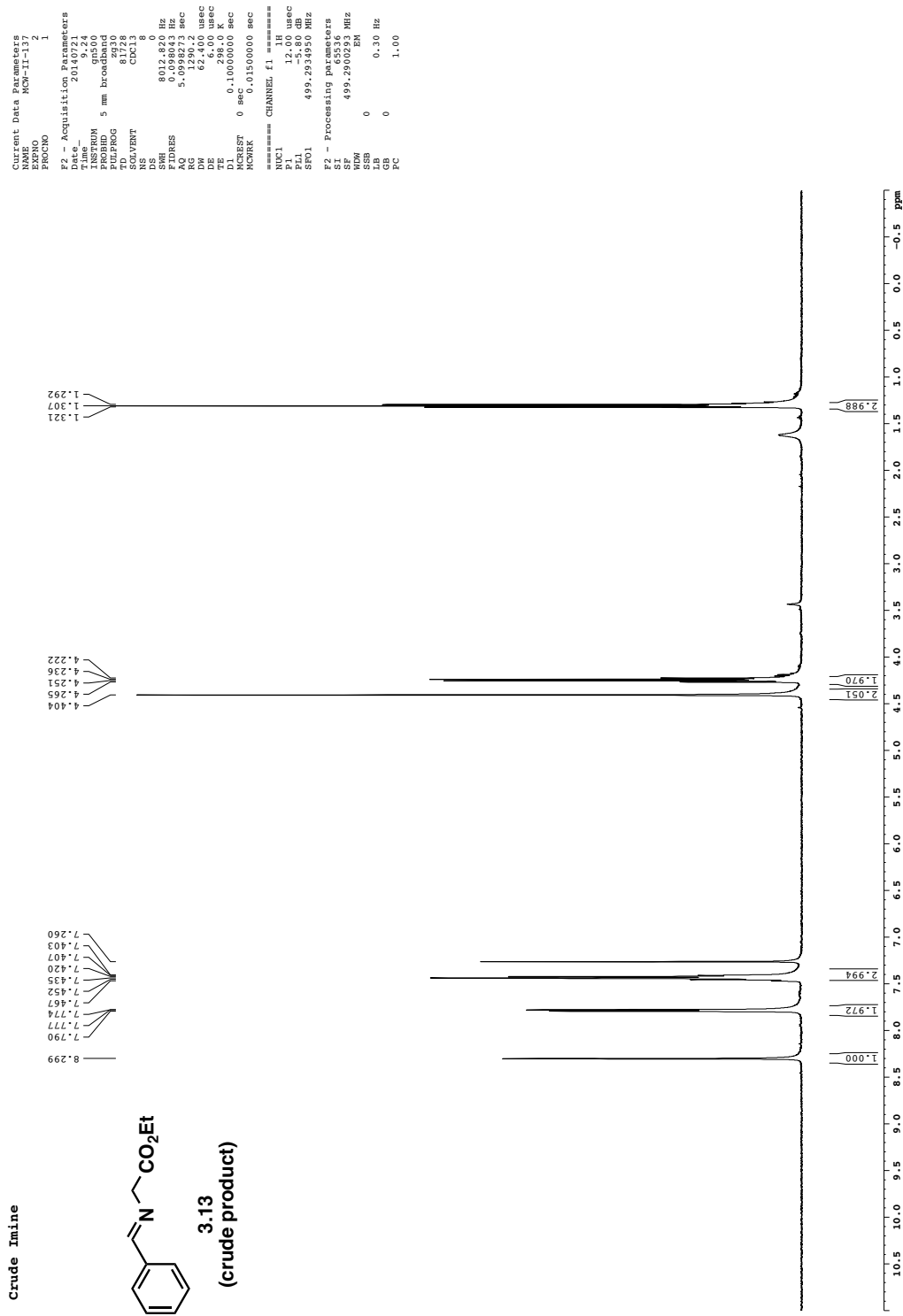
Crude Imine



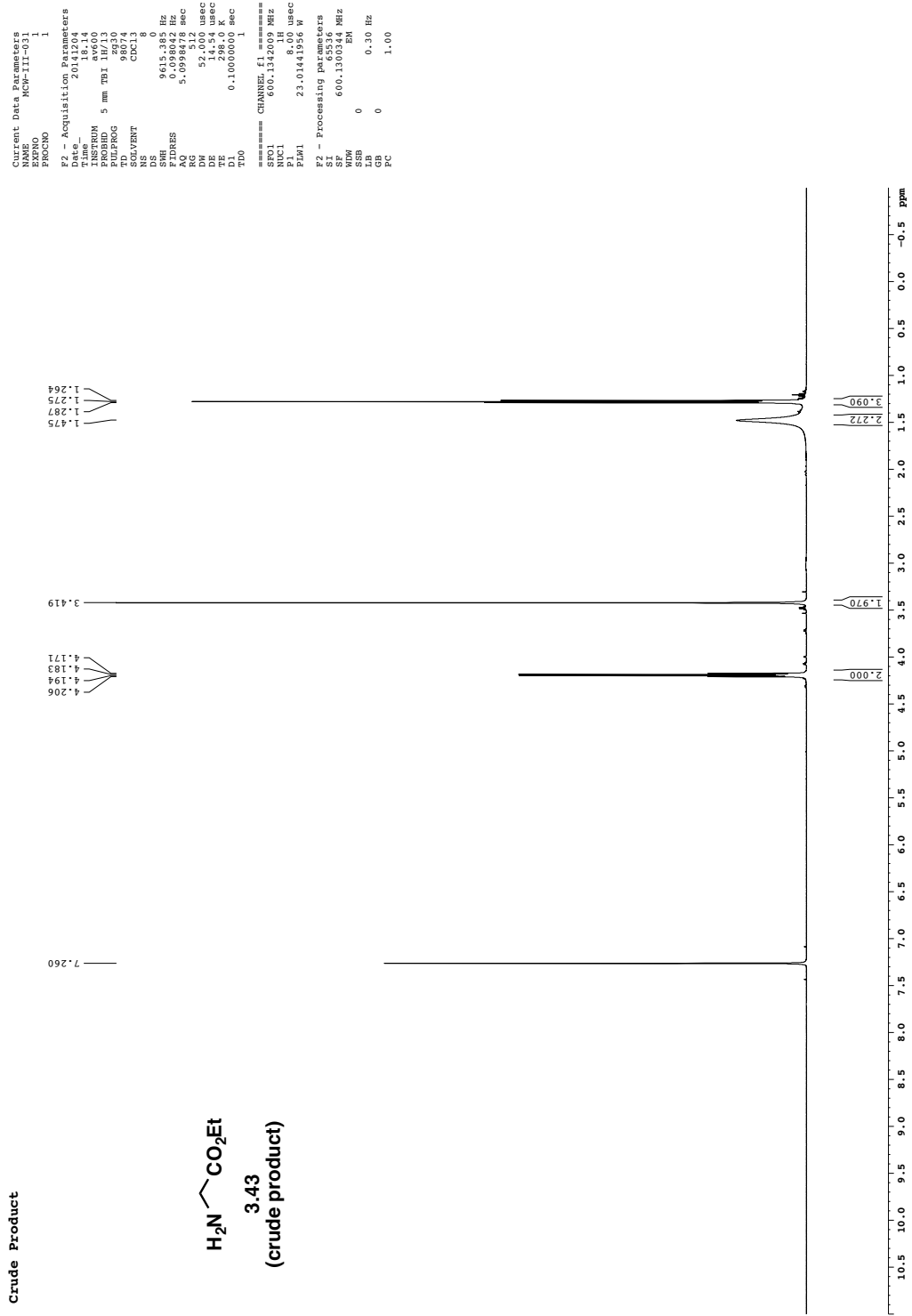
Crude Imine



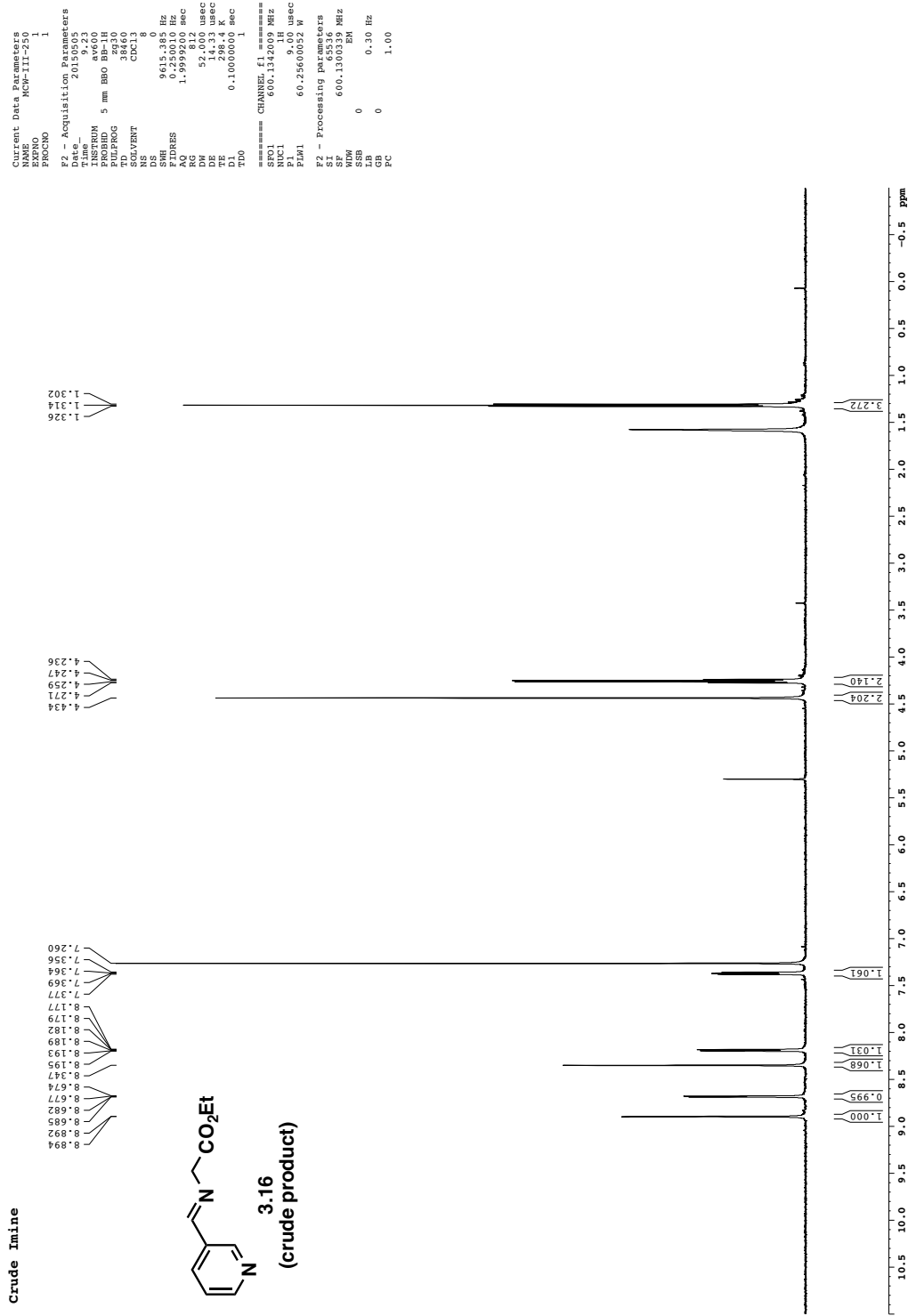
Crude Imine

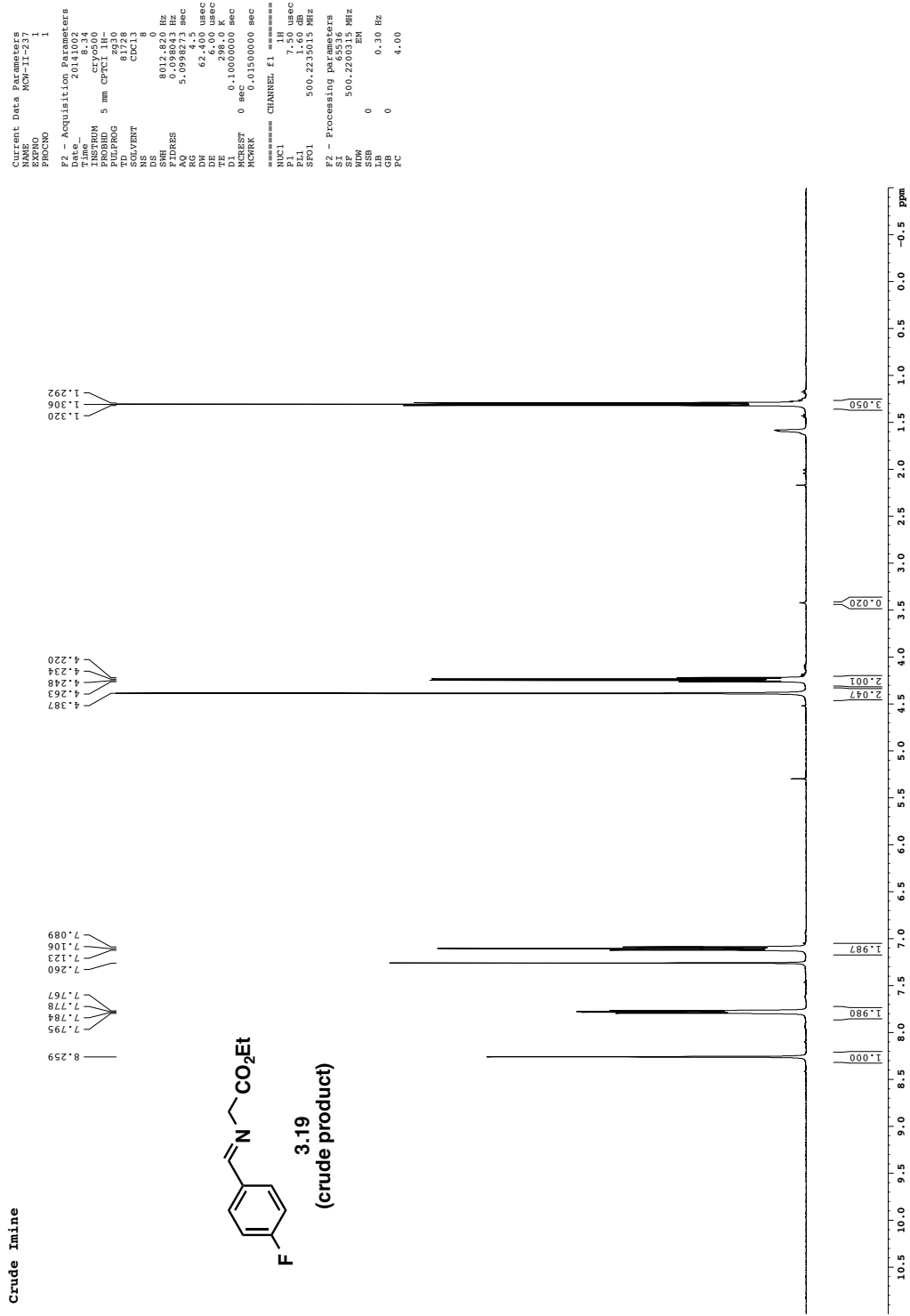


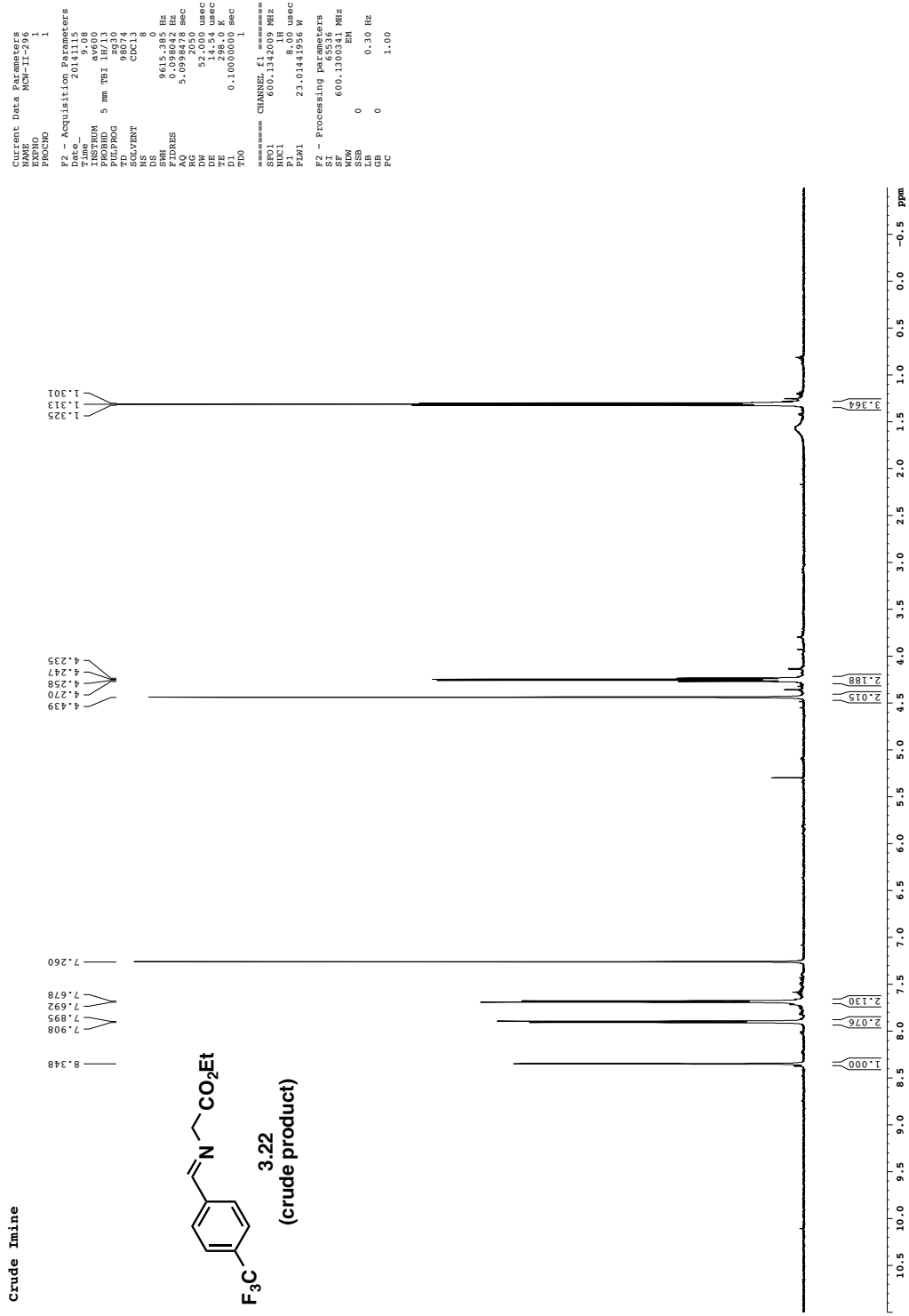
Crude Product



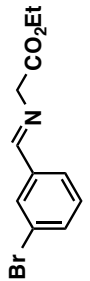
Crude Imine



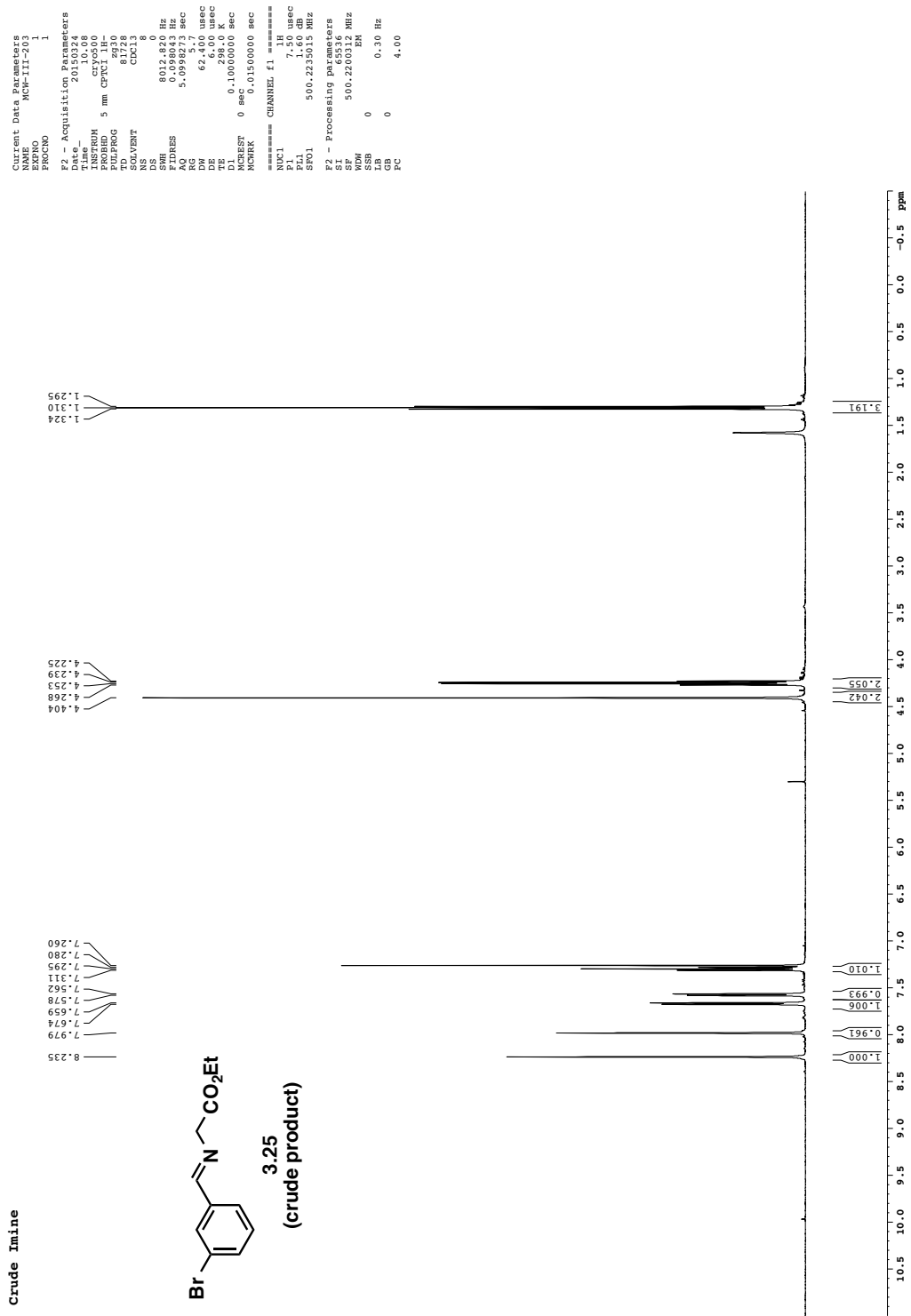


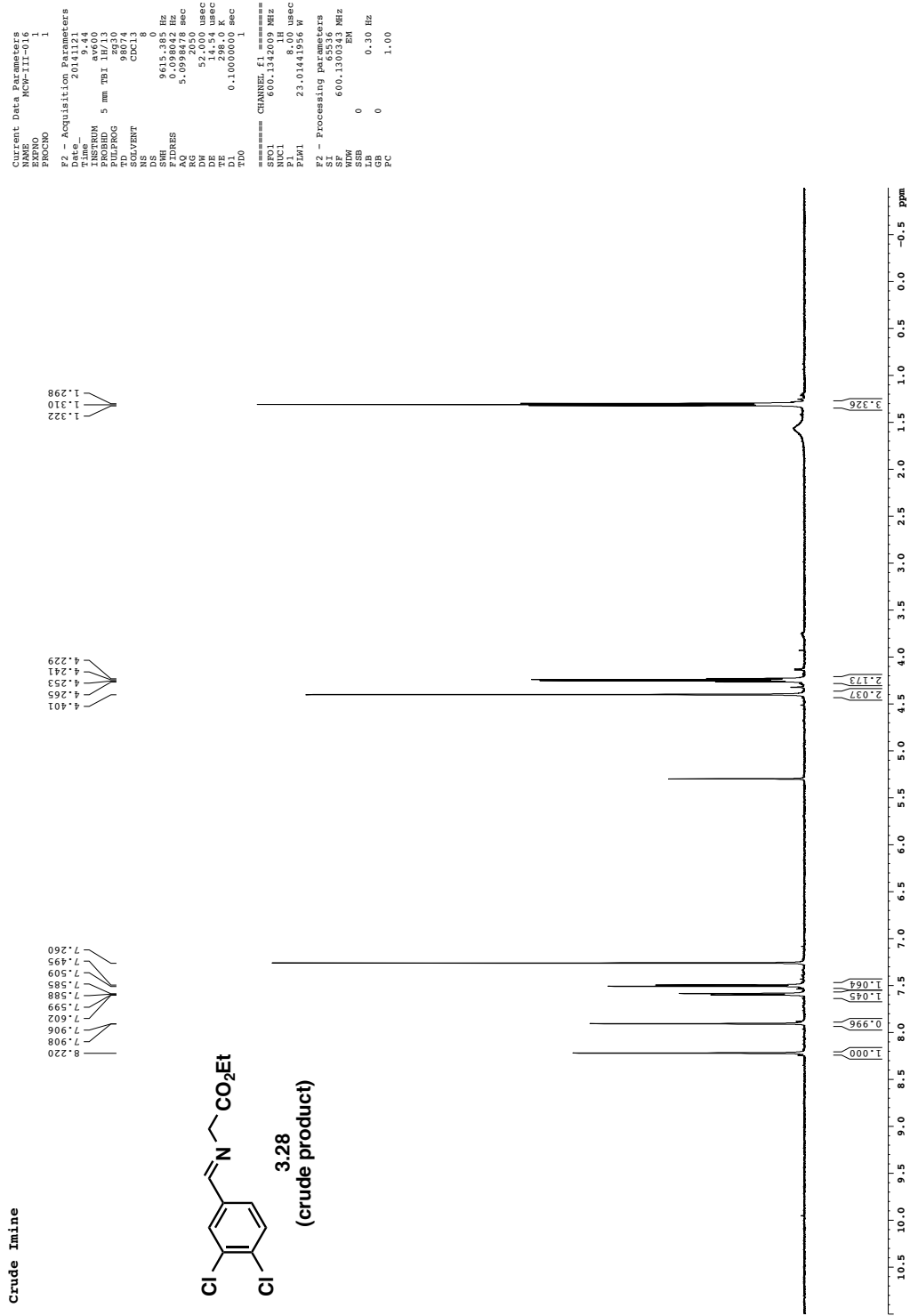


Crude Imine

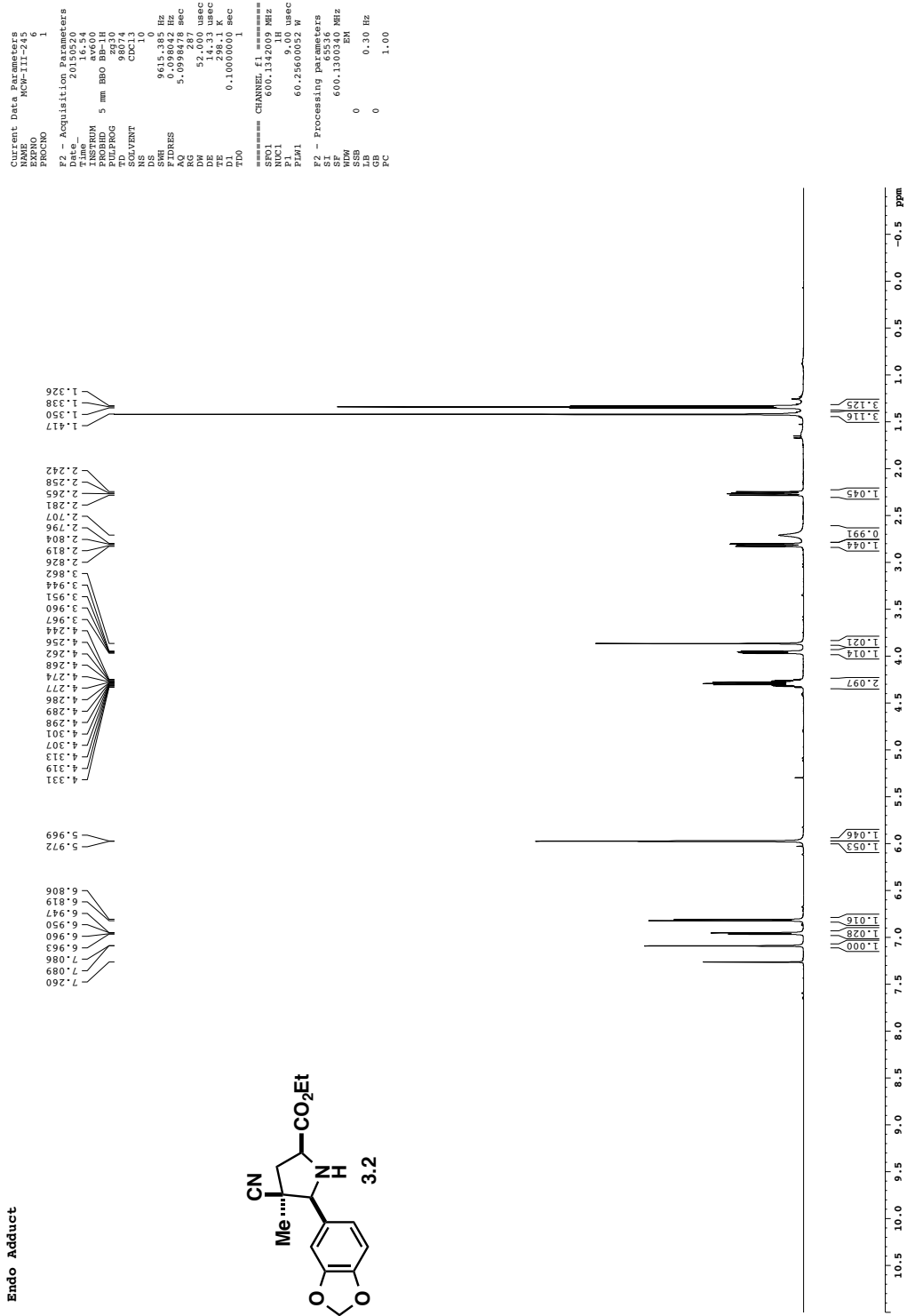


3.25
(crude product)

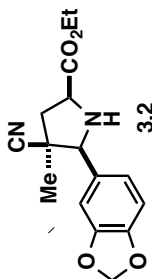


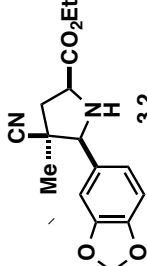


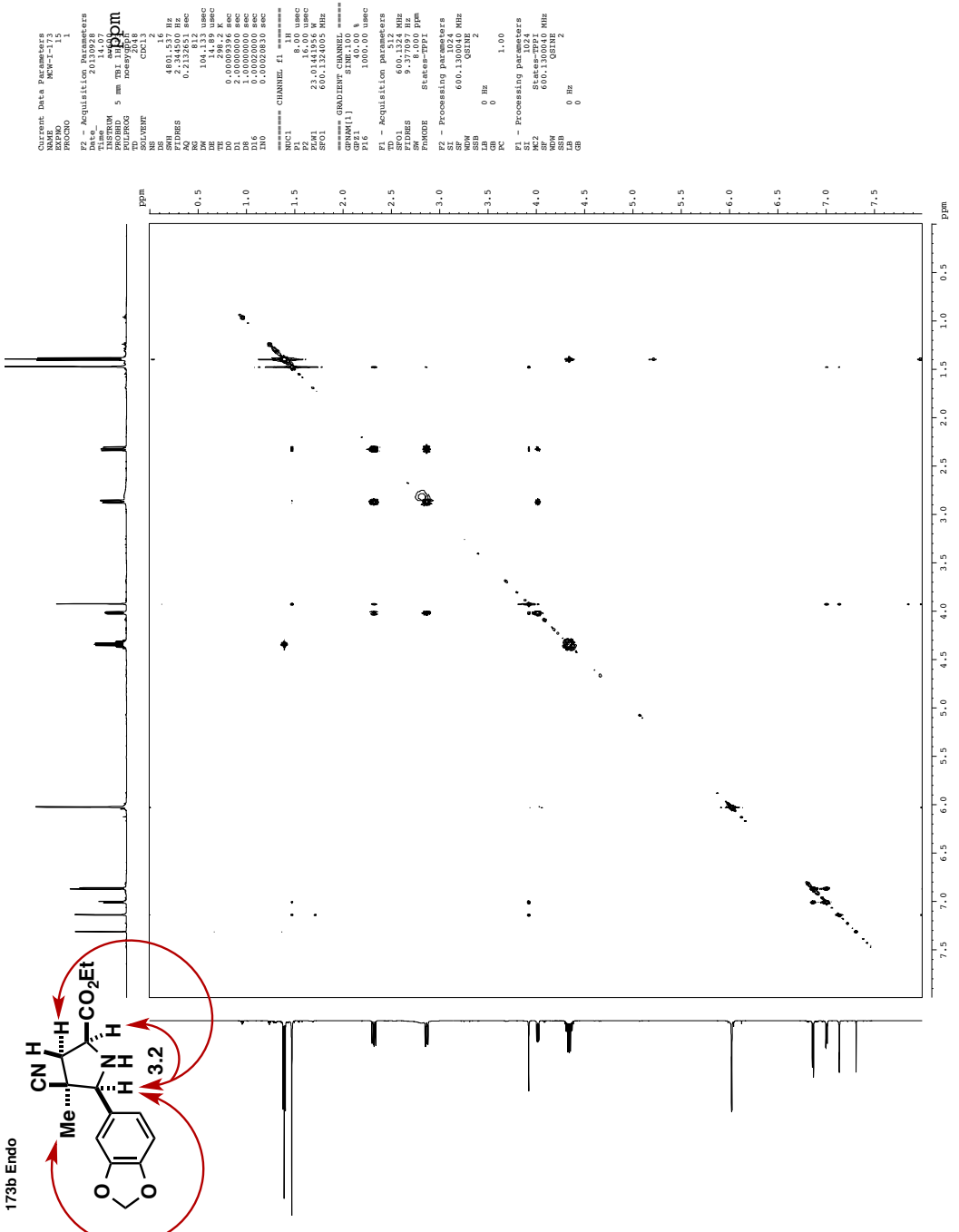
Endo Adduct



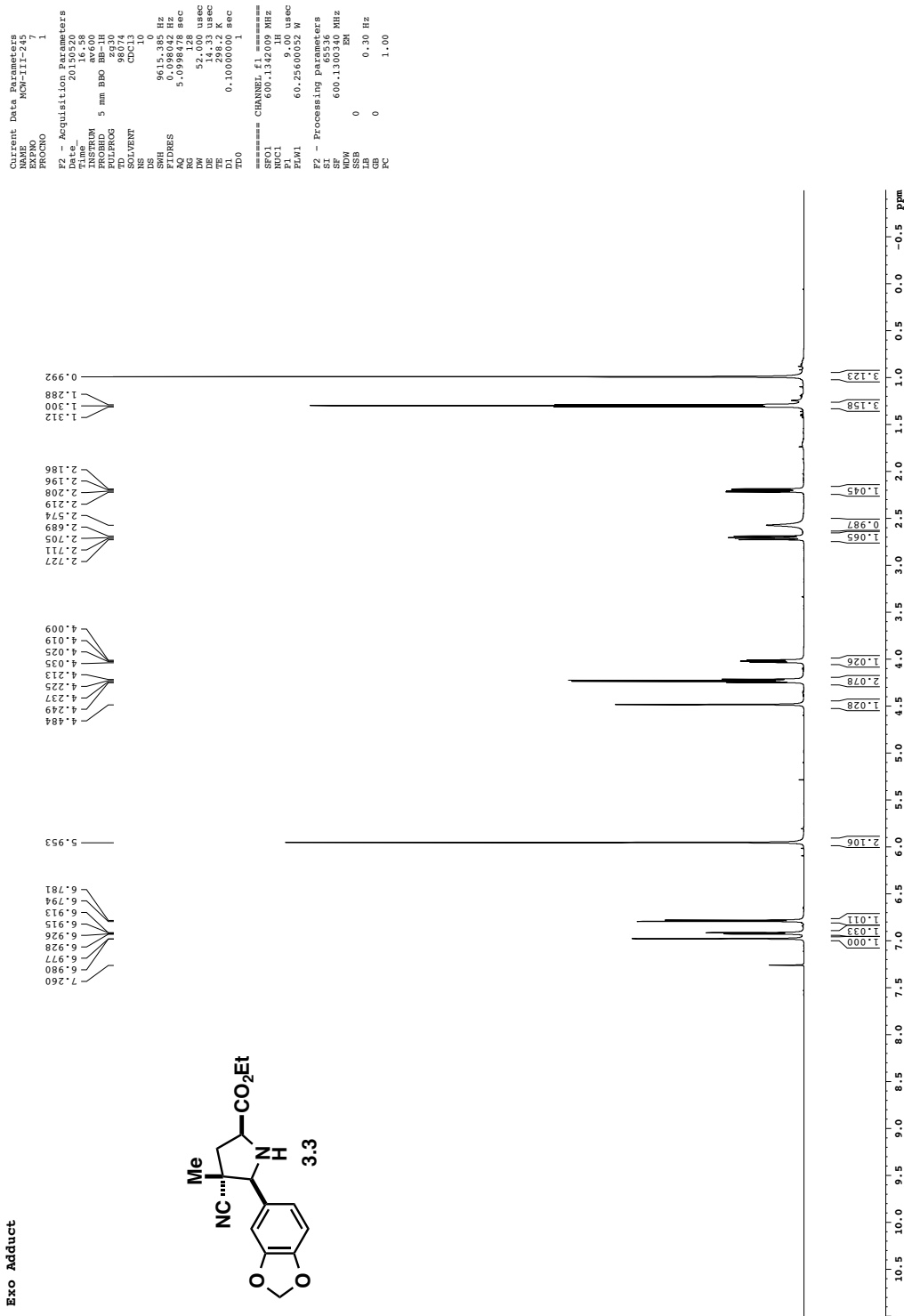
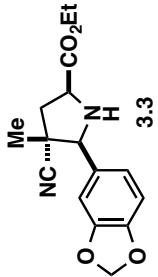
Purified Endo Product



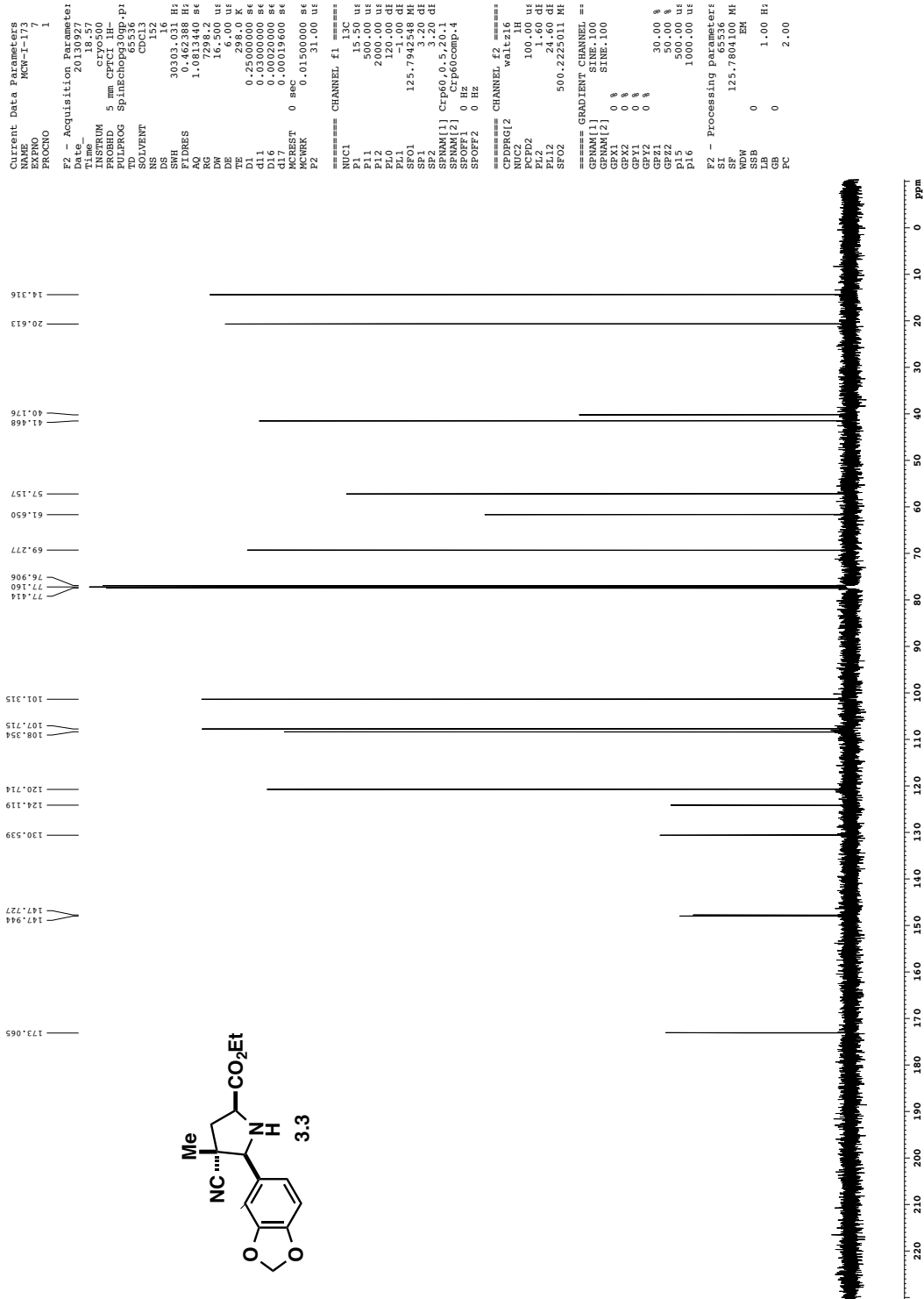
Current Data Parameters
 NAME MCW-T-173
 EXPNO 1
 FPGNO 1
 F2 - Acquisition Parameters
 Date 20130928
 Time 11.07
 INSTRUM cryo-500
 PROBHD 5 mm CPTCI 1H-
 PULPROG SpinEchoesP319p-p1
 TD 6516
 SOLVENT CDCl3
 NS 184
 DS 16
 SWH 303.03 Hz
 FIDRES 0.462388 Hz
 AQ 1.0813340 sec
 RG 9193.2
 DW 16.000 us
 DE 6.000 us
 TE 298.0 ms
 D1 0.2500000 sec
 d11 0.0300000 sec
 d16 0.0002000 sec
 dt7 0.00019600 sec
 MCREST 0 sec
 MWCK 0.01500000 sec
 P2 31.00 us
 ===== CHANNEL f1 =====
 NUC1 13C
 P1 15.50 us
 P11 500.00 us
 P12 2000.00 us
 P10 120.00 us
 P11 125.791248 MHz
 SP1 125.791248 MHz
 SP2 3.20 GHz
 SPNAM[1] Crp60.0,5,20.01
 SPNAM[2] Crp60.0,5,20.04
 SPoff1 0 Hz
 SPoff2 0 Hz
 ===== CHANNEL f2 =====
 CDDDRG[1] S1,RE:1.00 MHz
 NUC2 S1,RE:1.00 MHz
 PCP2 100.00 us
 P112 1.60 GHz
 P112 24.60 GHz
 SF02 500.225011 MHz
 ===== GRADIENT CHANNEL ===
 GRNAM[1] S1,RE:1.00 MHz
 GRNAM[2] 0 %
 GPX1 0 %
 GPY1 0 %
 GPY2 0 %
 GPZ1 30.00 %
 GPZ2 50.00 %
 P15 1000.00 us
 P16 1000.00 us
 S1 - Processing Parameters:
 SP 65136
 DW 125.7804100 MHz
 SSB 0 EM
 LB 1.00 Hz
 GB 0
 FC 2.00
 172.980
 148.169
 130.511
 108.520
 107.598
 77.1160
 77.414
 72.291
 61.837
 43.962
 42.285
 14.317
 Me
 CN
 CO₂Et
 3.2


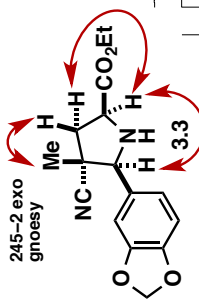
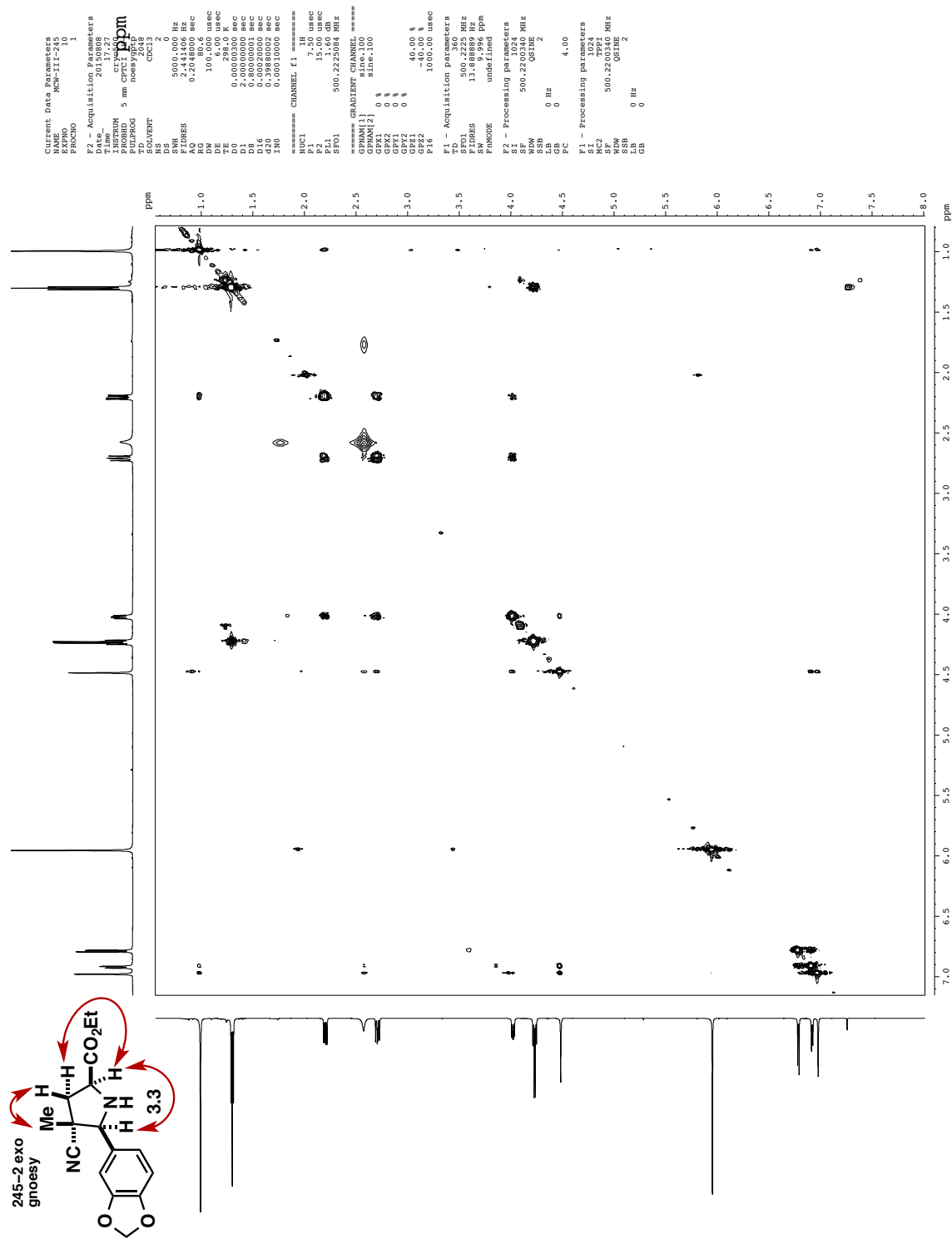


Exo Adduct

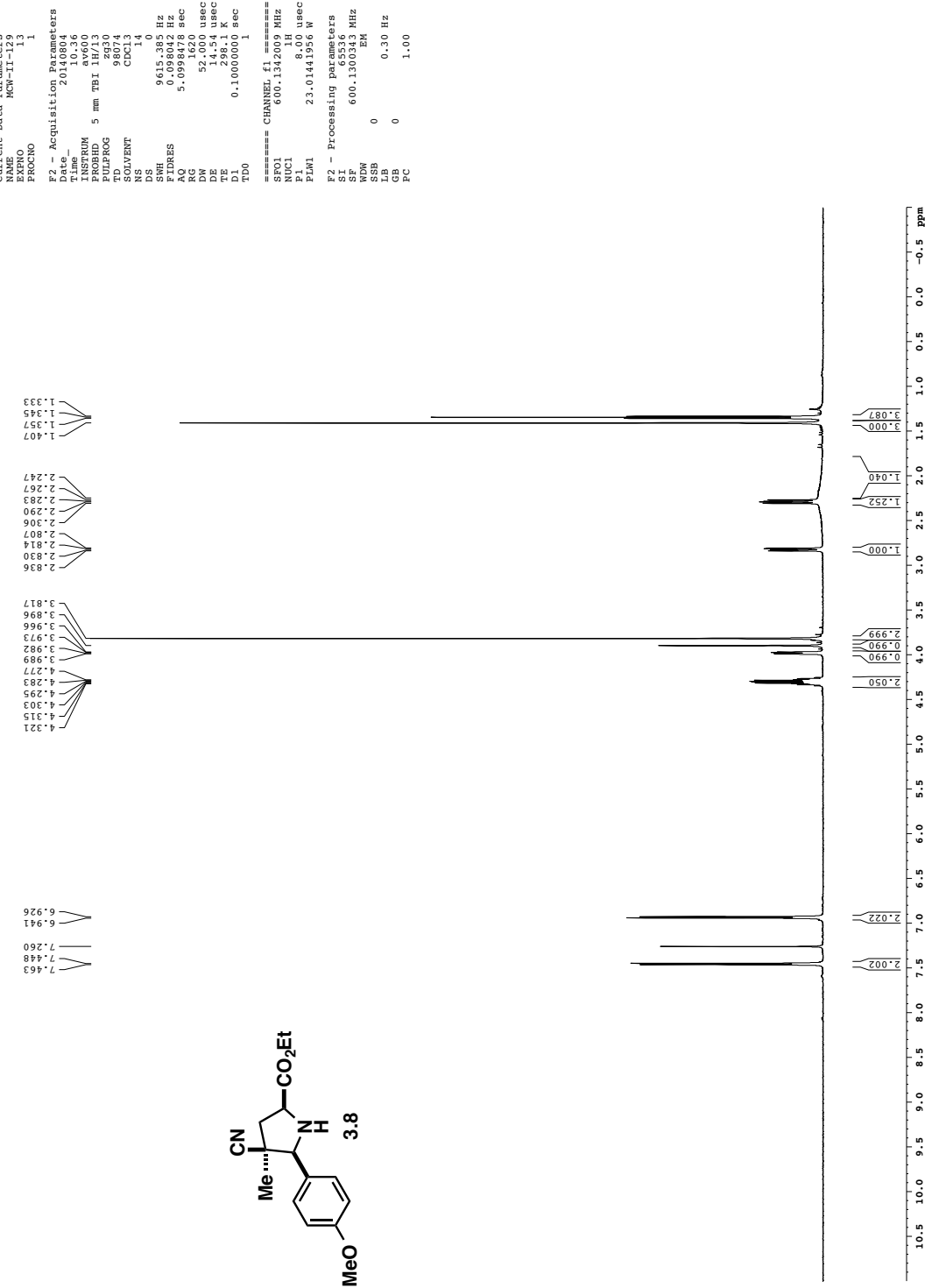
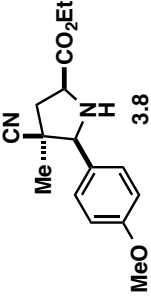


Purified Exo Product

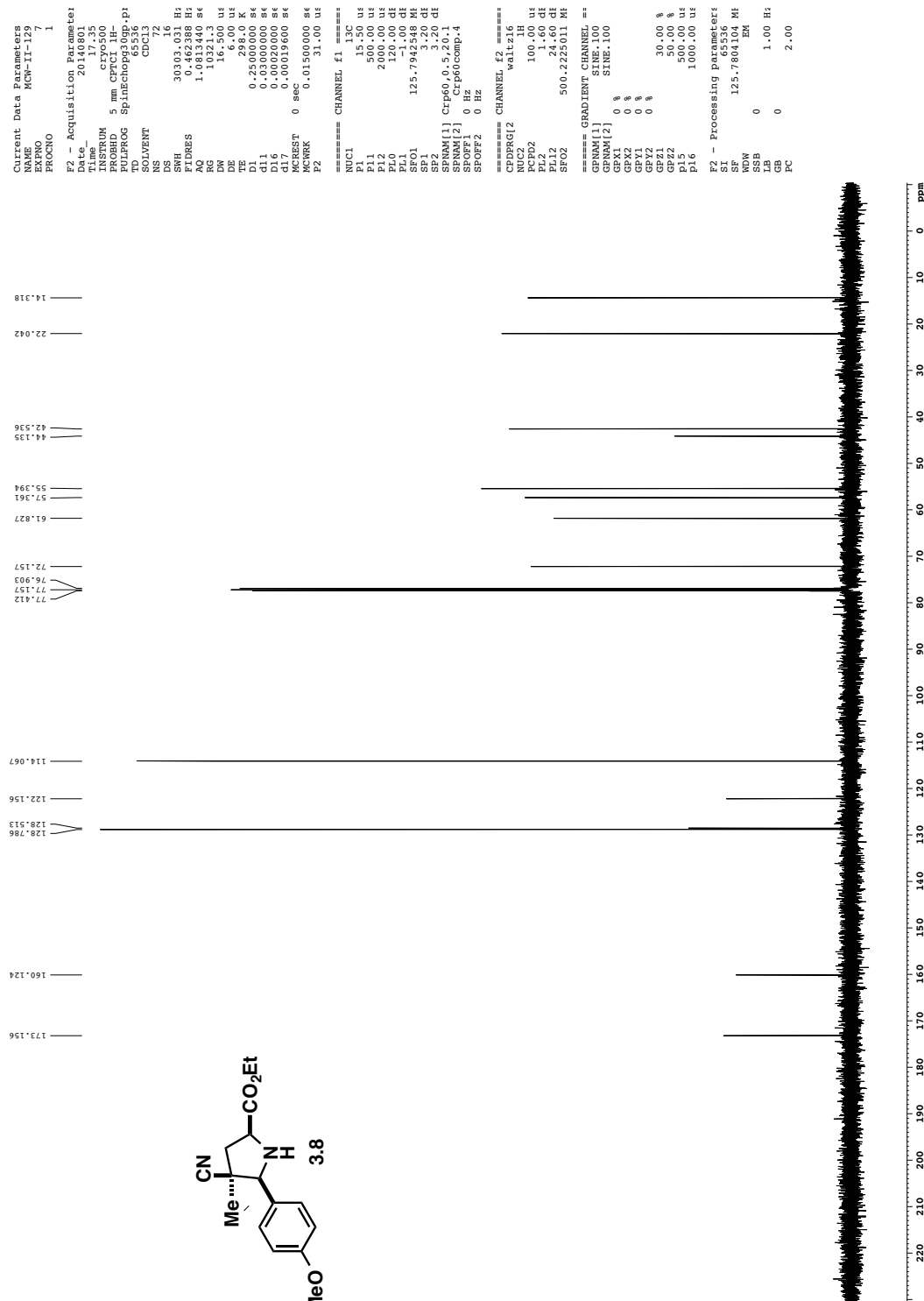
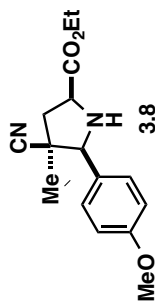


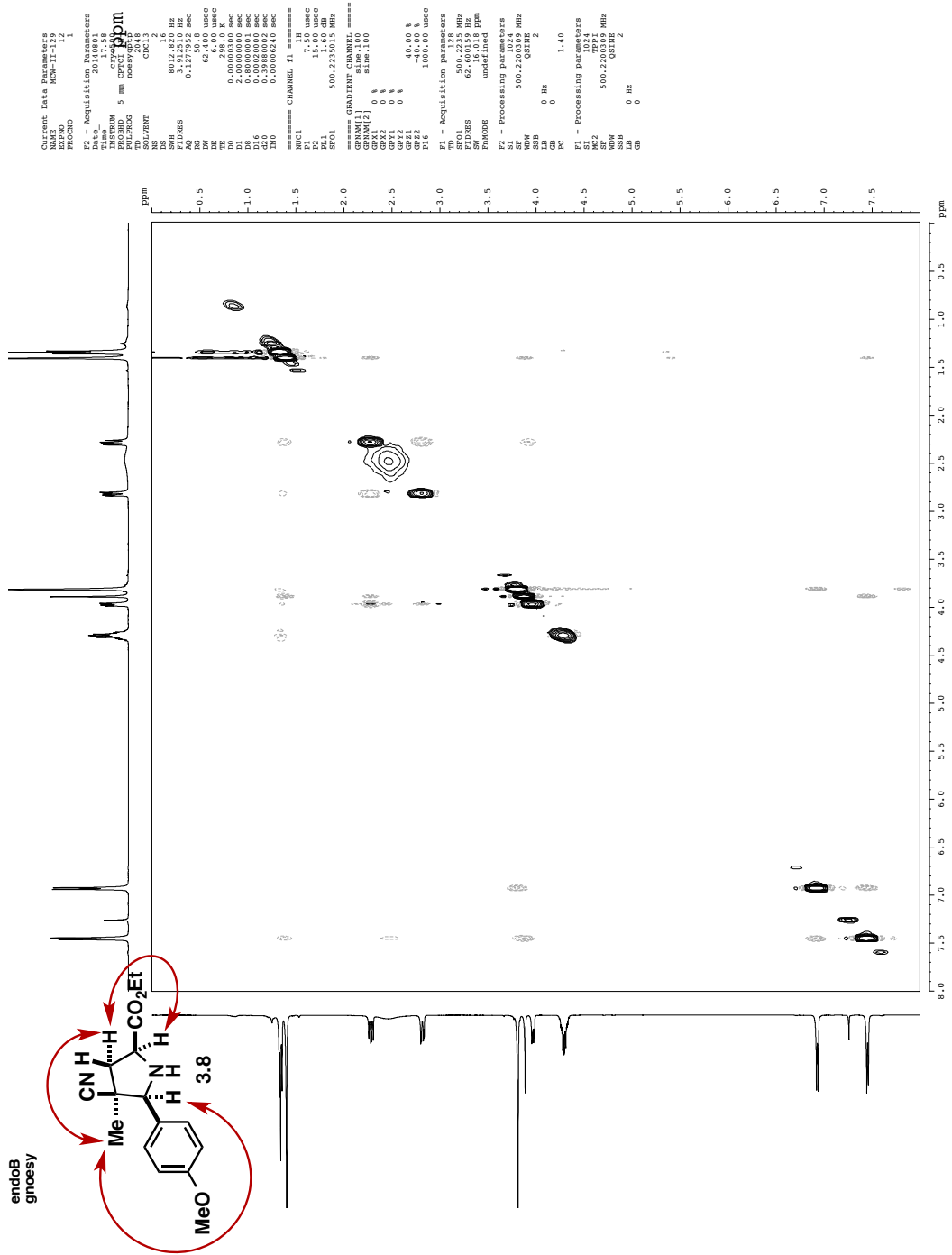


Purified Endo Adduct

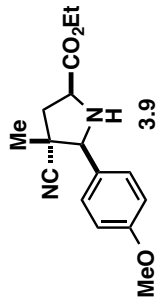


Purified Endo Adduct

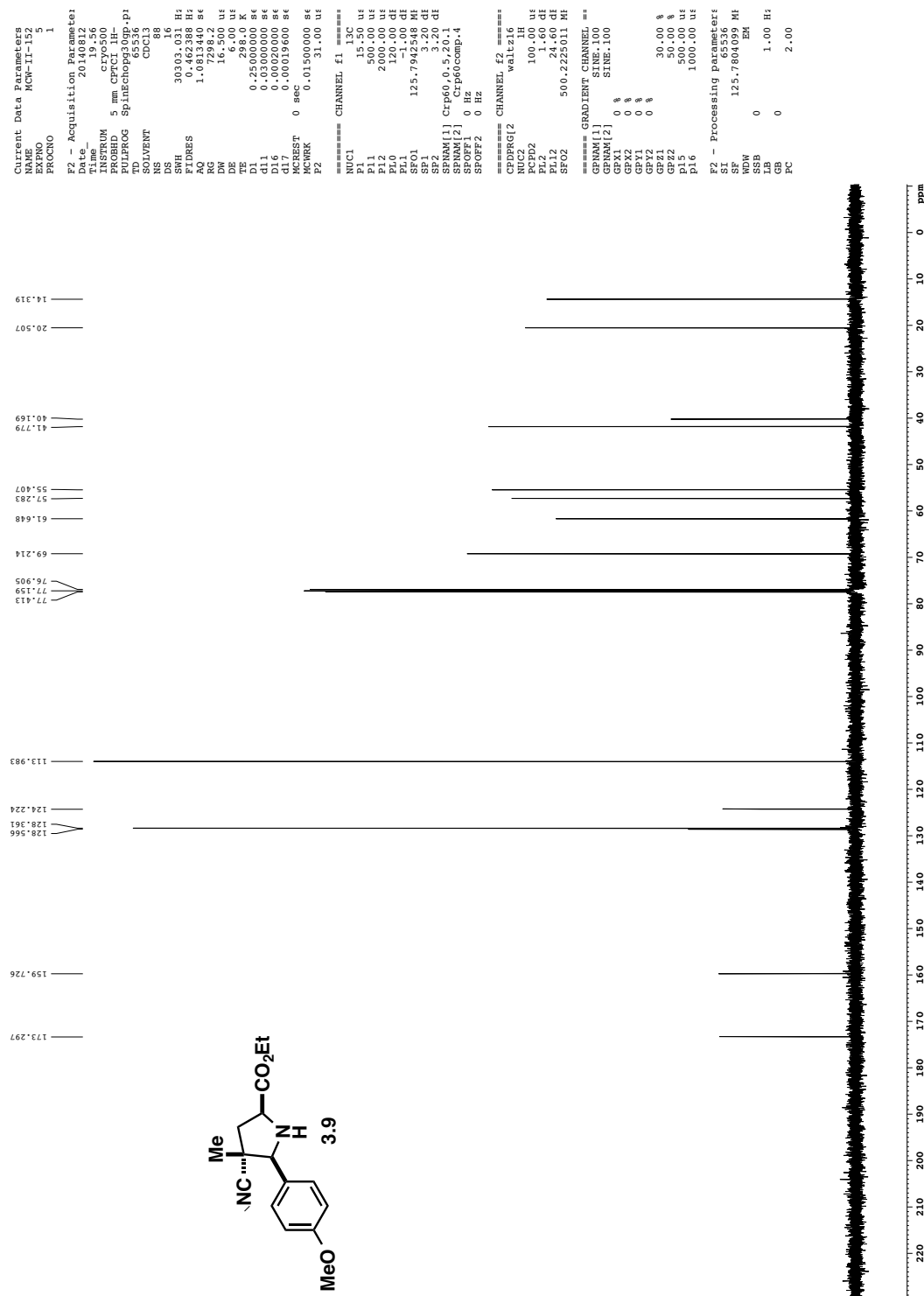
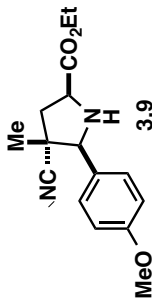


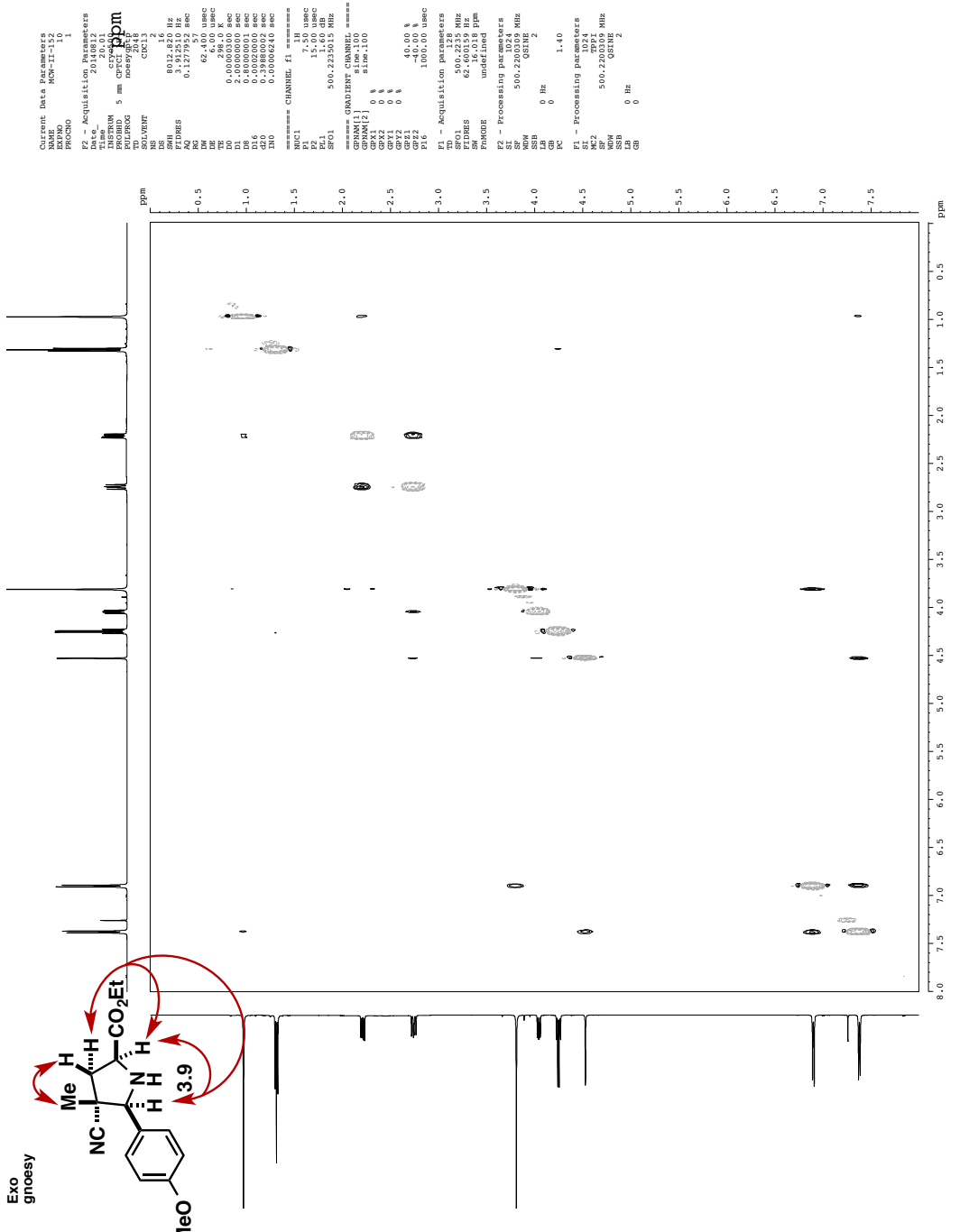


Purified Exo Adduct

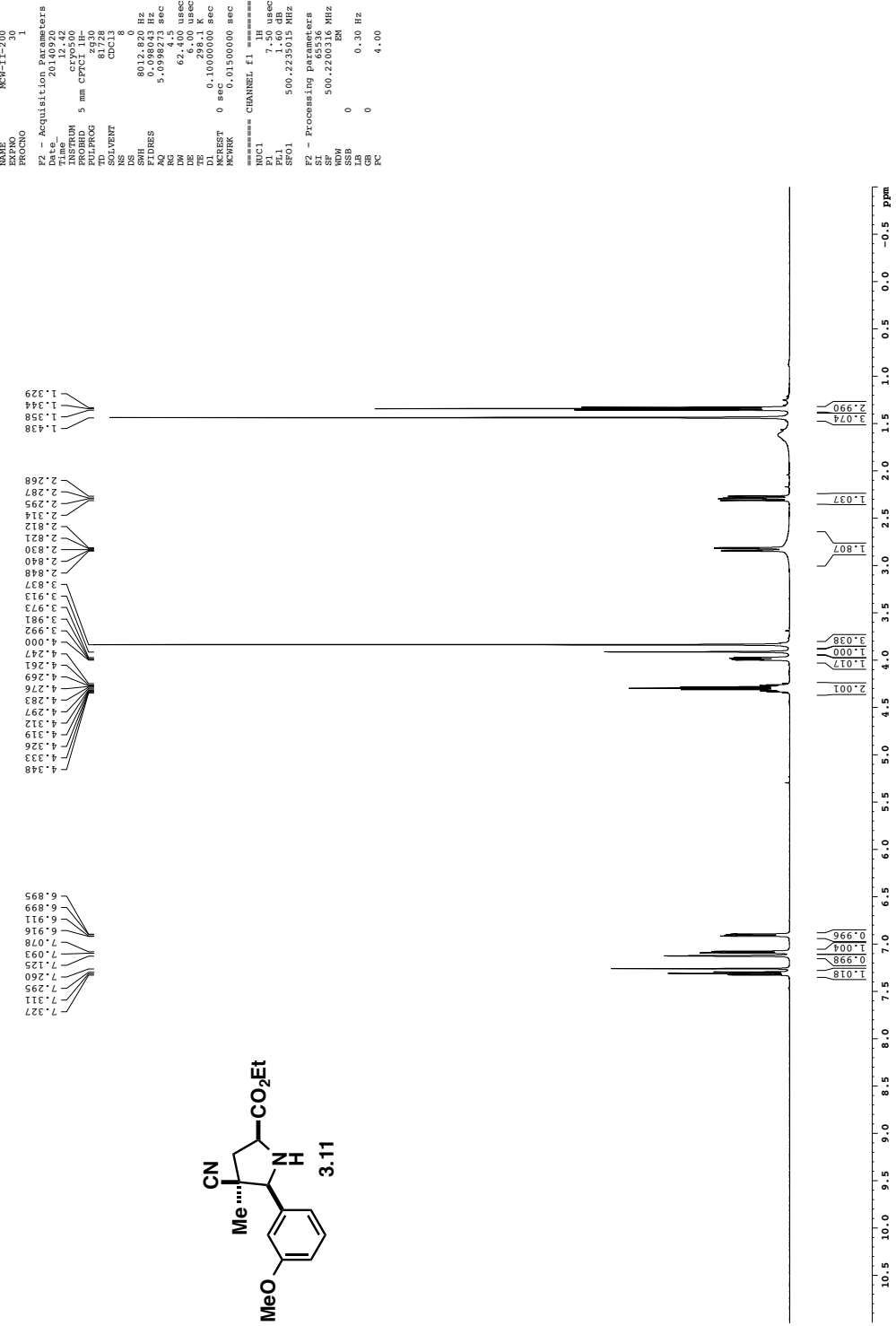
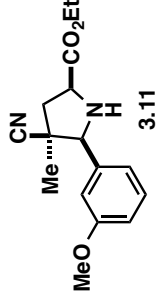


Purified Exo Adduct

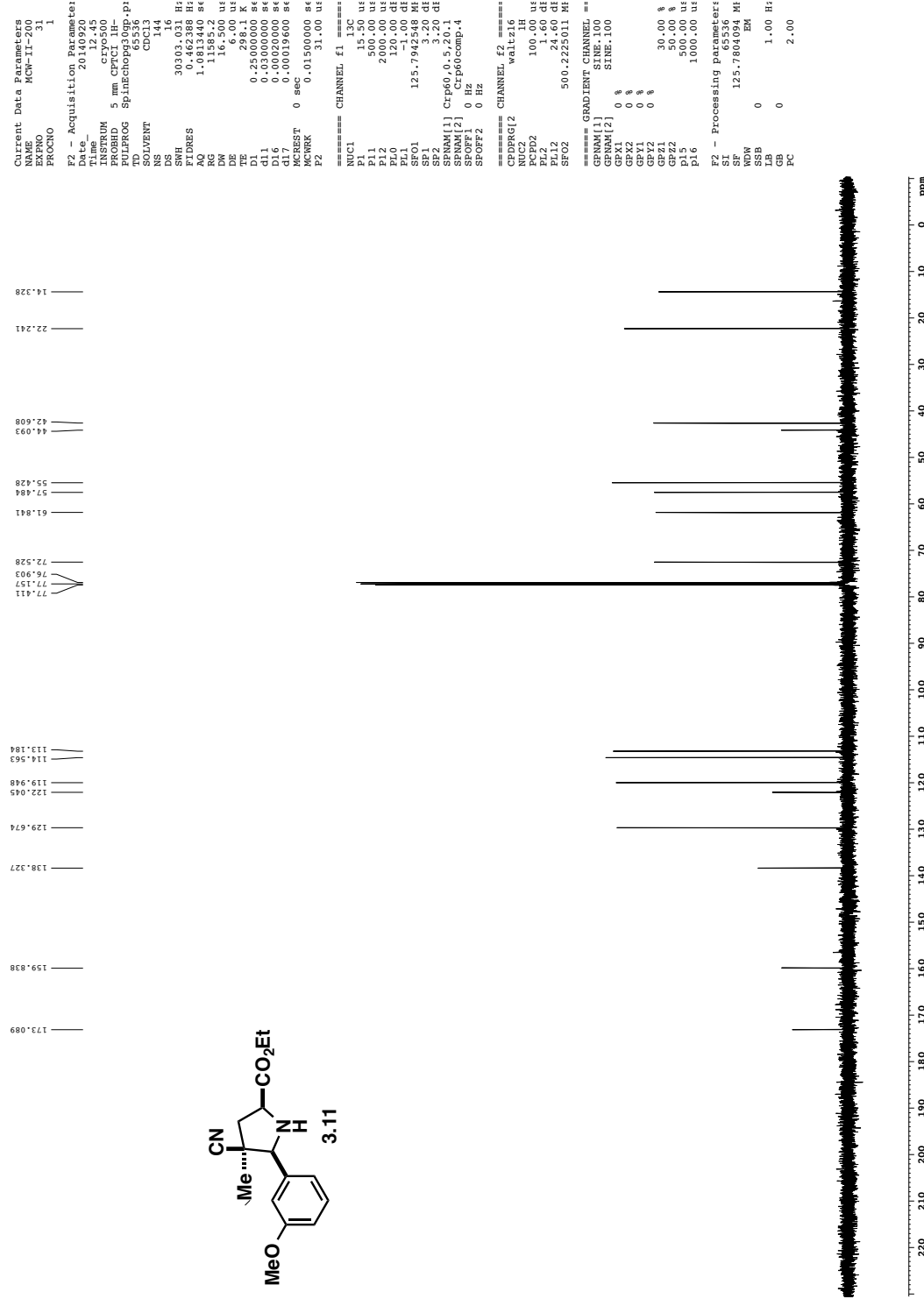
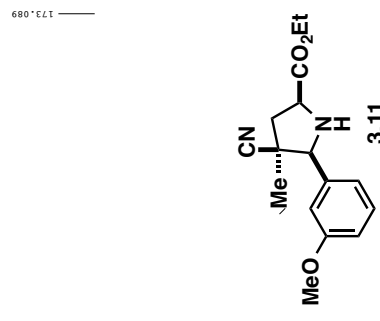


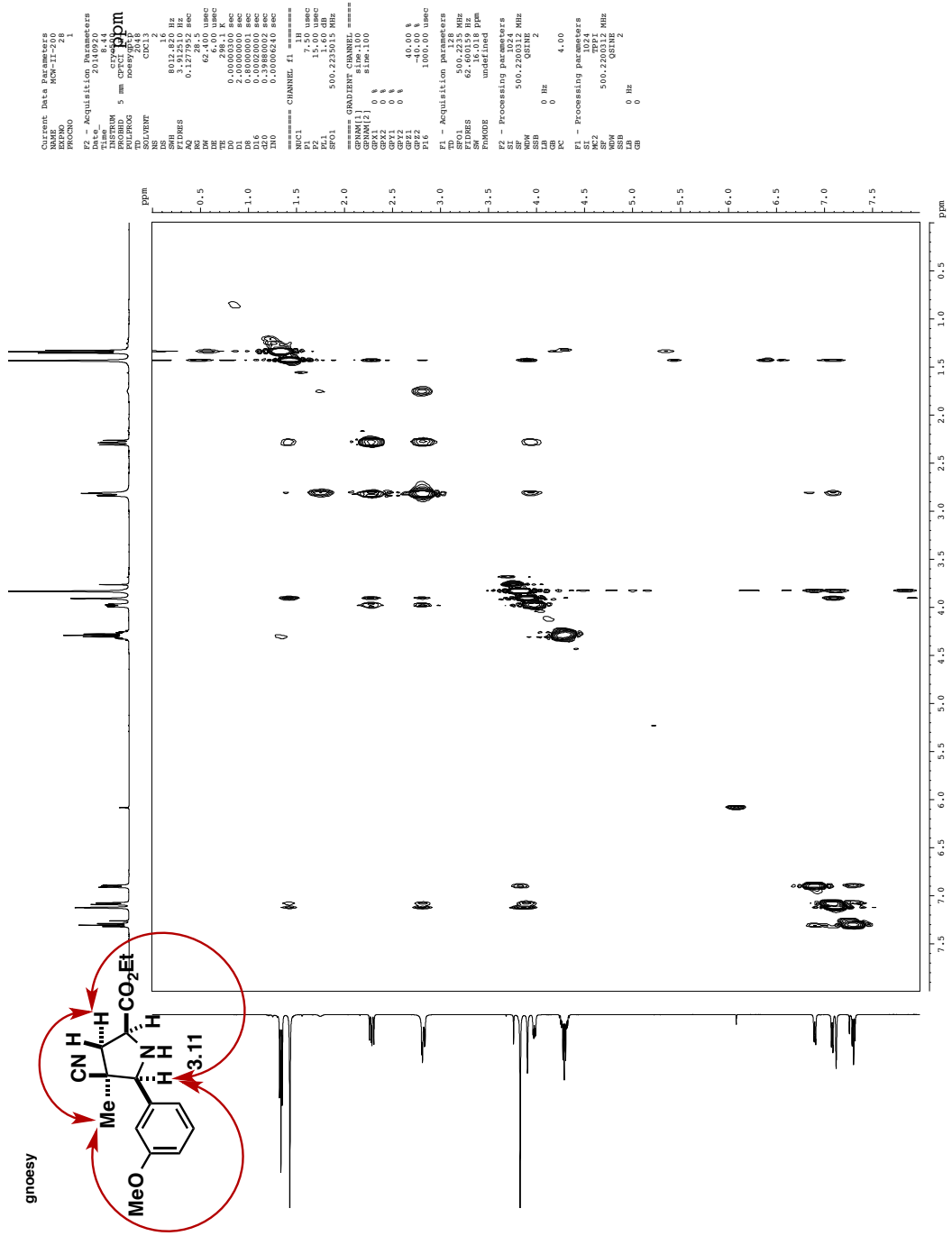


200B endo

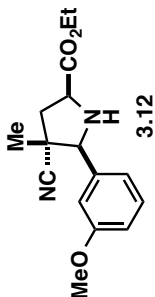
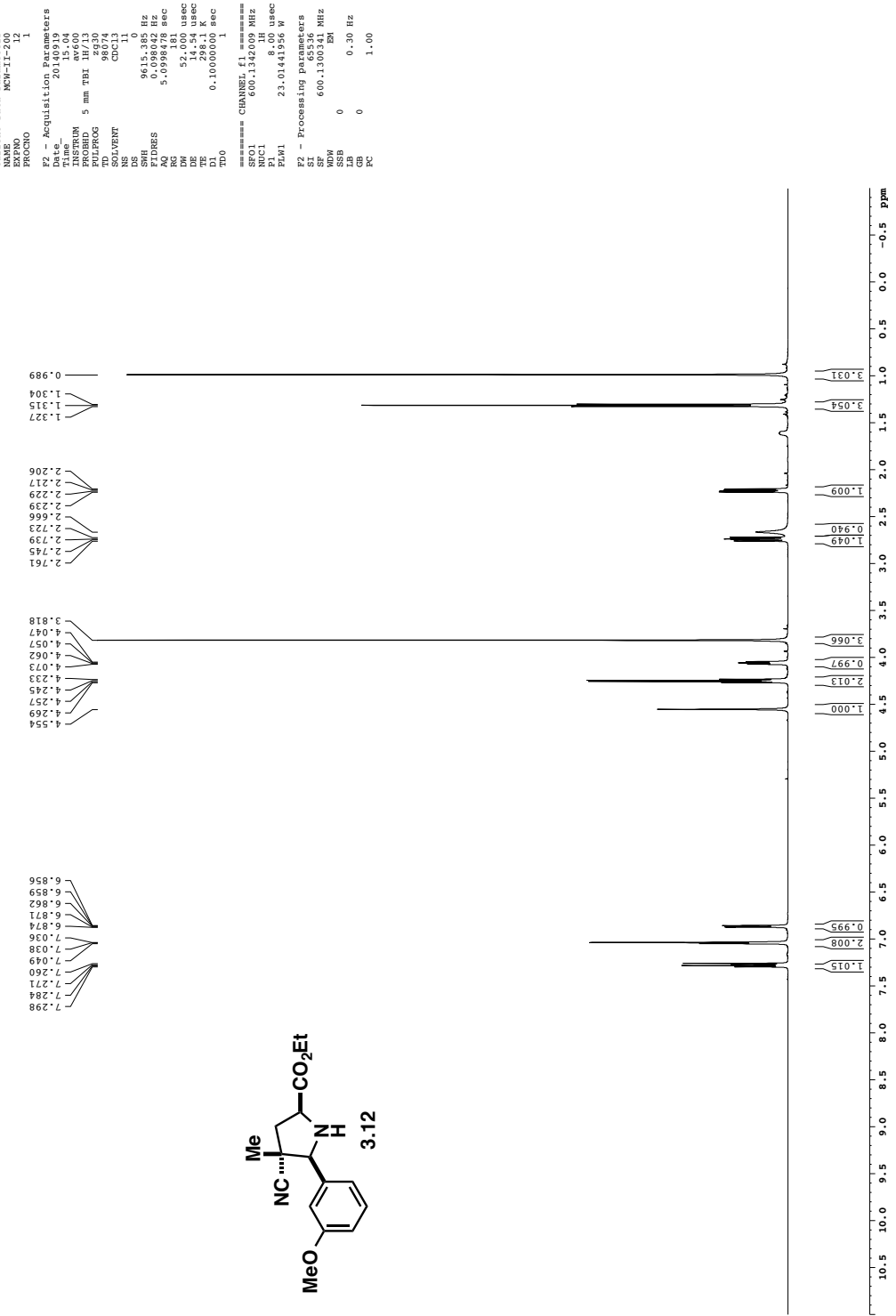


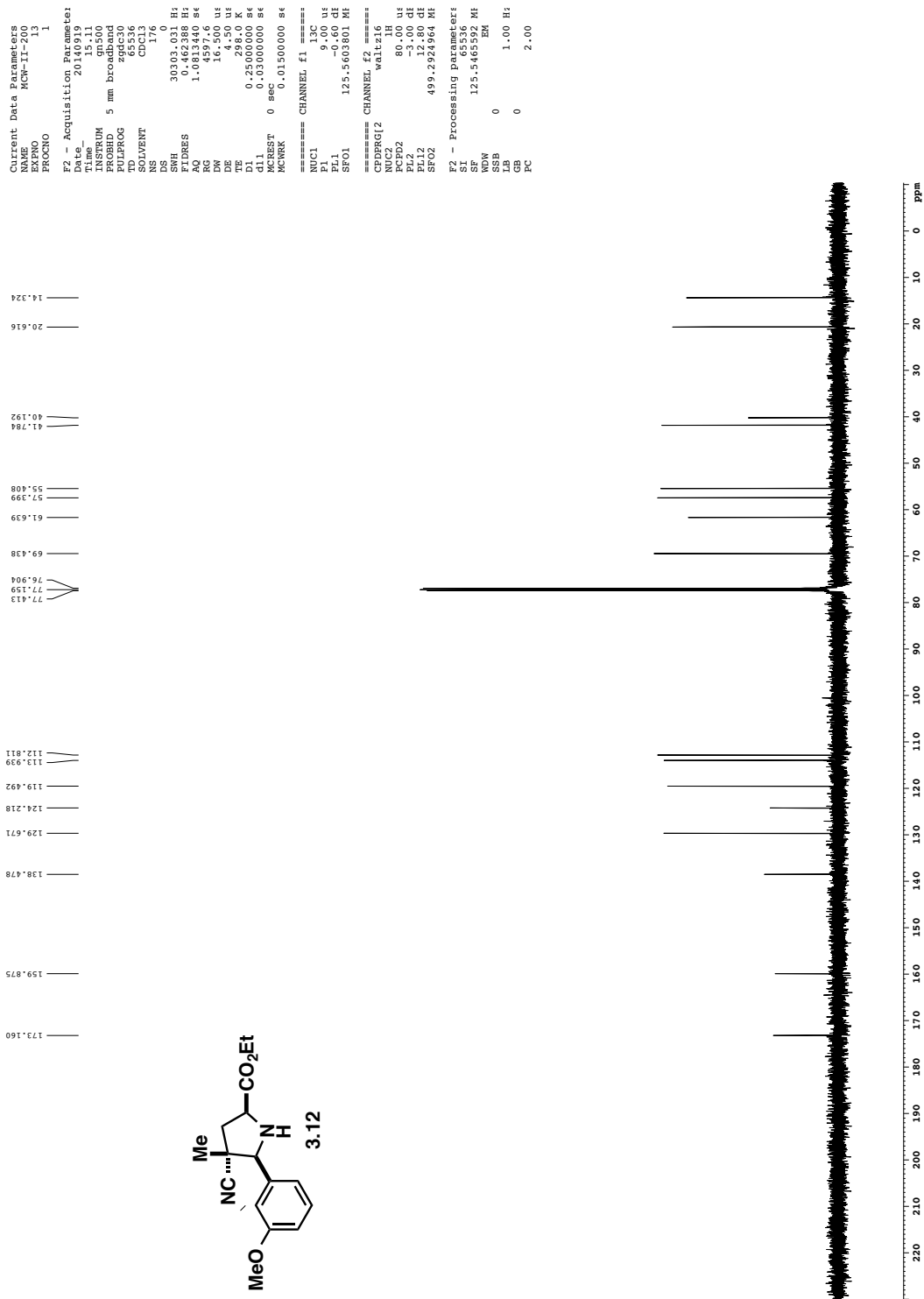
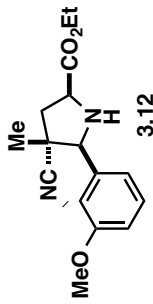
200s endo

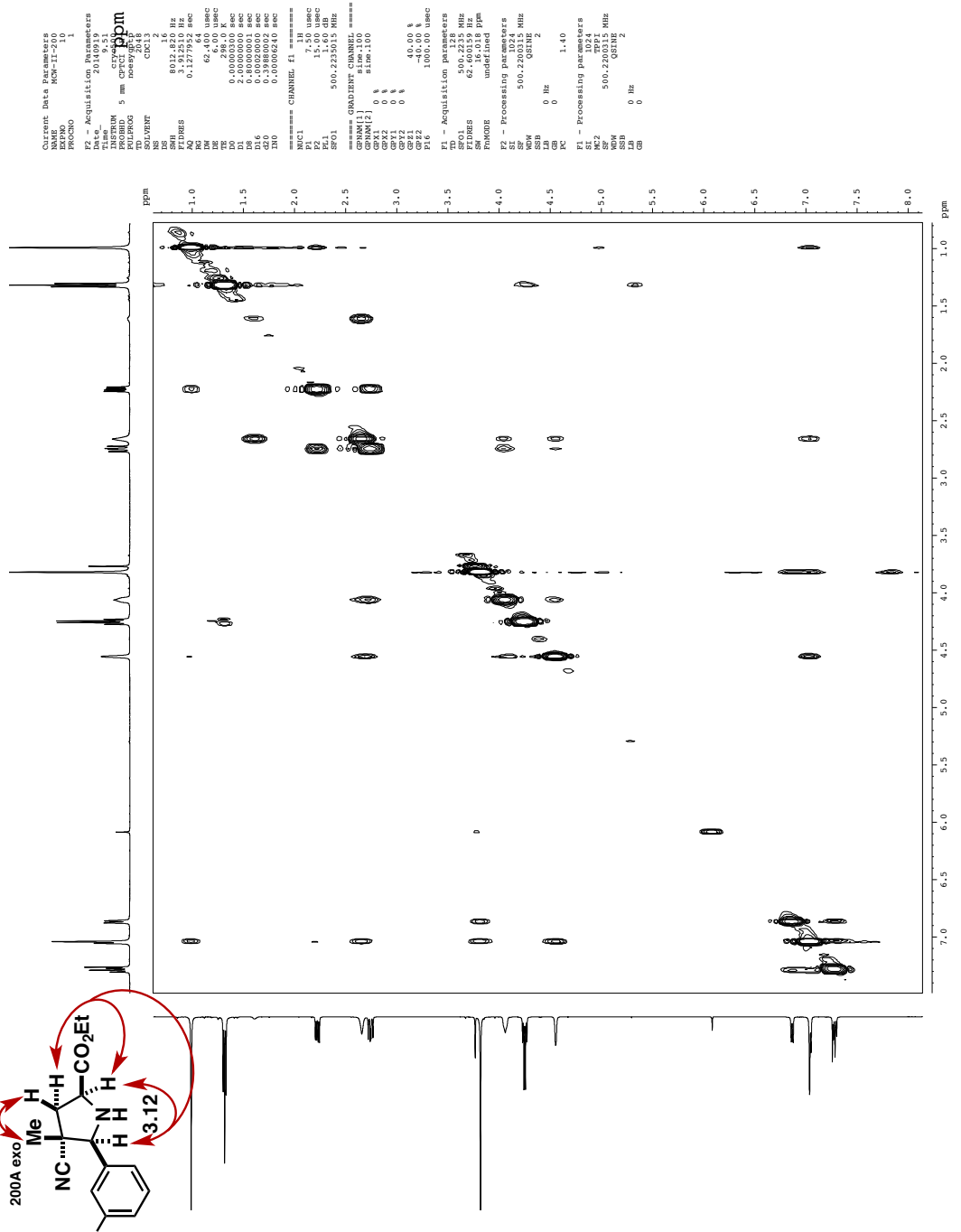




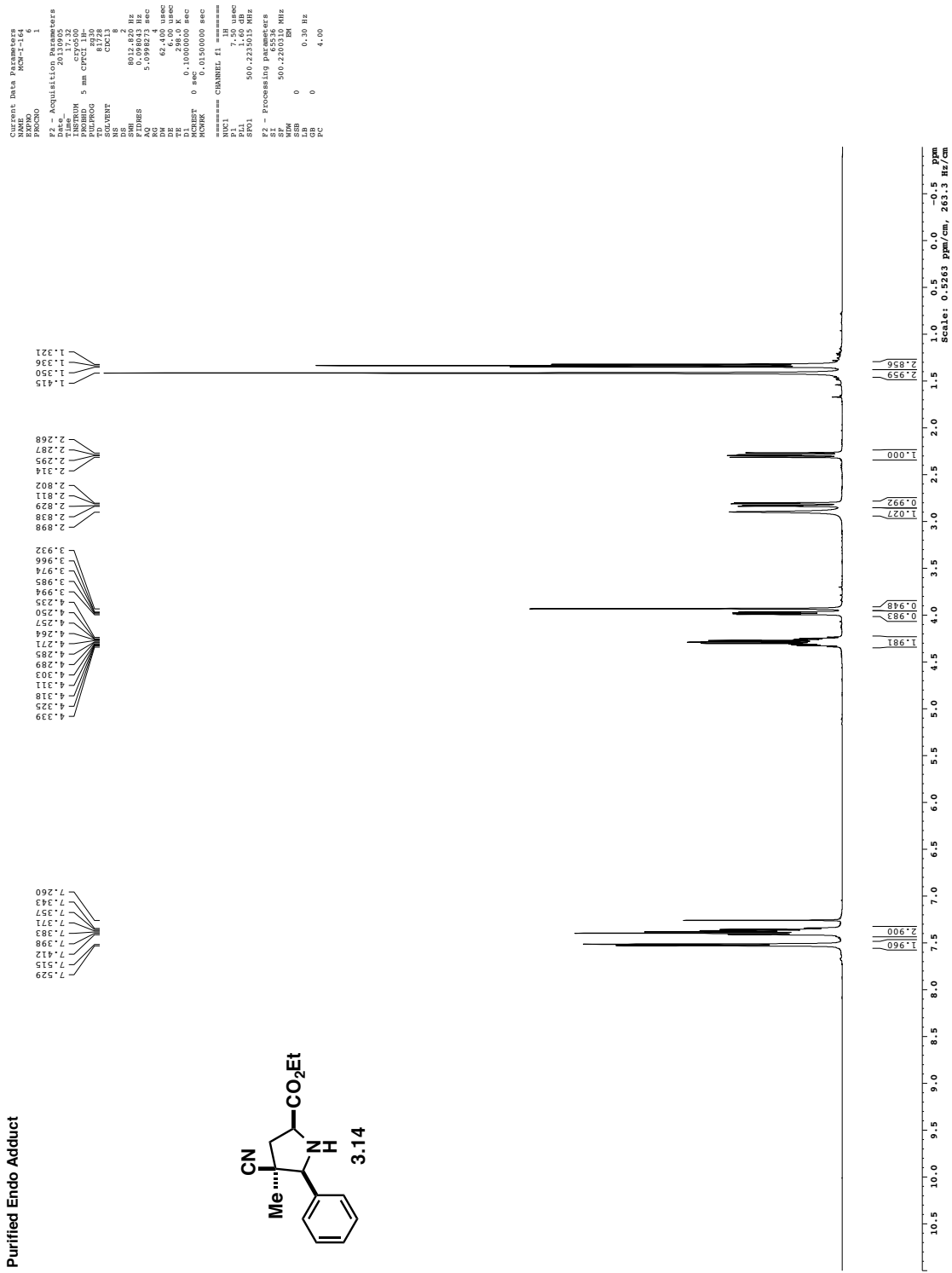
200A exo fr 34-39

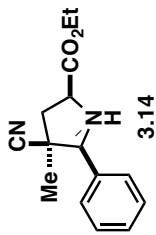




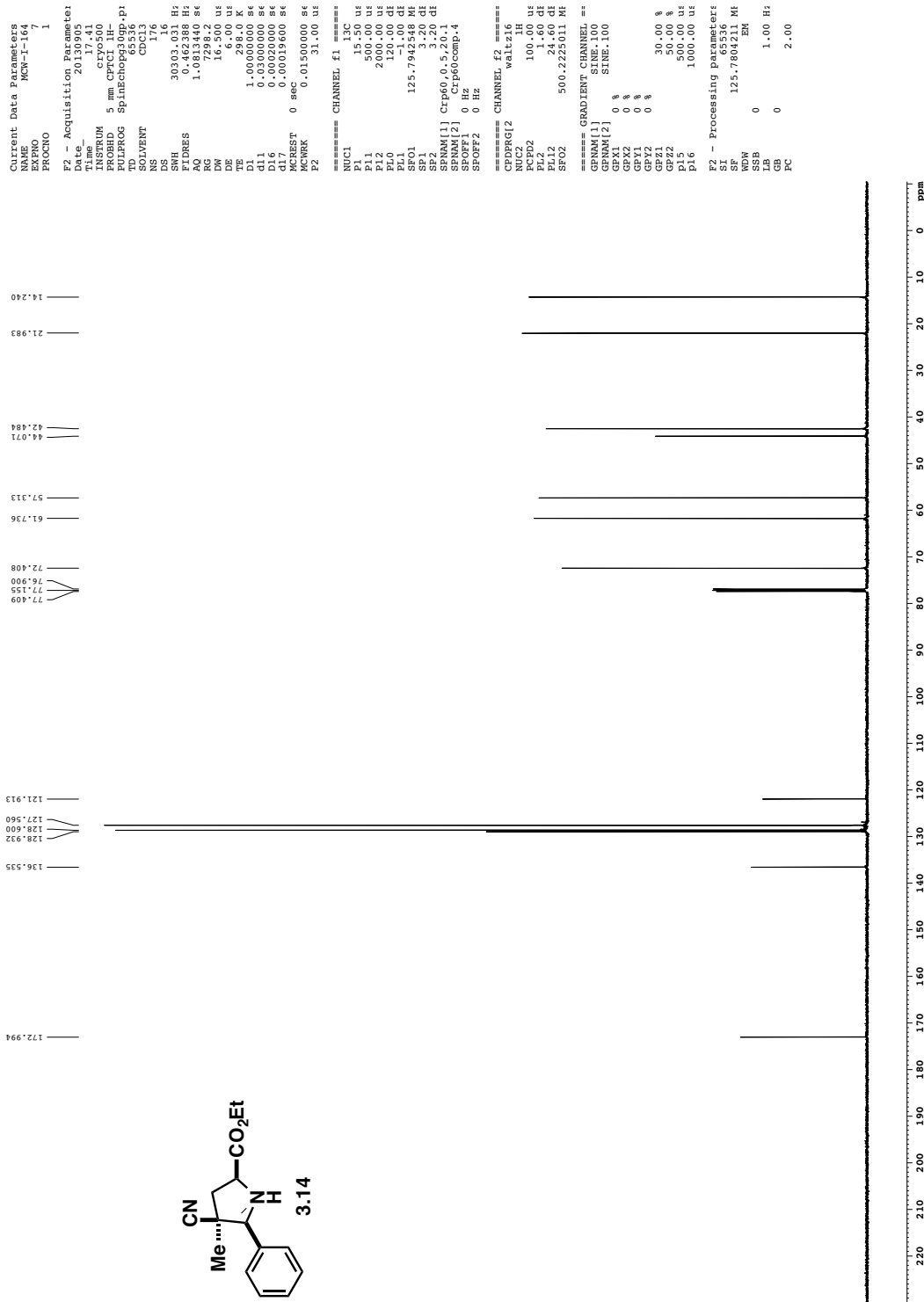


Purified Endo Adduct

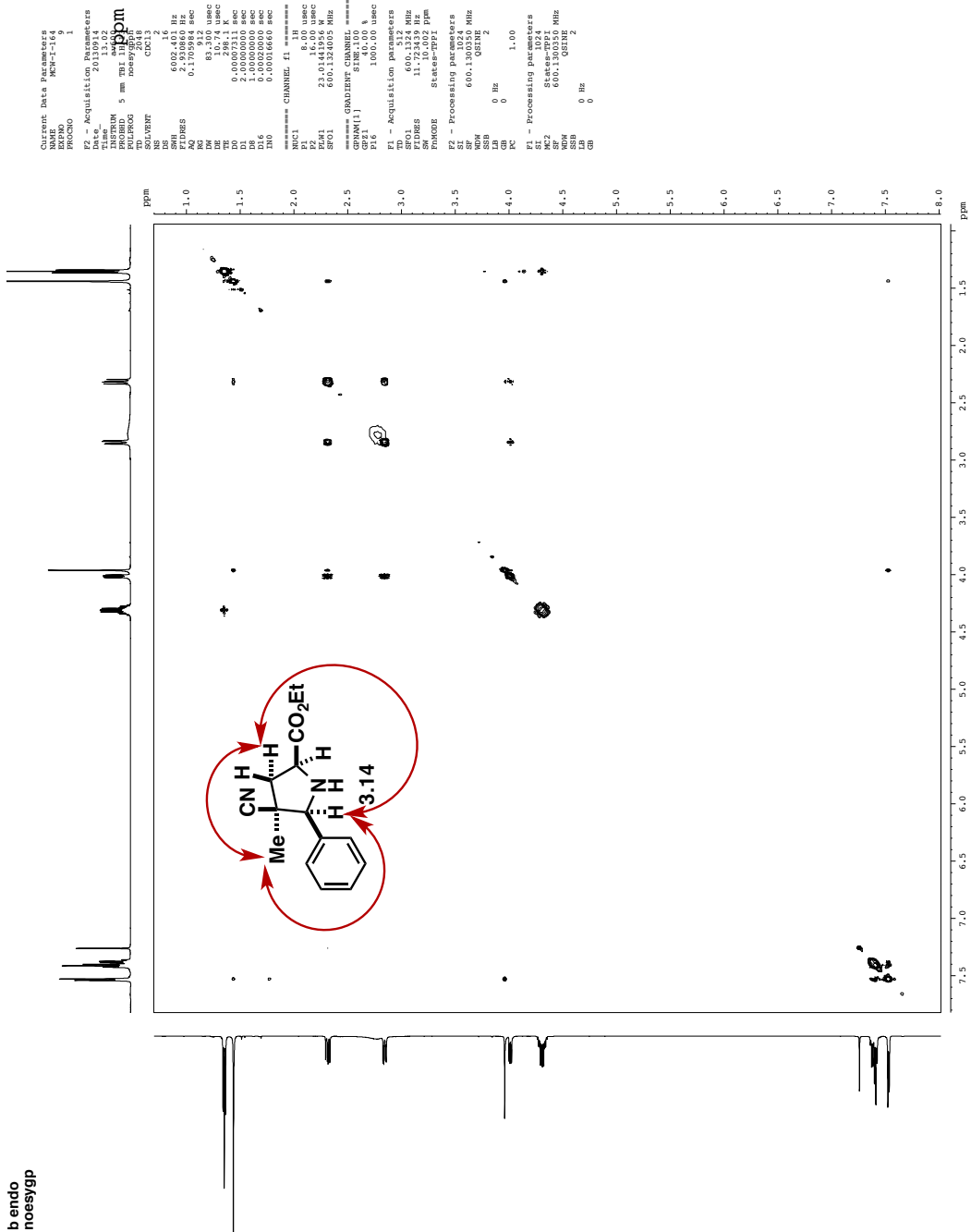




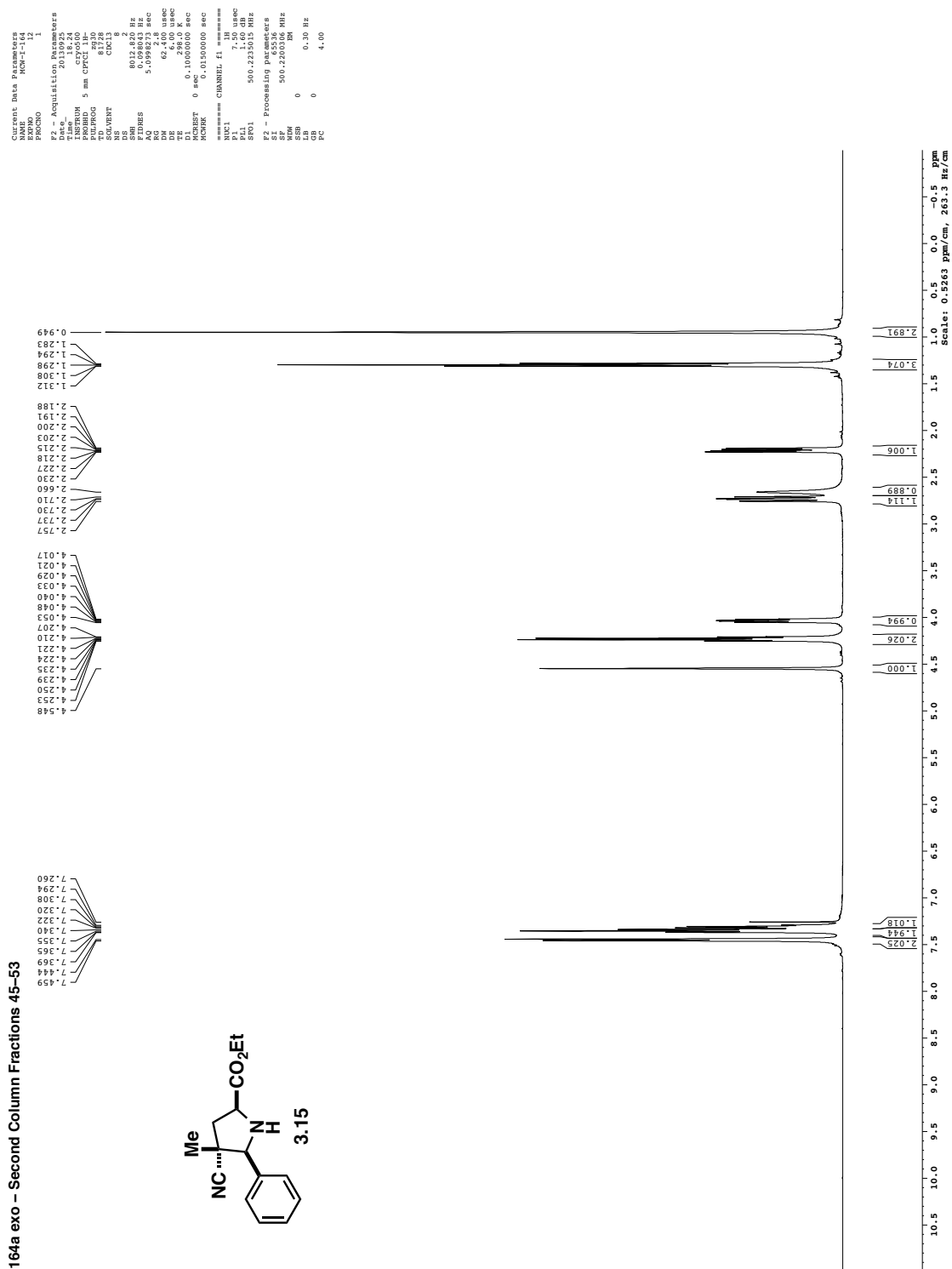
Purified Endo Adduct

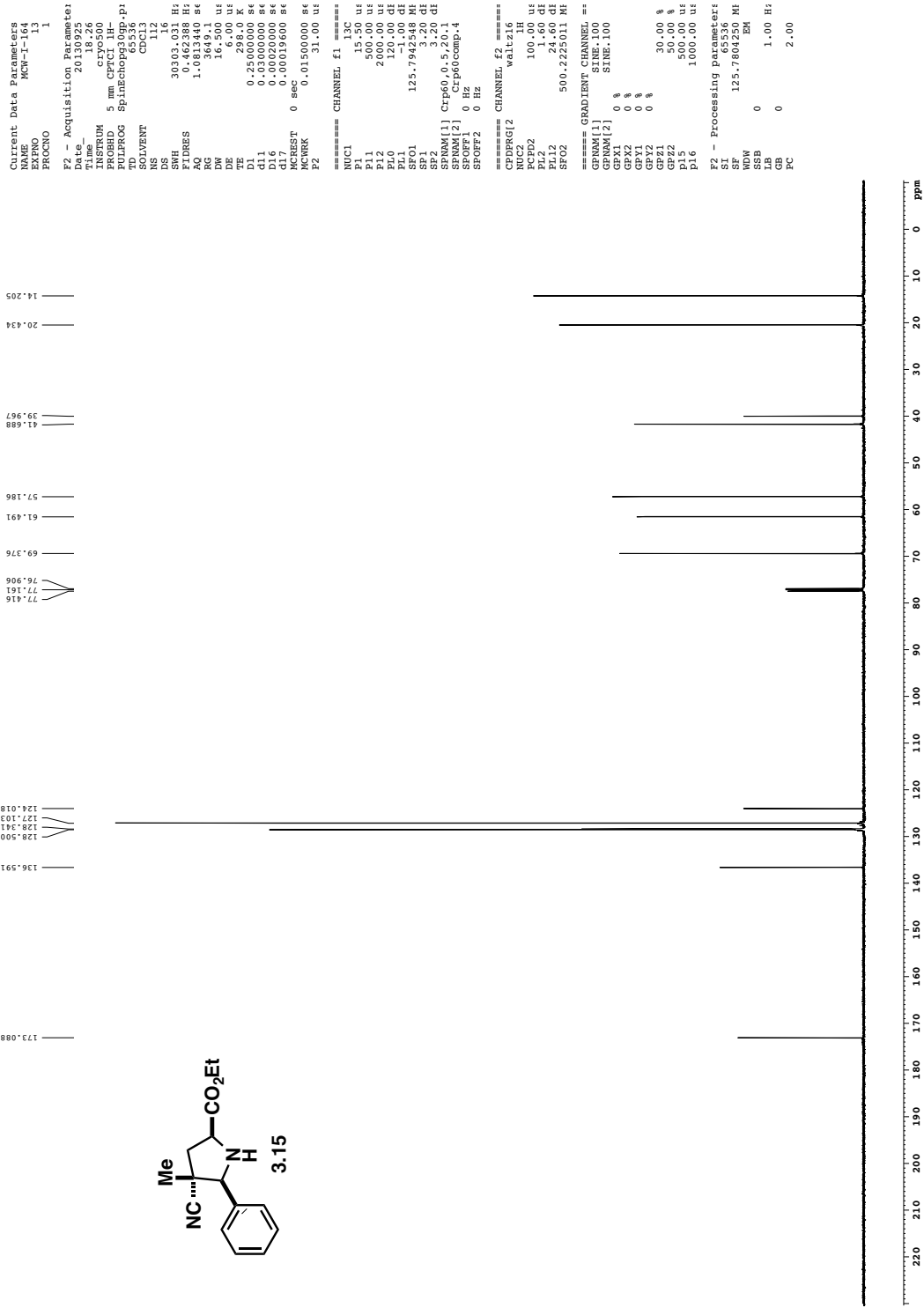


**b endo
noesygp**

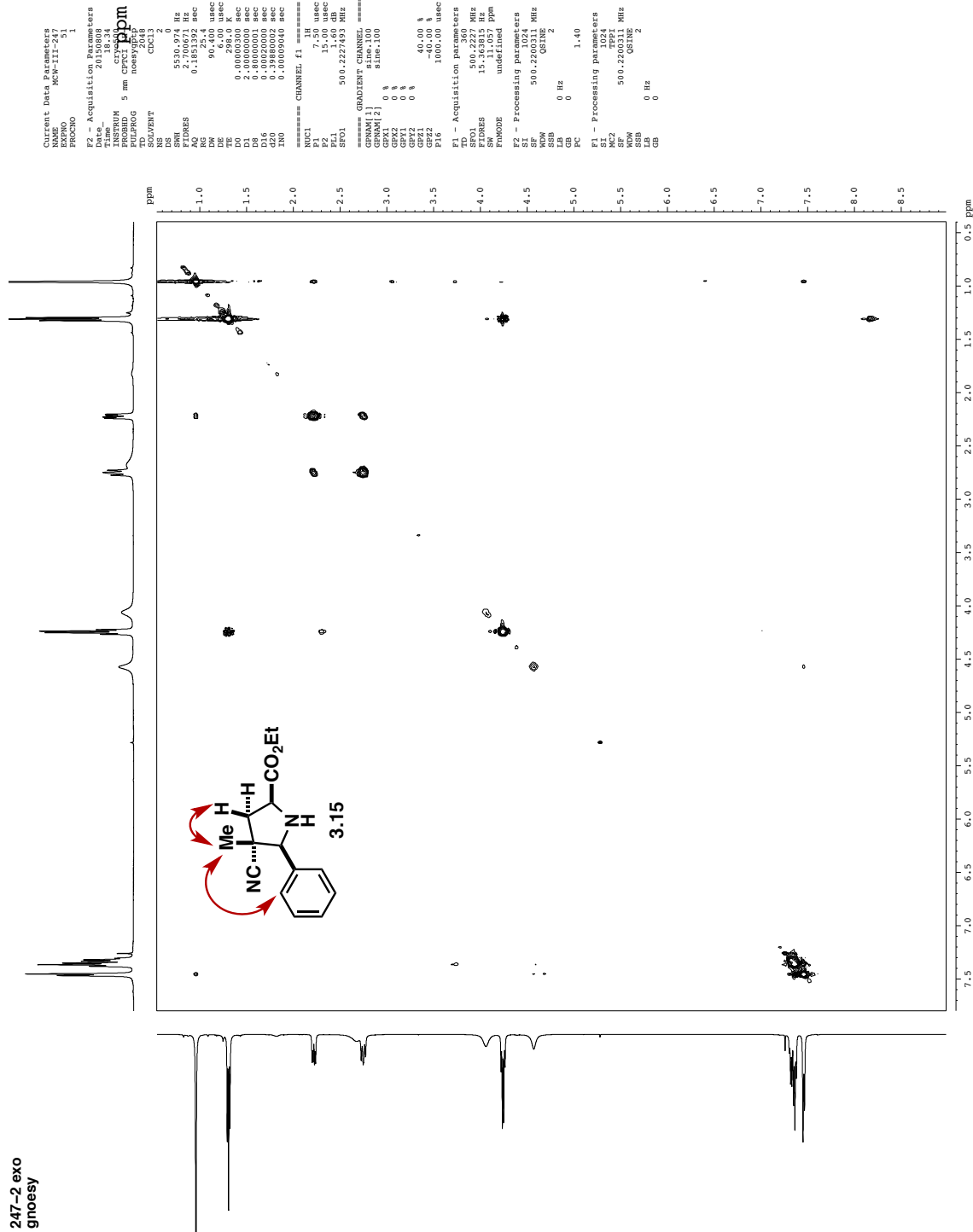


164a exo - Second Column Fractions 45-53

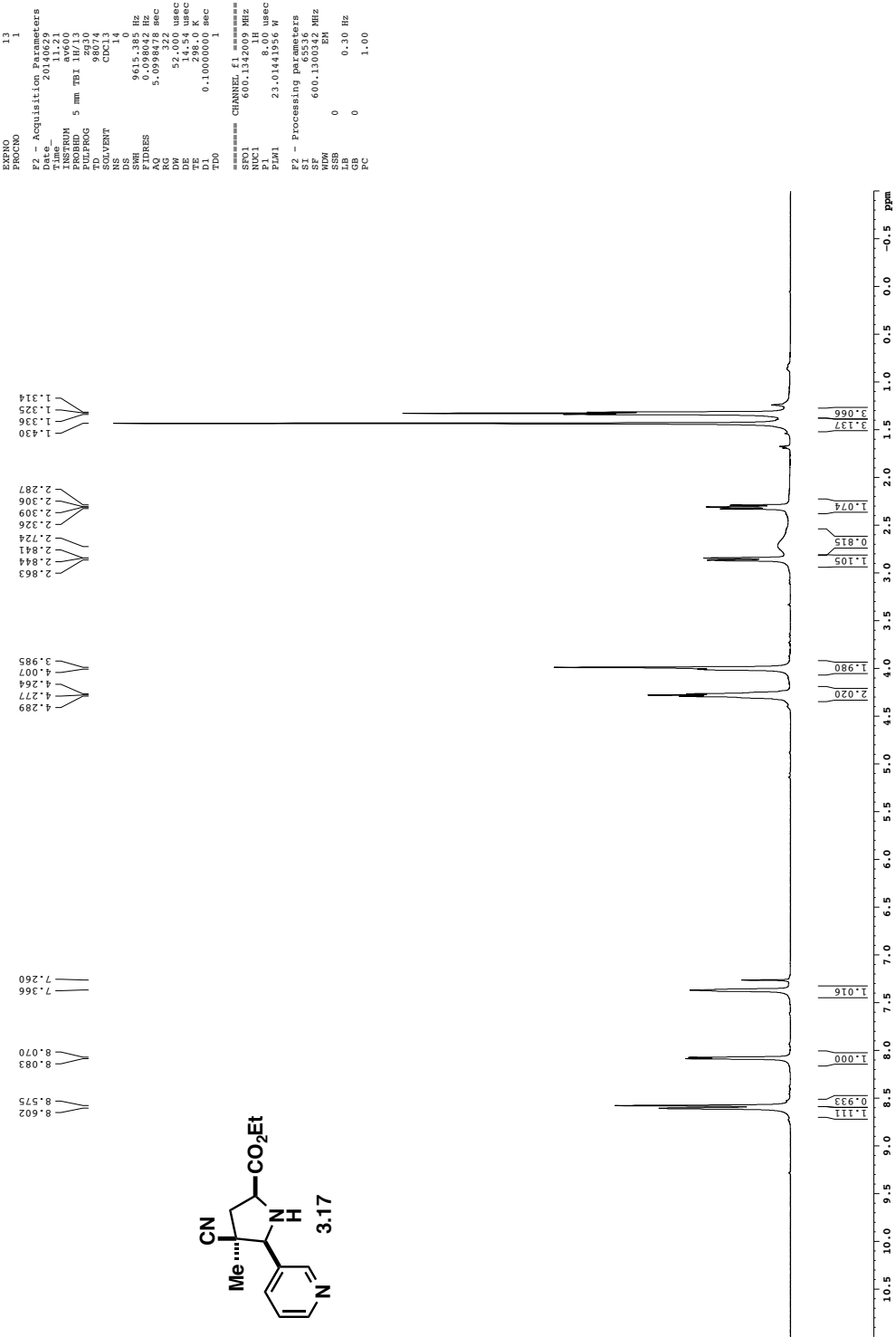
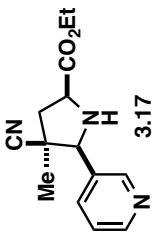




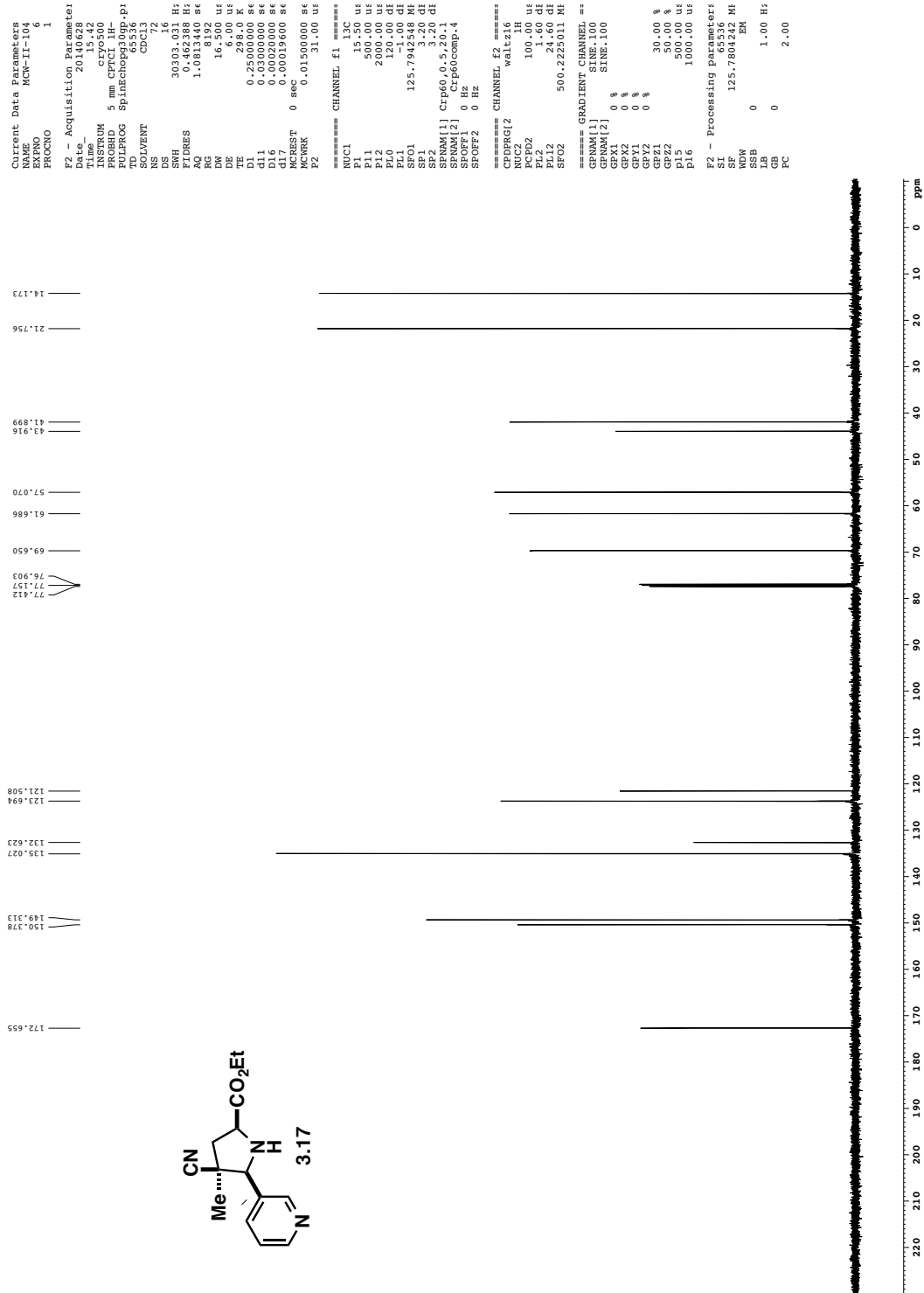
247-2 exo
gnoesy



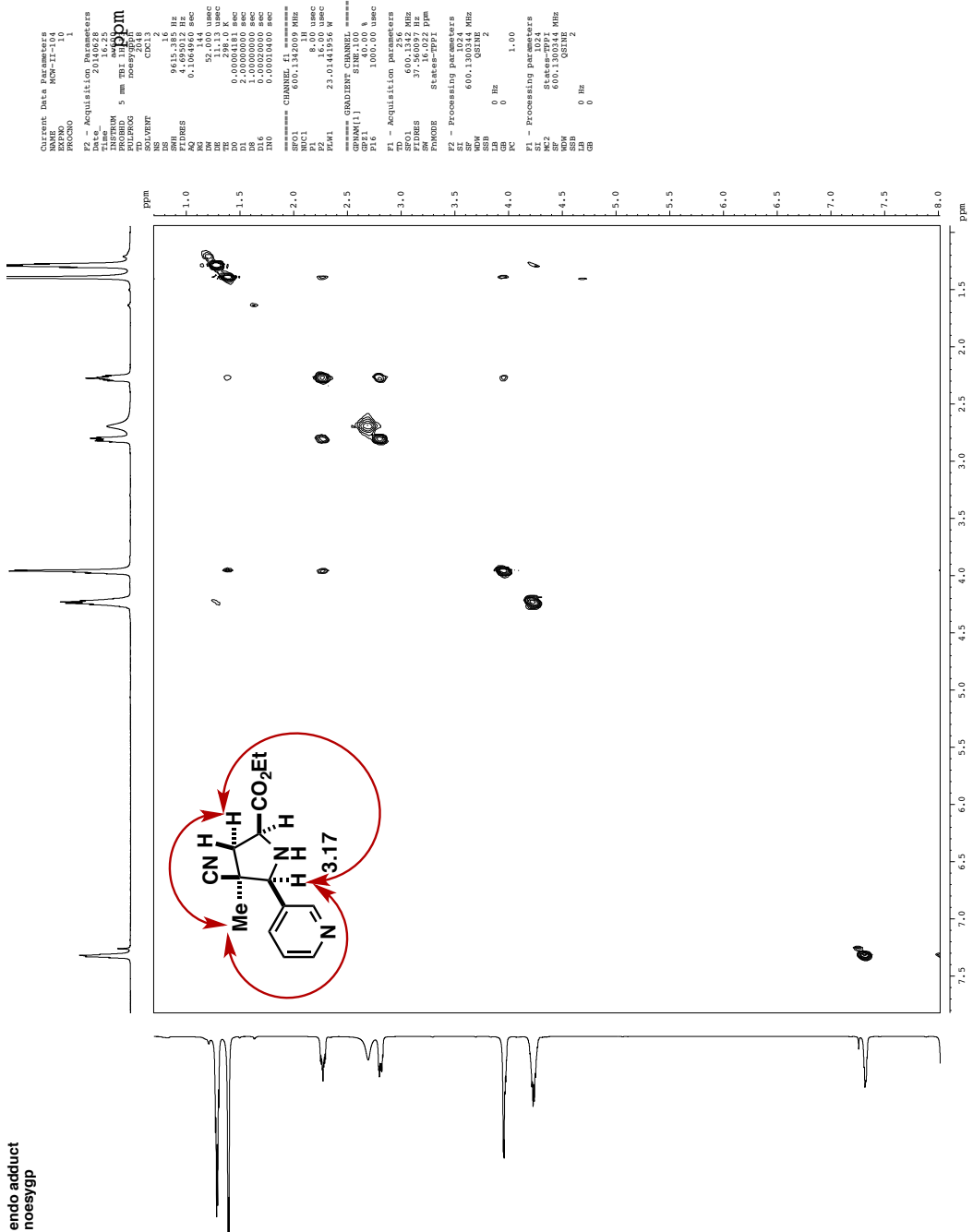
104B endo



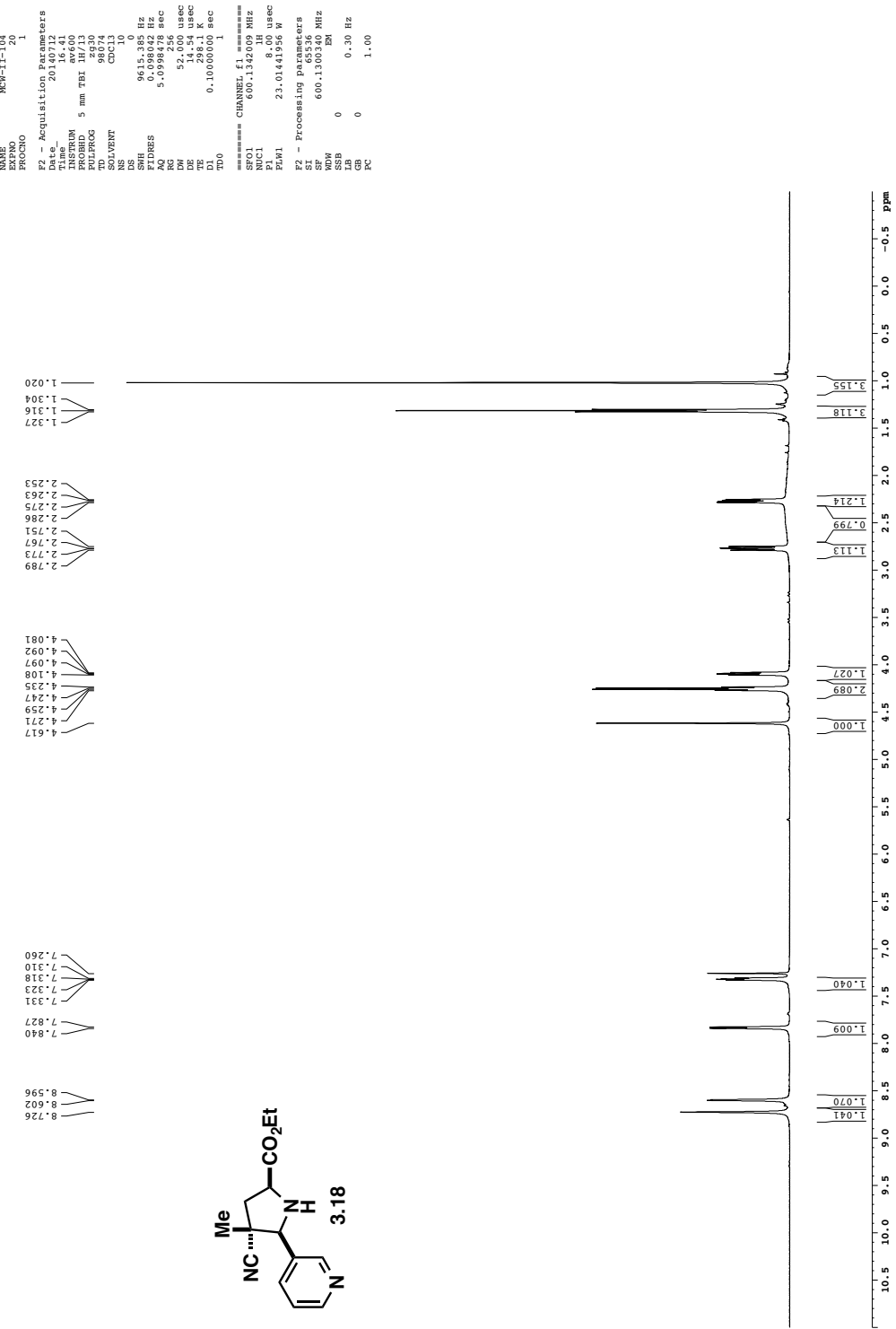
Endo Adduct

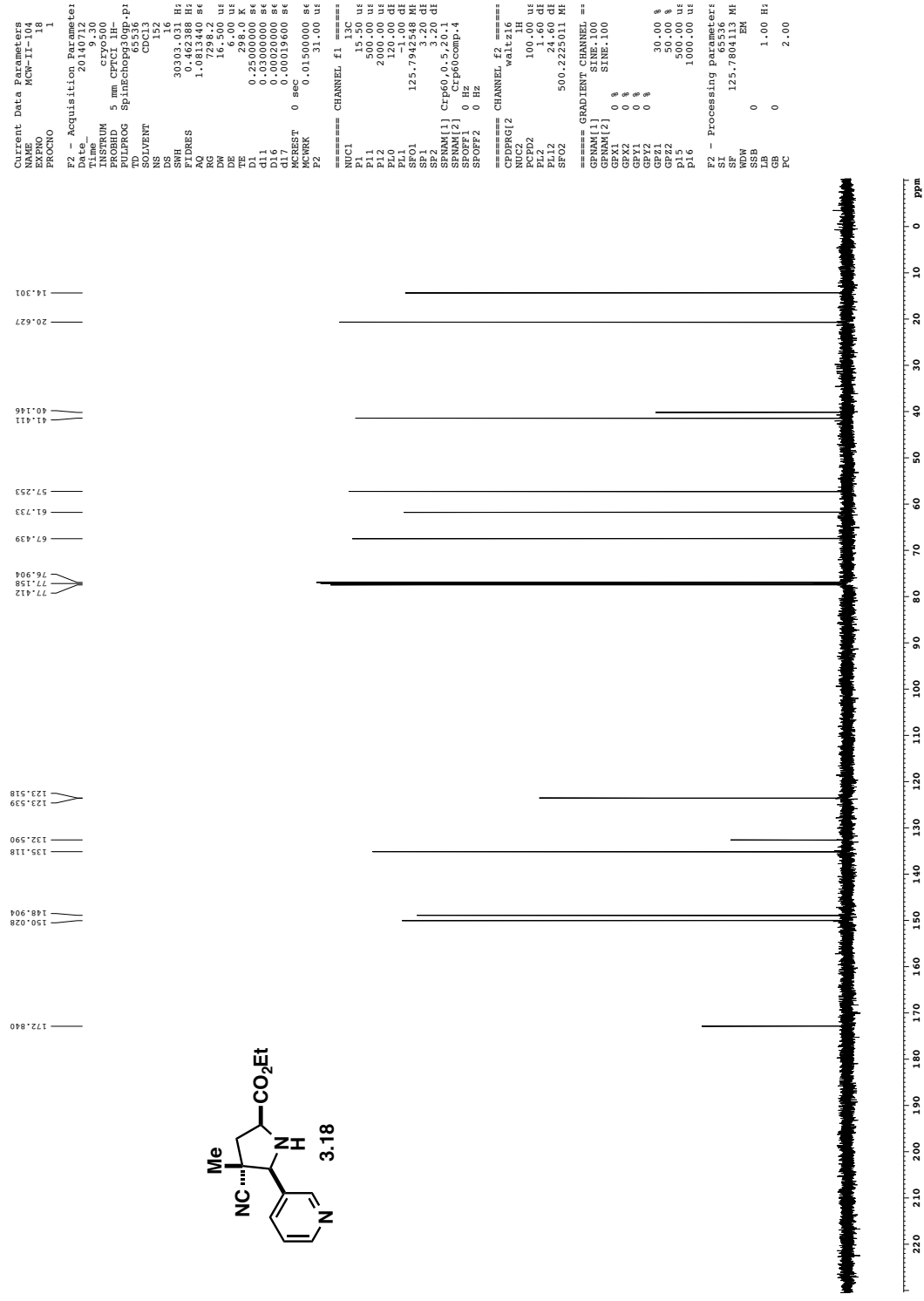


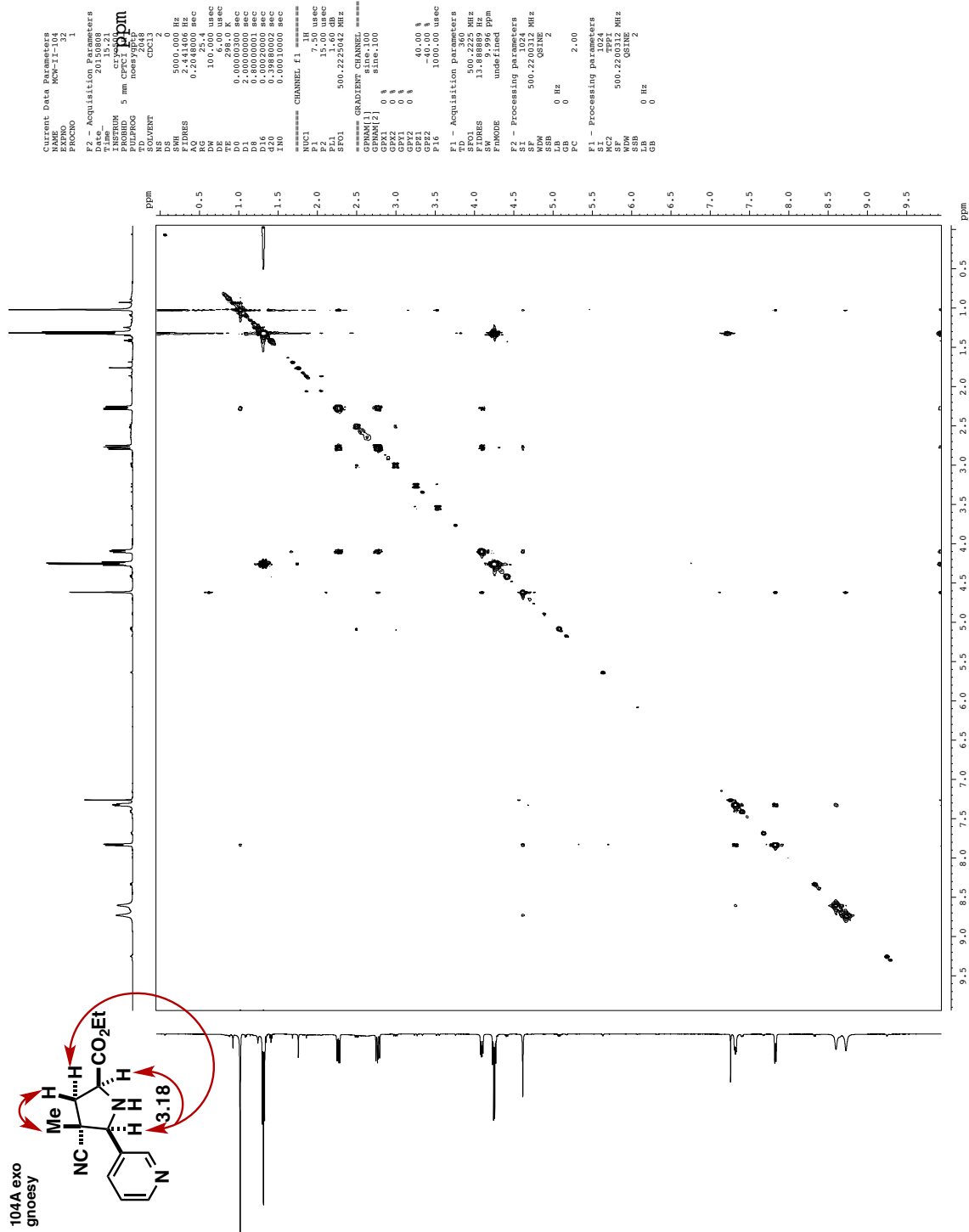
endo adduct
noesygpp



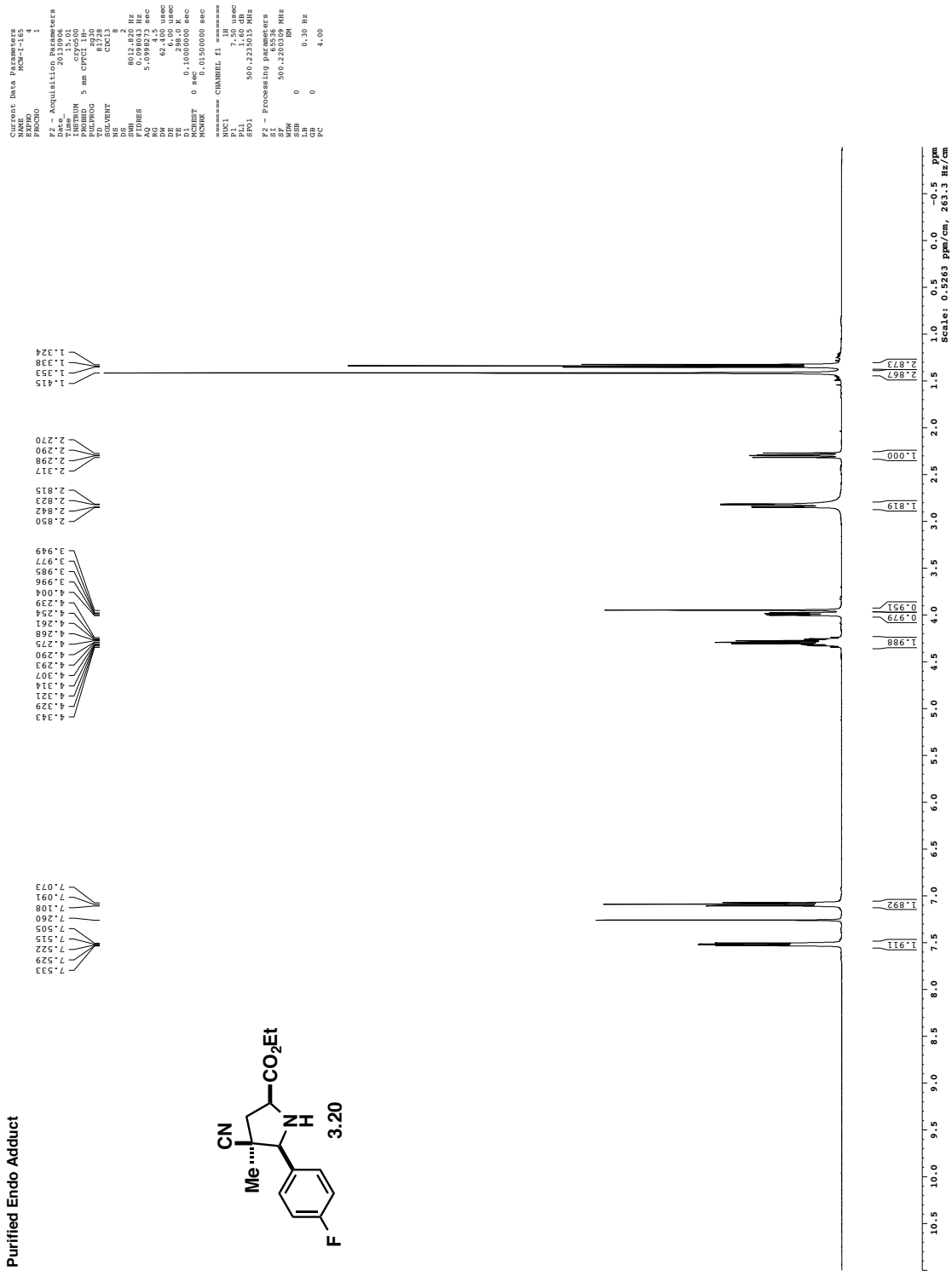
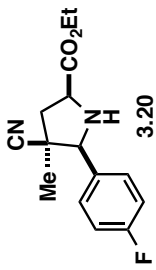
104A exo



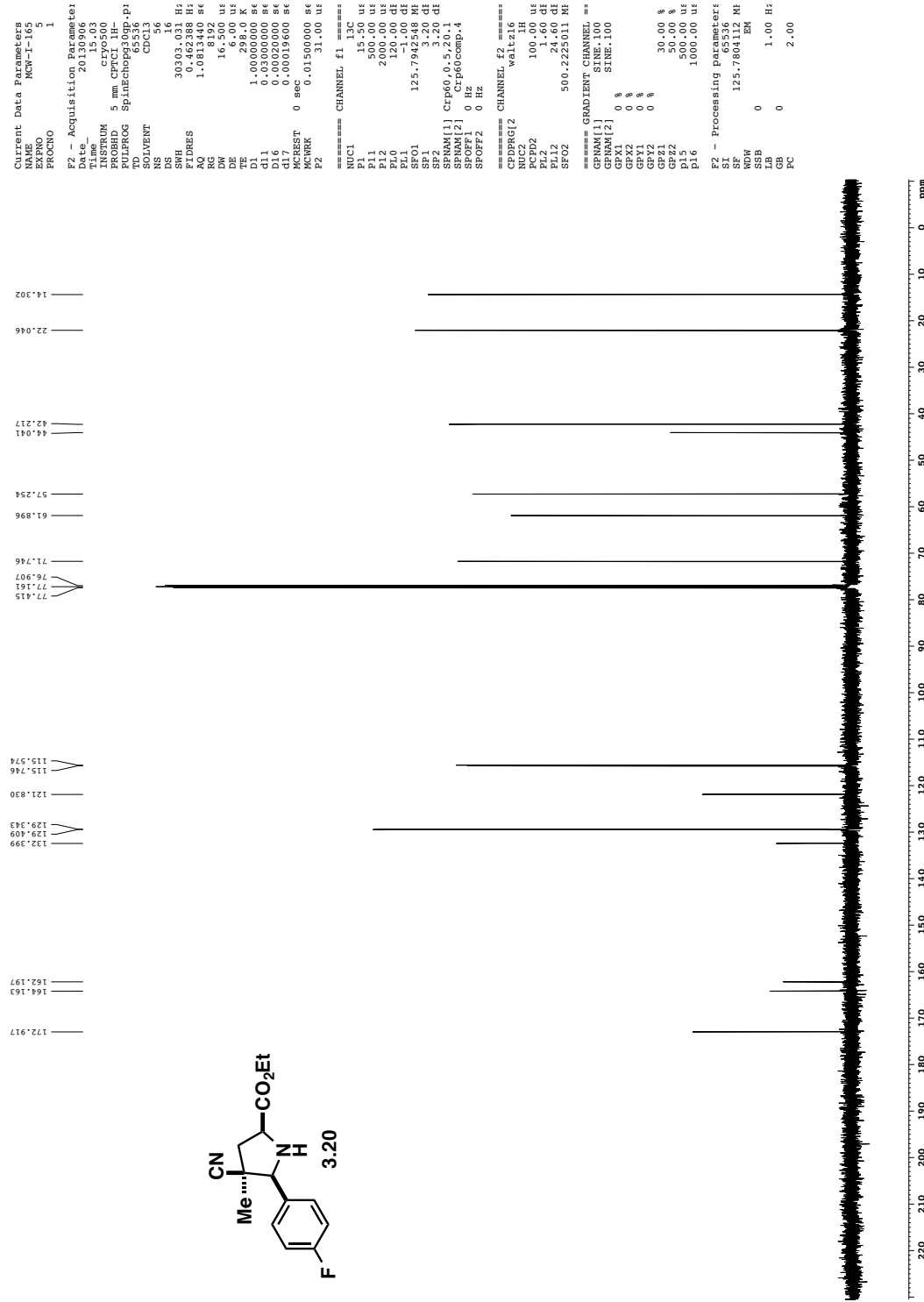
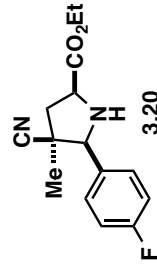




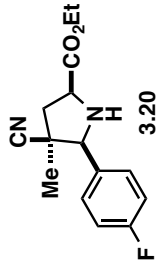
Purified Endo Adduct



Purified Endo Adduct



165b Endo - Purified Product



-112.659

```

Current Data Parameters
NAME      MCW-T-165
NAME      32
PROCNO   1

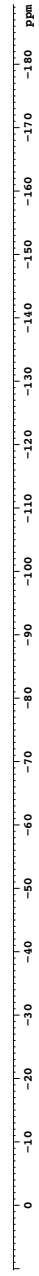
E2 = Acquisition Parameters
Date   2013.068
Time   17:26
INSTRUM  5 mm QNP400
RFIDR   251.0530
TD      6536
SOLVENT  CDCl3
NS      65
SWH     7518.570 Hz
FIDRES  0.438051 sec
AQ      1.184000
RG      6.50
DE      9.46 usec
TE      298.0 K
T1      1.000000 sec
D1L    0.000000 sec
D1Z1   0.0000200 sec
D1Z2   0.0000200 sec

CHANNEL F1 = 1H
NUC1   1H
PCP1   22.00 usec
PL1    -4.00 dB
SFO1   376.464491 MHz

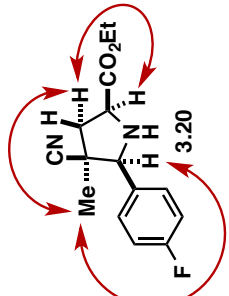
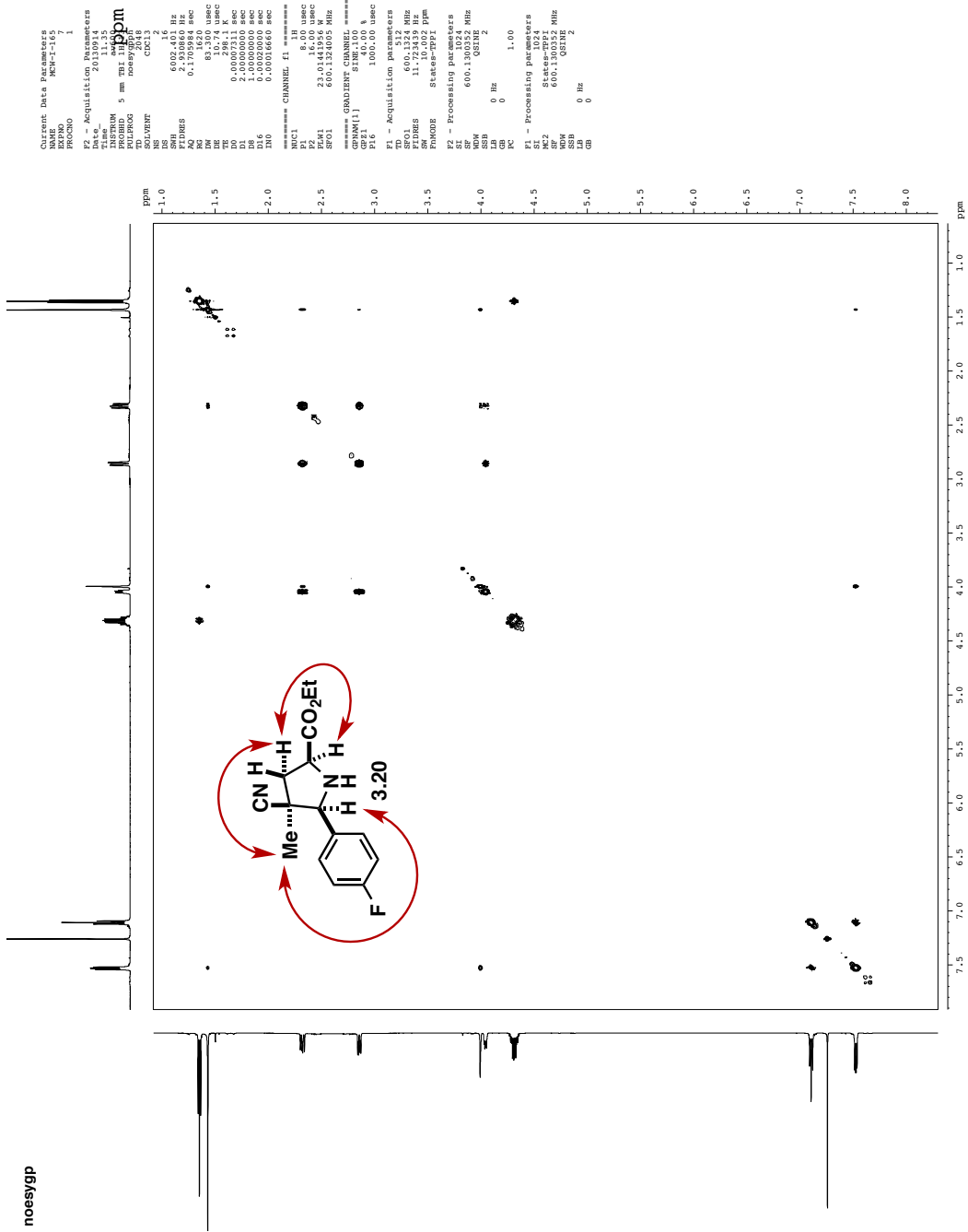
CHANNEL F2 = 1H
NUC2   1H
PCP2   80.00 usec
PL2    -3.00 dB
RFQ2   4006.1426007 MHz

E2 = Processing parameters
IS      31.36
SF      376.464491 MHz
WDW    0
SSB    0
LB     0.30 Hz
TP     0
PC    1.00

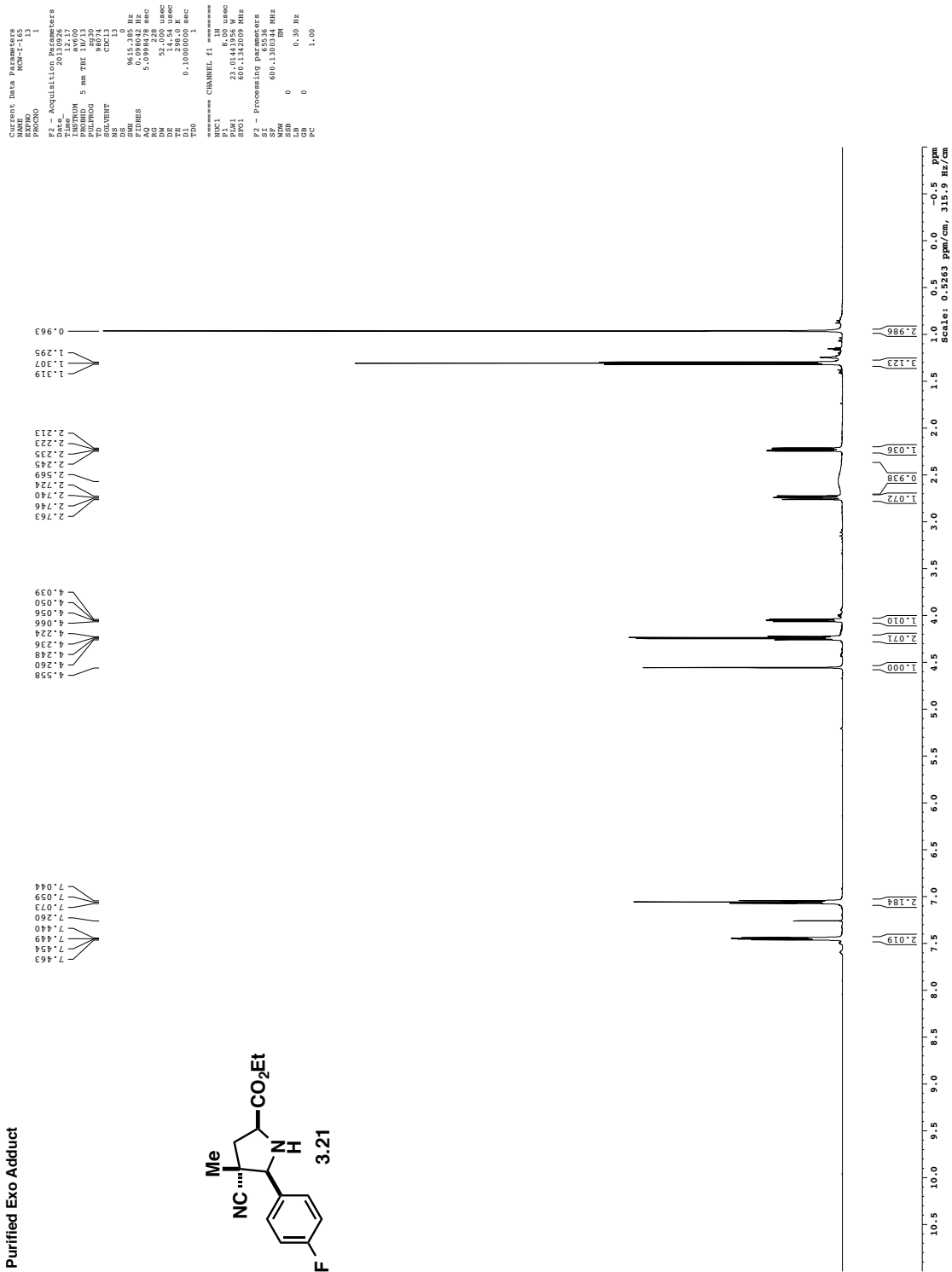
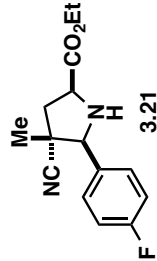
```



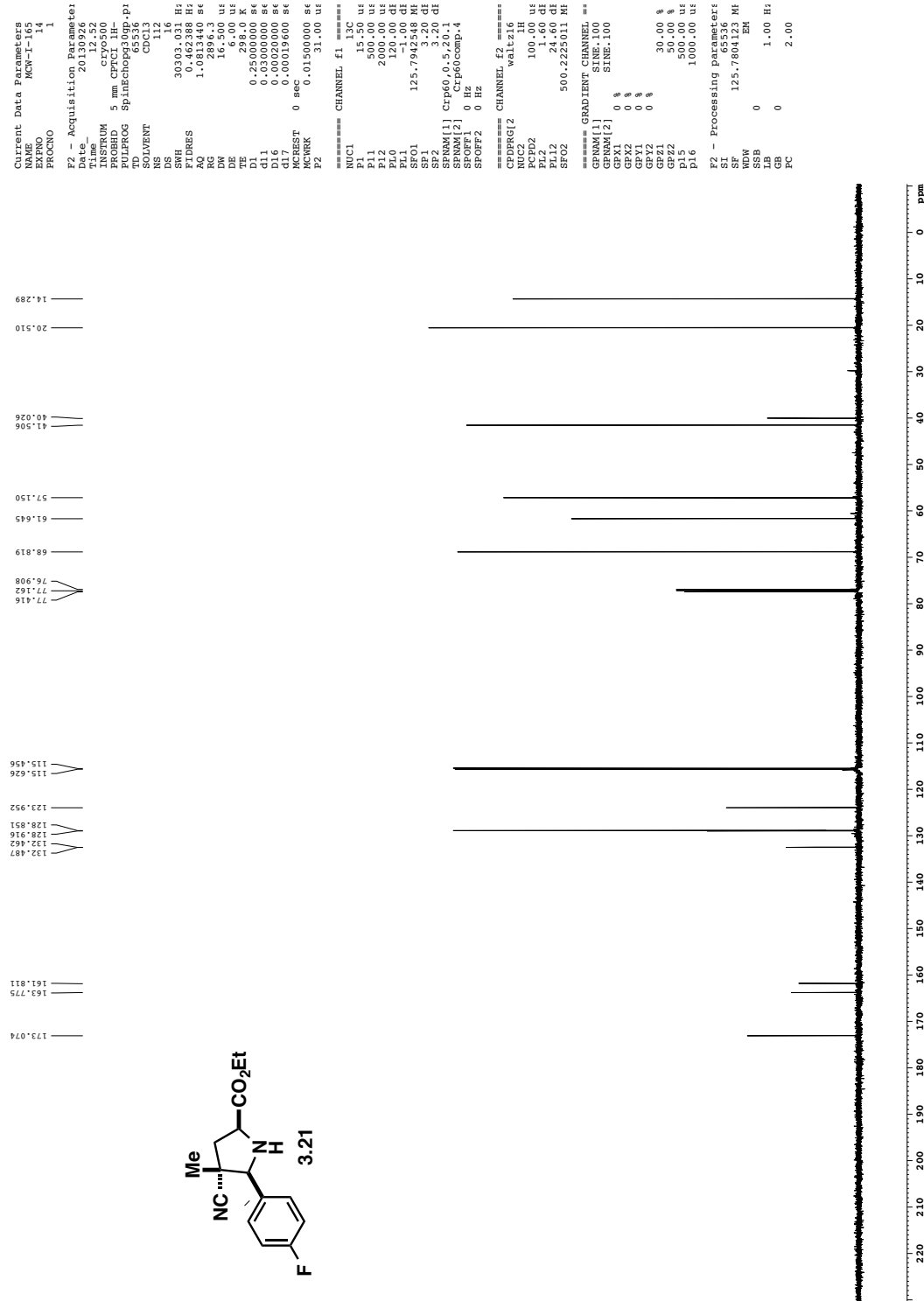
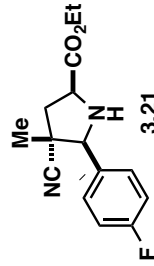
noesygp



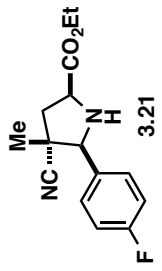
Purified Exo Adduct



Purified Exo Adduct



1165a Exo - Purified Product



```

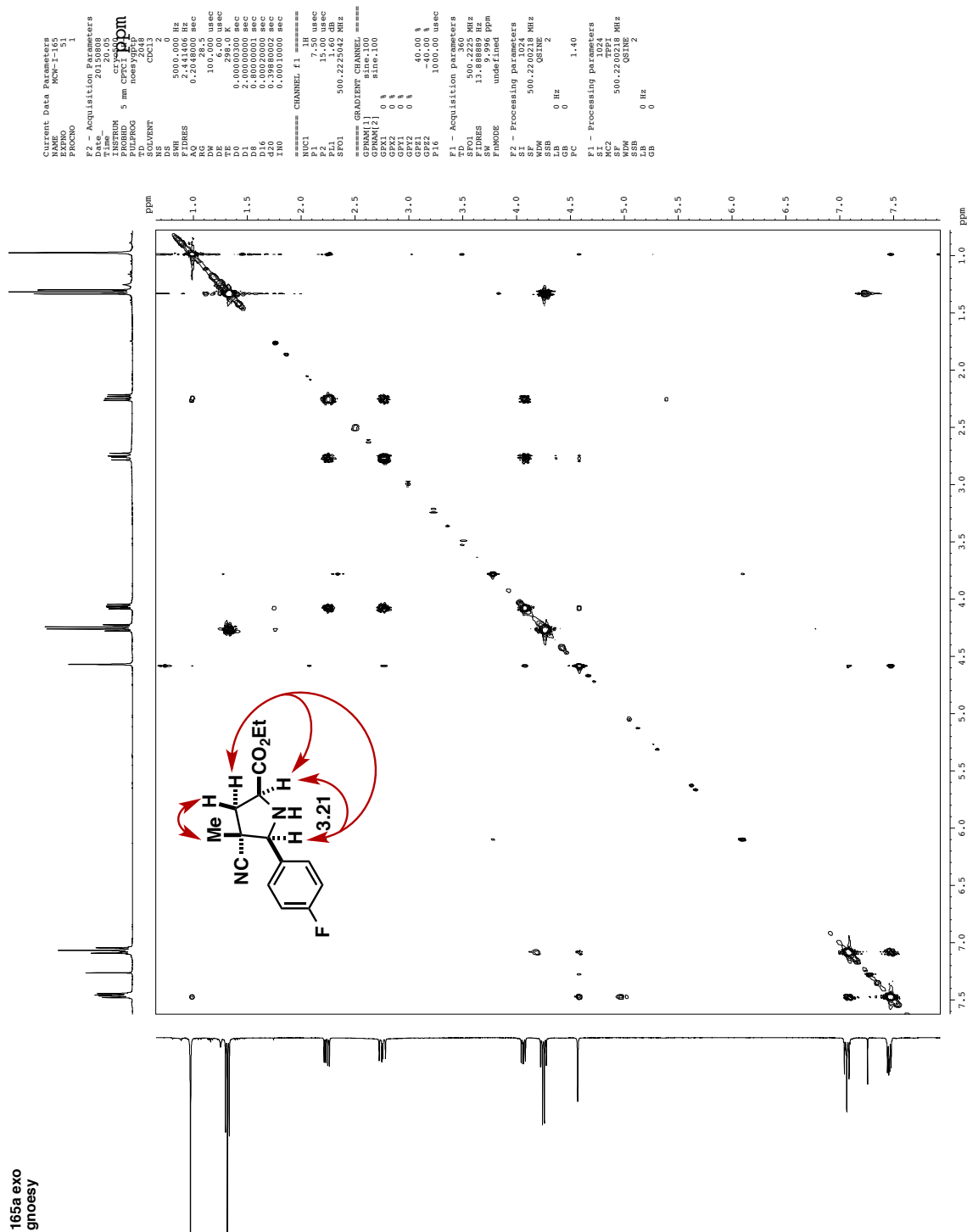
NAME      MCW-I-165
EXPTNO    35
P2 - Acquisition Parameters
Date_   20131008
Time_   20:17:35
TOFSUMN  5
TOFSUMD  mm QNP1H/P2
TE      90.00
FIDTRIG ECHO
TD      256.0
SWH     65.0340
SOLVENT  CDCl3
NS      72
DS      72
SF      75187.969 Hz
P1      1.47277 Hz
FIDRES  0.138144 sec
AQ      3.68400 sec
RG      9.46
DE      9.46
TE      298.0
DW      0.0000000 sec
D1      1.0000000 sec
D1J     0.1300000 sec
D1Z     0.0002000 sec
D1QZ    0.0000000 sec

=====
CHANNEL F1 19F
NUC1      F1
SF01     376.464691 MHz
PL      22.50 msec
P1      22.50 msec
SF02     376.464691 MHz
=====
CHANNEL F2 1H
CPDPRG1 CPDPRG1
IN      1.0
IR      1.0
RCPD2  80.00 usc
FID2    3.00 dB
PL2    16.00 dB
SF02    400.1320007 MHz
F2 - Processing parameters
SI      65536
SP      376.4983829 MHz
WDDW    EM
SSB3    0
LB      0.30 Hz
GB      0
PC      1.00

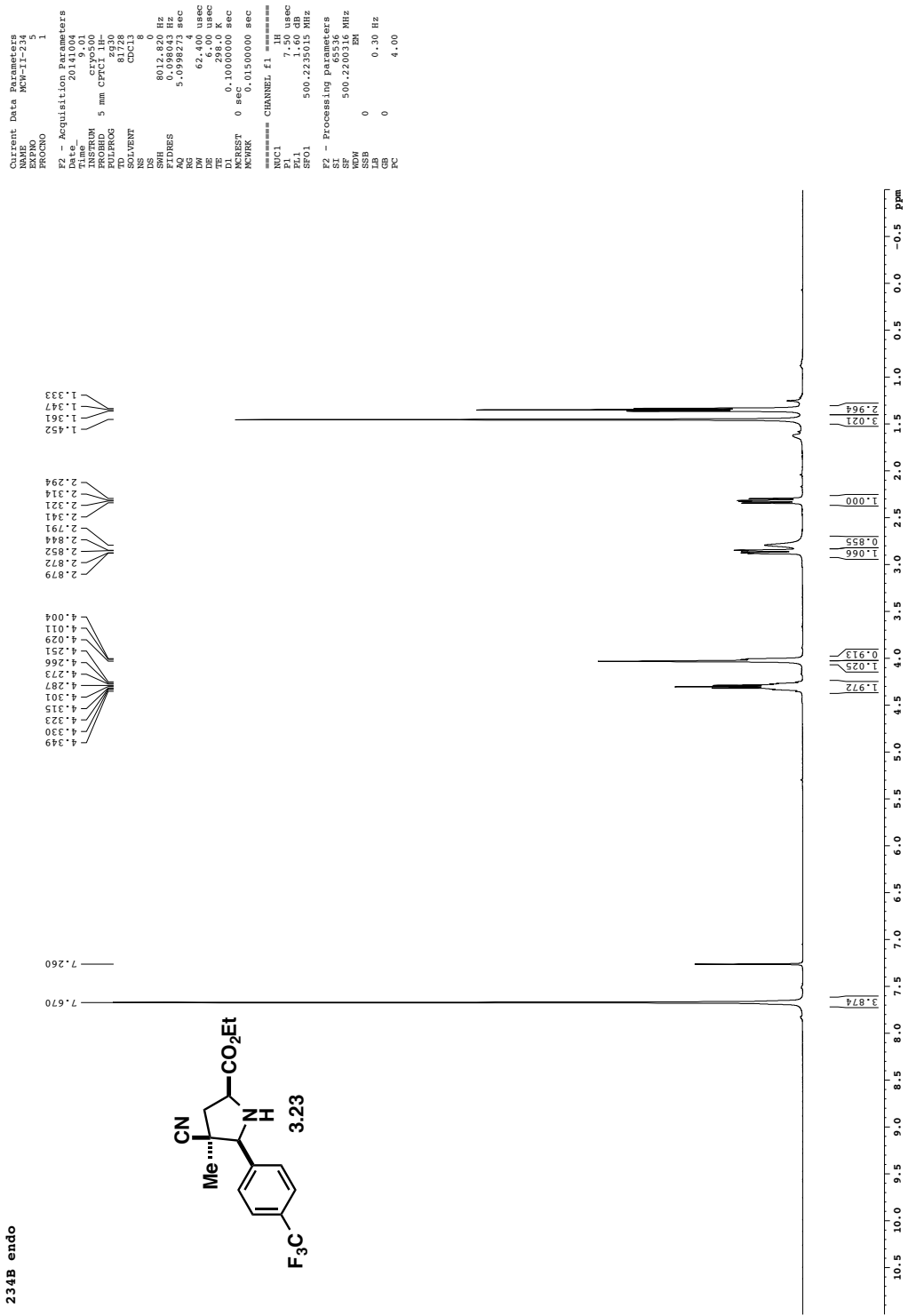
```



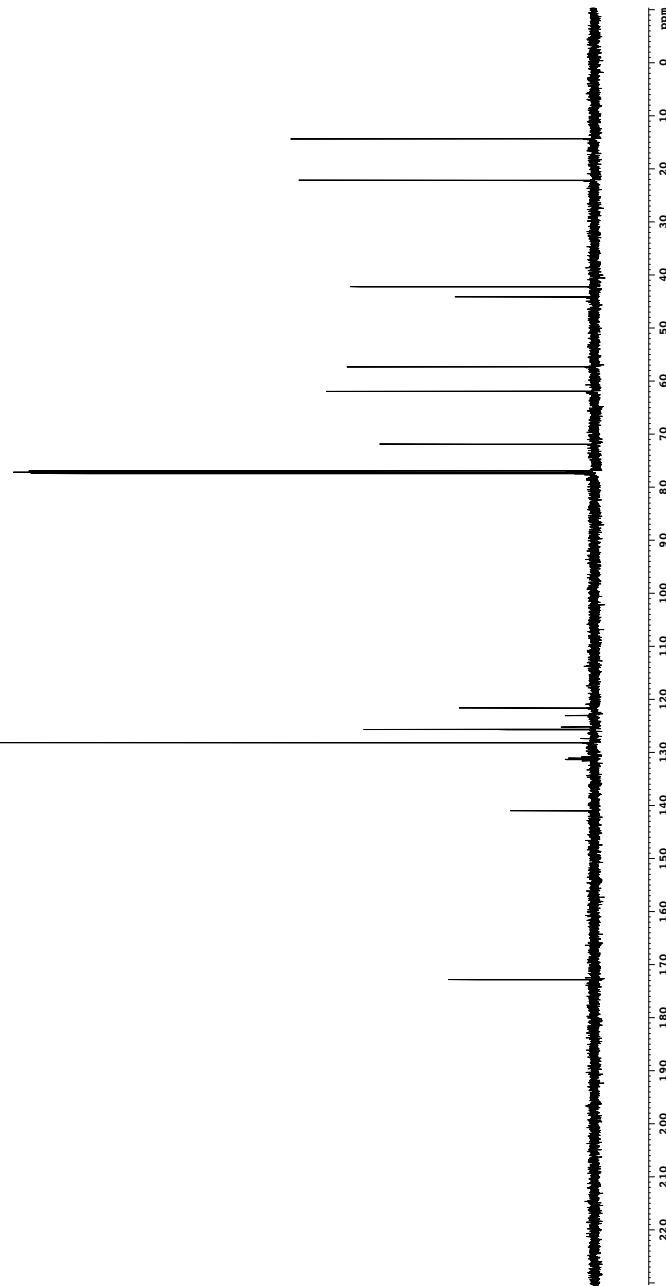
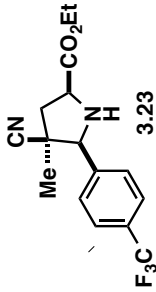
**165a exo
gnoesy**



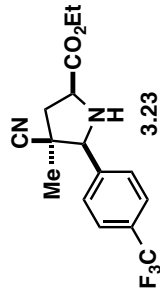
234B endo



234B endo



234B 19F{1H}



— — — — — -62.654

```

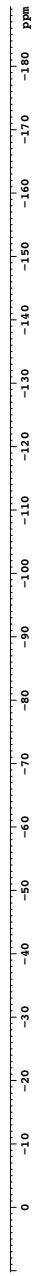
Current Data Parameters
NAME      MW-11-234
EXPNO     13
PROCNO    1
Date      2014.064
Time      10:06
INSTRUM  5 mm QNP700
PROBHD   2gfh630
PULPROG  zg30
TD       6536
SOLVENT   CDCl3
NS        24
DS        0
SWH      75187.969 Hz
FIDRES   0.439144 sec
AQ        1.47277 Hz
RG        184.0
TE        9.46 usec
TM        298.0 K
D1       2.000000 sec
T1       0.000000 sec
FIDSPS   0.0002000 sec
R1       0.0002000 sec

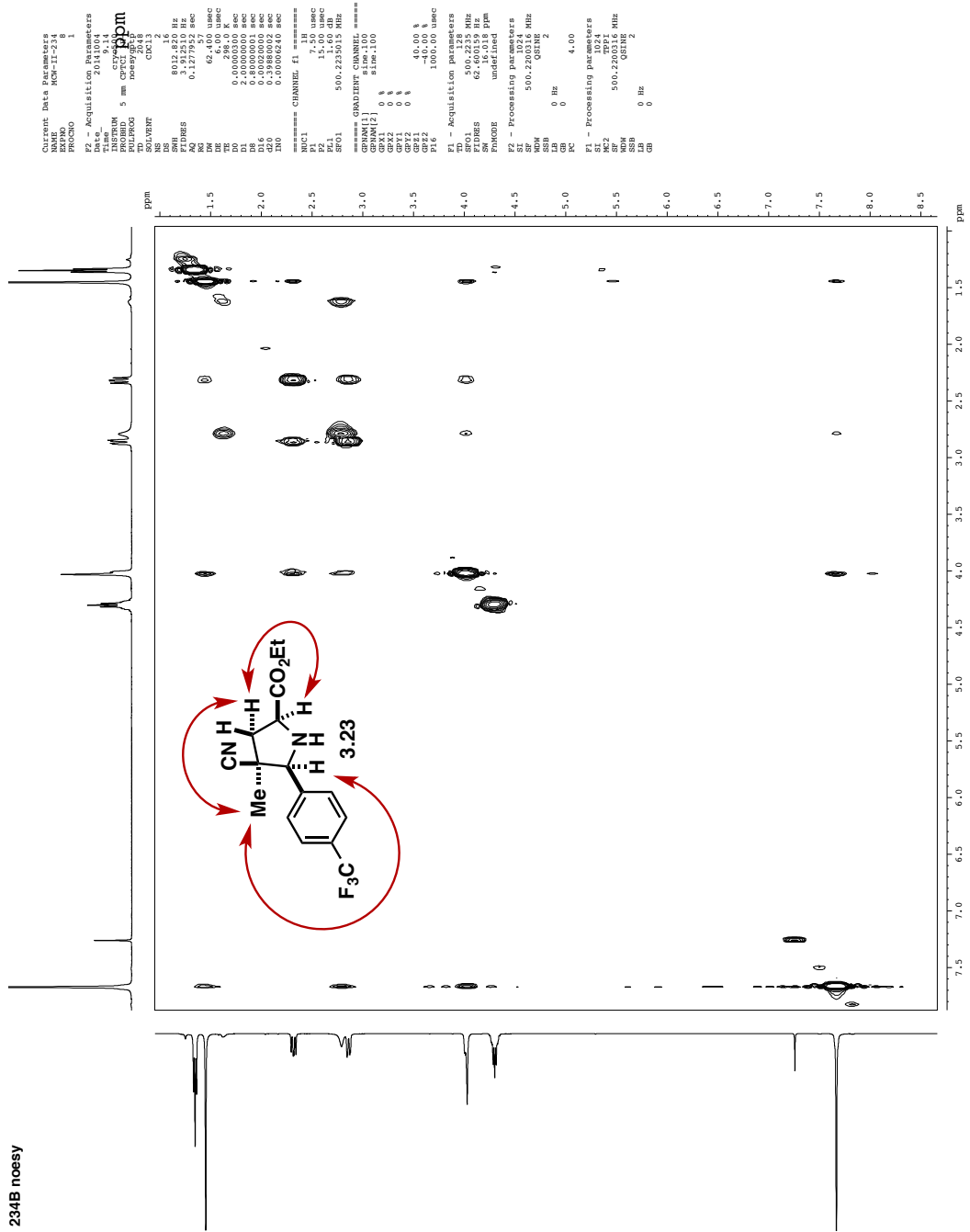
===== CHANNEL F1 =====
NUC1      1H
PC1       22.50 usec
PL1      -45.00 dB
SFO1     376.464491 MHz

===== CHANNEL F2 =====
NUC2      13C
PCP2     90.00 usec
PL2      120.00 dB
R2       400.1420007 MHz

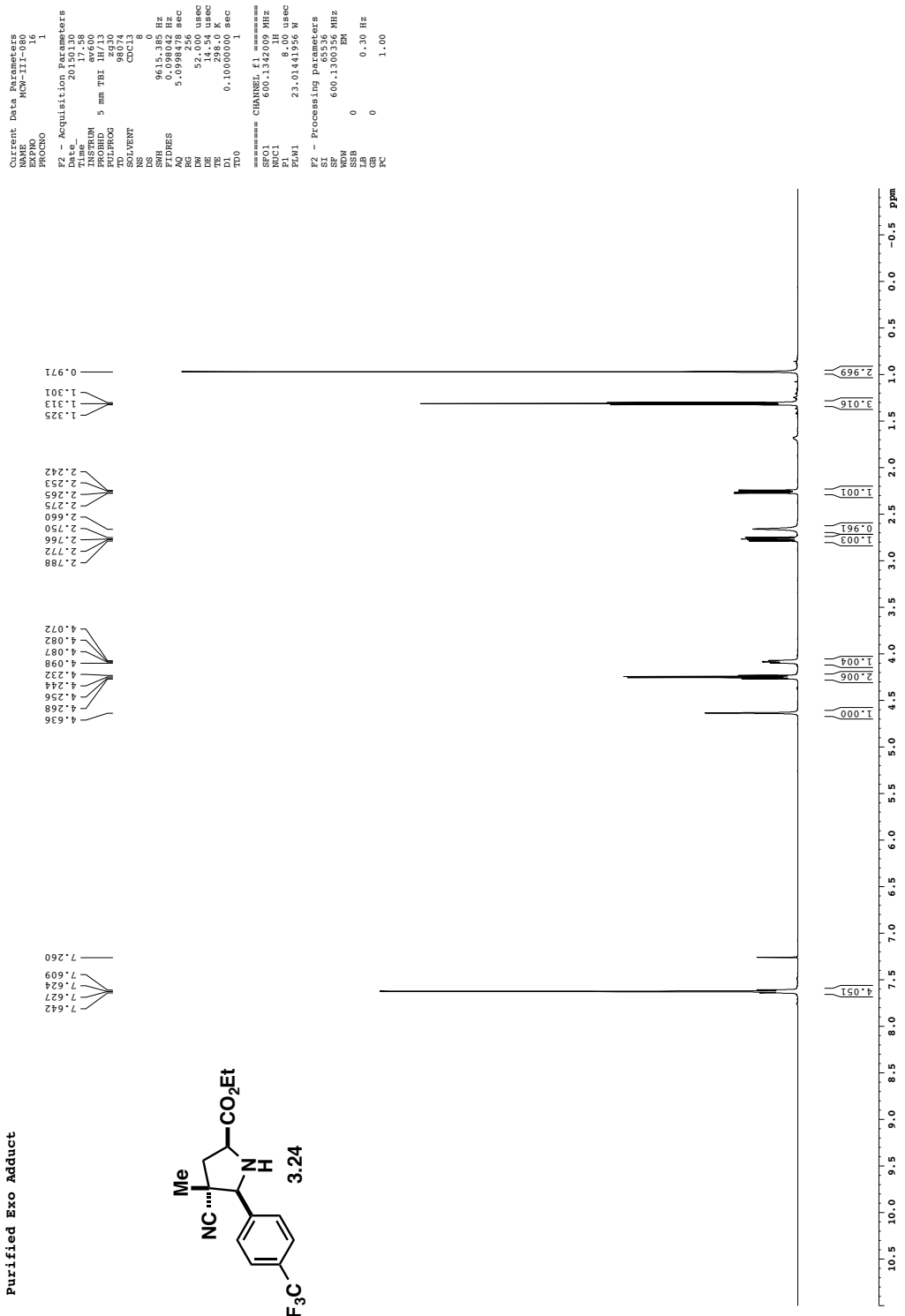
===== Processing Parameters =====
SI        3538355
SF      376.464491 MHz
WDW      EN
SSB      0
LB      0.30 Hz
DE      0
PC      1.00

```

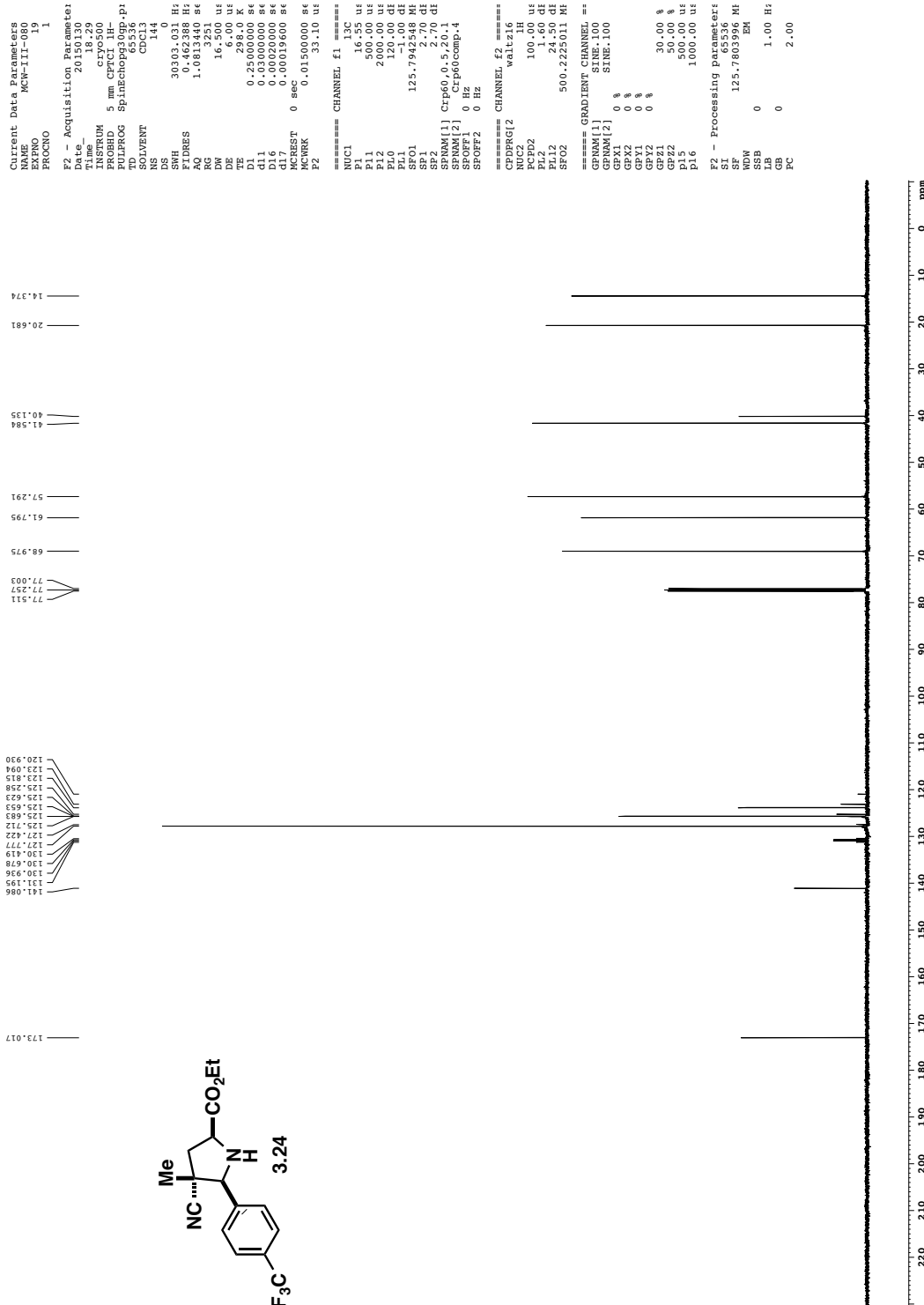




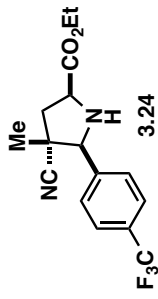
Purified Exo Adduct



Purified Exo Adduct



Purified Exo Adduct



Current Data Parameters
NAME : NCM-111-080
EXPRO : 18
PROCNO : 1

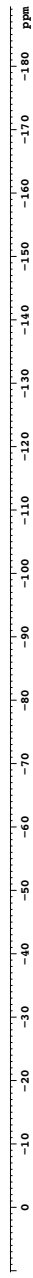
E2 = Acquisition Parameters
Date : 20150130
Time : 18:18
INSTRUM : 5 mm QNP
PROBHD : 4.00
PULPROG : zg3f16p
TD : 65736
SOLVENT : CDCl3
NS : 12
DS :
SWH : 75187.969 Hz
FIDRES : 1.147277 Hz
AQ : 0.4358144 sec
RG : 12.650
DE : 6.50 usec
TE : 9.46 usec
TM : 298.0 K
D1 : 2.0000000 sec
D11 : 0.0000000 sec
D12 : 0.0000000 sec

===== CHANNEL F1 =====
NUC1 : 1H
PCP1 : 90.00 usec
PL1 : 22.35 usec
SF01 : -6.00 dB
SF1 : 376.464491 MHz

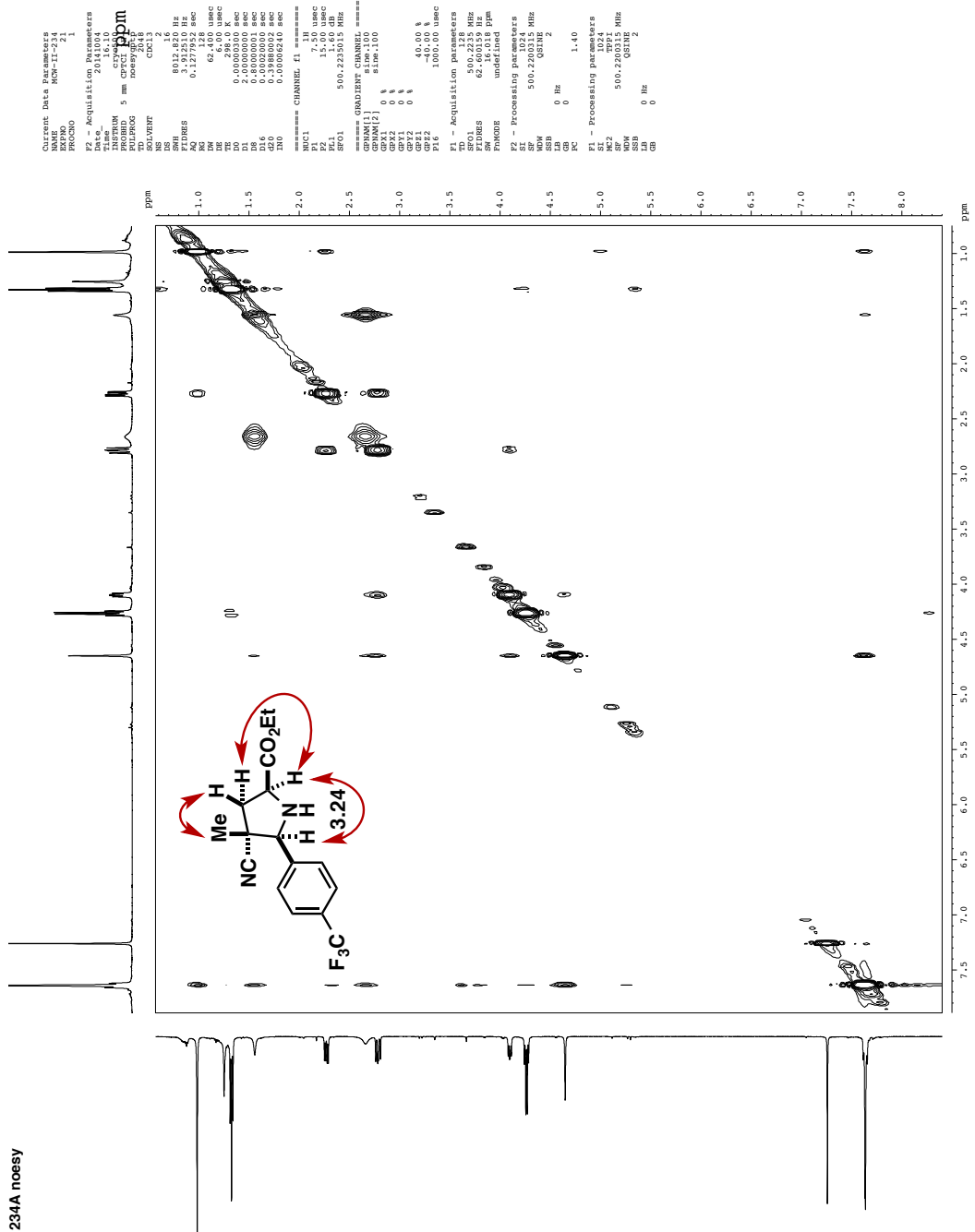
===== CHANNEL F2 =====
NUC2 : 13C
PCP2 : 90.00 usec
PL2 : 120.00 dB
SFQ2 : 4006.1320007 MHz

E2 = Processing Parameters
IS : 35
SF : 376.464491 MHz
NDW : 0 EN
SSB : 0
LB : 0 -30 Hz
GS : 0
PC : 1.00

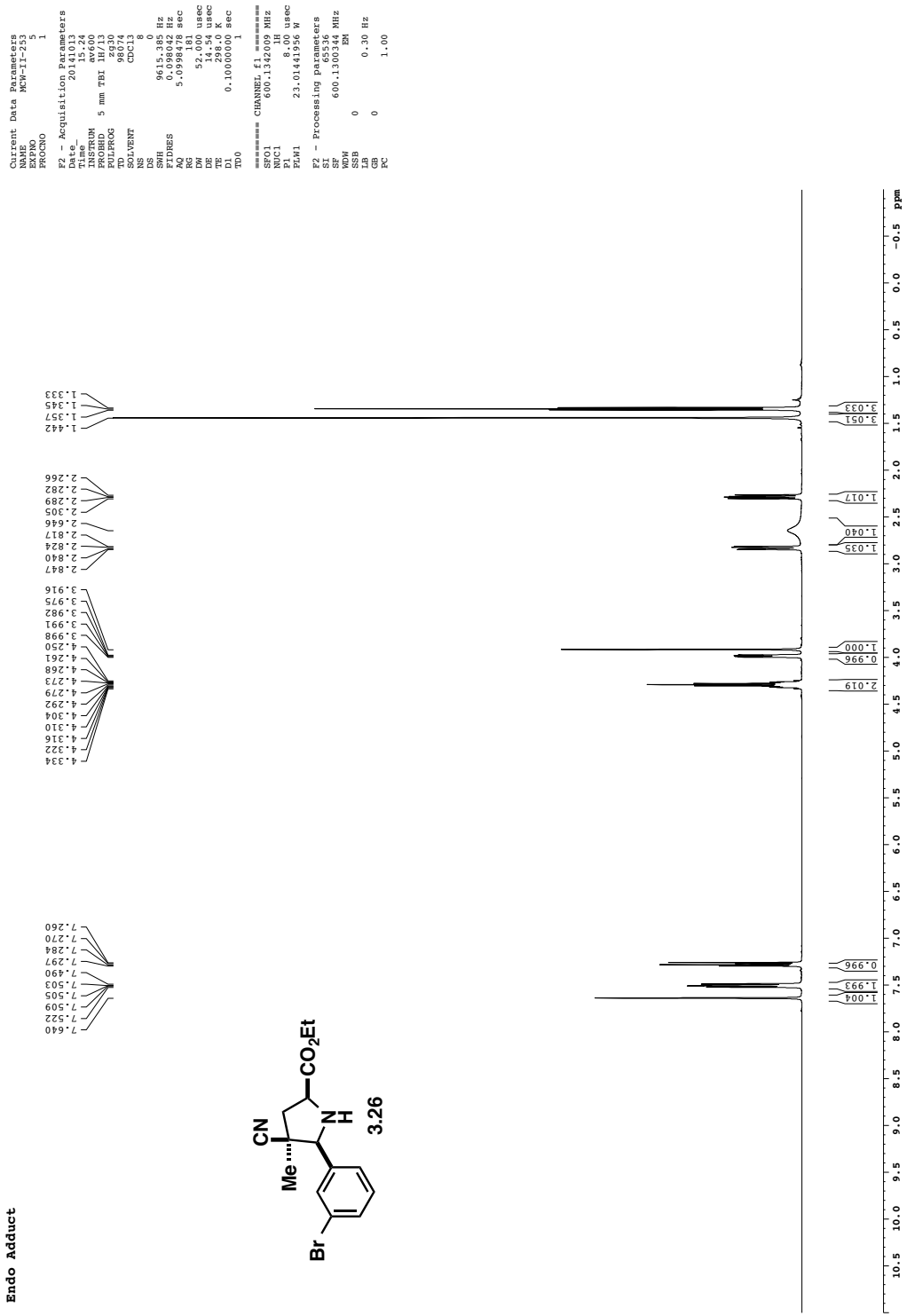
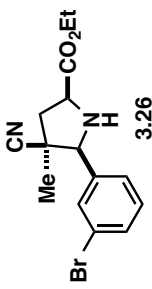
-62.643



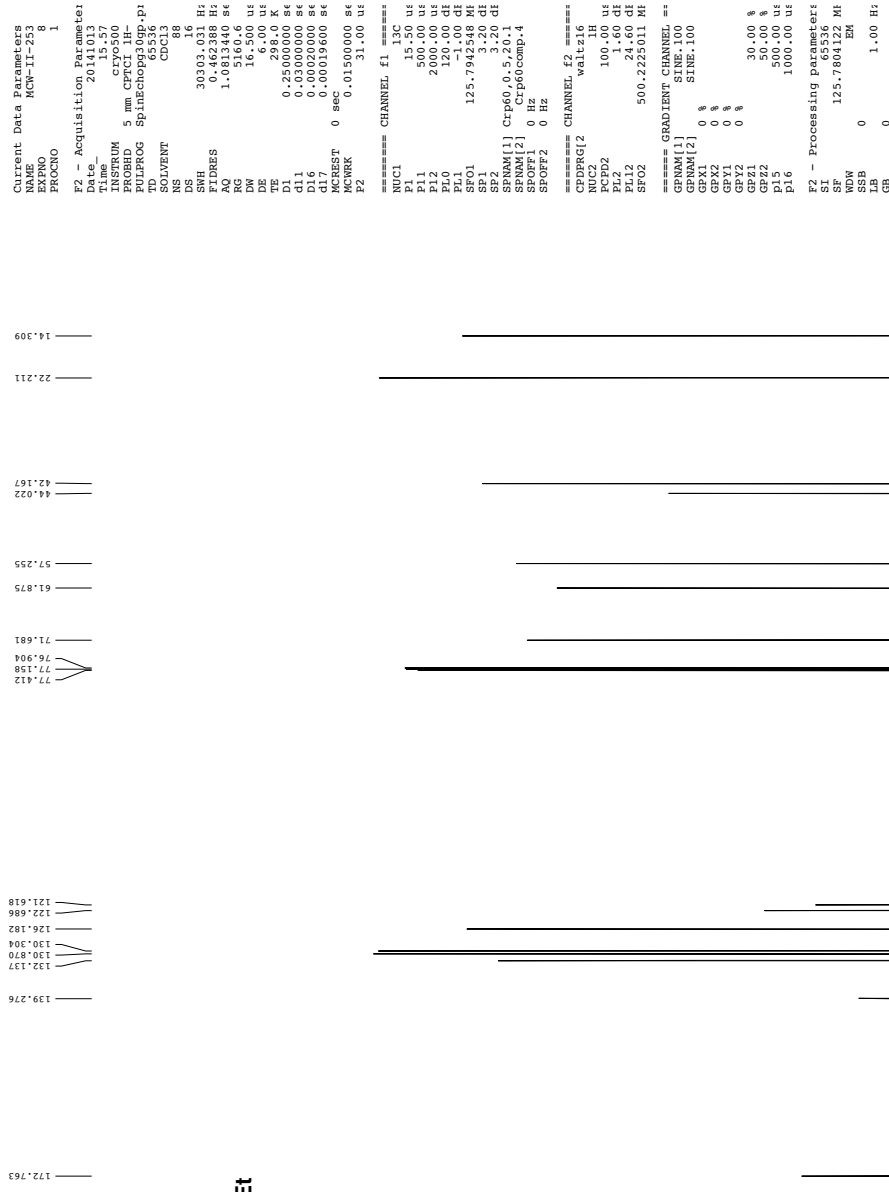
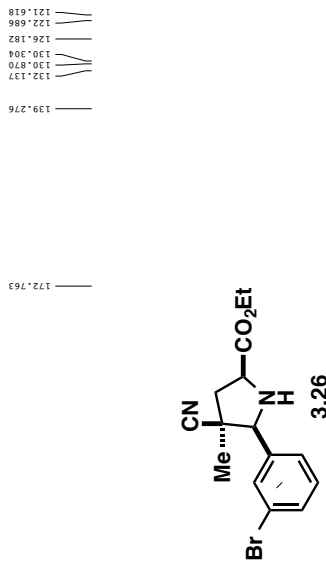
234A noesy



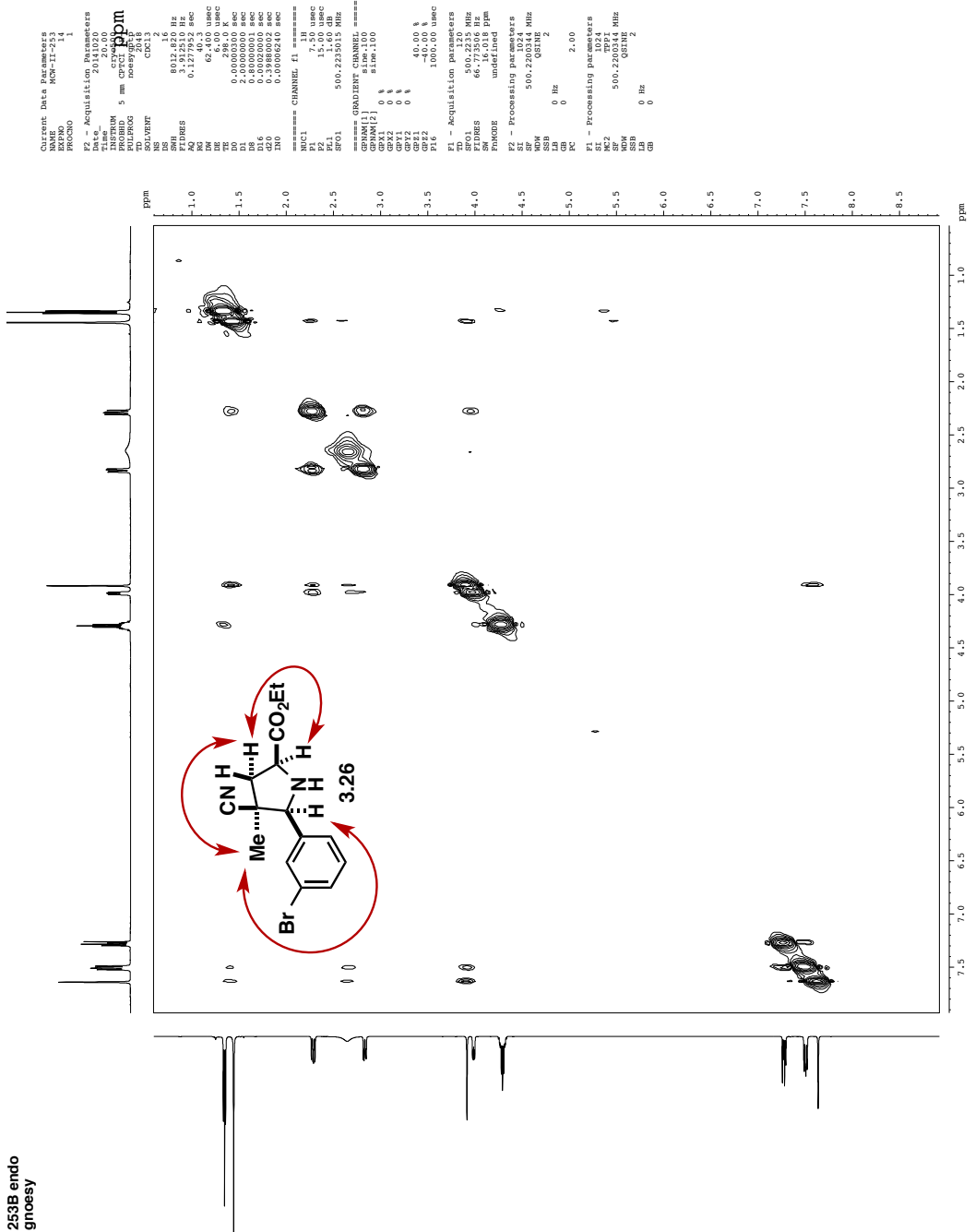
Endo Adduct



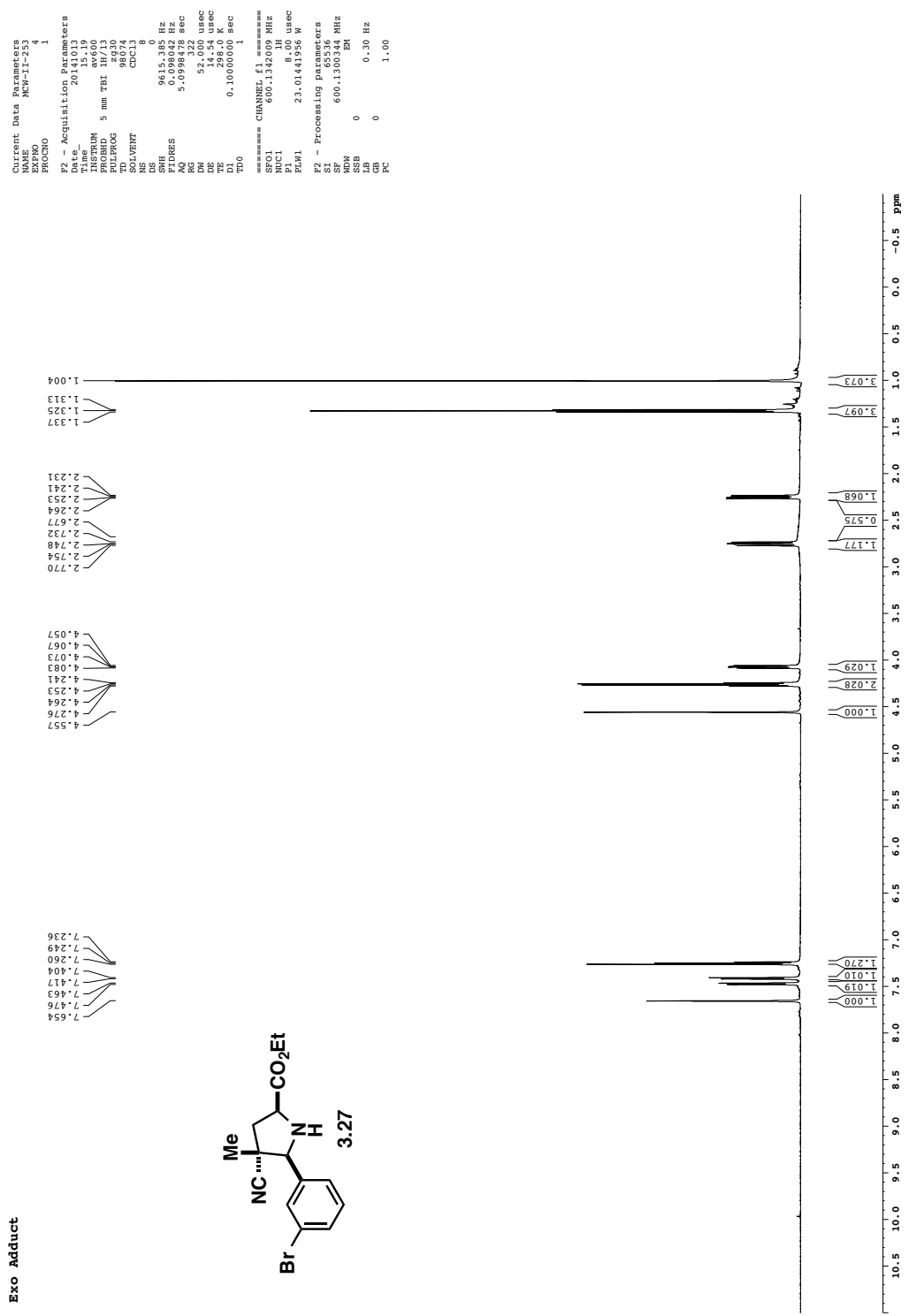
Endo Adduct



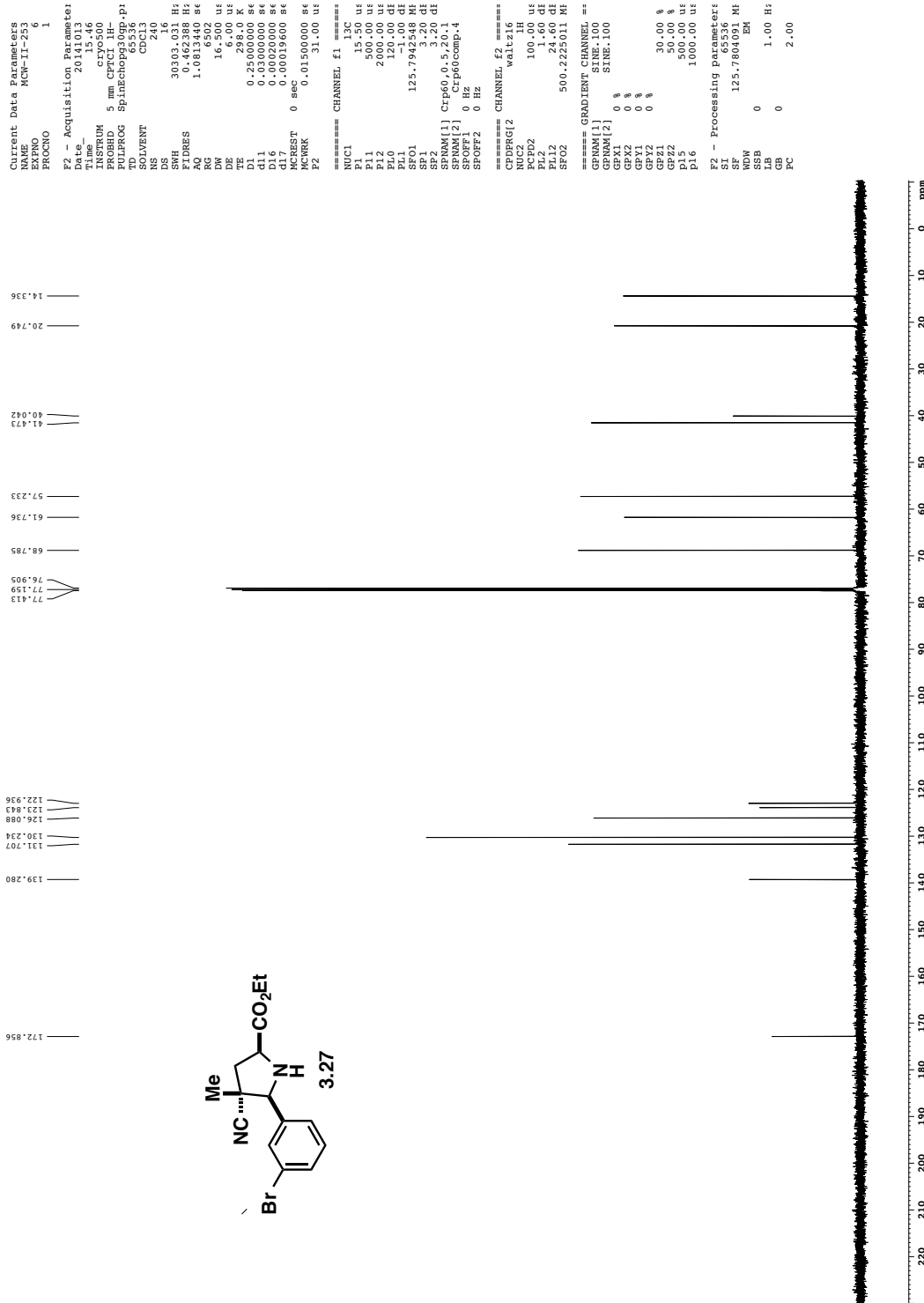
253B endo
gnoesy



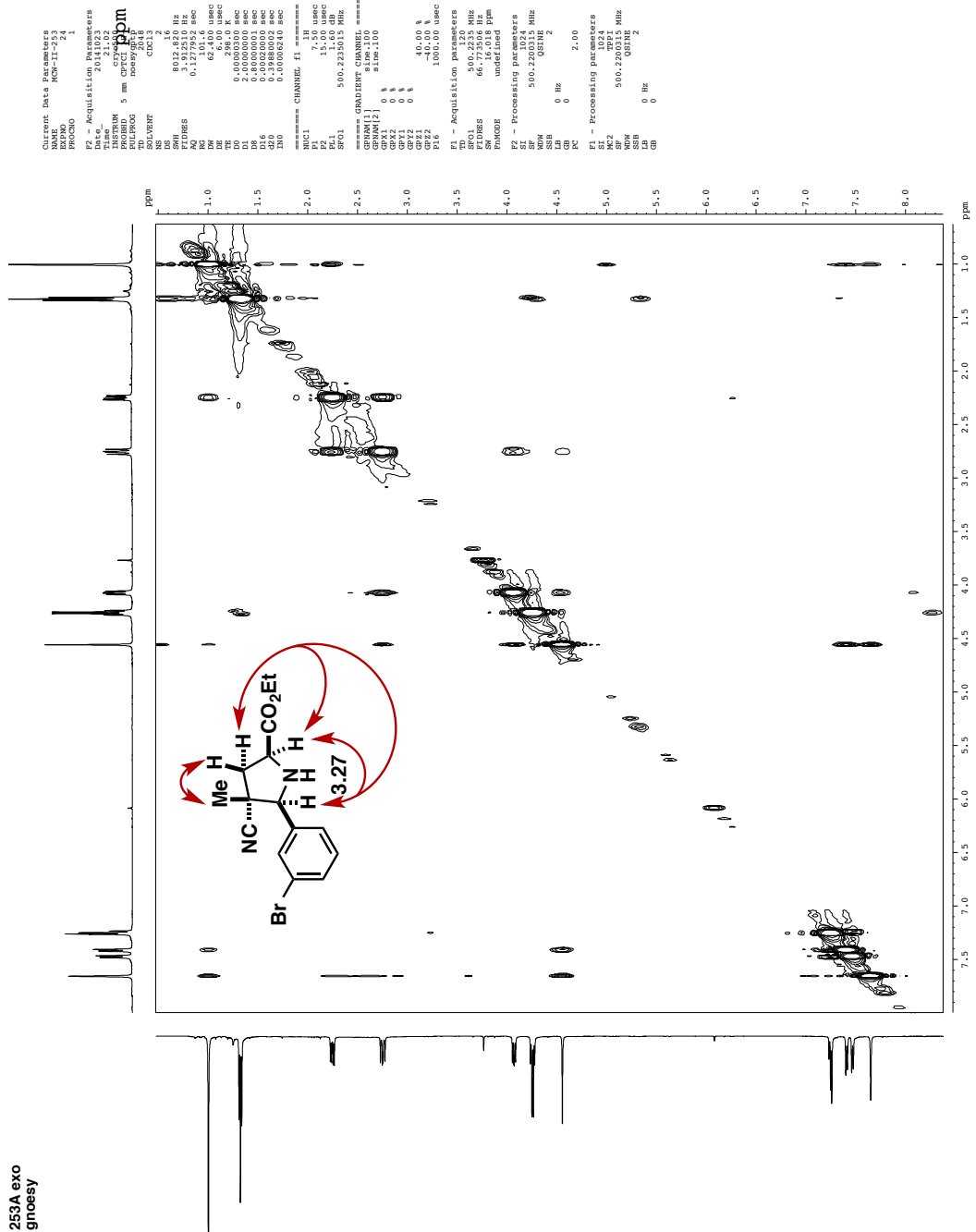
Exo Adduct



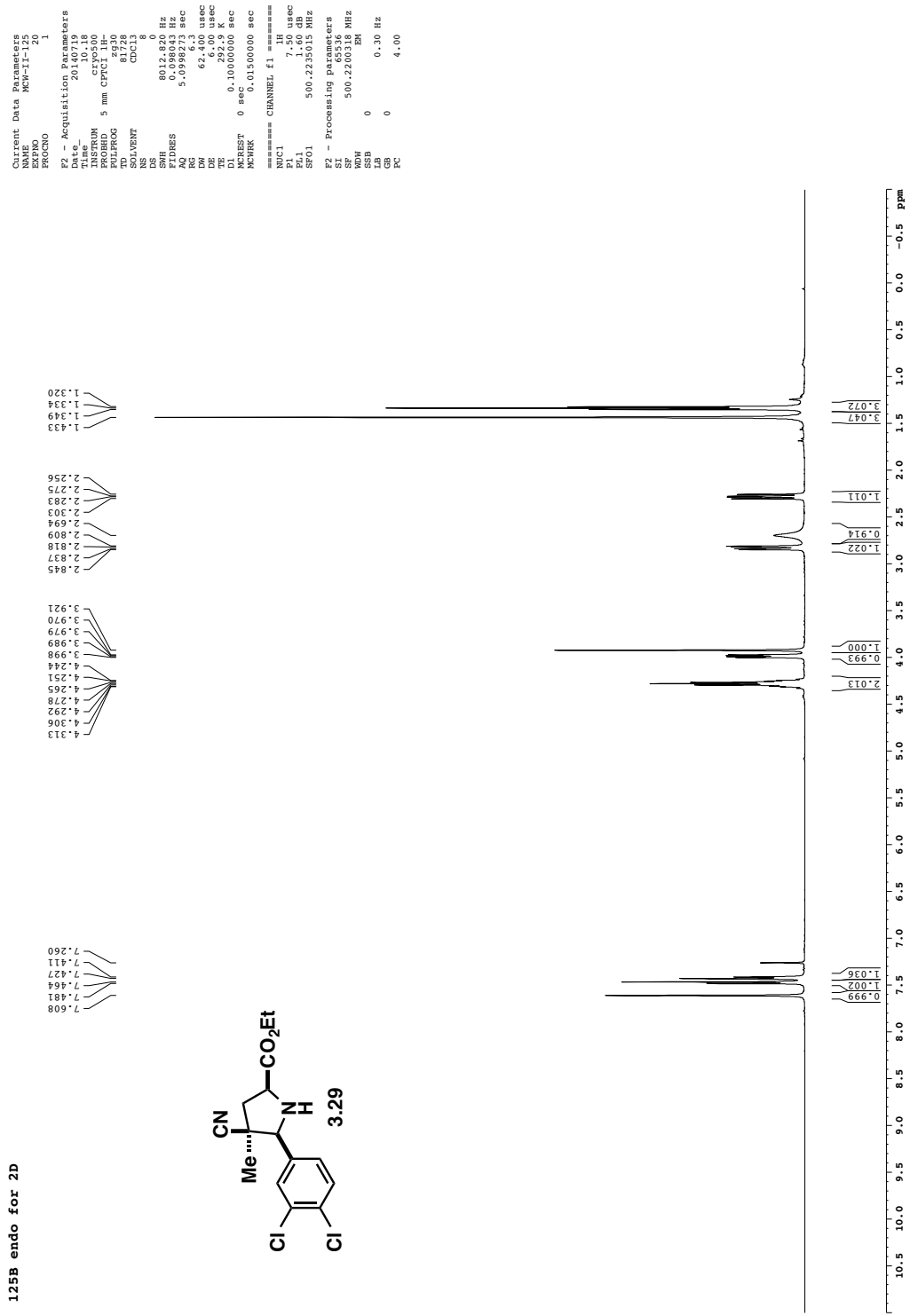
Exo Adduct



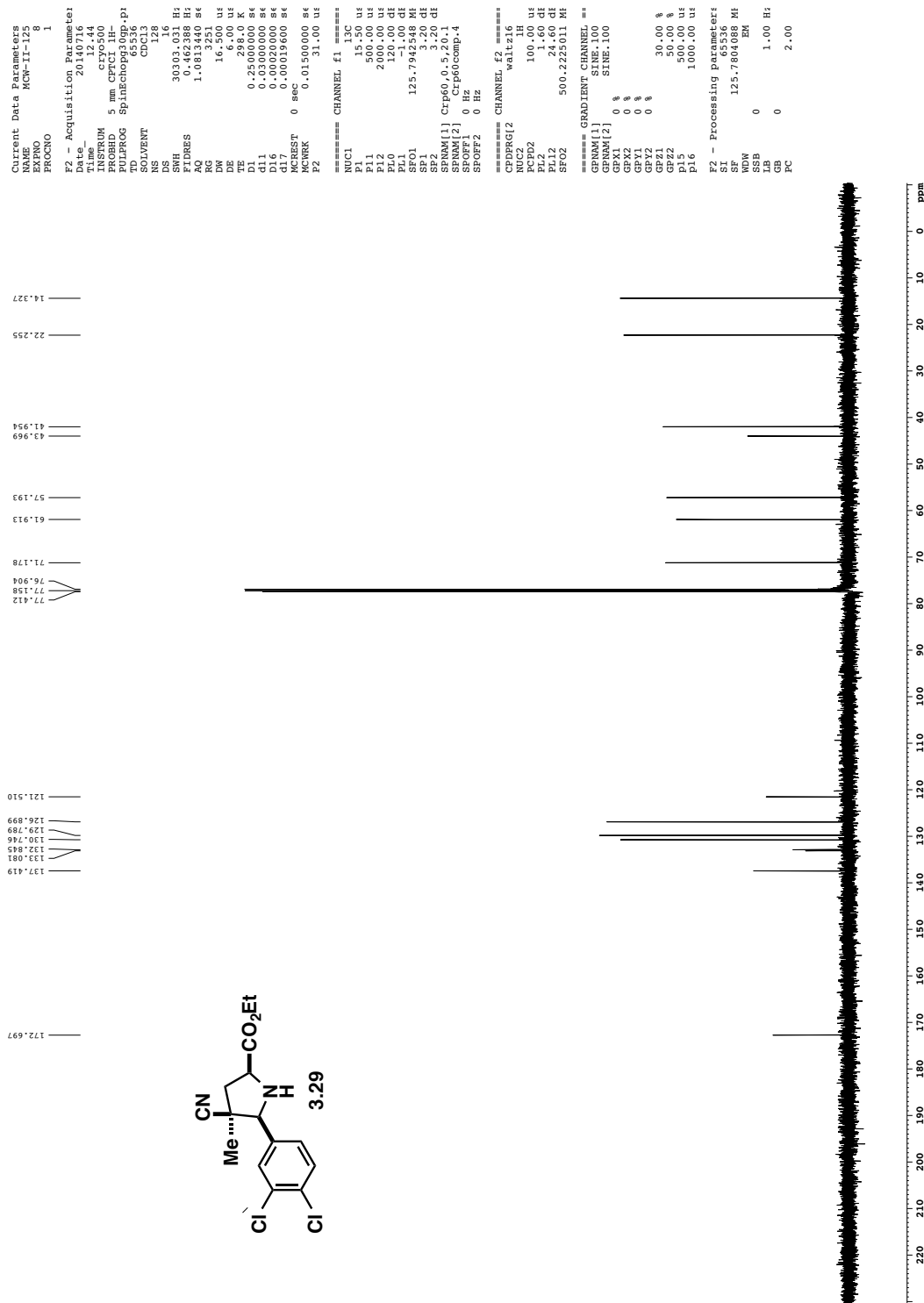
253A exo
gnoesy



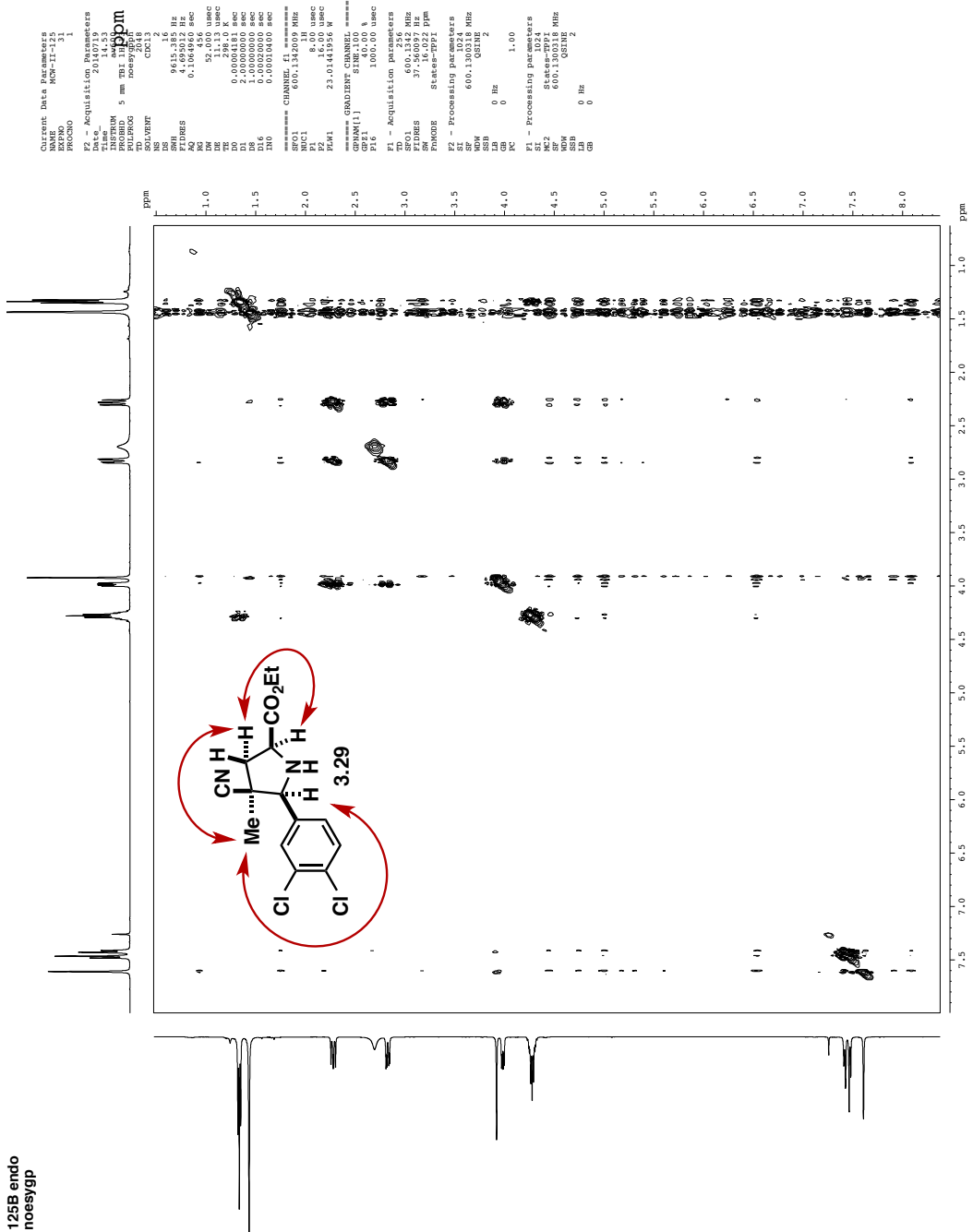
125b endo for 2D



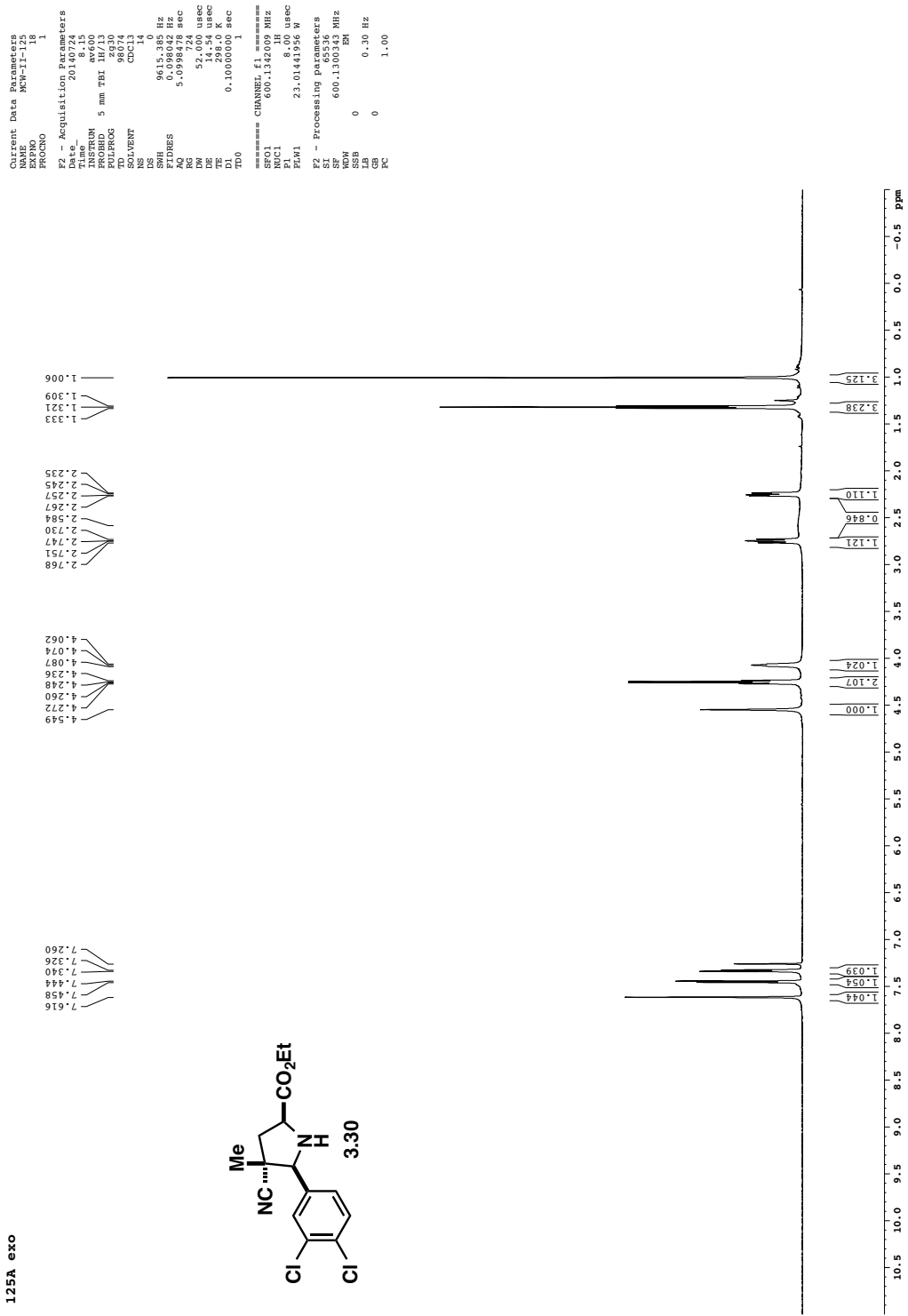
Endo Adduct



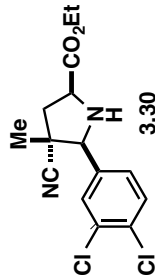
125B endo
noesygpp



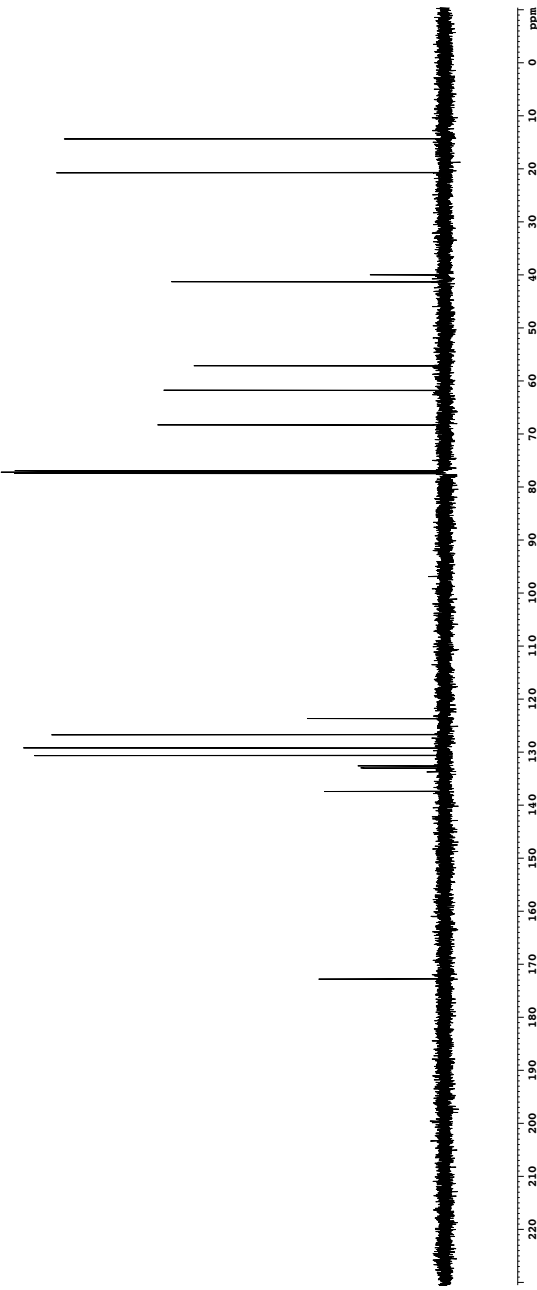
125a exo



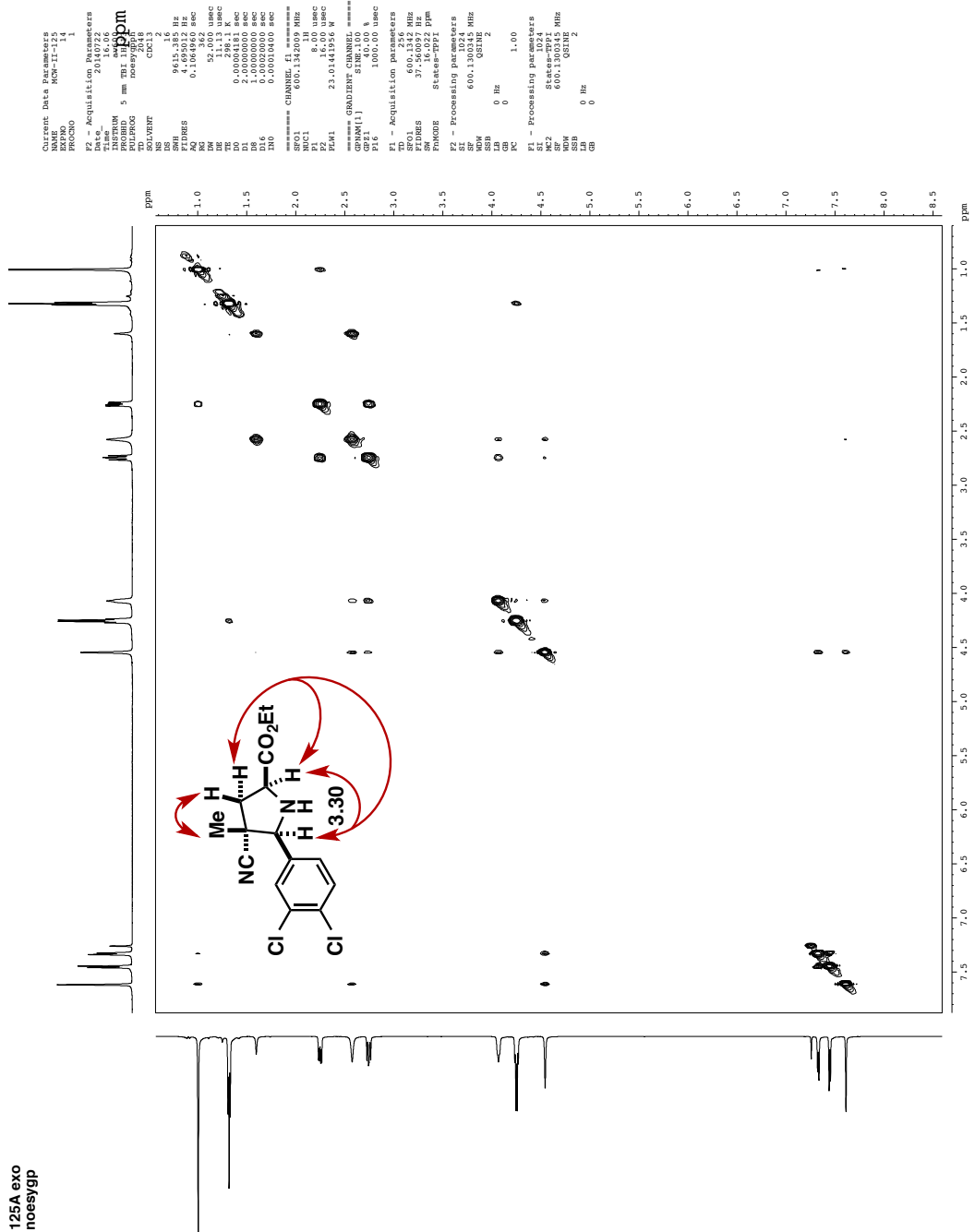
125A exo



1	ACW-II-38	ACW-II-38
2	EXPNO	EXPNO
3	P2	- Acquisition Parameters
4	41.274	
5	39.173	
6	57.117	
7	61.728	
8	68.251	
9	75.349	
10	76.349	
11	76.718	
12	77.413	
13	85.193	
14	93.193	
15	100.193	
16	109.193	
17	119.193	
18	129.193	
19	139.193	
20	149.193	
21	159.193	
22	169.193	
23	179.193	
24	189.193	
25	199.193	
26	209.193	
27	219.193	
28	229.193	
29	239.193	
30	249.193	
31	259.193	
32	269.193	
33	279.193	
34	289.193	
35	299.193	
36	309.193	
37	319.193	
38	329.193	
39	339.193	
40	349.193	
41	359.193	
42	369.193	
43	379.193	
44	389.193	
45	399.193	
46	409.193	
47	419.193	
48	429.193	
49	439.193	
50	449.193	
51	459.193	
52	469.193	
53	479.193	
54	489.193	
55	499.193	
56	509.193	
57	519.193	
58	529.193	
59	539.193	
60	549.193	
61	559.193	
62	569.193	
63	579.193	
64	589.193	
65	599.193	
66	609.193	
67	619.193	
68	629.193	
69	639.193	
70	649.193	
71	659.193	
72	669.193	
73	679.193	
74	689.193	
75	699.193	
76	709.193	
77	719.193	
78	729.193	
79	739.193	
80	749.193	
81	759.193	
82	769.193	
83	779.193	
84	789.193	
85	799.193	
86	809.193	
87	819.193	
88	829.193	
89	839.193	
90	849.193	
91	859.193	
92	869.193	
93	879.193	
94	889.193	
95	899.193	
96	909.193	
97	919.193	
98	929.193	
99	939.193	
100	949.193	
101	959.193	
102	969.193	
103	979.193	
104	989.193	
105	999.193	
106	1009.193	
107	1019.193	
108	1029.193	
109	1039.193	
110	1049.193	
111	1059.193	
112	1069.193	
113	1079.193	
114	1089.193	
115	1099.193	
116	1109.193	
117	1119.193	
118	1129.193	
119	1139.193	
120	1149.193	
121	1159.193	
122	1169.193	
123	1179.193	
124	1189.193	
125	1199.193	
126	1209.193	
127	1219.193	
128	1229.193	
129	1239.193	
130	1249.193	
131	1259.193	
132	1269.193	
133	1279.193	
134	1289.193	
135	1299.193	
136	1309.193	
137	1319.193	
138	1329.193	
139	1339.193	
140	1349.193	
141	1359.193	
142	1369.193	
143	1379.193	
144	1389.193	
145	1399.193	
146	1409.193	
147	1419.193	
148	1429.193	
149	1439.193	
150	1449.193	
151	1459.193	
152	1469.193	
153	1479.193	
154	1489.193	
155	1499.193	
156	1509.193	
157	1519.193	
158	1529.193	
159	1539.193	
160	1549.193	
161	1559.193	
162	1569.193	
163	1579.193	
164	1589.193	
165	1599.193	
166	1609.193	
167	1619.193	
168	1629.193	
169	1639.193	
170	1649.193	
171	1659.193	
172	1669.193	
173	1679.193	
174	1689.193	
175	1699.193	
176	1709.193	
177	1719.193	
178	1729.193	
179	1739.193	
180	1749.193	
181	1759.193	
182	1769.193	
183	1779.193	
184	1789.193	
185	1799.193	
186	1809.193	
187	1819.193	
188	1829.193	
189	1839.193	
190	1849.193	
191	1859.193	
192	1869.193	
193	1879.193	
194	1889.193	
195	1899.193	
196	1909.193	
197	1919.193	
198	1929.193	
199	1939.193	
200	1949.193	
201	1959.193	
202	1969.193	
203	1979.193	
204	1989.193	
205	1999.193	
206	2009.193	
207	2019.193	
208	2029.193	
209	2039.193	
210	2049.193	
211	2059.193	
212	2069.193	
213	2079.193	
214	2089.193	
215	2099.193	
216	2109.193	
217	2119.193	
218	2129.193	
219	2139.193	
220	2149.193	
221	2159.193	
222	2169.193	
223	2179.193	
224	2189.193	
225	2199.193	
226	2209.193	
227	2219.193	
228	2229.193	
229	2239.193	
230	2249.193	
231	2259.193	
232	2269.193	
233	2279.193	
234	2289.193	
235	2299.193	
236	2309.193	
237	2319.193	
238	2329.193	
239	2339.193	
240	2349.193	
241	2359.193	
242	2369.193	
243	2379.193	
244	2389.193	
245	2399.193	
246	2409.193	
247	2419.193	
248	2429.193	
249	2439.193	
250	2449.193	
251	2459.193	
252	2469.193	
253	2479.193	
254	2489.193	
255	2499.193	
256	2509.193	
257	2519.193	
258	2529.193	
259	2539.193	
260	2549.193	
261	2559.193	
262	2569.193	
263	2579.193	
264	2589.193	
265	2599.193	
266	2609.193	
267	2619.193	
268	2629.193	
269	2639.193	
270	2649.193	
271	2659.193	
272	2669.193	
273	2679.193	
274	2689.193	
275	2699.193	
276	2709.193	
277	2719.193	
278	2729.193	
279	2739.193	
280	2749.193	
281	2759.193	
282	2769.193	
283	2779.193	
284	2789.193	
285	2799.193	
286	2809.193	
287	2819.193	
288	2829.193	
289	2839.193	
290	2849.193	
291	2859.193	
292	2869.193	
293	2879.193	
294	2889.193	
295	2899.193	
296	2909.193	
297	2919.193	
298	2929.193	
299	2939.193	
300	2949.193	
301	2959.193	
302	2969.193	
303	2979.193	
304	2989.193	
305	2999.193	
306	3009.193	
307	3019.193	
308	3029.193	
309	3039.193	
310	3049.193	
311	3059.193	
312	3069.193	
313	3079.193	
314	3089.193	
315	3099.193	
316	3109.193	
317	3119.193	
318	3129.193	
319	3139.193	
320	3149.193	
321	3159.193	
322	3169.193	
323	3179.193	
324	3189.193	
325	3199.193	
326	3209.193	
327	3219.193	
328	3229.193	
329	3239.193	
330	3249.193	
331	3259.193	
332	3269.193	
333	3279.193	
334	3289.193	
335	3299.193	
336	3309.193	
337	3319.193	
338	3329.193	
339	3339.193	
340	3349.193	
341	3359.193	
342	3369.193	
343	3379.193	
344	3389.193	
345	3399.193	
346	3409.193	
347	3419.193	
348	3429.193	
349	3439.193	
350	3449.193	
351	3459.193	
352	3469.193	
353	3479.193	
354	3489.193	
355	3499.193	
356	3509.193	
357	3519.193	
358	3529.193	
359	3539.193	
360	3549.193	
361	3559.193	
362	3569.193	
363	3579.193	
364	3589.193	
365	3599.193	
366	3609.193	
367	3619.193	
368	3629.193	
369	3639.193	
370	3649.193	
371	3659.193	
372	3669.193	
373	3679.193	
374	3689.193	
375	3699.193	
376	3709.193	
377	3719.193	
378	3729.193	
379	3739.193	
380	3749.193	
381	3759.193	
382	3769.193	
383	3779.193	
384	3789.193	
385	3799.193	
386	3809.193	
387	3819.193	
388	3829.193	
389	3839.193	
390	3849.193	
391	3859.193	
392	3869.193	
393	3879.193	
394	3889.193	
395	3899.193	
396	3909.193	
397	3919.193	
398	3929.193	
399	3939.193	
400	3949.193	
401	3959.193	
402	3969.193	
403	3979.193	
404	3989.193	
405	3999.193	
406	4009.193	
407	4019.193	
408	4029.193	
409	4039.193	
410	4049.193	
411	4059.193	
412	4069.193	
413	4079.193	
414	4089.193	
415	4099.193	
416	4109.193	
417	4119.193	
418	4129.193	
419	4139.193	
420	4149.193	
421	4159.193	
422	4169.193	
423	4179.193	
424	4189.193	
425	4199.193	
426	4209.193	
42		

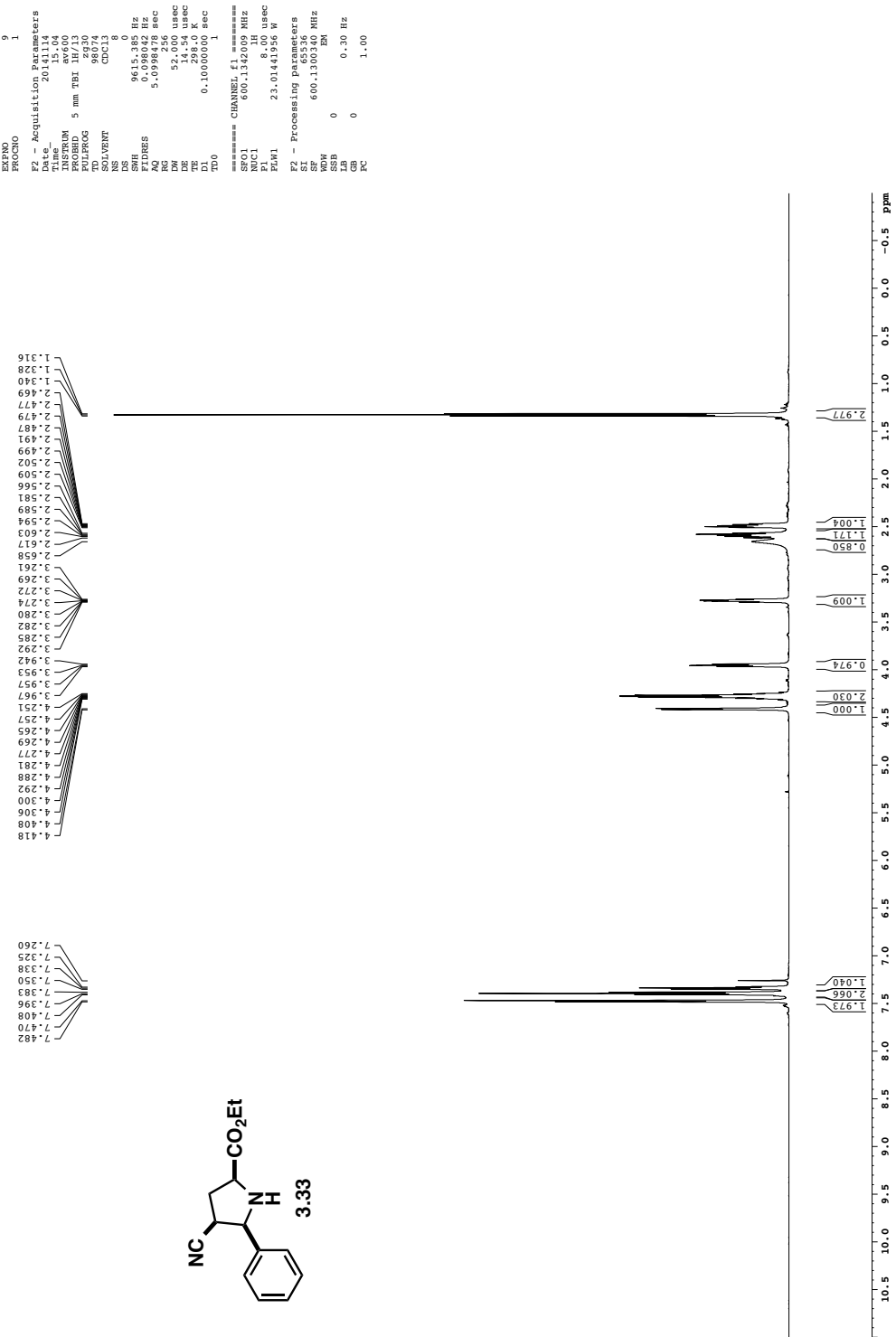
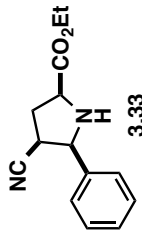


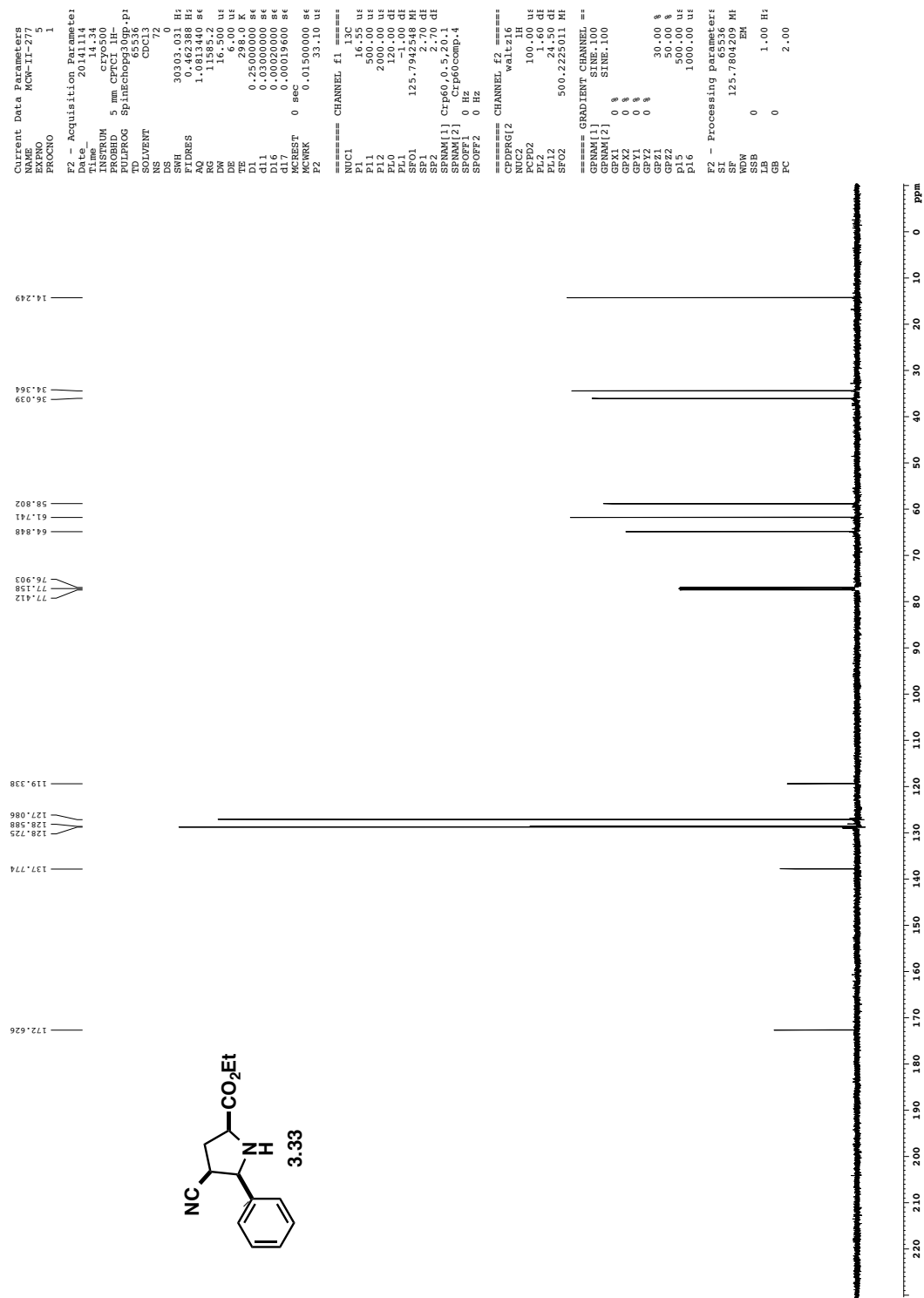
125A
exo
noesygp



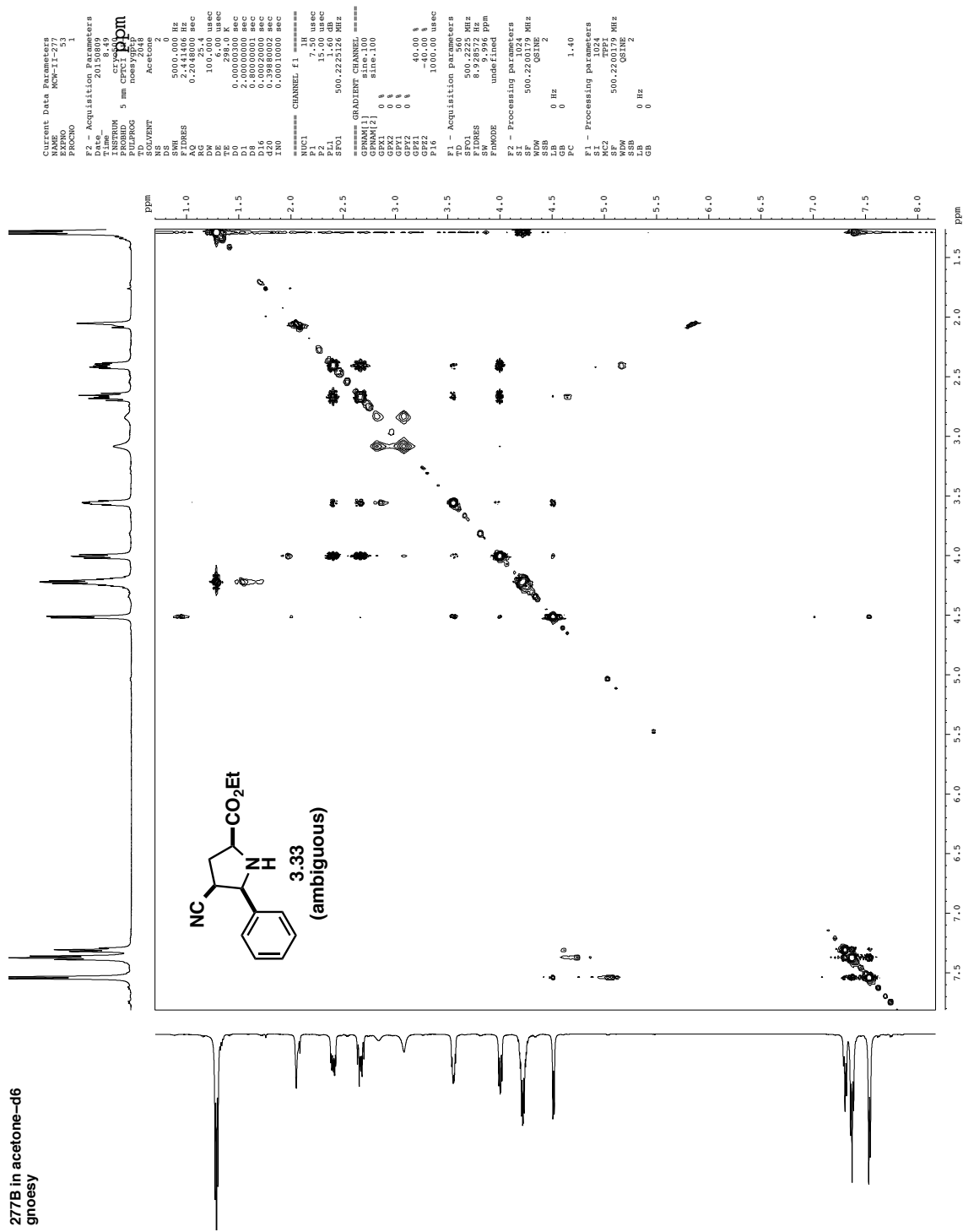
249

277B for 1H-1H 2D

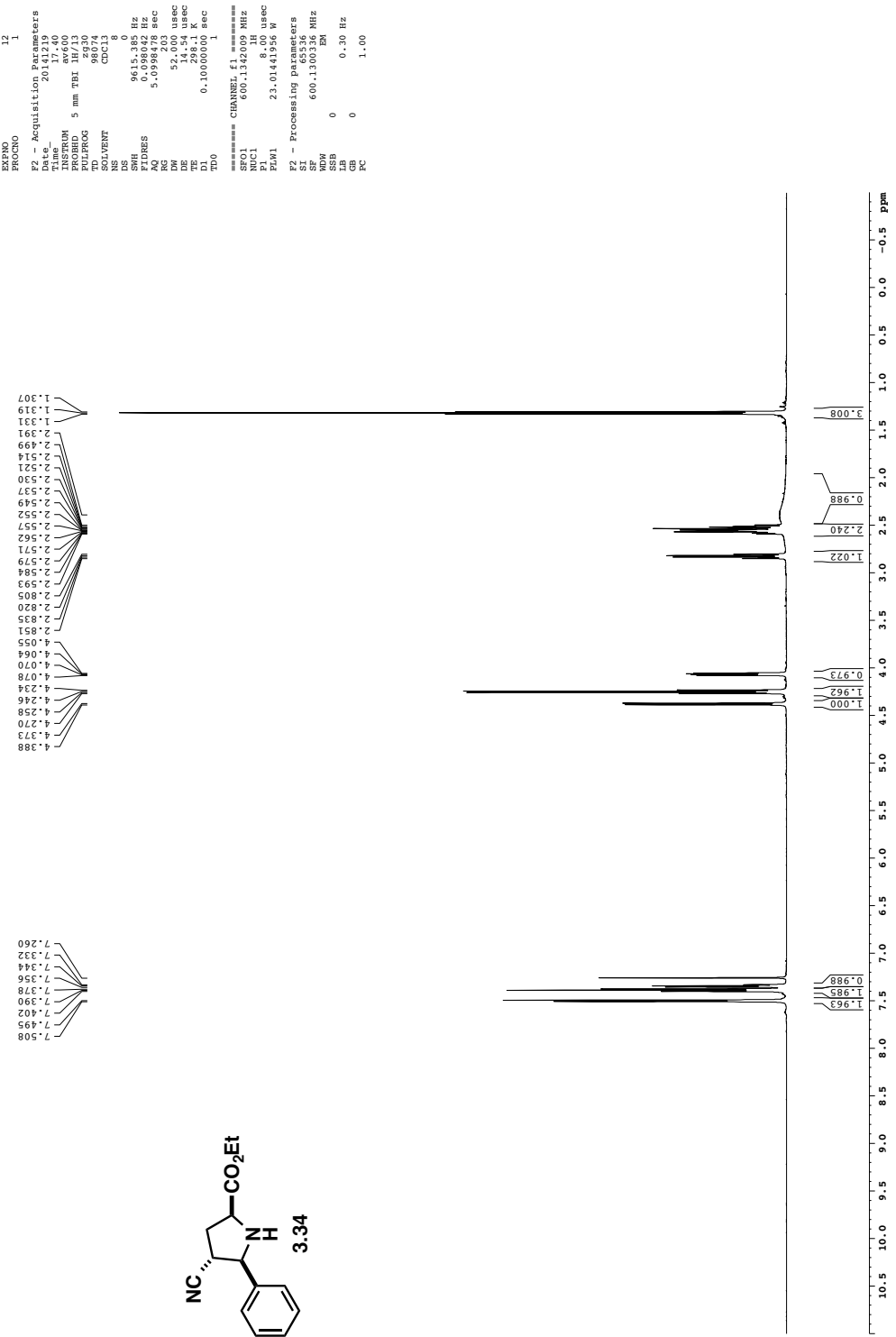
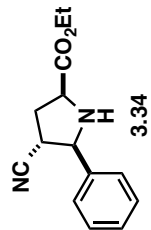


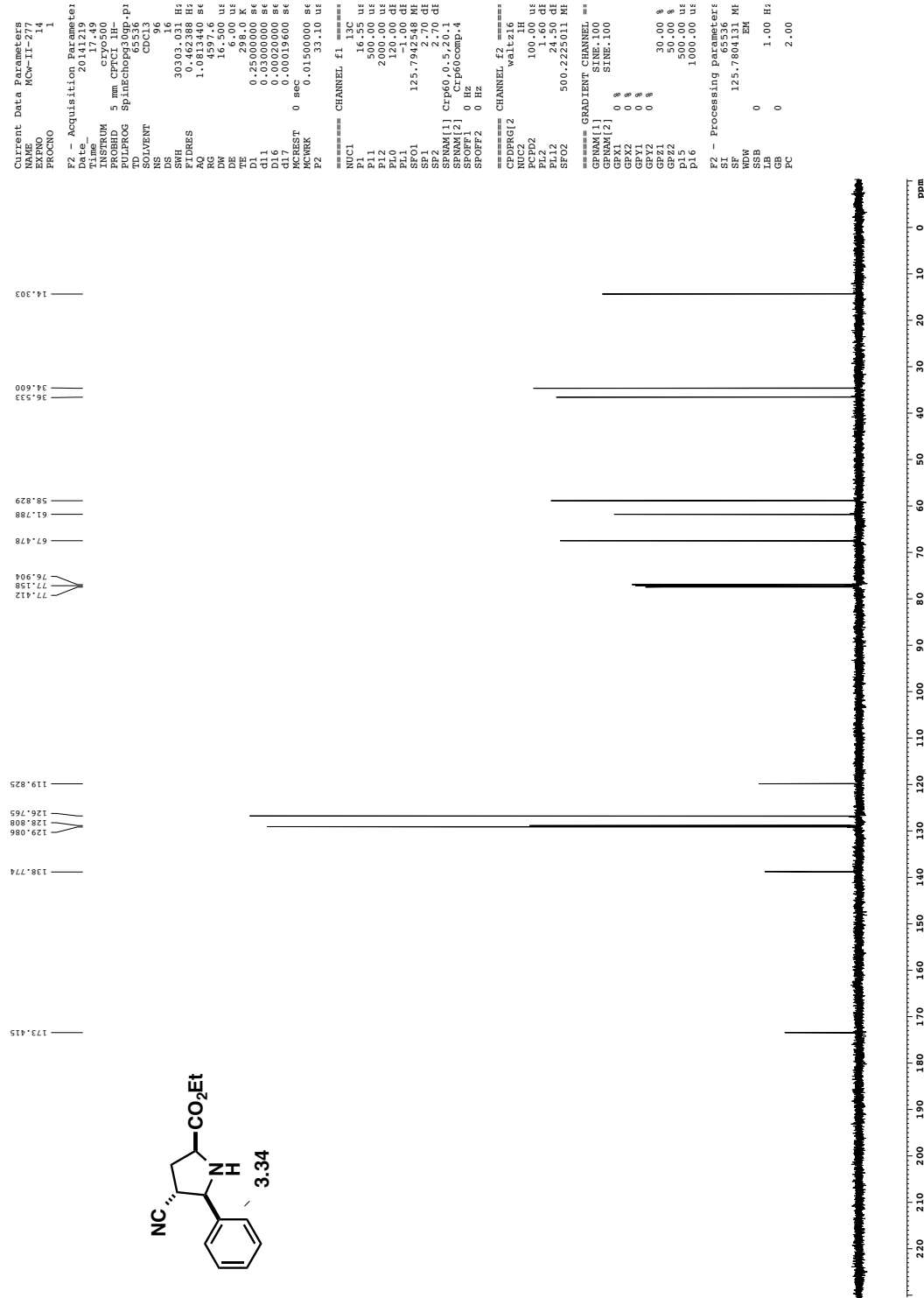


**277B in acetone-d₆
gnoesy**

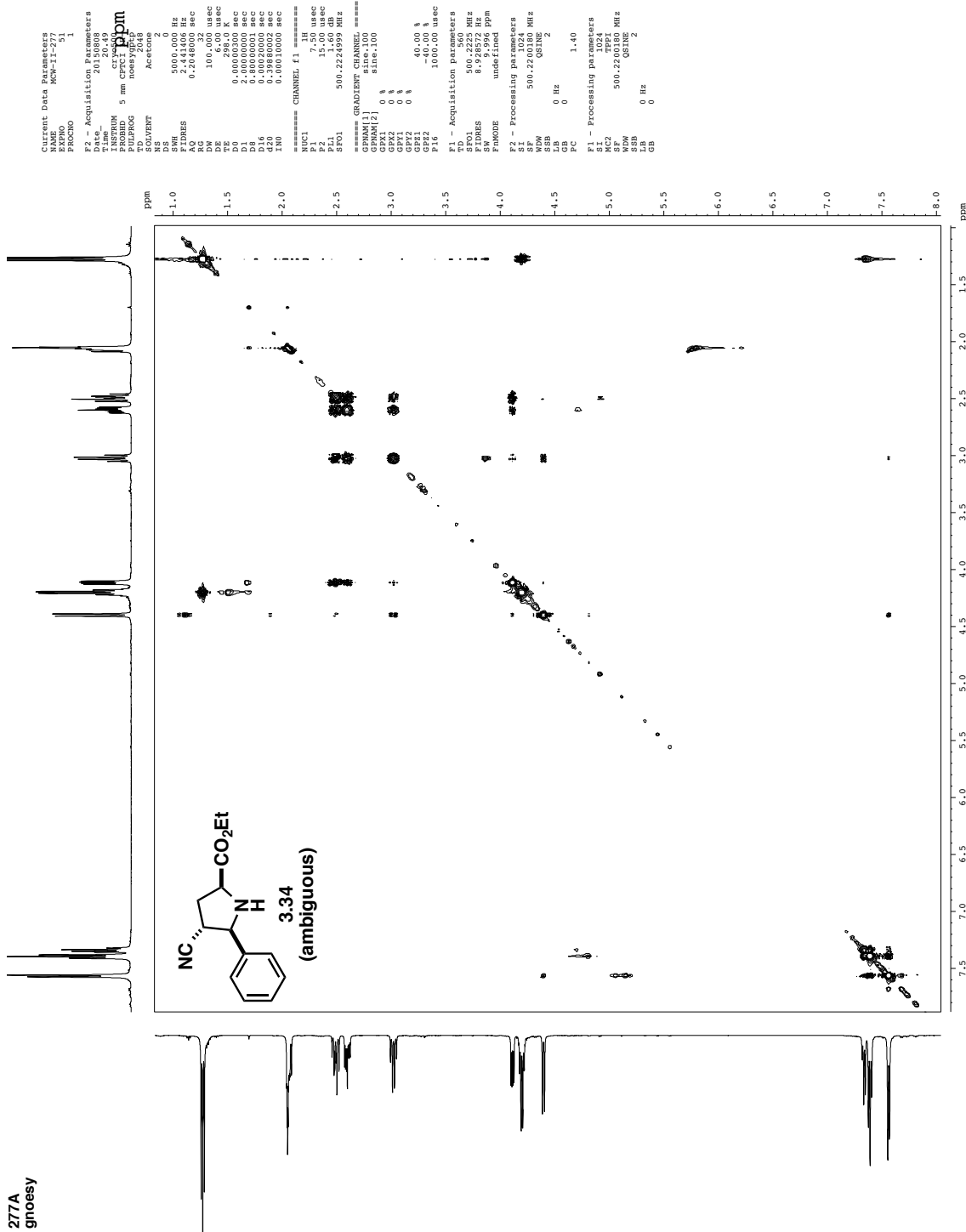


277A Fr 85-90

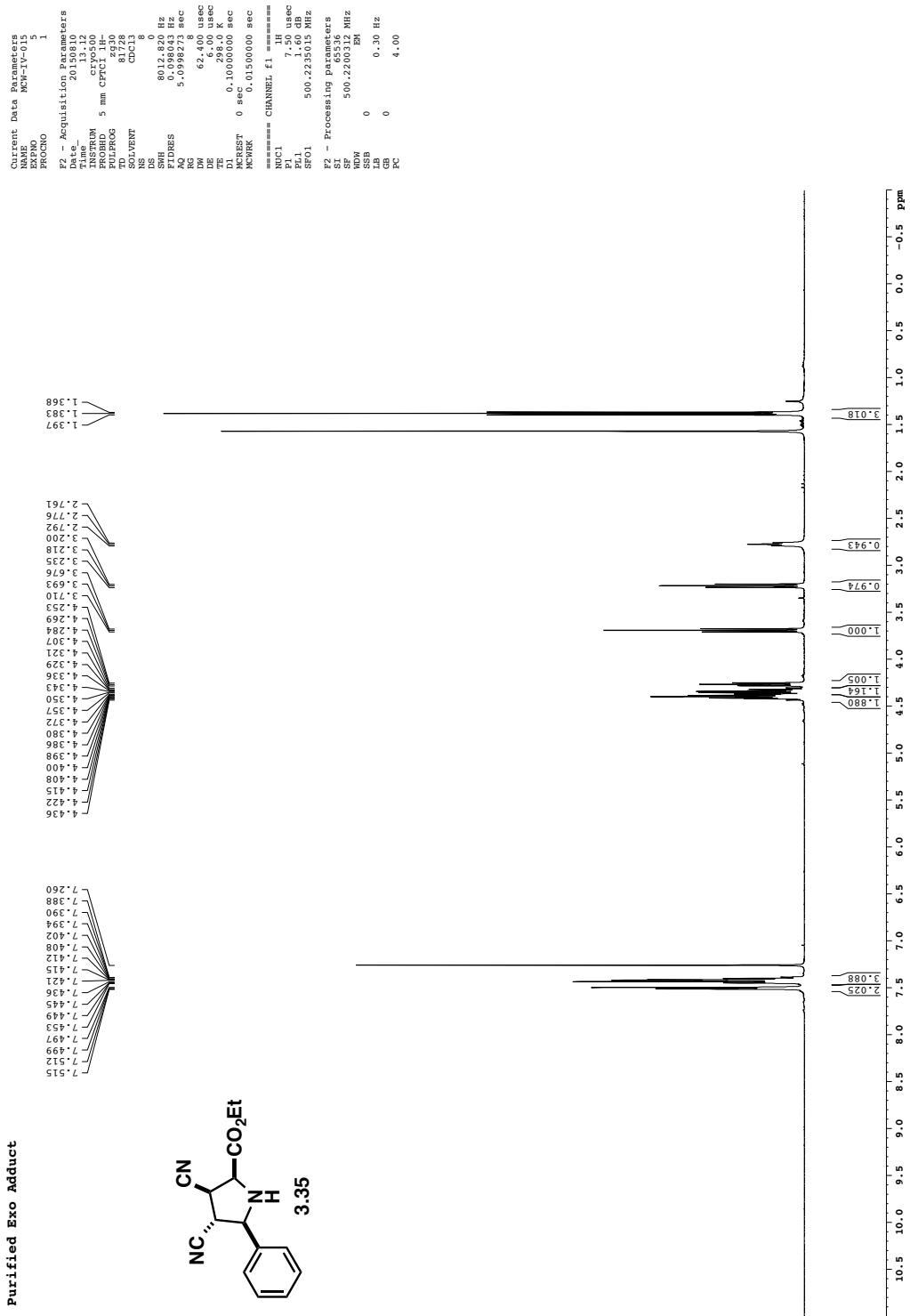
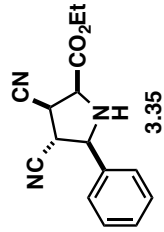




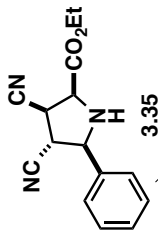
277A
gnosis



Purified Exo Adduct



Purified Exo Adduct



Current Data Parameters
NAME MCW-IV-015
EXPCNO 6
PROCNO 1

F2 - Acquisition Parameters
TE time 13.110
TR time 20.0
TI time 13.110
D1 time 13.110
TD 65336
PULPROG SpinEchop33Op.p1
INSTRUM cryo500
PROBID 5 mm CP/PC1 1H
SOLVENT CDCl3
NS 160
DS 160
SWH 303.03 Hz
ETDRES 1.081340 sec
AQ 0.462388 Hz
RG 9195.2
DW 16.500 us
DE 6.500 us
TE 250.000 us
TM 0.250000 us
D1 0.0300000 sec
D11 0.0000000 sec
D16 0.00020000 sec
D17 0.00019600 sec
MCREST 0 sec
DW0 0.01500000 sec
P2 33.10 us

===== CHANNEL f1 =====
NUC1 13C
P1 16.55 us
P11 500.00 us
P12 2000.00 us
P2 120.00 us
PH 1.00 deg
SP01 125.7942340 MHz
SP1 2.70 GHz
SP2 Crp0,-0.5,20.1
SPNAM[1] Crp0,-0.5,20.1
SPNAM[2] Crp60,comp,-4
SPOFF1 0 Hz
SPOFF2 0 Hz

===== CHANNEL f2 =====
CPDRG1/2 walt16
NUC2 1H
PCPD2 100.00 us
PL12 1.60 deg
PL12 24.50 deg
SF12 500.225011 MHz

===== GRADIENT CHANNEL ==
GPNAME[1] SINE100
GPNAME[2] SINE100
GPX1 0 %
GPX2 0 %
GPY1 0 %
GPY2 0 %
GPZ1 30.00 %
GPZ2 50.00 %
P15 500.00 us
P16 1000.00 us

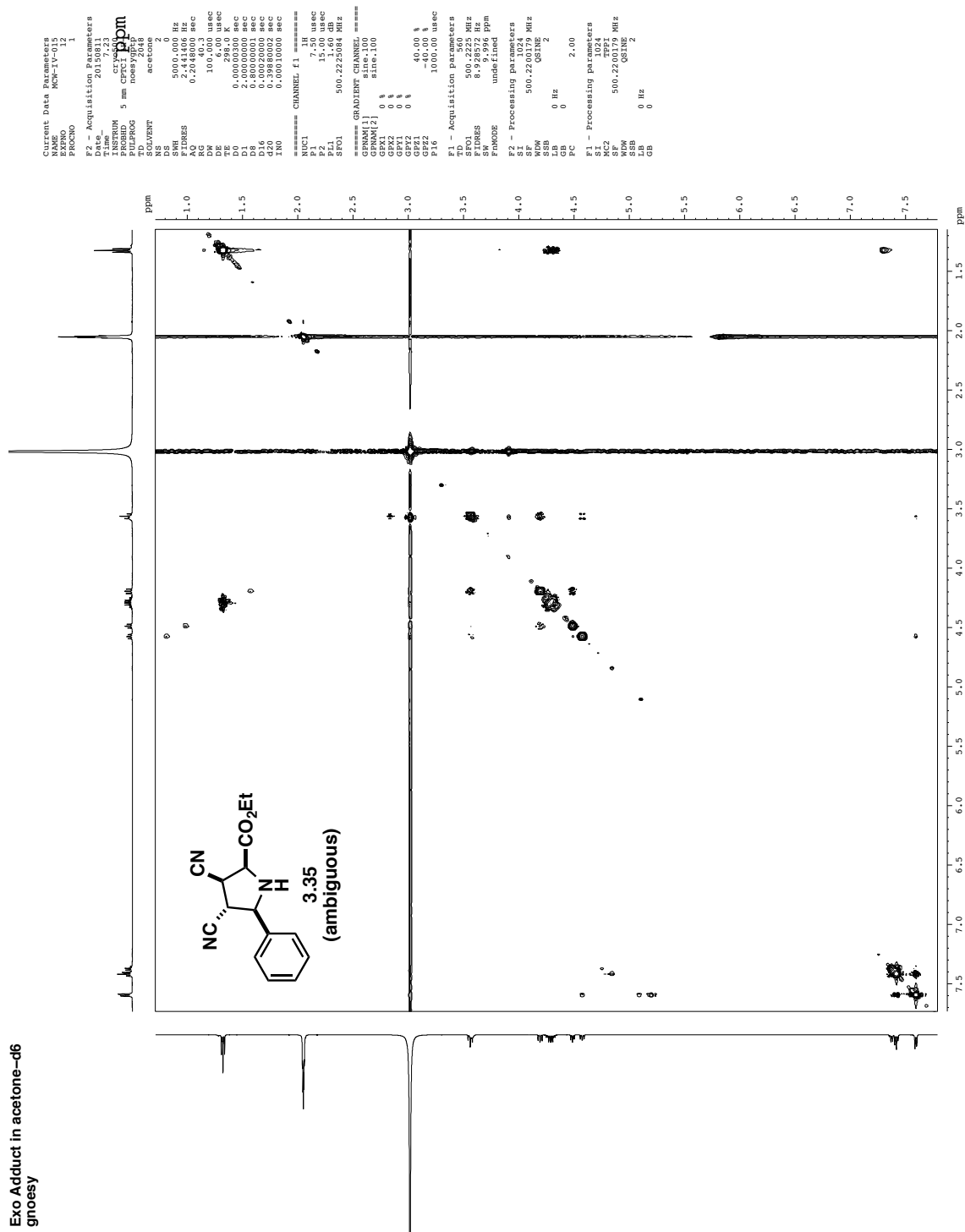
F2 - Processing Parameters
SF 125.7804480 Hz
SP EM
NDW 0
SSB 0
LB 1.00 Hz
GB 0
PC 2.00

169.279
136.455
126.779
124.471
123.607
116.942
77.159
77.045
67.977
61.779
61.793
41.541
37.577
14.242

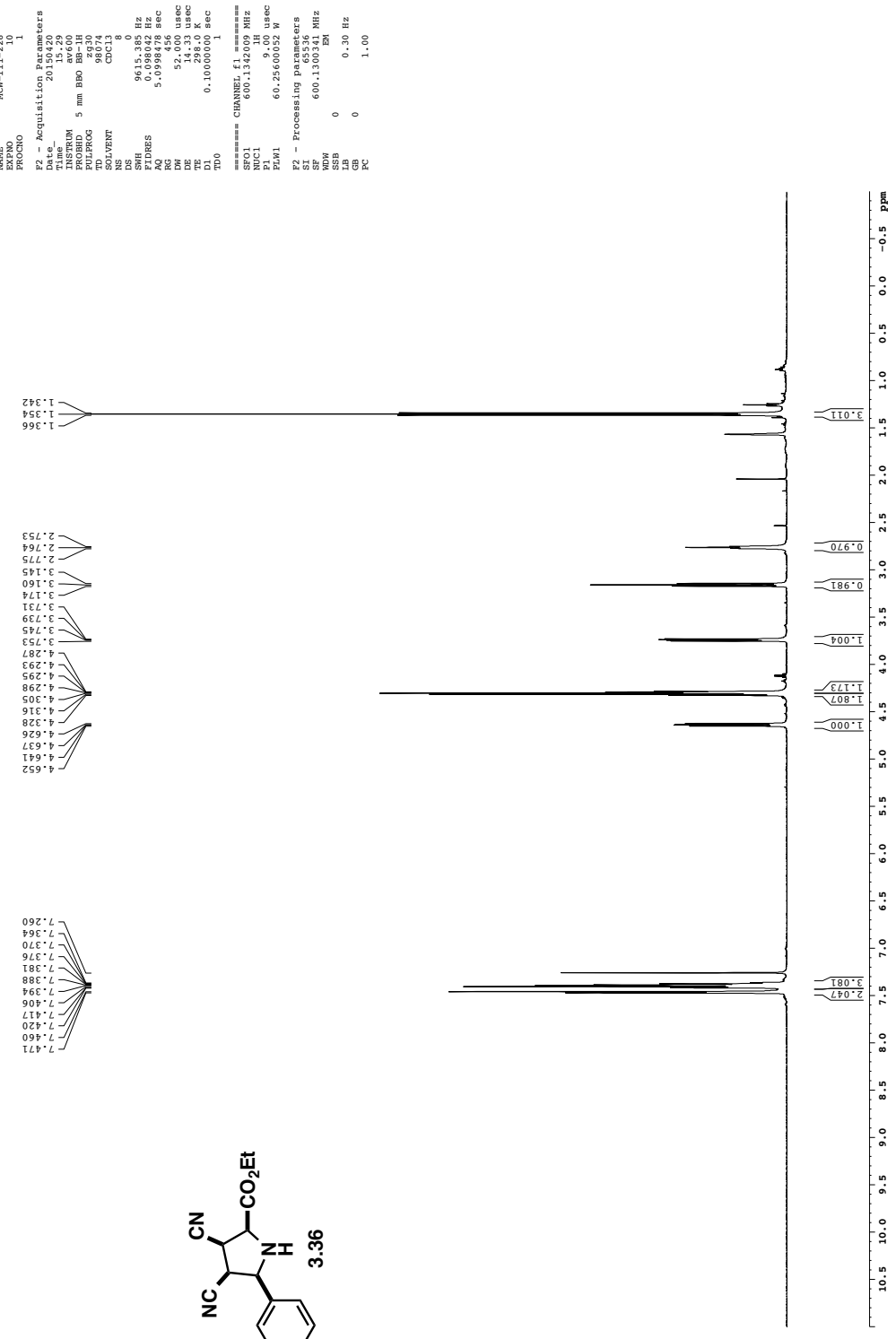
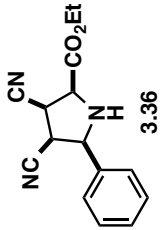
220 210 200 190 180 170 160 150 140 130 120 110 100 90 80 70 60 50 40 30 20 10 0 ppm

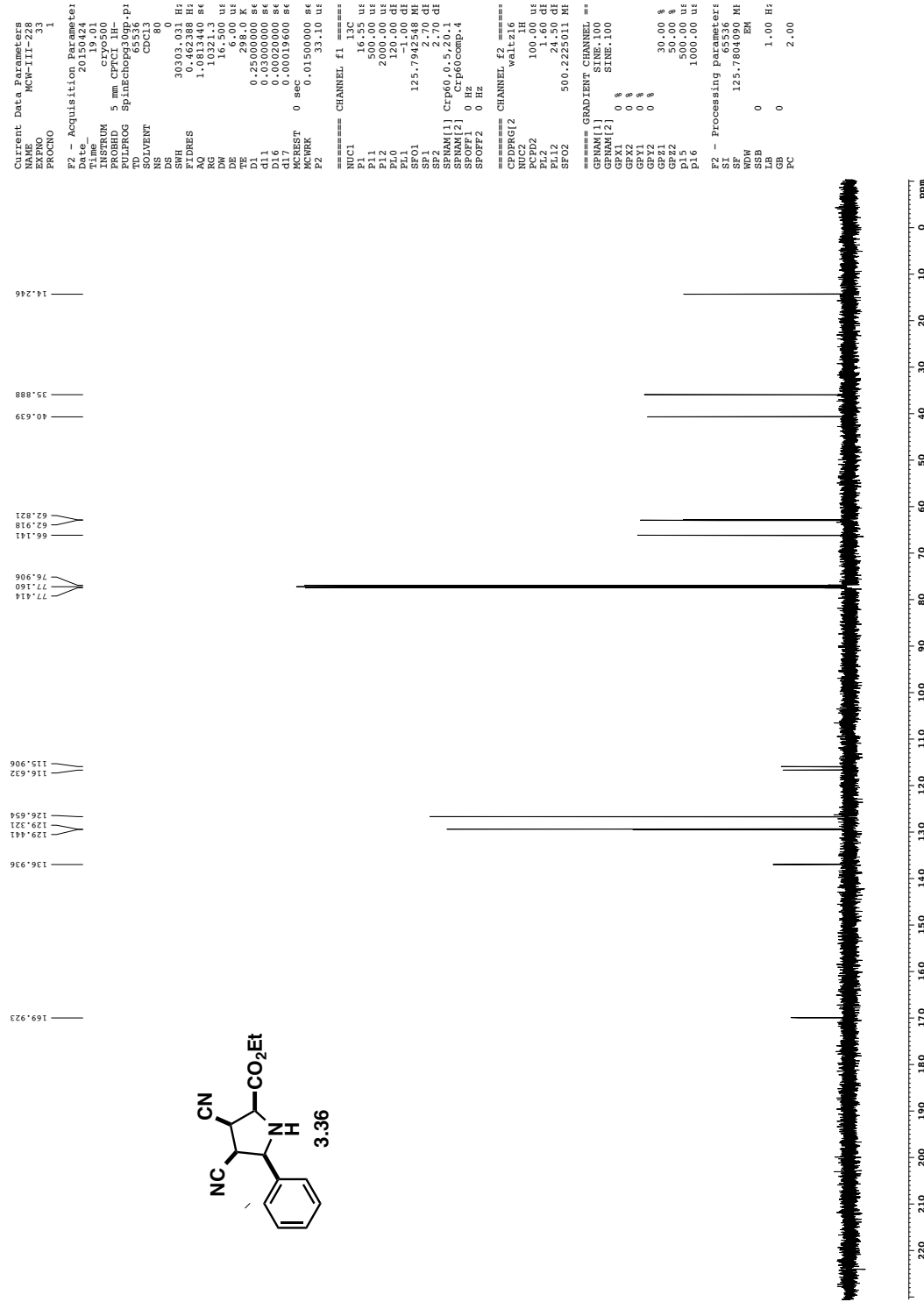
CN(C)C1CC(C(=O)C2=CC=C(C=C2)N1)C(C(=O)C)C

**Exo Adduct in acetone-d₆
gnoesy**

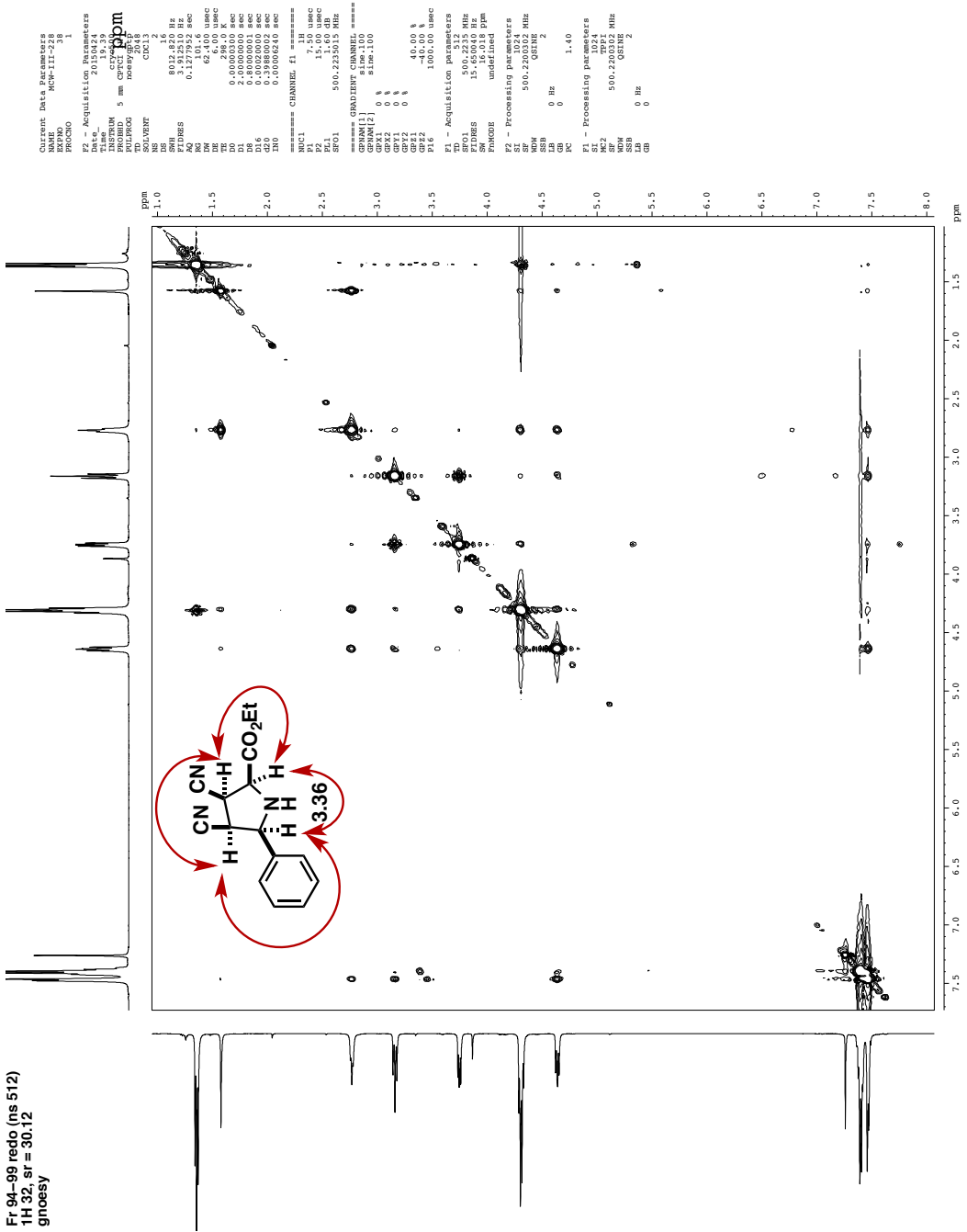


Fr 94-99 redo

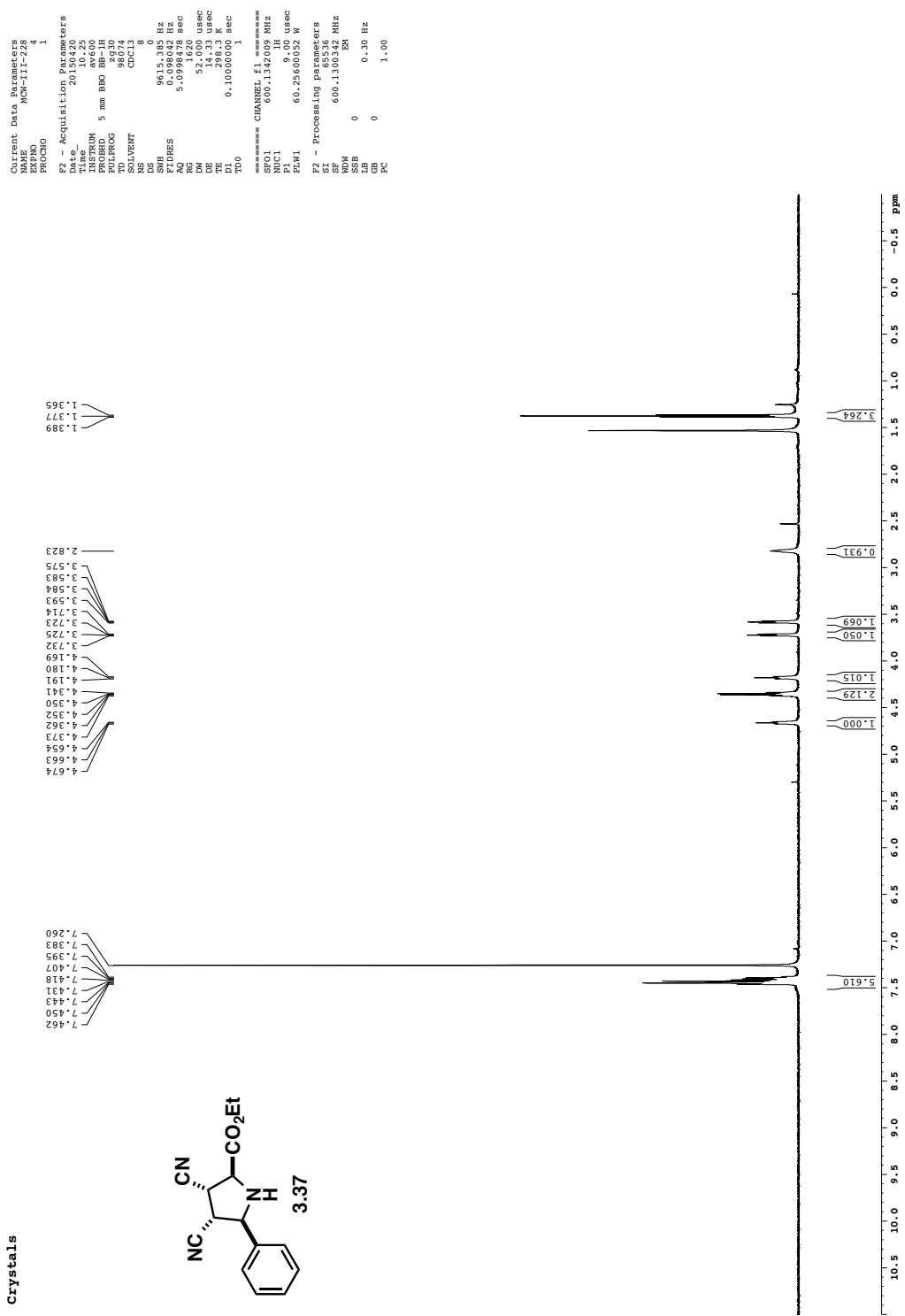
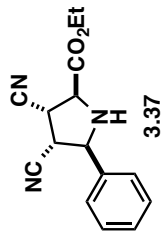




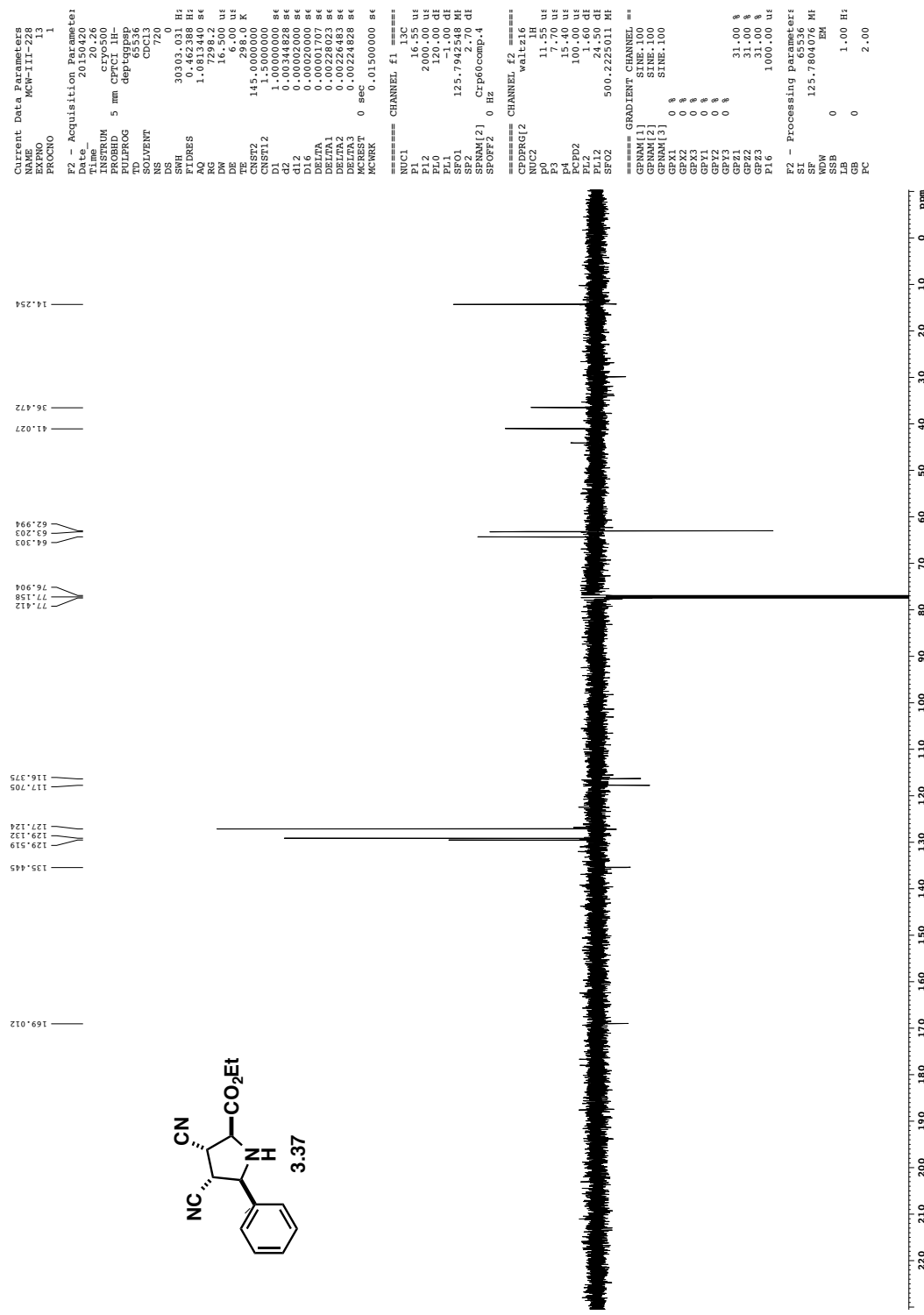
Fr 94-99 redo (ns 512)
 ^1H 32, $\text{sr} = 30.12$
 gnoesy

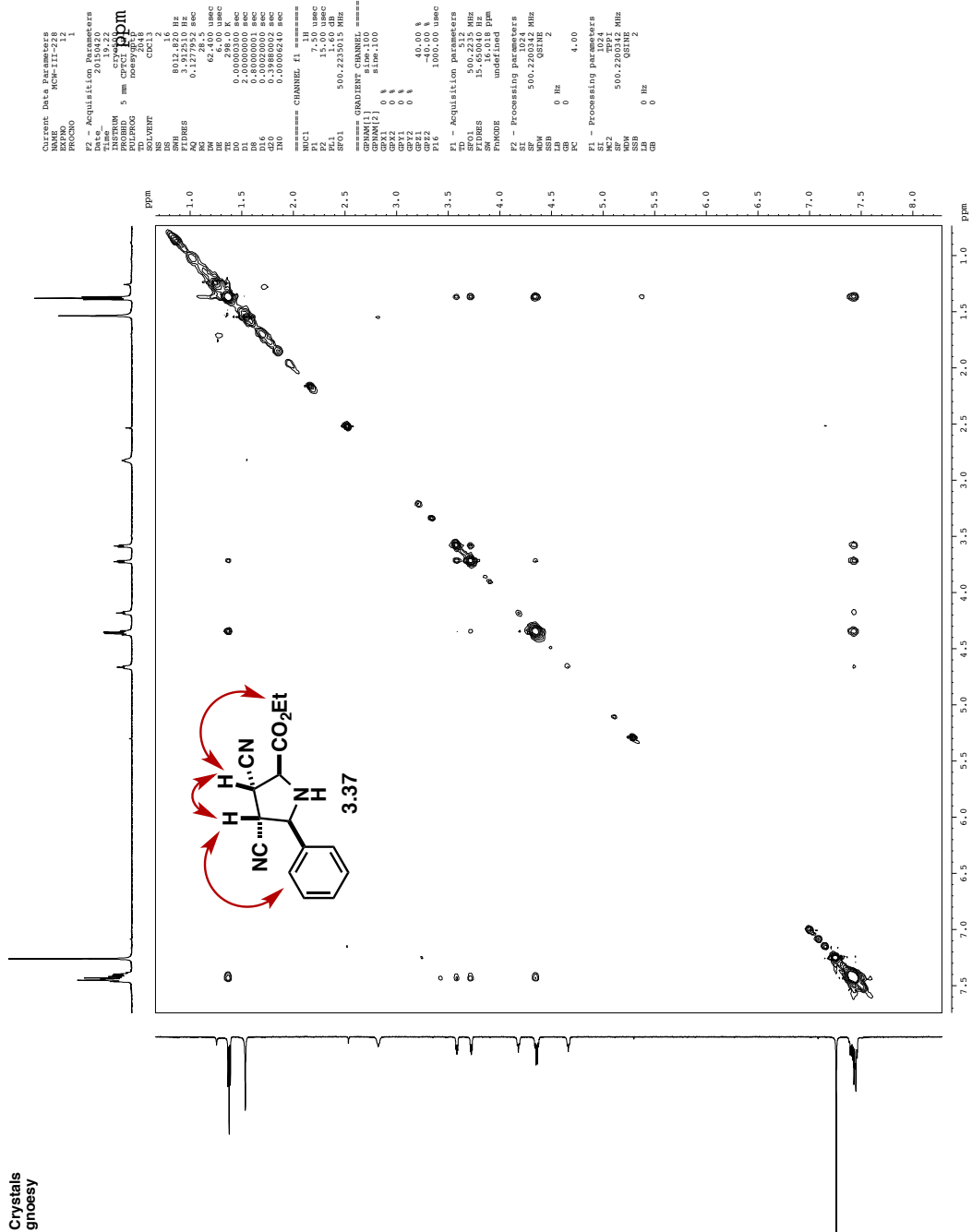


Crystals

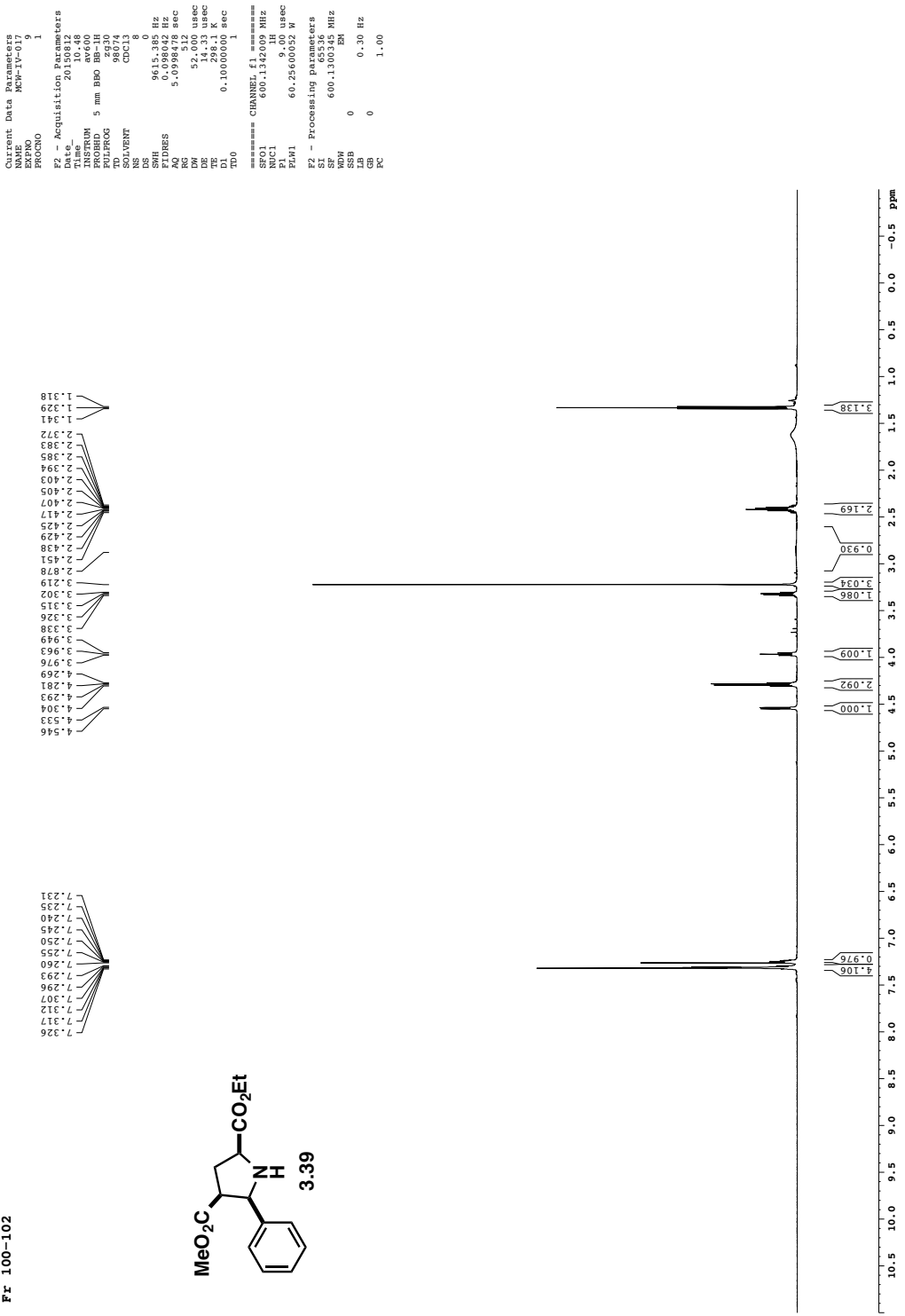


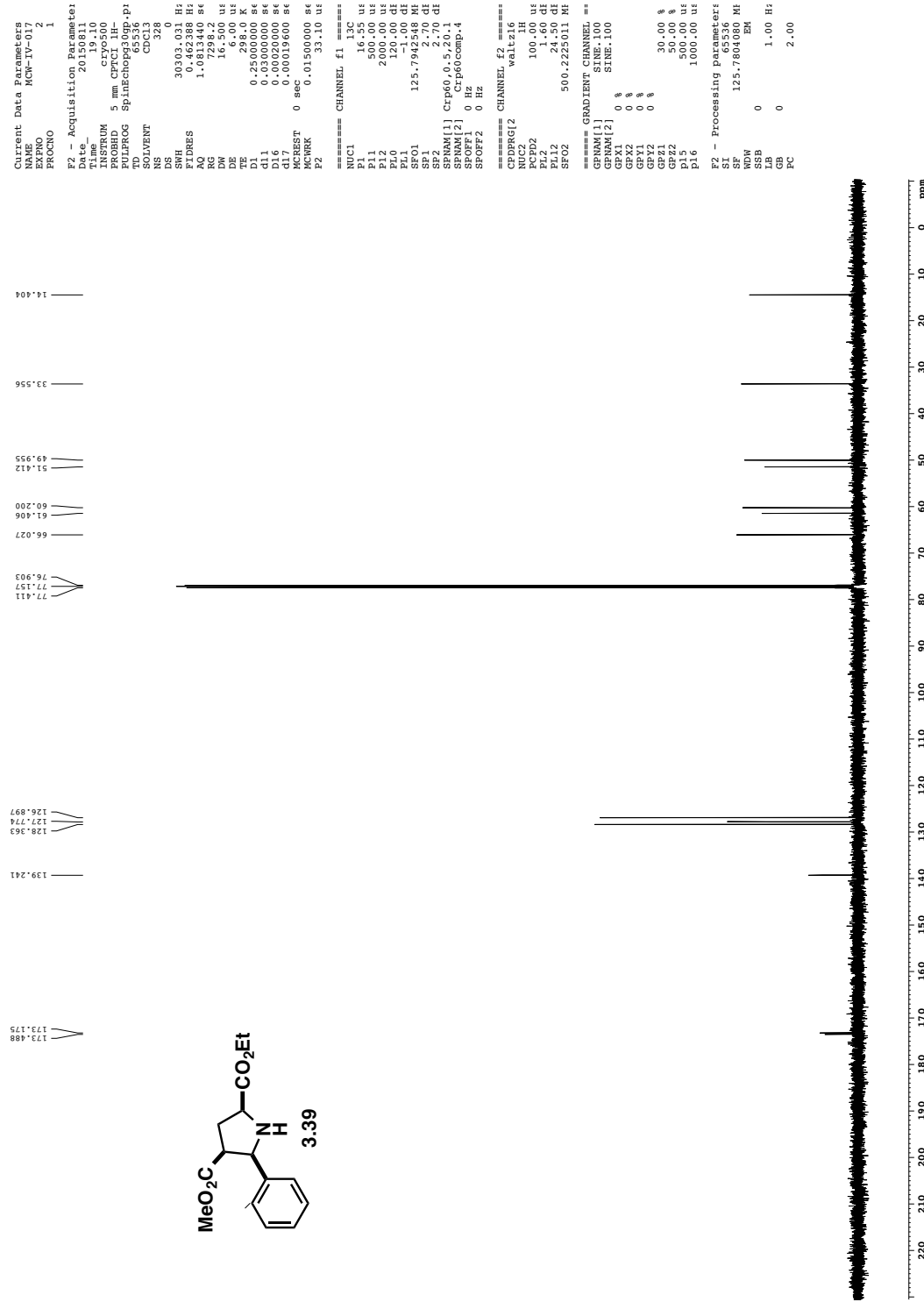
Crystals
deptq 13C spectrum with 1H decoupling (CH & CH₃ one way up; C, CH₂ and solvent the other)



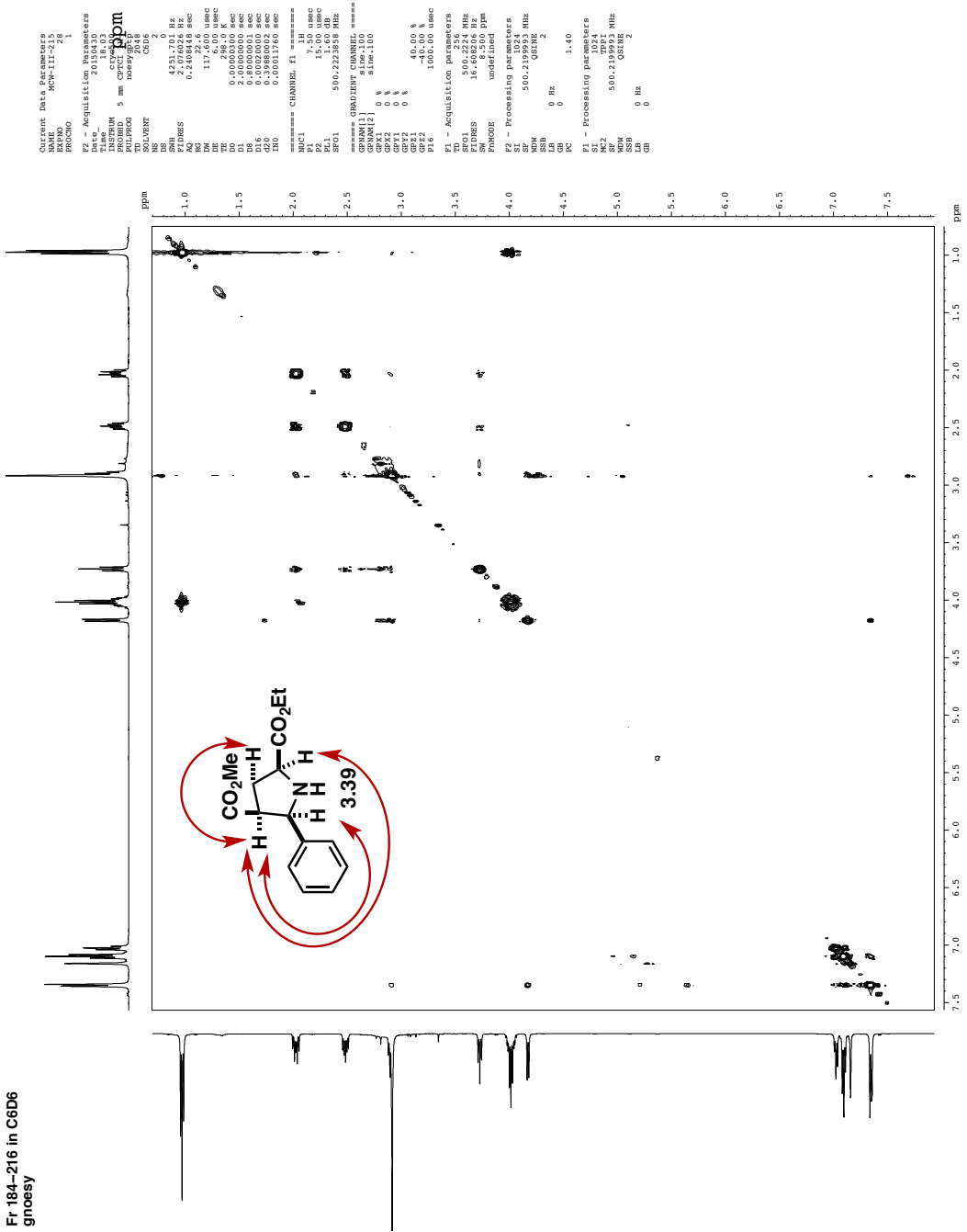


Fr 100-102

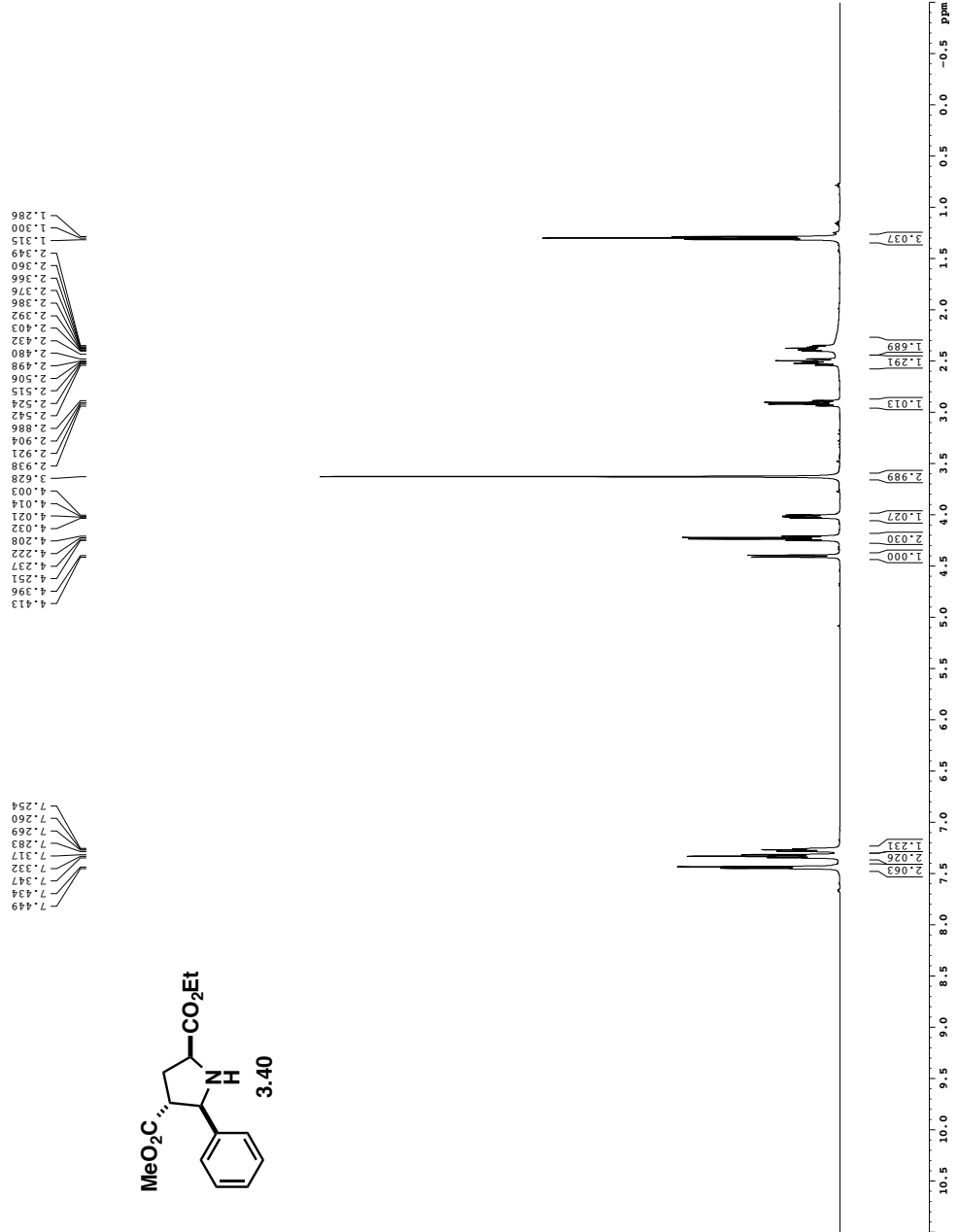
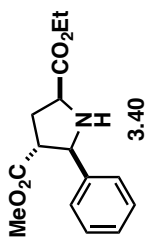


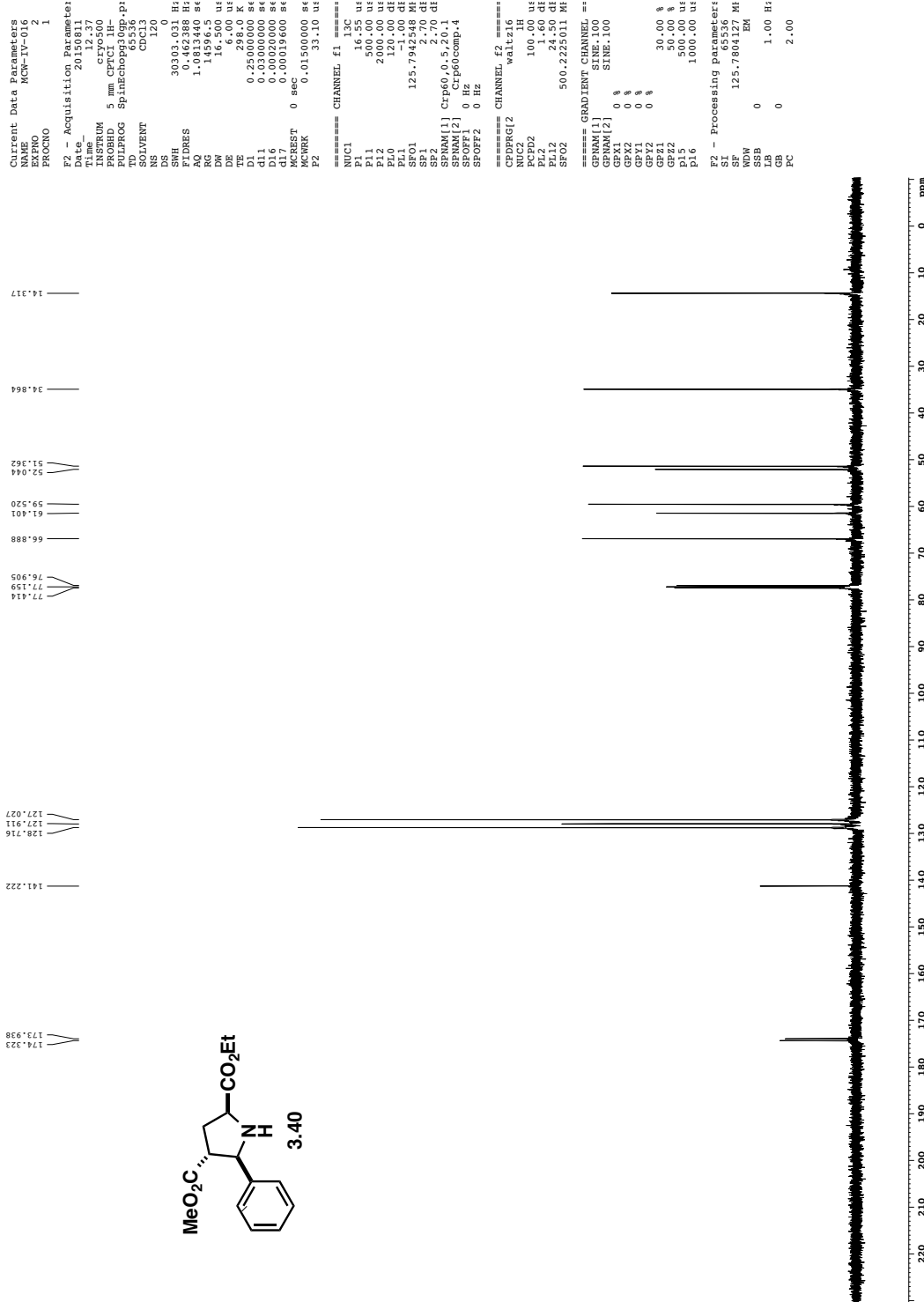
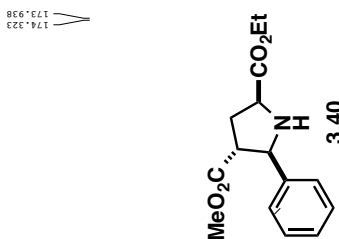


Fr 184–216 in C6D6
gnoesy

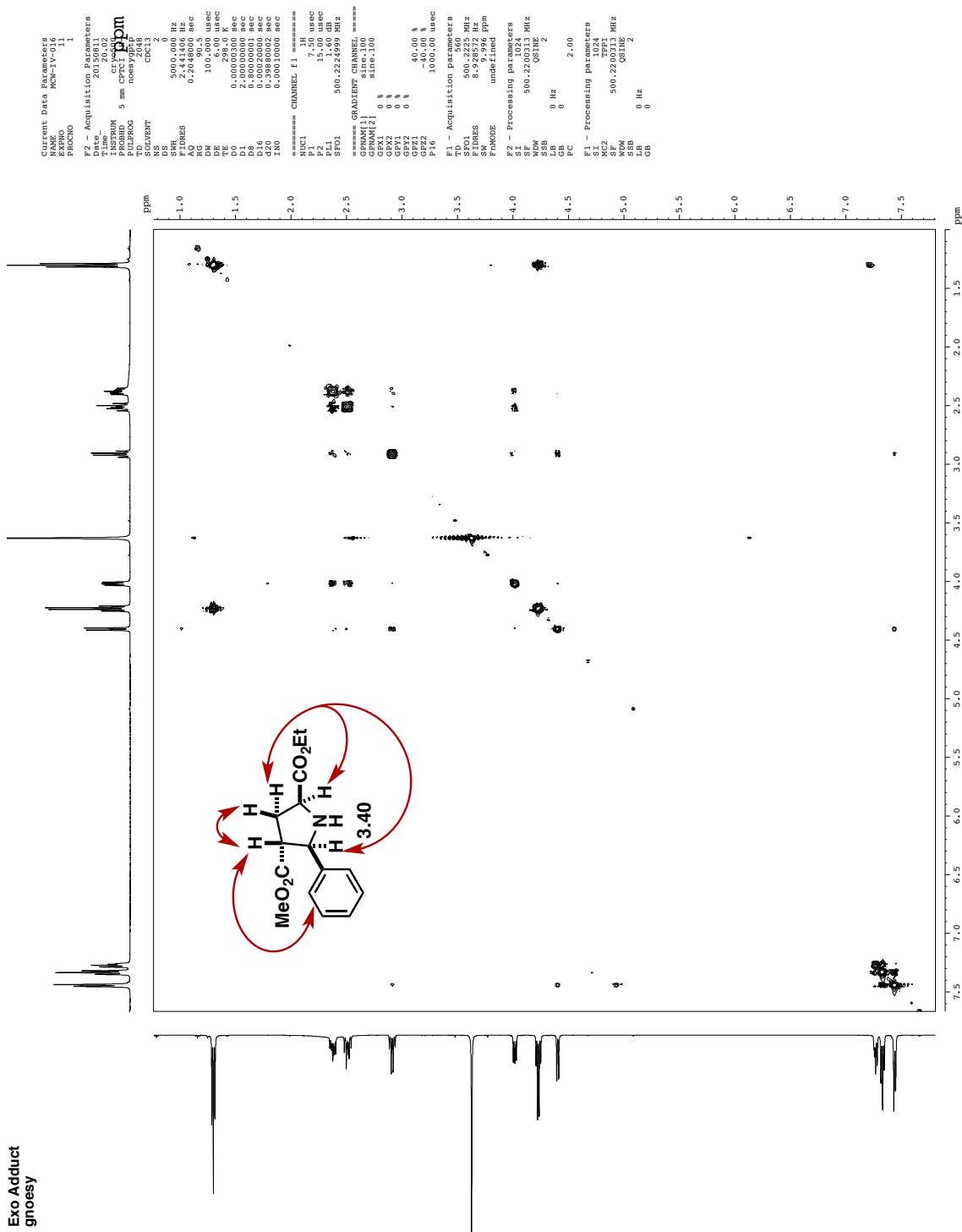


Purified Product



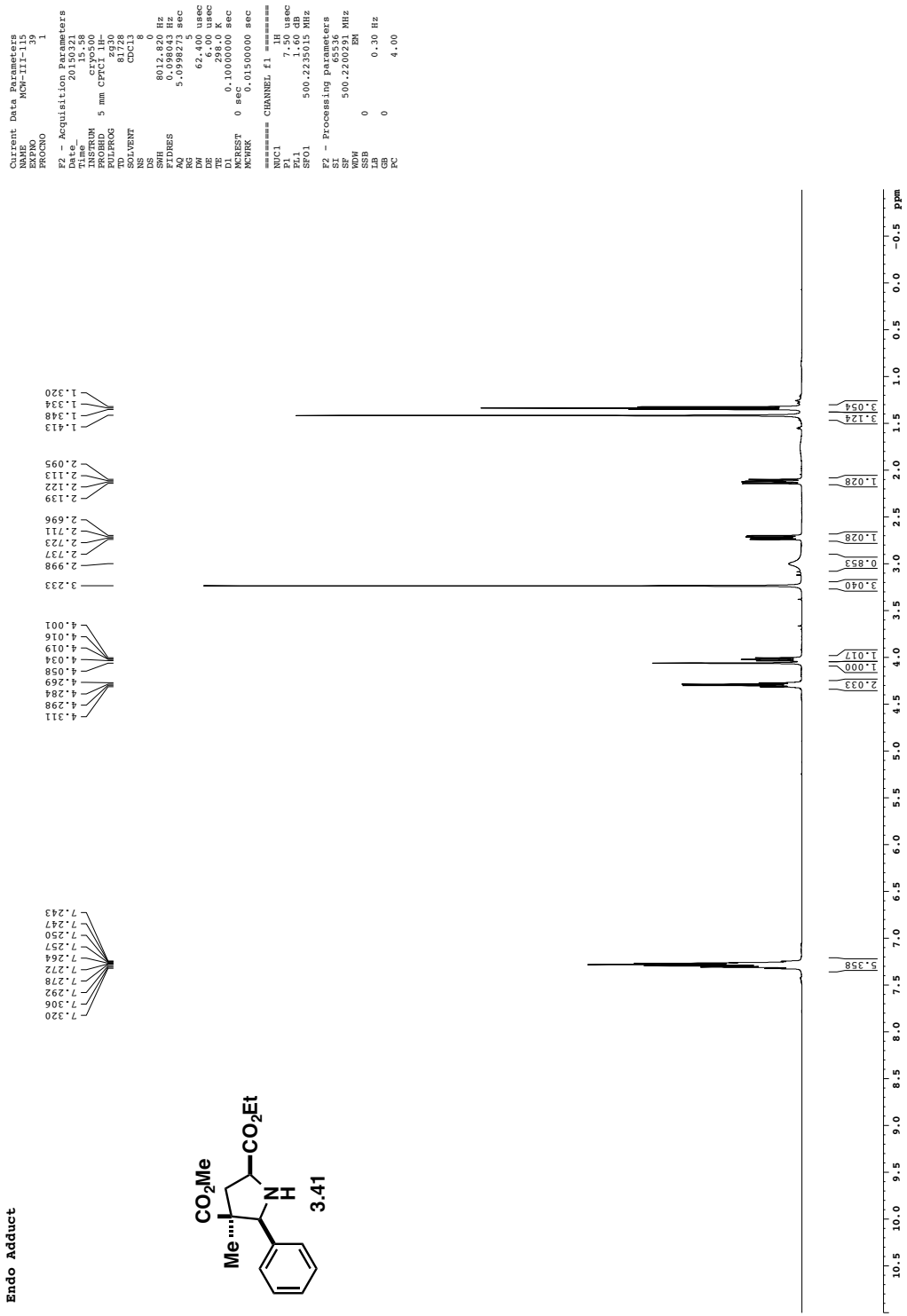


Exo Adduct
gnoesy

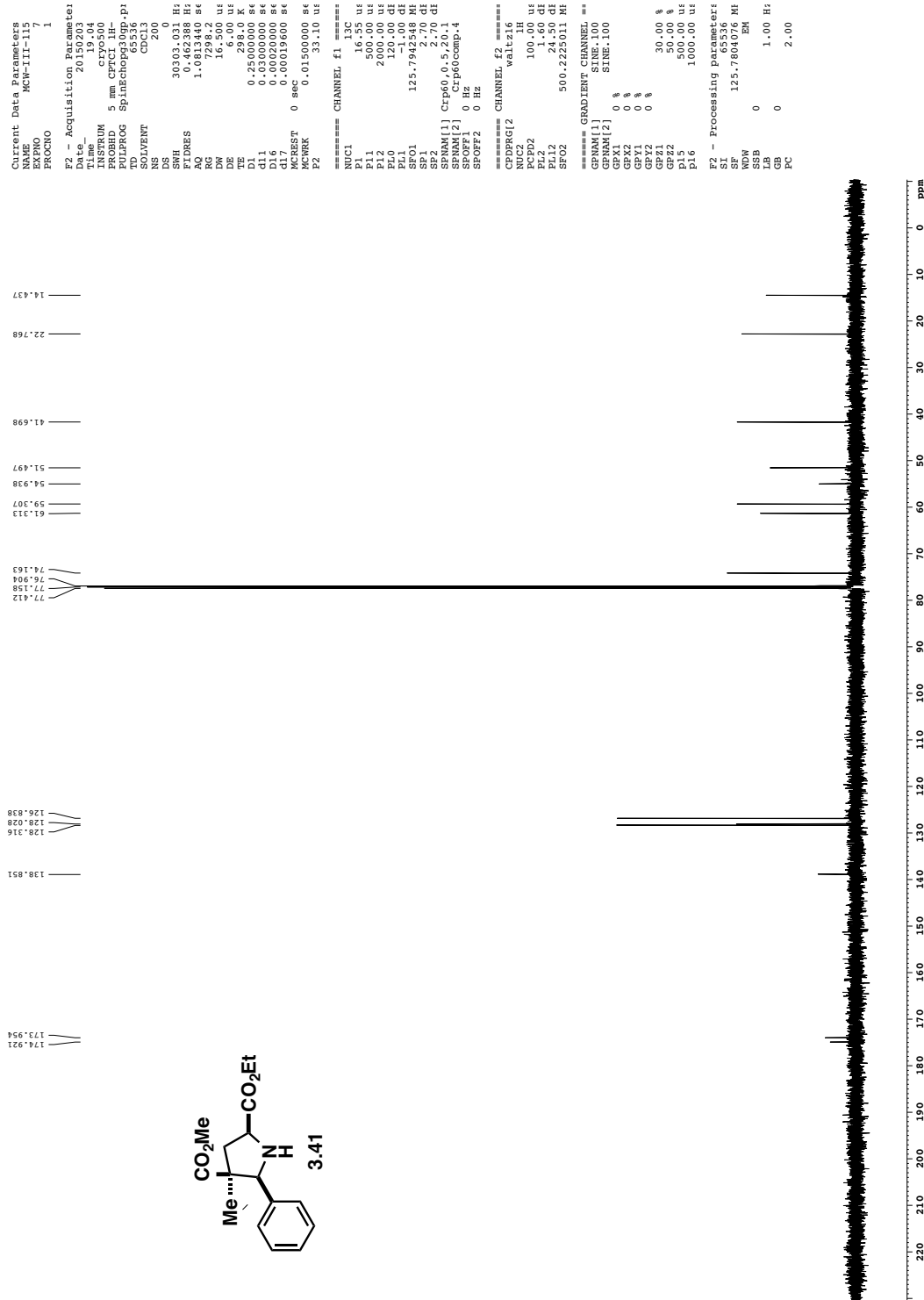


270

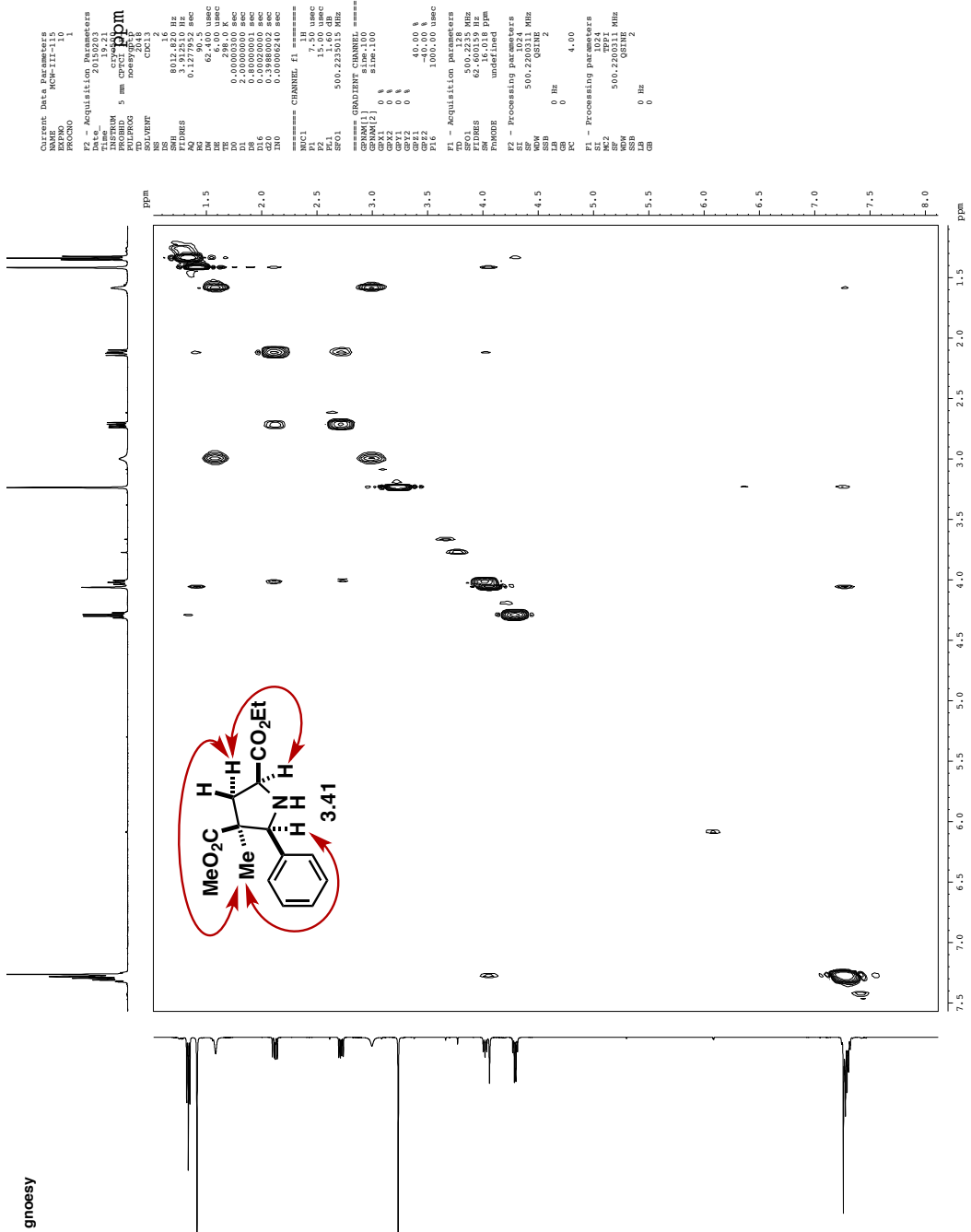
Endo Adduct



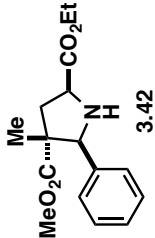
Endo Adduct



gnoesy



EX 49-51



0.85 ppm

0.948

1.982

1.960

1.970

1.300

1.312

1.323

2.647

2.746

2.761

2.767

2.769

3.445

4.002

4.014

4.017

4.029

4.231

4.232

4.236

4.242

4.244

4.254

4.256

4.268

4.696

7.240

7.243

7.246

7.254

7.260

7.265

7.268

7.296

7.309

7.334

7.337

7.341

7.345

7.349

7.353

7.357

7.361

7.365

7.369

7.373

7.377

7.381

7.385

7.389

7.393

7.397

7.401

7.405

7.409

7.413

7.417

7.421

7.425

7.429

7.433

7.437

7.441

7.445

7.449

7.453

7.457

7.461

7.465

7.469

7.473

7.477

7.481

7.485

7.489

7.493

7.497

7.501

7.505

7.509

7.513

7.517

7.521

7.525

7.529

7.533

7.537

7.541

7.545

7.549

7.553

7.557

7.561

7.565

7.569

7.573

7.577

7.581

7.585

7.589

7.593

7.597

7.601

7.605

7.609

7.613

7.617

7.621

7.625

7.629

7.633

7.637

7.641

7.645

7.649

7.653

7.657

7.661

7.665

7.669

7.673

7.677

7.681

7.685

7.689

7.693

7.697

7.701

7.705

7.709

7.713

7.717

7.721

7.725

7.729

7.733

7.737

7.741

7.745

7.749

7.753

7.757

7.761

7.765

7.769

7.773

7.777

7.781

7.785

7.789

7.793

7.797

7.801

7.805

7.809

7.813

7.817

7.821

7.825

7.829

7.833

7.837

7.841

7.845

7.849

7.853

7.857

7.861

7.865

7.869

7.873

7.877

7.881

7.885

7.889

7.893

7.897

7.901

7.905

7.909

7.913

7.917

7.921

7.925

7.929

7.933

7.937

7.941

7.945

7.949

7.953

7.957

7.961

7.965

7.969

7.973

7.977

7.981

7.985

7.989

7.993

7.997

8.001

8.005

8.009

8.013

8.017

8.021

8.025

8.029

8.033

8.037

8.041

8.045

8.049

8.053

8.057

8.061

8.065

8.069

8.073

8.077

8.081

8.085

8.089

8.093

8.097

8.101

8.105

8.109

8.113

8.117

8.121

8.125

8.129

8.133

8.137

8.141

8.145

8.149

8.153

8.157

8.161

8.165

8.169

8.173

8.177

8.181

8.185

8.189

8.193

8.197

8.201

8.205

8.209

8.213

8.217

8.221

8.225

8.229

8.233

8.237

8.241

8.245

8.249

8.253

8.257

8.261

8.265

8.269

8.273

8.277

8.281

8.285

8.289

8.293

8.297

8.301

8.305

8.309

8.313

8.317

8.321

8.325

8.329

8.333

8.337

8.341

8.345

8.349

8.353

8.357

8.361

8.365

8.369

8.373

8.377

8.381

8.385

8.389

8.393

8.397

8.401

8.405

8.409

8.413

8.417

8.421

8.425

8.429

8.433

8.437

8.441

8.445

8.449

8.453

8.457

8.461

8.465

8.469

8.473

8.477

8.481

8.485

8.489

8.493

8.497

8.501

8.505

8.509

8.513

8.517

8.521

8.525

8.529

8.533

8.537

8.541

8.545

8.549

8.553

8.557

8.561

8.565

8.569

8.573

8.577

8.581

8.585

8.589

8.593

8.597

8.601

8.605

8.609

8.613

8.617

8.621

8.625

8.629

8.633

8.637

8.641

8.645

8.649

8.653

8.657

8.661

8.665

8.669

8.673

8.677

8.681

8.685

8.689

8.693

8.697

8.701

8.705

8.709

8.713

8.717

8.721

8.725

8.729

8.733

8.737

8.741

8.745

8.749

8.753

8.757

8.761

8.765

8.769

8.773

8.777

8.781

8.785

8.789

8.793

8.797

8.801

8.805

8.809

8.813

8.817

8.821

8.825

8.829

8.833

8.837

8.841

8.845

8.849

8.853

8.857

8.861

8.865

8.869

8.873

8.877

8.881

8.885

8.889

8.893

8.897

8.901

8.905

8.909

8.913

8.917

8.921

8.925

8.929

8.933

8.937

8.941

8.945

8.949

8.953

8.957

8.961

8.965

8.969

8.973

8.977

8.981

8.985

8.989

8.993

8.997

9.001

9.005

9.009

9.013

9.017

9.021

9.025

9.029

9.033

9.037

9.041

9.045

9.049

9.053

9.057

9.061

9.065

9.069

9.073

9.077

9.081

9.085

9.089

9.093

9.097

9.101

9.105

9.109

9.113

9.117

9.121

9.125

9.129

9.133

9.137

9.141

9.145

9.149

9.153

9.157

9.161

9.165

9.169

9.173

9.177

9.181

9.185

9.189

9.193

9.197

9.201

9.205

9.209

9.213

9.217

9.221

9.225

9.229

9.233

9.237

9.241

9.245

9.249

9.253

9.257

9.261

9.265

9.269

9.273

9.277

9.281

9.285

9.289

9.293

9.297

9.301

9.305

9.309

9.313

9.317

9.321

9.325

9.329

9.333

9.337

9.341

9.345

9.349

9.353

9.357

9.361

9.365

9.369

9.373

9.377

9.381

9.385

9.389

9.393

9.397

9.401

9.405

9.409

9.413

9.417

9.421

9.425

9.429

9.433

9.437

9.441

9.445

9.449

9.453

9.457

9.461

9.465

9.469

9.473

9.477

9.481

9.485

9.489

9.493

9.497

9.501

9.505

9.509

9.513

9.517

9.521

9.525

9.529

9.533

9.537

9.541

9.545

9.549

9.553

9.557

9.561

9.565

9.569

9.573

9.577

9.581

9.585

9.589

9.593

9.597

9.601

9.605

9.609

9.613

9.617

9.621

9.625

9.629

9.633

9.637

9.641

9.645

9.649

9.653

9.657

9.661

9.665

9.669

9.673

9.677

9.681

9.685

9.689

9.693

9.697

9.701

9.705

9.709

9.713

9.717

9.721

9.725

9.729

9.733

9.737

9.741

9.745

9.749

9.753

9.757

9.761

9.765

9.769

9.773

9.777

9.781

9.785

9.789

9.793

9.797

9.801

9.805

9.809

9.813

9.817

9.821

9.825

9.829

9.833

9.837

9.841

9.845

9.849

9.853

9.857

9.861

9.865

9.869

9.873

9.877

9.881

9.885

9.889

9.893

9.897

9.901

9.905

9.909

9.913

9.917

9.921

9.925

9.929

9.933

9.937

9.941

9.945

9.949

9.953

9.957

9.961

9.965

9.969

9.973

9.977

9.981

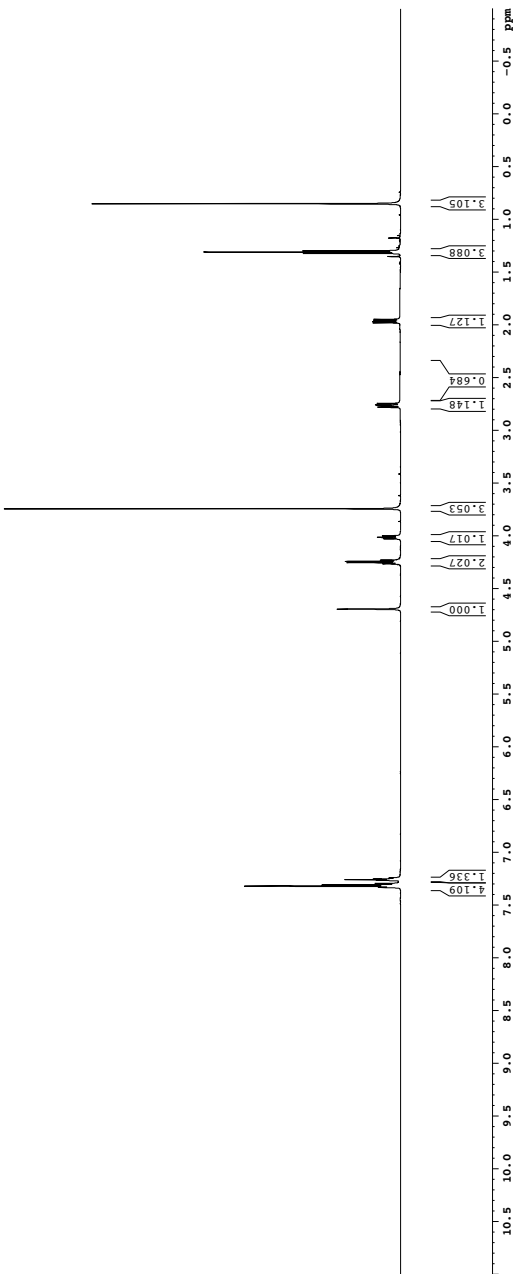
9.985

9.989

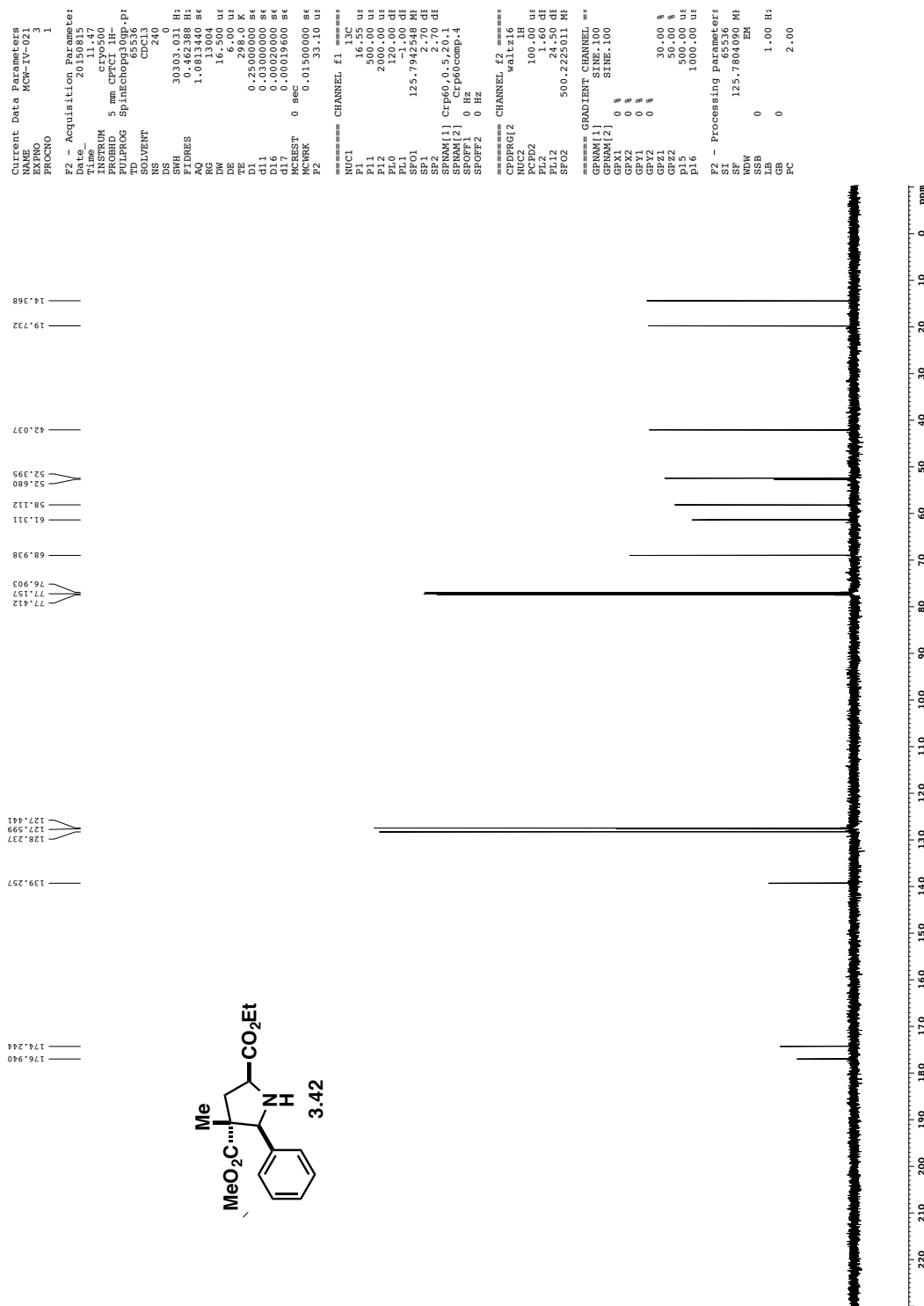
9.993

9.997

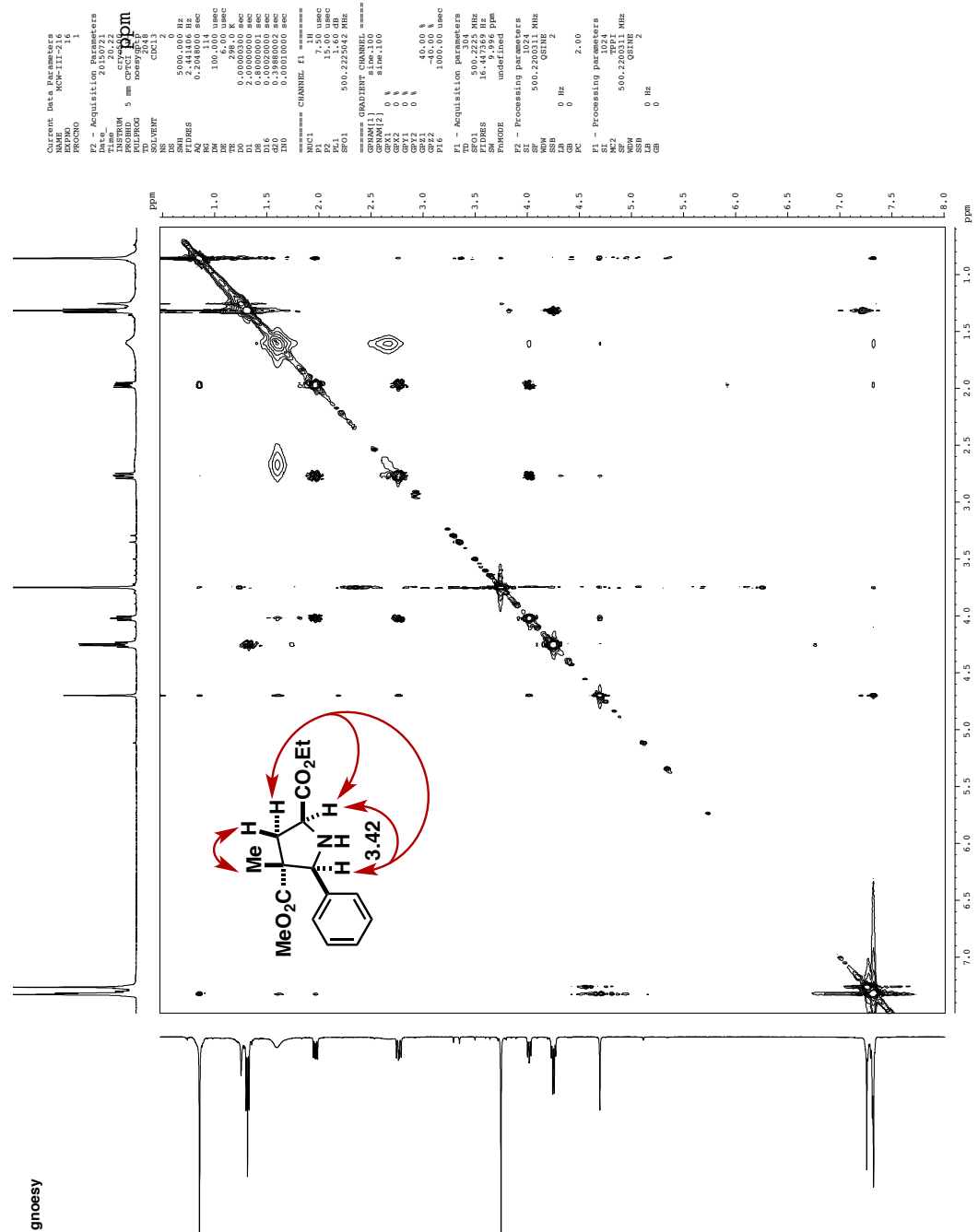
10.000



Purified Product



gnosis

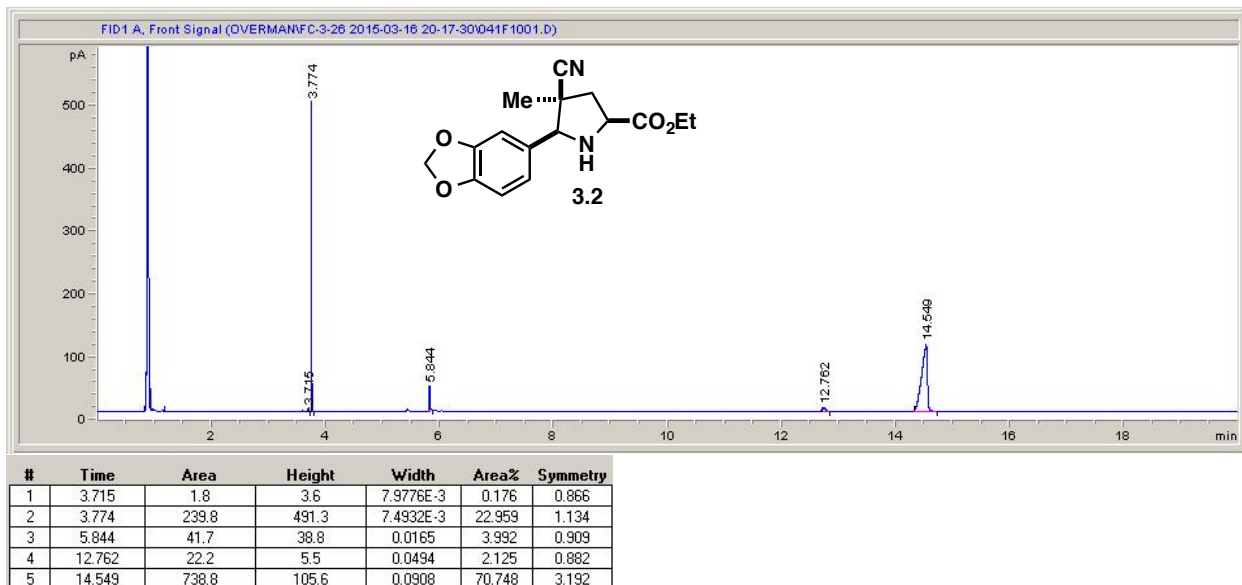


3.9 Appendix C: Representative GC-FID Chromatograms

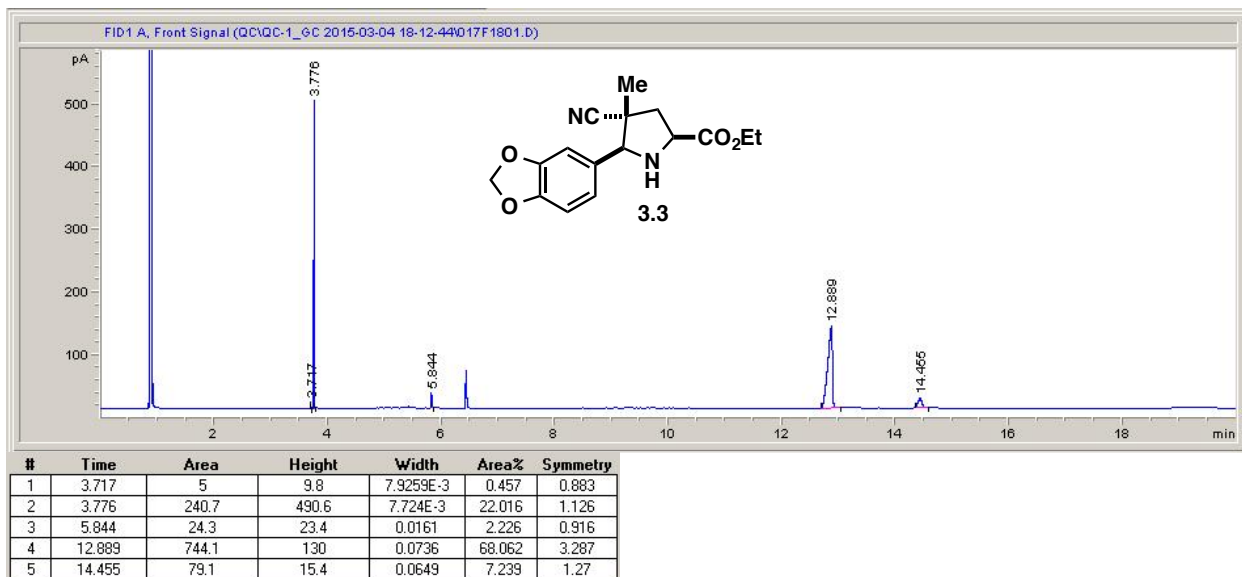
Table 3.18. GC-FID Response Factors for Starting Materials

entry	compound	retention time (t_R)	response factor (F)
1	1,3,5-trimethoxybenzene	3.8 min	(standard)
2	piperonal	3.7 min	0.976 ± 0.059
3	3.1	5.8 min	1.143 ± 0.016
4	4-methoxybenzaldehyde	3.5 min	1.242 ± 0.036
5	3.7	5.5 min	1.235 ± 0.026
6	3-methoxybenzaldehyde	3.1 min	1.033 ± 0.006
7	3.10	5.1 min	1.323 ± 0.012
8	benzaldehyde	1.8 min	0.905 ± 0.026
9	3.13	4.2 min	1.340 ± 0.031
10	3-pyridinecarboxaldehyde	2.2 min	0.813 ± 0.029
11	3.16	4.6 min	0.822 ± 0.030
12	4-fluorobenzaldehyde	1.7 min	1.229 ± 0.028
13	3.19	4.2 min	1.180 ± 0.014
14	4-(trifluoromethyl)benzaldehyde	1.7 min	1.128 ± 0.013
15	3.22	4.1 min	1.487 ± 0.012
16	3-bromobenzaldehyde	3.1 min	1.104 ± 0.032
17	3.25	5.2 min	1.205 ± 0.041
18	3,4-dichlorobenzaldehyde	3.5 min	0.959 ± 0.035
19	3.28	5.6 min	1.043 ± 0.034

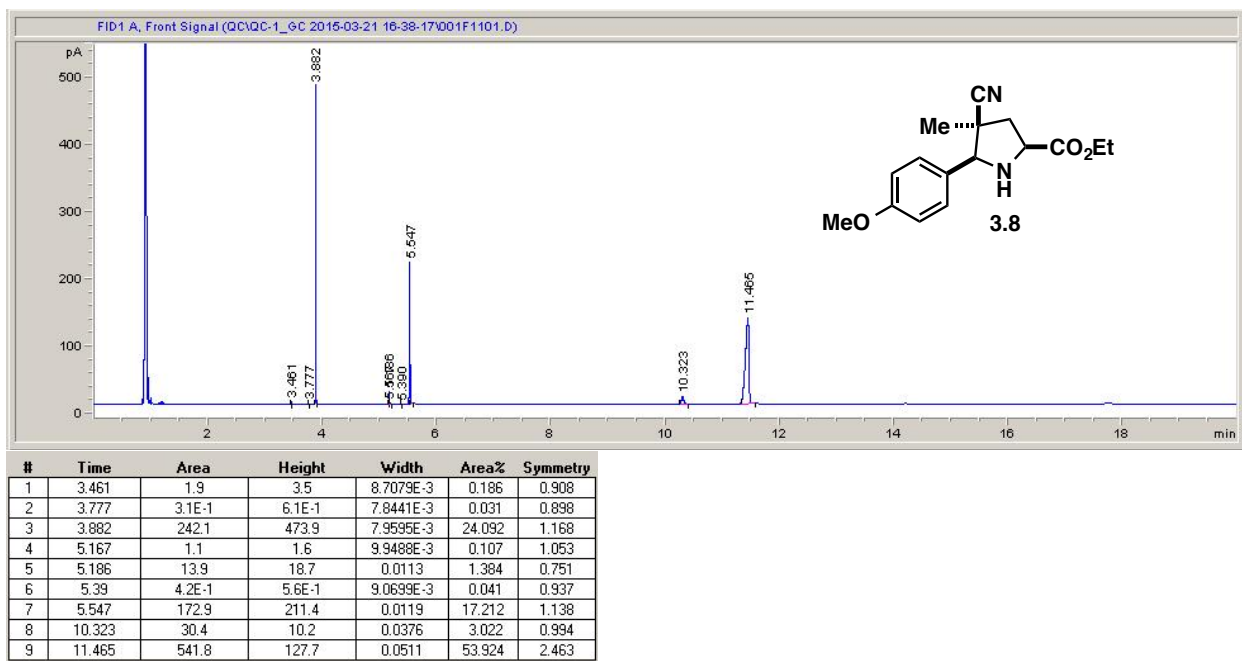
3.2, $t_R = 14.6$ min, F = 1.849 ± 0.084 :



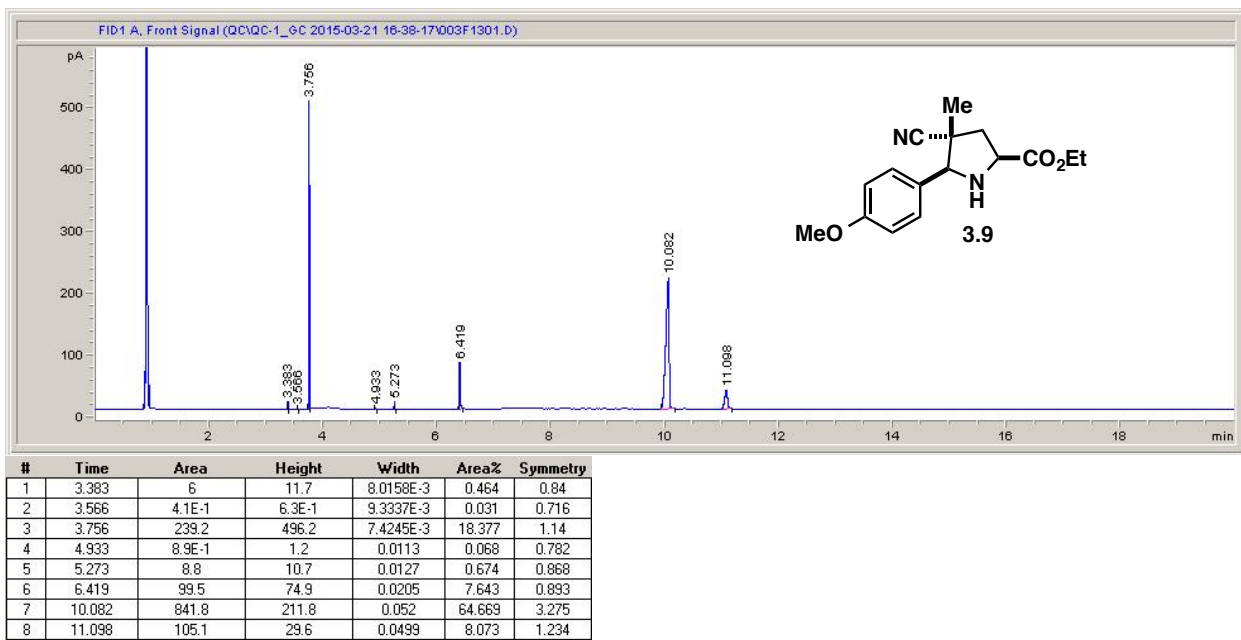
3.3, $t_R = 12.9$ min, $F = 1.778 \pm 0.076$:



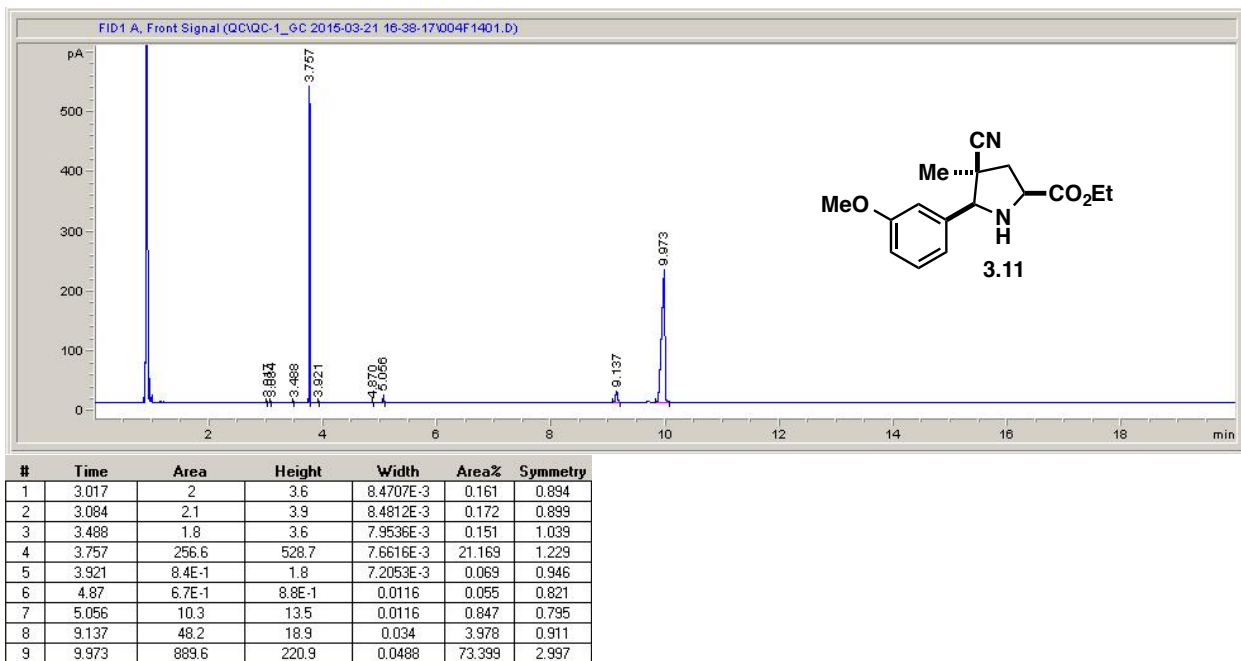
3.8, $t_R = 11.5$ min, $F = 1.823 \pm 0.057$:



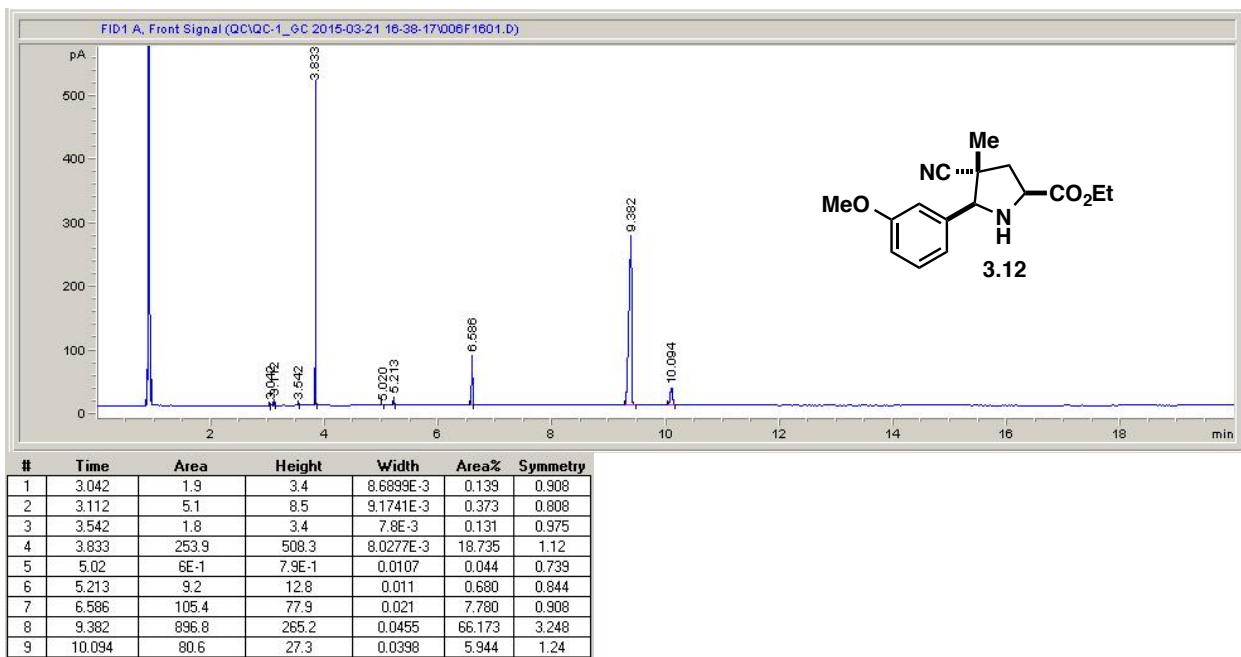
3.9, $t_R = 10.1$ min, $F = 1.888 \pm 0.064$:



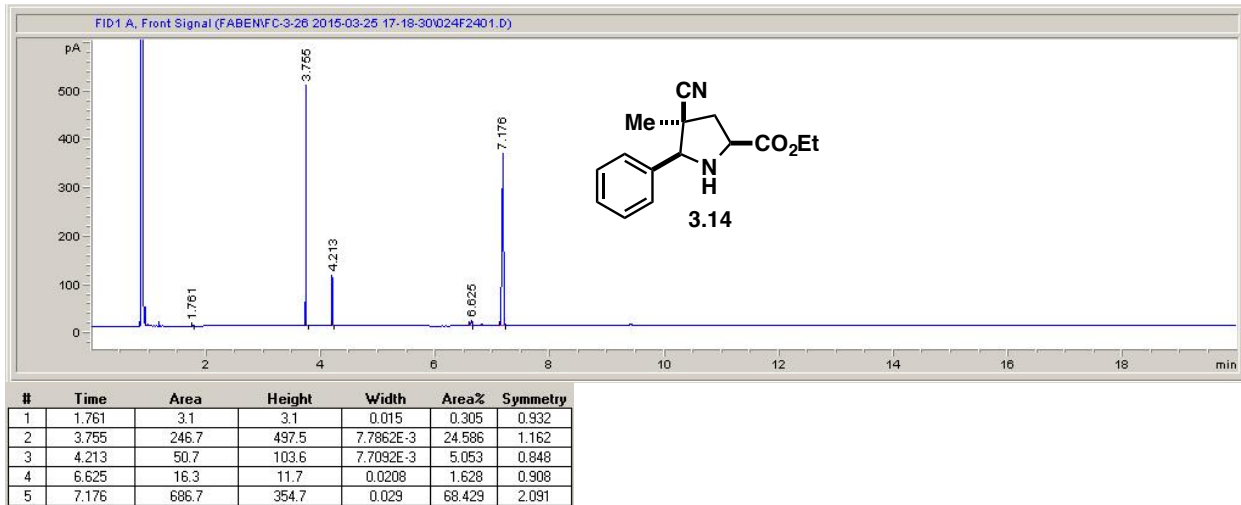
3.11, $t_R = 10.0$ min, $F = 2.000 \pm 0.025$:



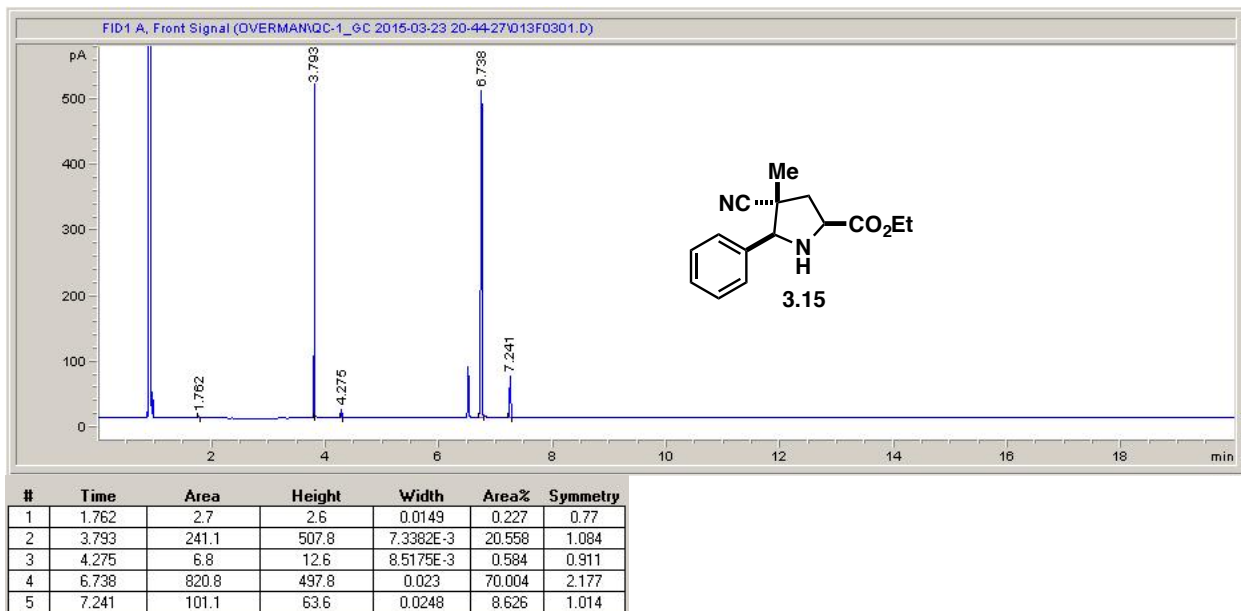
3.12, $t_R = 9.4$ min, $F = 2.024 \pm 0.032$:



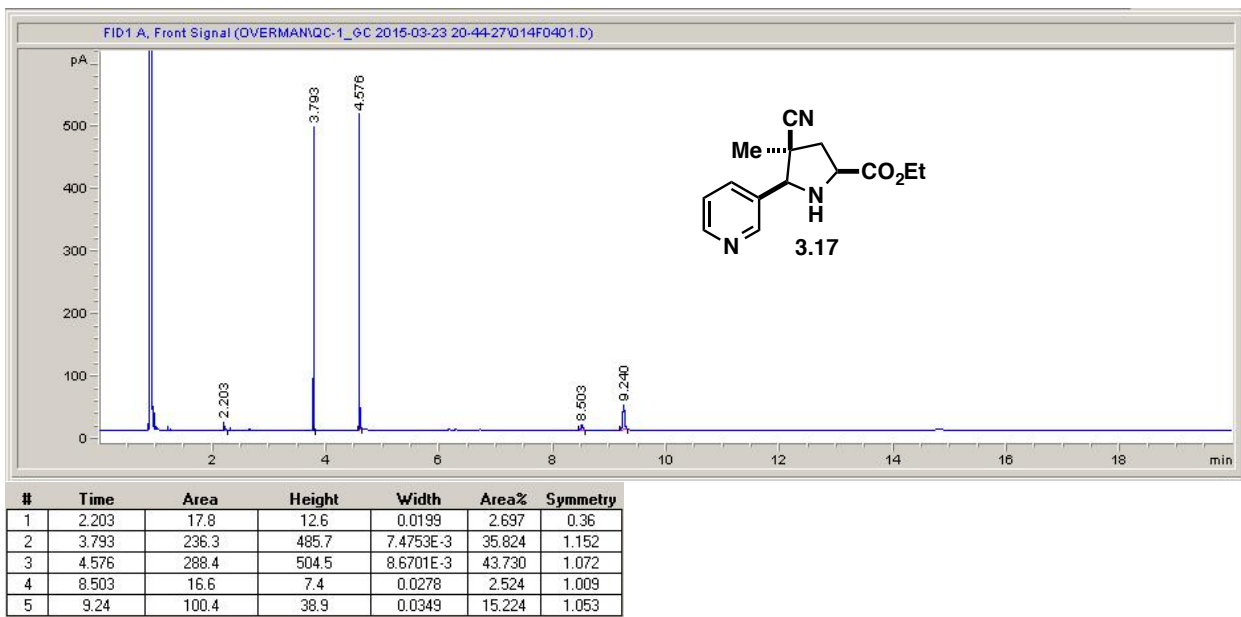
3.14, $t_R = 7.2$ min, $F = 1.984 \pm 0.044$:



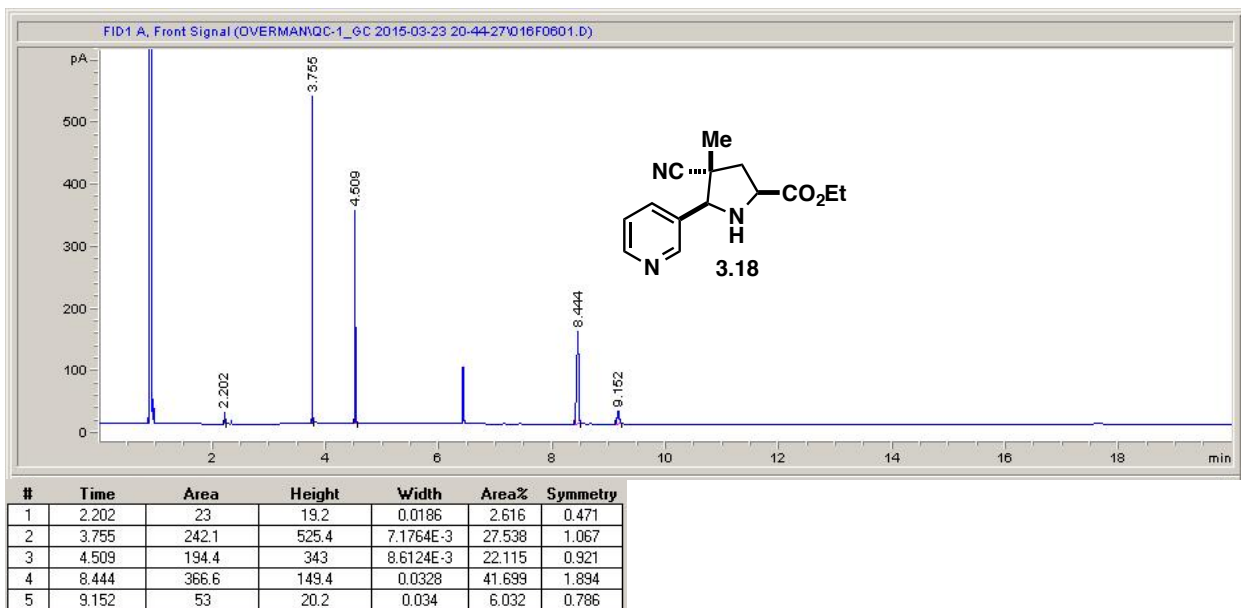
3.15, $t_R = 6.7$ min, $F = 1.978 \pm 0.032$:



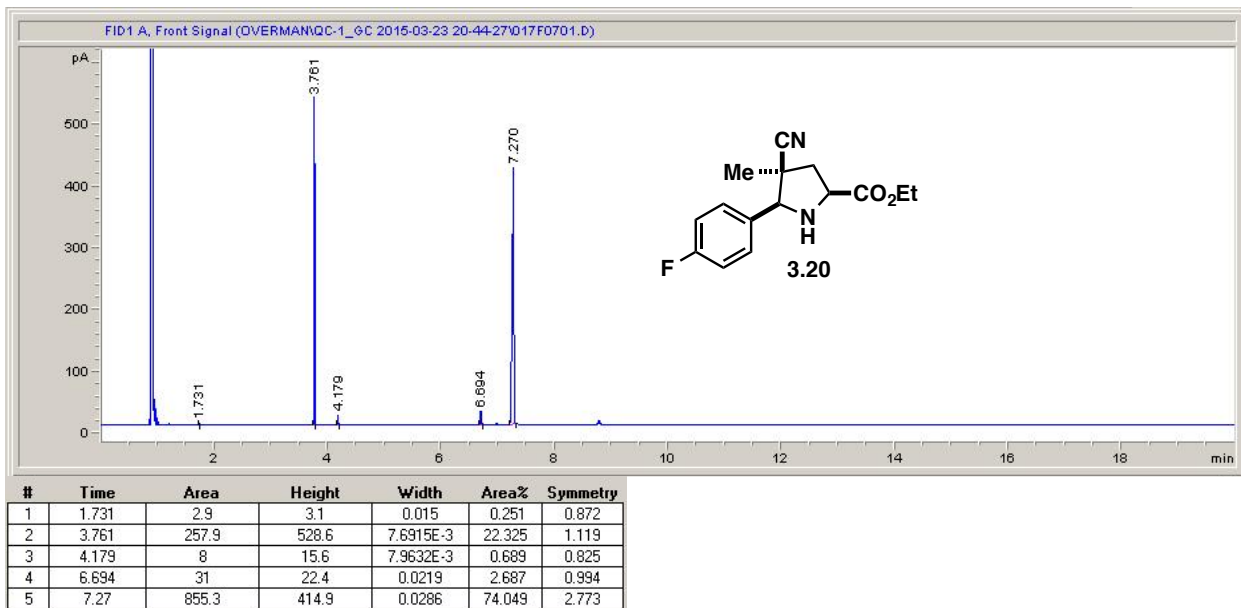
3.17, $t_R = 9.2$ min, $F = 1.671 \pm 0.066$:



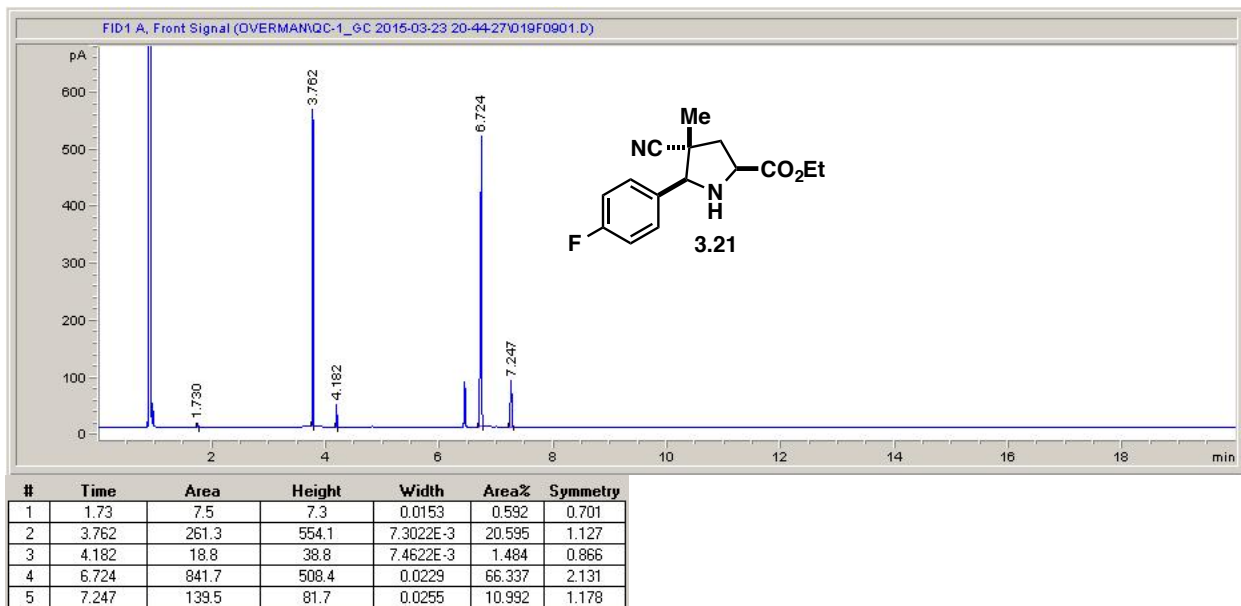
3.18, $t_R = 8.4$ min, $F = 1.600 \pm 0.079$:



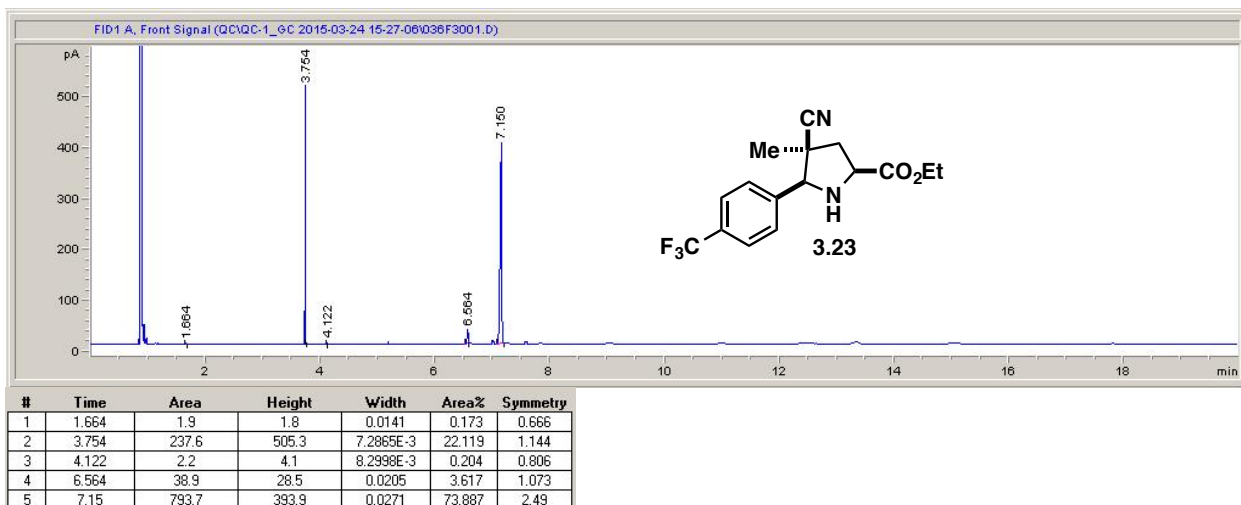
3.20, $t_R = 7.3$ min, $F = 2.014 \pm 0.042$:



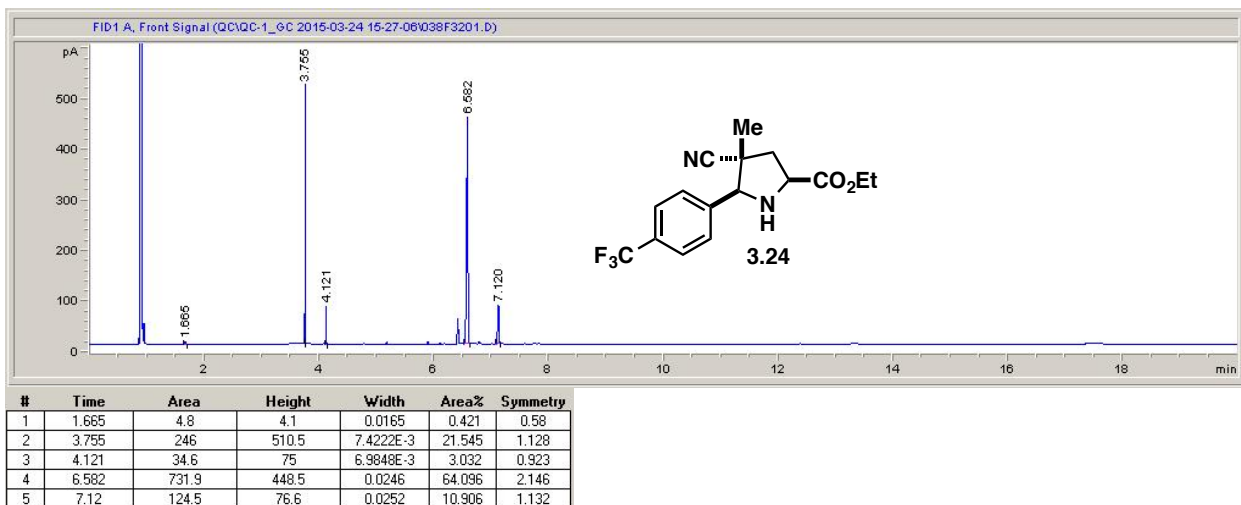
3.21, $t_R = 6.7$ min, $F = 1.729 \pm 0.017$:



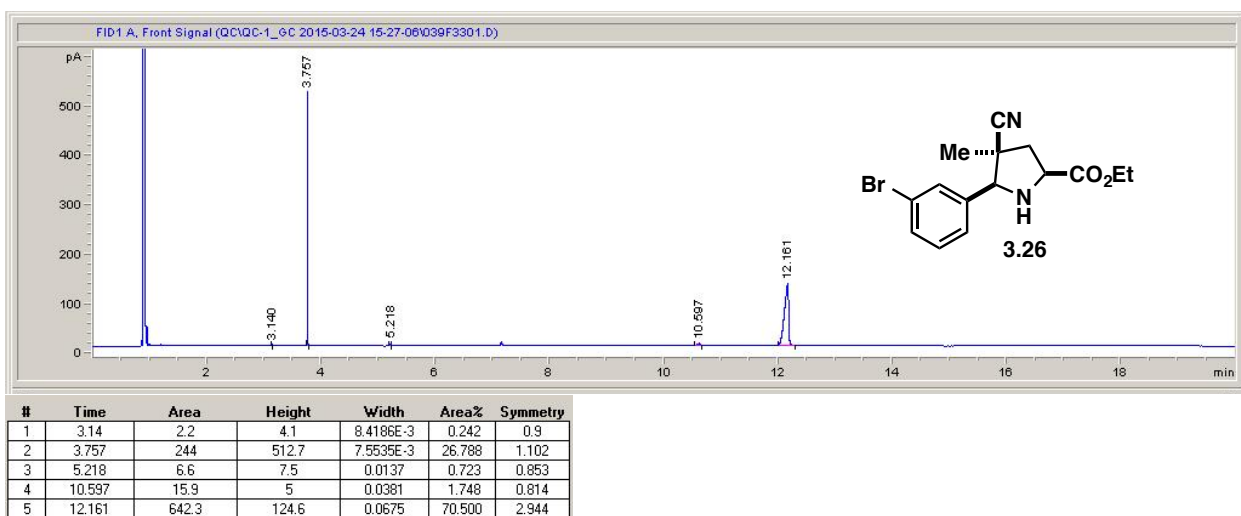
3.23, $t_R = 7.2$ min, $F = 1.943 \pm 0.031$:



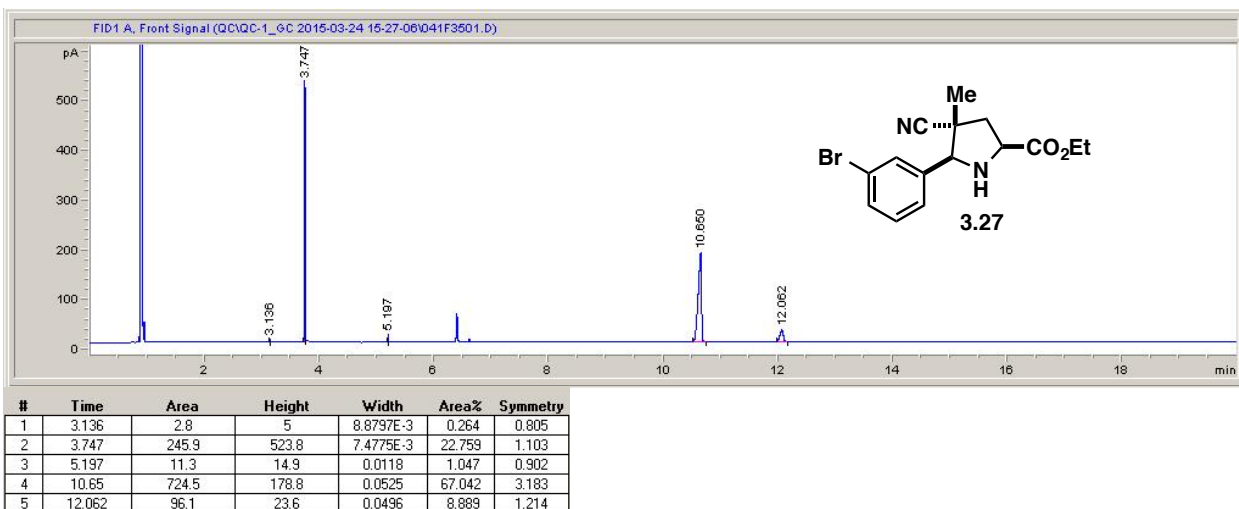
3.24, $t_R = 6.6$ min, $F = 1.919 \pm 0.022$:



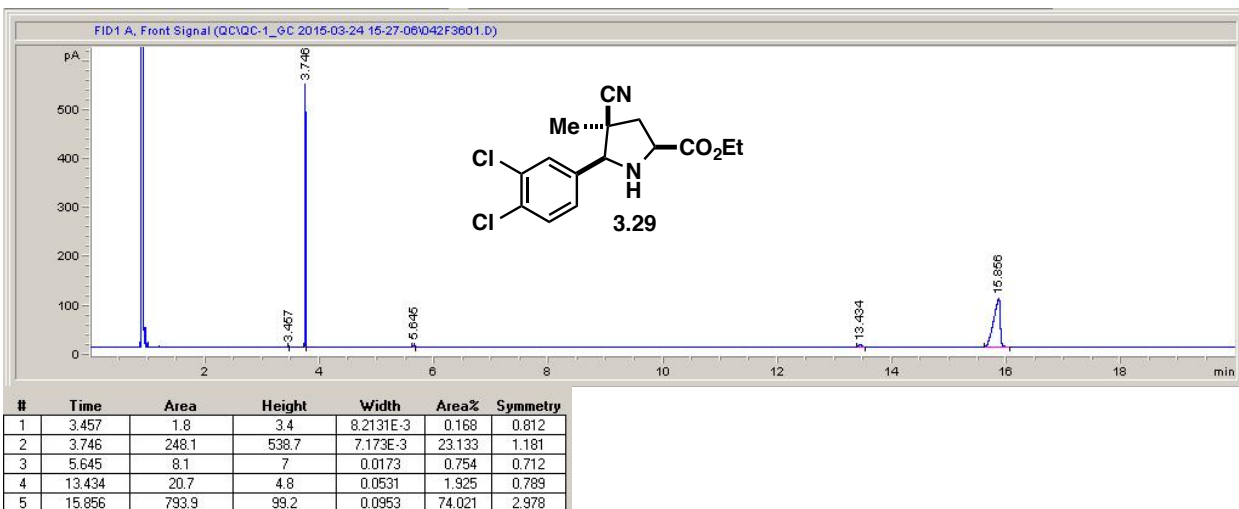
3.26, $t_R = 12.2$ min, $F = 1.837 \pm 0.036$:



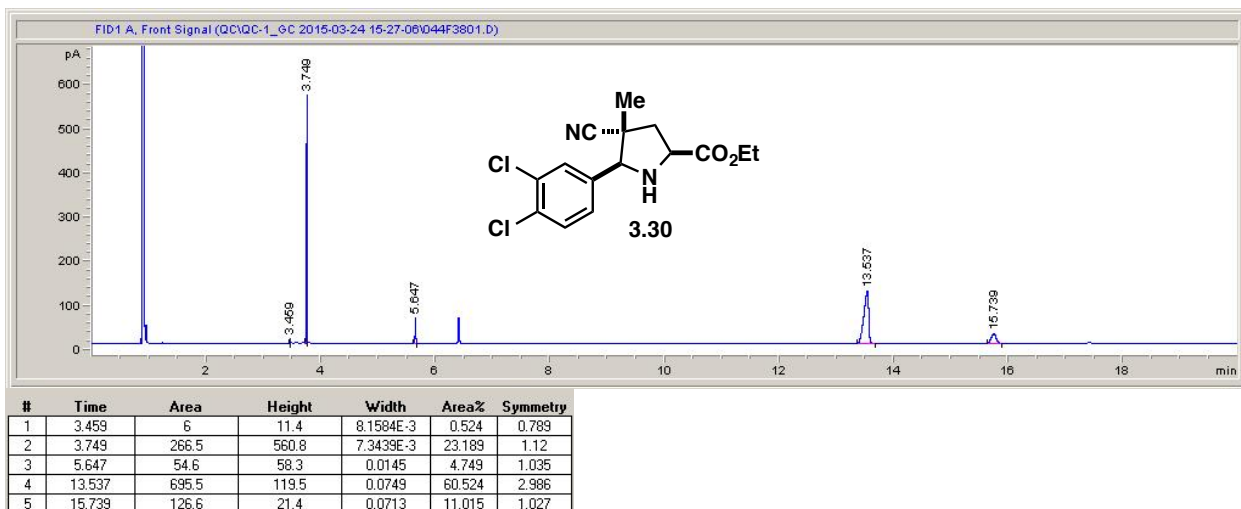
3.27, $t_R = 10.7$ min, F = 1.770 ± 0.015 :



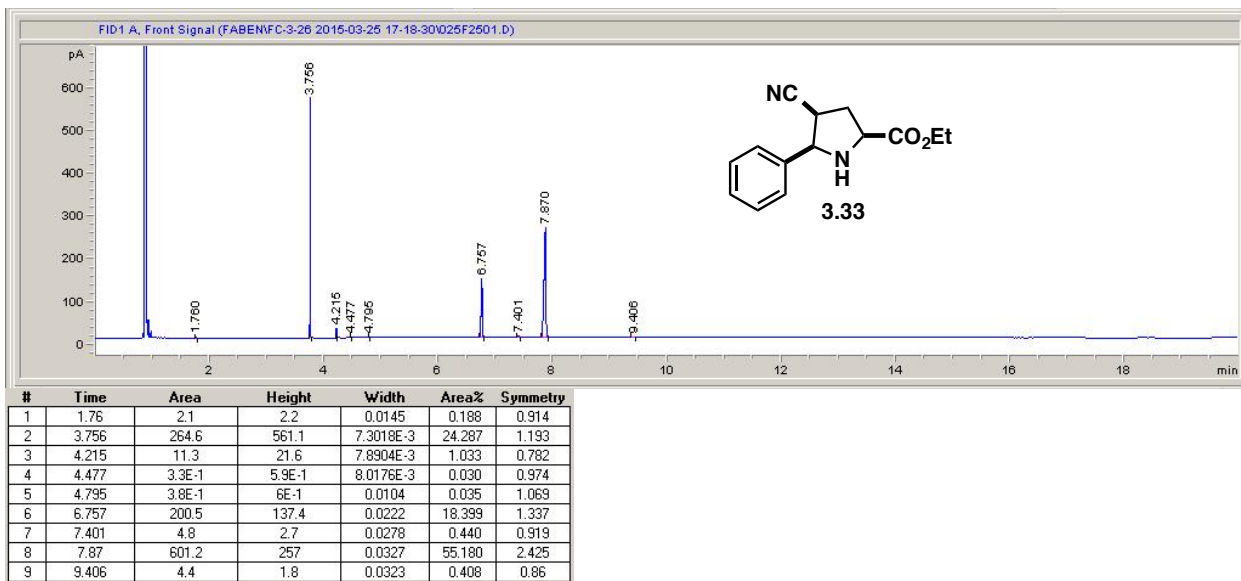
3.29, $t_R = 15.9$ min, F = 1.758 ± 0.032 :



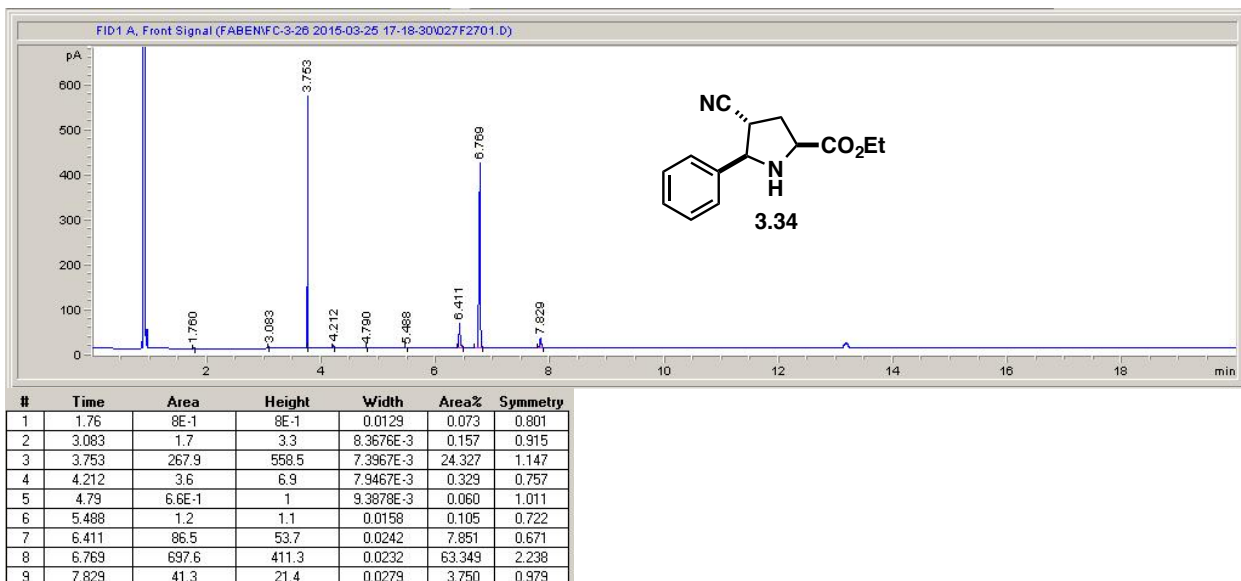
3.30, $t_R = 13.5$ min, F = 1.521 ± 0.099 :



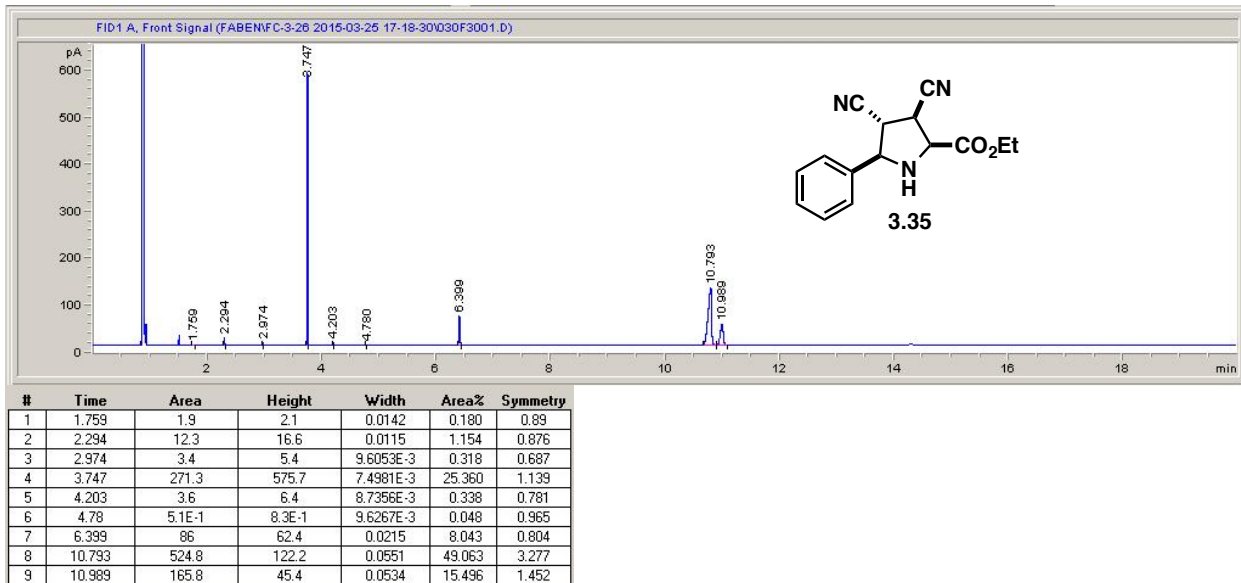
3.33, $t_R = 7.9$ min, F = 1.681 ± 0.025 :



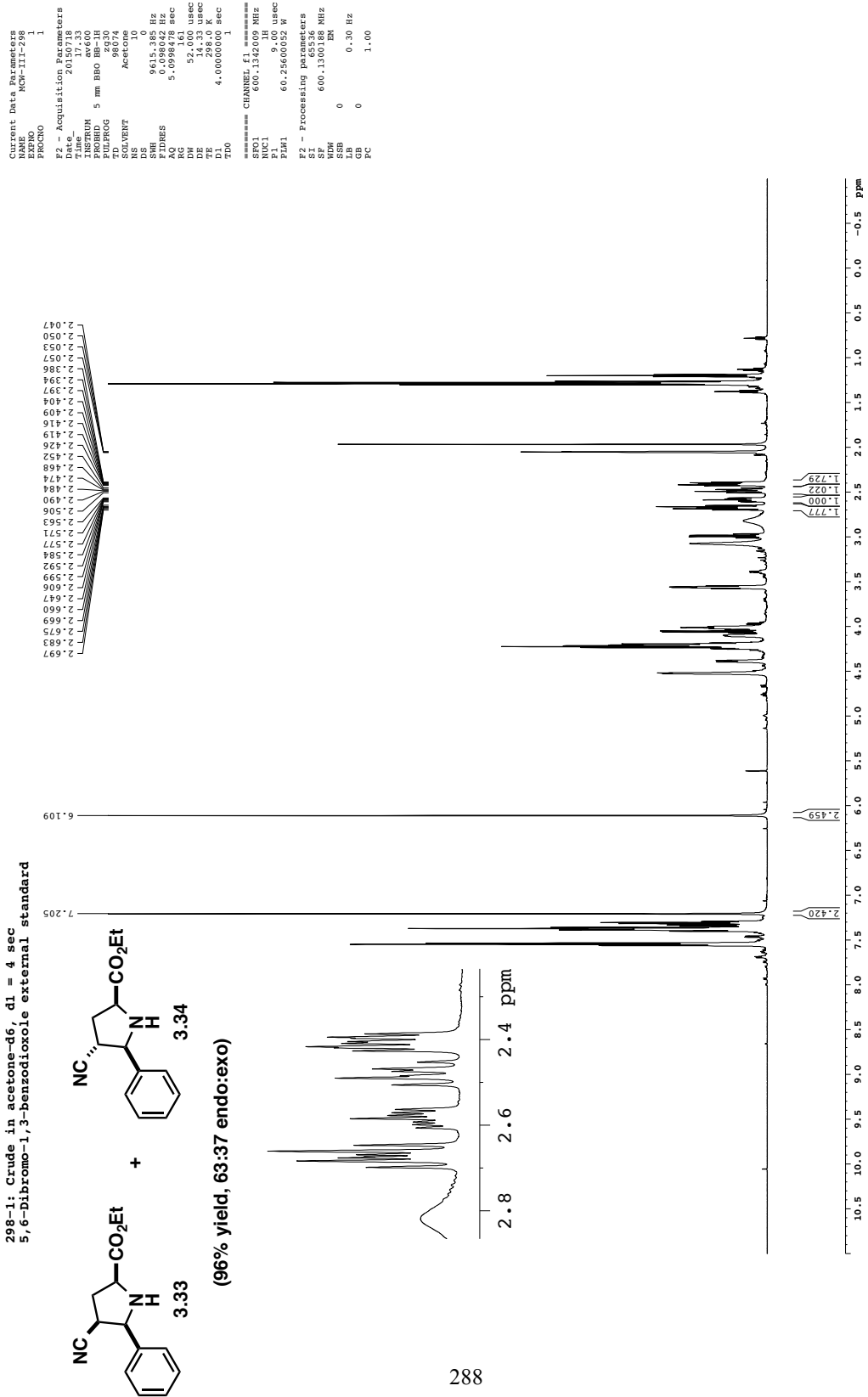
3.34, $t_R = 6.8$ min, $F = 1.714 \pm 0.034$:



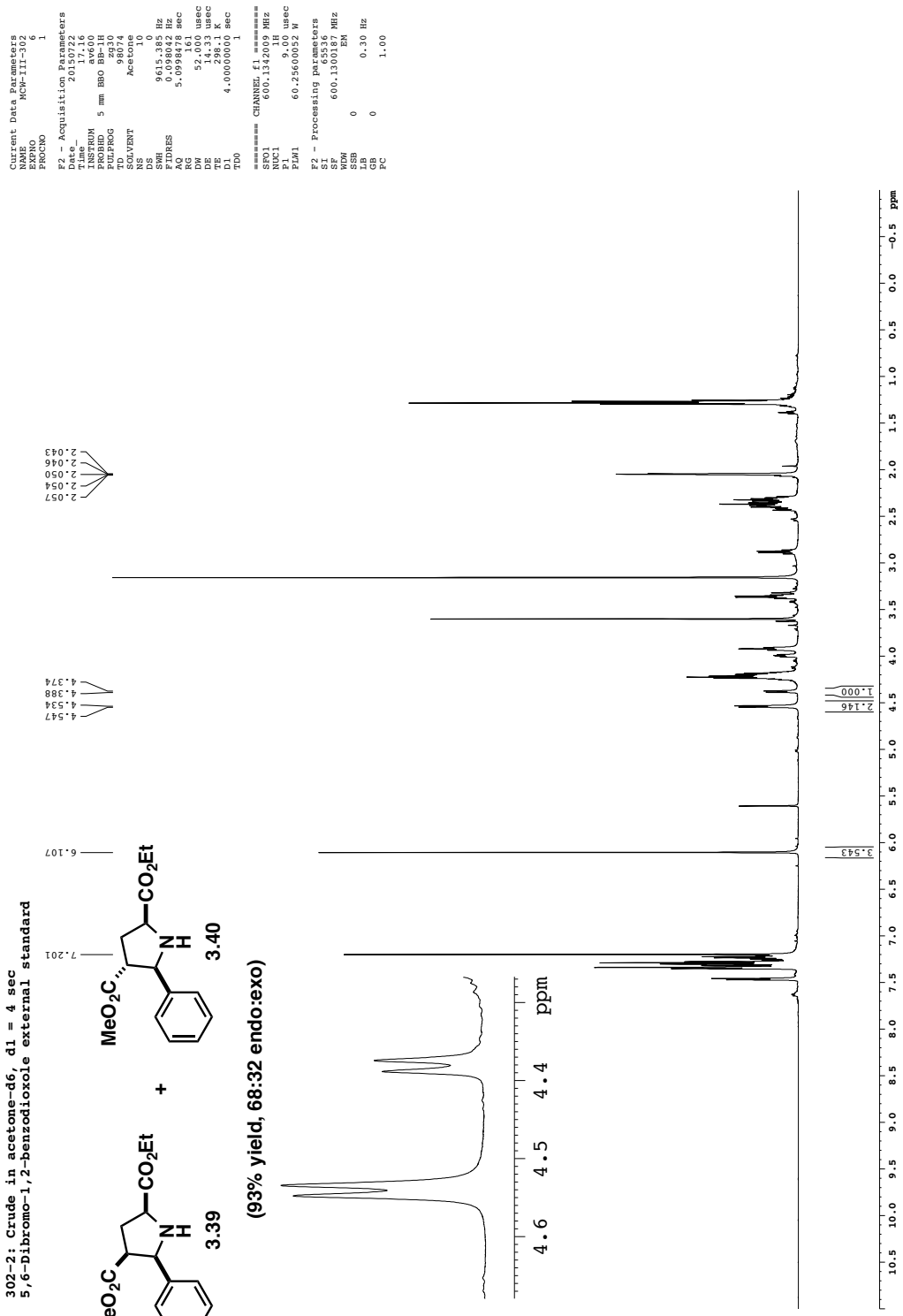
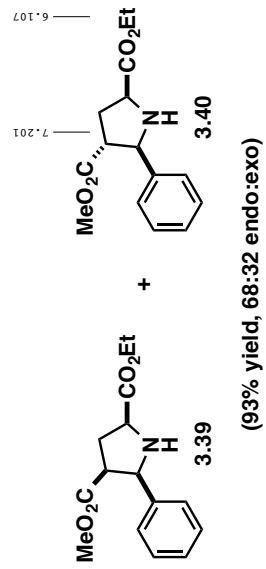
3.35, $t_R = 11.0$ min, $F = 1.503 \pm 0.026$:



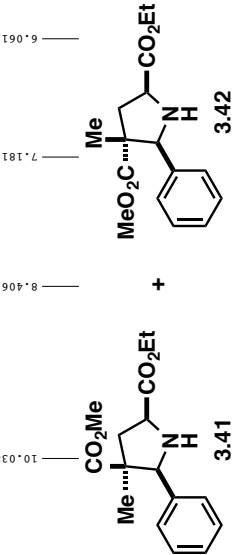
3.10 Appendix D: Representative Analytical ^1H NMR Spectral Data



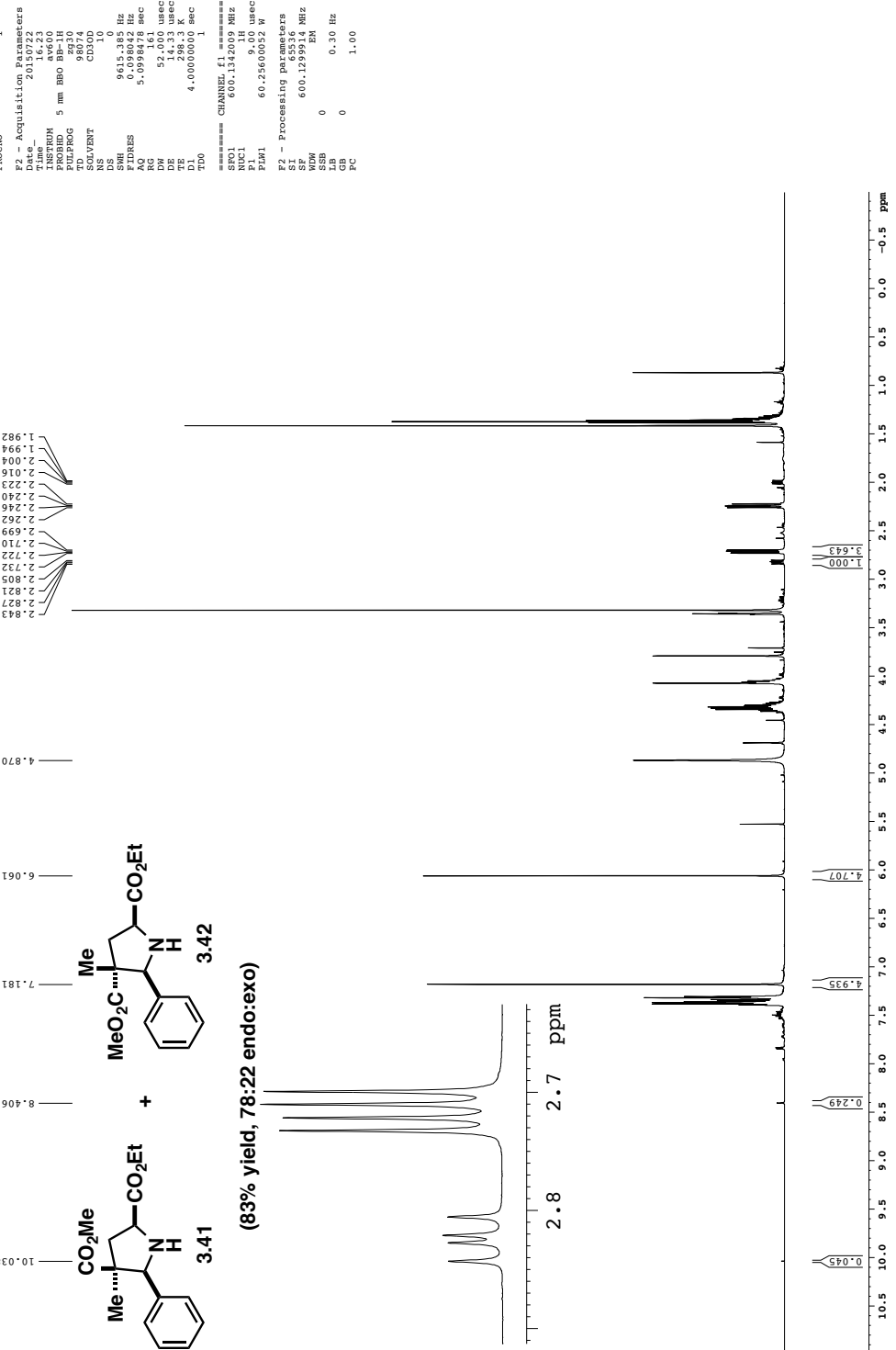
302-2: Crude in acetone-d₆, d₁ = 4 sec
 5,6-Dibromo-1,2-benzodioxole external standard



303-2: Crude in CD3OD, d1 = 4 sec
5,6-Dibromo-1,2-benzodioxole external standard



(83% yield, 78:22 endo:exo)



1. 1982
1. 1994
2. 2004
2. 2016
2. 2023
2. 2040
2. 2046
2. 2048
2. 2062
2. 699
2. 7110
2. 722
2. 732
2. 805
2. 821
2. 843

Current Data Parameters		Data Parameters	
	Value		Value
MCW-III-3	0	MCW-III	0
REPRO	1	REPRO	0
RCONO	1	RCONO	0
2 - Acquisition Parameters			
BBW	16.22	BBW	20.16
ULPBRID	16.22	ULPBRID	16.22
INSTRNMN	BB-BB-1H	INSTRNMN	BB-BB-1H
OLVENT	S	OLVENT	S
ADRES	S	ADRES	S
G	5.098478	G	5.098478
W	1.61	W	1.61
USEC	52.000000	USEC	52.000000
E	14.33	E	14.33
D	4.000000	D	4.000000
DD	1.00	DD	1.00
3 - Processing Parameters			
CHANNEL	11	CHANNEL	11
FCWL1	600.134000 MHz	FCWL1	600.134000 MHz
FCWL2	60.00000052 R	FCWL2	60.00000052 R
I	9.00 usec	I	9.00 usec
P	6.55346 MHz	P	6.55346 MHz
DW	EM	DW	EM
SBP	0.30 Hz	SBP	0.30 Hz
B	1.00	B	1.00
C	1.00	C	1.00

3.11 References and Notes

¹ For an example where the diastereoselectivity of a Cu(II)-catalyzed 1,3-DC was switched by employing two different *P,P'*-biaryl ligands and fumaronitrile as the dipolarophile, see: Oderaotoshi, Y.; Cheng, W.; Fujitomi, S.; Kasano, Y.; Minakata, S.; Komatsu, M. *Org. Lett.* **2003**, *5*, 5043.

² For examples where the diastereoselectivity can be altered by the 1,3-DC starting materials, see: (a) Cabrera, S.; Arrayás, R. G.; Martín-Matute, B.; Cossío, F. P.; Carretero, J. C. *Tetrahedron* **2007**, *63*, 6587. (b) Kim, H. Y.; Li, J.-Y.; Kim, S.; Oh, K. *J. Am. Chem. Soc.* **2011**, *133*, 20750. (c) Castelló, L. M.; Nájera, C.; Sansano, J. M.; Larrañaga, O.; de Cázar, A.; Cossío, F. P. *Synthesis* **2015**, 934.

³ For examples demonstrating a change in enantioselectivity in 1,3-DC reactions, see: (a) Zeng, W.; Chen, G.-Y.; Zhou, Y.-G.; Li, Y.-X. *J. Am. Chem. Soc.* **2007**, *129*, 750. (b) Kim, H. Y.; Shih, H.-J.; Knabe, W. E.; Oh, K. *Angew. Chem. Int. Ed.* **2009**, *48*, 7420. (c) Li, J.-Y.; Kim, H. Y.; Oh, K. *Org. Lett.* **2015**, *17*, 1288.

⁴ (a) Kauffmann, T.; Berg, H.; Köppelmann, E. *Angew. Chem.* **1970**, *82*, 396. (b) Kauffmann, T. *Angew. Chem. Int. Ed.* **1974**, *13*, 627. (c) Pearson, W. H.; Walters, M. A.; Oswell, K. D. *J. Am. Chem. Soc.* **1986**, *108*, 2769. (d) Tsuge, O.; Kanemasa, S.; Yorozu, K.; Ueno, K. *Bull. Chem. Soc. Jpn.* **1987**, *60*, 3359. (e) Tsuge, O.; Kanemasa, S.; Yoshioka, M. *J. Org. Chem.* **1988**, *53*, 1384. (f) Kanemasa, S.; Yoshioka, M.; Tsuge, O. *Bull. Chem. Soc. Jpn.* **1989**, *62*, 869. (g) Kanemasa, S.; Yamamoto, H. *Tetrahedron Lett.* **1990**, *31*, 3633. (h) Kanemasa, S.; Yamamoto, H.; Wada, E.; Sakurai, T.; Urushido, K. *Bull. Chem. Soc. Jpn.* **1990**, *63*, 2857. (i) Annunziata, R.; Cinquini, M.; Cozzi, F.; Raimondi, L.; Pilati, T. *Tetrahedron: Asymmetry* **1991**, *2*, 1329. (j) Kanemasa, S.; Hayashi, T.; Tanaka, J.; Yamamoto, H.; Sakurai, T. *J. Org. Chem.* **1991**, *56*, 4473.

⁵ Amornraksa, K.; Barr, D.; Donegan, G.; Grigg, R.; Ratananukul, P.; Sridharan, V. *Tetrahedron* **1989**, *45*, 4649.

⁶ For examples that describe the use of both silver and lithium salts, see: (a) Grigg, R.; Gunaratne, H. Q. N.; Sridharan, V. *Tetrahedron* **1987**, *43*, 5887. (b) Barr, D. A.; Grigg, R.; Gunaratne, H. Q. N.; Kemp, J.; McMeekin, P.; Sridharan, V. *Tetrahedron* **1988**, *44*, 557. (c) Barr, D. A.; Dorrity, M. J.; Grigg, R.; Malone, J. F.; Montgomery, J.; Rajviroongit, S.; Stevenson, P. *Tetrahedron Lett.* **1990**, *31*, 6569. (d) Grigg, R.; Montgomery, J.; Somasunderam, A. *Tetrahedron* **1992**, *48*, 10431. (e) Pätz, M.; Galley, G.; Jones, P. G.; Chrapkowsky, A. *Tetrahedron Lett.* **1993**, *34*, 5707. (f) Barr, D. A.; Dorrity, M. J.; Grigg, R.; Hargreaves, S.; Malone, J. F.; Montgomery, J.; Redpath, J.; Stevenson, P.; Thornton-Pett, M. *Tetrahedron* **1995**, *51*, 273.

⁷ Nyerges, M.; Rudas, M.; Tóth, G.; Herényi, B.; Kádas, I.; Bitter, I.; Töke, L. *Tetrahedron* **1995**, *51*, 13321.

⁸ Ayerbe, M.; Arrieta, A.; Cossío, F. P. *J. Org. Chem.* **1988**, *63*, 1795.

⁹ (a) Knöpfel, T. F.; Aschwanden, P.; Ichikawa, T.; Watanabe, T.; Carreira, E. M. *Angew. Chem. Int. Ed.* **2004**, *43*, 5971. (b) Stohlner, R.; Wahl, F.; Pfaltz, A. *Synthesis* **2005**, 1431. (c) Zeng, W.; Zhou, Y.-G. *Org. Lett.* **2005**, *7*, 5055. (d) Alemparte, C.; Blay, G.; Jørgensen, K. A. *Org. Lett.* **2005**, *7*, 4569. (e) Bonini, B. F.; Boschi, F.; Franchini, M. C.; Fochi, M.; Fini, F.; Mazzanti, A.; Ricci, A. *Synlett* **2006**, 543. (f) Nájera, C.; de Gracia Retamosa, M.; Sansano, J. M. *Org. Lett.* **2007**, *9*, 4025. (g) Zeng, W.; Zhou, Y.-G. *Tetrahedron Lett.* **2007**, *48*, 4619. (h) Nájera, C.; de Gracia Retamosa, M.; Sansano, J. M.; de Cázar, A.; Cossío, F. P. *Tetrahedron: Asymmetry* **2008**, *19*, 2913. (i) Nájera, C.; de Gracia Retamosa, M.; Sansano, J. M. *Angew. Chem. Int. Ed.* **2008**, *47*, 6055. (j) Agbodjan, A. A.; Cooley, B. E.; Copley, R. C. B.; Corfield, J. A.; Flanagan, R. C.; Glover, B. N.; Guidetti, R.; Haigh, D.; Howes, P. D.; Jackson, M. M.; Matsuoka, R. T.; Medhurst, K. J.; Millar, A.; Sharp, M. J.; Slater, M. J.; Toczko, J. F.; Xie, S. *J. Org. Chem.* **2008**, *73*, 3094. (k) Hernández-Toribio, J.; Arrayás, R. G.; Martín-Matute, B.; Carretero, J. C. *Org. Lett.* **2009**, *11*, 393. (l) Yu, S.-B.; Hu, X.-P.; Deng, J.; Wang, D.-Y.; Duan, Z.-C.; Zheng, Z. *Tetrahedron: Asymmetry* **2009**, *20*, 621. (m) Nájera, C.; de Gracia Retamosa, M.; Martín-Rodríguez, M.; Sansano, J. M.; de Cázar, A.; Cossío, F. P. *Eur. J. Org. Chem.* **2009**, 5622. (n) Wang, C.-J.; Xue, Z.-Y.; Liang, G.; Lu, Z. *Chem. Commun.* **2009**, 2905. (o) Liang, G.; Tong, M.-C.; Wang, C.-J. *Adv. Synth. Catal.* **2009**, *351*, 3101. (p) Robles-Machín, R.; Alonso, I.; Adrio, J.; Carretero, J. C. *Chem. Eur. J.* **2010**, *16*, 5286. (q) Oura, I.; Shimizu, K.; Ogata, K.; Fukuzawa, S. *Org. Lett.* **2010**, *12*, 1752. (r) Martín-Rodríguez, M.; Nájera, C.; Sansano, J. M.; Costa, P. R. R.; de Lima, E. C.; Dias, A. G. *Synlett* **2010**, 962. (s) Shimizu, K.; Ogata, K.; Fukuzawa, S. *Tetrahedron Lett.* **2010**, *51*, 5068. (t) Eröksüz, S.; Dogan, Ö.; Garner, P. P. *Tetrahedron: Asymmetry* **2010**, *21*, 2535. (u) Xue, Z.-Y.; Liu, T.-L.; Lu, Z.; Huang, H.; Tao, H.-Y.; Wang, C.-J. *Chem. Commun.* **2010**, *46*, 1727. (v) Yamashita, Y.; Imaizumi, T.; Kobayashi, S. *Angew. Chem. Int. Ed.* **2011**, *50*, 4893. (w) Yamashita, Y.; Imaizumi, T.; Guo, X.-X.; Kobayashi, S. *Chem. Asian J.* **2011**, *6*, 2550. (x) Liu, T.-L.; Xue, Z.-Y.; Tao, H.-Y.; Wang, C.-J. *Org. Biomol. Chem.* **2011**, *9*, 1980. (y) Tong, M.-C.; Li, J.; Tao, H.-Y.; Li, Y.-X.; Wang, C.-J. *Chem. Eur. J.* **2011**, *17*, 12922. (z) Liu, T.-L.; He, Z.-L.; Li, Q.-H.; Tao, H.-Y.; Wang, C.-J. *Adv. Synth. Catal.* **2011**, *353*, 1713. (aa) Xue, Z.-Y.; Fang, X.; Wang, C.-J. *Org. Biomol. Chem.* **2011**, *9*, 3622. (ab) Imae, K.; Konno, T.; Ogata, K.; Fukuzawa, S. *Org. Lett.* **2012**, *14*, 4410. (ac) Han, M.-L.; Wang, D.-Y.; Zeng, P.-W.; Zheng, Z.; Hu, X.-P. *Tetrahedron: Asymmetry* **2012**, *23*, 306. (ad) González-Esguevillas, M.; Adrio, J.; Carretero, J. C. *Chem. Commun.* **2013**, *49*, 4649. (ae) Lim, A. D.; Codelli, J. A.; Reisman, S. E. *Chem. Sci.* **2013**, *4*, 650. (af) Liu, K.; Teng, H.-L.; Yao, L.; Tao, H.-Y.; Wang, C.-J. *Org. Lett.* **2013**, *15*, 2250. (ag) Wang, Z.; Luo, S.; Zhang, S.; Yang, W.-L.; Liu, Y.-Z.; Li, H.; Luo, X.; Deng, W.-P. *Chem. Eur. J.* **2013**, *19*, 6739. (ah) Yamashita, Y.; Kobayashi, S. *Chem. Eur. J.* **2013**, *19*, 9420. (ai) Mancebo-Aracil, J.; Nájera, C.; Sansano, J. M. *Tetrahedron: Asymmetry* **2015**, *26*, 674. (aj) Bai, X.-F.; Song, T.; Xu, Z.; Xia, C.-G.; Huang, W.-S.; Xu, L.-W. *Angew. Chem. Int. Ed.* **2015**, *54*, 5255.

¹⁰ (a) Filippone, S.; Maroto, E. E.; Martín-Domenech, A.; Suárez, M.; Martín, N. *Nat. Chem.* **2009**, *1*, 578. (b) Arai, T.; Mishiro, A.; Yokoyama, N.; Suzuki, K.; Sato, H. *J. Am. Chem. Soc.* **2010**, *132*, 5338. (c) Wang, M.; Wang, Z.; Shi, Y.-H.; Shi, X.-X.; Fossey, J. S.; Deng, W.-P. *Angew. Chem. Int. Ed.* **2011**, *50*, 4897. (d) Maroto, E. E.; Filippone, S.; Martín-Domenech, A.; Suárez, M.; Martín, N. *J. Am. Chem. Soc.* **2012**, *134*, 12936. (e) Castelló, L. M.; Nájera, C.; Sansano, J. M.; Larrañaga, O.; de Cázar, A.; Cossío, F. P. *Org. Lett.* **2013**, *15*, 2902.

(f) Chaulagain, M. R.; Felten, A. E.; Gilbert, K.; Aron, Z. D. *J. Org. Chem.* **2013**, *78*, 9471.
(g) Maroto, E. E.; Filippone, S.; Suárez, M.; Martínez-Álvarez, R.; de Cózar, A.; Cossío, F. P.; Martín, N. *J. Am. Chem. Soc.* **2014**, *136*, 705. (h) Wang, Z.; Yu, X.; Tian, B.-X.; Payne, D. T.; Yang, W.-L.; Liu, Y.-Z.; Fossey, J. S.; Deng, W.-P. *Chem. Eur. J.* **2015**, *21*, 10457. (i) Dai, L.; Xu, D.; Tang, L.-W.; Zhou, Z.-M. *ChemCatChem* **2015**, *7*, 1078.

¹¹ BINAP = 2,2'-bis(diphenylphosphino)-1,1'-binaphthalene.

¹² Yan, X.-X.; Peng, Q.; Zhang, Y.; Zhang, K.; Hong, W.; Hou, X.-L.; Wu, Y.-D. *Angew. Chem. Int. Ed.* **2006**, *45*, 1979.

¹³ González-Esguevillas, M.; Pascual-Escudero, A.; Adrio, J.; Carretero, J. C. *Chem. Eur. J.* **2015**, *21*, 4561

¹⁴ When the Cu(I)/PCy₃ catalyst was used (Table 3.5, entry 6), a 60% yield of desired products was obtained. We hypothesize this is the result of excess PCy₃ acting as a catalytic base in the reaction. This is plausible because the pK_a of triethylammonium (10.75 in H₂O) is similar to that of tricyclohexylphosphonium (9.7 in nitromethane, see ref 15).

¹⁵ Henderson, W. A., Jr.; Streuli, C. A. *J. Am. Chem. Soc.* **1960**, *82*, 5791.

¹⁶ For reviews, see: (a) Johnson, J. S.; Evans, D. A. *Acc. Chem. Res.* **2000**, *33*, 325. (b) Stanley, L. M.; Sibi, M. P. *Chem. Rev.* **2008**, *108*, 2887. (c) Rasappan, R.; Laventine, D.; Reiser, O. *Coord. Chem. Rev.* **2008**, *252*, 702. (d) Surry, D. S.; Buchwald, S. L. *Chem. Sci.* **2010**, *1*, 13.

¹⁷ Initial calculations were performed using a 1:1 ligand-to-copper ratio. Later calculations showed that the coordination of a second molecule of PCy₃ is exergonic by 8.9 kcal/mol. To investigate the effects of the monodentate ligand-to-Cu(I) ratio, 1,3-DC reactions between imine **3.1** and methacrylonitrile were run using a 1.1:1 ratio of P(OCH₂CF₃)₃ or PCy₃ to Cu(I). This resulted in reduced catalyst solution solubility and the reactions were lower yielding compared to similar reactions run using a 2.2:1 ligand:Cu(I) ratio. Both experimental data and theoretical calculations showed that the diastereoselectivities of each reaction were independent on the ligand-to-metal ratio.

¹⁸ For reviews on 1,3-DC reactions, see: (a) Kanemasa, S. *Synlett* **2002**, 1371. (b) Coldham, I.; Hufton, R. *Chem. Rev.* **2005**, *105*, 2765. (c) Nájera, C.; Sansano, J. *Angew. Chem. Int. Ed.* **2005**, *44*, 6272. (d) Husinec, S.; Savic, V. *Tetrahedron: Asymmetry* **2005**, *16*, 2047. (e) Pandey, G.; Banerjee, P.; Gadre, S. R. *Chem. Rev.* **2006**, *106*, 4484. (f) Adrio, J.; Carretero, J. C. *Chem. Commun.* **2011**, *47*, 6784. (g) Nájera, C.; Sansano, J. M. *Monatsh. Chem.* **2011**, *142*, 659. (h) Nájera, C.; Sansano, J. M. *J. Organomet. Chem.* **2014**, *771*, 78. (i) Narayan, R.; Potowski, M.; Jia, Z.-J.; Antonchick, A. P.; Waldmann, H. *Acc. Chem. Res.* **2014**, *47*, 1296. (j) Adrio, J.; Carretero, J. C. *Chem. Commun.* **2014**, *50*, 12434. (k) Hashimoto, T.; Maruoka, K. *Chem. Rev.* **2015**, *115*, 5366.

¹⁹ (a) Rasmusson, G. H.; Reynolds, G. F.; Arth, G. E. *Tetrahedron Lett.* **1973**, *14*, 2145. (b) Belokon, Y. N.; Faleev, N. G.; Belikov, V. M.; Maksakov, V. A.; Petrovskii, P. V.;

Tsyryapkin, V. A. *Russian Chem. Bull.* **1977**, *26*, 813. (c) Grigg, R.; Kemp, J. *Tetrahedron Lett.* **1980**, *21*, 2461. (d) Grigg, R.; Kemp, J.; Malone, J.; Tangthongkum, A. *J. Chem. Soc. Chem. Commun.* **1980**, *14*, 648. (e) Grigg, R.; Kemp, J.; Malone, J. P.; Rajviroongit, S.; Tangthongkum, A. *Tetrahedron* **1988**, *44*, 5361. (f) van Es, J. J. G. S.; ten Wolde, A.; van der Gen, A. *J. Org. Chem.* **1990**, *55*, 4069. (g) Casas, J.; Grigg, R.; Nájera, C.; Sansano, J. M. *Eur. J. Org. Chem.* **2001**, *1971*. (h) Dogan, Ö.; Koyuncu, H. *J. Organomet. Chem.* **2001**, *631*, 135. (i) Dogan, Ö.; Koyuncu, H.; Kaniskan, Ü. *Turkish J. Chem.* **2001**, *25*, 365. (j) Bravi, G.; Goodland, H. S.; Haigh, D.; Hartley, C. D.; Lovegrove, V. L. H.; Shah, P.; Slater, M. J. 4-(5-Membered)-Heteroaryl Acyl Pyrrolidine Derivatives as HCV Inhibitors. Patl Appl. WO2003037894A1, May 8, 2003. (k) Burton, G.; Goodland, H. S.; Haigh, D.; Kiesow, T. J.; Ku, T. W.; Slater, M. J. 1-Carbonyl-4-Cyano-Pyrrolidine-2-Carboxylic Acid Derivatives as Hepatitis C Virus Inhibitors. Pat. Appl. WO2004009543A2, Jan. 29, 2004. (l) Boruah, M.; Konwar, D.; Sharma, S. D. *Tetrahedron Lett.* **2007**, *48*, 4535. (m) Chaulagain, M. R.; Aron, Z. D. *J. Org. Chem.* **2010**, *75*, 8271. (n) Joseph, R.; Murray, C.; Garner, P. *Org. Lett.* **2014**, *16*, 1550. (o) Swain, S. P.; Shih, Y.-C.; Tsay, S.-C.; Jacob, J.; Lin, C.-C.; Hwang, K. C.; Horng, J.-C.; Hwu, J. R. *Angew. Chem. Int. Ed.* **2015**, *54*, 9926.

²⁰ For reactions run using fumaronitrile as the dipolarophile, see reference 19f and: (a) Grigg, R.; Kemp, J.; Warnock, W. J. *J. Chem. Soc., Perkin Trans. I* **1987**, 2275. (b) Khlebnikov, A. F.; Novikov, M. S.; Khlebnikov, V. A.; Kostikov, R. R. *Russian J. Org. Chem.* **2001**, *37*, 507. (c) Aly, M. F.; Abbas-Temirek, H. H.; Elboray, E. E. *ARKIVOC* **2010**, *3*, 237. (d) Padilla, S.; Tejero, R.; Adrio, J.; Carretero, J. C. *Org. Lett.* **2010**, *12*, 5608. (e) Cabrera, S.; Arrayás, R. G.; Carretero, J. C. *J. Am. Chem. Soc.* **2005**, *127*, 16394.

²¹ For reactions run using nitrile-containing dipolarophiles other than acrylonitrile and fumaronitrile, see references 13, 19f, j, k; 20c; and: (a) Joucla, M.; Hamelin, J. *Tetrahedron Lett.* **1978**, *19*, 2885. (b) Joucla, M.; Fouchet, B.; Hamelin, J. *Tetrahedron* **1985**, *41*, 2707. (c) Bartkovitz, D. J.; Chu, X.-J.; Ding, Q.; Jiang, N.; Liu, J.-J.; Ross, T. M.; Zhang, J.; Zhang, Z. Substituted Pyrrolidine-2-Carboxamides. Pat. Appl. WO2011098398A1, Aug. 18, 2011. (d) Chu, X.-J.; Ding, Q.; Jiang, N.; Liu, J.-J.; Ross, T. M.; Zhang, Z. N-Substituted Pyrrolidines. Pat. Appl. US20120010235A1, Jan. 12, 2012. (e) Shu, L.; Li, Z.; Gu, C.; Fishlock, D. *Org. Process Res. Dev.* **2013**, *17*, 247. (f) Ding, Q.; Zhang, Z.; Liu, J.-J.; Jiang, N.; Zhang, J.; Ross, T. M.; Chu, X.-J.; Bartkovitz, D.; Podlaski, F.; Janson, C.; Tovar, C.; Filipovic, Z. M.; Higgins, B.; Glenn, K.; Packman, K.; Vassilev, L. T.; Graves, B. *J. Med. Chem.* **2013**, *56*, 5979. (g) Rajkumar, V.; Babu, S. A. *Synlett* **2014**, 2629.

²² (a) Overman, L. E.; Baumann, M.; Nam, S.; Horne, D.; Jove, R.; Xie, J.; Kowolik, C. ETP Derivatives. PCT Int. Appl. WO 2014066435 A1, October 22, 2012. (b) Baumann, M.; Dieskau, A. P.; Loertscher, B. M.; Walton, M. C.; Nam, S.; Xie, J.; Horne, D.; Overman, L. E. *Chem. Sci.* **2015**, *6*, 4451.

²³ Relative configuration of the cycloadducts was assigned by 2D ¹H NMR experiments (see Appendix B for details).

²⁴ Tentative structural assignments of pyrrolidines **3.36** and **3.37** were based off 2D ¹H NMR experiments alone.

²⁵ For a reports discussing the concerted versus step-wise mechanism of 1,3-DC reactions, see: (a) Houk, K. N.; González, J.; Li, Y. *Acc. Chem. Res.* **1995**, *28*, 81. (b) Vivanco, S.; Lecea, B.; Arrieta, A.; Prieto, P.; Morao, I.; Linden, A.; Cossío, F. P. *J. Am. Chem. Soc.* **2000**, *122*, 6078.

²⁶ Solidifies at -20 °C.

²⁷ McKerrow, J. D.; Al-Rawi, J. M.; Brooks, P. *Synth. Commun.* **2010**, *40*, 1161.

²⁸ It was demonstrated that some imine substrates resulted in messy crude products when using the procedure described for imine **3.1**. Cleaner crude products could be accessed by using this alternative procedure with the corresponding glycine ethyl ester free base **3.43**.

²⁹ Prepared according to the procedure described by Gagné: Andrews, R. S.; Becker, J. J.; Gagné, M. R. *Angew. Chem. Int. Ed.* **2010**, *49*, 7274.